

AD 749279

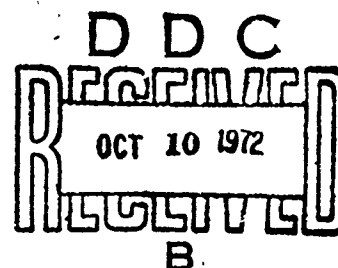
**LATERAL SEPARATION
VOLUME II
STUDY APPROACH**

**Advanced Systems Department
Resalab Incorporated
Dallas, Texas 75217**



JULY 1972

FINAL REPORT



Availability is unlimited. Document may
be released to the National Technical
Information Service, Springfield, Virginia
22151, for sale to the public.

Prepared for
DEPARTMENT OF TRANSPORTATION
FEDERAL AVIATION ADMINISTRATION
Systems Research & Development Service
Washington D C., 20591

Reproduced by
**NATIONAL TECHNICAL
INFORMATION SERVICE**
U S Department of Commerce
Springfield VA 22151

The contents of this report reflect the views of Resalab, Inc., Dallas, Texas which is responsible for the facts and the accuracy of the data presented herein. The contents do not necessarily reflect the official views or policy of the Department of Transportation. This report does not constitute a standard, specification or regulation.

ACCESSION FOR	
NTIS	Write Section <input checked="" type="checkbox"/>
DIC	Diff Section <input type="checkbox"/>
UNANNOUNCED	<input type="checkbox"/>
JUSTIFICATION	
BY	
DISTRIBUTION/AVAILABILITY CODES	
Dist	AVAIL. and/or SPECIAL
A	

- add A for Transport Hardware
The same for 'S' lot 72

TECHNICAL REPORT STANDARD TITLE PAGE

1. Report No. FAA-RD-72-58, II	2. Government Accession No.	3. Recipient's Catalog No.	
4. Title and Subtitle LATERAL SEPARATION VOLUME II STUDY APPROACH		5. Report Date July 1972	
		6. Performing Organization Code	
7. Author(s) Advanced Systems Department		8. Performing Organization Report No.	
9. Performing Organization Name and Address Resalab, Incorporated Dallas, Texas 75217		10. Work Unit No. Project 142-177-031	
		11. Contract or Grant No. DOT-FA71WA-2609	
12. Sponsoring Agency Name and Address FEDERAL AVIATION ADMINISTRATION Systems Research and Development Service Washington, D. C. 20591		13. Type of Report and Period Covered Final Report June 1971 to July 1972	
		14. Sponsoring Agency Code	
15. Supplementary Notes			
16. Abstract <p>The Lateral Separation Study provides a means of establishing the feasibility of minimizing runway spacings for the purpose of increasing terminal IFR operational capacity. A method for determining minimum lateral spacings between runways and measuring the relative safety for a given runway spacing is provided in Volume I of this report. Volume II presents the data essential to the determination of minimum runway spacings, including probability of collision data, normal operating zone data, and blunder recovery data, and develops the techniques used to generate this data.</p> <p>Probability density functions, which describe the location errors of aircraft operating under IFR conditions, were used to generate the probability of collision data and normal operating zone data. The Fokker-Planck equation was used to generate the lateral error probability density functions. Generation of the blunder recovery data was accomplished using a parametric variation on the pertinent system parameters.</p>			
17. Key Words Minimum Runway Lateral Separation Probability of Collision, Fokker-Planck, Blunder Recovery Area, Normal Operating Zone		18. Distribution Statement Availability is unlimited. Document may be released to the National Technical Information Service, Springfield, Virginia 22151, for sale to the public.	
19. Security Classif. (of this report) Unclassified	20. Security Classif. (of this page) Unclassified	21. No. of Pages 564 581	22. Price \$6.00 PC .95 MF

TABLE OF CONTENTS

Section		Page
1	Introduction	1-1
1.1	Problem Definition	1-3
2	Method of Solution	2-1
2.1	System Model Development	2-5
2.1.1	Model Concept Definition	2-5
2.1.2	Nominal Model	2-8
2.1.2.1	Introduction	2-8
2.1.2.2	Approach	2-8
2.1.2.3	Nominal Model Results	2-21
2.1.3	Expanded Models	2-27
2.1.3.1	Approach System Models	2-31
2.1.3.2	Curved Path Model and Multiple Aircraft/ Runway Model	2-36
2.1.4	Error Definition	2-48
2.1.4.1	Introduction	2-48
2.1.4.2	Approach	2-48
2.1.4.3	Results	2-53
2.1.5	State Equations	2-53
2.1.5.1	Introduction	2-53
2.1.5.2	Approach	2-56
2.1.5.3	State Equation Results	2-61
2.2	Fokker-Planck Development	2-67
2.2.1	Development Approach	2-68
2.2.1.1	Markov Representation of the State Vector	2-68
2.2.1.2	Reduction of the System Model	2-69
2.2.1.3	Fokker-Planck Implementation	2-75
2.2.2	Checkout/Verification of Fokker-Planck Method	2-89
2.2.2.1	Gaussian Density Comparison	2-89
2.2.2.2	Lateral Deviation Variance Response	2-95
2.3	Measured Distributions	2-99
2.3.1	Techniques Used to Collect, Reduce, and Process Distribution Data	2-101
2.3.1.1	Data Collection	2-101
2.3.1.2	Data Reduction	2-106
2.3.1.3	Data Processing	2-112
2.3.2	Measured Distribution Determination	2-113
2.3.2.1	Tabular Distribution Data	2-113
2.3.2.2	Gaussian Distributed Data	2-114
2.3.2.3	Systems with No Collected Data	2-114
2.3.3	Measured Distribution Data Validity	2-119

TABLE OF CONTENTS (Continued)

Section		Page
2.4	Nominal Model Verification and Sensitivity Analysis	2-123
2.4.1	Time Response	2-124
2.4.2	Frequency Response	2-127
2.4.3	Statistical Response	2-136
2.4.4	Sensitivity Analysis	2-142
2.4.4.1	System Parameter Sensitivity	2-142
2.4.4.2	System Error Sensitivity	2-144
2.5	Probability Density Functions and Normal Operating Zones	2-153
2.5.1	Lateral Probability Density Function Models	2-153
2.5.2	Probability Density Function Generation	2-157
2.5.2.1	Procedure for Lateral Density Function Generation	2-157
2.5.2.2	Procedure for Vertical Density Function Generation	2-162
2.5.2.3	Procedure for Longitudinal Density Function Generation	2-162
2.5.3	Normal Operating Zone Determination	2-164
2.5.3.1	NOZ Determination for Approach Systems	2-165
2.5.3.2	CTOL/STOL Skewed Normal Operating Zone	2-165
2.6	Probability of Collision	2-173
2.6.1	Analytical Development	2-174
2.6.1.1	STOL/STOL Independent	2-176
2.6.1.2	CTOL/CTOL Independent	2-180
2.6.1.3	CTOL/CTOL Dependent	2-183
2.6.1.4	CTOL/STOL Independent	2-187
2.6.2	Probability of Collision Data Generation	2-189
2.6.2.1	CTOL/CTOL - Probability of Collision Data Generation	2-192
2.6.2.2	CTOL/STOL - Probability of Collision Data Generation	2-195
2.6.2.3	STOL/STOL - Probability of Collision Data Generation	2-195
2.7	Blunder Analysis	2-201
2.7.1	Single Aircraft Analysis	2-202
2.7.1.1	Introduction	2-202
2.7.1.2	Approach	2-202
2.7.1.3	Results	2-209
2.7.2	Dual Aircraft Analysis	2-215

TABLE OF CONTENTS (Continued)

Section	Page
2.7.2.1 Introduction	2-215
2.7.2.2 Approach	2-215
2.7.2.3 Results	2-222
3 Study Outputs	3-1
3.1 Measured Distribution Data	3-5
3.1.1 Distribution Data Presentation	3-6
3.1.2 Measured Distribution Data Validity Observations	3-11
3.2 System Models	3-17
3.3 Sensitivity Data	3-41
3.4 Probability Density Function Data	3-47
3.4.1 Error Distribution Data	3-47
3.4.2 NOZ Data	3-50
3.5 Probability of Collision Data	3-55
3.5.1 CTOL/CTOL Probability of Collision Data	3-56
3.5.2 CTOL/STOL Independent Operations	3-57
3.5.3 STOL/STOL Independent Operations	3-57
3.6 Blunder Data	3-63
4 Summary	4-1

Appendix	Page
A Aircraft Model	A-1
B A Mathematical Description of Davison's Method	B-1
C Solutions of Partial Differential Equations by the Use of Finite Differences	C-1
D Variance Propagation of a Linear System	D-1
E Measured Distribution Data	E-1
F Sensitivity Analysis	F-1
G Approach System Models	G-1
H Probability Density Function Data and Normal Operating Zone Data	H-1
I Probability of Collision Data	I-1
J Single Aircraft Blunder Analysis Data	J-1
K Dual Aircraft Blunder Analysis Data	K-1
L Bibliography	L-1

LIST OF ILLUSTRATIONS

Figure		Page
2-1	Method of Solution	2-2
2.1.1-1	General System Model	2-7
2.1.2-1	Coordinate Systems	2-13
2.1.2-2	Course Deviation Indicator Model	2-15
2.1.2-3	Pilot Model	2-16
2.1.2-4	Simulated Delay Response	2-17
2.1.2-5	Aircraft Model	2-19
2.1.2-6	Nominal System Model	2-22
2.1.2-7	Nonlinear, Simulated Delay Nominal Model	2-23
2.1.2-8	Linear, Simulated Delay Nominal Model	2-24
2.1.2-9	Aircraft Bank Angle Response	2-28
2.1.2-10	Aircraft Heading Angle Response	2-29
2.1.2-11	Aircraft Lateral Deviation Response	2-30
2.1.3-1	Curved Approach Geometry	2-38
2.1.3-2	Curved Model Regions of Validity	2-40
2.1.3-3	Base Leg System Model	2-41
2.1.3-4	Turning System Model	2-42
2.1.3-5	Multiple Aircraft/Runway Model Possible Parallel Runway Configurations	2-44
2.1.3-6	Multiple Aircraft/Runway Model Possible Skewed Runway Configurations	2-45
2.1.3-7	Multiple Aircraft/Runway Model Block Diagram	2-46
2.1.3-8	Multiple Aircraft/Runway Model Description of Relative Distances and Rates	2-47
2.1.4-1	Typical Localizer "Noise" Power Spectral Density	2-51
2.1.5-1	Inner Loop Flow Graph	2-58
2.2.1-1	Lateral Distribution Standard Deviation Per Cent Difference Between Linear and Nonlinear Models	2-71
2.2.1-2	Comparison of Lateral Deviation Time Response for Second, Sixth, and Nonlinear Systems	2-77
2.2.1-3	Lateral Deviation Probability Density Function	2-81
2.2.2-1	Lateral Deviation Density Function at One Second	2-91
2.2.2-2	Lateral Deviation Density Function at Ten Seconds	2-92
2.2.2-3	Lateral Deviation Density Function at Twenty Seconds	2-93
2.2.2-4	Lateral Deviation Density Function at Thirty Seconds	2-94

LIST OF ILLUSTRATIONS (Continued)

Figure		Page
2.2.2-5	Comparison of the Fokker-Planck and Linear Gaussian Solution Technique	2-96
2.3.1-1	Data Collection, Reduction, and Processing Technique	2-102
2.3.1-2	Sample Photograph of Collected Data	2-103
2.3.1-3	Charleston Municipal/AFB Airport	2-105
2.3.1-4	Data Reduction Equipment	2-107
2.3.1-5	Data Reduction Measurements	2-108
2.3.2-1	Standard Deviation Versus Range for FC-ILS-I-STOL (Lateral)	2-117
2.4.1-1	Nominal Model Lateral Deviation Response	2-125
2.4.1-2	Nominal Model Heading Angle Response	2-126
2.4.1-3	Nominal Model Bank Angle Response	2-127
2.4.2-1	Basics of Root Locus	2-128
2.4.2-2	Root Locus of Y'/Y_d' Loop	2-130
2.4.2-3	Root Locus of Y'/Y_d' Loop - Detail View of Dominant Roots	2-132
2.4.2-4	State Equation Verification Time Response	2-133
2.4.2-5	Percent Overshoot and Peak Time versus Damping Ratio for a Second Order System	2-133
2.4.2-6	Root Locus of ψ/ψ_c Loop	2-134
2.4.2-7	Root Locus of ψ/ψ_c Loop - Detail View of Dominant Roots	2-135
2.4.2-8	Root Locus of ϕ/ϕ_c Loop	2-137
2.4.2-9	Root Locus of ϕ/ϕ_c Loop - Detail View of Dominant Roots	2-138
2.4.3-1	Effect of an Increase in K_{e_e} , N_ϕ , ψ_o or ϕ_o on the Statistical Response	2-140
2.4.3-2	Nominal Model Fit to Nominal Measured Distribution Data	2-143
2.4.4-1	System Parameter Sensitivity	2-146
2.4.4-2	Lateral Deviation Sensitivity Coefficients with Respect to K_{ψ_e}	2-147
2.4.4-3	System Error Sensitivity	2-150
2.4.4-4	Lateral Distribution Sensitivity Coefficients with Respect to σ_{ψ_o}	2-151
2.5.2-1	Comparison of Modified Burgerhout PDF and Gaussian PDF	2-160
2.5.2-2	Longitudinal Distribution for Dependent Operations	2-163

LIST OF ILLUSTRATIONS (Continued)

Figure		Page
2.5.3-1	Normal Operating Zone Determination	2-156
2.5.3-2	Normal Operating Zones	2-167
2.5.3-3	CTOL/STOL Skewed Geometry	2-168
2.6.1-1	Probability of Collision	2-175
2.6.1-2	Probability of Collision Geometry for STOL/STOL Independent Operations	2-176
2.6.1-3	Probability of Collision Geometry for CTOL/STOL Independent Operations	2-180
2.6.1-4	Graphical Illustration of Convolution Method	2-182
2.6.1-5	Probability of Collision Geometry for CTOL/CTOL Dependent Operations	2-183
2.6.1-6	Region of s_1s_2 -plane for which Probability of Collision Is Defined	2-186
2.6.1-7	Probability of Collision Geometry for CTOL/STOL Independent Operations	2-188
2.6.2-1	Cases Considered in Probability of Collision Analysis	2-191
2.6.2-2	Cases Considered in Probability of Collision for CTOL/CTOL Dependent Operations	2-194
2.6.2-3	Probability of Collision Geometry for CTOL/STOL Independent Operations	2-196
2.6.2-4	Runway Configurations Considered for CTOL/STOL Independent Operations	2-197
2.6.2-5	CTOL/STOL Threshold Displacement for which Probability of Collision Was Not Considered	2-198
2.7.1-1	Single Aircraft Geometric Analysis of the Two Types of Blunders	2-204
2.7.1-2	Single Aircraft Recovery Geometry	2-206
2.7.1-3	DAS Configuration	2-208
2.7.1-4	Reference Blunder Case for Single Aircraft	2-213
2.7.1-5	Blunder Sensitivity	2-214
2.7.2-1	Dual Aircraft Geometric Analysis	2-216
2.7.2-2	Dual Aircraft Blunder Analysis Illustration	2-220
2.7.2-3	Blundered Aircraft Turn Geometry	2-223
2.7.2-4	Dual Aircraft Reference Blunder Case	2-228
3.1.1-1	Standard Deviation Versus Range for FC-ILS-I-STOL (Lateral)	3-10
3.1.2-1	FC-ILS-I-CTOL (Vertical) Standard Deviation Versus Range	3-15
3.2-1	Coordinate Systems	3-21
3.2-2	Nominal System Model	3-22

LIST OF ILLUSTRATIONS (Continued)

Figure		Page
3.2-3	Nonlinear, Simulated Delay Nominal Model	3-23
3.2-4	Linear, Simulated Delay Nominal Model	3-24
3.2-5	Curved Model Regions of Validity	3-25
3.2-6	Base Leg System Model	3-26
3.2-7	Turning System Model	3-27
3.2-8	Multiple Aircraft/Runway Model Block Diagram	3-28
3.2-9	Possible Configuration for Multiple Aircraft/ Runway Model	3-29
3.2-10	Multiple Aircraft/Runway Model Possible Parallel Runway Configurations	3-30
3.2-11	Multiple Aircraft/Runway Model Possible Skewed Runway Configurations	3-31
3.3-1	Lateral Deviation Sensitivity Coefficients with Respect to K_{ψ_e}	3-43
3.3-2	Lateral Distribution Sensitivity Coefficients σ_y' with Respect to σ_{ψ_o}	3-46
3.4.2-1	NOZ Regions	3-51
3.5-1	Cases Considered in Probability of Collision Analysis	3-58
3.5.1-1	Explanation of Heading Information for Probability of Collision Tables	3-60
3.5.1-2	Cases Considered in Probability of Collision for CTOL/CTOL Dependent Operations	3-61
3.5.2-1	Runway Configurations for CTOL/STOL Independent Operations	3-62
3.6-1	Single Aircraft Geometric Analysis of the Two Types of Blunders	3-64
3.6-2	DAS Configuration	3-69
3.6-3	Dual Aircraft Geometric Analysis	3-71
4-1	Method of Solution	4-3
4-2	Cases Considered in Probability of Collision Analysis	4-11

LIST OF TABLES

Table	Page
2.1-1	Approach Systems 2-6
2.1.2-1	List of Symbols 2-9
2.1.2-2	Nominal Model Parameter Values 2-25
2.1.3-1	Expanded Model Parameter Values 2-32
2.1.4-1	Error Summary 2-54
2.2.1-1	Lateral Deviation Time Responses for the Original Nonlinear and Simplified Linear Models 2-76
2.3-1	Required Measured Distributions 2-100
2.3.2-1	Class 1 Systems 2-114
2.3.2-2	Mean and Standard Deviation Versus Range for FC-ILS-I-CTOL - Lateral 2-115
2.3.2-3	Distribution of Lateral Displacements for FC-ILS-I-CTOL - Lateral 2-116
2.3.2-4	Class 2 Systems 2-118
2.4.3-1	Nominal Model Initial State Distribution 2-141
2.4.4-1	Sensitivity Analysis Parameters 2-145
2.4.4-2	Sensitivity Analysis Errors 2-149
2.5.1-1	Procedure Outline for the Model Development of the Lateral PDF's 2-155
2.5.2-1	Probability Density Functions 2-158
2.6.1-1	Sample Table of the Normal Probability Function for Large Arguments 2-179
2.7-1	Blundered Aircraft Parameter Values 2-202
2.7.1-1	Single Aircraft Blunder Data 2-210
2.7.1-2	Single Aircraft Data Trends (Excluding DAS Error) 2-212
2.7.2-1	Dual Aircraft Blunder Analysis Sequence of Delays 2-218
2.7.2-2	Dual Aircraft Blunder Data 2-225
2.7.2-3	Dual Aircraft Data Trends (Excluding DAS Error) 2-227
3-1	Study Outputs 3-2
3.1-1	Required Measured Distributions 3-5
3.1.1-1	Mean and Standard Deviation Versus Range for FC-ILS-I-CTOL - Lateral 3-7
3.1.1-2	Distribution of Lateral Displacements for FC-ILS-I-CTOL - Lateral 3-8
3.1.2-1	Summary of the Percent of Aircraft at Various Ranges 3-12
3.1.2-2	System Sample Size 3-14

LIST OF TABLES (Continued)

Table		Page
3.2-1	Nominal Model Parameter Values	3-32
3.2-2	Nominal Model Initial State Distributions	3-34
3.2-3	Expanded Model Parameter Values	3-35
3.2-4	Error Summary	3-39
3.3-1	Sensitivity Analysis Parameters	3-42
3.3-2	Sensitivity Analysis Errors	3-45
3.4-1	Probability Density Functions	3-48
3.4.1-1	Lateral PDF's	3-49
3.5-1	Distributions for Lateral, Vertical, and Longitudinal Dimensions for Approach Systems	3-59
3.6-1	Blundered Aircraft Parameter Values	3-65
3.6-2	Single Aircraft Blunder Data	3-66
3.6-3	Dual Aircraft Blunder Data	3-72
4-1	Distributions for Lateral, Vertical, and Longitudinal Dimensions for the Approach Systems	4-9

SECTION 1

INTRODUCTION

Terminal operational capacity could be increased by reducing the present lateral separation criteria between simultaneous Instrument Flight Rules (IFR) operations on parallel runways and by establishing a basis for separation criteria for Conventional Take-Off and Landing/Short Take-Off and Landing (CTOL/STOL) operations for parallel or skewed runways. The objective of the Lateral Separation Study is to provide a means for establishing the feasibility of minimizing runway spacings for the purpose of increasing the terminal operational capacity.

The Lateral Separation Study provides a method for determining the minimum lateral spacing between runways and measuring the relative safety for a given runway spacing. A detailed procedural description of this method is contained in Volume I of this report. The basic objectives of Volume II are to present the data essential to the determination of minimum runway spacings and to describe the development of the techniques used to generate this data.

A presentation of the list of data essential to the determination of minimum runway spacings and a brief description of the problems associated with the generation of this data are contained in Section 1.1. Briefly, this data includes: probability of collision data, normal operating zone data, and blunder recovery data.

Section 2 provides a detailed description of the development of techniques used to generate the required data. The basic approach used in generating probability of collision and normal operating zone data was to obtain statistical descriptions of the location errors (probability density functions) of aircraft operating under IFR conditions. The probability density functions in turn were used directly to compute the probability of collision data and normal operating zone data. The lateral error probability density functions were obtained from the Fokker-Planck equation. The Fokker-Planck equation uses the system dynamics, provided by approach system models, and an initial lateral distribution, provided by measured distribution data, to propagate the probability density function in time. A deterministic analysis which included a parametric variation of the pertinent system parameters was used to generate the blunder recovery data.

The results of the various analyses described in Section 2 are discussed in Section 3 and presented in the

appendices. In addition to the probability of collision data, normal operating zone data and blunder recovery data, several other study results are presented including: measured distribution data, approach system models, sensitivity data, and probability density function data.

Section 4 presents a summary of the study results and the methods utilized to obtain these results.

SECTION 1.1

PROBLEM DEFINITION

As stated previously, the objective of this study is to provide a means to establish the feasibility of minimizing runway spacings for the purpose of increasing the terminal operational capacity. This objective is accomplished by providing a method for determining the minimum lateral spacing between runways and for measuring the relative safety for a given runway spacing. The basic problem then is to determine this method and to generate the necessary data.

It is necessary to provide a method for determining minimum runway spacings for the following aircraft and runway configurations:

- (1) CTOL/CTOL - parallel,
- (2) CTOL/STOL - parallel at different threshold locations,
- (3) CTOL/STOL - skewed, and
- (4) STOL/STOL - parallel.

The method should be capable of handling the following approach systems:

- (1) front course Instrument Landing System (FC-ILS),
- (2) back course Instrument Landing System (BC-ILS), and
- (3) VHF omnidirectional range/distance measuring equipment (VOR/DME).

Both independent and dependent operations should be considered, as well as arrivals, departures, missed approaches, and blunders.

Minimum runway spacings and relative safety considerations shall be based upon the following:

- (1) no transgression zones,
- (2) normal operating zones,
- (3) blunder recovery airspace, and
- (4) probability of collision.

The problems specific to Volume II of this report are associated with the generation of the data essential to minimum runway spacing determination and relative safety determination. The problems may be subdivided into four specific problem areas, which are:

- (1) developing system models,
- (2) determining normal operating zones (NOZ),
- (3) determining areas required for recovery from blunder situations,

- (4) determining runway separation evaluation data (probability of collision data).

The development of system models should include models for parallel arrival and departure runways and various other multiple runway configurations. These models should also include both straight-in and curved approach paths. The models should consider longitudinal separation and lateral deviations.

The normal operating zones should be determined for FC-ILS, Category I, CTOL approaches; FC-ILS, Category II, CTOL approaches; BC-ILS, Category I, CTOL approaches; FC-ILS, Category I, STOL approaches; and VOR/DME, CTOL approaches. These normal operating zones should be such that either 68% or 95% of the operations are contained in the zone.

The blunder recovery area should be determined for combinations of parameters which include a set of extreme deviation situations, a set of data acquisition systems having various accuracies and update rates, a set of rules and procedures, a set of aircraft/pilot performance characteristics, a set of communication times, and a set of measurement techniques.

The runway separation evaluation data should be determined for independent parallel CTOL operations for front course ILS/front course ILS, front course ILS/back course ILS, and front course ILS/(VOR/DME) approaches. This data should also be determined for dependent parallel CTOL front course ILS approaches with various longitudinal separations and for independent parallel CTOL/STOL and STOL/STOL front course ILS approaches for specific STOL runway threshold locations.

Once the solutions to the previous four problems are obtained, the problem of determining minimum spacing between runways should be solved. This minimum spacing would be based on an associated collision probability value determined by solving (4), a normal operating zone determined by solving (2), a blunder recovery area determined by solving (3), and a no transgression zone. A procedure for determining minimum runway spacings should be determined for:

- 1) Parallel runways and independent operations for:
 - FC-ILS-CTOL/FC-ILS-CTOL
 - FC-ILS-CTOL/BC-ILS-CTOL
 - FC-ILS-CTOL/(VOR/DME)-CTOL
 - FC-ILS-CTOL/FC-ILS-STOL (different runway threshold locations)
 - FC-ILS-STOL/FC-ILS-STOL

- 2) Parallel runways and dependent operations for:
FC-ILS-CTOL/FC-ILS-CTOL
- 3) Skewed runways and independent operations for:
FC-ILS-CTOL/FC-ILS-STOL with due consid-
eration for approaches, departures,
and missed approaches.

Once the minimum spacing problem is solved for CTOL/CTOL, CTOL/
STOL, and STOL/STOL, the effect on the terminal operational
capacity could be determined.

SECTION 2

METHOD OF SOLUTION

The objective of the methodology described in the following sections is the determination of the data required to obtain values for the minimum spacing between CTOL/CTOL, CTOL/STOL, and STOL/STOL runways under various operational procedures. This methodology is illustrated in block diagram form in Figure 2-1.

Basically, this methodology involves the derivation of system models that include all pertinent approach system characteristics such as pilot performance, aircraft performance, instrument approach system response and errors, controller interactions, etc. These models are discussed in further detail in Section 2.1.

Using these models, a set of state equations were derived, and the corresponding Fokker-Planck partial differential equation was developed. The development of the Fokker-Planck equation is described in Section 2.2.

The location error data collected at Chicago, Portland, Atlanta, NAFEC, Charleston and elsewhere was then processed to yield the measured aircraft error distributions. The lateral distributions were used to initialize the Fokker-Planck equation, to aid in verification of the system models, and to aid in the collision probability determination. A description of this effort is included in Section 2.3.

Verification of the system models was accomplished by comparing observed quantities from the physical system to those quantities predicted by the models as discussed in Section 2.4. In an effort to determine the dominant system parameters, a sensitivity analysis was completed using both a deterministic and a statistical model. The approach and results of this investigation are also included in Section 2.4.

Using the initial lateral measured error distributions and the verified Fokker-Planck equation, the aircraft positional error distributions, or probability density functions, from the initial range to the decision height were computed, as described in Section 2.5. These density surfaces are the statistical description of the positional errors of the aircraft at time or range intervals along the approach. The models and the corresponding Fokker-Planck equation were developed such that it was possible to vary the parameters of the models (equations) to determine the error distributions for each

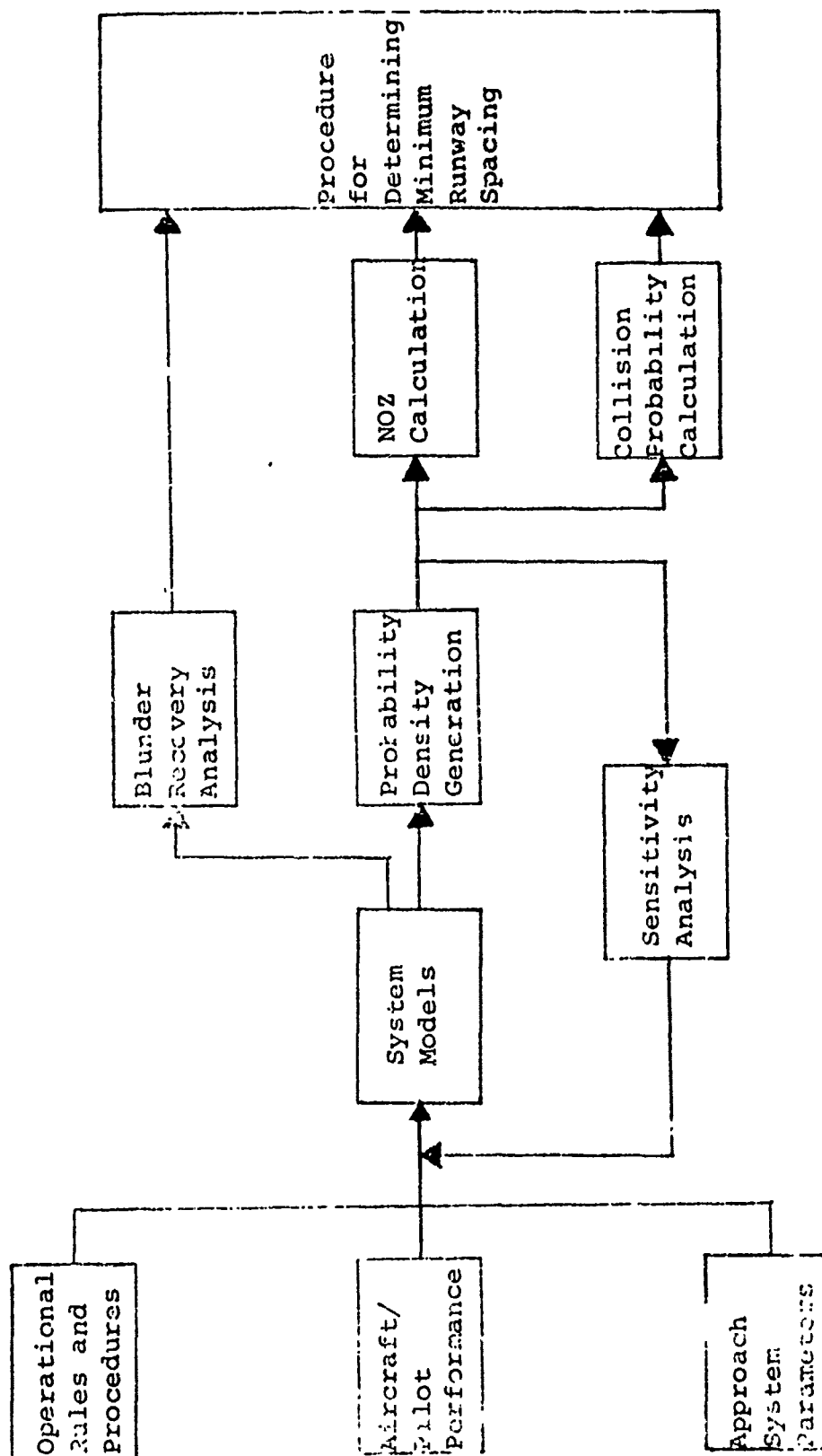


Figure 2-1 Method of Solution.

of the required operational procedures. The normal operating zones (the area containing 68% or 95% of the aircraft operations) were then computed directly from the lateral error distributions and are also discussed in Section 2.5. Vertical and longitudinal probability density functions were also obtained as discussed in Section 2.5.

The probability of collision for the various operational procedures and runway configurations were determined. The definition of these collision probabilities and the methods of obtaining them are described in Section 2.6.

The effect of those aircraft that deviate beyond the NOZ (blunders) were then investigated. The determination of the recovery airspace required for various blunder situations was accomplished using a deterministic approach. The determination of these recovery areas is described in Section 2.7.

The systematic combination of the results of the methodology described in Sections 2.1 through 2.7 yields the information necessary for determining minimum runway spacings and for measuring the relative safety for a given spacing for the various operational procedures and runway configurations. The procedure for determining the minimum runway spacing is discussed in Volume I, Section 4.

SECTION 2.1

SYSTEM MODEL DEVELOPMENT

After a thorough examination of the problem definition, discussed in Section 1.1, the method of solution, discussed in Section 2, was formulated. The first major effort involved in accomplishing the method of solution is the development of mathematical models which describe the required approach systems. To aid in model development and verification tasks, a comprehensive literature survey was conducted, resulting in the models described in this section. The approach systems investigated and modeled in this study are described in Table 2.1-1. The development of mathematical models which describe these approach systems is discussed in the sections which follow.

Due to similarities in these approach systems, a nominal system model is developed which represents all of the above approach systems. The nominal model equations and certain model parameter values are representative of all of the above approach systems; however, some model parameters are specific to each approach system. The nominal model is defined as a front course, instrument landing system, Category I and Category II combination, conventional take off and landing aircraft and runway (FC-ILS-INOM-CTOL).

Section 2.1.1 establishes the operational concepts for the system models. A detailed description of the nominal model development is contained in Section 2.1.2. Various required expansions of the nominal model to encompass the operational concepts are discussed in Section 2.1.3. Section 2.1.4 contains an error definition discussion for the various approach systems. Section 2.1.5 discusses the model state equation derivation for use in the Fokker-Planck analysis. Verification of the nominal system model is discussed in Section 2.4.

2.1.1 MODEL CONCEPT DEFINITION

Before a reasonable system model can be developed, it is necessary to plan all required phases of the analysis and relate the model to each phase by predetermining how the model will be utilized. It is also necessary to establish a set of ground rules and assumptions to serve as a guideline throughout model development and subsequent model usage. Additionally, it is necessary to define the general model structure by identifying the major components and their corresponding interconnections.

Table 2.1-1 Approach Systems

Designation	Primary User Class	Runway Type	Approach Guidance System
FC-ILS-I-CTOL	CTOL Category I	CTOL	Front Course, ILS Category I
FC-ILS-II-CTOL	CTOL Category II	CTOL	Front Course, ILS, Category II
BC-ILS-I-CTOL	CTOL Category I	CTOL	Back Course, ILS, Category I
VOR-CTOL	CTOL Category I	CTOL	VOR (tracking inbound to a station within the airport boundary)
FC-ILS-I-STOL	STOL Category I	STOL	Front Course, ILS, Category I

The purpose of this section is to accomplish these objectives.

The basic model concepts are derived by considering all factors which affect an aircraft's lateral deviation from a runway localizer beam. Consideration of these factors results in the model structure shown in Figure 2.1.1-1. The major components contained in the model structure are the aircraft, pilot, course deviation indicator and ground controller. The component interconnections are also shown in Figure 2.1.1-1.

Runway lateral separation requirements, as defined in this study, are based upon the assumptions that (1) the approach system's lateral and vertical tracking dynamics are independent and (2) the aircraft is to remain in the glideslope plane except when executing a missed approach. These assumptions allow the results obtained from this study to reflect the "worst case" possibility. Based upon these assumptions the system model simulates lateral control only.

After a thorough investigation of the objectives of this study, the model's operational concepts were established. The expanded system models (Section 2.1.3) are capable of IFR operations for CTOL or STOL aircraft operating on CTOL or STOL

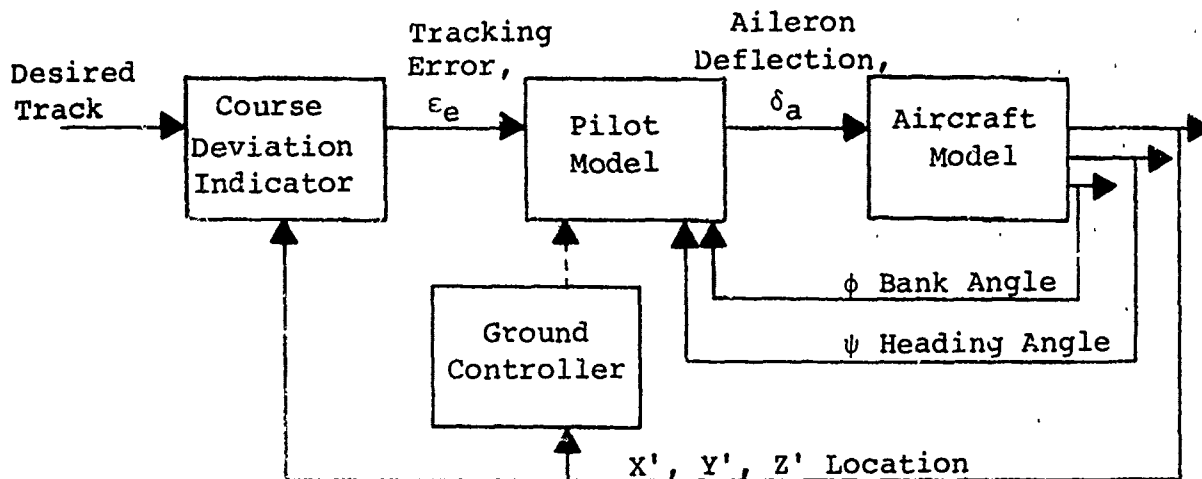


Figure 2.1.1-1 General System Model

runways with either an ILS (Category I or Category II) or VOR approach guidance system. The expanded models can simulate arrivals or departures and independent or dependent operations on single or multiple (parallel or skewed) runway configurations. They can simulate both straight-in approach paths and general curved three-dimensional approach paths, and have the capability of simulating missed approaches.

The approach system model is used in the generation of supporting data which will be used in the determination of the minimum lateral runway separation criteria. The state equations derived from the model are utilized in the Fokker-Planck analysis which generates probability density functions which in turn are used in the probability of collision analysis. The system model is also utilized in the blunder analysis, which defines lateral recovery airspace requirements for various blunder conditions.

The expanded models may be used as analysis tools to study approach systems. Certain terminal system parameters and/or system errors may be varied and the effects on the total system response observed. The models may be used in the prediction of distribution data for systems in which no measured field data exists. Certain system characteristics which are difficult to observe in the actual approach system (such as multiple aircraft relative velocities and locations, aircraft bank angle and heading angle, curved path characteristics, etc.) may be obtained easily from these expanded system models.

2.1.2 NOMINAL MODEL

2.1.2.1 Introduction

The purpose of the nominal model is to simulate a composite set of CTOL aircraft flying the final leg of a front course ILS approach under IFR conditions. The model is also used to develop and check the state equations used in the Fokker-Planck analysis and to establish a data base to which more complex models may be compared.

To determine the requirements of the nominal model, an analysis of the various components included in an ILS approach was undertaken. The various subsystems identified were then studied to allow development of simple yet accurate mathematical models of the subsystem response. For each subsystem various basic assumptions were used to determine the modeling requirements.

Three versions of the nominal model were developed for use in the various analyses required. The first and primary model is a nonlinear simulation with a time delay in the pilot model; the second is a nonlinear model with a simulated time delay; and, the third is a linear model. Each model was developed with a slightly different set of simplifying assumptions and will be discussed in later sections.

2.1.2.2 Approach

The development of all three versions of the nominal model was based on the general block diagram of the system presented in Section 2.1.1 (Figure 2.1.1-1).

These models are necessary to satisfy the various requirements of the problem definition (Section 1.1). The nonlinear, pure delay model is the most accurate simulation and establishes a data base to which following models may be compared. The nonlinear, simulated delay and linear models are required to determine the state equations to be used by the Fokker-Planck analysis.

List of Symbols

All symbols used in the various models, their units, and a brief description of each are listed in Table 2.1.2-1. The dot notation over a variable indicates the time derivative of that variable. A zero subscript indicates the initial condition.

Table 2.1.2-1 List of Symbols

Symbol	Units	Description
a_a	1/sec	Inverse of the aircraft bank rate to aileron response time constant
a_{p1} a_{p2} a_{p3} a_{p4} a_{p5}	-	Coefficients used in the simulated pilot/control delay
a_ϕ	1/sec	Inverse of the pilot lead time constant on bank angle feedback
K_a	1/sec ²	Aircraft bank rate to aileron response gain multiplied by a_a
K_p	rad/rad	Pilot gain on simulated delay
K_{ϵ_e} (angular)	rad/rad	Pilot tracking gain on the angular localizer error
K'_{ϵ_e} (displacement)	rad/ft	Pilot tracking gain on the displacement error from the localizer beam
K_ϕ	sec	Pilot gain on the bank angle divided by a_ϕ
K_ψ	rad/rad	Pilot gain on heading angle feedback
K_{ψ_e}	rad/rad	Pilot gain on heading angle error
L	ft	-X coordinate of the lateral guidance transmitting antenna
$LONG_{ij}$	ft	Ground range longitudinal separation of A/C _i and A/C _j
N_R	rad	Lateral guidance equipment receiver noise

Table 2. 2-1 List of Symbols (Continued)

Symbol	Units	Description
N_T	rad	Lateral guidance equipment transmitter noise
N_{tr}	rad/sec	Curved path turn rate error
$N_{Y'}$	ft	Pilot lateral tracking error (base leg)
N_{ϵ}	rad	Pilot localizer tracking error (final leg)
N_{ϕ}	rad	Pilot bank angle error
N_{ψ}	rad	Pilot heading angle error
R_{turn}	ft	Range from way point at which the turn will be commenced
SKEW	deg	Runway 2 skew angle from Runway 1
T_{turn}	sec	Time required to execute the turn
V	ft/sec	Aircraft airspeed
$V_{X'}$ $V_{Y'}$ $V_{Z'}$	ft/sec	Aircraft velocity along the glideslope coordinate system
XWPP	n. mi.	Slant range from touchdown to the base leg/final leg intersection (way point)
x y z	ft	Aircraft body centered coordinate system
x y z	ft	Runway coordinate system
x' y' z'	ft	Glideslope coordinate system

Table 2.1.2-1 List of Symbols (Continued)

Symbol	Units	Description
$\left. \begin{array}{l} x_b' \\ y_b' \\ z_b' \end{array} \right\}$	ft	Base leg coordinate system (in the glideloop plane)
$\left. \begin{array}{l} x_2 \\ y_2 \\ z_2 \end{array} \right\}$	ft	Runway 2 coordinate system
$y'd$	ft	Desired location of the aircraft in the glideslope axis system
β	rad	Base leg/final leg inter- section angle
γ	rad	Glideslope angle
δ_a	rad	Aileron deflection
ϵ	rad	Angular position of the air- craft in the glideslope axis system
ϵ_e	rad	Angular error of the aircraft position in the glideslope axis system
ϵ_{LOC}	rad	Desired angular position of the aircraft
θ_o	rad	Pitch angle in glideslope axis system
τ_c	sec	Curved path turn lead time
τ_p	sec	Pilot/control delay
ϕ_c	rad	Commanded bank angle
ϕ_e	rad	Error between commanded and anticipated bank angle
ϕ_{LIM}	rad	Bank angle limit
$\dot{\phi}_{LIM}$	rad/sec	Bank rate limit

Table 2.1.2-1 List of Symbols (Continued)

Symbol	Units	Description
ϕ_{turn}	rad	Commanded bank angle while in the curved path
$\left. \begin{matrix} \psi \\ \theta \\ \phi \end{matrix} \right\}$	rad	Heading, pitch and bank angles of the aircraft attitude in the glideslope axis system, respectively
$\left. \begin{matrix} \dot{\psi} \\ \dot{\theta} \\ \dot{\phi} \end{matrix} \right\}$	rad	Heading, pitch and bank rates in the glideslope system respectively
ψ_c	rad	Commanded heading angle
ψ_e	rad	Heading error defined in glideslope axis system
$\dot{\psi}_{\text{LIM}}$	rad/sec	Turn rate limit
ψ_R	rad	Reference heading angle in the glideslope axis system (zero error condition)
$\dot{\psi}_{\text{tr}}$	rad/sec	Curved path turn rate

Assumptions

Several assumptions were used to determine the configuration of the various models; some assumptions are common to all models, some apply only to a specific model.

Assumptions common to all models include:

- 1) the system's lateral and vertical tracking dynamics are independent, and
- 2) the aircraft remains in the glideslope plane except when executing a missed approach.

These assumptions result in a study reflecting the "worst case" possibility. Thus, the system models simulate lateral control only.

The aircraft will be assumed to perform coordinated turns in the glideslope plane in order to nullify any lateral displacement error. This assumption simplifies the aircraft dynamics equations. Further assumptions pertaining to the aircraft dynamics equations are discussed in Appendix A.

Assumptions particular to each model will be presented as required in the model development.

Coordinate Systems

Three coordinate systems are used in the models. These systems are a runway system, a glideslope system and an aircraft body centered system. The three systems and their relationships to one another are shown in Figure 2.1.2-1.

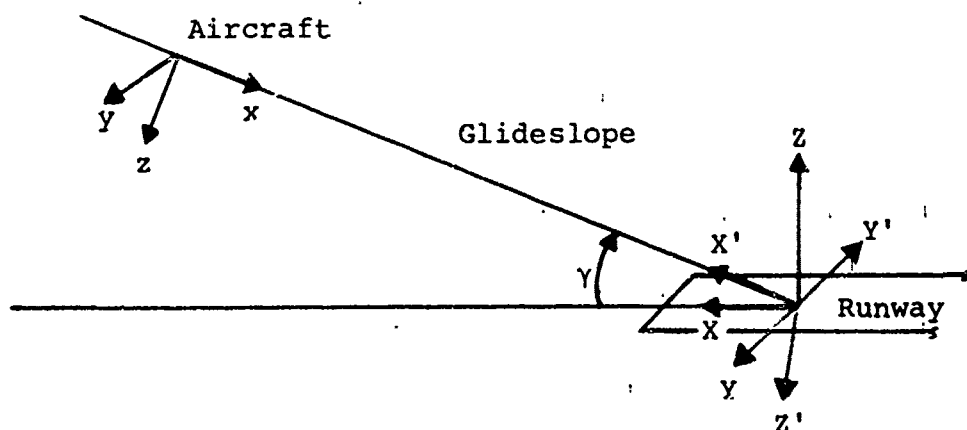


Figure 2.1.2-1 Coordinate Systems

The runway system is identified by the X, Y, Z axes. The axes have their origin at the touchdown point for approaches and the liftoff point for departures. The touchdown point for an approach is defined as the point on the runway at which an aircraft on an ideal track would first touch the runway (i.e. for FC-ILS it would be the glideslope intercept point). For a departure, the liftoff point is defined as the point an aircraft would lift off the runway for an ideal departure. The X axis is defined positive out along the runway centerline, the Z axis is positive up along the earth's gravitational vector, and the Y axis completes the right-handed system.

The glideslope system is identified by the X', Y', Z' axes. The axes also have their origin at the touchdown or liftoff point. The X' axis is defined positive out along an ideal track. For a FC-ILS approach, the X' axis is defined as being along the intersection of the ILS localizer and glideslope beams. For a FC-ILS departure the X' axis is defined similarly, assuming a glideslope equivalent beam exists with its intercept point coincident with the liftoff point and extending along the departure path. The Y' axis is coincident with the -Y axis, and the Z' axis completes the right-handed system.

The body centered system is identified by the x, y, z axes and has its origin at the aircraft center-of-gravity. The x axis is defined positive forward along the aircraft fuselage centerline, the y axis is positive out along the starboard wing, and the z axis completes the right-handed system.

Course Deviation Indicator (CDI) Model

Two techniques for simulating the CDI were developed. The CDI model in the nonlinear systems computes the angular error measured from the localizer beam in the glideslope plane, while in the linear system it computes the displacement error from the localizer beam.

The CDI angular simulator is an arctangent operator and is shown in Figure 2.1.2-2. Since the runway centerline is coincident with the X' axis, the Y' coordinate of the aircraft position is the lateral displacement error. The angular CDI simulator relates the lateral displacement error magnitude to the displayed angular error as a function of range from the lateral guidance transmitting antenna ($X' + L$). L is defined as minus the X coordinate of the lateral guidance transmitting antenna measured in the runway axis system. Thus, a 500 foot error at ten miles from the antenna displays less needle

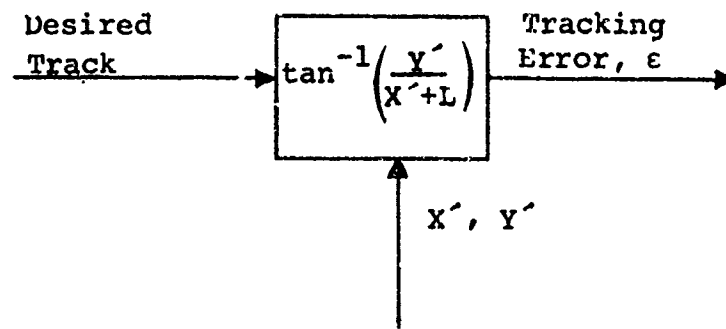


Figure 2.1.2-2 Course Deviation Indicator Model

deflection than the same 500 foot error would command at two miles from the antenna. This is representative of the variable sensitivity found in actual CDI operation.

The arctangent operator is a nonlinear function and in order to develop a linear model, a displacement error system was developed. In this system the Y' coordinate was used as the error signal. The linear CDI system is not a function of range. Thus, a 500 foot error would command the same magnitude of deflection at ten miles from the antenna as at two miles. This is not representative of actual conditions, but it is valid for short range intervals. Therefore, the linear model can simulate the actual system if it is utilized for short range segments.

Pilot Model

Selected feedback loops closed by the pilot for the localizer displacement control task are presented in Figure 2.1.2-3. The pilot commands a bank angle to aileron inner loop based on his perception of heading error in a secondary loop. The heading error is based on a heading reference established by his perception of localizer deviation (References 1 and 4)*. The bank angle is the pilot's primary controlling parameter.

Two pilot models were developed for use in the models. The most accurate model is based on the pilot model from Reference 1, and is illustrated in Figure 2.1.2-3. This model approximates the pilot response by a pure time delay and a lead. The time delay represents the pilot/control delay and the lead simulates the pilot's anticipatory ability.

*References are listed after every major section (section number of two levels or less, i.e. 1.1, 2.3, etc.).

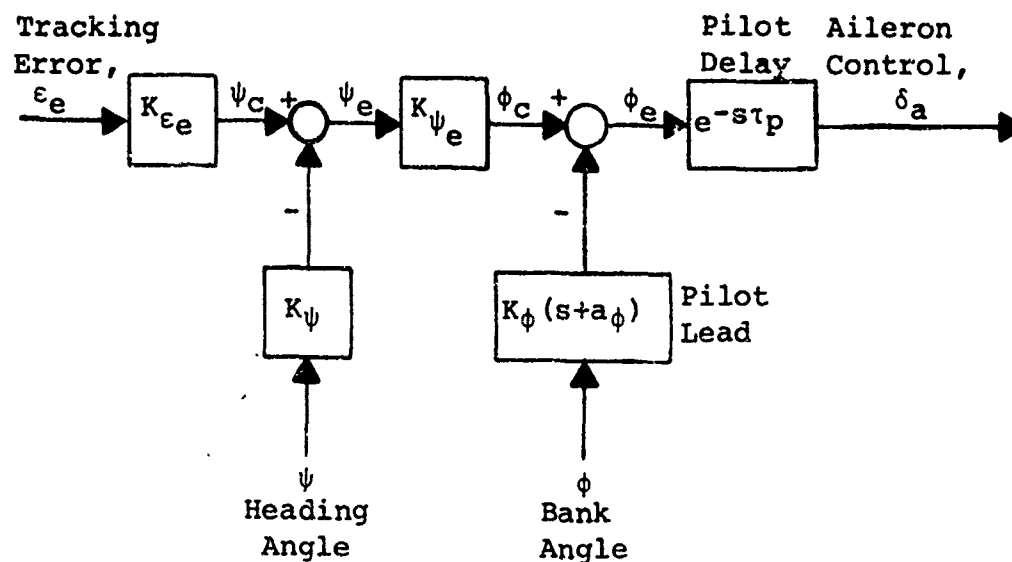
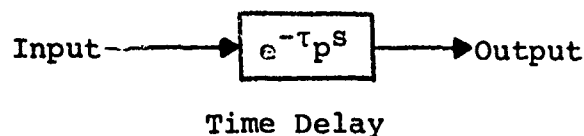
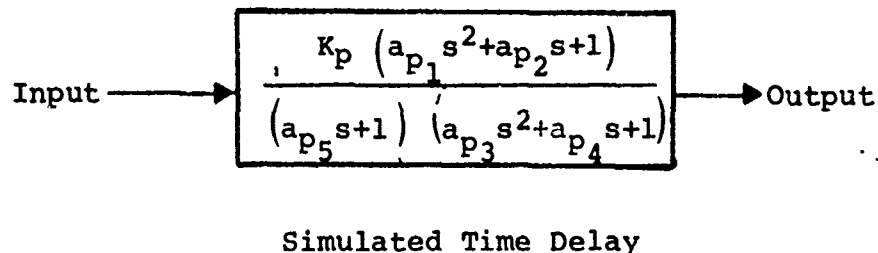


Figure 2.1.2-3 Pilot Model

In order to develop a pilot model in a form suitable for use in the Fokker-Planck analysis, the pilot/control time delay was replaced by a simulated time delay as developed in Reference 2. The output of the simulated delay function is compared to that of an actual delay for a .3 second delay in Figure 2.1.2-4. The pure time delay has the form:



and the simulated delay has the form:



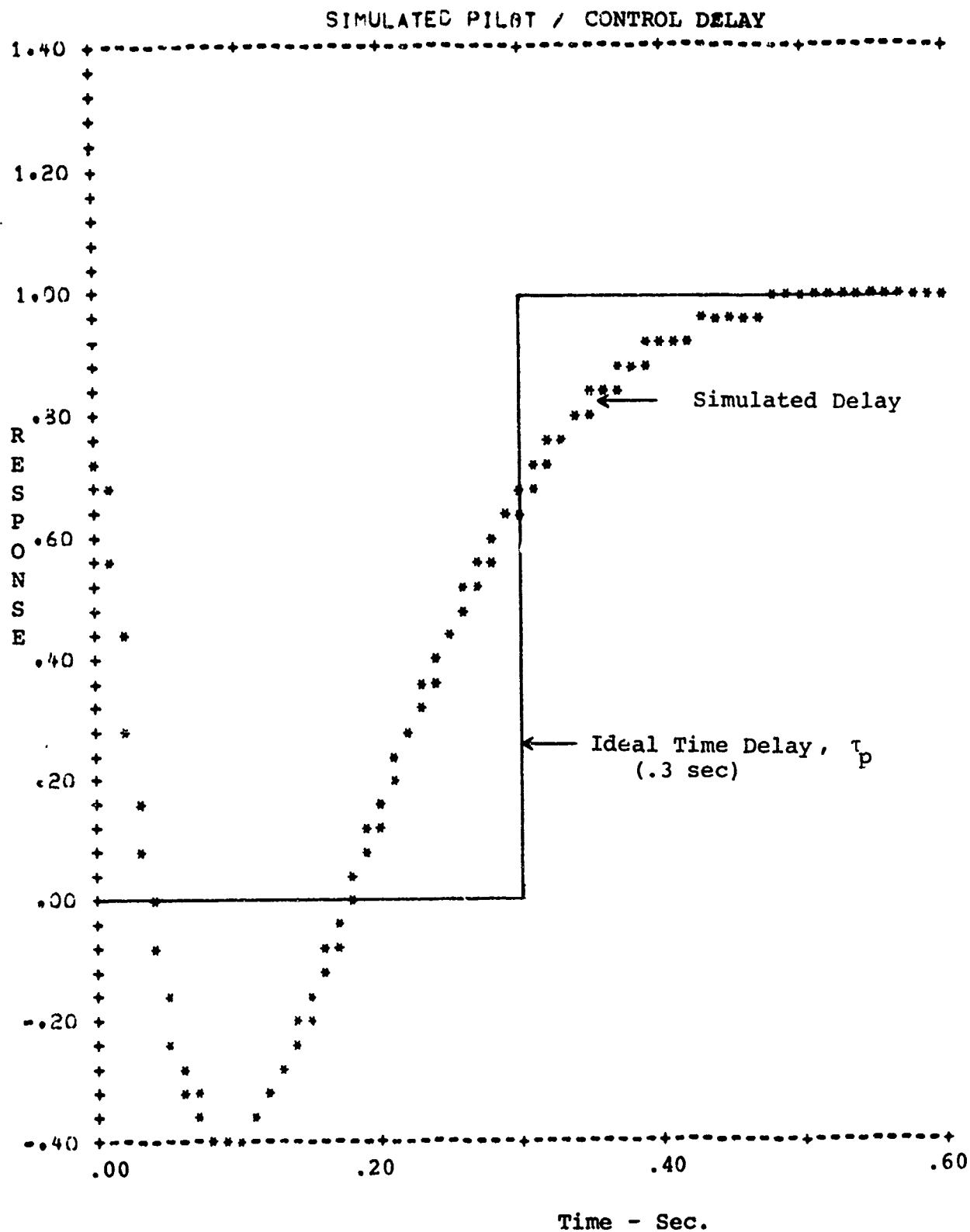


Figure 2.1.2-4 Simulated Delay Response

where

$$a_{p5} = \frac{\tau_p}{100} \quad (2.1.2-1)$$

$$a_{p1} = \left(\frac{\tau_p - a_{p5}}{2\sqrt{3}} \right)^2 \quad (2.1.2-2)$$

$$a_{p2} = -\frac{1}{2} (\tau_p - a_{p5}) \quad (2.1.2-3)$$

$$a_{p3} = \left(\frac{\tau_p - a_{p5}}{2\sqrt{3}} \right)^2 \quad (2.1.2-4)$$

$$a_{p4} = \frac{1}{2} (\tau_p - a_{p5}) \quad (2.1.2-5)$$

$$K_p = 1$$

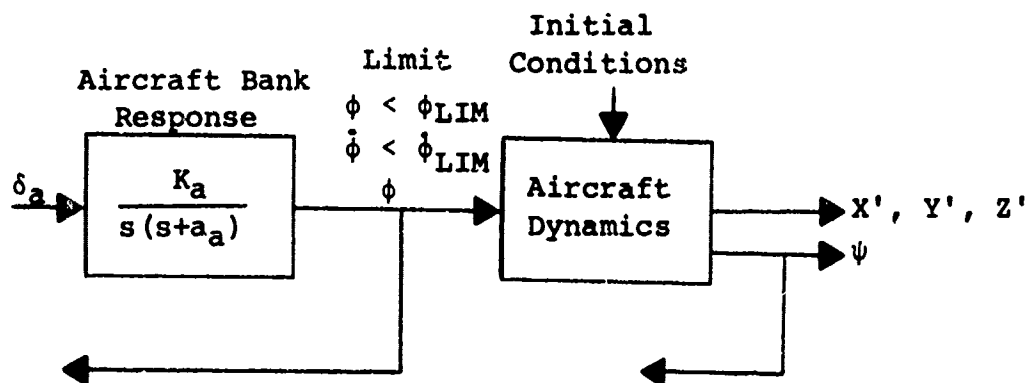
Verification of the simulated time delay as an approximation to the actual delay is contained in the results portion of this section (Section 2.1.2.3).

Aircraft Model

In the determination of approach system lateral distribution data, it is necessary to consider the aircraft's dominant lateral dynamics only. Due to the dominant long term nature of the approach system dynamics, the aircraft's short term transient motion becomes negligible; therefore, it is assumed that the aircraft's lateral dynamics can be simulated by representing the aircraft bank rate response to aileron input by a time lag (References 3 and 19) with a limited bank rate, $\dot{\phi}_{LIM}$, and turn rate, $\dot{\psi}_{LIM}$. These limits are imposed by pilot acceptability and passenger comfort considerations. For a given aileron input the aircraft bank rate will achieve 63% of its steady-state value in $1/a_a$ seconds. A bank angle limit, ϕ_{LIM} , is imposed by the turning rate limit as follows:

$$\phi_{LIM} = \tan^{-1} \left(\frac{V \dot{\psi}_{LIM}}{32.2} \right) \quad (2.1.2-6)$$

The pilot is assumed to cause the aircraft to perform level coordinated turns in the glideslope plane to nullify lateral deviation errors (Reference 4). This assumption is utilized in the derivation of the aircraft equations of motion shown in Figure 2.1.2-5. The derivation and associated assumptions are presented in Appendix A. The aircraft equations of



AIRCRAFT DYNAMICS:

Input -

$$\phi = f(t) \quad , \quad \text{radians}$$

Initial Conditions -

$$x'_0, y'_0, z'_0 \quad \text{ft}$$

$$V \quad , \quad \text{ft/sec}$$

$$\psi_0, \theta_0, \phi_0 \quad , \quad \text{radians}$$

Equations of Motion -

$$\dot{\psi} = \frac{32.2 \tan \phi}{V}$$

$$\dot{\theta} = 0$$

$$\psi = \psi_0 + \int \dot{\psi} \, dt$$

$$\vartheta = \theta_0$$

$$V_{X'} = V \cos \theta_0 \cos \psi$$

$$V_{Y'} = V \cos \theta_0 \sin \psi$$

$$V_{Z'} = -V \sin \theta_0$$

$$x' = x'_0 + \int V_{X'} \, dt$$

$$y' = y'_0 + \int V_{Y'} \, dt$$

$$z' = z'_0 + \int V_{Z'} \, dt$$

Figure 2.1.2-5 Aircraft Model

motion describe the heading and location of the aircraft as a function of bank angle and time.

The definition of the Euler angles for aircraft flying straight down the runway centerline and in the glideslope plane are listed below.

Approach

$$\psi = \pi$$

$$\theta = 0$$

$$\phi = 0$$

$$\psi_R = \pi$$

Departure

$$\psi = 0$$

$$\theta = 0$$

$$\phi = 0$$

$$\psi_R = 0$$

Total System

While flying an ILS approach, the pilot sees an error displayed on the CDI. After some nominal physiological delay he uses the magnitude and direction of the error to command an aileron deflection which causes the aircraft to bank, resulting in a heading change (References 1 and 4). The new heading tends to reduce the error and the CDI indicates a smaller error.

The CDI, pilot, and aircraft models are connected and related in a manner which accurately simulates the actual system. The CDI model computes the error from the ILS centerline which is input to the pilot model. Also input into the pilot model are the heading and the bank angle of the aircraft. The pilot model simulates the pilot's anticipation of the aircraft heading and bank angle change and then commands some aileron deflection. The aileron deflection is then used to determine the aircraft bank rate and heading change. The aircraft attitude and direction are used to compute the updated position and the CDI takes the information and generates a new error for the pilot model.

Inherent in every physical system of this type are several error sources (or noise sources). The types of errors which primarily affect the lateral approach system dynamics are the associated lateral guidance equipment transmitting (N_T) and receiving (N_R) errors as well as pilot errors. Pilot error sources are assumed to occur at each input (References 1 and 5) to the pilot, bank angle (ϕ), heading angle (ψ), and localizer tracking error (ϵ_e); therefore, the corresponding pilot errors are noted as N_ϕ , N_ψ , and N_ϵ . Included in these

pilot error terms are such things as pilot attitude, indicator equipment accuracy and any other contributors which affect the pilot's ability or desire to react to actual conditions. Since the bank angle is the pilot's primary controlling parameter, pilot attitude errors are primarily included in N_ϕ .

Three implementations of the total system are illustrated in the detailed block diagrams of Figures 2.1.2-6 through 2.1.2-8. These diagrams contain all gains, lags, delays, and feedback loops necessary to simulate the total system. The nonlinear version, Figure 2.1.2-6, is the primary and most accurate model; however, all three versions of the nominal model are valid for all aircraft types and for ILS or VOR approach systems. The nonlinear model was linearized by replacing the angular error indicator with a pure displacement function. The gains are adjusted so that the linear model generates an error signal response approximate to that of the nonlinear model at a particular range.

$$K'_{\epsilon_e} \text{ (displacement)} = \frac{K_{\epsilon_e} \text{ (angular)}}{X'+L} \quad (2.1.2-7)$$

For this reason the linear model can accurately simulate the actual system if it is utilized for short range segments. The heading angle (ψ) and the bank angle (ϕ) are assumed to be small ($< 25^\circ$) so that small angle approximations are valid. The linear system response has been compared to the nonlinear system response to verify that the linearization assumptions did not introduce significant errors (Section 2.1.2.3 and Section 2.2).

2.1.2.3 Nominal Model Results

The nominal model (Figure 2.1.2-6) has been programmed in a FORTRAN IV language computer routine for ease of use in the various analyses. A flow chart and source listing for this model is included in the User's Manual.

The nominal model parameter symbols, values, units, references, and pertinent comments are listed in Table 2.1.2-2. Unless otherwise denoted the parameters are valid for all three versions (Figures 2.1.2-6, 7, 8) of the nominal model.

Each loop in the nominal model has been verified by comparison of the simulated response to the expected response for the parameter values listed in Table 2.1.2-2 with the exception of τ_p and K_{ϵ_e} . For verification purposes the time

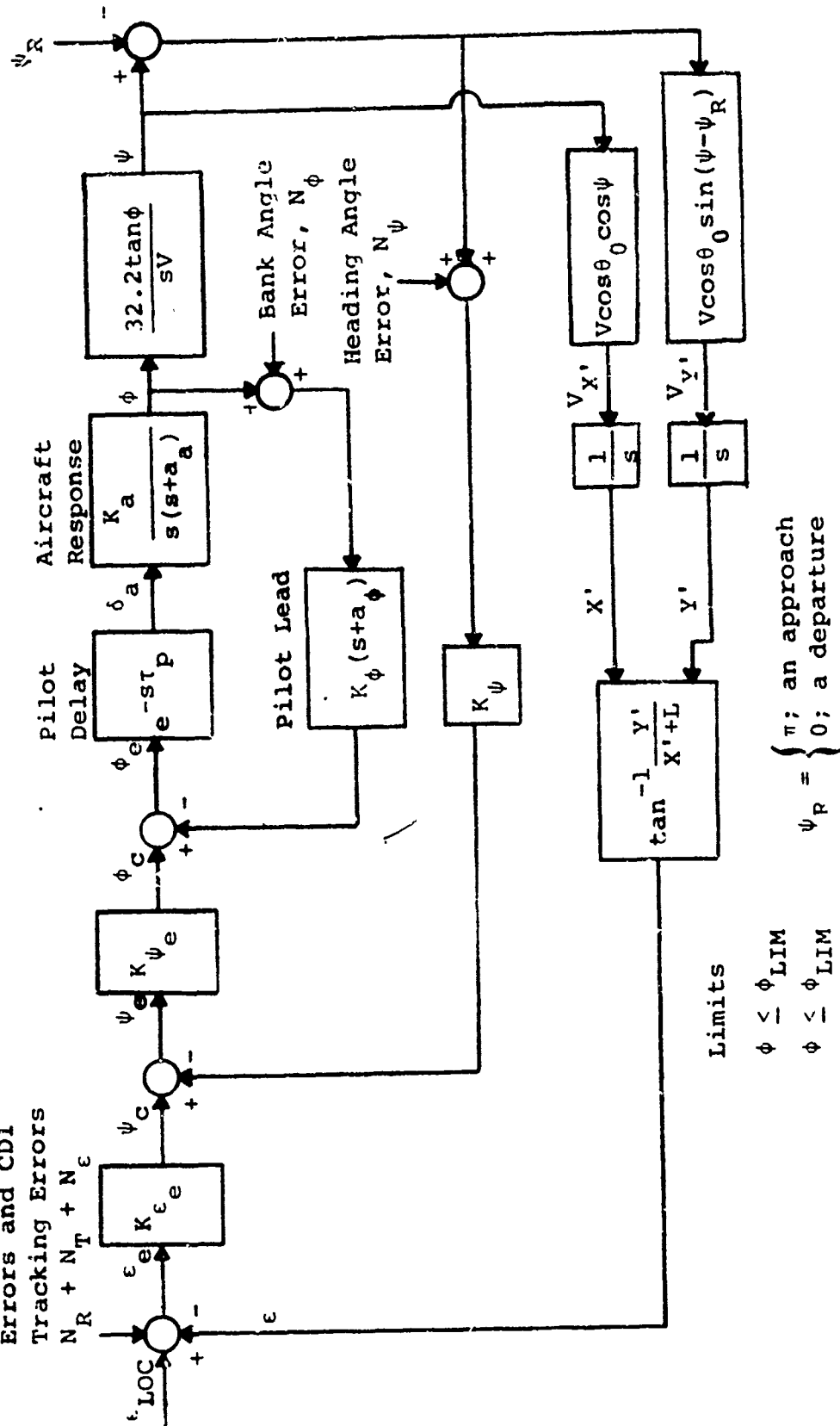
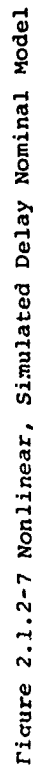


Figure 2.1.2-6 Nominal system Model



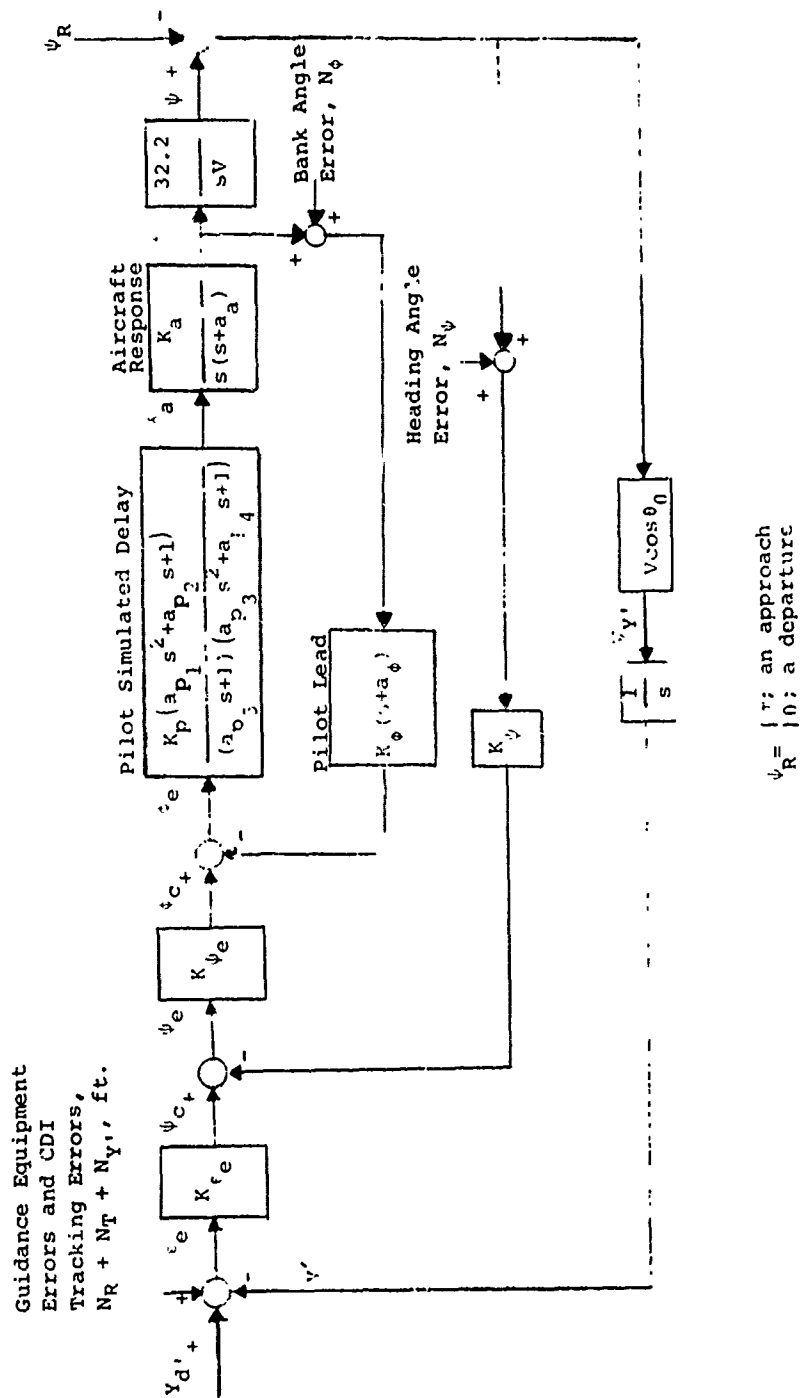


Figure 2.1.2-8 Linear, Simulated Delay Nominal Model

Table 2.1.2-2 Nominal Model Parameter Values

Symbol	Value	Units	Reference	Comments
a_a	1.0	sec^{-1}	4	CTOL aircraft
a_{p1}	.04	-	2	Simulated delay models (Equation 2.1.2-2)
a_{p2}	-.35	-	2	Simulated delay models (Equation 2.1.2-3)
a_{p3}	.04	-	2	Simulated delay models (Equation 2.1.2-4)
a_{p4}	.35	-	2	Simulated delay models (Equation 2.1.2-5)
a_{p5}	.007	-	2	Simulated delay models (Equation 2.1.2-1)
a_ϕ	1.5	sec^{-1}	1	
K_a	1.0	sec^{-2}	-	Assumed
K_p	1.0	-	-	Simulated delay models
$K_{\epsilon e}$	4.8	-	-	Nonlinear models, deter- mined in Section 2.4.3
$K'_{\epsilon e}$.000075 at 9 N. Mi to .000354 at .75 N. Mi.	$\frac{\text{rad}}{\text{ft}}$	-	Linear model (Equation 2.1.2-7)
K_ϕ	1.33	sec	1	
K_ψ	1.9	-	1	
$K_{\psi e}$	1.0	-	1	
L	9000.	feet	-	FC-ILS Approach

Table 2.1.2-2 Nominal Model Parameter Values (Continued)

Symbol	Value	Units	Reference	Comments
N_R	$\pm .00048$	rad	6, 7	1 σ value, determined in Section 2.1.4 (ILS _R)
N_T	$\pm .001497$	rad	15	1 σ value, determined in Section 2.1.4 (ILS _T for Category I/Category II Combination)
N_ϵ	$\pm .00349$	rad	-	1 σ value, determined in Section 2.1.4
N_ϕ	$\pm .1047$ at 9 N. Mi. $\pm .0436$ at 0 N. Mi.	rad	-	1 σ value, determined in Section 2.4.3 (Varies linearly with range)
N_ψ	$\pm .01745$	rad	-	1 σ value, determined in Section 2.1.4
V	236.4	ft/sec	-	Assumed (140 knots for CTOL aircraft)
γ	2.5	deg	-	CTOL runway
θ_o	0.	rad	-	Assumed
τ_p	.7	sec	-	Assumed
ϕ_{LIM}	.367	rad	-	Equation 2.1.2-6
$\dot{\phi}_{LIM}$.1745	rad/sec	-	Assumed (10 deg/sec)
$\dot{\psi}_{LIM}$.0524	rad/sec	-	Assumed (3 deg/sec)
ψ_R	3.1416	rad	-	Approach

responses of each loop were determined using a pilot/control delay of $\tau_p = 0.3$ seconds (instead of .7 seconds) and a pilot tracking gain on the localizer error of $K_{e_e} = 164.5$ (instead of 4.8) since the references utilized for comparison assumed these values. The nominal model simplifications (simulated delay and linearization) are also verified by observing the time responses discussed below.

Figure 2.1.2-9 illustrates the response of the bank angle to a commanded bank angle (for a pilot/control delay of 0.3 seconds) for both an actual pilot/control time delay and a simulated delay. Note that a good comparison exists between the two curves; therefore, the simulated delay is a good approximation to the actual delay. The .3 second delay can be seen on the curves as well as the 1 second CTOL bank rate to aileron response time constant as expected.

Figure 2.1.2-10 shows the heading angle response to a commanded heading angle. Note that the heading time constant appears to be about 6 seconds which compares favorably to the data in Reference 4, which gives a 6 second time constant for a similar aircraft.

Figure 2.1.2-11 shows the lateral deviation responses for an initial lateral deviation of 500 feet at a range of 15 nautical miles for the nominal system model (Figure 2.1.2-6), the nonlinear, simulated delay nominal model (Figure 2.1.2-7), and the linear, simulated delay nominal model (Figure 2.1.2-8). Note that the time responses for all three models compare very closely; therefore, the linearization assumptions and the simulated delay approximations are verified. Further verification of these model simplifications for a statistical response is contained in Section 2.2. Note that this response appears to have a damping ratio of about 0.3 which agrees with data given in Reference 1 for a similar system.

A complete verification of the nominal model is contained in Section 2.4.

2.1.3 EXPANDED MODELS

The nominal model described in Section 2.1.2 has been expanded to encompass the specific operational concepts defined in Section 2.1.1. The model expansion task may be broken into two parts:

1. Approach System Models (Section 2.1.3.1)
2. Curved Path and Multiple Aircraft/Runway Models (Section 2.1.3.2)

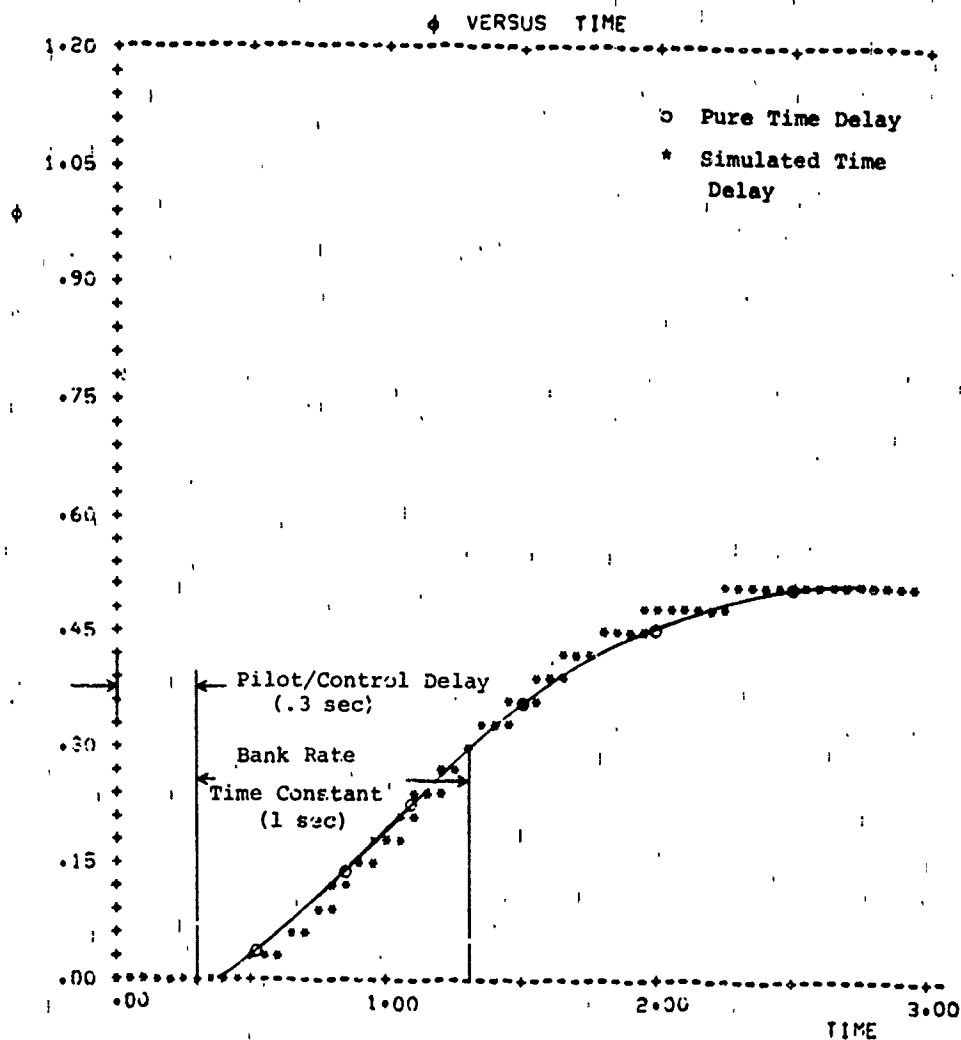


Figure 2.1.2-9 Aircraft Bank Angle Response

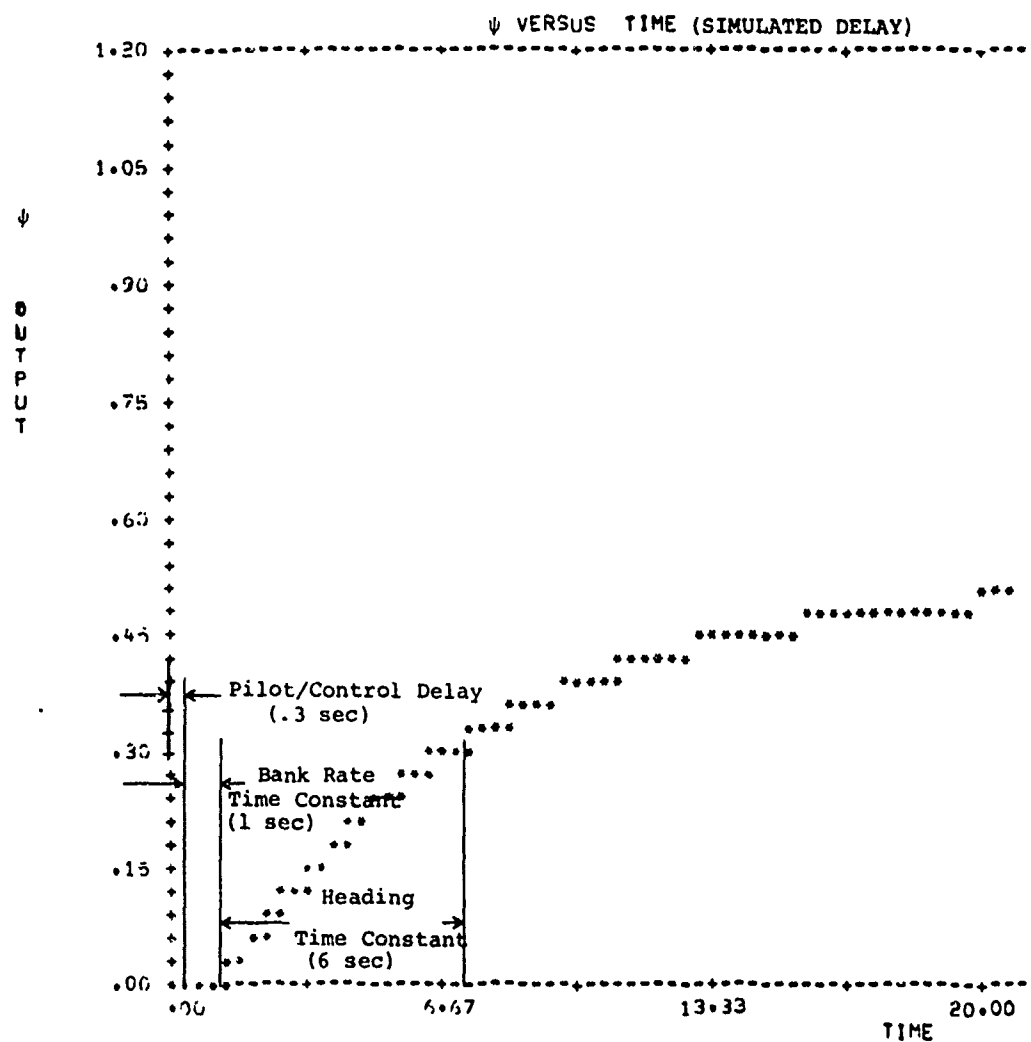


Figure 2.1.2-10 Aircraft Heading Angle Response

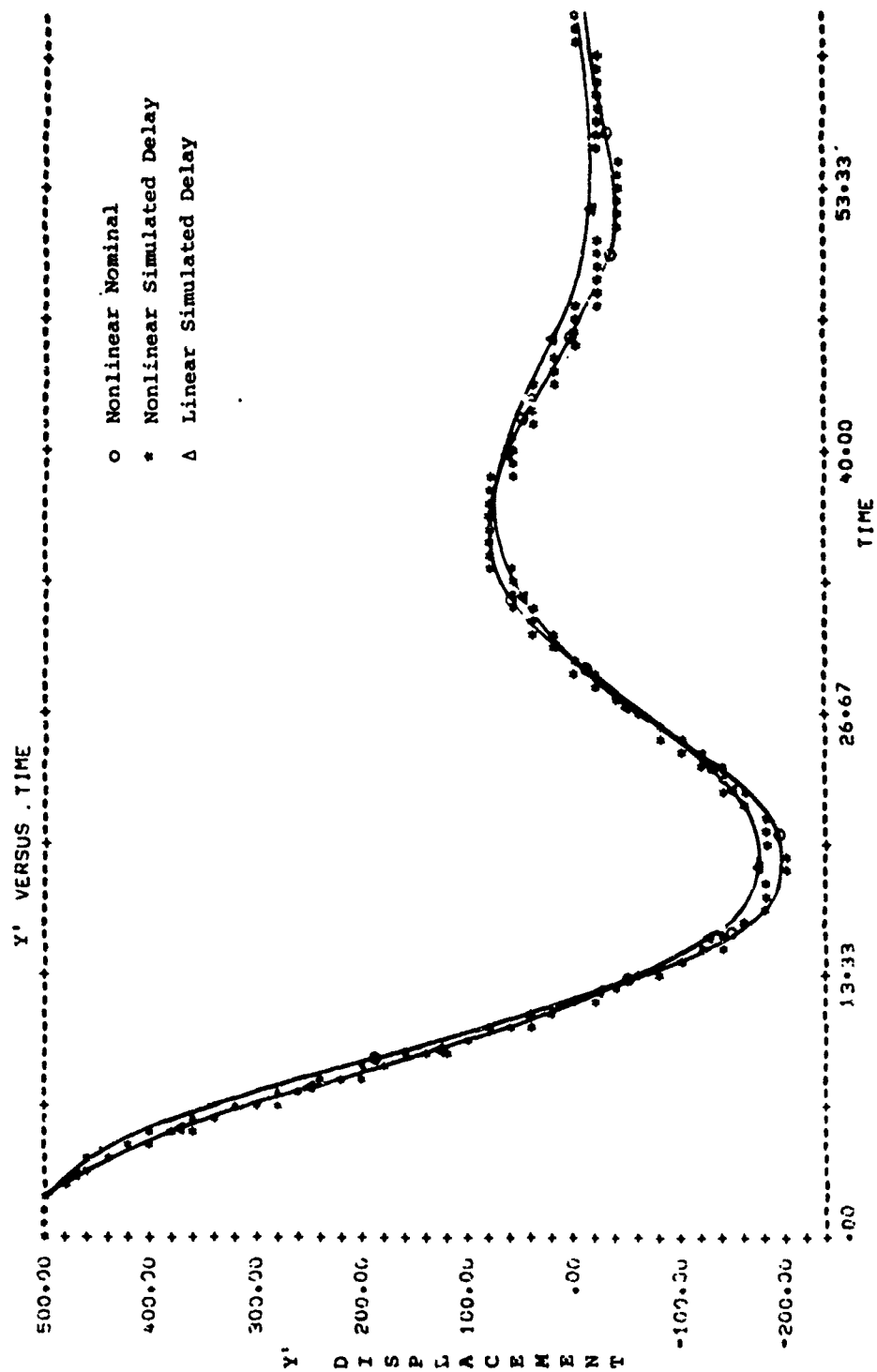


Figure 2.1.2-11 Aircraft Lateral Deviation Response

The approach system models are based on the systems listed in Table 2.1-1 and are developed for use in the generation of probability density functions which are used in the probability of collision analysis. The curved path model and multiple aircraft/runway model are developed for use as approach system analysis tools.

2.1.3.1 Approach System Models

The specific approach systems modeled in this study from Table 2.1-1 are as follows:

1. FC-ILS-I-CTOL
2. FC-ILS-II-CTOL
3. BC-ILS-I-CTOL
4. VOR-CTOL
5. FC-ILS-I-STOL

Due to similarities in the above approach systems, the nominal model block diagrams developed in Section 2.1.2 (Figures 2.1.2-6, 7, and 8) are valid for all of these systems. The nominal model equations and certain model parameter values are representative of all of the above approach systems; however, some model parameter values are specific to each approach system and thus distinguish the different approach system models from one another.

An analysis of each particular item necessary to model the specified approach systems resulted in the model parameter values shown in Table 2.1.3-1. The model parameter values for each specific approach system are determined from Table 2.1.3-1 and by fitting models to measured distribution data (from Section 2.3) for each approach system, as discussed in Section 2.5.

A brief description of each of the approach systems is contained below.

FC-ILS-I-CTOL (Front Course - Instrument Landing System - Category I - Conventional Take Off and Landing)

In this system a ground-based transmitter generates a set of beams in such a manner that the airborne receiver can determine, and indicate to the pilot, the position of the aircraft with respect to the extended runway centerline and an optimum glideslope. Under the stated assumptions it is not necessary to consider the glideslope guidance; therefore, the remaining discussion will be limited to the localizer. The optimum track of the aircraft is precisely along the extended runway centerline (localizer). However, due to various

Table 2.1.3-1 Expanded Model Parameter Values

Item	Symbol	Value	Units	Comments
CTOL Aircraft	a_a	1	sec^{-1}	References 4 and 21
	K_a	1	sec^{-2}	Assumed
	V	236.4	ft/sec	Assumed (140 knots)
	ϕ_{LIM}	.367	rad	Equation 2.1.2-6
	$\dot{\phi}_{\text{LIM}}$.1745	rad	Assumed (10 deg/sec)
	$\dot{\psi}_{\text{LIM}}$.0524	rad	Assumed (3 deg/sec)
STOL Aircraft	a_a	.6	sec^{-1}	References 20 and 21
	K_a	1.667	sec^{-2}	Assumed
	V	108.1	ft/sec	Assumed (64 knots)
	ϕ_{LIM}	.1742	rad	Equation 2.1.2-6
	$\dot{\phi}_{\text{LIM}}$.1745	rad	Assumed (10 deg/sec)
	$\dot{\psi}_{\text{LIM}}$.0524	rad	Assumed (3 deg/sec)
CTOL Runway	γ	2.5	deg	Reference 22
FC-ILS	L	9000	ft	Assumed
BC-ILS	L	-1000	ft	Assumed
VOR	L	4000	ft	Assumed
STOL Runway	γ	7.5	deg	Reference 23
FC-ILS	L	9000	ft	Value is consistent with the measured field data

Table 2.1.3-1 Expanded Model Parameter Values (Continued)

Item	Symbol	Value	Units	Comments
Pilot	a_{p1}	.04	-	Simulated delay models (Equation 2.1.2-2)
	a_{p2}	-.35	-	Simulated delay models (Equation 2.1.2-3)
	a_{p3}	.04	-	Simulated delay models (Equation 2.1.2-4)
	a_{p4}	.35	-	Simulated delay models (Equation 2.1.2-5)
	a_{p5}	.007	-	Simulated delay models (Equation 2.1.2-1)
	a_{ϕ}	1.5	sec ⁻¹	Reference 1
	K_p	1.0	-	Simulated delay models
	$K_{\epsilon e}$	-	-	Determined in Section 2.5 by fitting measured distribution data (Nonlinear models)
	$K'_{\epsilon e}$	-	$\frac{\text{rad}}{\text{ft}}$	Equation 2.1.2-7 (Linear model)
	K_{ϕ}	1.33	sec	Reference 1
	K_{ψ}	1.9	-	Reference 1

Table 2.1.3-1 Expanded Model Parameter Values (Continued)

Item	Symbol	Value	Units	Comments
Lateral Guidance Equipment ILS-I	K_{ψ_e}	1.0	-	Reference 1
	N_{ϵ}	.00149	rad	Determined in Section 2.1.4 (1 σ value)
	N_{ϕ}	-	rad	Determined in Section 2.5 by fitting measured distribution data (1 σ value)
	N_{ψ}	$\pm .01745$	rad	Determined in Section 2.1.4 (1 σ value)
	τ_p	.7	sec	Assumed
	N_R	$\pm .00048$	rad	Determined in Section 2.1.4 (1 σ value)
	N_T	$\pm .001745$	rad	Determined in Section 2.1.4 (1 σ value)
	ILS-II			
	N_R	$\pm .00048$	rad	Determined in Section 2.1.4 (1 σ value)
	N_T	$\pm .001249$	rad	Determined in Section 2.1.4 (1 σ value)
VOR	N_R	$\pm .02155$	rad	Determined in Section 2.1.4 (1 σ value)

Table 2.1.3-1 Expanded Model Parameter Values (Continued)

Item	Symbol	Value	Units	Comments
VOF (Cont'd)	N_T	$\pm .0218$	rad	Determined from Section 2.1.4 (1 σ value)

random error sources, this optimum track is seldom achieved. Changes in the position of the aircraft with respect to the localizer are presented to the pilot via the CDI or Flight Director (FD). The pilot, observing the CDI, commands an aileron deflection. The command causes the aircraft to move laterally in a coordinated turn. The basic system components (CDI, pilot, aircraft and monitoring controller) and their interconnections are illustrated in Figure 2.1.1-1.

FC-ILS-II-CTOL (Front Course - Instrument Landing System - Category II - Conventional Take Off and Landing)

This system is essentially the same as the category I system previously described. However, in this system the calibration and degree of allowable drift of the localizer are held within tighter bounds as discussed in Section 2.1.4.

BC-ILS-I-CTOL (Back Course - Instrument Landing System - Category I - Conventional Take Off and Landing)

The back course ILS localizer beam is generated by the same ground equipment as the front course; therefore, this system is essentially the same as the systems discussed above. However, on a back course approach the aircraft, at a given range from touchdown, is closer to the localizer antenna. Thus, the system is more sensitive to guidance errors.

VOR - CTOL (VHF Omnidirectional Range - Conventional Take Off and Landing)

This system differs from the previously discussed ILS in that the ground station transmits information in such a manner that the receiving equipment in the aircraft can determine the magnetic bearing to (or from) the VOR station. Thus, if a VOR station is located at or near an airport, this station can be used with appropriate procedures to affect landing during IFR weather conditions. This requires that the aircraft fly to (or from) the VOR station on a specified

radial which is input to the omnibearing selector (OBS). The deviations from the selected radial are presented to the pilot on the CDI. The remainder of the model is as discussed in the ILS above.

FC-ILS-I-STOL (Front Course - Instrument Landing System - Category I - Short Take Off and Landing)

This system is similar to the FC-ILS-I-CTOL except that the glideslope is normally elevated to about 7.5° versus 2.5° for CTOL and the primary user class is STOL aircraft. Also the final approach length is much shorter (2-3 N. Mi.) than for CTOL (5 N. Mi. or greater).

2.1.3.2 Curved Path Model and Multiple Aircraft/Runway Model

The curved path and multiple aircraft/runway models are developed for use as analysis tools to study approach systems. Certain terminal system parameters and/or system errors may be varied and the effects on the total system response observed. The models may be used in the prediction of distribution data for systems in which no measured field data exists. Certain system characteristics which are difficult to observe in the actual approach system (such as multiple aircraft relative velocities and locations, aircraft bank angle and heading angle, curved path characteristics, etc.) may be obtained easily from these system models.

Curved Path Model

The nominal model of Section 2.1.2 has been extended to include a three-dimensional curved approach path. This model may be used to study the approach of aircraft along a curved path. The curved path uses two legs (a base and a final) and a commanded standard-rate turn from base leg to final leg to simulate a curved approach. This model can also simulate departures and missed approaches.

The curved path approach model was developed by adding a base leg and a commanded standard-rate turn to the nominal model. The single base leg was deemed sufficient to allow a complete study of various curved approaches. Lateral control while the aircraft is on the base leg is not range dependent; that is, a displacement error rather than an angular error is used to command aircraft motion. The displacement error method is more representative of a controller observing a radar display and giving heading vectors and turn commands. The displacement error has a constant sensitivity for all ranges whereas an ILS has a range dependent sensitivity.

A standard-rate turn is normally used to maneuver the aircraft onto the final leg of the approach. Figure 2.1.3-1 illustrates the curved approach geometry and the different error logic used on each approach leg.

The desired turn rate is an input parameter to the standard-rate turn maneuver and any reasonable rate may be chosen. The bank angle which would give the desired turn rate is computed based on the input turn rate plus some random turn rate error and the aircraft velocity. The range at which the turn is commenced is a function of aircraft velocity, the angle through which the aircraft must turn, the desired turn rate and the pilot/controller turn anticipation time. The range from the intercept (base leg/final leg intersection) at which the turn is commanded, the time required to execute the turn, and the commanded bank angle are given by the following equations.

$$R_{\text{turn}} = \frac{V}{\dot{\psi}_{\text{tr}}} \tan \left| \frac{\beta}{2} \right| + V \tau_c$$

$$T_{\text{turn}} = \left| \frac{\beta}{\dot{\psi}_{\text{tr}}} \right|$$

$$\phi_{\text{turn}} = - \tan^{-1} \left[\frac{(\dot{\psi}_{\text{tr}} + N_{\text{tr}})V}{32.2} \right]$$

where

β = angle which must be turned, rad

$\dot{\psi}_{\text{tr}}$ = turn rate, rad/sec

τ_c = pilot/controller turn anticipation time, sec

T_{turn} = time required to execute the turn, sec

R_{turn} = range from intercept at which the turn will be commenced, ft

ϕ_{turn} = commanded bank angle while in the turn, rad

V = aircraft velocity, ft/sec

N_{tr} = turn rate error, rad/sec

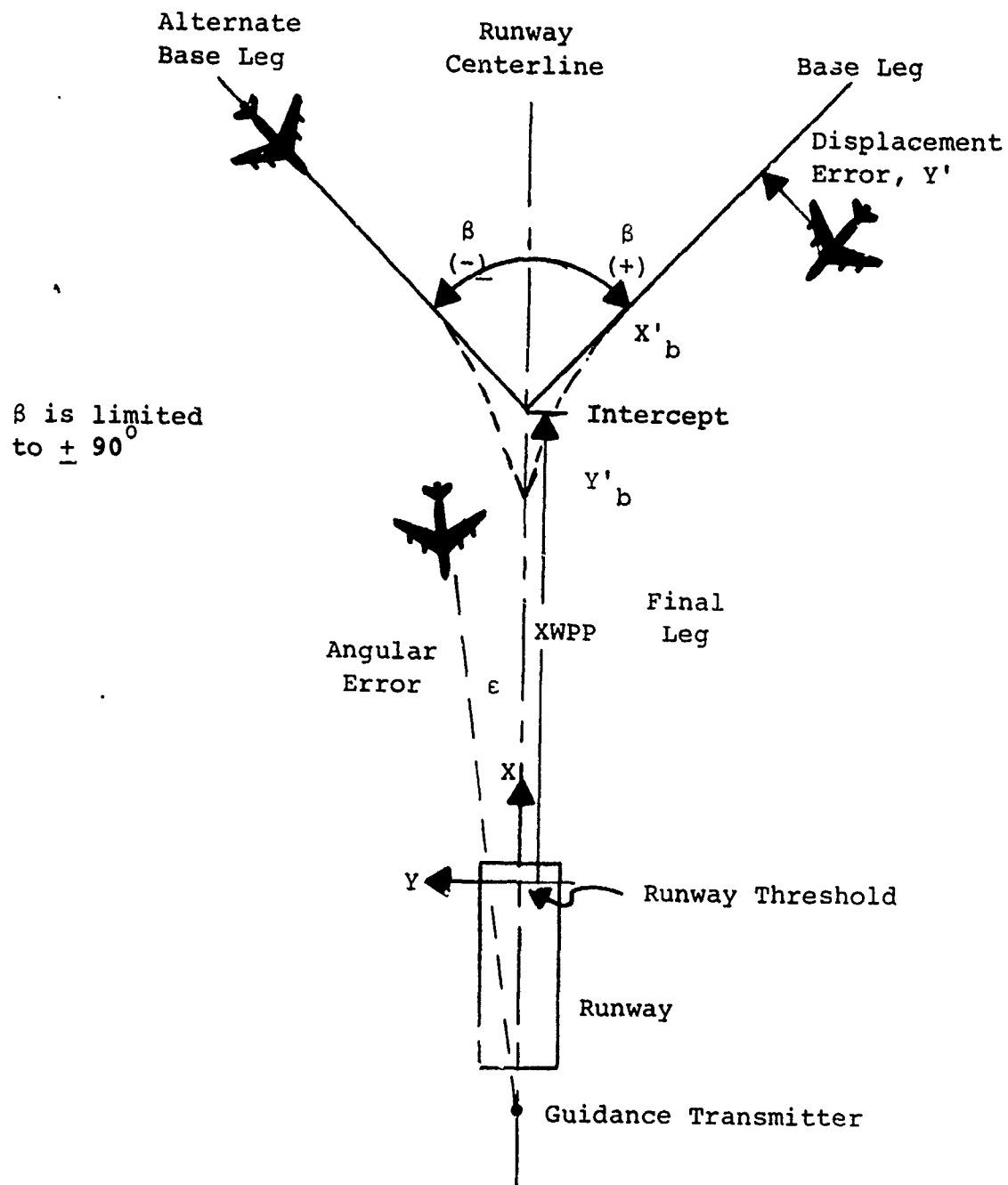


Figure 2.1.3-1 Curved Approach Geometry

The normal aircraft/pilot delays and response characteristics described in Section 2.1.2 are in force throughout the turn maneuver. The glideslope of the base leg is assumed to be a value such that the curved path and base leg lie in the final leg glideslope plane.

Departures are considered to be controlled in the same manner as approaches (discussed in Section 2.1.2); that is, the pilot receives the same form of lateral guidance information as during an approach. Departures are therefore simulated the same as approaches with the following exceptions: the aircraft is initialized at a heading angle (ψ) near zero, Ψ_R reference (Ψ_R) is set to zero, the value of L is set accordingly, and the glideslope angle (γ) is set to correspond to the rate of climb desired for the departure.

A limited missed approach capability is within the operational limits of the curved path model. If a missed approach simulation is desired, a positive pitch angle and missed approach range must be input. The aircraft will then climb out while flying down the localizer beam.

All control logic, coordinate system, and dynamics assumptions made during the development of the nominal model in Section 2.1.2 are valid.

The curved path model consists basically of three separate models which are valid in different regions of the curved approach geometry as illustrated in Figure 2.1.3-2. When the aircraft is operating in the base leg region of the curved approach path, then the base leg model shown in Figure 2.1.3-3 is used. From the time the aircraft's range to the intercept becomes equal to R_{turn} until T_{turn} seconds later, the turning model shown in Figure 2.1.3-4 is valid. After the aircraft has completed the turn the nominal model shown in Figure 2.1.2-6 is valid.

The curved path system model is capable of simulating IFR operations for CTOL or STOL aircraft operating on CTOL or STOL runways with either an ILS (Category I or Category II) or a VOR guidance system. Arrivals can be simulated on either straight-in approach paths or three-dimension general curved paths. Departures and missed approaches may also be simulated, but only on straight paths. The curved path model may be used as an analysis tool for studying curved approaches, departures, and missed approaches.

The curved path model has been programmed in FORTRAN IV and the source listing, flow charts, and operating instructions are contained in the User's Manual.

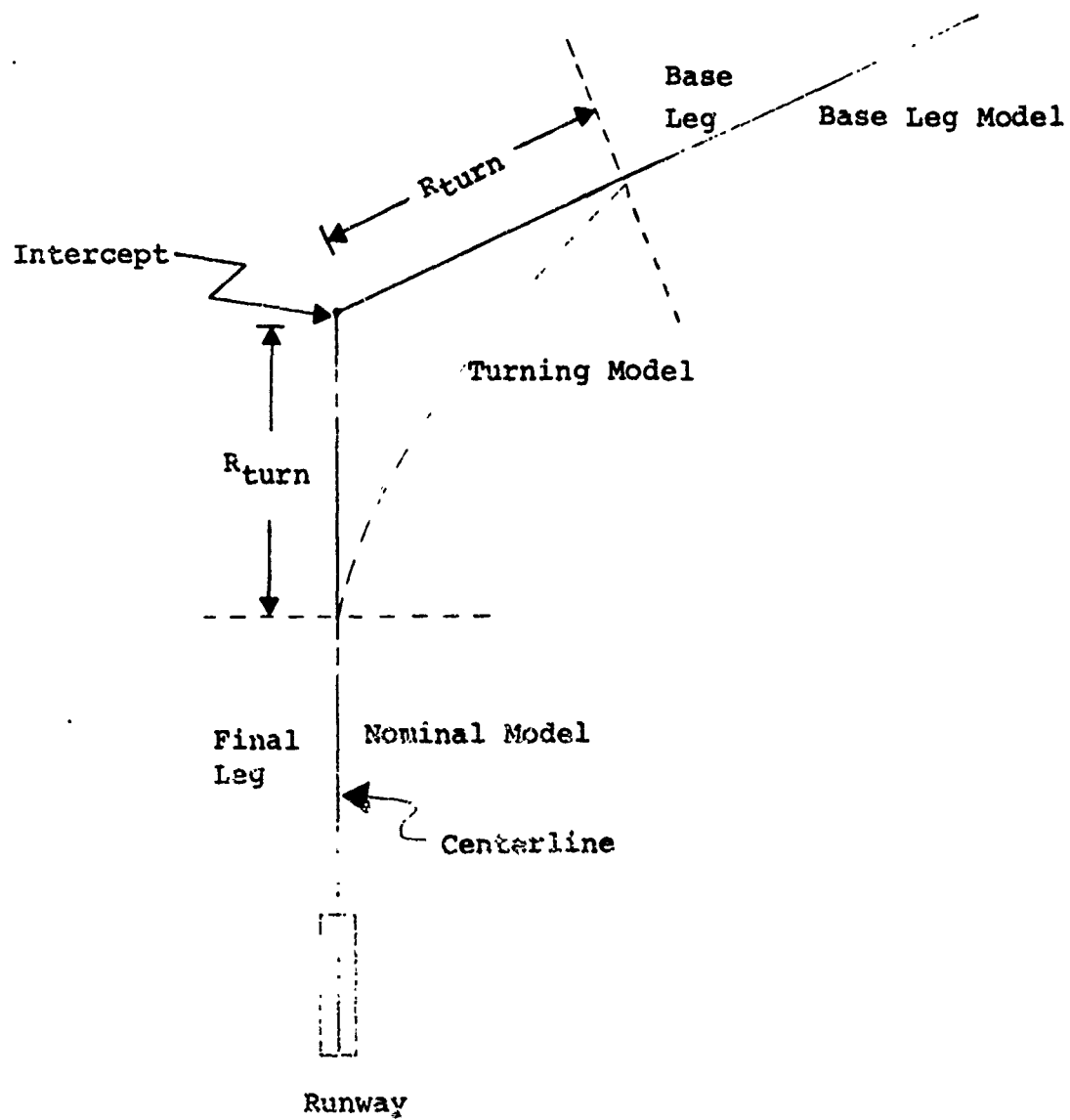
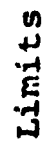
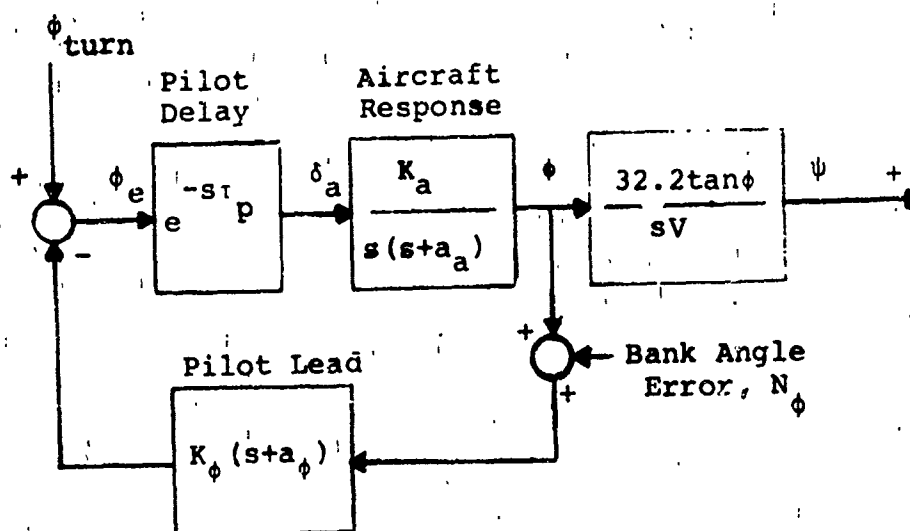


Figure 2.1.3-2 Curved Model Regions of Validity

$$N^R + N^T + N^Y, \quad \mathbb{F}^t$$
[illegible][illegible]

Valid for $x'_b > R_{\text{turn}}$

Figure 2.1.3-3 Basic Leg System Model



Limit

$$\phi \leq \phi_{LIM}$$

$$\dot{\phi} \leq \dot{\phi}_{LIM}$$

Figure 2.1.3-4 Turning System Model

The parameter values for the curved path model may be obtained from Table 2.1.3-1 or assumed.

Multiple Aircraft/Runway Model

The multiple aircraft/runway model may be used to study the effects of longitudinal separation on lateral safety requirements for parallel/non-parallel, CTOL/STOL, and independent/dependent final approaches as well as other analyses. This model can simulate up to four aircraft flying independent or dependent final approaches or departures to or from two parallel or skewed CTOL and/or STOL runways. Both CTOL and STOL type aircraft may be simulated approaching or departing either of the two runways.

In order to study parallel and non-parallel runway configurations a two runway model is required. By using two runways the following configurations may be studied: parallel runways of any lateral separation and threshold displacement; non-parallel runways; and CTOL/STOL or mixed operation runways. The possible parallel runway configurations are indicated in Figure 2.1.3-5. In all discussions Runway 1 is the primary runway and Runway 2 is the secondary (displaced, skewed, STOL, etc.) runway. Non-parallel runway configurations are shown in Figure 2.1.3-6. Runway 2 may have its centerline at any angle within (and including) $\pm 90^\circ$ relative to the Runway 1 centerline. All critical approach operations may be studied using only two runways.

Independent and dependent operations may be simulated using only four aircraft (two per runway) with appropriately selected velocities and approach path locations. The influence of longitudinal speed and longitudinal separation on separation safety standards may thus be studied.

These assumptions have been used to develop the system model shown in Figure 2.1.3-7 which simulates four aircraft flying approaches (or departures) to two separate runways. The multiple aircraft/runway model outputs pertinent aircraft parameters including: relative velocities of all aircraft in the X, Y, Z coordinate system, the relative longitudinal separation of all aircraft measured in ground range, and the runway 1 centered coordinates of all aircraft. These parameters are indicated in Figure 2.1.3-8.

The multiple aircraft/runway model may be used for the analysis of (a) parallel arrival runways, (b) runways used for both arrival and departure operations, (c) multiple runway configurations; and includes longitudinal separation and lateral deviations for (a) CTOL and CTOL/STOL independent

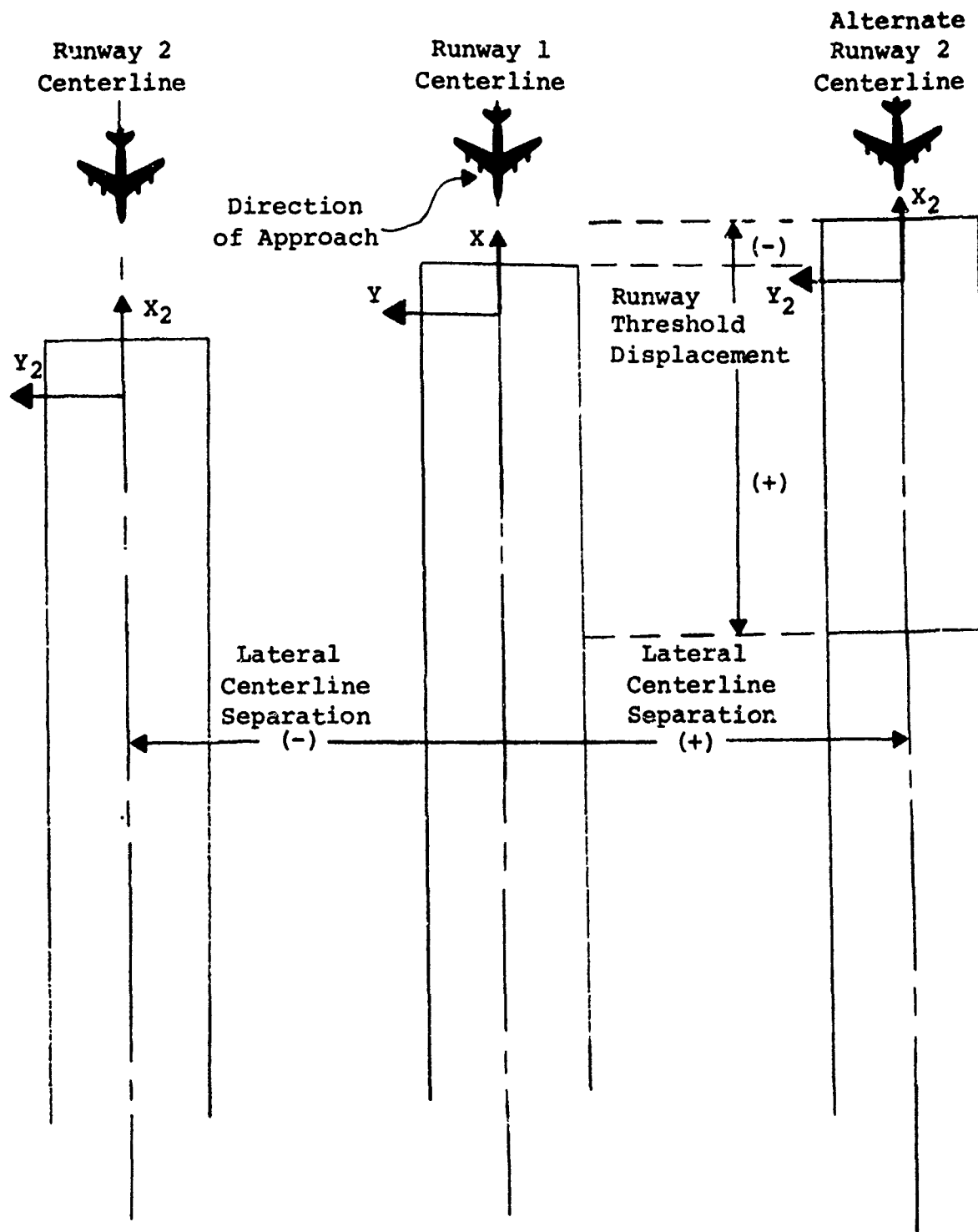
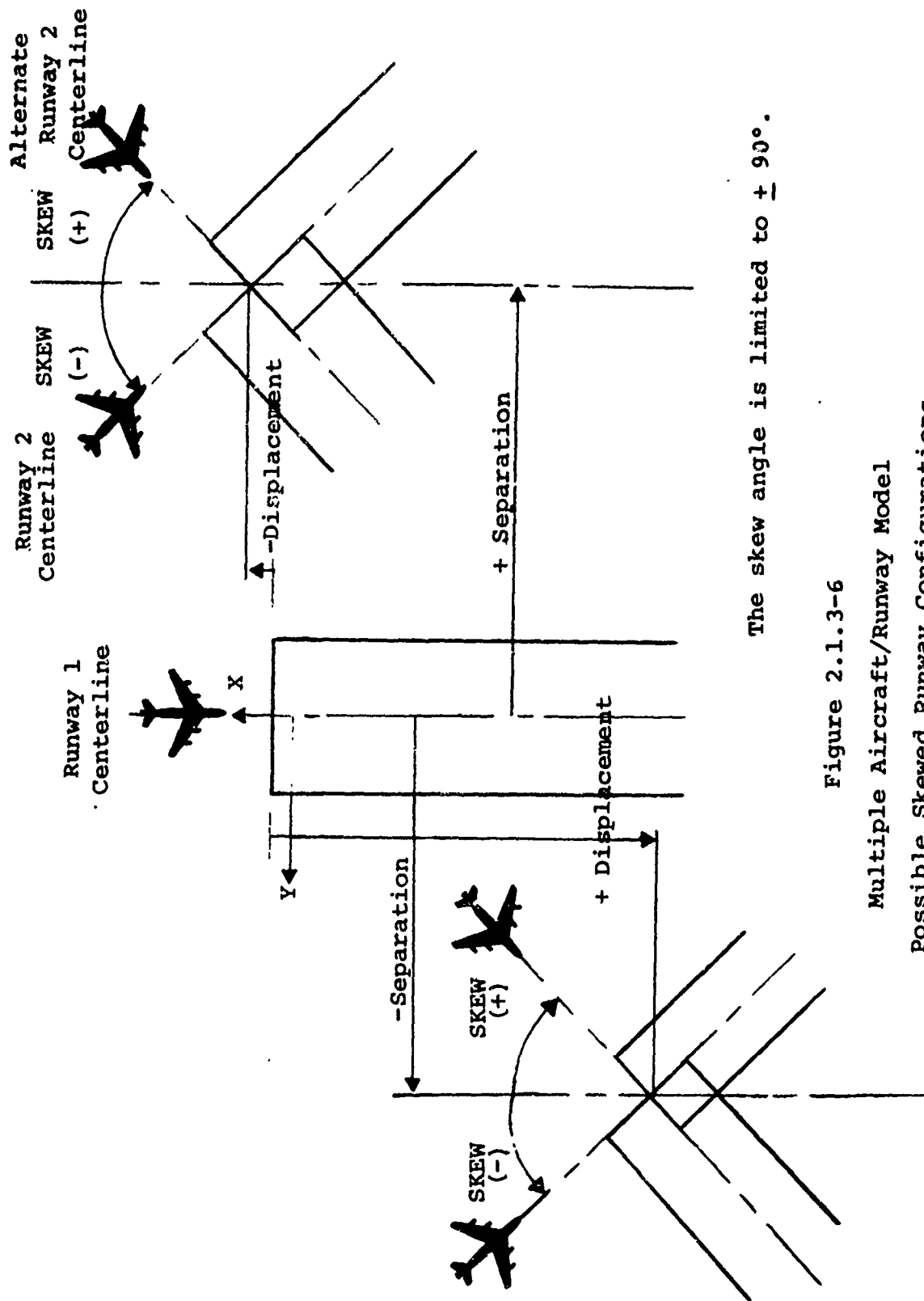


Figure 2.1.3-5
Multiple Aircraft/Runway Model
Possible Parallel Runway Configurations



The skew angle is limited to $\pm 90^\circ$.

Figure 2.1.3-6
Multiple Aircraft/Runway Model
Possible Skewed Runway Configurations

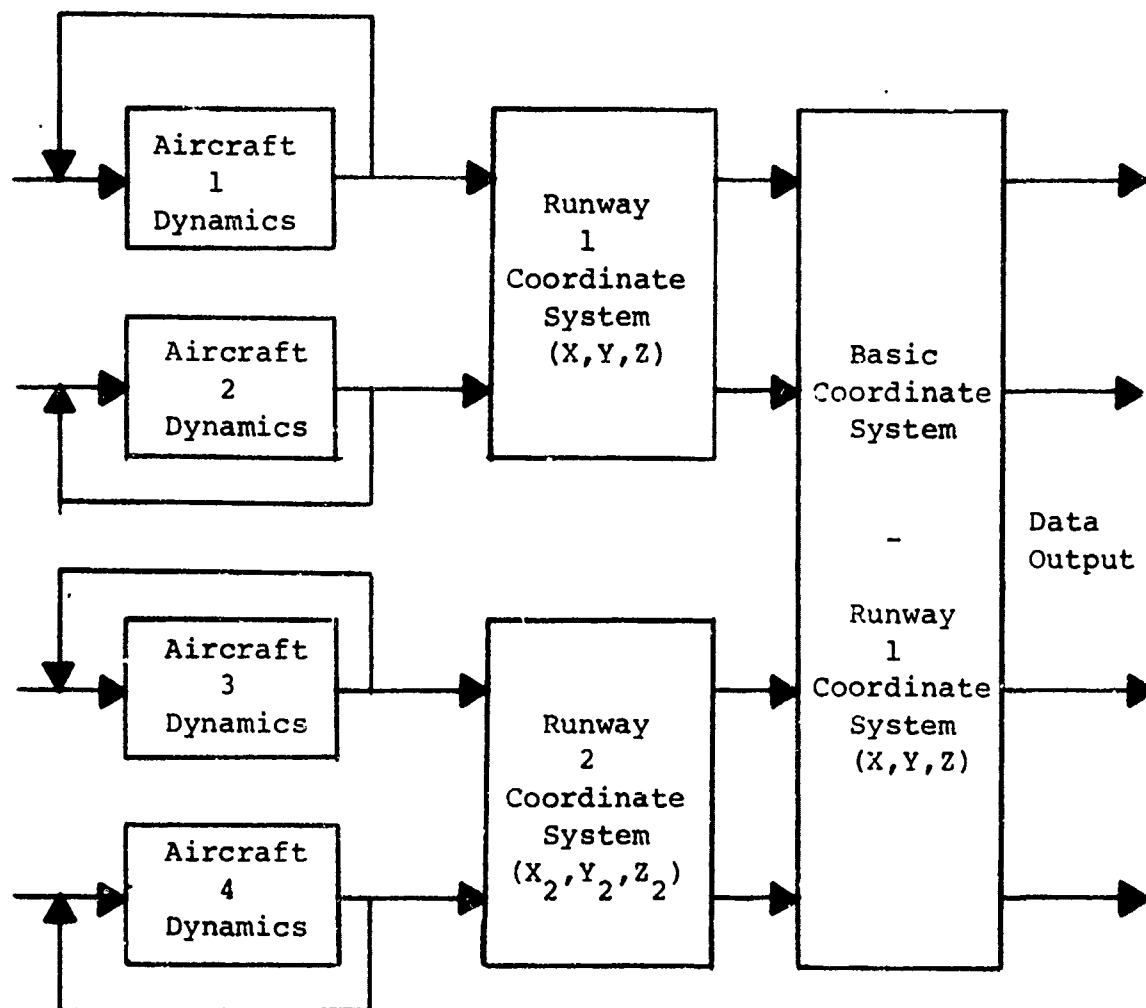


Figure 2.1.3-7 Multiple Aircraft/Runway Model Block Diagram

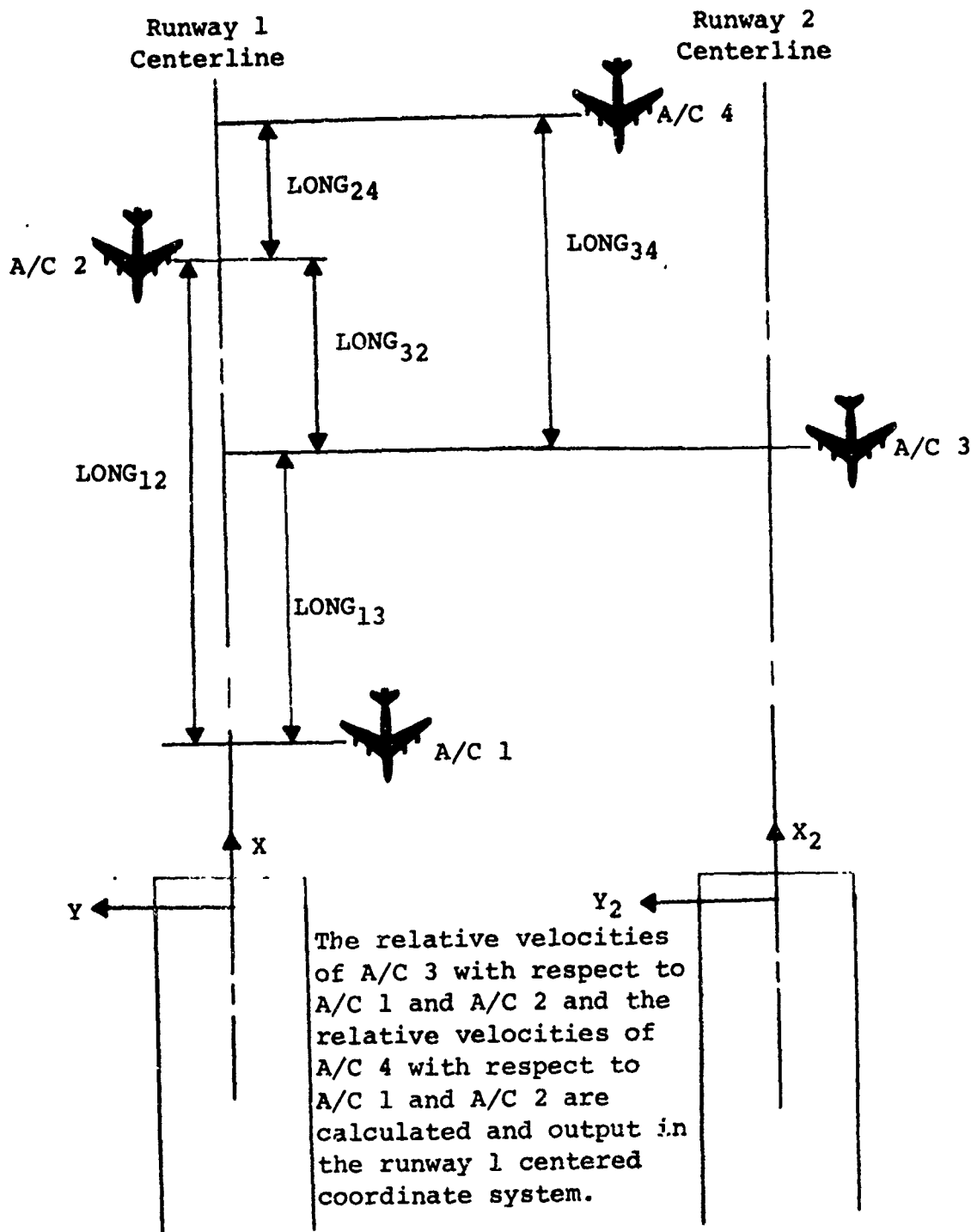


Figure 2.1.3-8
Multiple Aircraft/Runway Model
Description of Relative Distances and Rates

parallel runway operations, (b) CTOL and CTOL/STOL dependent, parallel operations, (c) independent CTOL/STOL non-parallel runway configuration operations, and (d) CTOL/STOL dependent non-parallel runway configuration operations.

The multiple aircraft/runway model has been programmed in FORTRAN IV and the source listing, flow charts, and operating instructions are contained in the User's Manual.

The model parameter values for the multiple aircraft/runway model may be obtained from Table 2.1.3-1 or assumed by the user.

2.1.4 ERROR DEFINITION

2.1.4.1 Introduction

Errors are inherent in every electronic and mechanical system. These errors are, in fact, the accumulation of errors from every component related to the entire system. The error definitions presented in this section will pertain to the following six systems: (1) VHF Omnidirectional Range Receiving Equipment (VOR_R), (2) VHF Omnidirectional Range Transmitting Equipment (VOR_T), (3) Instrument Landing Systems Receiving Equipment (ILS_R), (4) Instrument Landing Systems Transmitting Equipment (ILS_T), (5) Airport Surveillance Radar Systems (ASR) and (6) Human Response and Judgment Errors (N_ϕ , N_ψ , N_e , N_{tr}).

In order to realistically predict actual events by modeling and simulation techniques, errors must be included in the model. Error parameters that are to be entered into the model must be well defined and correctly communicate actual conditions to the model. The purpose of this section is to define the errors in the six major approach system equipments above. Figures 2.1.2-6, 7, and 8 illustrate the location of the error inputs to the nominal system models.

2.1.4.2 Approach

When estimations of errors are to be made, much research must be done to define the errors and determine the reliability of the error estimations. The approach used to define the error estimations for this system is to obtain error data from equipment specifications and error analyses resulting from projects conducted to determine errors inherent in specific systems. The specific systems are standard equipment utilized by the aviation industry. All error sources are assumed to be white-gaussian noise inputs and are

implemented in the system model by calling a gaussian distributed random number every integration step for each error source.

The following paragraphs pertain to the error analyses of the six categories listed in Section 2.1.4.1.

VHF Omnidirectional Range Receiving Equipment (VOR_R)

Because of its wide usage as a primary navigation system in the aviation industry, many studies have been conducted in both laboratory and real environments to determine the accuracy of the VOR_R equipment. Studies made by the Department of Transportation, Federal Aviation Administration (References 8, 11, 12), the manufacturers of VOR_R navigation equipment (References 6, 7, 14), and by institutions of learning and testing (References 9, 12, 15) have contributed to the evaluation of errors inherent in the receivers in this category. These errors are important to this study effort because of their effect on the total system performance.

References 6 and 7 estimate the VOR_R error to have a 1 sigma deviation of $\pm .25^\circ$ in azimuth, while Reference 14 estimates the error to be $\pm .125^\circ$ at 1 sigma deviation. Reference 9 and 12 estimate the error to be $\pm 1.25^\circ$ at 1 sigma, Reference 11 estimates $\pm 2.25^\circ$ and Reference 8 estimates $\pm 2.3^\circ$ at the 1 sigma deviation. It can be seen that the receiver error can be related to the type of analysis and equipment tested.

VHF Omnidirectional Range Transmitting Equipment (VOR_T)

The local geography of the area has, in some instances, limited the full use of the VOR_T system. Perturbations called course roughness, scalloping and bends create deviations such that in some instances the course deviations must be averaged to maneuver the aircraft on the indicated course. Flight inspection standards indicate that the course structure and alignment of radials shall be with the following limitations: (a) the alignment of all electronic radials will be within 2.5° of the current magnetic azimuth, (b) momentary deviations of the course due to roughness and scalloping, or combinations thereof will not exceed 3.0° from the average course, (c) bends will not exceed 3.5° from the computed average course alignment and must remain within 3.5° of the correct magnetic azimuth, and (d) the effects of any one or a combination of the three above will not render the radial unusable or unsafe (References 9, 10, 11).

The error of the VOR_T is estimated to be $\pm 1.0^\circ$ at 1 sigma (References 9, 11). Reference 10 states that frequency deviations from 60 Hz at the transmitter can cause CDI errors of up to 1.5° with certain receivers.

Instrument Landing System Receiver Equipment (ILS_R)

Instrument Landing System Receivers are utilized on fewer aircraft than the VOR_R equipment, and fewer studies have been conducted to determine the errors inherent in the ILS_R equipment. References 6 and 7 were utilized to determine the estimated error for the ILS_R equipment. The errors noted in the Collins 51R-7A/8A are $\pm .021^\circ$ at 1 sigma deviation and $\pm .0335^\circ$ at the 1 sigma deviation for the Collins 51RV-2B receivers.

Instrument Landing System Transmitting Equipment (ILS_T)

Instrument Landing System Transmitting Equipment is maintained at all facilities regularly used by commercial air services except for those sites where, because of traffic, climatic, or economic reasons, safety would not be affected by the absence of an ILS_T system (Reference 15).

Little information has been found in the literature concerning the error inherent in the ILS_T systems. Reference 1 presents a typical localizer noise power spectral density curve (Figure 2.1.4-1) which supplies information about the frequency content of the localizer noise.

Specifications state that the maximum allowable localizer deviation at the threshold point is 35 feet for Category I systems, and 25 feet for Category II systems. These numbers correspond to $.1^\circ$ for Category I systems and $.0715^\circ$ for Category II systems for a range of 10,000 feet from the localizer antenna to the threshold point. It is assumed that the 1 sigma deviations are $.1^\circ$ for Category I systems and $.0715^\circ$ for Category II systems. Reference 15 also stated that the maximum allowable localizer deviation was $\pm .1^\circ$ at 1 sigma deviation.

Airport Surveillance Radar (ASR)

The function of the surveillance radar is to obtain and supply information concerning the location of aircraft in the vicinity of air traffic centers. The capability of the ASR to detect and locate an aircraft is determined by the design and operational characteristics of the components and equipment utilized in the radar system.

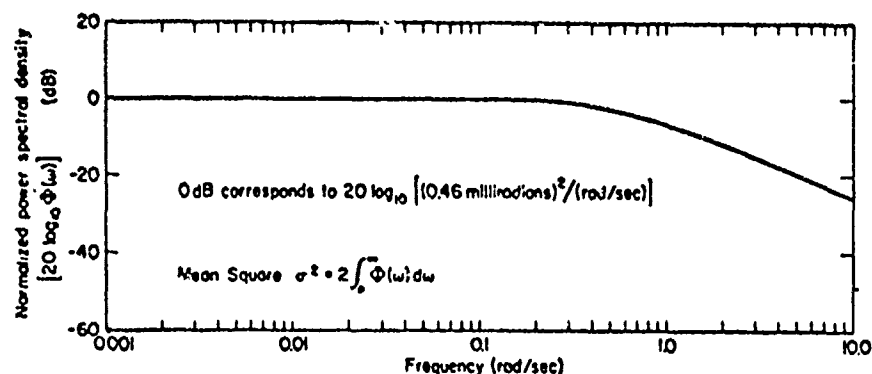


Figure 2.1.4-1

Typical Localizer "Noise" Power Spectral Density

As standard or normal systems to evaluate, the ASR-2 and ASR-5 are chosen. The error in both systems (Reference 13) is $\pm .5^\circ$ (1 σ).

Human Response and Pilot Judgment Errors, (N_ψ , N_ϕ , N_ϵ , N_{tr})

In studies of this nature where data is not available or where the parameters being considered are not observable, it is necessary to use inductive reasoning to estimate values or accuracies. Such is the case with the pilot induced errors of interpreting the instruments presenting heading, bank angle and localizer information. Certain pilot errors estimated in this section will be adjusted in Sections 2.4 and 2.5 to fit measured distributor data for specific approach systems. Since accurate estimates of human attitude errors do not exist, it is necessary to estimate these errors by observing measured data or by analyzing the instruments or indicators which the pilot must read in the localizer tracking task.

The most widely used heading instrument (directional gyros, DG's, and magnetic compasses) have course markings every 5 degrees. For headings between the marks, the pilot finds himself estimating the heading by mental linear interpolation. It is reasonable to assume that most of these heading estimates will contain random errors, N_ψ , within $\pm 1^\circ$ (1 σ). Since the DG is usually located directly in front of the pilot there should be no parallax problems.

Bank angle indicators have the coarsest (greatest angle between successive instrument marks) markings. However,

indirect bank angle measurement is available from the rate-of-turn indicator. The hierarchy of instruments generally order the rate-of-turn as being the primary bank attitude indicator. Direct measurement of the bank angle will have random errors in the order of $\pm 5^\circ$ (1σ). Since the bank angle is the pilot's primary controlling parameter, the pilot attitude random errors are primarily contained within N_ϕ ; therefore, more accurate estimates of N_ϕ are made for specific approach systems by fitting the measured distribution data in Sections 2.4 and 2.5.

The error N_ϵ , based on inattention to the localizer indicators (CDI or flight director) is estimated to have a 1σ value of about $\pm 0.2^\circ$. This corresponds to $< 10\%$ of full scale deflection on the CDI. There is no apparent parallax or biasing that would cause the mean to be non-zero.

The aircraft turn rate random error, N_{tr} , about a commanded standard rate turn is assumed to be gaussian with a 1 sigma deviation of $.2$ deg/sec.

White Gaussian Noise

The ILS lateral system equipment and pilot errors were assumed to be white gaussian noise sources. The word white implies that the noise contains all frequencies equally up to a frequency of w rad/sec where w is at least two times larger than the bandwidth of the ILS system. Therefore, the noise would appear white to the system. The word gaussian refers to a law for probability of samples of various amplitude which holds for many natural sources of noise (Reference 18). Justification of the white gaussian noise assumption for the ILS lateral equipment errors is illustrated by observing in Figure 2.1.4-1 the effective bandwidth of localizer noise power spectral density, $.2$ rad/sec, (Reference 1) and comparing it to the effective bandwidth of the ILS lateral system model ($\sim .05$ rad/sec). Since the bandwidth of the noise is more than a factor of two times the bandwidth of the system, the noise may be assumed to be white noise. Due to characteristics of the ILS lateral equipment, the major noise contributor is thermal noise which is generally gaussian and white (Reference 17); therefore, the ILS lateral system equipment errors were assumed to be white gaussian.

Pilot errors were also assumed to be white gaussian noise sources. The white noise assumption is again justified by the fact that the ILS lateral system bandwidth is assumed small compared to the pilot noise bandwidth. The gaussian

assumption is justified by the central limit theorem (Reference 16) which states that for a sequence of independent random variables, x_i , the distribution of the random variable, z_i , defined by

$$z_i = \frac{1}{n} (x_1 + x_2 + \dots + x_n)$$

tends to be gaussian as n increases regardless of the distributions of the x_i 's. Since the ILS lateral system model is concerned with a large sample of independent pilots, the congregate pilot errors assumed for the model are gaussian.

2.1.4.3 Results

The results of the error definition study are presented in Table 2.1.4-1. Error estimates are presented for VOR_R , VOR_T , ILS_R , ILS_T , ASR , N_ψ , N_ϕ , N_ϵ , and N_{tr} . Values for the lateral guidance equipment receiver, N_R , and transmitter, N_T , noises to be input into the models are dependent upon the specific approach system modeled. For the VOR system model,

$$N_R = VOR_R$$

$$N_T = VOR_T$$

For the ILS system models,

$$N_R = ILS_R$$

$$N_T = ILS_T$$

When used as input to the linear model or the base leg model, N_R , N_T , and N_ϵ must be converted to feet and are range dependent. A more accurate estimate for the pilot attitude error, N_ϕ , is made in Sections 2.4 and 2.5.

2.1.5 STATE EQUATIONS

2.1.5.1 Introduction

The Fokker-Planck analysis requires, as input, the system model state equations, which describe the complete dynamics of the approach systems described in Section 2.1.3.1. Since all specific approach system models to be considered are represented by the same block diagrams, one set of state equations apply to all approach system models. To simplify the Fokker-Planck analysis the pilot delay is approximated

Table 2.1.4-1 Error Summary

Item	Value* 1 σ , deg**	Reference	Remarks
VOR _R	± 1.235	-	Value for models - average of values from references below
	$\pm .25$	6, 7	Collins VOR/ILS 51RV-2B; Collins VOR/LOC 51R-7A,-8A
	$\pm .125$	14	Collins VOR/ILS 51RV-1
	± 1.25	9, 12	General/Industrial Aviation Usage; FAA, NECAP 1964 program
	± 2.25	11	General/Industrial Aviation Usage
	± 2.3	8	FAA, NECAP II, General Aviation Usage
VOR _T	± 1.25	-	Value for models - average of values from references below
	± 1.0	9, 11	General/Industrial Aviation Usage
	± 1.5	10	General/Industrial Aviation Usage (assumed)
ILS _R	$\pm .0275$	-	Value for models - average of values from references below
	$\pm .021$	7	Collins 51R-7A,-8A (assumed)
	$\pm .0335$	6	Collins 51RV-2B
ILS _T	$\pm .1$	15	Category I (assumed)
ILS _T	$\pm .0715$	-	Category II (assumed)

Table 2.1.4-1 Error Summary (Continued)

Item	Value* 1σ , deg**	Reference	Remarks
ASR	$\pm .5$	-	Value for models - average of values from references below
	$\pm .5$	13	NAFEC ASR-2
	$\pm .5$	12	NAFEC ASR-5
Heading Angle, N_{ψ}	$\pm 1.$	-	Assumed
Bank Angle, N_{ϕ}	$\pm 5.$	-	Assumed
CDI, N_{ϵ}	$\pm .2$	-	Assumed
Turn Rate, N_{tr}	$\pm .2^{***}$	-	Assumed

More accurate estimates of these pilot errors are made for the nominal approach system model in Section 2.4

* All random errors are assumed to be white gaussian noise sources with the mean equal to zero and standard deviation equal to 1σ .

** All angular errors are implemented in the models in radians.

*** Units are deg/sec; implemented in rad/sec.

by the simulated delay shown in Figures 2.1.2-7 and 2.1.2-8. Therefore, the state equations are derived for both the linear and nonlinear simulated delay system models. Figure 2.1.2-7 and Figure 2.1.2-8 are the block diagrams of the nonlinear and linear simulated delay system models, respectively. These block diagrams are discussed and all terms are defined in Section 2.1.2.

2.1.5.2 Approach

The block diagrams are reduced to equation form to produce the system state equations.

Linear State Equations

The following equations are written directly from the block diagram given in Figure 2.1.2-8.

$$\epsilon_e = Y_d' - Y'$$

$$\psi_c = \epsilon_e K_{\epsilon_e}$$

$$\psi_e = \psi_c - (\psi - \psi_R + N_\psi) K_\psi$$

$$\phi_c = \psi_e K_{\psi_e}$$

$$\phi_e = \phi_c - (\phi + N_\phi) (K_\phi (s + a_\phi))$$

$$\delta_a = \phi_e \frac{K_p (a_{p1}s^2 + a_{p2}s + 1)}{(a_{p5}s + 1) (a_{p3}s^2 + a_{p4}s + 1)}$$

$$\phi = \delta_a \frac{K_a}{s(s + a_a)}$$

$$\dot{\psi} = \phi \frac{32.2}{V}$$

$$\psi = \dot{\psi} \left(\frac{1}{s} \right)$$

$$V_{Y'} = (\psi - \psi_R) (V \cos \theta_0)$$

$$Y' = V_{Y'} \left(\frac{1}{s} \right)$$

After defining the above variables, it is convenient to reduce by superposition the inner loop contained in

the linear block diagram model (Figure 2.1.2-8) to equational form.

$$\phi = \frac{\phi_c G}{1 + GH} - \frac{N_\phi GH}{1 + GH}$$

where

$$G = \frac{K_p (a_{p1}s^2 + a_{p2}s + 1)}{(a_{p5}s + 1)(a_{p3}s^2 + a_{p4}s + 1)} \cdot \frac{K_a}{s(s + a_a)}$$

$$H = K_\phi (s + a_\phi)$$

The resulting equation is:

$$\phi = \frac{\phi_c (b_1 s^2 + b_2 s + b_3) - N_\phi (d_1 s^3 + d_2 s^2 + d_3 s + d_4)}{s^5 + c_1 s^4 + c_2 s^3 + c_3 s^2 + c_4 s + c_5} \quad (2.1.5-1)$$

where

$$A_o = a_{p3} a_{p5}$$

$$b_1 = a_{p1} K_p K_a A_o^{-1}$$

$$b_2 = a_{p2} K_p K_a A_o^{-1}$$

$$b_3 = K_p K_a A_o^{-1}$$

$$c_1 = (a_a a_{p3} a_{p5} + a_{p3} + a_{p4} a_{p5}) A_o^{-1}$$

$$c_2 = (a_a (a_{p3} + a_{p4} a_{p5}) + a_{p4} + a_{p5} + K_\phi a_{p1} K_p K_a) A_o^{-1}$$

$$c_3 = (1 + a_a (a_{p4} + a_{p5}) + a_{p1} K_p K_a K_\phi a_\phi + K_\phi a_{p2} K_p K_a) A_o^{-1}$$

$$c_4 = (a_a + K_\phi K_p K_a + a_{p2} K_p K_a K_\phi a_\phi) A_o^{-1}$$

$$c_5 = (K_p K_a K_\phi a_\phi) A_o^{-1}$$

$$d_1 = K_\phi K_a K_p a_{p_1} A_o^{-1}$$

$$d_2 = K_\phi K_a K_p (a_{p_2} + a_{p_1} a_\phi) A_o^{-1}$$

$$d_3 = K_\phi K_a K_p (1 + a_{p_2} a_\phi) A_o^{-1}$$

$$d_4 = K_\phi K_a K_p a_\phi A_o^{-1}$$

Equation 2.1.5-1 is divided by s^5 in both the numerator and denominator to obtain:

$$\phi = \frac{\phi_c (b_1 s^{-3} + b_2 s^{-4} + b_3 s^{-5}) - N_\phi (d_1 s^{-2} + d_2 s^{-3} + d_3 s^{-4} + d_4 s^{-5})}{1 + c_1 s^{-1} + c_2 s^{-2} + c_3 s^{-3} + c_4 s^{-4} + c_5 s^{-5}}$$

Rewriting this equation the following is obtained:

$$\begin{aligned} \phi = & \phi_c b_1 s^{-3} + \phi_c b_2 s^{-4} + \phi_c b_3 s^{-5} - \phi_c d_1 s^{-2} - \phi_c d_2 s^{-3} - \phi_c d_3 s^{-4} - \phi_c d_4 s^{-5} \\ & - N_\phi d_1 s^{-2} - N_\phi d_2 s^{-3} - N_\phi d_3 s^{-4} - N_\phi d_4 s^{-5} \end{aligned}$$

This allows the flow graph, Figure 2.1.5-1, to be constructed.

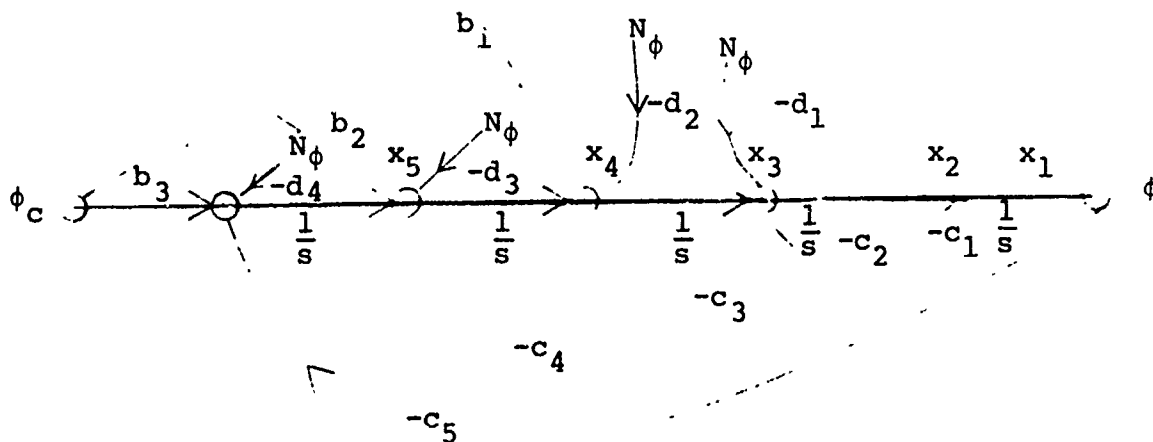


Figure 2.1.5-1 Inner Loop Flow Graph

Using Mason's Loop Rule, $\frac{\phi}{\phi_c} = \frac{\Sigma \text{ forward paths}}{-\Sigma \text{ feedback paths}}$,

The flow graph is verified by writing $\frac{\phi}{\phi_c}$ from the flow graph as follows (with $N_\phi = 0$):

$$\frac{\phi}{\phi_c} = \frac{b_1 s^{-3} + b_2 s^{-4} + b_3 s^{-5}}{1 - (-c_1 s^{-1} - c_2 s^{-2} - c_3 s^{-3} - c_4 s^{-4} - c_5 s^{-5})}$$

Now multiplying the numerator and denominator by s^5 the following equation is obtained:

$$\frac{\phi}{\phi_c} = \frac{b_1 s^2 + b_2 s + b_3}{s^5 + c_1 s^4 + c_2 s^3 + c_3 s^2 + c_4 s + c_5}$$

which is identical to Equation 2.1.5-1, the general $\frac{\phi}{\phi_c}$ transfer function.

To obtain the state equations for the inner loop of the block diagram, the flow graph is utilized. States x_1, x_2, x_3, x_4 , and x_5 are defined following the integration as shown in Figure 2.1.5. The following state equations are written from the flow graph.

$$\dot{x}_1 = x_2 - c_1 x_1 \quad (2.1.5-2)$$

$$\dot{x}_2 = x_3 - c_2 x_1 - d_1 N_\phi \quad (2.1.5-3)$$

$$\dot{x}_3 = x_4 - c_3 x_1 - d_2 N_\phi + b_1 \phi_c \quad (2.1.5-4)$$

$$\dot{x}_4 = x_5 - c_4 x_1 - d_3 N_\phi + b_2 \phi_c \quad (2.1.5-5)$$

$$\dot{x}_5 = b_3 \phi_c - c_5 x_1 - d_4 N_\phi \quad (2.1.5-6)$$

Where $x_1 = \phi$ and x_2, x_3, x_4 , and x_5 are intermediate states.

From the block diagram of the model, let:

$$x_6 = \psi$$

$$x_7 = y'$$

$$u = y'_d + N_R + N_T + N_{y'}, \text{ ft}$$

therefore:

$$\dot{x}_6 = \frac{32.2}{V} x_1 \quad (2.1.5-7)$$

$$\dot{x}_7 = (x_6 - \psi_R) V \cos \theta_0 \quad (2.1.5-8)$$

and

ϕ_c may be written as:

$$\phi_c = K_{\psi_e} (K_{\epsilon_e} (u - x_7) - K_{\psi} (x_6 - \psi_R + N_{\psi})) \quad (2.1.5-9)$$

Nonlinear State Equations

Figure 2.1.2-7 is utilized in the derivation of the nonlinear state equations. The method of derivation is identical to that utilized in the linear case. Since the inner loop of the nonlinear block diagram is identical to the inner loop of the linear block diagram, with the exception of the limits on ϕ and $\dot{\phi}$, the reduction of this loop results in Equations 2.1.5-2 through 2.1.5-6 with states x_1, x_2, x_3, x_4 , and x_5 defined as in the previous paragraph. Referring to the block diagram let:

$$x_6 = \psi$$

$$x_7 = y'$$

$$x_8 = X'$$

$$u = \epsilon_{LOC} + N_R + N_T + N_{\epsilon}, \text{ rad}$$

The following equations may be written from the block diagram:

$$\dot{x}_6 = \frac{32.2}{V} \tan x_1 \quad (2.1.5-10)$$

$$\dot{x}_7 = (V \cos \theta_0) (\sin(x_6 - \psi_R)) \quad (2.1.5-11)$$

$$\dot{x}_8 = (V \cos \theta_0) \cos x_6 \quad (2.1.5-12)$$

$$\phi_c = K_{\psi_e} \left(K_{\epsilon_e} \left(u - \tan^{-1} \left(\frac{x_7}{x_8 + L} \right) \right) - K_{\psi} (x_6 - \psi_R + N_{\psi}) \right) \quad (2-1-5-13)$$

2.1.5.3 State Equation Results

The state equations required by the Fokker-Planck analysis are given in this section. A definition of all terms is contained in Section 2.1.2. Two sets of state equations, derived for use in various required analyses, are the linear and nonlinear state equations with an approximation for the pilot delay. The following terms, defined in Section 2.1.5.2, will retain their definitions: A_0 , b_1 , b_2 , b_3 , c_1 , c_2 , c_3 , c_4 , c_5 , d_1 , d_2 , d_3 , and d_4 . In addition,

$$\psi_R = \begin{array}{l} \pi; \text{ an approach} \\ 0; \text{ a departure} \end{array}$$

The initialization of the states may be derived from the list of zero error conditions listed below. The zero error conditions are defined by the aircraft flying straight down the runway centerline.

$$x_1 = \phi = 0$$

$$x_2 = x_3 = x_4 = x_5 = 0$$

$$x_6 = \psi = \psi_R$$

$$x_7 = Y' = 0$$

$$x_8 = X' = \text{slant range}$$

$$\theta_0 = 0, \text{ indicates the aircraft is flying down the glideslope.}$$

Linear State Equations

The linear state equations may be defined by combining Equations 2.1.5-2 through 2.1.5-9.

$$\dot{x}_1 = x_2 - c_1 x_1$$

$$\dot{x}_2 = x_3 - c_2 x_1 - d_1 N_\phi$$

$$\dot{x}_3 = x_4 - c_3 x_1 - d_2 N_\phi - b_1 K_{\psi_e} K_\psi (x_6 + N_\psi) - b_1 K_{\psi_e} K_\epsilon x_7 + b_1 K_{\psi_e} K_\epsilon u + b_1 K_{\psi_e} K_\psi \psi_R$$

$$\dot{x}_4 = x_5 - c_4 x_1 - d_3 N_\phi - b_2 K_{\psi_e} K_\psi (x_6 + N_\psi) - b_2 K_{\psi_e} K_\epsilon x_7 + b_2 K_{\psi_e} K_\epsilon u + b_2 K_{\psi_e} K_\psi \psi_R$$

$$\dot{x}_5 = -c_5 x_1 - d_4 N_\phi - b_3 K_{\psi_e} K_\psi (x_6 + N_\psi) - b_3 K_{\psi_e} K_\epsilon x_7 + b_3 K_{\psi_e} K_\epsilon u + b_3 K_{\psi_e} K_\psi \psi_R$$

$$\dot{x}_6 = \frac{32.2}{V} x_1$$

$$\dot{x}_7 = (x_6 - \psi_R) (V \cos \theta_0)$$

where $x_1 = \phi$ and x_2, x_3, x_4 , and x_5 are intermediate states in the inner loop and $x_6 = \psi$, $x_7 = Y'$, and $u = Y_d' + N_R + N_T + N_Y$. The linear state equation may be written in matrix form as follows:

$$\begin{bmatrix} \dot{x}_1 \\ \dot{x}_2 \\ \dot{x}_3 \\ \dot{x}_4 \\ \dot{x}_5 \\ \dot{x}_6 \\ \dot{x}_7 \end{bmatrix} = \begin{bmatrix} -c_1 & 1 & 0 & 0 & 0 & 0 & 0 \\ -c_2 & 0 & 1 & 0 & 0 & 0 & 0 \\ -c_3 & 0 & 0 & 1 & 0 & -b_1 K_{\psi_e} K_\psi & -b_1 K_{\psi_e} K_\epsilon \\ -c_4 & 0 & 0 & 0 & 1 & -b_2 K_{\psi_e} K_\psi & -b_2 K_{\psi_e} K_\epsilon \\ -c_5 & 0 & 0 & 0 & 0 & -b_3 K_{\psi_e} K_\psi & -b_3 K_{\psi_e} K_\epsilon \\ \frac{32.2}{V} & 0 & 0 & 0 & 0 & 0 & 0 \\ 0 & 0 & 0 & 0 & 0 & V \cos \theta_0 & 0 \end{bmatrix} \begin{bmatrix} x_1 \\ x_2 \\ x_3 \\ x_4 \\ x_5 \\ x_6 \\ x_7 \end{bmatrix}$$

$$\begin{array}{c}
 + \\
 \cdot \\
 \cdot \\
 \cdot
 \end{array}
 \begin{bmatrix}
 0 & 0 & 0 & 0 \\
 0 & -d_1 & 0 & 0 \\
 b_1 K_{\psi_e} K_{\epsilon_e} & -d_2 & -b_1 K_{\psi_e} K_{\psi} & b_1 K_{\psi_e} K_{\psi} \\
 b_2 K_{\psi_e} K_{\epsilon_e} & -d_3 & -b_2 K_{\psi_e} K_{\psi} & b_2 K_{\psi_e} K_{\psi} \\
 b_3 K_{\psi_e} K_{\epsilon_e} & -d_4 & -b_3 K_{\psi_e} K_{\psi} & b_3 K_{\psi_e} K_{\psi} \\
 0 & 0 & 0 & 0 \\
 0 & 0 & 0 & -V \cos \theta_o
 \end{bmatrix}
 \begin{bmatrix}
 u \\
 N_{\phi} \\
 N_{\psi} \\
 \psi_R
 \end{bmatrix}$$

Nonlinear State Equations

The nonlinear state equations with the approximation of the pilot delay may be defined by combining Equations 2.1.5-2 through 2.1.5-6 and 2.1.5-10 through 2.1.5-13.

$$\dot{x}_1 = x_2 - c_1 x_1 \quad , \text{ where } \begin{array}{l} x_1 \leq \phi_{LIM} \\ \dot{x}_1 \leq \phi_{LIM} \end{array}$$

$$\dot{x}_2 = x_3 - c_2 x_1 - d_1 N_{\phi}$$

$$\begin{aligned}
 \dot{x}_3 = & x_4 - c_3 x_1 - d_2 N_{\phi} - b_1 K_{\psi_e} K_{\psi} (x_6 + N_{\psi}) - b_1 K_{\psi_e} K_{\epsilon_e} \tan^{-1} \left(\frac{x_7}{x_8 + L} \right) \\
 & + b_1 K_{\psi_e} K_{\epsilon_e} u + b_1 K_{\psi_e} K_{\psi} \psi_R
 \end{aligned}$$

$$\begin{aligned}
 \dot{x}_4 = & x_5 - c_4 x_1 - d_3 N_{\phi} - b_2 K_{\psi_e} K_{\psi} (x_6 + N_{\psi}) - b_2 K_{\psi_e} K_{\epsilon_e} \tan^{-1} \left(\frac{x_7}{x_8 + L} \right) \\
 & + b_2 K_{\psi_e} K_{\epsilon_e} u + b_2 K_{\psi_e} K_{\psi} \psi_R
 \end{aligned}$$

$$\begin{aligned}
 \dot{x}_5 = & -c_5 x_1 - d_4 N_{\phi} - b_3 K_{\psi_e} K_{\psi} (x_6 + N_{\psi}) - b_3 K_{\psi_e} K_{\epsilon_e} \tan^{-1} \left(\frac{x_7}{x_8 + L} \right) \\
 & + b_3 K_{\psi_e} K_{\epsilon_e} u + b_3 K_{\psi_e} K_{\psi} \psi_R
 \end{aligned}$$

$$\dot{x}_6 = \frac{32.2}{V} \tan x_1$$

$$\dot{x}_7 = (V \cos \theta_0) \sin(x_6 - \psi_R)$$

$$\dot{x}_8 = (V \cos \theta_0) \cos x_6$$

where $x_1 = \phi$ and x_2, x_3, x_4 , and x_5 are intermediate states in the inner loop and $x_6 = \psi$, $x_7 = Y'$, $x_8 = X'$ and $u = \epsilon_{LOC} + N_R + N_T + N_E$.

The state equations are verified in Section 2.4.

REFERENCES

1. Clement, W. F., H. R. Jex, and P. Graham, "Application of a Systems Analysis Theory for Manual Control Displays to Aircraft Instrument Landing", Fourth Annual NASA-University Conference on Manual Control, (NASA SP-192), March 21-23, 1968.
2. Jackson, A. S., Analog Computation, McGraw-Hill Book Company, Inc., 1960.
3. Etkin, Bernard, Dynamics of Flight, John Wiley and Sons, Inc., 1959.
4. Teper, G. L. and R. L. Stapleford, "An Assessment of the Lateral-Directional Handling Qualities of a Large Aircraft in the Landing Approach", J. Aircraft, Vol. 3, No. 3, May-June, 1966.
5. Paskin, H. M., "A Discrete Stochastic Optimal Control Model of the Human Operator", 1970 Proceedings, National Aerospace Electronics Conference, May 18-20, 1970 (NAECON '70).
6. -, Collins Radio Co., "51RV-2B VOR/ILS Receiver Specifications", Collins Overhaul Manual, pp. 3-8, 1969.
7. -, Collins Radio Co., "51R-7A, -8A VHF NAV/COMM Receivers", General Description, pp. 1-3 - 1-8, 1968.
8. Pitham, Leonard and Frank Parr, "Navigation Equipment Capability Program", Flight Standards Service, December 1968.
9. Winick, A. B. and D. M. Brandewie, "VOR/DME System Improvements", Proceedings of the IEEE, Volume 58, No. 3, March 1970.
10. McFarland, R. H. and F. J. Kike, "Results of VOR Path Stability Investigations", Eascon '68 Record, p. 531.
11. Winick, A. B. and D. M. Brandewie, "VORTAC System Improvements", FAA, Department of Transportation, Eascon '69 Record, pp. 153-160.

12. -, Federal Aviation Agency, Standards Development Division FS-920, "Navigation Equipment Capability Analysis Program", August, 1964.
13. -, FAA, Department of Transportation, "Technical Facilities at NAFEC", National Aviation Facilities Experimental Center, June, 1969.
14. -, Collins Radio Co., "Collins 51RV-1 Navigation Receiver," Equipment Specifications, pp. 6-8B, January 27, 1969.
15. -, Airlines Electronic Engineering Committee, "Supplement No. 1 to ARINC Characteristic No. 547 Airborne VHF Navigation Receiver", Aeronautical Radio, Inc., April 20, 1966.
16. Papoulis, Athamassois, Probability, Random Variables, and Stochastic Processes, McGraw-Hill Book Co., New York, 1965.
17. Schwartz, Mischa, Information Transmission Modulation and Noise, McGraw-Hill Book Co., New York, 1959.
18. Pierce, J. R., Symbols, Signals and Noise, Harper and Row Publishers, New York, 1961.
19. Blakelock, John H., Automatic Control of Aircraft and Missiles, John Wiley and Sons, Inc., New York, 1965.
20. -, Advisory Group for Aerospace Research and Development, "V/STOL Handling, I-Criteria and Discussion", NATO, AGARD-R-577-70, December, 1970.
21. Hall, G. Warren and Edward M. Booth, "An In-Flight Investigation of Lateral-Directional Dynamics for the Landing Approach", Technical Report AEDL-TR-70-145, October, 1970.
22. -, Airman's Information Manual, Part 1, DOT/FAA, November, 1970.
23. -, "STOL Steep Approaches in the DeHavilland DHC-5 Buffalo", DOT/FAA, Memorandum Report FS-640, April, 1970.

SECTION 2.2

FOKKER-PLANCK DEVELOPMENT

The Fokker-Planck equation is a second order differential equation whose solution (in the Lateral Separation Study) is the joint probability density function of the "state variables" represented in the system model. A fundamental characteristic of this equation is that the dynamics of the system model dictate the manner in which the density function evolves (or propagates) as a function of time (or range).

The primary marginal density function of interest in this study is that of the lateral deviation state since the objective of this study is to provide the procedure and data necessary to minimize lateral spacings between parallel runways. The Fokker-Planck equation was used to generate the lateral deviation density function required to solve the problem defined in Section 1.1. The application of this equation to obtain a probability density function requires two things:

- (1) the state equations of the system model and
- (2) an initial distribution for each state of the system.

The state equations are provided in Section 2.1.5 and simplified in Section 2.2.1.2. The model parameter values and initial state distributions are provided in Appendix G for each approach system considered. Application of the technique developed in this section to generate each of the required probability density functions is discussed in Section 2.5.

The development of the Fokker-Planck analysis technique is contained in this section. The development approach (Section 2.2.1) and verification (Section 2.2.2) of the Fokker-Planck technique are illustrated by utilizing the nominal system model developed in Section 2.1.

The fundamental assumption necessary in applying the Fokker-Planck equation to the system model is that the state variables are represented by a Markov process. This assumption implies that the associated probability transition density is always a solution to the Fokker-Planck equation under mild regularity conditions (Reference 1). A more elaborate discussion of this assumption is contained in Section 2.2.1.1.

Since the system model represents an integral part of the Fokker-Planck analysis, an approach system model which accurately represents lateral motion about the extended runway centerline was required. The model given in Section 2.1.2 (Figure 2.1.2-6) represents the original model developed for this purpose. In order to apply the Fokker-Planck equation,

the system model was simplified such that it accurately represented the original model. The method of simplifying the system model is discussed in Section 2.2.1.2.

Section 2.2.1.3 contains a description of the Fokker-Planck implementation process. Included in this description is a general discussion of the Fokker-Planck equation and how the system model state equations are implemented, a discussion of the application of the Fokker-Planck equation to a linear system, and a description of the computer solution to the Fokker-Planck equation.

The verification of the Fokker-Planck method is contained in Section 2.2.2. Two methods of verifying the Fokker-Planck method are discussed. Utilizing the fact that gaussian distributed inputs into linear systems produce gaussian distributed outputs, the Fokker-Planck method was verified as follows:

- (1) showing that for a linear system with gaussian inputs, the Fokker-Planck solution produced gaussian outputs (Section 2.2.2.1) and
- (2) comparing the lateral deviation variance response for a linear gaussian system predicted by the Fokker-Planck equation to the response predicted by the classical linear gaussian method of variance propagation (Section 2.2.2.2).

2.2.1 DEVELOPMENT APPROACH

2.2.1.1 Markov Representation of the State Vector

The application of the Fokker-Planck approach toward solving the probability transition density describing the distribution of aircraft errors requires (1) that the aircraft system model be expressed in state equation form, and (2) that the state vector which evolves as a function of time be a Markov process. The concept of a probability transition density replaces the usual conditional probability density in that the present value of the stochastic process in question is conditioned only on the last value of the process and not on a time history of the process. The preceding statement characterizes the Markov concept for a random process.

Requirement (1) above has been satisfied for both the linear and nonlinear system models (Section 2.1.5). Requirement (2) can be interpreted as follows. If \underline{x} represents an n -dimensional system state vector, then the joint probability transition density of this process is given by

$$\begin{aligned}
 & p[x_1(t), x_2(t), \dots, x_n(t) \mid x_1(\tau_1), x_2(\tau_1), \dots, x_n(\tau_1)] \\
 &= p[x_1(t), x_2(t), \dots, x_n(t) \mid \begin{array}{l} x_1(\tau_1), x_1(\tau_1), \dots, x_1(\tau_1); \\ x_2(\tau_2), x_2(\tau_2), \dots, x_2(\tau_2); \\ \vdots \\ x_n(\tau_n), x_n(\tau_n), \dots, x_n(\tau_n) \end{array}]
 \end{aligned}
 \tag{2.2.1-1}$$

where $x_1(\bullet), x_2(\bullet), \dots, x_n(\bullet)$ represent the n states describing the system and the times t and τ_i are such that $t > \tau_1 > \tau_2 \dots > \tau_n$. In words, Equation 2.2.1-1 states that the present values which the state vector or stochastic process \underline{x} assumes at time t is only dependent on the values assumed at some earlier time τ_1 where τ_1 can be arbitrarily chosen. The Markov assumption is used extensively in physical systems covering a broad class of practical problems. A detailed discussion of Markovian processes and applications can be found in References 1, 3, 4, 6, 7, and 8. Although it is clear that the position of the aircraft at time t can be approximately determined from the values assumed at $t = t - \Delta t$, the exact position can only be statistically determined. The Markov assumption implies that the present position error is dependent only on the errors in the state variables at time $t = t - \Delta t$; i.e., an aircraft's true position at some time t is only dependent on the values assumed by the state variables in the infinitesimal past, at $t - \Delta t$, and not on a history of the aircraft's past flight path. This assumption is clearly valid for an aircraft's motion when subjected to random perturbations, thus satisfying requirement (2) above. It should be noted that the pilot/control delay in the system model given in Figure 2.1.2-6 was replaced with a simulated delay as shown in Figure 2.1.2-7 in order to preserve the Markov assumption.

2.2.1.2 Reduction of the System Model

The nonlinear version of the system model developed in Section 2.1.2 (Figure 2.1.2-6) represents the most accurate model developed in the Lateral Separation Study for an instrument landing approach system. Theoretically, the Fokker-Planck equation can be applied to a system of any finite order. However, limitations on computer memory and available computer time

necessary for solving the Fokker-Planck equation require a lower order system model. Therefore, in order to apply the Fokker-Planck equation, it was necessary to simplify this system model.

As discussed in Section 2.1., the first step in simplifying the system model in Figure 2.1.2 was to replace the pilot/control delay with a simulated delay resulting in the model shown in Figure 2.1.2-7. The state equations derived from this model resulted in an eighth order set of nonlinear state equations, as shown in Section 2.1.5. The nonlinearities, due to transcendental functions of various angles, were then removed by assuming that the value of the small angles approximated these functions. The remaining nonlinearities in the system model, which included a turn rate limit (and, therefore, bank angle limit) of 3 degrees/second and a banking rate limit of 10 degrees/second, were removed. This resulted in the seventh order linear model shown in Figure 2.1.2-8. The simplified models were shown to accurately approximate the original nonlinear system model in Section 2.1.2. Further validation of the model simplification is contained below.

A Monte Carlo simulation was run to compare the lateral distribution standard deviation response of the linear model to the nonlinear model. As shown in Figure 2.2.1-1, the differences between the two models were minimal. Since the lateral distribution standard deviation time response of the "linearized" system model was almost identical to that of the nonlinear model, it was decided that the seventh order linear model represented a sufficiently accurate model for use in the Fokker-Planck analysis.

The implementation of the Fokker-Planck equation to include the linear seventh order system state equations presents two fundamental problem areas.

- (1) the computer solution described in Section 2.2.1.3 for solving the seventh order system requires much more time and computer memory than is feasible; and
- (2) the accuracy obtained in the solution may be questionable due to round-off and truncation errors arising from the tremendous number of computations required.

In order to alleviate the preceding problems, it was necessary to reduce the order of the seventh order linear model.

The model reduction task occurred in two stages. The seventh order linear model was first reduced to a sixth order linear model by eliminating the $(a_{p_5} s + 1)$ term in the pilot control

simulated delay model given in Section 2.1.2. This term has practically no effect on the system for the range of values considered. From Sections 2.1.2 and 2.1.3

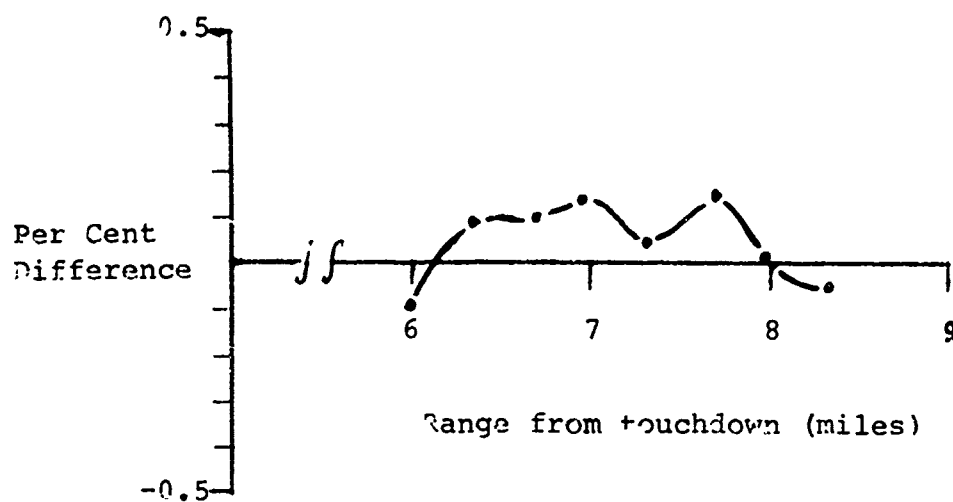


Figure 2.2.1-1

Lateral Distribution Standard Deviation Per Cent Difference
Between Linear and Nonlinear Models

$$\tau_p = .7 \text{ seconds, and}$$

$$a_{p_5} = \frac{\tau_p}{100} = .007 \text{ seconds.}$$

A pole which has a time constant of 0.007 seconds has little effect on this system since the system's dominant time constant is much larger (Section 2.4.1); therefore, this term was omitted, resulting in a sixth order linear model.

The second stage of the model reduction task is concerned with reducing the sixth order linear model such that the two fundamental problem areas mentioned previously are solved. A literature search regarding this problem resulted in the method proposed by E. J. Davison (Reference 2) for reducing the number of states in a linear system such that the reduced linear model retains the dominant characteristics (eigenvalues) of the original model.

Davison's method was developed to reduce the order of the system model such that the Fokker-Planck implementation would be feasible on a digital computer. The only restraint imposed in reducing the order of the linear model was that the lateral deviation time response obtained from the reduced and original models remain in close agreement. A detailed discussion of the state reduction technique is given in Appendix B. Application of Davison's method results in a reduced model which accurately approximates the lateral deviation time response given by the sixth order linear model.

The original sixth order linear model to be reduced by Davison's method has the following form:

$$\dot{\underline{x}} = A \underline{x} + B \underline{v} \quad (2.2.1-2)$$

where

$\dot{\underline{x}}$ denotes a 6x1 column vector representing the six "states" describing the system;

A is a 6x6 matrix of constants;

B is a 6xN matrix of constants;

and

\underline{v} is a Nx1 column vector representing the N inputs to the system model.

Davison's method reduces the system model defined by Equation

2.2.1-2 to a system model of the form

$$\dot{\underline{x}}^* = A^* \underline{x}^* + B^* \underline{v} \quad (2.2.1-3)$$

where

\underline{x}^* is an $L \times 1$ column vector ($L < 6$) resulting from eliminating a predetermined number of states from the sixth order system in Equation 2.2.1-2;

A^* is an $L \times L$ matrix which has the same L dominant eigenvalues as the A matrix;

and

B^* is an $L \times N$ matrix which is determined such that the effect of the dominant modes in the reduced system given by Equation 2.2.1-3 is the same as the effect produced by the dominant modes in the system given by Equation 2.2.1-2.

Appendix B contains a more complete mathematical description of Davison's method.

To illustrate the reduction technique, the non-linear nominal system model from Figure 2.1.2-6, with the parameter values from Table 2.1.2-2 (except for $K_{\epsilon_e} = 114.7$

at a range of 9 NMi), was first reduced to a linear sixth order system and later reduced to a linear second order system. The time responses of these three systems were then compared. The value of $K_{\epsilon_e} = 114.7$ was chosen so that the

time responses would be oscillatory and, therefore, magnify the deviations between the nonlinear system response and the reduced linear systems' responses.

The sixth order linear model representing the approach model to be reduced is of the form

$$\dot{\underline{x}} = A \underline{x} + B \underline{v}$$

where

$$A = \begin{bmatrix} 0 & 236.4444 & 0 & 0 & 0 & 0 \\ 0 & 0 & .13627 & 0 & 0 & 0 \\ 0 & 0 & -10.9913 & 0 & 0 & 1 \\ -.04498 & -47.4753 & -49.9740 & 0 & 0 & 0 \\ +.01558 & 16.4502 & -40.9870 & 1 & 0 & 0 \\ -.0018 & -1.9 & -24.1010 & 0 & 1 & 0 \end{bmatrix}$$

$$B = \begin{bmatrix} -236.4444 & 0 & 0 & 0 \\ 0 & 0 & 0 & 0 \\ 0 & 0 & -1.333 & 0 \\ 47.4753 & -47.4753 & -49.974 & .04498 \\ -16.4502 & 16.4502 & -16.000 & -.01558 \\ 1.9 & -1.9 & 9.544 & .0018 \end{bmatrix}$$

$$\underline{x} = \begin{bmatrix} x_1 \\ x_2 \\ x_3 \\ x_4 \\ x_5 \\ x_6 \end{bmatrix} = \begin{bmatrix} \text{Lateral Deviation} \\ \text{Heading Angle} \\ \text{Bank Angle} \\ \text{PP1} \\ \text{PP2} \\ \text{PP3} \end{bmatrix}$$

and

$$\underline{v} = \begin{bmatrix} 0 \\ 0 \\ 0 \\ 1 \end{bmatrix}$$

where \underline{v} represents a unit step input to the system. PP1, PP2, and PP3 refer to intermediate states. Note that the system states must be arranged in order of decreasing dominance.

Using Davison's technique, a reduction was accomplished retaining the first two states in the sixth order model (lateral deviation and heading angle). The resulting reduced second order linear model is of the form

$$\dot{\underline{x}}^* = A^* \underline{x}^* + B^* \underline{v}$$

where

$$A^* = \begin{bmatrix} 0 & 236.4 \\ -.0001431 & -.1090 \end{bmatrix}$$

$$B^* = \begin{bmatrix} -69.80 & 46.66 & 21.02 & -.04417 \\ .1649 & -.1693 & -.1700 & .00016 \end{bmatrix}$$

$$\underline{x}^* = \begin{bmatrix} x_1 \\ x_2 \end{bmatrix} = \begin{bmatrix} \text{Lateral Deviation} \\ \text{Heading Angle} \end{bmatrix}$$

and

$$\underline{v} = \begin{bmatrix} 0 \\ 0 \\ 0 \\ 1 \end{bmatrix}$$

Table 2.2.1-1 and Figure 2.2.1-2 show the comparison of the lateral deviation time response for the original nonlinear model and the reduced sixth and second order linear models. As indicated in Figure 2.2.1-2, the second and sixth order responses were essentially equivalent to the nonlinear model time response since the points of maximum deviation of the second and sixth order systems from the nonlinear system response were only .024 feet and .0031 feet, respectively.

Based upon the preceding results, it is assumed in the subsequent Fokker-Planck analysis that a sufficiently accurate system model is given by a second order linear system.

$$\begin{bmatrix} \dot{x}_1 \\ \dot{x}_2 \end{bmatrix} = \begin{bmatrix} a_{11} & a_{12} \\ a_{21} & a_{22} \end{bmatrix} \begin{bmatrix} x_1 \\ x_2 \end{bmatrix} + \begin{bmatrix} b_{11} & b_{12} & b_{13} & b_{14} \\ b_{21} & b_{22} & b_{23} & b_{24} \end{bmatrix} \begin{bmatrix} v_1 \\ v_2 \\ v_3 \\ v_4 \end{bmatrix} \quad (2.2.1-4)$$

where x_1 and x_2 represent lateral deviation and heading angle, respectively, the a_{ij} and b_{ij} terms are constants, and the v_i 's represent inputs. This assumption is further justified in the system model root locus analysis discussed in Section 2.4.2.

2.2.1.3 Fokker-Planck Implementation

As stated in the preceding section, the second order system model given in Equation 2.2.1-4 is the basic model to which the Fokker-Planck equation will be applied. This section discusses the general form of the Fokker-Planck equations for an n^{th} order system model and develops an equation to be implemented for the second order system model.

Table 2.2.1-1

Lateral Deviation Time Responses for the Original Nonlinear
and Simplified Linear Models

Time, sec	Nonlinear System, feet	Sixth Order System, feet	Second Order System, feet
0.0	0.0	0.0	0.0
6.0	0.2994	0.3025	0.2817
15.0	1.258	1.258	1.237
19.2	1.381	1.379	1.358
25.2	1.208	1.205	1.184
31.2	0.9507	0.9491	0.9277
37.2	0.8555	0.8571	0.8358
45.0	0.9535	0.9564	0.9350
55.2	1.055	1.054	1.032
60.0	1.038	1.035	1.014

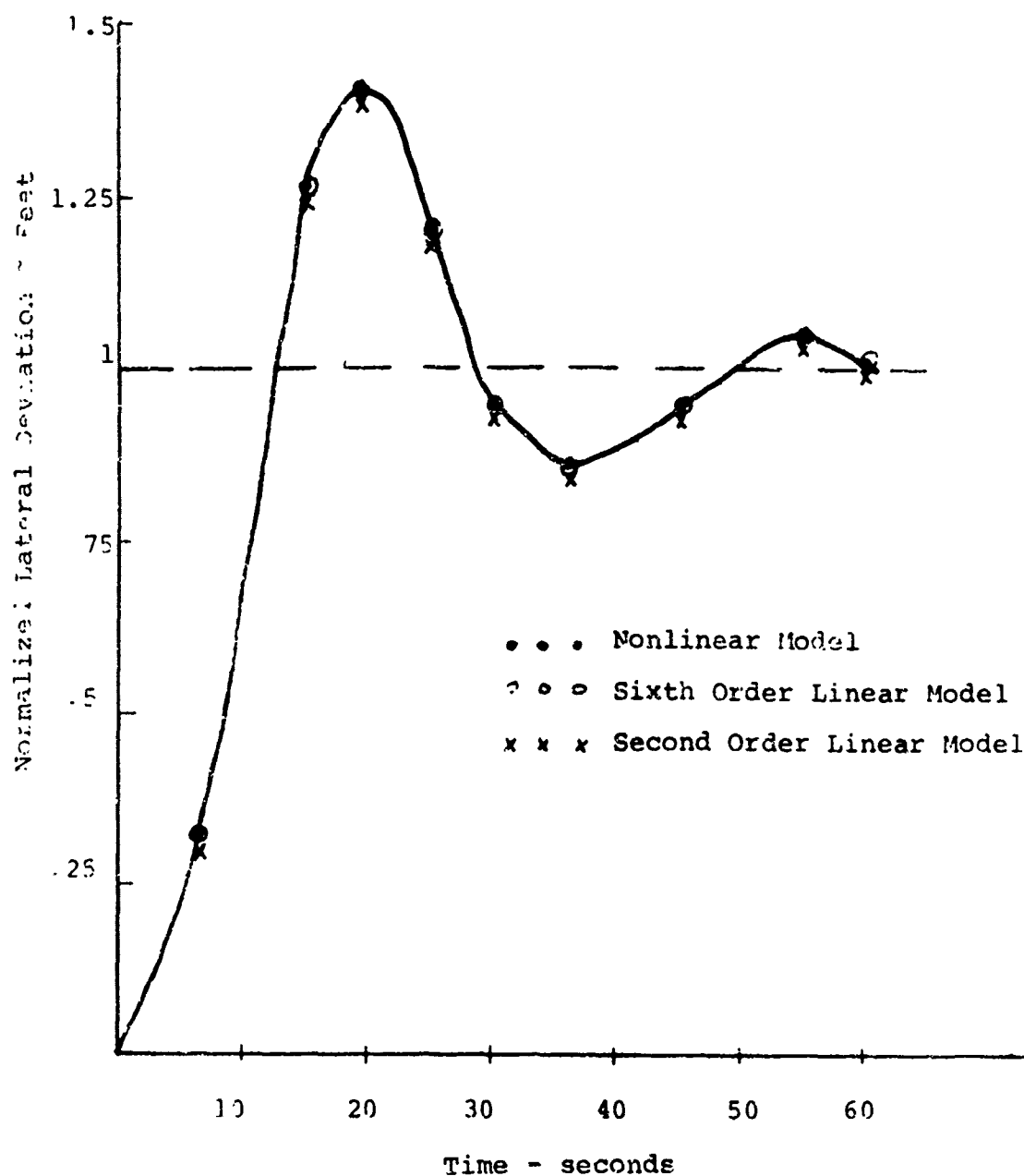


Figure 2.2.1-2

Comparison of Lateral Deviation Time Response for
2nd, 6th, and Nonlinear Systems

The implementation of this equation for the second order model is then given at the end of this section.

Fokker-Planck Equation

The Fokker-Planck equation can be thought of as a method for describing how the shape of the density function associated with the random errors in the system model changes as a function of time. R. L. Stratonovich (Reference 8) has referred to the Fokker-Planck equation as the "conservation of probability" in the sense that regardless of the time at which the equation is solved or the manner in which the shape of the density function is altered, the area under the curve which is obtained as a solution is always equal to unity.

In order to determine the propagation of a state variable's probability density function, the Fokker-Planck equation can be applied to the following state variable equation:

$$\dot{\underline{x}} = \underline{f}[\underline{x}(t), t] + \underline{G}[\underline{x}(t), t] \underline{u}(t)$$

where

$\underline{x}(t)$ is a $N \times 1$ random state vector;

$\underline{f}[\underline{x}(t), t]$ is a $N \times 1$ vector which is a linear or nonlinear function of $\underline{x}(t)$ and t ;

$\underline{G}[\underline{x}(t), t]$ is a $N \times R$ matrix which is a linear or nonlinear function of $\underline{x}(t)$ and t ;

and

$\underline{u}(t)$ is a zero-mean gaussian white-noise-input $P \times 1$ vector with $\text{Cov}\{\underline{u}(t), \underline{u}(\tau)\} = \underline{\Psi}_u(t) \delta_D(t - \tau)$

(Thus the covariance matrix $\underline{\Psi}_u(t)$ is a $R \times R$ matrix.)

The following Fokker-Planck equation has been derived, as shown by Sage and Melsa (Reference 5), for the preceding vector state variable equation:

$$\begin{aligned} \frac{\partial p[\underline{x}(t) | \underline{x}(t_0)]}{\partial t} = & -\text{tr} \left(\frac{\partial}{\partial \underline{x}(t)} \{ \underline{f}[\underline{x}(t), t] p[\underline{x}(t) | \underline{x}(t_0)] \} \right) \\ & + 0.5 \text{tr} \left(\frac{\partial}{\partial \underline{x}(t)} \left[\frac{\partial}{\partial \underline{x}(t)} \right]^T \left\{ \underline{G}[\underline{x}(t), t] \underline{\Psi}_u(t) \underline{G}^T[\underline{x}(t), t] p[\underline{x}(t) | \underline{x}(t_0)] \right\} \right) \end{aligned} \quad (2.2.1-5)$$

where

$p[\underline{x}(t) | \underline{x}(t_0)]$ is the conditional joint probability density of the state vector $\underline{x}(t)$ given the initial state vector $\underline{x}(t_0)$

and

tr is the trace (sum of the diagonal elements) of a matrix.

This equation is solved with the initial condition

$$p(\underline{x}(t_0) | \underline{x}(t_0)) = \delta_D(x_1(t_0) - x_{1_0}) \delta_D(x_2(t_0) - x_{2_0})$$

since the initial state vector is the given conditioning variable and since the elements of the state vector, x_1 , x_2 , etc., can be considered to be independent at the initial time t_0 . Although Equation 2.2.1-5 is of the form usually found in the literature, it can be altered to provide a more direct solution for the lateral deviation density function. For a second order system, the above equation would result in a solution of the form $p(x_1(t), x_2(t) | x_1(t_0), x_2(t_0))$. If the density function $p(x_1(t))$, which could for example be the lateral deviation density function, is the required quantity, then the above solution must be integrated as follows to yield $p(x_1(t))$:

$$\begin{aligned} p(x_1(t), x_2(t), x_1(t_0), x_2(t_0)) &= p(x_1(t), x_2(t) | x_1(t_0), x_2(t_0)) \\ &\quad \cdot p(x_1(t_0), x_2(t_0)) \\ p(x_1(t)) &= \int_{-\infty}^{\infty} \int_{-\infty}^{\infty} \int_{-\infty}^{\infty} p(x_1(t), x_2(t), x_1(t_0), x_2(t_0)) dx_{2t} dx_{1t_0} dx_{2t_0} \\ &= \int_{-\infty}^{\infty} \int_{-\infty}^{\infty} \int_{-\infty}^{\infty} p(x_1(t), x_2(t) | x_1(t_0), x_2(t_0)) p(x_1(t_0), x_2(t_0)) \\ &\quad \cdot dx_{2t} dx_{1t_0} dx_{2t_0} \end{aligned}$$

where

$p(x_1(t_0), x_2(t_0)) = p(x_1(t_0)) p(x_2(t_0))$ since the 2 states are assumed to be independent initially.

Much of the effort in obtaining $p(\underline{x}_1(t))$ can be eliminated by obtaining a slightly altered Fokker-Planck equation. By multiplying the above Fokker-Planck equation by $p(\underline{x}(t_0))$, the following equation is obtained (due to the fact that $p(\underline{x}(t_0))$ is independent of t and $\underline{x}(t)$):

$$\begin{aligned} & \frac{\partial p(\underline{x}(t) | \underline{x}(t_0)) p(\underline{x}(t_0))}{\partial t} \\ &= -\text{tr} \left(\frac{\partial}{\partial \underline{x}(t)} \{ \underline{f}[\underline{x}(t), t] p(\underline{x}(t) | \underline{x}(t_0)) p(\underline{x}(t_0)) \} \right) \\ &+ 0.5 \text{tr} \left(\frac{\partial}{\partial \underline{x}(t)} \left[\frac{\partial}{\partial \underline{x}(t)} \right]^T \{ G[\underline{x}(t), t] \Psi_u(t) G^T[\underline{x}(t), t] \right. \right. \\ & \left. \left. p(\underline{x}(t) | \underline{x}(t_0)) p(\underline{x}(t_0)) \right\} \right) \end{aligned}$$

By substituting the joint density $p(\underline{x}(t), \underline{x}(t_0))$ for $p(\underline{x}(t) | \underline{x}(t_0)) p(\underline{x}(t_0))$ and by integrating the equation over $\underline{x}(t_0)$, the following Fokker-Planck equation, which will be the equation used in the remainder of the Fokker-Planck analysis is obtained:

$$\begin{aligned} \frac{\partial p(\underline{x}(t))}{\partial t} &= -\text{tr} \left(\frac{\partial}{\partial \underline{x}(t)} \{ \underline{f}[\underline{x}(t), t] p(\underline{x}(t)) \} \right) \\ &+ 0.5 \text{tr} \left(\frac{\partial}{\partial \underline{x}(t)} \left[\frac{\partial}{\partial \underline{x}(t)} \right]^T G[\underline{x}(t), t] \Psi_u(t) G^T[\underline{x}(t), t] p(\underline{x}(t)) \right) \end{aligned}$$

This equation is solved with an initial condition of $p(\underline{x}(t))|_{t=t_0} = p(\underline{x}(t_0))$. Assuming the states are independent at time t_0 , the joint density $p(\underline{x}(t_0))$ is equal to the product of the marginal density functions, $p(x_1(t_0)) p(x_2(t_0)) \dots p(x_n(t_0))$. A second order example solution for this equation, $p(x_1(t), x_2(t))$, can be integrated directly to obtain the desired lateral deviation probability density function, $p(x_1(t))$, as follows:

$$p(x_1(t)) = \int_{-\infty}^{\infty} p(x_1(t), x_2(t)) dx_2$$

The preceding method is illustrated in Figure 2.2.1-3.

The derivation of the Fokker-Planck equation assumes that the error inputs to the system are white gaussian noise. This assumption is discussed in Section 2.1.4.

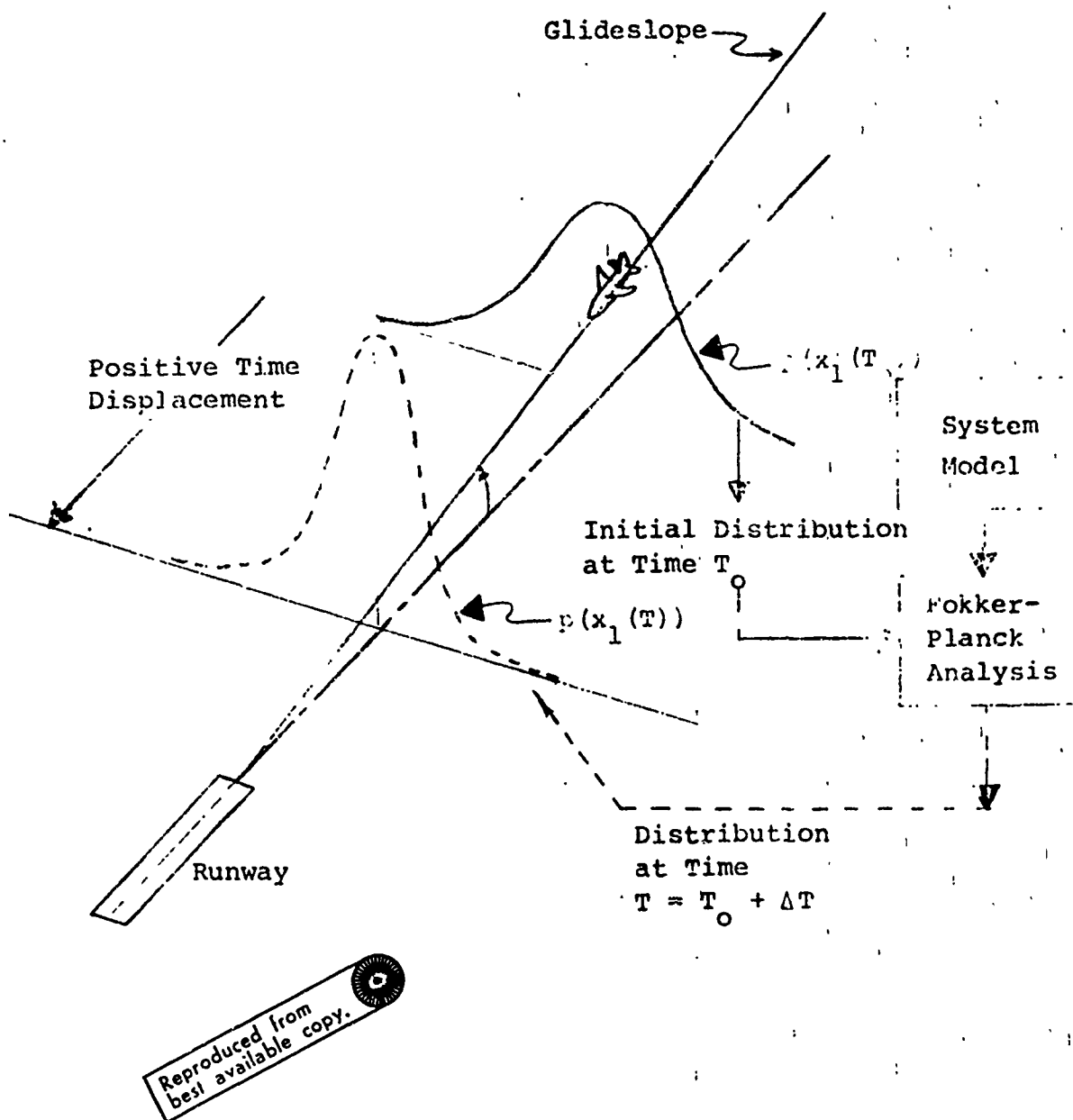


Figure 2.2.1-3

FIGURE 2.2.1-3. Method of Propagating a Distribution

Application of the Fokker-Planck Equation to a Linear System

As described in Section 2.2.1.2, the seventh order linear system was reduced to a second order system (Equation 2.2.1-4) which accurately approximates the original system.

This reduced model is given by

$$\dot{\underline{x}} = \underline{A}\underline{x} + \underline{B}\underline{u} \quad (2.2.1-7)$$

which can be expressed in matrix notation as

$$\begin{bmatrix} \dot{x}_1 \\ \dot{x}_2 \end{bmatrix} = \begin{bmatrix} a_{11} & a_{12} \\ a_{21} & a_{22} \end{bmatrix} \begin{bmatrix} x_1 \\ x_2 \end{bmatrix} + \begin{bmatrix} b_{11} & b_{12} & b_{13} & b_{14} \\ b_{21} & b_{22} & b_{23} & b_{24} \end{bmatrix} \begin{bmatrix} u_1 \\ u_2 \\ u_3 \\ u_4 \end{bmatrix}$$

where

$$\begin{bmatrix} x_1 \\ x_2 \end{bmatrix} = \begin{bmatrix} \text{lateral deviation} \\ \text{heading angle} \end{bmatrix}$$

a_{ij} 's and b_{ij} 's are constants, and the u_i 's represent the noise inputs to the system model. The general Fokker-Planck equation (Equation 2.2.1-6) which was applied to this second order linear system is given by:

$$\frac{\partial p}{\partial t} = -\text{tr} \left(\frac{\partial}{\partial \underline{x}} (\underline{A} \underline{x} p) \right) + 0.5 \text{tr} \left(\frac{\partial}{\partial \underline{x}} \left(\frac{\partial}{\partial \underline{x}} \right)^T (\underline{B} \Psi_u \underline{B}^T p) \right) \quad (2.2.1-8)$$

where

$p = p(x_1, x_2)$ is the joint probability density of x_1 and x_2 ,

\underline{A} and \underline{B} are the matrices defined in Equation 2.2.1-4, tr represents the sum of the diagonal elements of a square matrix, Ψ_u is the covariance of the system model noise inputs and is defined as

$$\Psi_u = \begin{bmatrix} \sigma_{u_1}^2 & 0 & 0 & 0 \\ 0 & \sigma_{u_2}^2 & 0 & 0 \\ 0 & 0 & \sigma_{u_3}^2 & 0 \\ 0 & 0 & 0 & \sigma_{u_4}^2 \end{bmatrix}$$

and

$\frac{\partial}{\partial \underline{x}}$ is a linear operator defined as

$$\frac{\partial}{\partial \underline{x}} \equiv \begin{bmatrix} \frac{\partial}{\partial x_1} \\ \frac{\partial}{\partial x_2} \end{bmatrix}$$

The remainder of this subsection develops the right-hand side of Equation 2.2.1-8 to the form to be implemented for solution on a digital computer. This computer solution is then described in the following subsection.

In order to develop the right-hand side of Equation 2.2.1-8, first consider the first term on the right-hand side of the equation.

Since

$$\underline{A} \underline{x} p = \begin{bmatrix} a_{11} & a_{12} \\ a_{21} & a_{22} \end{bmatrix} \cdot \begin{bmatrix} x_1 \\ x_2 \end{bmatrix} \cdot p = \begin{bmatrix} (a_{11}x_1 + a_{12}x_2)p \\ (a_{21}x_1 + a_{22}x_2)p \end{bmatrix},$$

it follows that

$$\frac{\partial (\underline{A} \underline{x} p)}{\partial \underline{x}} = \begin{bmatrix} a_{11}p + \frac{\partial p}{\partial x_1}(a_{11}x_1 + a_{12}x_2) & \sim \\ \sim & a_{22}p + \frac{\partial p}{\partial x_2}(a_{21}x_1 + a_{22}x_2) \end{bmatrix}.$$

Therefore, the first term on the right side of Equation 2.2.1-8 is obtained by summing the diagonal elements of the preceding matrix:

$$\begin{aligned} -\text{tr} \left(\frac{\partial (\underline{A} \underline{x} p)}{\partial \underline{x}} \right) &= - \left[a_{11}p + \frac{\partial p}{\partial x_1}(a_{11}x_1 + a_{12}x_2) \right. \\ &\quad \left. + a_{22}p + \frac{\partial p}{\partial x_2}(a_{21}x_1 + a_{22}x_2) \right]. \end{aligned} \quad (2.2.1-9)$$

The second term on the right-hand side of Equation 2.2.1-8 is developed as follows. Let the matrix product $B \Psi_u B^T$ be denoted as

$$B \Psi_u B^T = \begin{bmatrix} m_{11} & m_{12} \\ m_{21} & m_{22} \end{bmatrix}.$$

The linear operator $\frac{\partial}{\partial \underline{x}} \left[\frac{\partial}{\partial \underline{x}} \right]^T$ is defined by

$$\frac{\partial}{\partial \underline{x}} \left[\frac{\partial p}{\partial \underline{x}} \right]^T = \begin{bmatrix} \frac{\partial^2 p}{\partial x_1^2} & \frac{\partial^2 p}{\partial x_1 \partial x_2} \\ \frac{\partial^2 p}{\partial x_2 \partial x_1} & \frac{\partial^2 p}{\partial x_2^2} \end{bmatrix}.$$

Therefore

$$\begin{aligned} B \Psi_u B^T \frac{\partial}{\partial \underline{x}} \left[\frac{\partial p}{\partial \underline{x}} \right]^T &= \begin{bmatrix} m_{11} & m_{12} \\ m_{21} & m_{22} \end{bmatrix} \begin{bmatrix} \frac{\partial^2 p}{\partial x_1^2} & \frac{\partial^2 p}{\partial x_1 \partial x_2} \\ \frac{\partial^2 p}{\partial x_2 \partial x_1} & \frac{\partial^2 p}{\partial x_2^2} \end{bmatrix} \\ &= \begin{bmatrix} m_{11} \frac{\partial^2 p}{\partial x_1^2} + m_{12} \frac{\partial^2 p}{\partial x_2 \partial x_1} & \sim \\ \sim & m_{21} \frac{\partial^2 p}{\partial x_1 \partial x_2} + m_{22} \frac{\partial^2 p}{\partial x_2^2} \end{bmatrix}. \end{aligned}$$

It follows that the second term is obtained by summing the diagonal elements of the preceding matrix and multiplying by 0.5; i.e.,

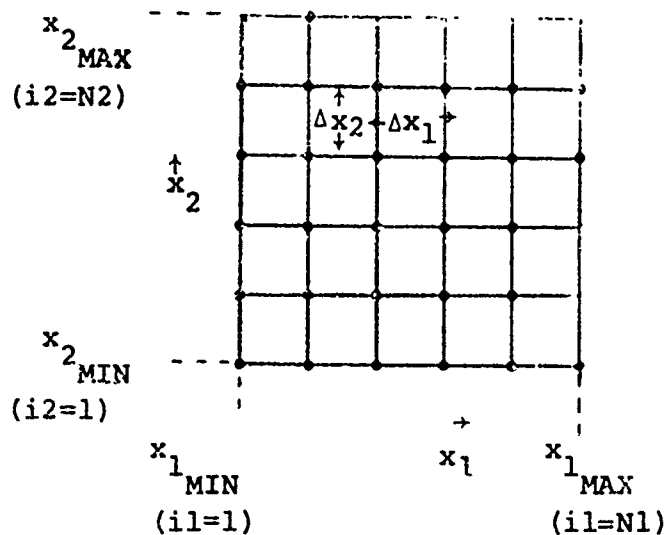
$$0.5 \text{tr} \left[B \Psi_u B^T \frac{\partial}{\partial \underline{x}} \left(\frac{\partial p}{\partial \underline{x}} \right)^T \right] = 0.5 m_{11} \frac{\partial^2 p}{\partial x_1^2} + (m_{12} + m_{21}) \frac{\partial^2 p}{\partial x_1 \partial x_2} + m_{22} \frac{\partial^2 p}{\partial x_2^2} \quad (2.2.1-10)$$

Adding Equations 2.2.1-9 and 2.2.1-10, the desired result is obtained:

$$\begin{aligned} \frac{\partial p}{\partial t} = & -a_{11}p - \frac{\partial p}{\partial x_1} (a_{11}x_1 + a_{12}x_2) - a_{22}p - \frac{\partial p}{\partial x_2} (a_{21}x_1 + a_{22}x_2) \\ & + \frac{m_{11}}{2} \frac{\partial^2 p}{\partial x_1^2} + \frac{m_{12} + m_{21}}{2} \frac{\partial^2 p}{\partial x_1 \partial x_2} + \frac{m_{22}}{2} \frac{\partial^2 p}{\partial x_2^2} \end{aligned} \quad (2.2.1-11)$$

Computer Solution for the Fokker-Planck Equation

The explicit form of the finite-difference technique is used in a computer program to solve the previously described Fokker-Planck equation (Equation 2.2.1-11). In using this method to solve a partial differential equation, a network of grid points is first established throughout the region of interest occupied by the independent variables. The exact solution to the partial-differential equation is approximated at each grid point by the method of finite differences (Appendix C). For the Fokker-Planck implementation of the second order system given in Equation 2.2.1-4, the network of grid points has been set up as follows where x_1 and x_2 represent lateral deviation and heading angle, respectively.



Time is the third independent variable and is perpendicular to the grid shown; i.e., this grid is repeated every Δt sec.

In the above figure, Δx_1 and Δx_2 are obtained as follows:

$$\Delta x_1 = \frac{x_{1\text{MAX}} - x_{1\text{MIN}}}{(N1-1)}$$

$$\Delta x_2 = \frac{x_{2\text{MAX}} - x_{2\text{MIN}}}{(N2-1)}$$

where the dimension of the solution grid is $N1 \times N2$. If the approximate joint density solution at a grid point is denoted as $p_{i1,i2,n}$, where

$$i1 = \frac{x_1 - x_{1\text{MIN}}}{\Delta x_1} + 1,$$

$$i2 = \frac{x_2 - x_{2\text{MIN}}}{\Delta x_2} + 1,$$

and

n = present time = t ,

then the partial derivatives in Equation 2.2.1-11 at a particular grid point can be approximated as follows:

$$\frac{\partial p(x_1(t), x_2(t))}{\partial x_1} \approx \frac{p_{i1+1,i2,n} - p_{i1-1,i2,n}}{2\Delta x_1}$$

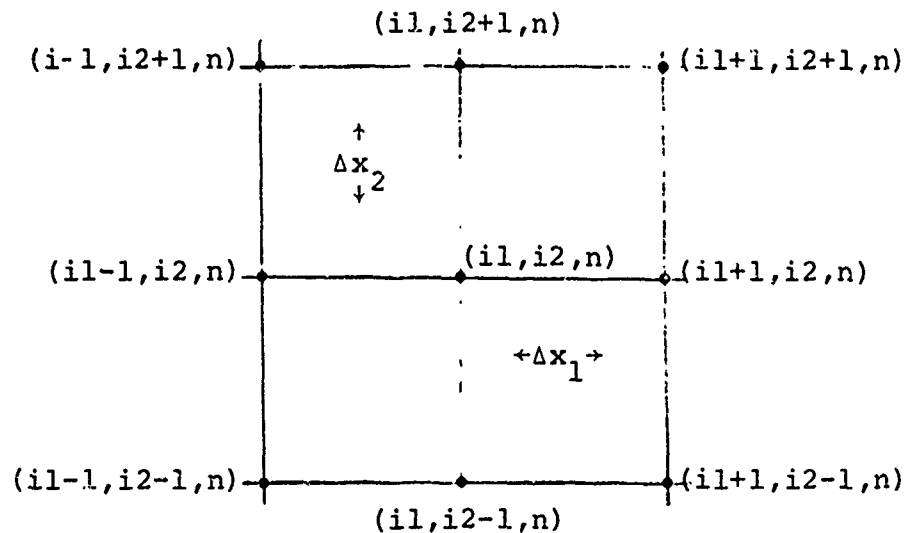
$$\frac{\partial p(x_1(t), x_2(t))}{\partial x_2} \approx \frac{p_{i1,i2+1,n} - p_{i1,i2-1,n}}{2\Delta x_2}$$

$$\frac{\partial^2 p(x_1(t), x_2(t))}{\partial x_1^2} \approx \frac{p_{i1-1,i2,n} - 2p_{i1,i2,n} + p_{i1+1,i2,n}}{(\Delta x_1)^2}$$

$$\frac{\partial^2 p(x_1(t), x_2(t))}{\partial x_2^2} \approx \frac{p_{i1,i2-1,n} - 2p_{i1,i2,n} + p_{i1,i2+1,n}}{(\Delta x_2)^2}$$

$$\frac{\partial^2 p(x_1(t), x_2(t))}{\partial x_1 \partial x_2} \approx \frac{P_{i1+1, i2+1, n} - P_{i1-1, i2+1, n} - P_{i1+1, i2-1, n} + P_{i1-1, i2-1, n}}{4\Delta x_1 \Delta x_2}$$

Thus the partial derivatives at the grid point $(i1, i2, n)$ involve the surrounding grid points as shown:



Letting $n+1$ represent $(t + \Delta t)$, the partial of the joint density with respect to time (i.e., the left-hand side of Equation 2.2.1-11) is approximated as follows:

$$\frac{\partial p(x_1(t), x_2(t))}{\partial t} \approx \frac{P_{i1, i2, n+1} - P_{i1, i2, n}}{\Delta t}$$

Substituting these equations into the second order Fokker-Planck equation (Equation 2.2.1-11), the following is obtained:

$$\begin{aligned} \frac{P_{i1, i2, n+1} - P_{i1, i2, n}}{\Delta t} = & -a_{11}p - \left(\frac{P_{i1+1, i2, n} - P_{i1-1, i2, n}}{2\Delta x_1} \right) (a_{11}x_1 + a_{12}x_2) \\ & - a_{22}p - \left(\frac{P_{i1, i2+1, n} - P_{i1, i2-1, n}}{2\Delta x_2} \right) (a_{21}x_1 + a_{22}x_2) + \\ & + \frac{m_{11}}{2} \left(\frac{P_{i1-1, i2, n} - 2P_{i1, i2, n} + P_{i1+1, i2, n}}{(\Delta x_1)^2} \right) + \frac{m_{12} + m_{21}}{2} . \end{aligned}$$

$$\begin{aligned}
& \cdot \frac{P_{i1+1,i2+1,n} - P_{i1-1,i2+1,n} - P_{i1+1,i2-1,n} + P_{i1-1,i2-1,n}}{4\Delta x_1 \Delta x_2} \\
& + \frac{m_{22}}{2} \cdot \frac{P_{i1,i2-1,n} - 2P_{i1,i2,n} + P_{i1,i2+1,n}}{(\Delta x_2)^2} \quad (2.2.1-12)
\end{aligned}$$

The equation is then multiplied through by Δt , and $P_{i1,i2,n}$ is added to both sides of the equation, so that an explicit equation for $P_{i1,i2,n+1}$ results.

The following initial conditions are used in the solution of this equation since the states are assumed to be independent initially:

$$p(x_1(t_0), x_2(t_0)) = p(x_1(t_0)) p(x_2(t_0))$$

The initial density function for the lateral deviation state is defined from the measured distribution data (Section 2.3). It should be noted at this point that the Fokker-Planck equation can be initialized using any continuous density function which appears to represent the most accurate lateral error distribution. The initial state distributions are discussed in Section 2.4.3 (nominal model) and Section 2.5 and are provided in Appendix G.

The joint density values for the grid points must be supplied at time t_0 . Grid point values at $t = (t_0 + \Delta t)$ are computed explicitly using Equation 2.2.1-12. The values at $t = (t_0 + \Delta t)$ are then used to compute the grid point values at $t = (t_0 + 2\Delta t)$.

The boundary conditions which have been used for this computer solution are as follows:

$$P_{i1,i2,n} = 0 \quad \text{if } i1=1, i1=N1, i2=1, \text{ or } i2=N2$$

In other words, the joint probability density function is set equal to zero at the outer points of the grid. Depending on the number of grid points and distribution accuracy requirements, these outer points may correspond to 8σ or greater.

The lateral deviation marginal density function can be obtained from the joint density function at each point in time (every Δt). Likewise, the density function for the remaining state, heading angle, can be obtained easily in a similar manner. The lateral deviation density function is obtained as follows:

$$p(x_1(t)) = \int_{-\infty}^{\infty} p(x_1(t), x_2(t)) dx_2$$

The computer program uses trapezoidal integration to obtain $p(x_1(t))$ as follows:

$$p_{i1,n} = \Delta x_2 (0.5 p_{i1,1,n} + p_{i1,2,n} + \dots + p_{i1,N2-1,n} + 0.5 p_{i1,N2,n})$$

Then, $p(x_1(t))$ is obtained at each grid point in the x_1 direction. Specification of the number of grid points is dependent on the distribution curve accuracy requirements.

A complete description of the computer program including flow charts, listings, and operating instructions is included in the User's Manual.

2.2.2 CHECKOUT/VERIFICATION OF FOKKER-PLANCK METHOD

2.2.2.1 Gaussian Density Comparison

In order to verify the computer solution of the Fokker-Planck equation described in Section 2.2.1.3, gaussian processes were used for the input and initial conditions. When gaussian processes are input into a linear system, the output is gaussian. The output of the second order linear system, the lateral deviation, should therefore have a gaussian density function for gaussian inputs if the solution of the Fokker-Planck is correct.

The reduced second order linear system described in Section 2.2.1.2 was used to check out the Fokker-Planck equation. This system is given by

$$\dot{\underline{x}} = \underline{A}\underline{x} + \underline{B}u$$

where

$$\underline{A} = \begin{bmatrix} a_{11} & a_{12} \\ a_{21} & a_{22} \end{bmatrix} = \begin{bmatrix} 0 & 236.4 \\ -.0001431 & -.109 \end{bmatrix}$$

$$\underline{B} = \begin{bmatrix} b_1 \\ b_2 \end{bmatrix} = \begin{bmatrix} -.04417 \\ .00016 \end{bmatrix}$$

and \underline{u} is a scalar noise input such that

$$\text{cov}\{u(t), u(\tau)\} = \psi_{11} = (150)^2$$

The lateral deviation (x_1) and heading angle (x_2) were assumed to have gaussian density functions at time equal zero. The mean and standard deviation were chosen arbitrarily as follows:

$$\sigma_{x_1} = 150. \text{ feet} \quad \sigma_{x_2} = .1 \text{ radians}$$

$$\mu_{x_1} = 0. \text{ feet} \quad \mu_{x_2} = 0. \text{ radians}$$

The computer solution for this check-out example used the following grid parameters:

$$x_{1 \text{ MAX}} = 600. \text{ feet}$$

$$x_{1 \text{ MIN}} = -600. \text{ feet}$$

$$x_{2 \text{ MAX}} = .4 \text{ radians}$$

$$x_{2 \text{ MIN}} = -.4 \text{ radians}$$

$$\Delta t = .1 \text{ second}$$

} refer to
Section 2.2.1.3

Figures 2.2.2-1, 2.2.2-2, 2.2.2-3, and 2.2.2-4 represent the lateral deviation density function obtained from the computer program at 1 second, 10 seconds, 20 seconds, and 30 seconds, respectively. The standard deviation and mean for each of these curves was obtained from the computer program. A gaussian curve with the same standard deviation and mean was also plotted on each graph in order that the lateral deviation density function could be compared to a gaussian curve. The results obtained indicate negligible differences between the theoretical gaussian densities and the Fokker-Planck solution; therefore, the Fokker-Planck solution is considered to be verified.

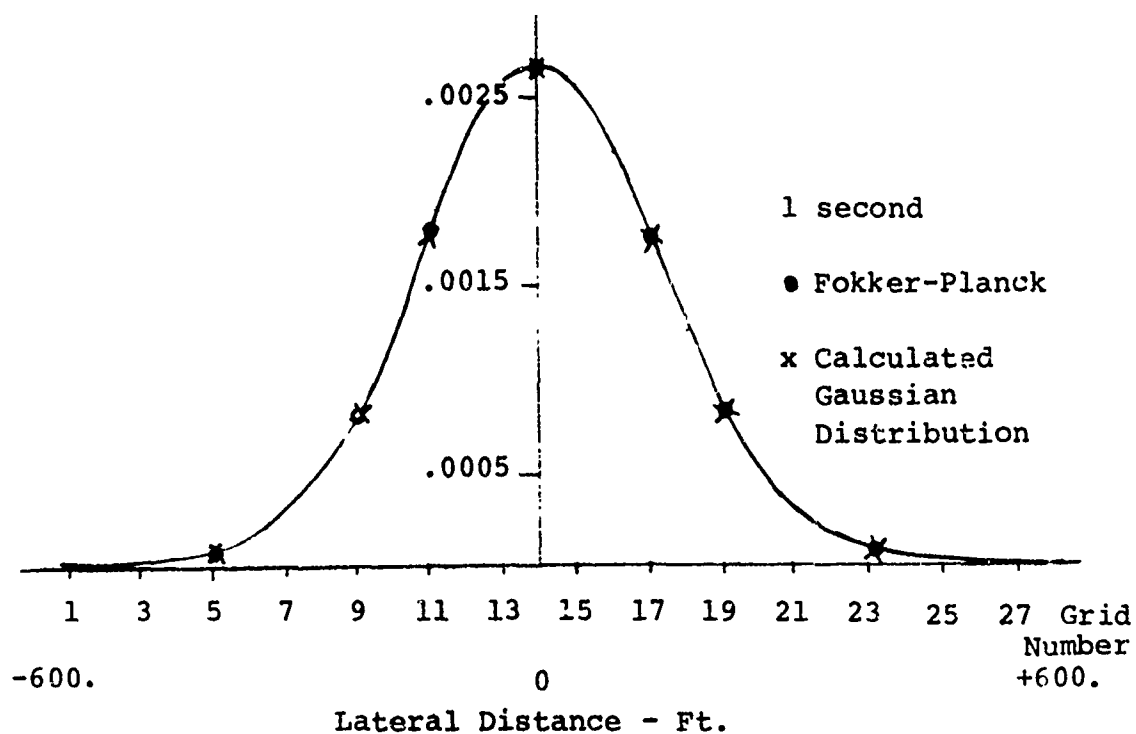


Figure 2.2.2-1

Lateral Deviation Density Function at One Second

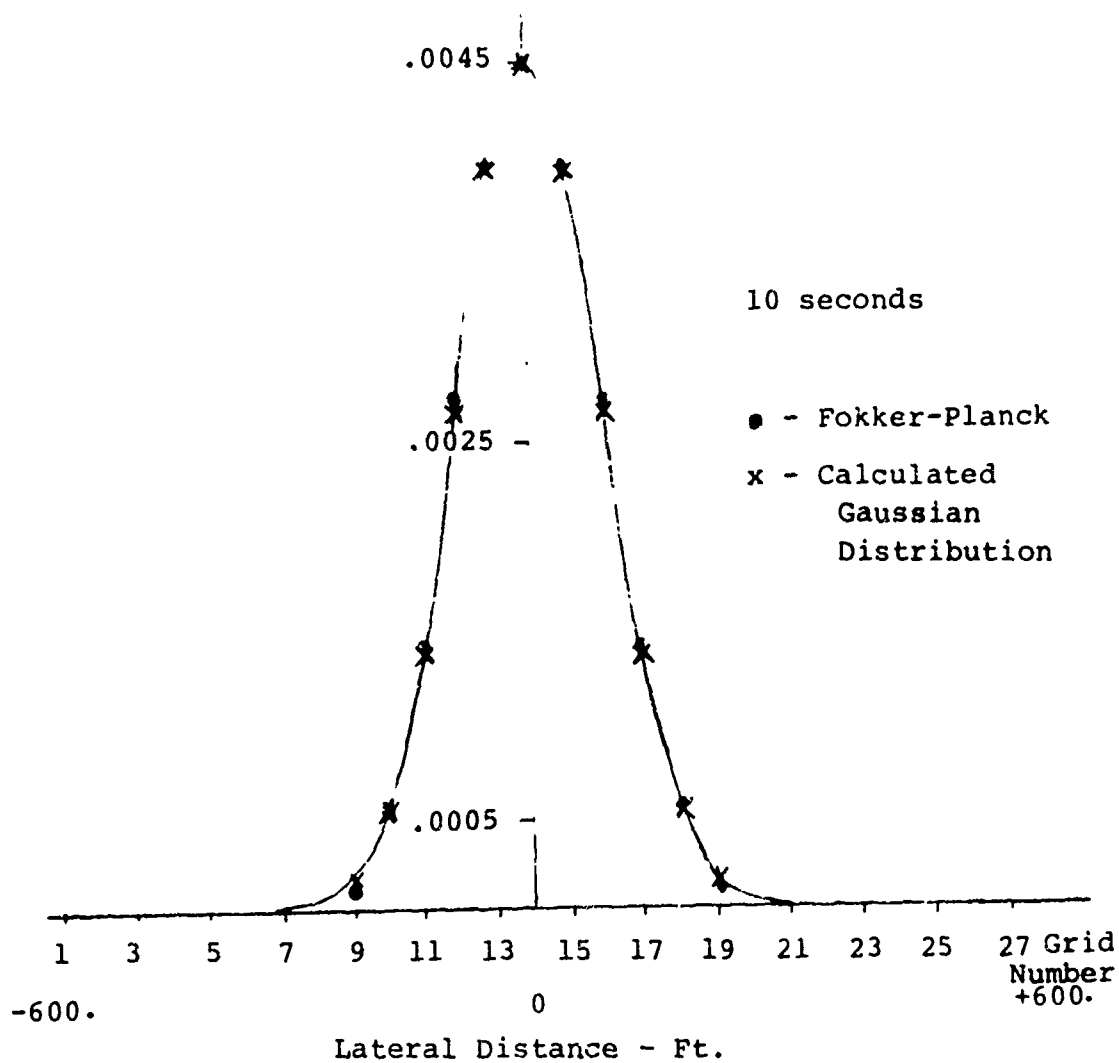


Figure 2.2.2-2

Lateral Deviation Density Function at Ten Seconds

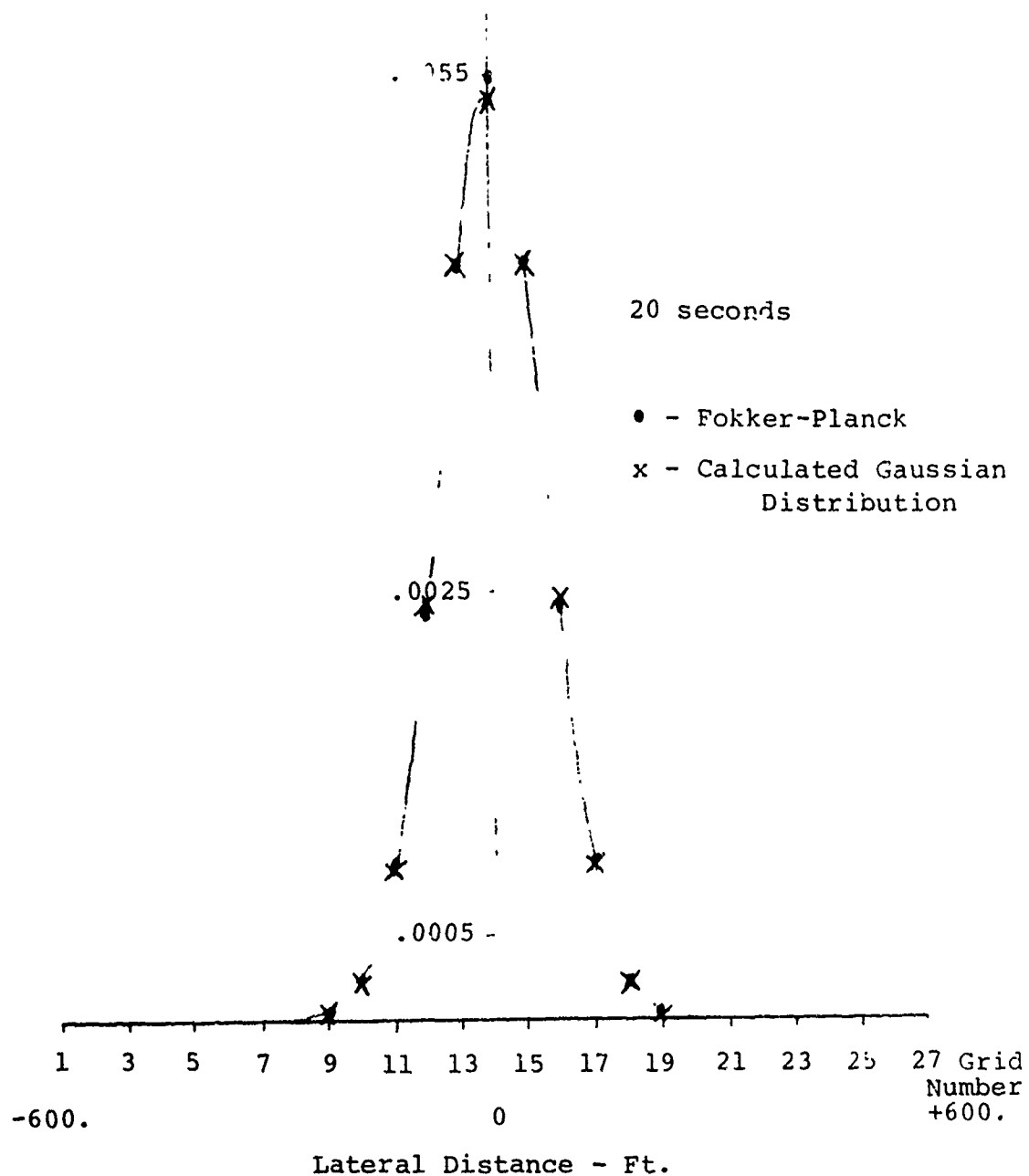


Figure 2.2.2-3

Lateral Deviation Density Function at Twenty Seconds

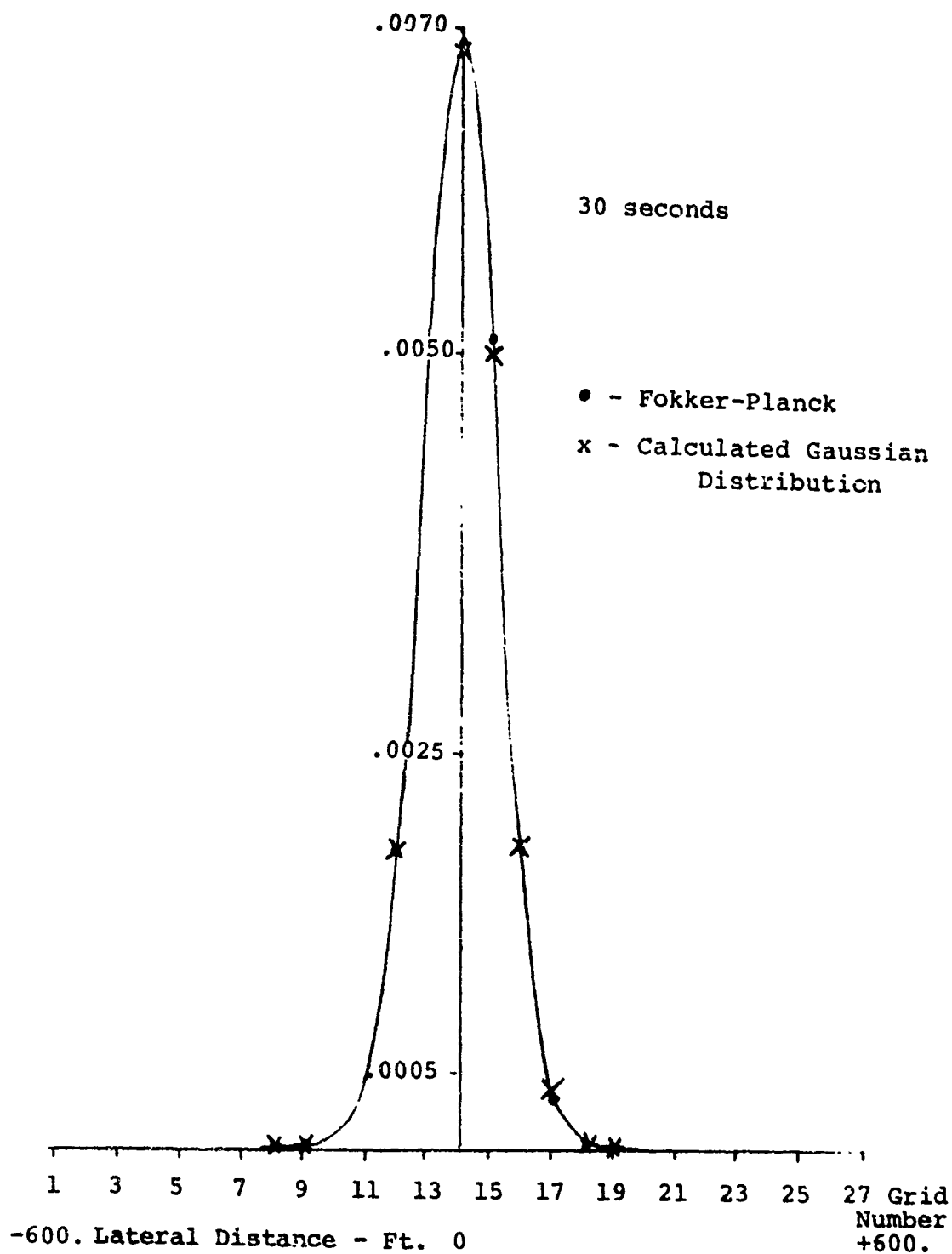


Figure 2.2.2-4
Lateral Deviation Density Function at Thirty Seconds

2.2.2.2 Lateral Deviation Variance Response

Another check on the Fokker-Planck solution was to compare the variance of the lateral deviation from the Fokker-Planck solution (reduced second order system) with that from the classical linear gaussian solution (sixth order system) described in Appendix D. The system parameters and initial conditions described in Section 2.2.2.1 were used to make this comparison. Since both methods used gaussian processes with the same linear system, the variances of the two output lateral deviation density functions should be approximately equal. These functions will be approximately equal, rather than exactly equal, due to different error sources in the two methods. The variance propagation technique accumulates errors introduced by the integration (Runge-Kutta) technique. The Fokker-Planck has error sources introduced by the integration technique (trapezoidal) used in the solution of partial differential equations by the method of finite differences and by the grid spacing. The standard deviation of the lateral deviation density function is plotted versus time in Figure 2.2.2-5 for each method. As shown in the figure, the maximum deviation between the two curves is only five feet (3% difference); therefore, the Fokker-Planck method of propagating distributions is verified.

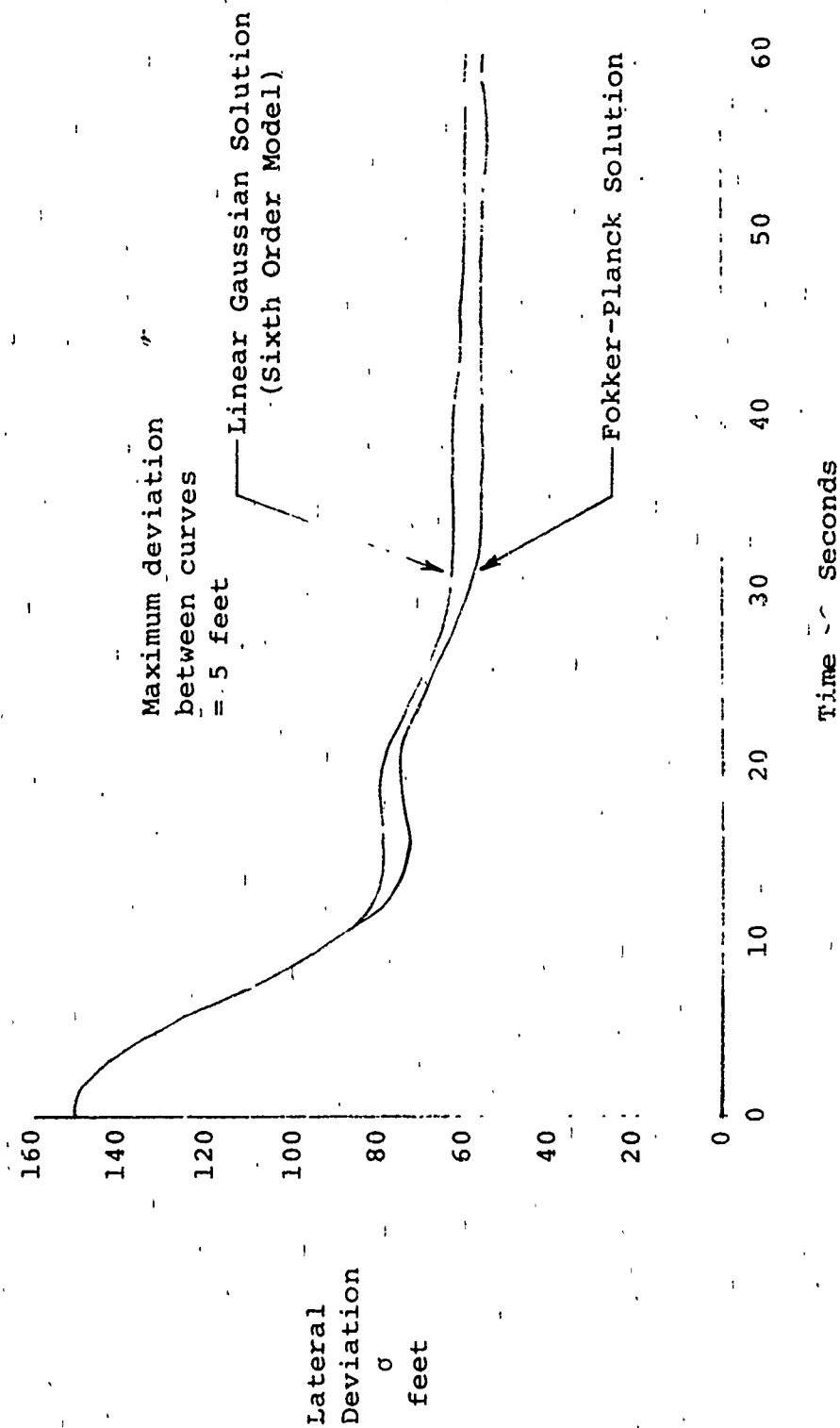


Figure 2.2.2-5
Comparison of the Fokker-Planck and
Linear-Gaussian Solution Technique

REFERENCES

1. Barucha-Reid, A. T., Elements of the Theory of Markov Processes and Their Applications, McGraw-Hill, New York, 1960.
2. Davison, E. J., "A Method for Simplifying Linear Dynamic Systems", IEEE Transactions on Automatic Control, Vol. AC-11, No. 1, January, 1966.
3. Helstrom, C. W., "Markov Processes and Applications", Communication Theory, Chapter 2.
4. Pawula, R. F., Generalizations and Extensions of the Fokker-Planck Kolmogorov Equations, Ph.D. dissertation from California Institute of Technology, 1965.
5. Sage, A. P. and J. L. Melsa, Estimation Theory with Applications to Communications and Control, McGraw-Hill, New York, 1971.
6. Sveshnikov, A. A., Problems in Probability Theory, Math Statistics and Theory of Random Functions, W. B. Saunders Company, Philadelphia, 1968.
7. Takacs, Lojos, Stochastic Processes, Methuen and Company Ltd., London, 1960.
8. Stratonovich, R. L., Topics in the Theory of Random Noise, Volumes I and II, Gordon and Breach, New York, 1967.

SECTION 2.3

MEASURED DISTRIBUTIONS

The characteristics of various approach systems have been recorded in the form of trajectory information from a finite sample of aircraft flying IFR approaches. This information has been reduced and processed to enable both vertical and lateral error distributions (measured distribution data) to be obtained at discrete points in range. Data has been collected jointly by the FAA and Resalab for the various approach systems considered in this study.

Since the measured distribution data has been derived from a finite number of samples, only certain reliable information is available from this data. Generally, the sample size is sufficient to warrant accurate estimates of the mean and variance of the data; however, in some cases, the sample size is too small to accurately estimate the variance. The sample size is generally not sufficient to accurately determine the shape of the distribution, particularly in the region of the tails. The data is available only at discrete points in range. Due to these limitations on the measured distribution data, it is necessary to utilize other techniques such as the Fokker-Planck technique or the linear gaussian variance propagation technique to generate the probability density function for use in the probability of collision determination. Where no data exists, the distributions were derived, based on reasonable assumptions.

The measured distribution data was utilized in this study for three reasons:

- 1) to verify that the models, as formulated, are, in fact, good representations of the actual systems (Sections 2.4 and 2.5),
- 2) to provide the initial distributions for the various techniques utilized to generate the probability density functions (Section 2.5), and
- 3) to provide vertical error distributions for use in the probability of collision determination (Section 2.6).

This section identifies the lateral, vertical, and longitudinal measured distributions for the systems listed in Table 2.3-1. Measured distribution data is available for all of

Table 2.3-1 Required Measured Distributions

Distribution	System
Lateral	FC-ILS-INOM-CTOL* FC-ILS-I-CTOL FC-ILS-II-CTOL BC-ILS-I-CTOL VOR-CTOL FC-ILS-I-STOL
Vertical	FC-ILS-I-CTOL FC-ILS-I-STOL
Longitudinal	FC-ILS-I-CTOL

*Nominal Measured Distribution Data

these systems with the exception of the system specified for the longitudinal distribution. In this case, data was derived, based on assumed operational procedures.

The techniques used by Resalab to collect, reduce, and process the data from Charleston, S. C., is discussed in Section 2.3.1. Basically, the technique uses a precision approach radar (PAR) as a measurement and display system. The displayed position is recorded photographically and reduced with a computer controlled microdensitometer. Once the Charleston data is reduced, it can be combined with the data collected by the FAA at other airports to provide a more representative data base.

The distribution data used in the lateral separation project is discussed in Section 2.3.2 and may be divided into three classes, depending upon the characteristics of the data. These classes characterize:

- 1) systems for which field data has been collected but no assumptions made concerning the distribution,
- 2) systems for which field data has been collected and the distributions assumed gaussian,
- 3) systems for which no field data has been collected, therefore, the required distribution must be inferred from assumptions.

The validity of using the collected data as representations of generalized systems is examined in Section 2.3.3.

The resulting distributions for each of the required systems are discussed in Section 3.1 and presented in Appendix E.

2.3.1 TECHNIQUES USED TO COLLECT, REDUCE, AND PROCESS DISTRIBUTION DATA

A review of the available distribution data indicated that additional lateral data were required for BC-ILS-I-CTOL and VOR-CTOL. These approach systems are alternates to a front course approach; and at several airports, one (or both) of these is available to a runway parallel to a FC-ILS runway. Measurement of the lateral distribution of errors on approaches using BC and VOR was conducted at Charleston by Resalab. When meteorological conditions dictated the use of the FC approach, these data were also collected. The techniques of collecting, reducing, and processing the data are discussed below and illustrated in Figure 2.3.1-1. The errors induced by the collection and reduction of the data are also examined.

2.3.1.1 Data Collection

Method

The method used to collect the distribution data is to record the aircraft position at various times. The aircraft position is presented on the PAR scope and recorded on photographic film. The camera was rigidly mounted approximately 24 inches from the PAR scope face and the shutter held open for the duration of an approach. This technique results in a recording of the aircraft position for every sweep of the PAR antenna. A representative example of a recorded approach is given in Figure 2.3.1-2. The range history of aircraft position has the appearance of a "smoke trail" in the photograph. The actual aircraft trajectory lies in the center of the aircraft track shown in the figure. The upper trace shows the elevation vs range history of the aircraft; the lower trace shows the azimuth vs range history.

Additional data was collected concerning the meteorological conditions that existed during the approach. This data included the ceiling, visibility, wind conditions, and the altitude at which the pilot converted from instrument guidance to visual guidance (breakout altitude). The breakout altitude and the type of equipment used to accomplish the approach was determined from the pilot when operations permitted.

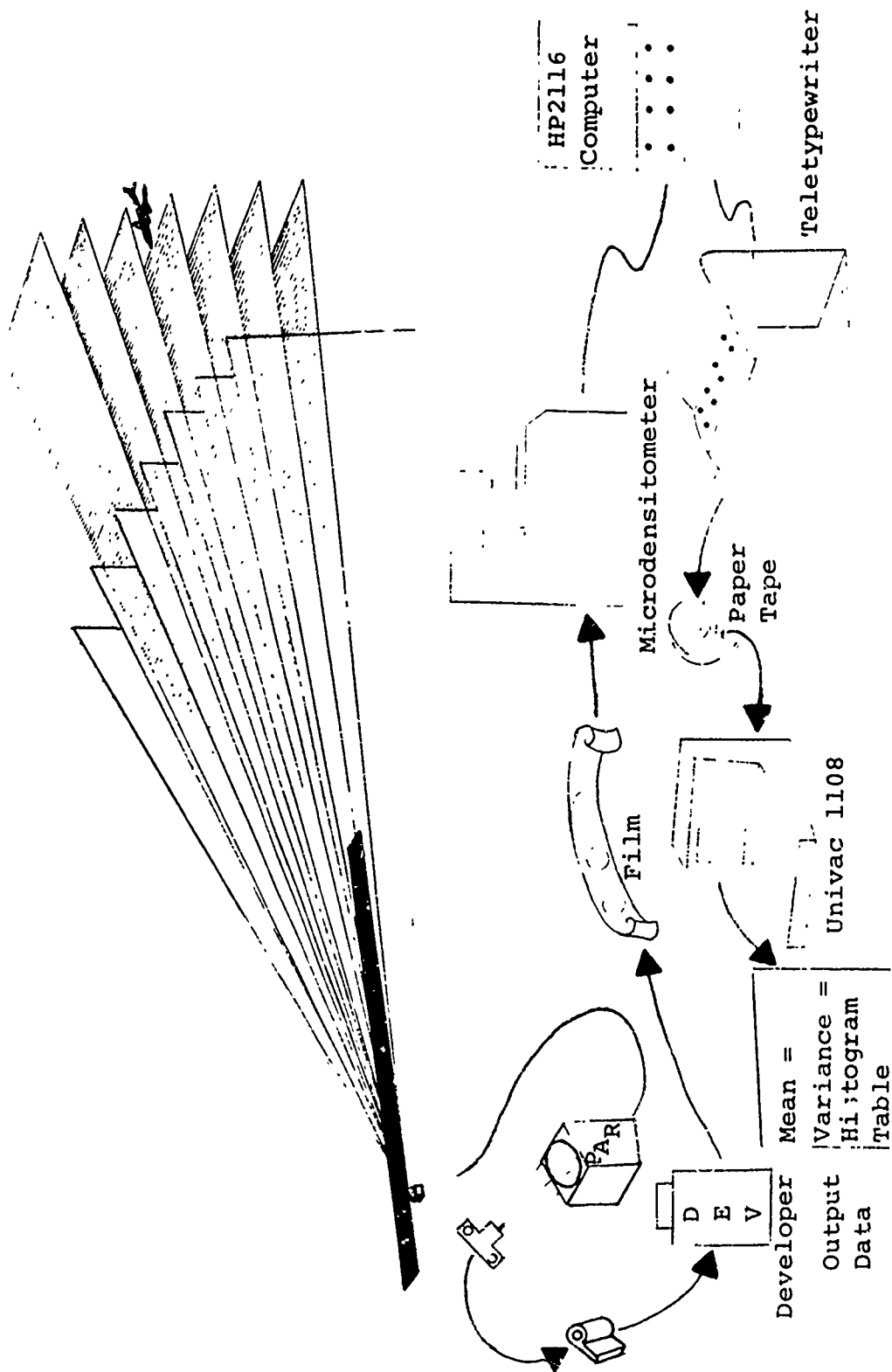
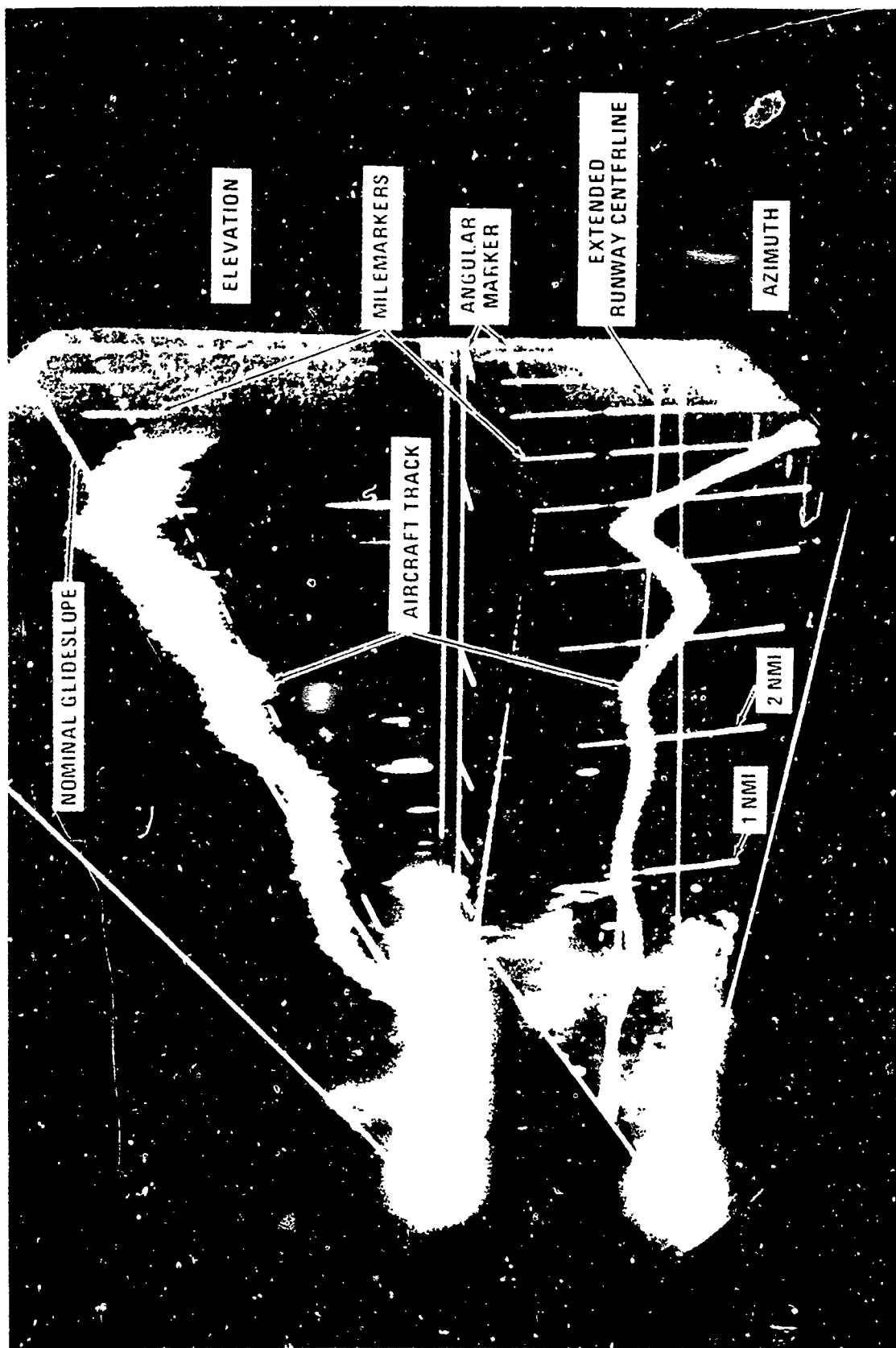


Figure 2.3.1-1 Data Collection, Reduction, and Processing Technique



K10-5

Figure 2.3.1-2. Sample Photograph of Collected Data

Equipment

The PAR, in this application, acts as a data collection and presentation device while the camera acts as a recording device. The recording medium is the film.

The PAR at Charleston is an AN/MPN-13. This system has a 45kw X band transmitter that is time-shared between two antennas. One of these antennas sweeps horizontally, the other vertically. The action of these two antennas determines the position of the aircraft, in one case, in azimuth angle and range, and in the other case, in elevation angle and range; thus, the aircraft position in space is defined.

The camera used to record the PAR scope data is a standard Cannon FX single lens reflex equipped with a 50mm lens. At the beginning of the approach, the shutter of the camera is opened and held open during the approach. This produces a time exposure of the aircraft trajectory over the entire approach as shown in Figure 2.3.1-2.

Errors

The specifications on the PAR indicate that the range error is within 2 percent of true range when true range is greater than 0.5 nautical mile. The azimuth error, expressed in distance from true position, is no greater than 0.6 percent of range plus 1.0 percent of the target deviation from the cursor (extended centerline as presented on the scope). The elevation error is less than 0.3 percent of range plus 1.0 percent of the deviation from the optimum glide path. The errors presented represent an upper bound. Since the PAR is regularly maintained and adjusted, the actual errors will be significantly smaller.

Airport and Equipment Layout

In some measurements, the relative location of the various equipment and runways is required. One of the more critical dimensions is the offset of the PAR from the runway centerline. This distance is used to determine the scale factor discussed in Section 2.3.1.2. Other measurements required include the position of the localizer and VOR. Figure 2.3.1-3 shows the position of the PAR and other pertinent equipment with respect to the runways. The lines through the PAR site and parallel to each runway are presented on the scope face. These lines indicate the PAR offset distance (RO) used for determination of the scale factor. The distance from the PAR to the 33-15 runway is 515 feet, and the distance to the

FC-ILS
Approach

N

9000' x 200'

515'

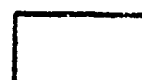
PAR

715'

7000' x 150'



VOR



Terminal
Buildings

Localizer
Antenna

BC-ILS
Approach

Not to Scale

Figure 2.3.1-3 Charleston Municipal/AFB Airport

03-21 runway is 715 feet. The PAR scope is physically located in the terminal building.

2.3.1.2 Data Reduction

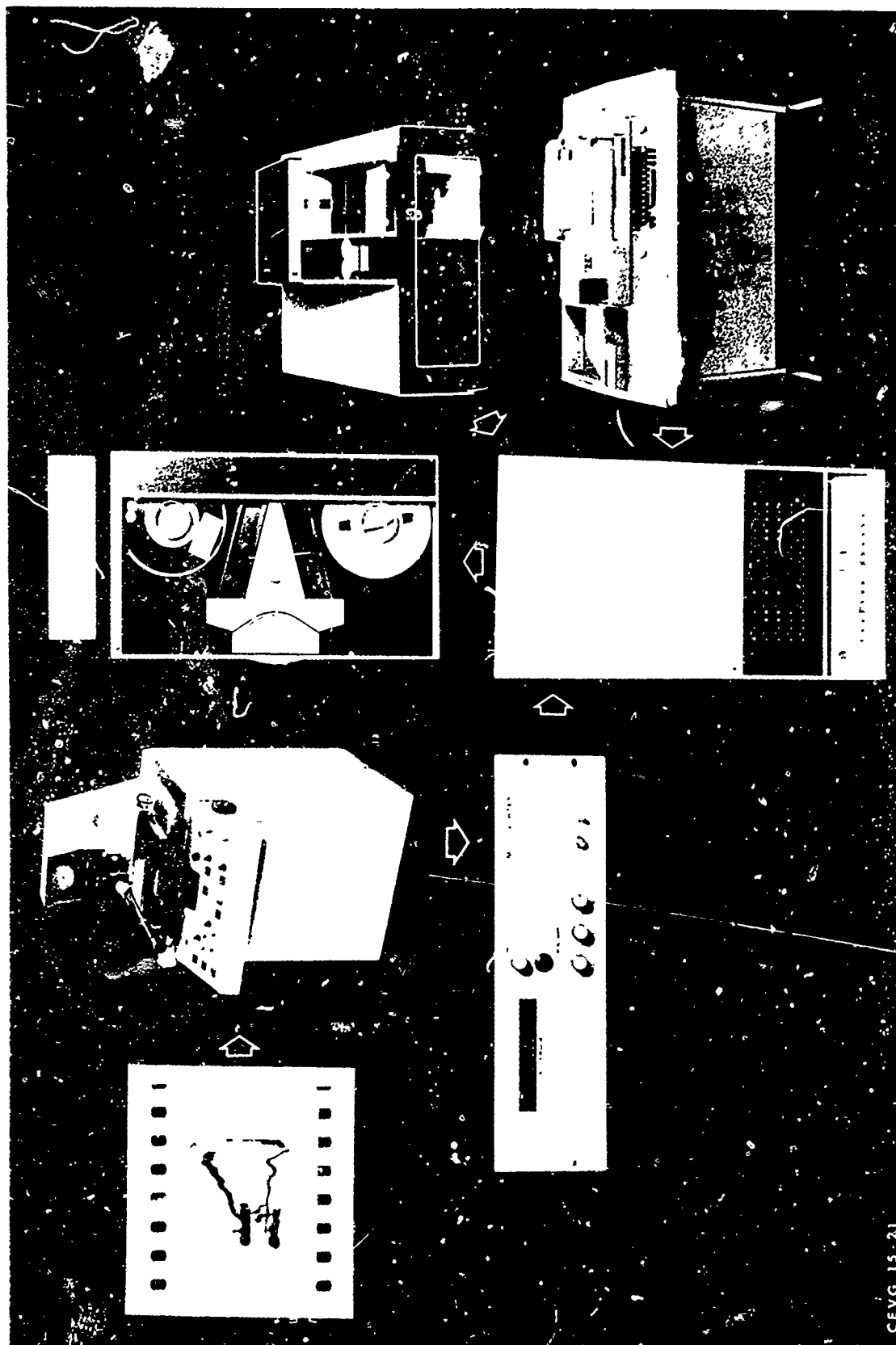
The data reduction effort in this study was concerned with determining the lateral position data of approaching aircraft. This data was obtained from the collected data (discussed in Section 2.3.1.1). The procedures and equipment used and the errors involved in this effort are discussed below.

Equipment and Methods

The equipment involved in the data reduction effort, shown in Figure 2.3.1-4, includes a HP 2116B computer, Photometric Data Systems series 1010 Microdensitometer and associated computer equipment. The microdensitometer has a stage that is driven in the x and y axes in 10 micron (1 micron = 10^{-6} meters) steps which enables precise location measurements to be obtained. A location measurement can be made by aligning the desired point on a transparency (mounted on the stage) with a set of cross-hairs. The area of alignment is magnified to increase the accuracy of the positioning. The microdensitometer stage position is monitored and can be controlled by the computer.

The data reduction method requires certain measurements to be made from the film at each of the specified ranges. Due to the number of ranges considered and the number of data samples collected, the number of measurements required was extremely large. The basic philosophy was to automate the methods as much as practical. The limit of practicality, in this case, is governed by the ratio of background density to signal density (on the film) and by the presence of unwanted returns and radar clutter (Figure 2.3.1-2). The presence of these unwanted signals precluded the usage of some of the automatic functions available on the microdensitometer. Therefore, the human operator was required to make decisions concerning what was considered to be signal and what was noise. The following paragraphs discuss the general data reduction procedure.

The automatic portion of the reduction system requires that the film be aligned in such a manner that the film edge is parallel with the x-axis movement of the microdensitometer's movable stage. Once this alignment is made, the stage is manually driven to range zero (indicated radar site) and to



REV B VG15-21

Figure 2 3 1 4 Data Reduction Equipment

CEVG 15-21

each of the indicated range marks. These positions are recorded by the computer. Since the range marks are logarithmically spaced, the computer was utilized to automatically position the film at the proper range settings. Now the measurements required from the film can be obtained speedily. The computer, using the differences between the range points and a logarithmic scale factor, computes and drives the stage to the first of the specified ranges. The operator then aligns the crosshairs on the runway extended centerline, the PAR offset line, the left and then the right side of the aircraft trace (shown in Figure 2.3.1-5). Each of these measurements are recorded on

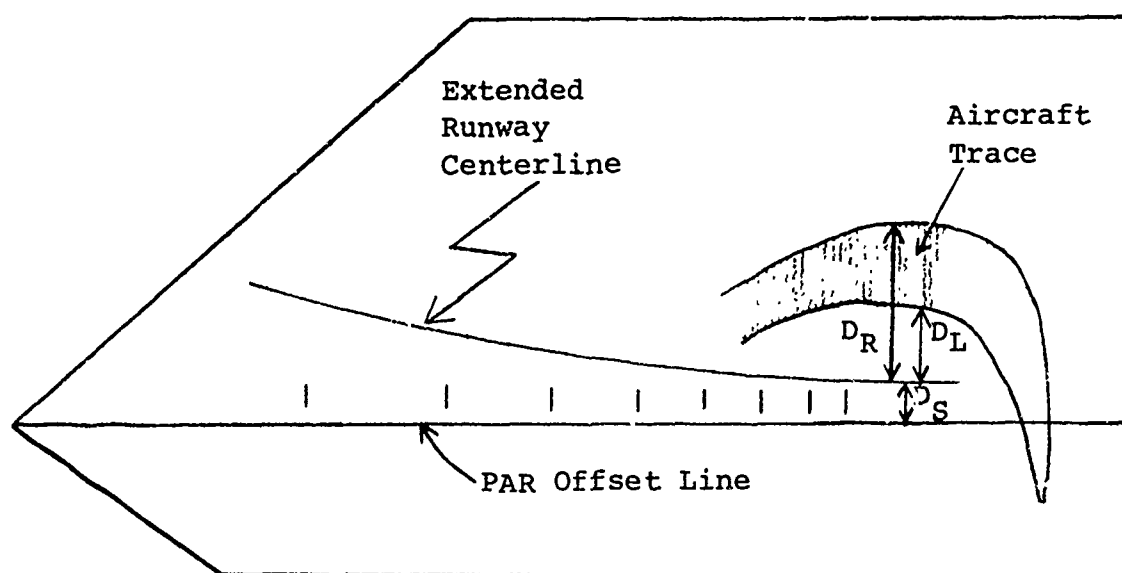


Figure 2.3.1-5 Data Reduction Measurements

a command from the operator. When all programmed measurements are completed at one range, the computer automatically calculates the aircraft's lateral deviation and drives the stage to the next of the specified ranges where the procedure is repeated. The computer prepares a copy of the lateral deviations at each specified range for visual checking. A paper tape is produced containing the deviation data for future processing. When all required measurements on this frame are completed, the stage is driven to the next frame and these procedures repeated.

The displacement of the aircraft to the left or right of the localizer (extended runway centerline) is determined from the previously described PAR scope photographs. Referring to Figure 2.3.1-5, it can be seen that the center of the aircraft trace (in a lateral sense) can be determined from

the average of the measurements of D_R and D_L . The scale factor, RO/D_S , can be determined from the scope measurement, D_S , and the actual distance RO . D_S is the distance measured on the scope between the extended runway centerline and the PAR offset line. The equation used to determine the lateral deviations (Y') is

$$Y' = \frac{RO}{D_S} \cdot \frac{D_L + D_R}{2} \quad (2.3.1-1)$$

where

$$RO = \begin{cases} 515 \text{ feet; if runway 33-15 is used} \\ 715 \text{ feet; if runway 03-21 is used} \end{cases}$$

and D_S , D_L , and D_R are defined in Figure 2.3.1-5. The scale factor, RO/D_S , converts the measurements made on the scope face (or film image) to actual distances in feet.

Errors

Regardless of the precision of the instrument, no measurement device or method gives the true value for the quantity measured. Mechanical imperfections in instruments and the limitations introduced by human factors are such that repeated measurements of the same quantity generally result in different values. Variations among successive values are caused by errors in the observations. Errors fall into three general classes which may be categorized by origin. These classes are: (1) measurement mistakes, (2) systematic, and (3) random.

Measurement mistakes are mistakes caused by misreading scales, transposing figures, erroneous computations, or careless observers. They are usually large and easily detected by repeated measurements.

Systematic errors follow some fixed law and are generally constant in magnitude and/or sign within a series of observations. The origin of systematic errors is primarily within the measuring device. Causes of systematic errors include faulty instrument calibration, errors inherent in the graduation of scales, and changes in performance resulting from variations in the environment, primarily, temperature and humidity. Systematic errors can be eliminated or substantially reduced when the cause is known.

Random errors are those remaining after measurement mistakes and systematic errors have been removed. They result from accidental and unknown combinations of causes beyond the control of the observer. Random errors are characterized by: (1) variation in sign--positive and negative

errors occurring with equal frequency, (2) small errors occurring more frequently than large errors, and (3) extremely large errors rarely occurring.

The design and operation of the data reduction system considered the error sources noted above. For instance, errors in scale reading by the operator were eliminated entirely, since the scale reading function is accomplished by the computer at the command of the operator. Most measurement mistakes can be identified and consequently eliminated by plotting the reduced data and comparing it to the original data. Systematic errors are minimized because the resultant measurement depends on differences of measurements; therefore, any system bias is eliminated.

For the above reasons, the measurement mistakes and systematic errors are assumed to have been essentially eliminated by the data reduction technique; therefore, the remainder of this section is concerned with the effects of human induced random errors. Random errors, usually introduced by placement or reading of a scale or hairline are minimized but not eliminated by providing the operator with significant magnification of the film area being measured. Furthermore, the propagation of human (random) errors from the source (particular measurement) through the end result can be determined. These results then aid in determining possible improvements to the data collection system and/or instill confidence in the data itself. The errors in the measurement/display system (PAR) have been previously discussed. This analysis of data reduction system errors assumes that the indicated aircraft position (on the PAR) is absolutely correct. Thus, this analysis is of the error introduced solely by the human operator of the reduction system.

Considering that

$$D_L^A = D_L^M + \epsilon_{D_L}$$

where the superscript A indicates the actual value of D_L (Figure 2.3.1-5) and the superscript M indicates measured values. Note also that

$$D_R^A = D_R^M + \epsilon_{D_R}$$

and

$$D_S^A = D_S^M + \epsilon_{D_S}$$

The measurement errors, ϵ_{D_L} , ϵ_{D_R} , and ϵ_{D_S} are assumed to be gaussian distributed random variables with mean equal to zero and variance equal to σ_D^2 .

$$\epsilon_{D_L} = N(0, \sigma_D^2)$$

$$\epsilon_{D_R} = N(0, \sigma_D^2)$$

$$\epsilon_{D_S} = N(0, \sigma_D^2)$$

ϵ_{D_L} , ϵ_{D_R} , and ϵ_{D_S} represent the human induced errors of positioning the reading instrument on the proper point. From Equation 2.3.1-1, and the above discussion, it follows that

$$\begin{aligned} \epsilon_{Y'} &= (Y')^A - (Y')^M \\ &= \frac{RO}{D_S^A} \left(\frac{D_L^A + D_R^A}{2} \right) - \frac{RO}{D_S^M} \left(\frac{D_L^M + D_R^M}{2} \right) \end{aligned}$$

With appropriate substitutions, the above equation can be rewritten as

$$\epsilon_{Y'} = \frac{RO}{2} \left[\frac{D_L^A + D_R^A}{D_S^A} - \left(\frac{D_L^A - \epsilon_{D_L} + D_R^A - \epsilon_{D_R}}{D_S^A - \epsilon_{D_S}} \right) \right]$$

The errors have been assumed to be gaussian and independent. A Monte Carlo simulation was run for a typical case with the measurements listed below.

Range = 3 miles

$Y' = 700$ feet

$$\epsilon_{D_L} = N(0, .0125^2)$$

$$\epsilon_{D_R} = N(0, .0125^2)$$

$$\epsilon_{D_S} = N(0, .0125^2)$$

$$D_L^A = 1.0 \text{ mm}$$

$$D_R^A = 1.8 \text{ mm}$$

$$D_S^A = 1.0 \text{ mm}$$

$$RO = 515 \text{ feet}$$

The results of this simulation determined that the mean of the human induced error in the aircraft position is 0.229 feet, and the standard deviation is 7.942 feet. The example presented is assumed to be representative of a typical data reduction point.

2.3.1.3 Data Processing

The lateral error distribution data is processed and presented in two forms. One form is the mean and variance at each specified range. The equation to determine the mean is

$$\bar{Y}' = \frac{1}{n} \sum_{i=1}^n Y_i'$$

and the variance is

$$\sigma_{Y'}^2 = \frac{1}{n} \sum_{i=1}^n (Y_i' - \bar{Y})^2$$

The other form is a tabular presentation of histogram data with partitions spaced laterally ten meters (32.8 feet) apart. These data forms are consistent with the forms of data previously collected. The partitioning for the histogram data was done at 10 meter intervals with a partition boundary coincident with the extended runway centerline. This is consistent with previous data collection efforts conducted by the FAA.

2.3.2

MEASURED DISTRIBUTION DETERMINATION

As stated previously, it was necessary to determine measured distributions for the systems listed in Table 2.3-1. This section presents the methods used to determine the distributions for each of these systems. Measured distribution data can be summarized and presented in a variety of forms. The most advantageous presentation depends in part on assumptions concerning the characterization of the distribution shape and on the ultimate use of the data. The distribution data used in the lateral separation project may be divided into three classes depending upon the characteristics of the data. These classes characterize:

1. systems for which field data has been collected and the distribution is presented in a tabular form of a histogram and/or mean and standard deviation tables;
2. systems for which field data has been collected and the distribution is assumed gaussian;
3. systems for which no field data has been collected.

These classes are briefly discussed in the sections which follow.

2.3.2.1

Tabular Distribution Data

A common method of presenting measured distribution data is a tabular form of histogram or mean and standard deviation data. The systems from Table 2.3-1 which fall into this class and require lateral distributions, are contained in Table 2.3.2-1. The sources of the collected data which were combined to obtain the resulting distributions are also indicated in the table.

Data for these systems are presented in two forms. One form is the sample mean and standard deviation at each of the specified ranges; the other form is a table of histogram data from observed data. An example of the mean and standard deviation data is given in Table 2.3.2-2 for the FC-ILS-I-CTOL system. An example of the histogram form of data presentation is given in Table 2.3.2-3. The complete data set for each of the above systems is given in Appendix E. The histogram data is presented at the same specific ranges as the mean and standard deviation data. The range to touchdown is given in meters across the top of the page. The lateral deviations are given in multiples of the partition intervals on the vertical axis. The partition intervals are five or ten meters as noted in Table 2.3.2-3. The numbers in the body of the table represent

Table 2.3.2-1 Class 1 Systems

System	Data Sources
Lateral	
FC-ILS-INOM-CTOL	Atlanta and Chicago O'Hare Airports
FC-ILS-I-CTOL	Chicago O'Hare, Portland, and Charleston Airports
FC-ILS-II-CTOL	Atlanta Airport
BC-ILS-I-CTOL	Reference 1 and Charleston Airport
VOR-CTOL	Reference 1, NAFEC*, and Charleston Airport
Vertical	
FC-ILS-I-CTOL	Chicago O'Hare and Portland Airports

*National Aviation Facilities Experimental Center, Atlantic City, N. J.

the number of aircraft observed in the indicated partition at the indicated range.

2.3.2.2 Gaussian Distributed Data

Where the processing of the published data has presumed gaussian distributions, these assumptions are maintained. Specifically, the systems of Table 2.3-1 for which gaussian distributions have been assumed are contained in Table 2.3.2-4. When the data is presumed to be distributed according to the gaussian distribution laws, the entire distribution is completely described by the mean and variance. Generally, the reported means of the data have been small. A representative example of the lateral deviation standard deviation is given in Figure 2.3.2-1 for a FC-ILS-I-STOL (Lateral). The distribution data for all of the above systems is presented in Appendix E.

2.3.2.3 Systems with No Collected Data

In the consideration of dependent parallel IFR operations for CTOL aircraft, it was necessary to determine the longitudinal spacing distribution about a nominal longitudinal

Table 2.3.2-2

Mean and Standard Deviation Versus Range for
FC-ILS-I-CTOL - Lateral*

Range, meters	Number of Samples	Mean, meters	Standard Deviation, meters
600	513	-.0161	11.8943
1200	618	-3.0435	22.0739
1800	633	-5.2973	26.4976
2400	642	-6.7594	31.9236
3000	644	-2.8728	35.8871
3600	638	1.6535	37.7171
4200	622	8.9878	43.6031
4800	631	8.3098	46.9545
5400	630	8.4069	53.4125
6000	631	6.9212	61.9026
6600	629	2.9729	68.5199
7500	513	14.46	75.30
8100	500	11.83	83.99
8700	490	7.67	90.20
9300	468	6.37	93.00
9900	447	4.83	97.60
10500	423	12.93	92.45
11100	387	16.36	91.98
11700	342	17.42	94.11
12300	324	21.30	100.43
12900	307	26.29	96.41
13500	283	28.54	102.12
14100	245	28.99	103.63
14700	224	33.03	103.14
15300	181	27.42	97.75
15900	134	25.53	113.84

*Charleston data is included in the range interval from 1200 meters to 5600 meters, inclusive, but not elsewhere, since the data collection ranges were not coincident elsewhere.

Reproduced from
best available copy.

Table 2.3.2-3 Distribution of Lateral Displacements for
FC-ILS-I-CTOL - Lateral**

Partition Interval	Range, hundreds of meters										
	6*	12*	18*	24	30	36	42	48	54	60	66
-20 to -79	5.	1.	4.	0.	2.	1.	2.	2.	2.	4.	5.
-79	1.	0.	1.	1.	0.	1.	1.	0.	0.	0.	2.
-10	0.	0.	0.	0.	0.	0.	0.	0.	1.	1.	3.
-17	0.	1.	1.	0.	1.	0.	1.	0.	0.	1.	2.
-16	0.	0.	1.	2.	0.	0.	0.	0.	1.	4.	1.
-15	0.	0.	1.	1.	1.	1.	0.	1.	1.	1.	2.
-14	0.	2.	1.	0.	0.	0.	0.	0.	1.	1.	0.
-13	0.	3.	1.	1.	0.	1.	1.	2.	3.	2.	2.
-12	0.	3.	6.	2.	3.	2.	1.	1.	2.	3.	2.
-11	0.	1.	3.	1.	1.	3.	2.	6.	2.	3.	7.
-10	0.	2.	4.	0.	0.	1.	1.	0.	2.	3.	3.
-9	1.	3.	6.	3.	7.	3.	3.	6.	4.	13.	5.
-8	1.	4.	6.	4.	2.	1.	4.	9.	11.	8.	7.
-7	2.	2.	14.	3.	8.	6.	5.	7.	8.	6.	20.
-6	3.	17.	24.	9.	3.	7.	17.	14.	15.	15.	15.
-5	1.	16.	39.	13.	18.	21.	14.	24.	18.	23.	32.
-4	15.	47.	37.	35.	23.	36.	28.	20.	31.	32.	22.
-3	21.	56.	57.	49.	54.	45.	42.	32.	27.	41.	32.
-2	93.	90.	86.	75.	78.	74.	51.	42.	48.	40.	47.
-1	112.	76.	54.	110.	98.	65.	47.	52.	57.	45.	53.
0	128.	98.	73.	115.	93.	86.	76.	73.	70.	75.	54.
1	64.	83.	61.	89.	94.	74.	71.	70.	67.	48.	50.
2	25.	40.	41.	50.	61.	68.	70.	84.	62.	47.	45.
3	13.	21.	32.	39.	31.	49.	50.	49.	50.	43.	40.
4	9.	20.	20.	15.	23.	36.	44.	44.	24.	36.	38.
5	3.	10.	12.	6.	18.	19.	24.	26.	33.	29.	33.
6	0.	8.	11.	8.	11.	12.	22.	18.	22.	29.	21.
7	0.	2.	6.	1.	4.	7.	9.	11.	16.	24.	22.
8	0.	4.	6.	2.	2.	4.	11.	11.	17.	13.	7.
9	3.	2.	7.	2.	0.	4.	7.	9.	6.	5.	18.
10	1.	1.	3.	2.	2.	6.	6.	4.	6.	10.	10.
11	0.	0.	1.	1.	1.	2.	5.	1.	4.	2.	6.
12	0.	1.	4.	1.	1.	1.	1.	2.	3.	4.	3.
13	1.	2.	3.	1.	2.	1.	2.	3.	4.	0.	2.
14	1.	0.	3.	1.	1.	0.	1.	5.	2.	2.	2.
15	0.	0.	1.	0.	0.	0.	1.	1.	1.	4.	3.
16	0.	0.	1.	0.	1.	1.	1.	0.	1.	1.	3.
17	0.	0.	0.	0.	0.	0.	1.	0.	1.	2.	1.
18	0.	0.	0.	0.	0.	0.	0.	0.	0.	1.	1.
19	0.	0.	0.	0.	0.	0.	0.	0.	2.	2.	0.
20 to 56	0.	2.	2.	0.	0.	0.	0.	2.	5.	8.	8.

*At these ranges, the partitions are at five meter intervals; elsewhere, the partitions are at ten meter intervals.

**Charleston data is included in the range interval from 1200 meters to 6600 meters, inclusive, but not elsewhere, since the data collection ranges were not coincident elsewhere.

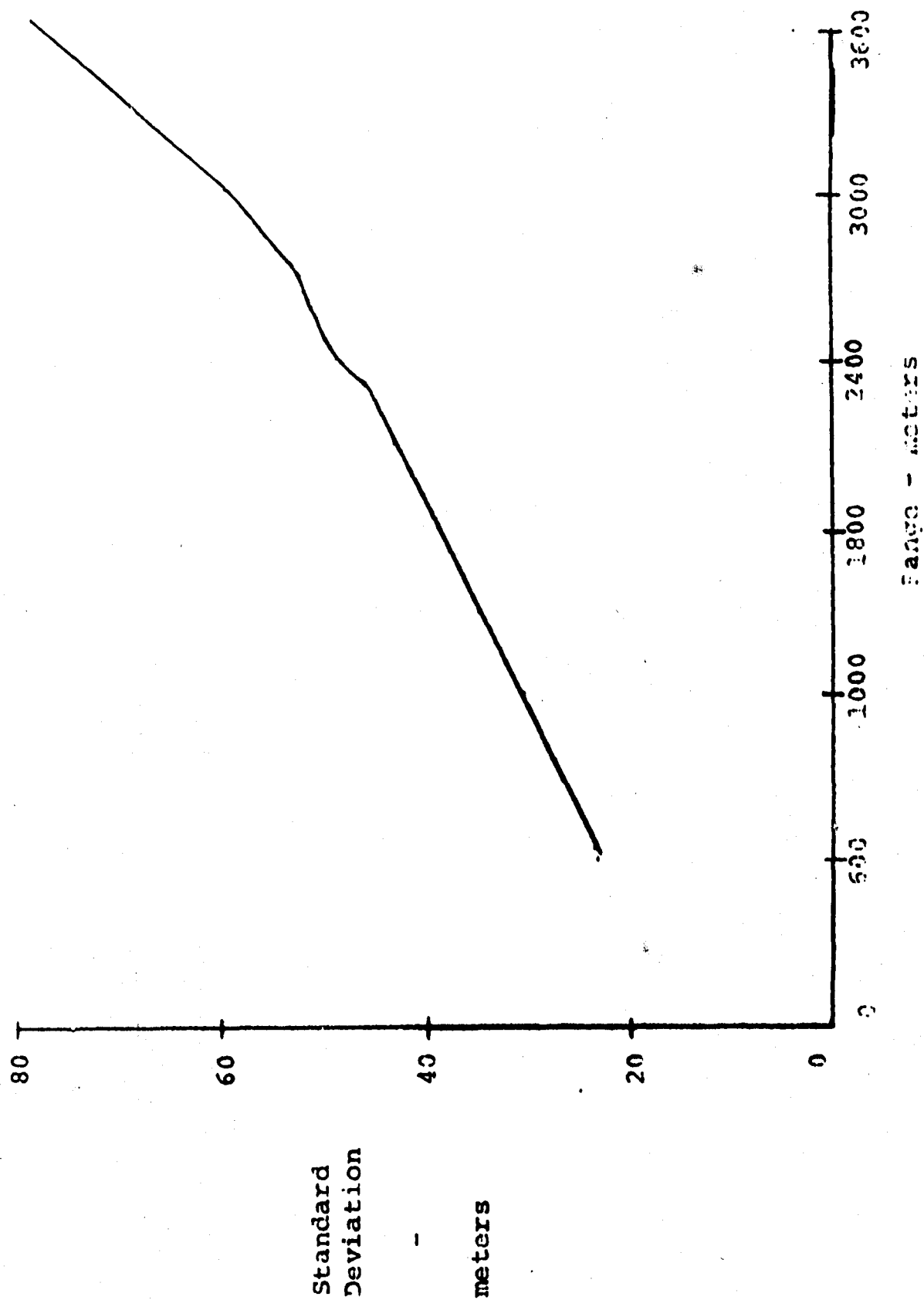


Figure 2.1.2-1

Standard Deviation Versus Range for FC-III I-STIL (Lateral)

Table 2.3.2-4 Class 2 Systems

Distribution Required	System	Data Sources
Lateral	FC-ILS-I-STOL	Reference 2
Vertical	FC-ILS-I-STOL	Reference 2

location. Since no measured data of this type was available, it was necessary to make certain assumptions concerning this data for the FC-ILS-I-STOL (longitudinal) system. It was assumed that the aircraft velocity was normally distributed about a nominal mean approach velocity, \bar{V} , with a standard deviation, σ_V .

$$V = N(\bar{V}, \sigma_V^2)$$

Standard procedures require that the final approach be held "close" with respect to the recommended final approach speed. Based on conversations with experienced pilots, the standard deviation of the velocity distribution was assumed to be five knots. With this assumption and the following equation

$$X' = X'_0 - \int_0^t V dt$$

it can be shown that the distribution on X' is also gaussian.

$$X' = N(\bar{X}', \sigma_{X'}^2)$$

$$\bar{X}' = X'_0 - \bar{V}t$$

$$\sigma_{X'} = \frac{\sigma_V t}{\sqrt{2}}$$

where

- x' ~ longitudinal location, feet
- \bar{x}' ~ mean longitudinal location, feet
- $\sigma_{x'}$ ~ longitudinal location standard deviation, feet
- x'_0 ~ initial longitudinal location, feet
- \bar{v} ~ aircraft mean velocity, feet/second (assumed to be 236.444 feet/second for CTOL aircraft)
- σ_v ~ velocity distribution standard deviation, ft/sec (assumed to be 8.444 feet/second)
- t ~ time from the point where the aircraft velocity control is initiated, sec

2.3.3 MEASURED DISTRIBUTION DATA VALIDITY

The resulting combined data representing each system of Table 2.3-1 must be checked carefully to verify that the data represents that system. Possible problem sources which might affect the validity of the data are discussed below. The problem sources and their effects on the measured distribution data are discussed in further detail in Section 3.1.

Turn-on Range

To be able to combine data collected at various airports or to obtain meaningful comparisons between various approach systems, the collected data should be taken from sources having comparable turn-on ranges. Furthermore, the turn-on range for each set of data needs to be identified in order to exclude that data associated with the "delivery" technique before turn-on.

The turn-on range is governed, in part, by the traffic rate. If the traffic rate is high, there is a tendency to have the aircraft "in trail" at longer ranges, sometimes as much as 20 to 25 miles. This gives the pilot considerably greater time to establish a better track on the ILS (or VOR) beam and, therefore, a finer definition of the required wind correction angle. Under these circumstances, the distribution at the outer marker will be much narrower than the distribution for those aircraft that turn-on within one or two miles of the outer marker. Turn-on range data is presented in Section 3.1.2.

Turn-on Direction and Overshoot

At some airports with parallel runways, the standard traffic patterns are prescribed so that the turn-on to the final approach to a right-hand runway of a pair of parallel runways will normally require a right turn (as viewed by the pilot). Conversely, the left runway normally requires a left turn. Presently, procedures state that the turn-on to the final approach to each of the parallel independent runways shall occur with a minimum of 1000 feet vertical separation between the two aircraft. This procedure minimizes the effects of overshoots which occur at turn-on. However, if in the future the procedures are changed such that the 1000 feet vertical separation requirement is eliminated or reduced, it will be necessary to consider the effects of overshoots. For this reason, an analysis was conducted on the front course and back course data collected at Charleston, S. C., in order to determine the amount of overshoot at turn-on and the direction of turn-on. The results of this analysis are contained in Section 3.1.2.

Overshoot as used in this analysis is defined as the distance that an aircraft travels beyond the extended runway centerline measured on the opposite side from the turn-on direction.

Sample Size

When collecting data for the purpose of determining the error distribution, it is necessary to collect sufficient data to assure an adequate sample. When the class of distributions cannot be predetermined, but must be derived, the usual method of determining an adequate sample size is by the method of convergence. In this method, the data collection activity is continued until the mean, variance, or any other required distribution parameters converge to a constant value and the parameters do not change with the addition of new data.

Since most of the data was obtained in a reduced form from previous data collection efforts, it was not possible to use convergence technique to determine the existence of an adequate sample size. However, by comparing the trend of the standard deviations of the data at various ranges and the number of data points available at those ranges, it is possible to make some general observations concerning the sample size. These observations are contained in Section 2.3.3.

Ground Proximity

Operational problems at short ranges include an acute awareness by the pilot of the ground proximity and the

effects on the pilot at breakout into VFR conditions. All vertical data must be examined with these considerations in mind.

Simulated Versus Actual IFR Conditions

Some of the data collected at Charleston (FC-ILS-I-CTOL (Lateral), BC-ILS-I-CTOL (Lateral) and VOR-CTOL (Lateral)) and all of the data collected at NAFEC (FC-ILS-I-STOL (Lateral), FC-ILS-I-STOL (Vertical), and VOR-CTOL (Lateral)) were collected under simulated IFR conditions. Although simulated conditions (blocking possible visual references) create the same visual and physical illusions as actual IFR conditions, the pilot's attitude could be different for the two situations. The attitude differences could be attributed to the fact that the pilot knows that conversion to VFR can be made at his option, regardless of the aircraft's position on the approach, simply by removing the hooding device. Under actual IFR, the breakout attitude is governed by prevailing weather and the pilot must reach the weather ceiling before conversion to VFR can occur.

Assumed Distributions

No data has been collected on the distribution of aircraft about the nominal longitudinal position. The distribution for FC-ILS-I-CTOL (Longitudinal) was derived from the assumed distribution for velocity errors. The mean and standard deviation of the velocity distribution were assumed based on conversations with experienced pilots.

REFERENCES

1. Callaway, E. E., "ILS Back Course and VOR Approach Data", DOT-FAA, FS-640, 5 August 1971.
2. -, "STOL Steep Approaches in the Breguet 941", DOT-FAA, FS-640, November 1969.

SECTION 2.4

NOMINAL MODEL VERIFICATION AND SENSITIVITY ANALYSIS

A necessary task in any simulation or modeling study is that of verifying that the model is a good representation of the physical system. Several methods exist for accomplishing this verification task. The most logical approach is to compare the known (or expected) observable quantities of the physical system to those same observable quantities predicted by the simulation. If a good comparison is observed, the system model is said to be verified.

The procedure discussed above was used in the verification of the instrument landing approach system nominal model and its associated state equations derived in Section 2.1. Since the responses of the three versions of the nominal model have been shown to be in close agreement in Sections 2.1.2 and 2.2, verification pertaining to any one model holds for all three. Basically, three approaches were taken to verify these models - time response analysis, frequency response analysis, and statistical response analysis. Analysis of the models is accomplished by fitting the nominal system model to a set of data hereafter referred to as the nominal measured distribution data (from Section 2.3).

The time response analysis (Section 2.4.1) discusses the three versions of the nominal model and their associated parameter values. A time response for each loop is presented and discussed to verify that the nominal system model is representative of the actual approach system.

The frequency response analysis (Section 2.4.2) consists of a root locus analysis of each loop in the linear version of the nominal model to show the system transient response and gain variation for each system model feedback loop. The linear system model state equations are verified by comparing the transient time response characteristics obtained by integrating the linear state equations (from Section 2.1.5) to those characteristics predicted by the root locus analysis.

The statistical response analysis (Section 2.4.3) describes the method of fitting the nominal model to the nominal measured distribution data (from Section 2.3) and gives the resulting parameter values including initial conditions.

A sensitivity analysis was performed to identify the effects of pertinent model parameters and model errors on the approach system's lateral distribution. The sensitivity results, the nominal system model, and measured distribution data were utilized in fitting models to the specific approach systems listed in Table 2.1-1. This model fitting task is discussed in Section 2.5.

From these analyses, all three versions of the nominal system model are shown to be good representations of the instrument landing approach system.

2.4.1 TIME RESPONSE

As described previously the nominal model (Figure 2.1.2-6) represents a composite set of CTOL aircraft approaching on a front course, ILS, Category I, CTOL system. The nominal model parameters, from Section 2.1.2 (Table 2.1.2-2), were used in the time response analysis. A time response of each feedback loop of the nominal model is discussed below. The time response analysis is performed for a deterministic system (no errors).

Figure 2.4.1-1 shows the lateral deviation response for an initial lateral offset of 500 feet at a range of 9 n. mi. The response is overdamped with a time constant of about 127 seconds. Note that the response represents the mean of a composite set of perfect systems (no errors); however, when system errors are applied (Section 2.4.3) the lateral response becomes statistical.

The aircraft heading angle response is shown in Figure 2.4.1-2 for a step input. This response represents an aircraft flying an arbitrary but constant heading angle of 3.14159 radians (180°) and suddenly a commanded change in heading of .05 radians is input into the system. As shown in Figure 2.4.1-2, the system first goes through a delay equal to the pilot/control delay ($\tau_p = .7$ seconds) plus a lag response for the aircraft bank angle rate ($1/a_a = 1$ second). The remaining response shows an overdamped response with a time constant of about 6 seconds (which agrees with data presented in Reference 1) before achieving a final constant heading angle of 3.19159 radians.

Figure 2.4.1-3 illustrates the aircraft bank angle response when the pilot detects a requirement to change the bank angle. This response depicts an aircraft flying wings level ($\phi = 0$) and suddenly the requirement for a bank angle change of .05 radians is input into the pilot model system. The response shows an initial delay of .7 seconds corresponding

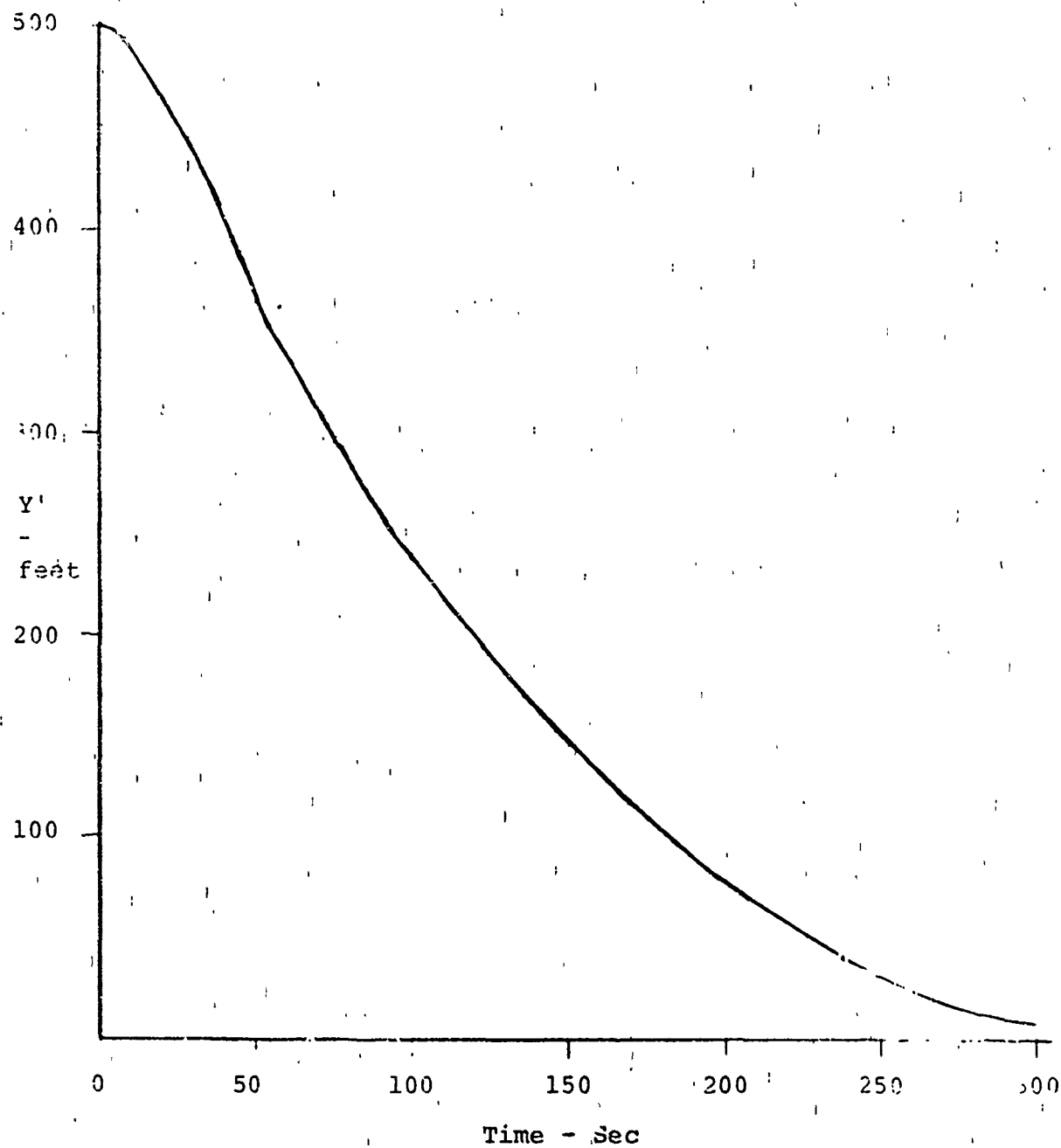


Figure 2.4.1-1 Nominal Model Lateral Deviation Response

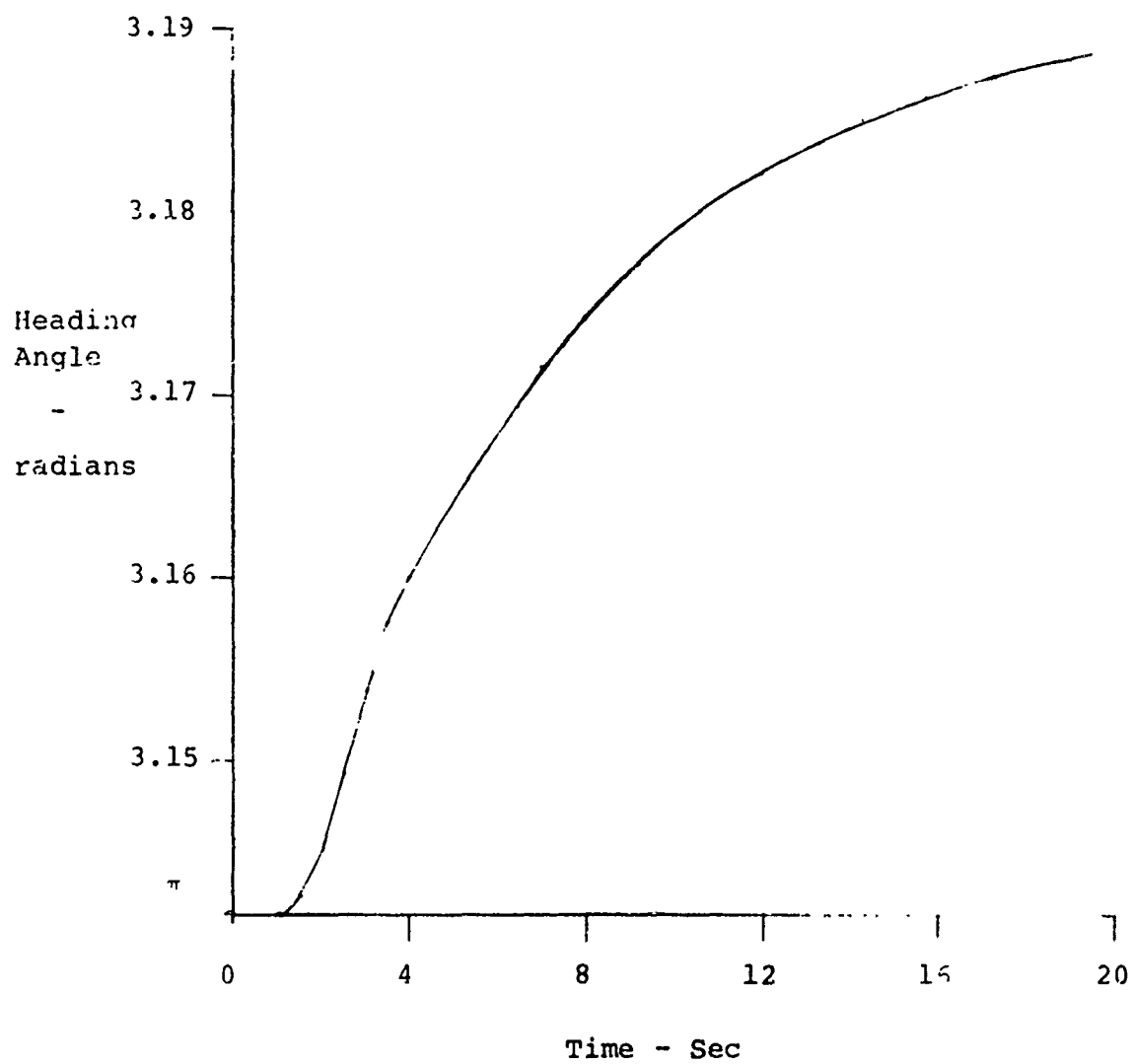


Figure 2.4.1-2 Nominal Model Heading Angle Response

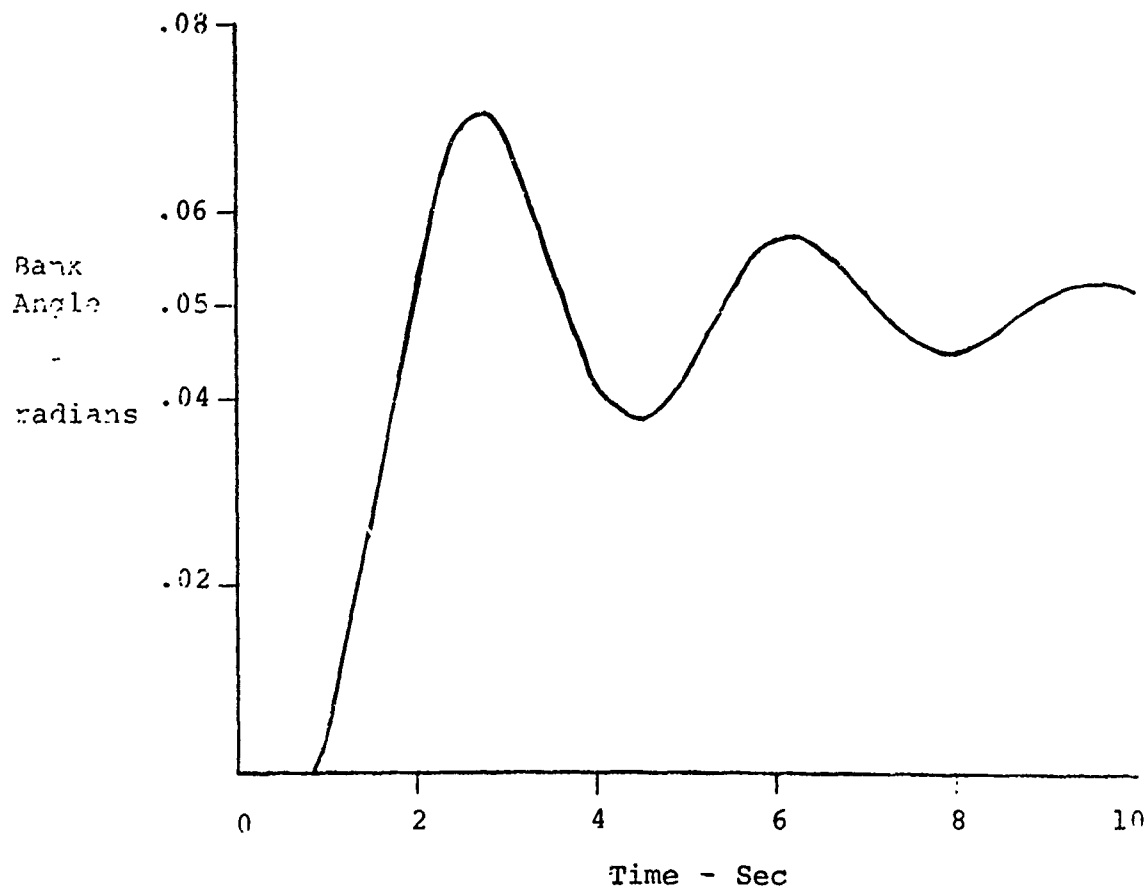


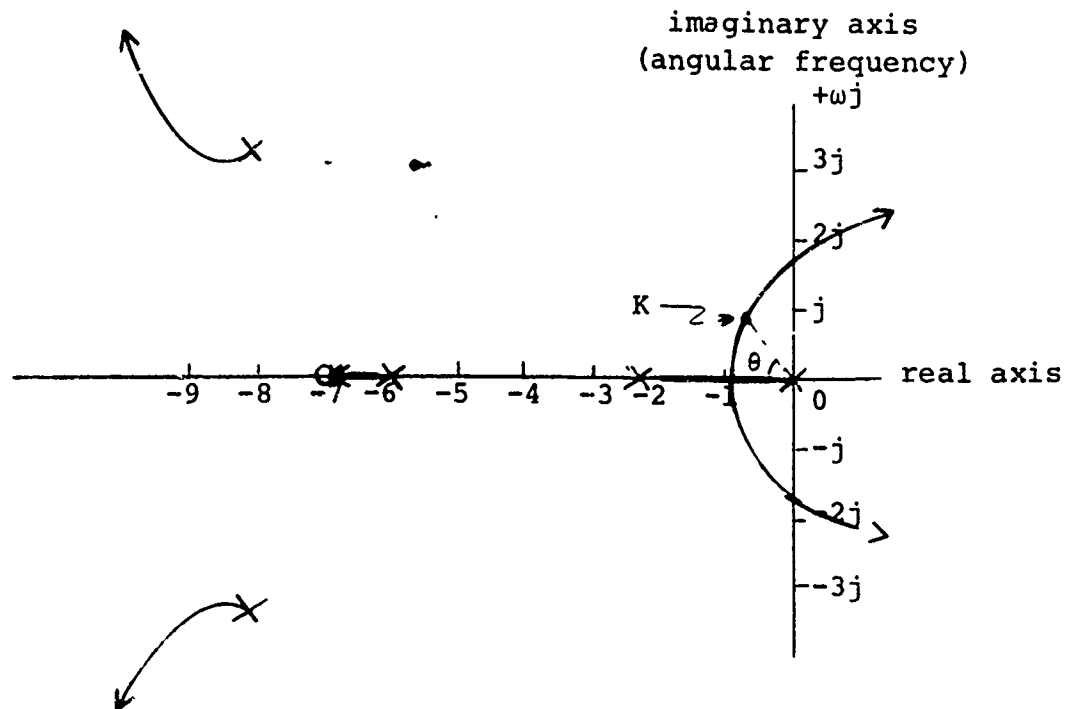
Figure 2.4.1-3 Nominal Model Bank Angle Response

to the pilot/control delay ($\tau_p = .7$ seconds) followed by an underdamped response characteristic of a pilot searching for a specific bank angle. This agrees with the transient response characteristics predicted by the root locus analysis discussed in Section 2.4.2.

2.4.2 FREQUENCY RESPONSE

The linear state equations derived in Section 2.1.5 were verified by performing a frequency response analysis (root locus). The time response of a closed-loop linear control system, such as that shown in Figure 2.1.2-8, is directly related to the location of the closed-loop roots of the characteristic equation in the s-plane (imaginary plane); therefore, a comparison can be made between the time response predicted by the root locus and the time response obtained by integrating the state equations.

The root locus technique is a graphical method for drawing the locus of roots in the imaginary plane as a particular parameter or gain is varied and provides a measure of sensitivity of the system roots to the parameter being varied. The root locus method provides indications of the relative stability and transient performance of a linear system. The locus of the roots of the characteristic equation begins at the poles and ends at the zeroes as the gain increases from zero to infinity. Figure 2.4.2-1 illustrates the basic components of a root locus.



- x pole
- o zero
- K gain corresponding to particular root on locus (operating point)
- ζ damping ratio, $\zeta = \cos \theta$ (for a 2nd order system only)
- direction corresponding to increasing gain

Figure 2.4.2-1 Basics of Root Locus

The complex conjugate roots nearest the origin of the imaginary plane are labeled the dominant roots of the system since they dominate the transient response. The relative dominance of the roots is determined by the ratio of the real parts of the complex roots and will result in reasonable dominance for ratios exceeding five to one.

When one pair of roots dominate, the system can be approximated by a second order linear system and concepts such as damping ratio and frequency can be evaluated from the root locus graph. Roots located on the real axis provide an overdamped response to a step input. Second order complex roots have a damping ratio equal to the cosine of the angle measured from the negative real axis to a vector drawn from the origin to the root, and roots to the right of the angular frequency axis indicate an unstable system.

A root locus analysis was performed on each of the three feedback loops (Y'/Y_d' , ψ/ψ_c , ϕ/ϕ_c) in the linear, simulated delay nominal model, Figure 2.1.2-8. The root locus of the entire system, or the Y'/Y_d' loop, is shown in Figure 2.4.2-2. It was derived by varying the pilot gain on the displacement error from the localizer (K_{ϵ}'). The control system is a 7th order system and thus has seven poles and two zeroes as shown.

The operating points (K_{ϵ}') are determined by fitting the nominal model to the set of nominal measured distribution data from Section 2.3. A discussion of this model fitting task is contained in Section 2.4.3.

The nominal system operating points vary with range (X'). From Equation 2.1.2-7, a value of K_{ϵ_e} equal to 4.8 yields

$$K_{\epsilon_e}' = \begin{cases} .000075 & \text{at } 9 \text{ N Mi.} \\ .000354 & \text{at } .75 \text{ N Mi.} \end{cases}$$

The variation of the operating points on the root locus corresponds to the variation of system sensitivity with range as expected in the physical system. For these operating points the two roots nearest the origin are shown to dominate because the ratio of their real parts to the next most dominant pair is always greater than five to one. This result validates the approximation made in Section 2.2.1.2 which stated that the system model could be accurately represented by a second order system.

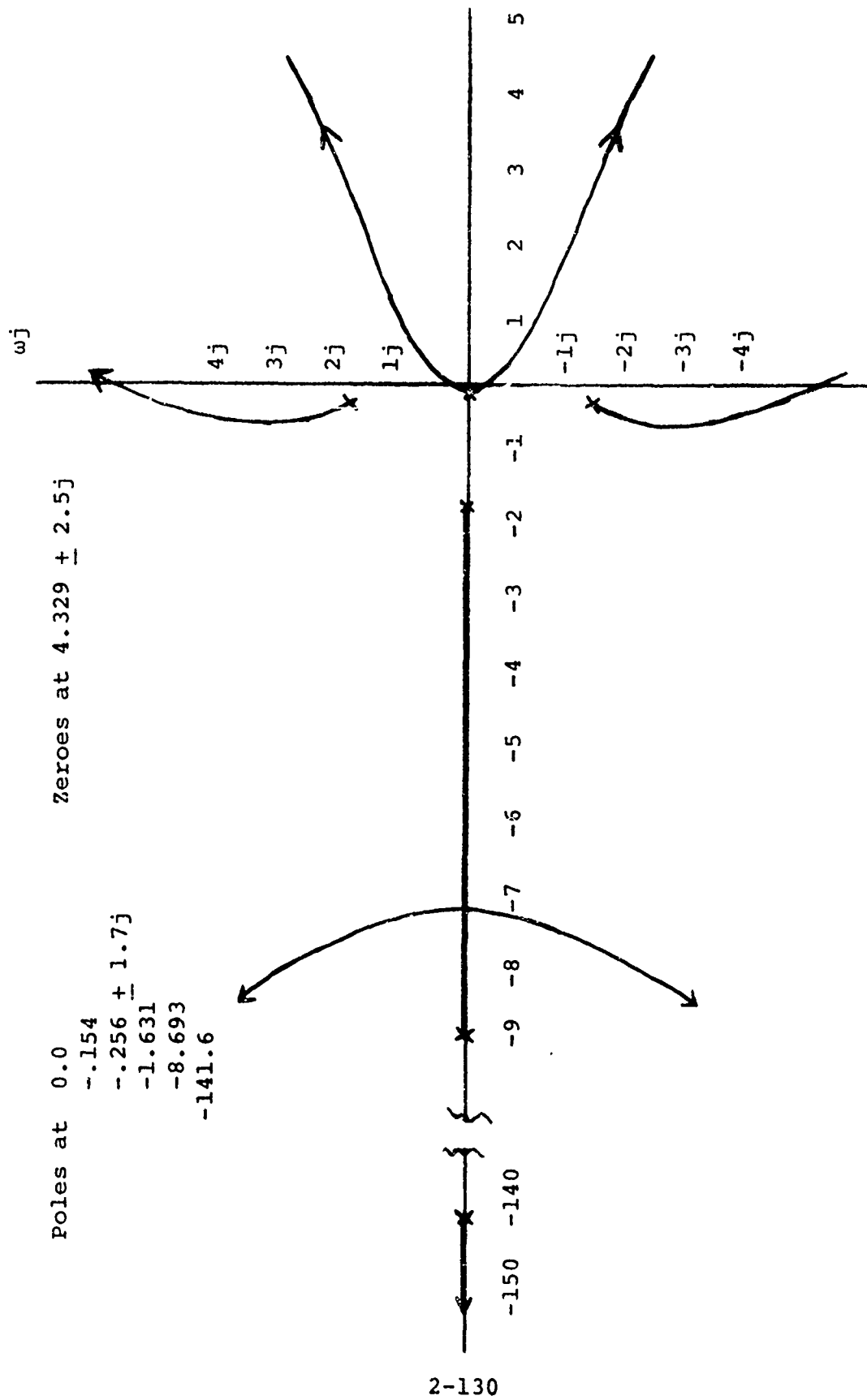


Figure 2.4.2-2 Root Locus of $\frac{y'}{y} \text{ Loop}$

The detail view of the dominating roots is shown in Figure 2.4.2-3. At ranges greater than 1.25 miles ($K'_{\epsilon} = .0003$) the system is seen to be overdamped ($\zeta \geq 1$); however, as range decreases the system sensitivity to lateral error increases, resulting in a slightly underdamped system ($\zeta < 1$). At the point where the system goes visual ($X' = .75$ N Mi.), the damping ratio is approximately .9. For values between .0003 and .0065 the system is underdamped and for values greater than .0065 the system is unstable.

In order to verify the system model state equations, the system response characteristics predicted by a root locus analysis were compared to those characteristics obtained by integrating the state equations. A gain value of $K'_{\epsilon} = .004$, located as shown in Figure 2.4.2-3, was selected as the gain for the comparison. At this gain the two loci shown dominate the system. Therefore, the damping ratio and frequency can be determined from the root locus since the system can be approximated by a 2nd order system. Furthermore, the integration of the state equations for this gain value provides a time response from which the damping ratio and frequency can be obtained. The time response is shown in Figure 2.4.2-4.

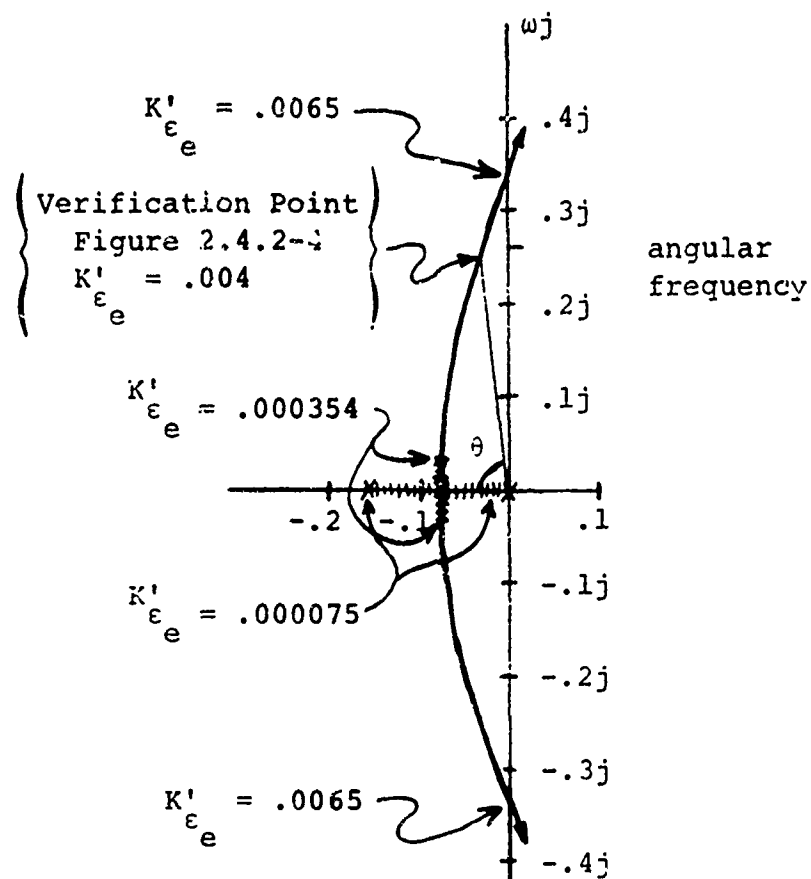
The damping ratio is computed from the root locus as

$$\zeta = \cos \theta = .105.$$

The damping ratio can be calculated from the time response by determining the percentage of overshoot and using the graph in Figure 2.4.2-5. In this particular case there is a 72.8% overshoot which indicates a damping ratio of approximately .1 which compares with the value independently derived from the root locus.

The angular frequency can be calculated from Figure 2.4.2-5 by reading a value of $\omega_n T_p$, which is the angular frequency times the peak time. From Figure 2.4.2-4 the peak time is 11.8 seconds, the $\omega_n T_p$ value is 3.18 and ω_n is .27. The angular frequency from the root locus plot is 0.269, which compares favorably to the value obtained from the time response.

The root locus of the ψ/ψ_c loop was obtained by varying the pilot gain on the heading angle error, K_{ψ} , and is shown in Figure 2.4.2-6. This loop is a 6th order system and has the six poles and two zeros shown. For small values of K_{ψ} the dominant roots are the four shown in Figure 2.4.2-7. For values of K_{ψ} greater than 4.3, the two imaginary roots nearest the frequency axis dominate. Furthermore, for values



Poles at 0 and $-.154$

Breaking Point at $K'_{\epsilon_e} = .0003$

Locus Crosses Imaginary Axis at $K'_{\epsilon_e} = .0065$

Operating Points //

Figure 2.4.2-3 Root Locus of $\frac{Y'}{Y_d}$ Loop - Detail View of Dominant Roots

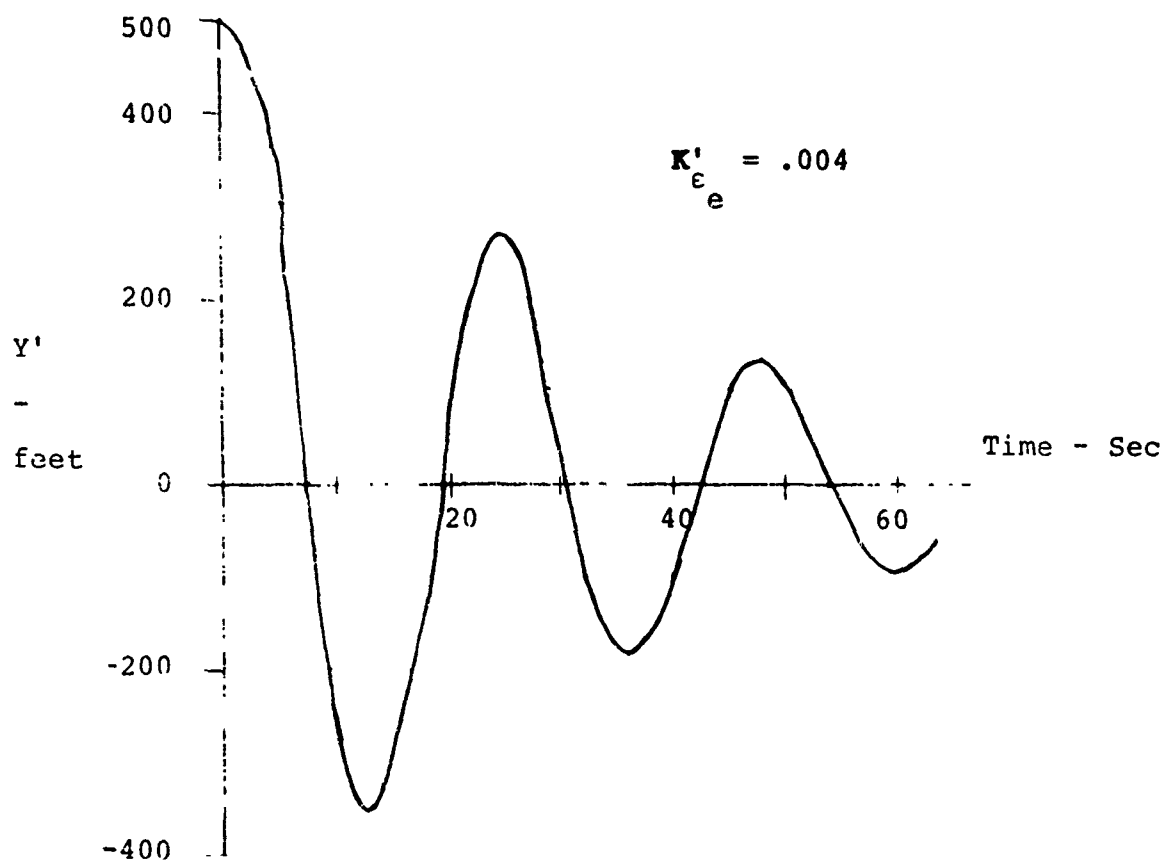


Figure 2.4.2-4 State Equation Verification Time Response

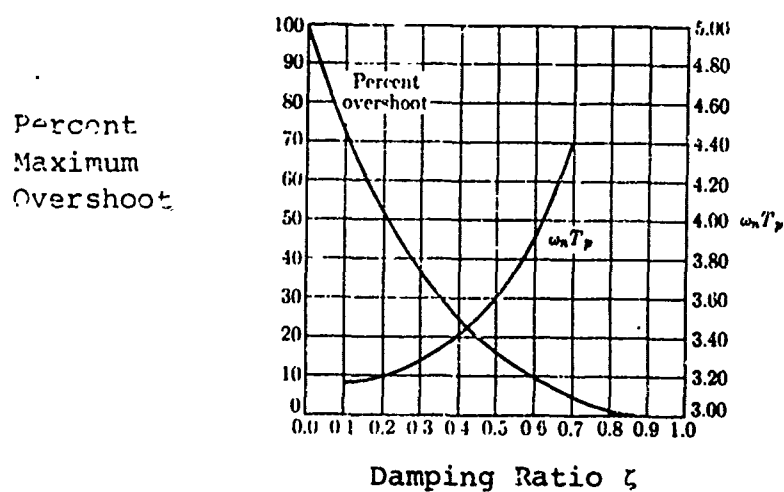


Figure 2.4.2-5 Percent Overshoot and Peak Time versus Damping Ratio for a Second-Order System (Reference 2)

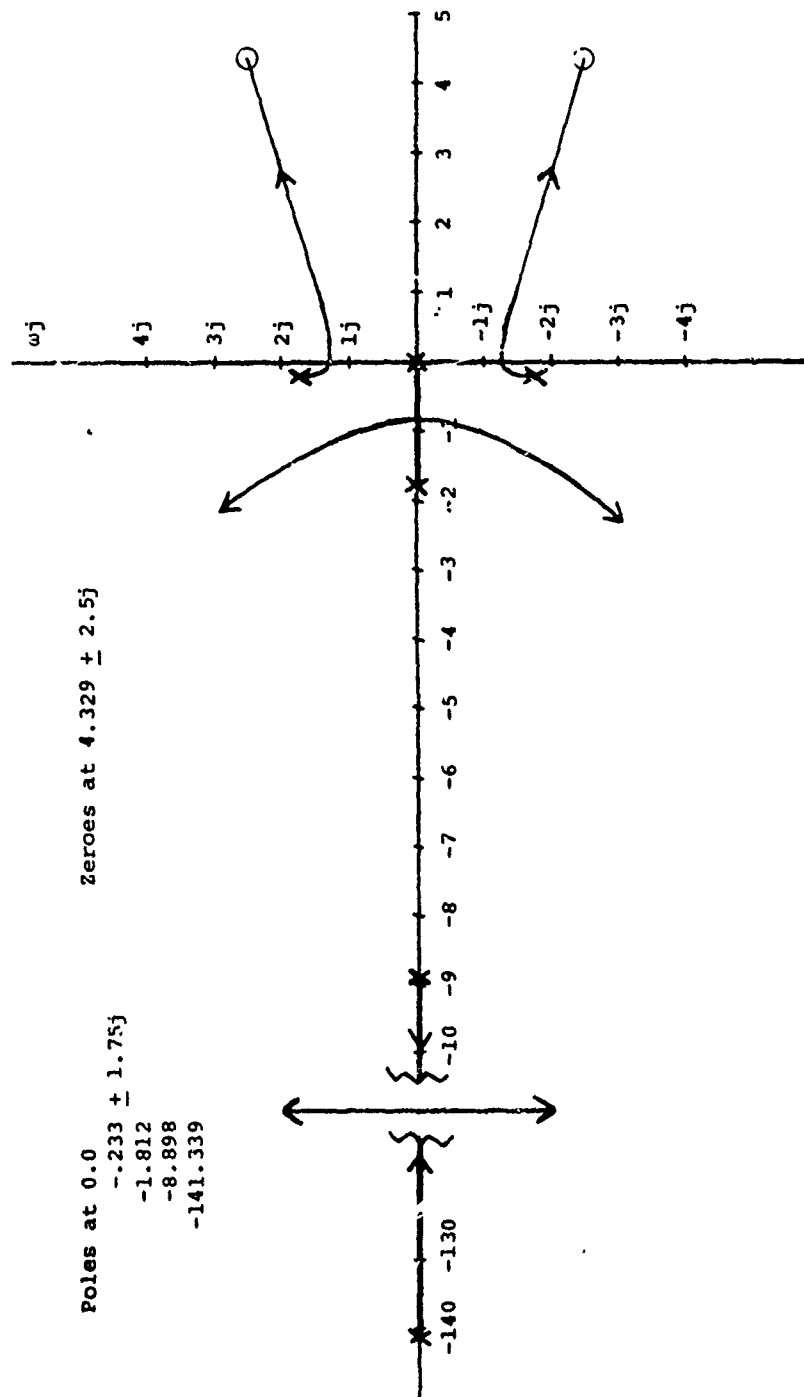
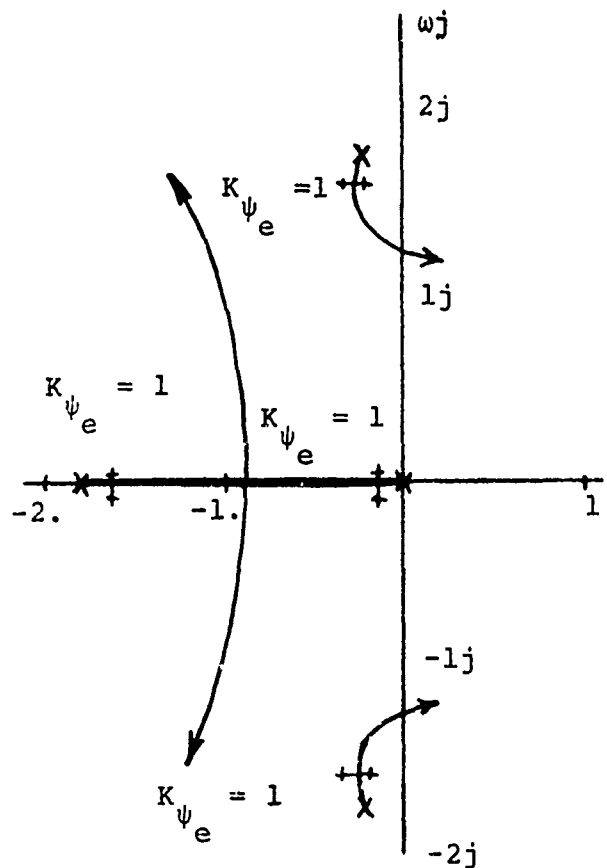


Figure 2.4.2-6 Root Locus of $\frac{\psi}{\psi_c}$ Loop



Poles at 0

$-.233 \pm 1.75j$

-1.812

Zeros at $4.329 \pm 2.5j$

Breakaway Point at $K_{\psi_e} = 2.7$

Locus Crosses Imaginary Axis at $K_{\psi_e} = 6.2$

† Operating Point at $K_{\psi_e} = 1.0$

Figure 2.4.2-7 Root Locus of $\frac{\psi}{\psi_c}$ Loop - Detail View of Dominant Roots

of K_{ψ_e} greater than 6.2 the system is unstable. The operating point of the nominal system is a constant value of 1. and is located on the loci as shown in Figure 2.4.2-7.

The ϕ/ϕ_c loop represents a fifth order system. The root locus was obtained by varying the aircraft response gain, K_a . The five poles and two roots are shown in Figure 2.4.2-8. For values of K_a greater than .1 the dominant roots are those shown in Figure 2.4.2-9. This loop becomes unstable for values of K_a greater than 1.35. The nominal system operating point is $K_a = 1$. As shown in Figure 2.4.2-9, the root locus predicts an underdamped system which is reflected in the oscillatory time response shown in Figure 2.4.1-3.

2.4.3 STATISTICAL RESPONSE

A statistical response analysis was performed in order to determine the model parameter values, errors, and initial state distributions, which fit the nominal system model predicted distribution to the nominal measured distribution data discussed in Section 2.3.

The nominal model parameter and error values are listed in Table 2.1.2-2. However, due to the nature of some of these parameters and errors (primarily those due to pilot attitude and pilot errors), it was necessary to determine particular ones by fitting the model to measured field data.

The initial distribution for the lateral deviation is known from the measured field data; however, the initial distributions for the remaining states of the system must be determined.

This analysis was conducted by considering the variance propagation of the linear model with gaussian inputs (Appendix D). The mean and variance of the response of a linear system with gaussian input distributions give a complete statistical description of the process, because the system output is also gaussian. In order to determine the parameters, errors and initial distributions, nominal measured distribution data, in the form of the lateral distribution standard deviation (σ_Y) as a function of range (X'), was matched by the statistical system response of the linear nominal model with gaussian input.

The model fitting task was accomplished by utilizing the nominal model parameter and error values determined in Sections 2.1.2 and 2.1.4, an initial lateral deviation

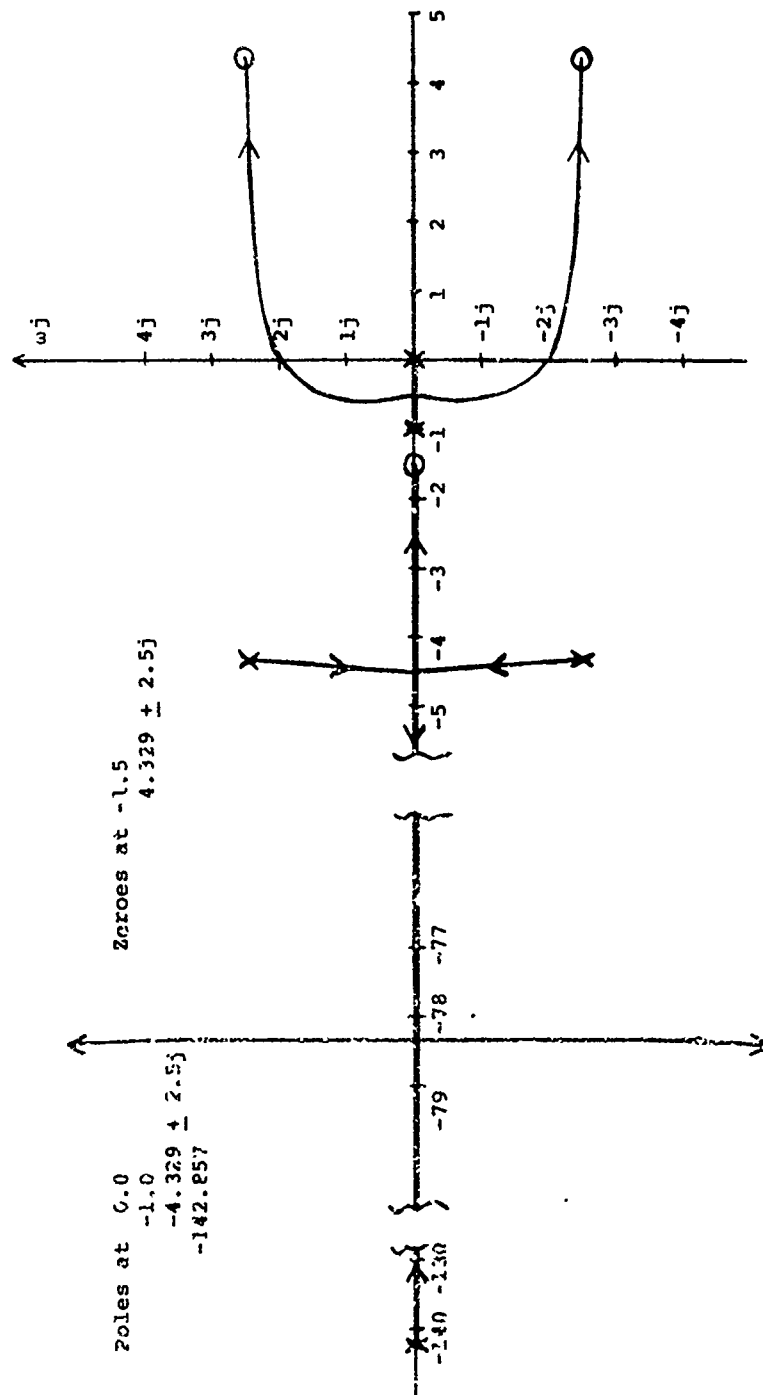
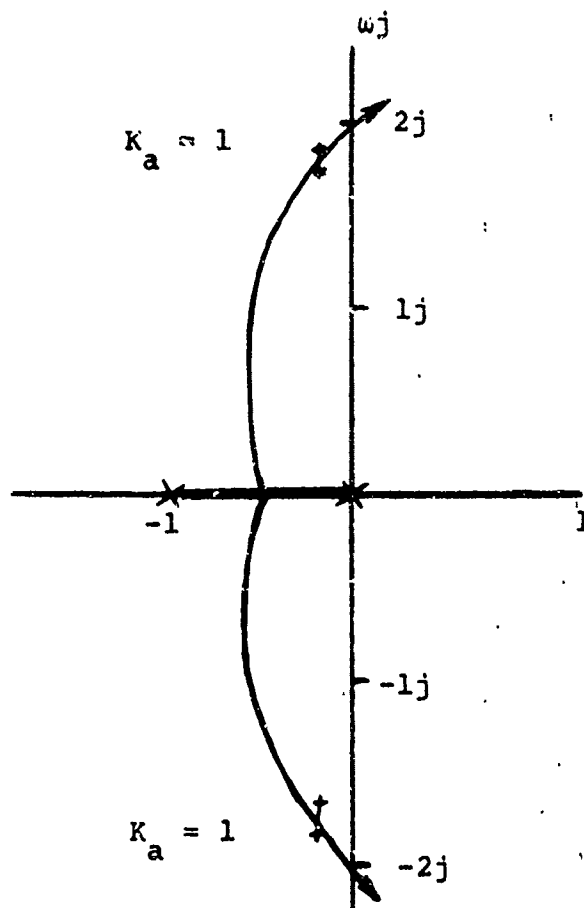


Figure 2.4.2-8 Root Locus of $\frac{\phi}{\phi_c}$ Loop



Poles at 0 and -1

Breakaway Point at $K_a = .15$

Locus Crosses Imaginary Axis at $K_a = 1.35$

† Operating Point at $K_a = 1.0$

Figure 2.4.2-9 Root Locus of $\frac{\phi}{\psi_c}$ - Detail View of Dominant Roots

distribution which was assumed gaussian (Y'_0), assumed initial distributions on the remaining states of the system (defined in Section 2.1.5 as ψ_0 , ϕ_0 , and intermediate states), and the nominal measured distribution data (from Appendix E) in the form of $\sigma_{Y'}$ versus X'). The pertinent model parameters, errors and initial distributions were adjusted, within reasonable bounds, from their original estimates, and their effects on the lateral deviation distribution were determined. Some of these effects are shown in Figure 2.4.3-1. By observing these effects on the lateral distribution, reasonable adjustments were made to the pertinent model parameters, errors and initial distributions until an acceptable fit was obtained.

It was assumed that only the model parameters and errors due to pilot attitude and pilot errors would be adjusted to fit the field data.

Since the pilot's primary controlling parameter is the aircraft bank angle (ϕ), the bank angle pilot error (N_ϕ) is assumed to contain the major effects of the pilot's attitude and errors. Since the pilot gain on the lateral error from the localizer (K_{ϵ_e}) affects the system's transient response, as shown in Section 2.4.2, it is assumed that K_{ϵ_e} is also significantly affected by pilot attitude. The values of the various model pilot error distributions, determined in Section 2.1.4, were investigated. The pilot errors estimated in that section were tested and found to be valid with the exception of the pilot bank angle error, N_ϕ . For the above reasons, the original estimates of all model parameters and errors except N_ϕ and K_{ϵ_e} will remain unchanged.

The effect of K_{ϵ_e} is shown in Figure 2.4.3-1 to affect the general slope of the statistical response. The optimum value for K_{ϵ_e} was 4.8 which corresponds to K'_{ϵ_e} varying between .000075 at nine miles and .000354 at .75 miles from touchdown. (Equation 2.1.2-7)

After several attempts at fitting the measured distribution, it was apparent that the standard deviation of the bank angle error decreased as the pilot neared touchdown. For the optimum fit to the nominal measured data, the standard deviation of N_ϕ ranges from 6° at nine miles from touchdown to 2.5° at touchdown. The effect of a greater noise N_ϕ is shown in Figure 2.4.3-1.

Since only the initial distribution on the lateral deviation (Y'_0) was available, it was necessary to determine the initial distribution on the remaining states. The linear seventh order state equations from Section 2.1.5

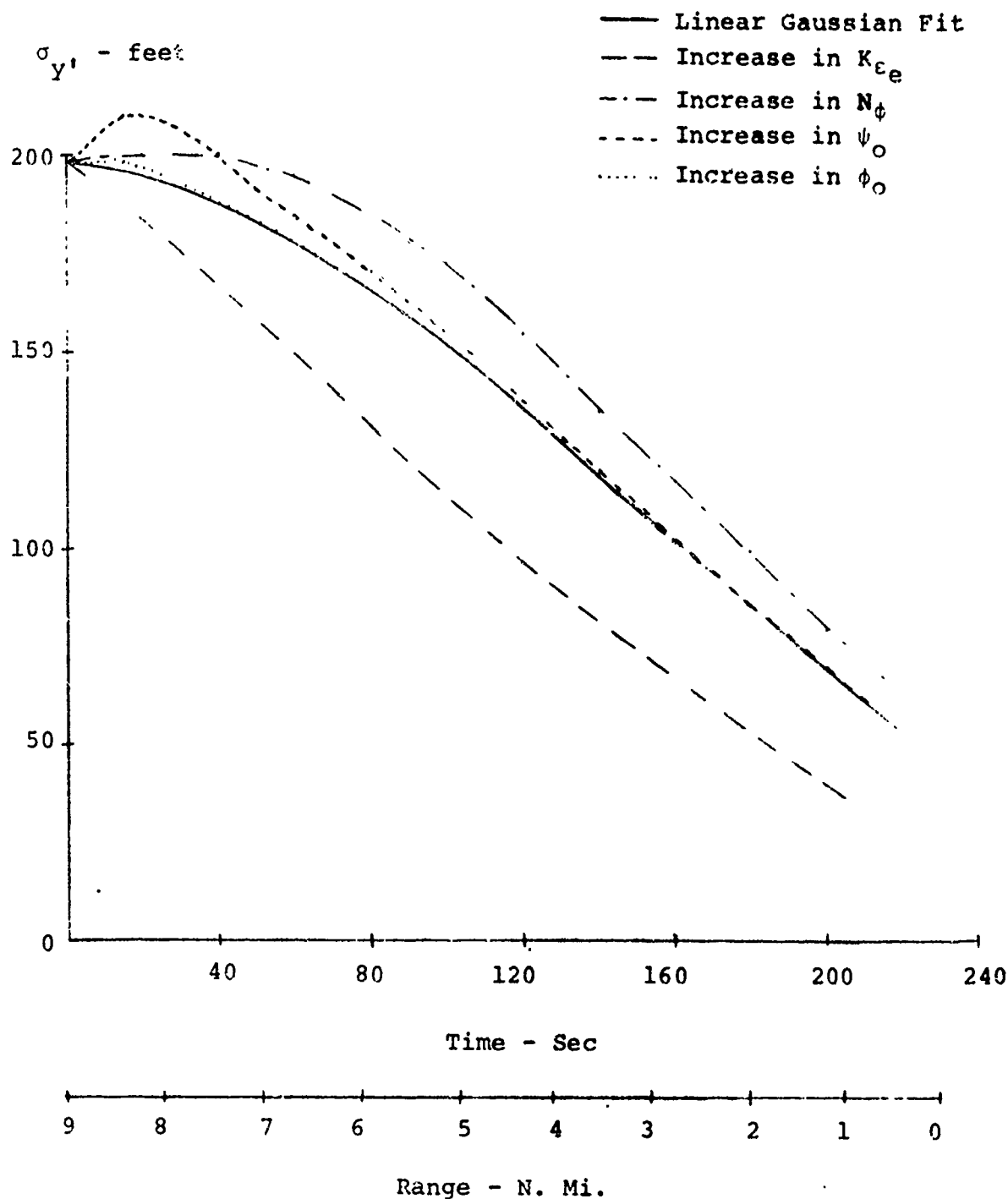


Figure 2.4.3-1 Effect of an Increase in $K_{\epsilon e}$, N_{ϕ} , ψ_0 or ϕ_0 on the Statistical Response

were reduced to a linear sixth order system as described in Section 2.2.1.2; therefore, the initial state distributions for ψ_0 , ϕ_0 , and three intermediate states were needed at the initial range (9Nmi). The original estimates of the initial state distributions were made by observing the state values of the linear nominal model for reasonable operating conditions. These original estimates were then adjusted to fit the nominal measured distribution data in the manner described previously.

The effects of the initial distributions on the lateral deviation distribution were determined as shown in Figure 2.4.3-1. As can be seen, larger initial heading angle and bank angle standard deviations cause σ_y to increase initially and hold that increased value for a period of time. Based upon these observed effects the initial state distributions were adjusted within reasonable physical bounds until an acceptable fit was obtained. Since the intermediate states (IS) are a result of the simulated delay approximation, they have no observable physical characteristics. Thus, the original estimates, which seem adequate for the system, were retained. The resulting initial state distributions are shown in Table 2.4.3-1 and

Table 2.4.3-1
Nominal Model Initial State Distributions (at $X'_0 = 9\text{Nmi}$)

State	Symbol	σ^*	Units
X_{10}	Y'_0	198	feet
X_{20}	ψ_0	.02	radians
X_{30}	ϕ_0	.01	radians
X_{40}	IS	.12	
X_{50}	IS	.26	
X_{60}	IS	.54	

*Assumed Gaussian- mean = 0, variance = σ^2

the resulting nominal model fit to the nominal measured field data is shown in Figure 2.4.3-2.

2.4.4 SENSITIVITY ANALYSIS

The purpose of the sensitivity analysis is to identify the effects of selected pertinent model parameters and model errors on the lateral distribution of aircraft on the approach system. The sensitivity analysis was performed by utilizing the nominal system model defined in Section 2.1.2, with specific initial conditions, as the reference condition. Each of the pertinent parameters and errors of the nominal system model was varied about its nominal value and the resulting sensitivity coefficient of the lateral deviation or lateral distribution standard deviation was calculated at various points in range.

A sensitivity coefficient is defined by the following equation:

$$S_P^X = \frac{\Delta X}{\Delta P},$$

where ΔX is the change in a specific system variable due to the change of ΔP , and ΔP is the change in the selected parameter or error. The sensitivity coefficient, S_P^X , identifies the change in a system variable, X , caused by a change in a parameter, P . It should be noted that the sensitivity coefficient is only valid for small changes in the varied parameter about the reference condition.

The system parameter sensitivity analysis (Section 2.4.4.1), performed by utilizing a deterministic model (no random errors), was used to find the sensitivity coefficients for the pertinent parameters of the nominal nonlinear system model.

The system error sensitivity analysis (Section 2.4.4.2) utilized the linear system nominal model with gaussian inputs and the variance propagation technique described in Appendix D. It was performed to find the sensitivity coefficients for the pertinent errors of the linear system model.

2.4.4.1 System Parameter Sensitivity

The nominal nonlinear system model (Figure 2.1.2-6) was used to determine the sensitivity of the lateral deviation (Y') to some of the pertinent parameters of the system model. The analysis was performed deterministically (no

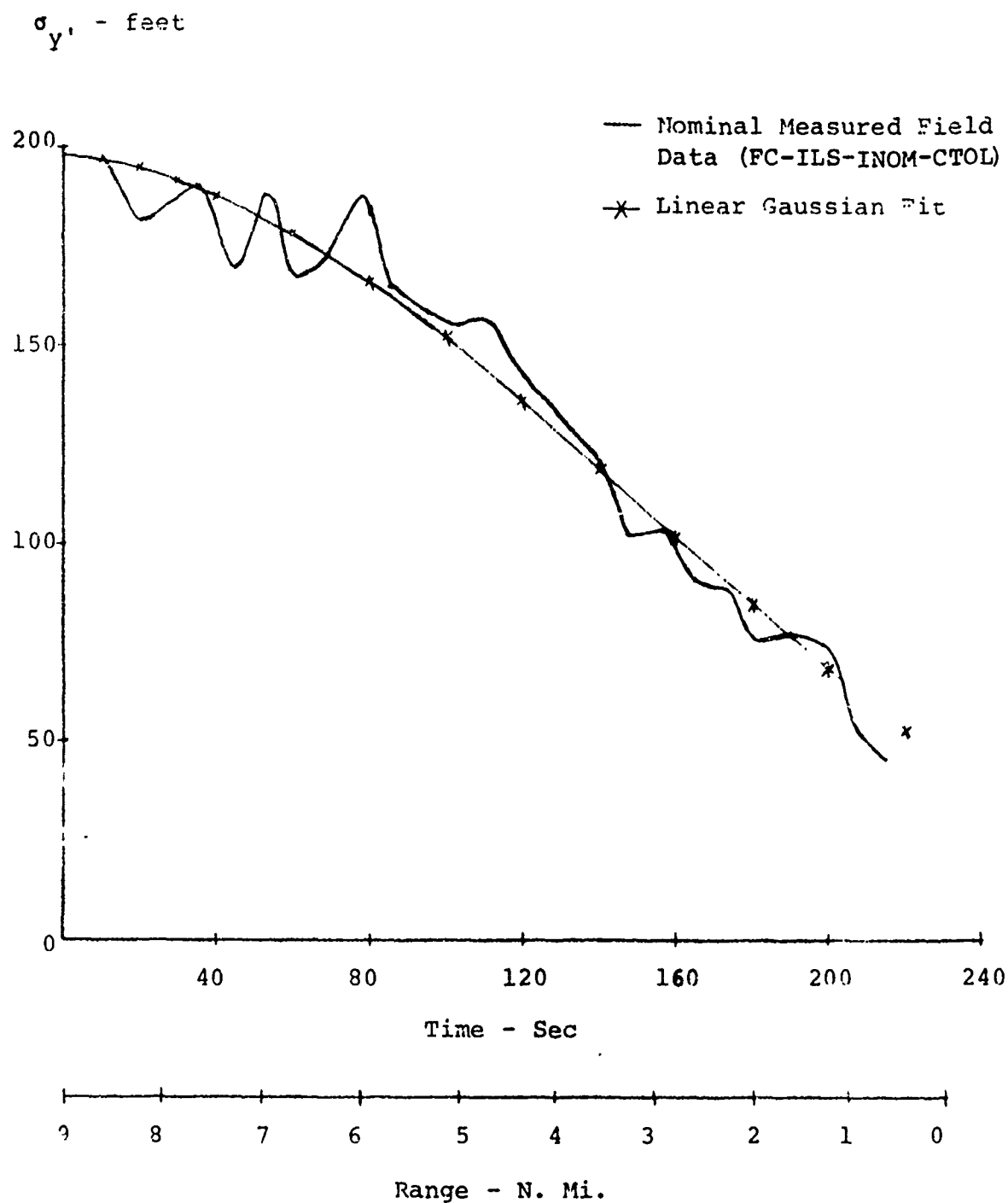


Figure 2.4.3-2 Nominal Model Fit to Nominal
Measured Distribution Data

random inputs). The symbols of these parameters along with their descriptions, reference values, and units are listed in Table 2.4.4-1. The initial conditions are all zero except for the following:

$$Y'_0 = 500 \text{ ft.}$$

$$X'_0 = 13.53 \text{ NMi.}$$

$$\psi_0 = 3.14159 \text{ rad.}$$

Each of the parameters was varied (ΔP), and the resulting lateral deviation response predicted by the system model was observed at various points of range and time. By comparing this lateral deviation response to the response predicted by the nominal system model, $\Delta Y'$ was determined and the sensitivity coefficient was calculated by the following equation.

$$S_P^{Y'} = \frac{\Delta Y'}{\Delta P}$$

The $\Delta Y'$ is the change in the lateral deviation due to the change of ΔP , and ΔP is the change in the selected parameter. An illustration of the parameter sensitivity analysis technique is shown in Figure 2.4.4-1.

The sensitivity coefficients of each parameter from Table 2.4.4-1 were calculated and plotted at common points in range. The resulting sensitivity curves, presented in Appendix F, illustrate the sensitivity of the lateral deviation to each of the pertinent parameters as a function of range and time. A typical example from parameter sensitivity curves of Appendix F is shown in Figure 2.4.4-2. It illustrates the sensitivity of the lateral deviation to the pilot gain on heading angle error as a function of range and time about the given reference condition.

2.4.4.2 System Error Sensitivity

By using the method of variance propagation for a linear gaussian system described in Appendix D, the linear system nominal model was used to find the sensitivity of the lateral distribution standard deviation ($\sigma_{Y'}$) to the standard deviation (σ_N) of some of the pertinent system errors. The symbols representing these errors, along with their descriptions,

Table 2.4.4-1 Sensitivity Analysis Parameters

Symbol	Reference Value	Units	Description
V	236.4444	ft/sec	Aircraft airspeed
K_{ϵ_e} (angular)	4.8	rad/rad	Pilot tracking gain on the angular localizer error
K_{ψ_e}	1.0	rad/rad	Pilot gain on heading angle error
K_{ψ}	1.9	rad/rad	Pilot gain on heading angle feedback
K_{ϕ}	1.333	sec	Pilot gain on the bank angle divided by a_{ϕ}
K_a	1.0	1/sec ²	Aircraft bank rate to aileron response gain multiplied by a_a
a_a	1.0	1/sec	Inverse of the aircraft bank rate to aileron response time constant
a_{ϕ}	1.5	1/sec	Inverse of the pilot lead time constant on bank angle feedback
τ_p	0.7	sec	Pilot/control delay
L	9000.0	ft	-X coordinate of the lateral guidance transmitting antenna

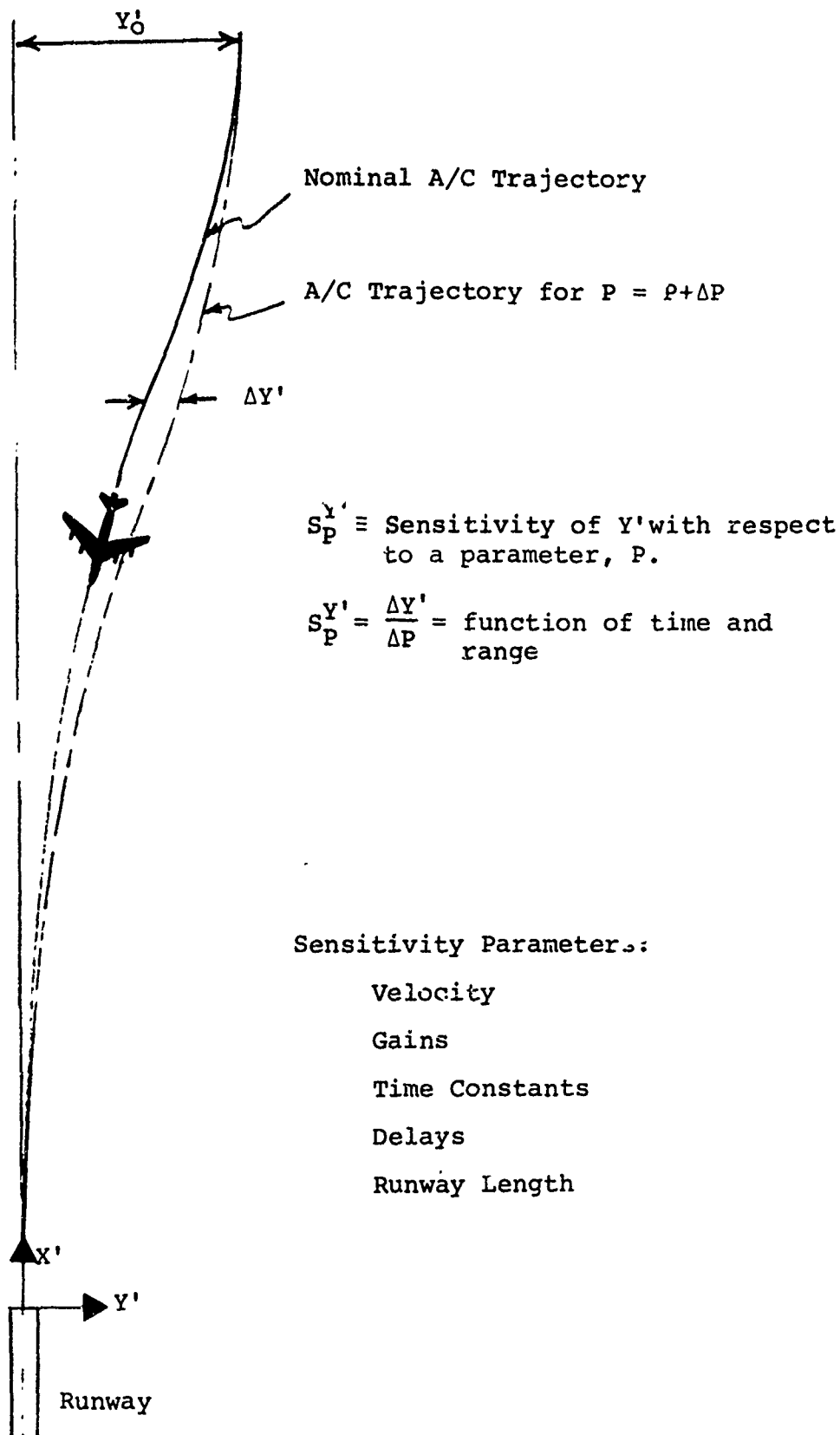


Figure 2.4.4-1 System Parameter Sensitivity

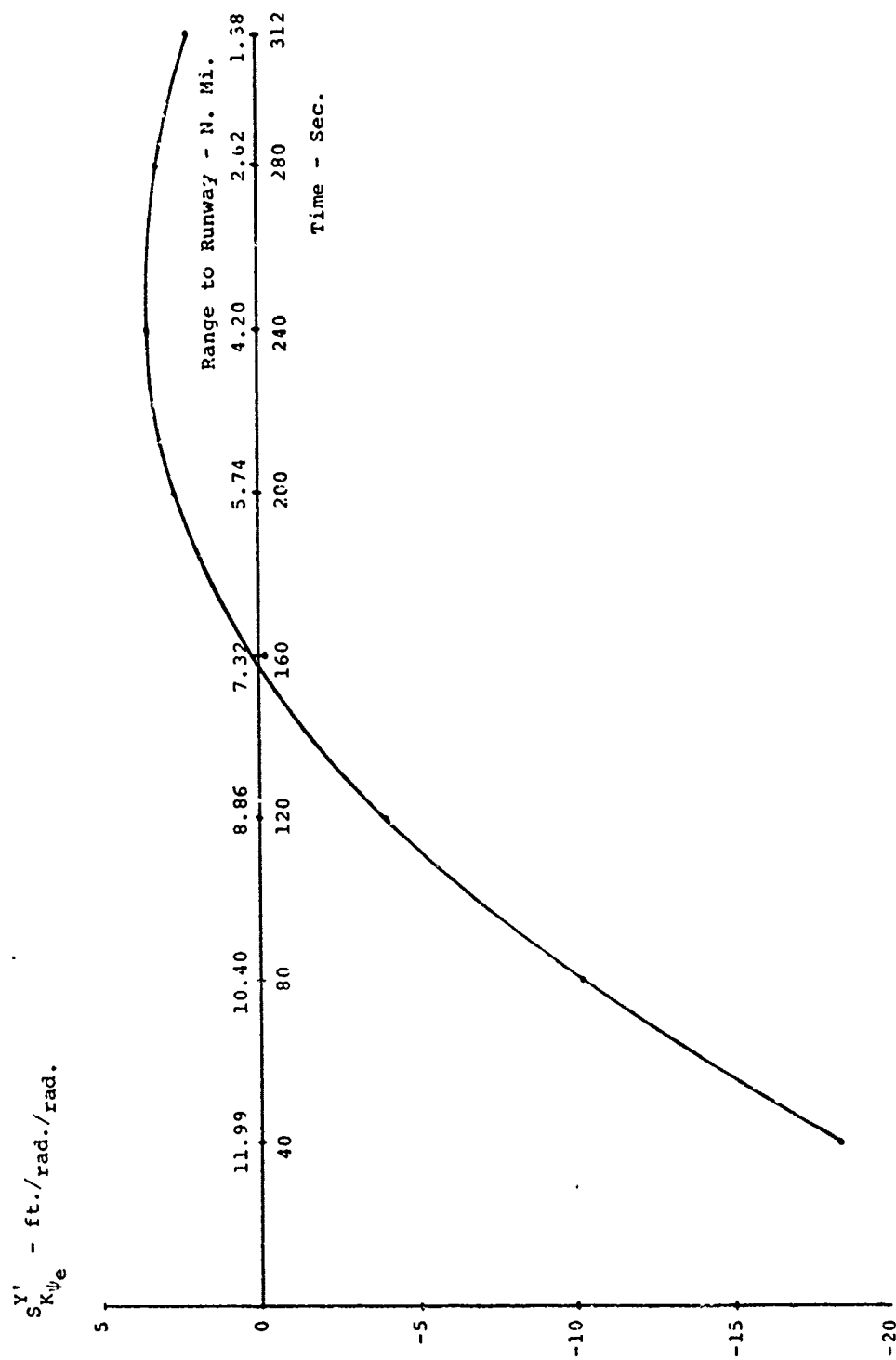


Figure 2.4.4-2 Lateral Deviation Sensitivity Coefficients With Respect to K_{ψ_e}

reference values, and units are listed in Table 2.4.4-2. The initial state distributions are defined in Table 2.4.3-1. Each of the error distribution standard deviations was changed some $\Delta\sigma_N$, and the resulting lateral distribution standard deviation response was observed at specific points in range and time. By comparing this lateral distribution standard deviation response to the response predicted by the nominal model, $\Delta\sigma_{Y'}$, was determined at each range point allowing the sensitivity coefficient to be calculated by the equation

$$S_{\sigma_N}^{\sigma_{Y'}} = \frac{\Delta\sigma_{Y'}}{\Delta\sigma_N}.$$

The $\Delta\sigma_{Y'}$ is the change in the lateral distribution standard deviation due to the change of $\Delta\sigma_N$, and $\Delta\sigma_N$ is the change in the selected error. An illustration of the error sensitivity analysis technique is shown in Figure 2.4.4-3.

The sensitivity coefficients for each error were calculated and plotted at common points in range. The resulting sensitivity curves, presented in Appendix F, illustrate the sensitivity of the lateral distribution standard deviation to the standard deviation changes in some of the pertinent system errors as a function of range and time. A typical example from the error sensitivity curves in Appendix F is shown in Figure 2.4.4-4. It illustrates the sensitivity of the lateral deviation distribution to the initial heading angle distribution about the given reference condition.

Table 2.4.4-2 Sensitivity Analysis Errors

Symbol	Reference Value (Rad.)	Description
$\sigma_{N_{\psi}}$.01745	Pilot heading angle error distribution standard deviation
$\sigma_{N_{\phi}}$.1047 @ 9Nmi .0436 @ 0Nmi	Pilot bank angle error distribution standard deviation
σ_{ILS_R}	.00048	ILS equipment receiver error distribution standard deviation
σ_{ILS_T}	.001497	ILS equipment transmitter error distribution standard deviation
$\sigma_{N_{\epsilon}}$.00349	Pilot localizer tracking error (final leg) distribution standard deviation
σ_{ψ_0}	.02	Initial condition on heading state distribution standard deviation

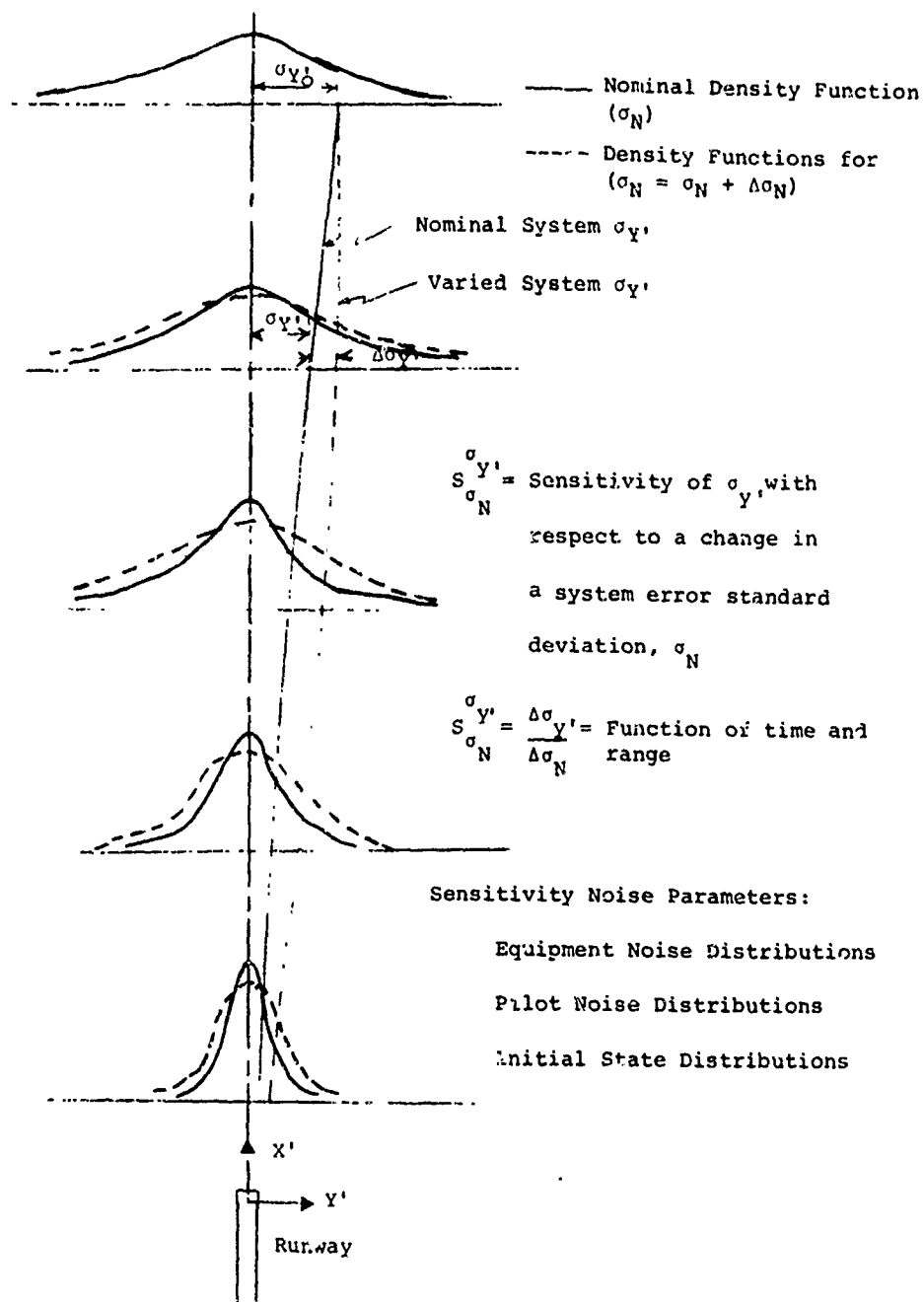


Figure 2.4.4-3 System Error Sensitivity

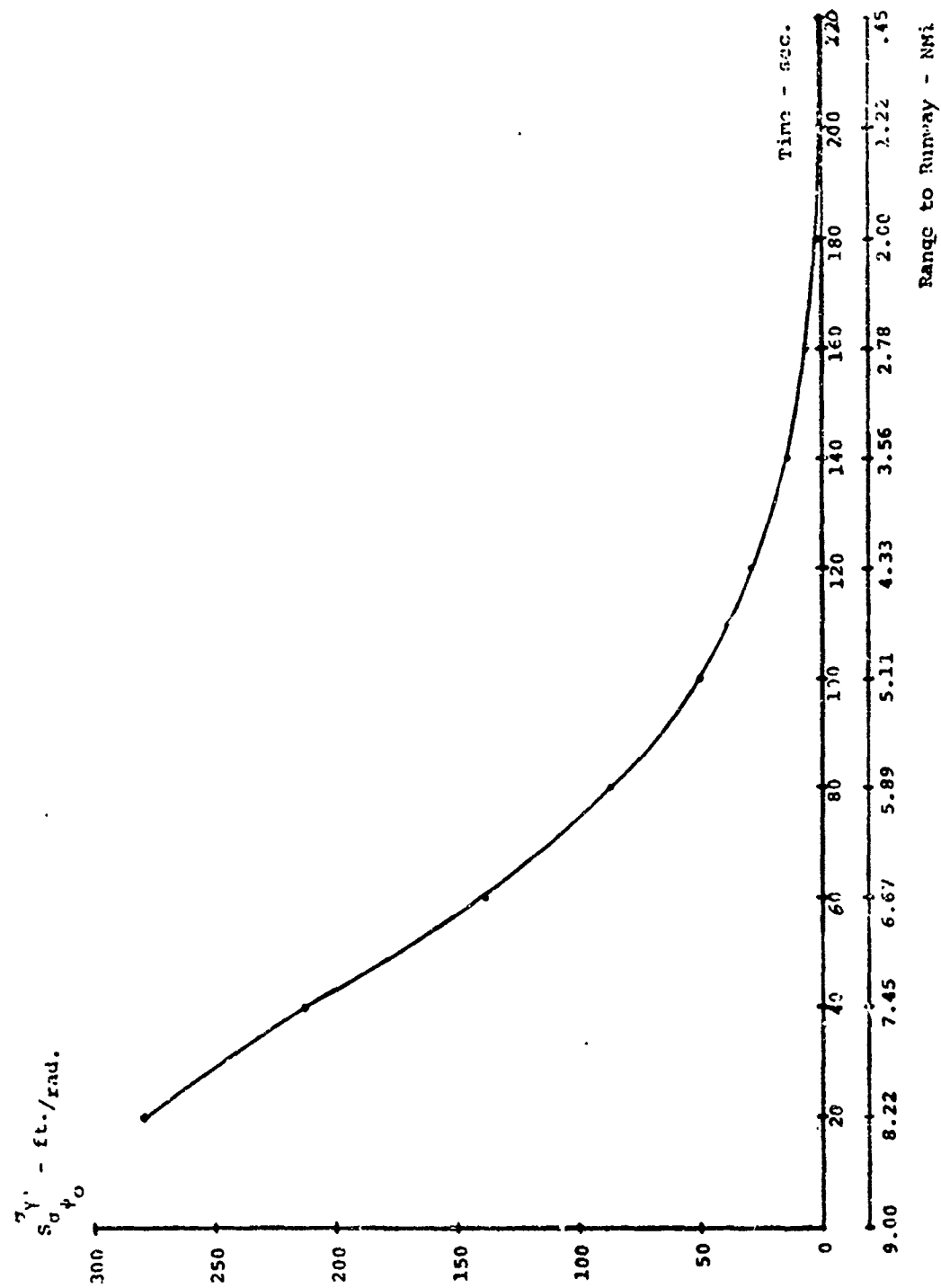


Figure 2.4.4-4 Lateral Distribution Sensitivity Coefficients σ_y With Respect to σ_{ψ_0}

REFERENCES

1. Teper, G. L. and R. L. Stapleford, "An Assessment of the Lateral-Directional Handling Qualities of a Large Aircraft in the Landing Approach", J. Aircraft, Vol. 3, No. 3, May-June, 1966.
2. Dorf, Richard C., Modern Control Systems, Addison-Wesley Publishing Company, Reading, Massachusetts, 1967, p91.

SECTION 2.5

PROBABILITY DENSITY FUNCTIONS AND NORMAL OPERATING ZONES

A positional error probability density function (PDF), as utilized in this study, is a statistical description of the errors about an "ideal track". It is defined for a composite set of aircraft flying the final leg of an instrument approach under IFR conditions. A complete three dimensional statistical description of these errors is required to aid in the generation of data necessary to determine minimum runway spacings. For this reason, the positional error probability density space consists of three dimensions (lateral, vertical, and longitudinal).

The primary dimension utilized in the lateral separation criteria determination is the lateral dimension. For this reason, lateral approach system models are developed which accurately generate the lateral PDF for the required approach systems. Development of these models is accomplished by adapting the nominal system model, developed in Section 2.1 and verified in Section 2.4, to the measured distribution data from Section 2.3. This process is described in Section 2.5.1.

One purpose of this section is to describe the generation of the PDF's required in the probability of collision determination (Section 2.6) and in the NOZ determination. The generation of these PDF's is discussed in Section 2.5.2. This discussion is divided into three parts: lateral (Section 2.5.2.1), vertical (Section 2.5.2.2), and longitudinal (Section 2.5.2.3). The method for generating the required lateral PDF's utilizes the Fokker-Planck equation (Section 2.2) with the lateral approach system models from Section 2.5.1. The vertical error PDF's are determined from the measured distribution data from Appendix E. The longitudinal error density is determined from an assumed constant velocity error distribution from Section 2.3.

A second purpose of this section is to describe the generation of the required normal operating zones (NOZ) to be used in the determination of minimum runway spacings. The generation of the NOZ is discussed in Section 2.5.3 for approach systems in general (Section 2.5.3.1) and for CTOL/STOL skewed operations (Section 2.5.3.2).

2.5.1 LATERAL PROBABILITY DENSITY FUNCTION MODELS

Before a lateral probability density function can be generated for a particular approach system, it is necessary

to develop a model which accurately simulates the dynamics of that approach system. Furthermore, it is necessary to derive the state equations from that model to be incorporated into the Fokker-Planck equation to allow the PDF to be generated. This section is a description of the method utilized to develop the approach system models listed below.

1. Front Course-ILS-Category I-CTOL (FC-ILS-I-CTOL)
2. Front Course-ILS-Category II-CTOL (FC-ILS-II-CTOL)
3. Back Course-ILS-Category I-CTOL (BC-ILS-I-CTOL)
4. VOR-CTOL (VOR-CTOL)
5. Front Course-ILS-Category I-STOL (FC-ILS-I-STOL)

The nominal model developed in Section 2.1 and verified in Section 2.4 must be adapted to the measured distribution data (from Section 2.3) for each of the approach system models before the lateral probability density functions can be generated. The procedure required to adapt a model to the measured data consists of the six basic steps summarized in Table 2.5.1-1. The completion of this procedure results in a model and its corresponding Fokker-Planck equation with all system parameters, errors, and initial conditions specified. The Fokker-Planck equation is then used to generate the lateral positional error.

The first step in the procedure for determining the model parameters, errors, and initial conditions is the selection of the set of measured data that corresponds to the approach system model to be considered. Once the initial and discrete comparison range distributions are selected, the second step of the procedure is initiated. This step consists of specifying the model parameters, errors, and initial conditions for the initial attempt at adapting the model to the measured distribution data. Initial estimates of the parameters and errors are determined from the results of the analysis of Section 2.1.3 (Table 2.1.3-1). The system initial conditions are estimated by observing the responses of each state, predicted by the nominal model from Section 2.1.2. These parameters, errors, and initial conditions are then used in the nonlinear eighth order state equation from Section 2.1.5. Once these state equations are determined, the set of reduced state equations can be formulated.

The third step is to reduce the nonlinear eighth order system state equations to a set of second order linear system state equations which can be applied to the Fokker-Planck equation. The model reduction process, discussed in Section 2.2.1.2 must be accomplished at several range points

Table 2.5.1-1

Procedure Outline for the Model Development of the Lateral Probability Density Functions	
Step I :	Select the measured lateral distribution data at the initial range and at each of the comparison ranges for the particular approach system model to be considered.
Step II :	Determine a best estimate for the model parameters, errors, and initial conditions for the system model.
Step III:	With the estimate for the model parameters, reduce the resultant nonlinear eighth order set of state equations to a set of second order linear state equations for each specified range interval and apply each set to the Fokker-Planck equation.
Step IV :	Solve the Fokker-Planck equation generated in Step III using the initial distribution selected in Step I.
Step V :	Using a variance and PDF shape comparison, determine whether or not the Fokker-Planck distribution data matches the measured distribution data at the comparison points. If the measured and calculated distributions match, then the model and corresponding Fokker-Planck equation can be used for lateral error probability density function generation. If the distributions do not match, proceed to Step VI.
Step VI :	Using the sensitivity data of Appendix F, adjust the model parameters, errors, initial conditions, or combinations of these. If any parameter is changed, return to Step III; if only the errors and/or initial conditions are altered, return to Step IV.

along the approach path, since the linear model is a good approximation to the nonlinear model for only short range intervals. The selected range interval is 4700 feet.

The reduced system state equations are included in the Fokker-Planck equation as described in Section 2.2.1.3. This equation is initialized using the measured distribution data at the initial range. Using this Fokker-Planck equation, the lateral error density functions are calculated at discrete ranges along the approach path. The technique used to solve the resultant Fokker-Planck equation is described in Section 2.2.1.3. Generation of the range-ordered set of lateral error PDF data completes the fourth step in the model development procedure.

A comparison of the Fokker-Planck generated PDF to the measured PDF constitutes the fifth step of the procedure. This comparison is made based on (1) the variance of Fokker-Planck generated data and the variance of the measured PDF and (2) the shapes of their respective PDF's. The two-fold comparison is required only at the specific comparison ranges along the approach. The total approach can be subdivided into essentially three regions. One or two points in the initial region, mid-range region, and final region are all that are required to yield sufficient comparison information to adapt the system model to the measured data. Thus, if the measured and calculated variances compare favorably in the three range regions, the system parameters, errors, and initial conditions are correct for the system model and corresponding measured data. If this is the case, the Fokker-Planck equation is ready to be used to determine the lateral PDF's. If the variances in any of the regions do not compare favorably, then either the parameters, errors, initial conditions, or a combination of these must be changed to adapt the system model to the measured data. This leads to the sixth step in the procedure.

The sixth step involves using sensitivity techniques to adapt the parameters, errors, or initial conditions in such a manner that the comparison in step five is satisfied and the Fokker-Planck/system model development completed. The sensitivity data developed in Section 2.4.4 and presented in Section 3.3 and Appendix F can be directly applied to the process of adapting the system to the measured distribution data. This sensitivity data is range dependent; therefore, by determining in step five the region or regions in which the variances are not matched, the corresponding sensitive system factors can be determined. Also, since the sign of the sensitivity data indicates whether the factors should be increased or decreased to

better fit the measured data. If the system parameters are varied, the next step is to return to step three and proceed as before. If only the system errors and/or initial conditions are altered, then the procedure is to return to step four and continue.

This procedure is iterative in nature but converges rapidly to an adapted model if the initial parameters, errors, and initial conditions are chosen judiciously and if the sensitivity data is used effectively.

This procedure was used for approach system models 1. through 5. listed previously. The model block diagram and resulting parameters, errors, and initial conditions for each of these five cases are presented in Appendix G. Once the models for these five approach types and their associated parameters, errors, and initial conditions are determined, the probability density functions for the lateral dimension can be generated.

2.5.2 PROBABILITY DENSITY FUNCTION GENERATION

The total aircraft positional error space probability density function consists of three dimensions; lateral, vertical, and longitudinal. Separation of these dimensions is possible due to the physics of the lateral separation problem, as discussed in Section 2.1. The primary purpose for generating the three PDF's is the calculation of the probability of collision values for the various required approach systems, operations, and runway spacings discussed in Section 2.6. A secondary reason for determining the lateral PDF's is the determination of the locus of points termed the normal operating zone (NOZ). The approach systems for which PDF's are determined, the PDF type, and methods of determination are included for each of the three dimensions in Table 2.5.2-1. The procedure for determining the probability density function for the lateral dimension is considered in Section 2.5.2.1. The vertical PDF generation is discussed in Section 2.5.2.2 followed by the longitudinal PDF generation in Section 2.5.2.3.

Once the distribution data is generated for the three dimensions, the probability of collision data may be calculated for both dependent and independent operations. The normal operating zones may also be calculated using the lateral error probability density functions.

2.5.2.1 Procedure for Lateral Density Function Generation

It is necessary to generate lateral PDF's for the lateral approach systems listed in Table 2.5.2-1. The approach

Table 2.5.2-1

Probability Density Functions

Dimension	Approach System	PDF Type	Method of Determination
<u>lateral</u>	FC-ILS-I-CTOL	Fokker-Planck Output	Fokker-Planck
	FC-ILS-II-CTOL	Fokker-Planck Output	Fokker-Planck
	EC-ILS-I-CTOL	Fokker-Planck Output	Fokker-Planck
	VOR-CTOL	Fokker-Planck Output	Fokker-Planck
	FC-ILS-I-STOL	Fokker-Planck Output	Fokker-Planck
<u>vertical</u>	FC-ILS-I-CTOL	Gaussian	Measured Distribution Data
	FC-ILS-I-STOL	Gaussian	Measured Distribution Data
<u>Longitudinal</u>	FC-ILS-I-CTOL	Gaussian	Assumed Velocity Distribution

taken to generate the required PDF's utilizes the Fokker-Planck equation and the approach system models developed in Section 2.5.1. The model block diagrams, parameters, errors, and initial conditions are presented in Appendix G.

The procedure utilized to generate the lateral PDF's consists of four basic steps. The completion of this procedure results in a lateral PDF which is used in the probability of collision determination and in a NOZ determination.

The first step in the procedure is to determine the lateral deviation PDF to be used to initialize the Fokker-Planck equation at the initial range (turn-on range). The method to determine this PDF utilizes the modified Burgerhout PDF to fit the initial measured distribution data for the first four systems. The modified Burgerhout PDF was selected as the initial CTOL lateral error PDF because of the occurrence of a significant amount of measured error data in the tails of the measured data. Fitting a gaussian function through the tails of the distribution yields variances much larger than was found for the measured data. Thus, a distribution was required which had the narrow variance indicated by the measured data, but also fit the tails of the distribution. The modified Burgerhout PDF illustrated in Figure 2.5.2-1 has both of these features. The modified Burgerhout PDF fit for each measured data set is determined by using the standard deviation (σ) of the measured data to scale a nominal modified Burgerhout PDF ($\sigma=1.0$). This fit is required only at the initial range (turn-on range) due to the basic properties of the Fokker-Planck equation. The PC-ILS-I-STOL (Lateral) system utilizes a gaussian fit to the initial measured distribution data. This choice of the gaussian distribution was based on two factors. First, there were no extreme data points as in the CTOL case; and second, the chi-square test indicated that the gaussian distribution was valid (Reference 1). The statistical means for both the CTOL and STOL lateral PDF's were set to the runway centerline to reduce the problem of including system biases that were peculiar to the sites where the measured data was collected. The effect of these types of system biases in the determination of the minimum runway spacing is discussed in Section 4, Volume I.

Step two of the procedure consists of selecting the appropriate model with its associated parameters, errors, and initial conditions from Appendix G and incorporating these values into the nonlinear state equations from Section 2.1.5.

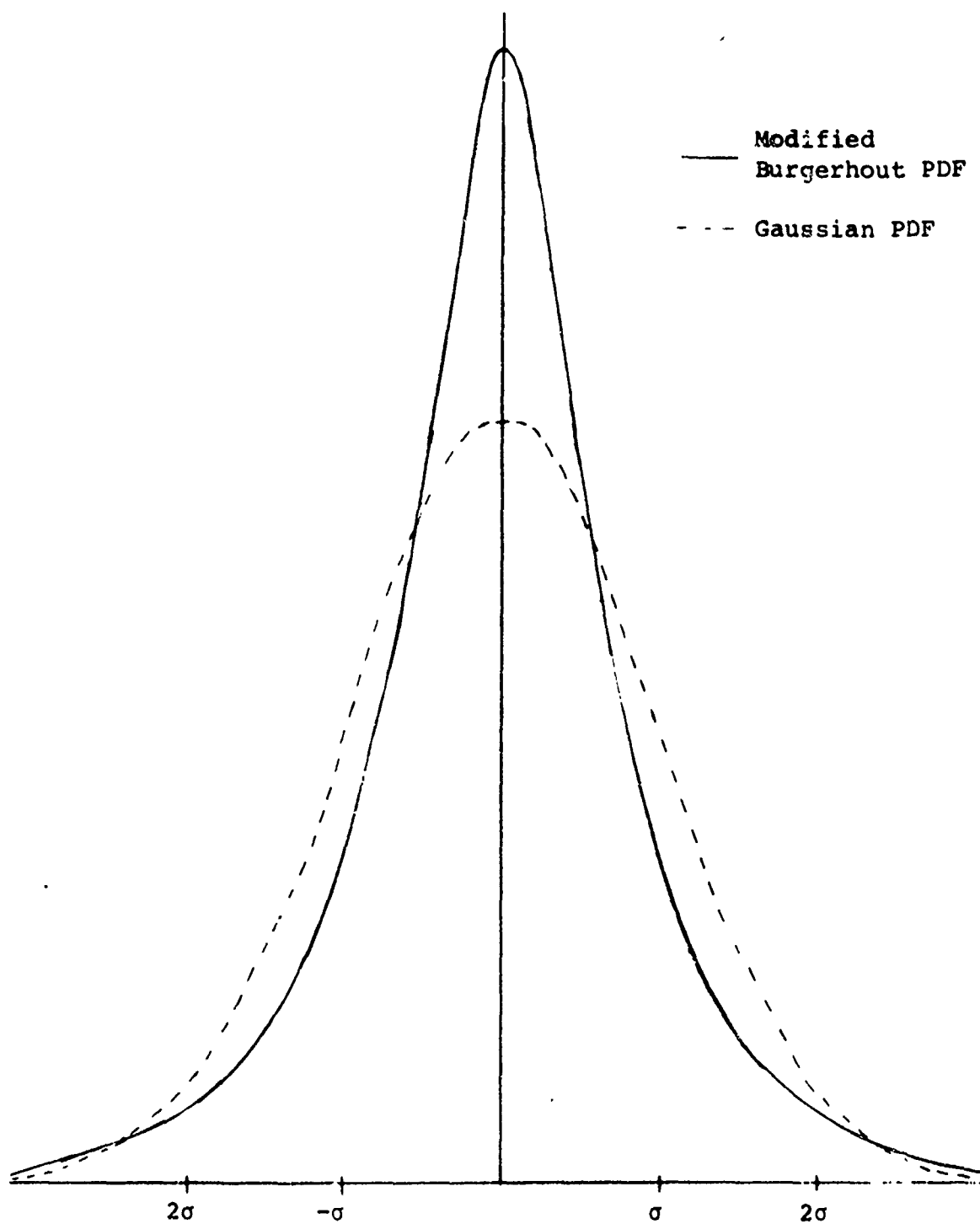


Figure 2.5.2-1 Comparison of Modified Burgerhout PDF and Gaussian PDF

Next, in step three of the procedure, the nonlinear state equations are reduced to a set of linear second order state equations for each 4700 foot range interval along the approach path. This model reduction task is described in Section 2.2.1.2.

The reduced state equations are then incorporated into the Fokker-Planck equation as described in Section 2.2.1.3. This equation is initialized using the initial lateral deviation PDF determined in the first step of this procedure. The lateral PDF is then generated by solving the Fokker-Planck equation as described in Section 2.2.1.3.

Several items must be considered prior to the actual generation of the lateral error probability density data. First, the initial range and final range from touchdown must be selected and the corresponding PDF for the initial range calculated. The selection of these ranges is restricted only by model considerations. That is, the initial range must occur after the aircraft has completed turn-on and the final range must be selected at or before the point where the aircraft becomes VFR.

In addition to the initial and final range values, the delta range interval for the solution of the Fokker-Planck equation must be selected. A delta range interval of approximately 23.6 feet (.1 second at 140 knots) was selected to generate the lateral probability density functions. The primary reason for the choice of these range increments was to yield accurate results for the total collision probability for dependent operations. Without the use of the Fokker-Planck equation, such range accuracy would not be possible since the measured data had range increments in the order of 2000 feet.

The grid spacing increment along the lateral axis, utilized in the computer solution of the Fokker-Planck equation, is based primarily on the accuracy required for collision probability determination and the lateral distribution at the initial range. The values selected for the five lateral approach systems were 38 increments approximately 174 feet in length which yielded a total lateral error coverage of approximately 3300 feet on either side of the runway centerline. Once this final parameter is selected, the Fokker-Planck equation is solved using the computer solution discussed in Section 2.2. The lateral error PDF data is presented in Appendix H at the initial range and other ranges required for the probability of collision determination for each of the systems.

2.5.2.2 Procedure for Vertical Density Function Generation

For the collision probability determination, the composite CTOL/STOL operations require a vertical dimension error PDF. This results from the fact the CTOL operation has a different glideslope (2.5°) than the STOL (7.5°) operation; and, therefore, the worst case assumption of vertical coincidence is not valid.

A gaussian vertical error PDF was selected for the vertical dimension. This type of distribution was selected due to the fact that one, there was no requirement to model the vertical dimension, and two, the measured data presented in Appendix E over range intervals of interest tested gaussian with only a few exceptions (Reference 1). The gaussian distributions were determined by using the measured error distribution data from Appendix E as the vertical error PDF. The measured data standard deviations were linearly interpolated to arrive at vertical distributions of the required range points for the two vertical systems indicated in Table 2.5.2-1.

The means for both the CTOL and STOL vertical PDF's were set to the glideslope value to reduce the problem of including system biases that were peculiar to the measured data collection sites. No attempt was made to include the non-symmetrical distribution effect which occurs near touchdown for either of the two systems. The vertical PDF data at selected ranges for the systems indicated in Table 2.5.2-1 is presented in Appendix H.

2.5.2.3 Procedure for Longitudinal Density Function Generation

The need for a longitudinal error density function was predicated by the requirement to determine probability of collision data for dependent operations. Thus, a longitudinal error density function was required for the front course - ILS - Category I - CTOL approach system. Using a velocity error standard deviation (σ_v) of 5 knots, a mean (\bar{V}) of 140 knots, and assuming a gaussian distribution, the longitudinal error probability density function was generated as discussed in Section 2.3.2.3. The resultant longitudinal error distribution is also gaussian with a standard deviation equal to $[(\sigma_v t)/\sqrt{2}]$ and a mean equal to $[X_0' - \bar{V}t]$, where X_0' is the initial range and t is time. As indicated, this process is a time varying process in which the mean of the PDF travels at a constant velocity (\bar{V}), and the standard deviation increases proportionately with t .

This process describes a spreading longitudinal location error which is expected for dependent operations as assumed in this study. It is further assumed for dependent operations that at some range (X'_0) greater than the outer marker, the controller establishes a desired longitudinal separation between two aircraft approaching adjacent parallel runways and a nominal approach speed (\bar{V}) for the two aircraft. This range is assumed to be 9 nmi (54,720 feet), as shown in Figure 2.5.2-2, which corresponds to the approximate range at which the 1000 foot vertical separation is lost. The nominal approach speeds for the two aircraft are assumed equal to \bar{V} . It is further assumed that once the desired longitudinal separation and nominal approach speed have been established, the controller no longer controls the process; i.e., no real-time velocity or location control occurs after the desired separation and speeds are established. Thus, the longitudinal location error of aircraft flying with an assumed velocity error standard deviation of 5 knots would tend to increase with time. Based upon the preceding assumptions, the longitudinal PDF for the two aircraft illustrated in Figure 2.5.2-2 is defined as follows:

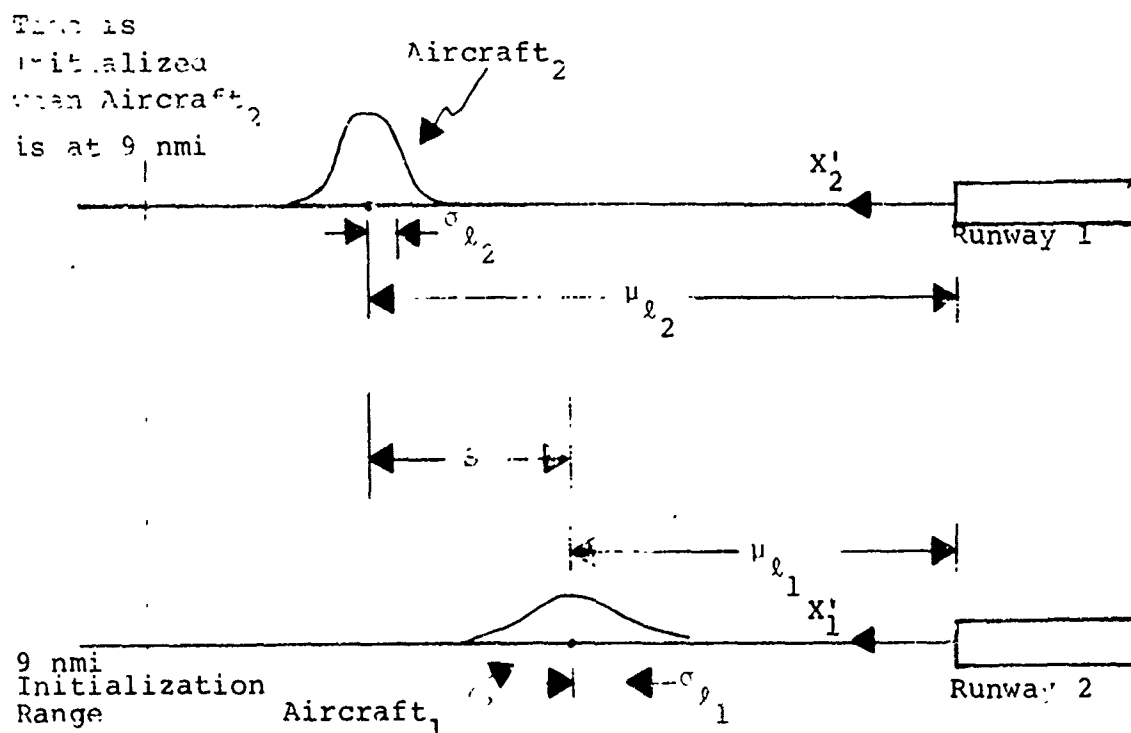


Figure 2.5.2-2

Longitudinal Distribution for Dependent Operations

$$X_i' = N(\mu_{\ell_i}, \sigma_{\ell_i}^2); i = 1, 2$$

where

$$\mu_{\ell_i} = X_0' - \bar{V}(t + \Delta t_i)$$

$$\sigma_{\ell_i} = \frac{\sigma_V(t + \Delta t_i)}{\sqrt{2}}$$

with the corresponding values

$$X_0' = 54,720 \text{ feet}$$

$$\bar{V} = 140 \text{ knots} = 236.4 \text{ feet/second}$$

$$\sigma_V = 5 \text{ knots} = 8.44 \text{ feet/second}$$

$$t = 0 \text{ seconds; when aircraft}_2 \text{ range} = 54,720 \text{ feet}$$

$$\Delta t_1 = S/\bar{V} \text{ seconds; time required for aircraft}_1 \text{ to fly a distance of } S \text{ feet}$$

$$\Delta t_2 = 0 \text{ seconds}$$

$$S = \text{desired longitudinal separation, feet}$$

The resulting longitudinal PDF for the FC-ILS-I-CTOL system is presented in Appendix A at selected ranges.

2.5.3 NORMAL OPERATING ZONE DETERMINATION

The normal operating zone (NOZ) is defined as being either a zone that contains 68% or 95% of the operations. These percentage values correspond roughly to the 1σ and 2σ points respectively for a gaussian distribution function. Except for the STOL case, the lateral error distributions are non-gaussian; therefore, the percentage definition will be used for determining the normal operating zones. The procedure for determining the NOZ for the approach systems indicated in Section 2.5.1 is based primarily on the integration of the lateral error density functions for each of the systems as discussed

in Section 2.5.3.1. It is also necessary to determine the NOZ for CTOL/STOL skewed operations. The NOZ for this case is determined in a slightly different manner as discussed in Section 2.5.3.2.

2.5.3.1 NOZ Determination for Approach Systems

The 68% and 95% NOZ's are determined for the approach systems by integrating the lateral error density functions generated in Section 2.5.2.1 as illustrated in Figure 2.5.3-1. The integration of the PDF's is accomplished using a spline fit to the lateral grid points utilized in the computer solution to the Fokker-Planck equation. The 68% and 95% points are calculated at specified range intervals along the approach. The loci of these points are two lines, symmetric about the runway centerline, which define the 68% and 95% NOZ respectively. At 5000 feet range from either end of the runway for CTOL operations and at 1500 feet for STOL operations, the NOZ is defined by two lines parallel to the runway centerline as depicted in Figure 2.5.3-2. These points correspond to the approximate ranges at which the CTOL and STOL aircraft go VFR and the corresponding model becomes invalid.

The 68% and 95% NOZ's for each of the systems listed in Section 2.5.1 are presented in Appendix H.

2.5.3.2 CTOL/STOL Skewed Normal Operating Zone

To determine the minimum runway spacing between CTOL/STOL skewed runways, the normal operating zone for STOL departures must be determined at the point of minimum separation between the CTOL runway extended centerline and the STOL nominal departure path. The geometry of the CTOL/STOL skewed configuration is illustrated in Figure 2.5.3-3. As shown in the figure, the point of minimum separation occurs within the curved portion of the nominal departure path. Due to the complexity of the task of generating the PDF for the curved path departure, the NOZ for this case is determined in a slightly different manner.

The basic approach to determine this NOZ is to utilize a model of the curved path dynamics of the departing STOL aircraft to perform a Monte Carlo simulation. The standard deviation (σ_y) of the lateral errors, measured from the nominal departure path, at the minimum separation point is determined from the Monte Carlo simulation. For this analysis, the 68% NOZ is assumed to be equal to σ_y , and the 95% NOZ is

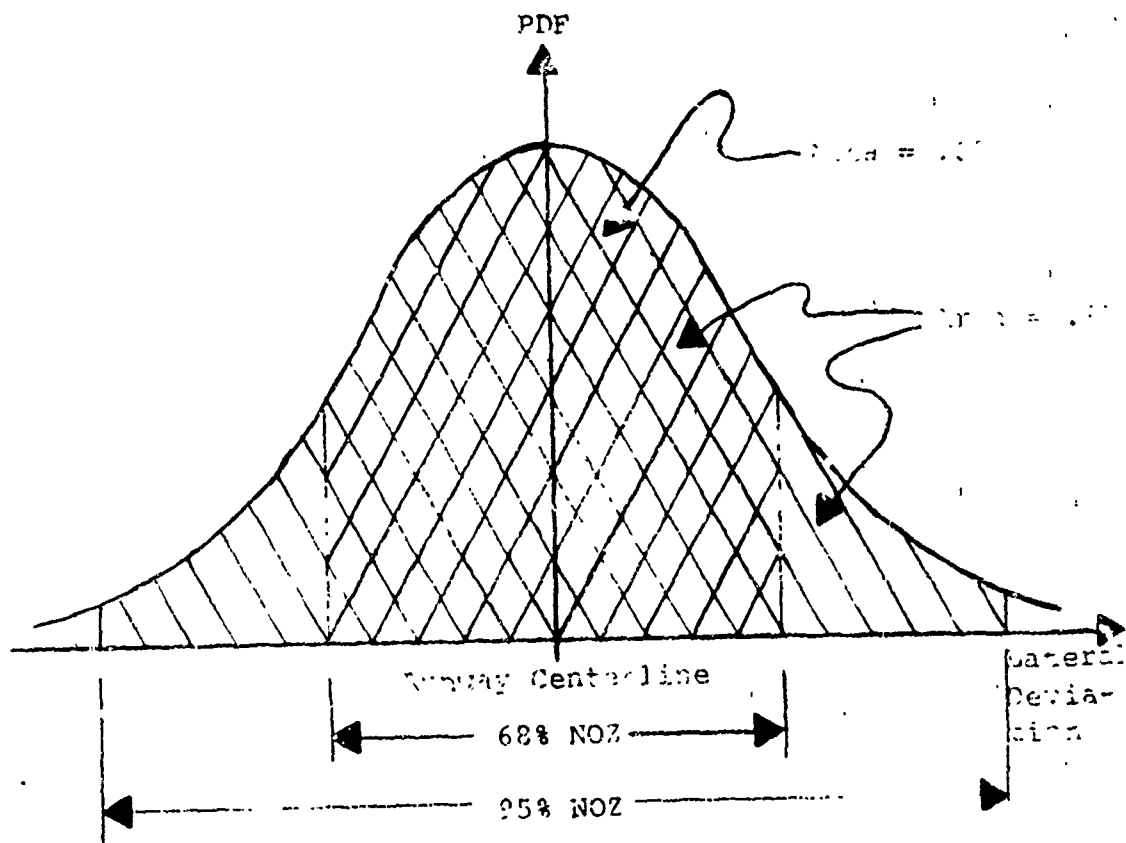


Figure 2.5.3-1 Normal Operating Zone Determination

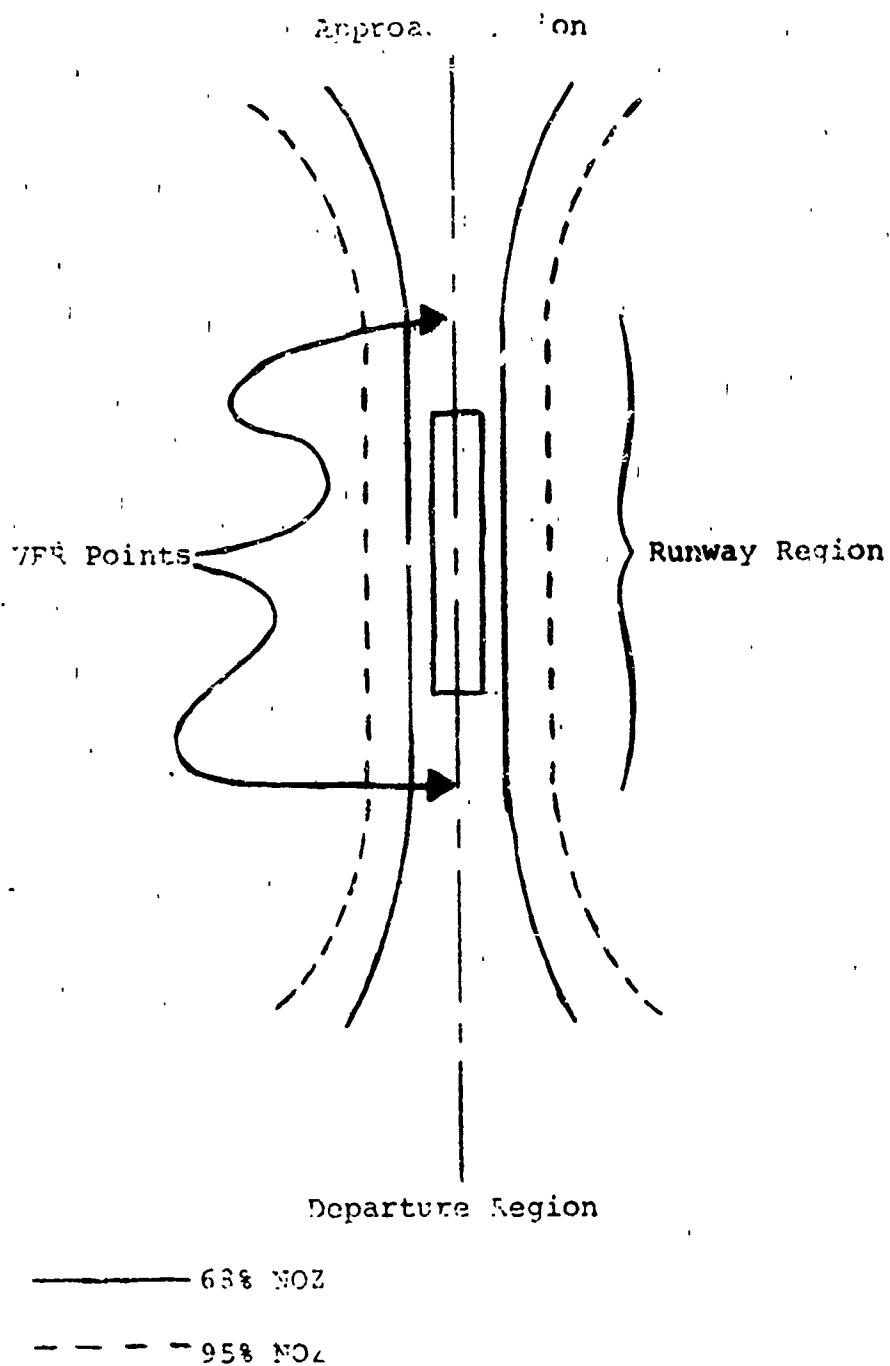


Figure 2.5.3-2 Normal Operating Zones

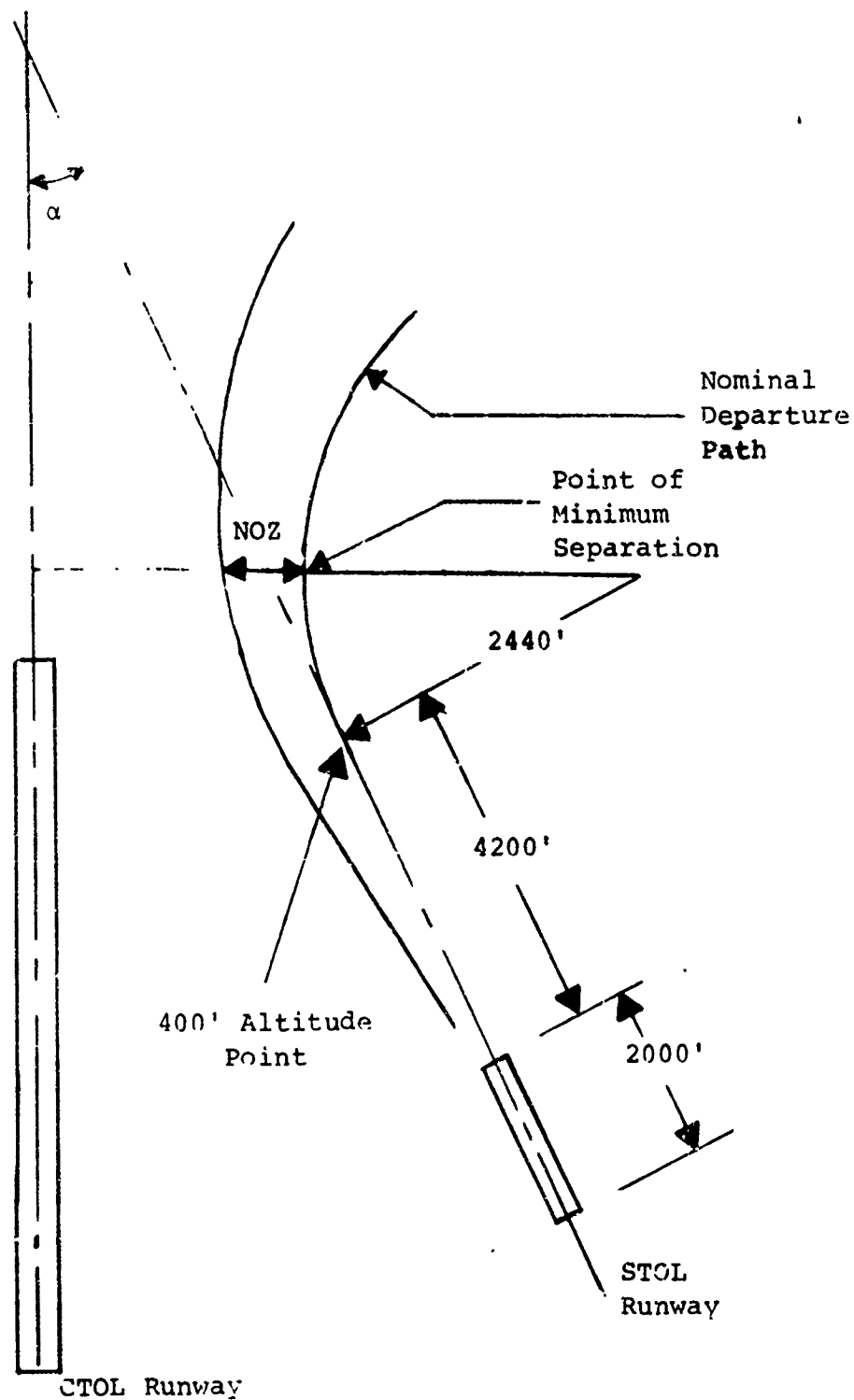


Figure 2.5.3-3 CTOL/STOL Skewed Geometry

assumed to be equal to $2\sigma_y$.

The STOL nominal departure path is defined in Figure 2.5.3-3. The straight portion of the departure is followed until the aircraft reach an altitude of 400 feet (this occurs at a range of 4200 feet, Reference 2). At this point, the aircraft execute a standard rate turn. Reference 3 indicates that pilots who were requested to execute a standard rate turn actually performed turns distributed about a mean ($\bar{\dot{\psi}}$) of 2.89 degrees per second with a standard deviation ($\sigma_{\dot{\psi}}$) of .392 degrees per second. The nominal departure speed (\bar{V}) for the STOL aircraft is assumed to be 73 knots (Reference 1). The curved portion of the nominal departure path is defined by the radius of curvature (\bar{R})

$$\bar{R} = \frac{\bar{V}}{\bar{\dot{\psi}}} = 2440 \text{ feet.}$$

The curved path dynamics assumed for the Monte Carlo simulation are described by the following equation

$$R = \frac{V}{\dot{\psi}}$$

where R is the radius of curvature of the curved path, V is the velocity, and $\dot{\psi}$ is the turn rate. The velocity and turn rate are assumed to be normally distributed as

$$V = N(\bar{V}, \sigma_V)$$

$$\dot{\psi} = N(\bar{\dot{\psi}}, \sigma_{\dot{\psi}})$$

where

$$\bar{V} = 123 \text{ ft/sec; (73 knots)}$$

$$\sigma_V = 8.44 \text{ ft/sec; (5 knots)}$$

$$\bar{\dot{\psi}} = .0504 \text{ rad/sec; (2.89 deg/sec), and}$$

$$\sigma_{\dot{\psi}} = .00684 \text{ rad/sec; (.392 deg/sec).}$$

The initial distribution of R is also assumed to be normal. The standard deviation is assumed from the lateral PDF for an approach at the equivalent range.

$$R_o = N(\bar{R}, \sigma_R)$$

where

$$\bar{R} = 2440 \text{ feet, and}$$

$$\sigma_R = 93 \text{ feet.}$$

The results of the Monte Carlo simulation were the corresponding σ_y and $2\sigma_y$ values at the minimum separation point for skew angles (α) of 10°, 20°, 30°, 40°, 50°, 60°, 70°, 80°, and 90°. The NOZ's resulting from this analysis are presented in Appendix H.

REFERENCES

1. -, "STOL Steep Approaches in the Breguet 941", Memorandum Report - Attachment 1, DOT-FAA, FS-640, November 1969.
2. -, "Ground Noise Measurements During Landing and Take-off Operations of a McDonnell-Douglas 188 (Breguet 941) STOL Airplane", Langley Working Paper, LWP-741, 18 April 1969.
3. Watkins, Jimmy, "Analysis of the Minimum Required Lateral Spacing Between Parallel Runways Used for Simultaneous IFR Approaches", DOT-FAA, SRDS, ATC Development Division, Subprogram No. 150-502, November 1970.

SECTION 2.6

PROBABILITY OF COLLISION

In order to reduce the present minimum spacing criteria between two parallel runways, a means of measuring the relative safety of two aircraft attempting to land on parallel runways is needed. This relative safety is defined to be the probability of collision in the Lateral Separation Study.

It is assumed throughout this analysis that the airspace requirements for a departure are no greater than for an approach; therefore, probability of collision models described in this section are based on approaches, and all subsequent results obtained are assumed to be equally valid for both departures and approaches.

The probability of collision between two aircraft approaching parallel runways is considered for the following cases:

- (a) STOL/STOL independent operations
- (b) CTOL/CTOL independent operations
- (c) CTOL/CTOL dependent operations
- (d) CTOL/STOL independent operations

The notation used above defines the aircraft and runway configuration for each of the parallel runways. For example, CTOL/STOL defines one runway as being a CTOL runway with CTOL aircraft as the primary user class and the other runway as a STOL runway with STOL aircraft as the primary user class. Independent operations refer to aircraft approaching parallel runways such that no controller intervention occurs for the purpose of ensuring longitudinal spacing between the aircraft. Dependent operations refer to a situation in which two aircraft approach parallel runways and at least one of the aircraft is subjected to controller intervention in an attempt to establish a given longitudinal spacing between the approaching aircraft. It is assumed for dependent operations that at some range beyond the outer marker, the controller has established:

- (1) the desired longitudinal spacing between the two aircraft, and
- (2) the nominal approach speeds for the two aircraft.

It is further assumed that once the spacing and approach speeds have been established, the remainder of the approach occurs with no controller intervention.

Simplifying assumptions and a general method of approach toward developing a probability of collision model is

presented in Section 2.6.1. A detailed analytical development for probability of collision models for cases (a), (b), (c), and (d) above is then given in Sections 2.6.1.1, 2.6.1.2, 2.6.1.3, and 2.6.1.4, respectively.

The aircraft lateral, vertical, and longitudinal error probability density functions are determined in Section 2.5 and presented in Appendix H. These density functions are used in the generation of the required probabilities of collision, as discussed in Section 2.6.2. Specific runway and approach system configurations for each of the above four cases are also discussed in Section 2.6.2, and results obtained from all combinations outlined in Section 2.6.2 are discussed in Section 3.5 and presented in Appendix I. The probability of collision results contained in Appendix I can be utilized in the determining of minimum runway spacing as described in Volume I of this report (Section 4).

2.6.1 ANALYTICAL DEVELOPMENT

Figure 2.6.1-1 represents the geometry and coordinate system upon which the general form of the probability of collision between two aircraft is based. As illustrated in the figure, d represents the separation between two aircraft approaching parallel runways. The symbol d is a random variable since there are random errors in the aircraft flight path.

The most general expression for the probability of collision as defined in the Lateral Separation Study is given by

$$P[d \leq \lambda] = \int_{-\infty}^{\lambda} f_d(\xi) d\xi \quad (2.6.1-1)$$

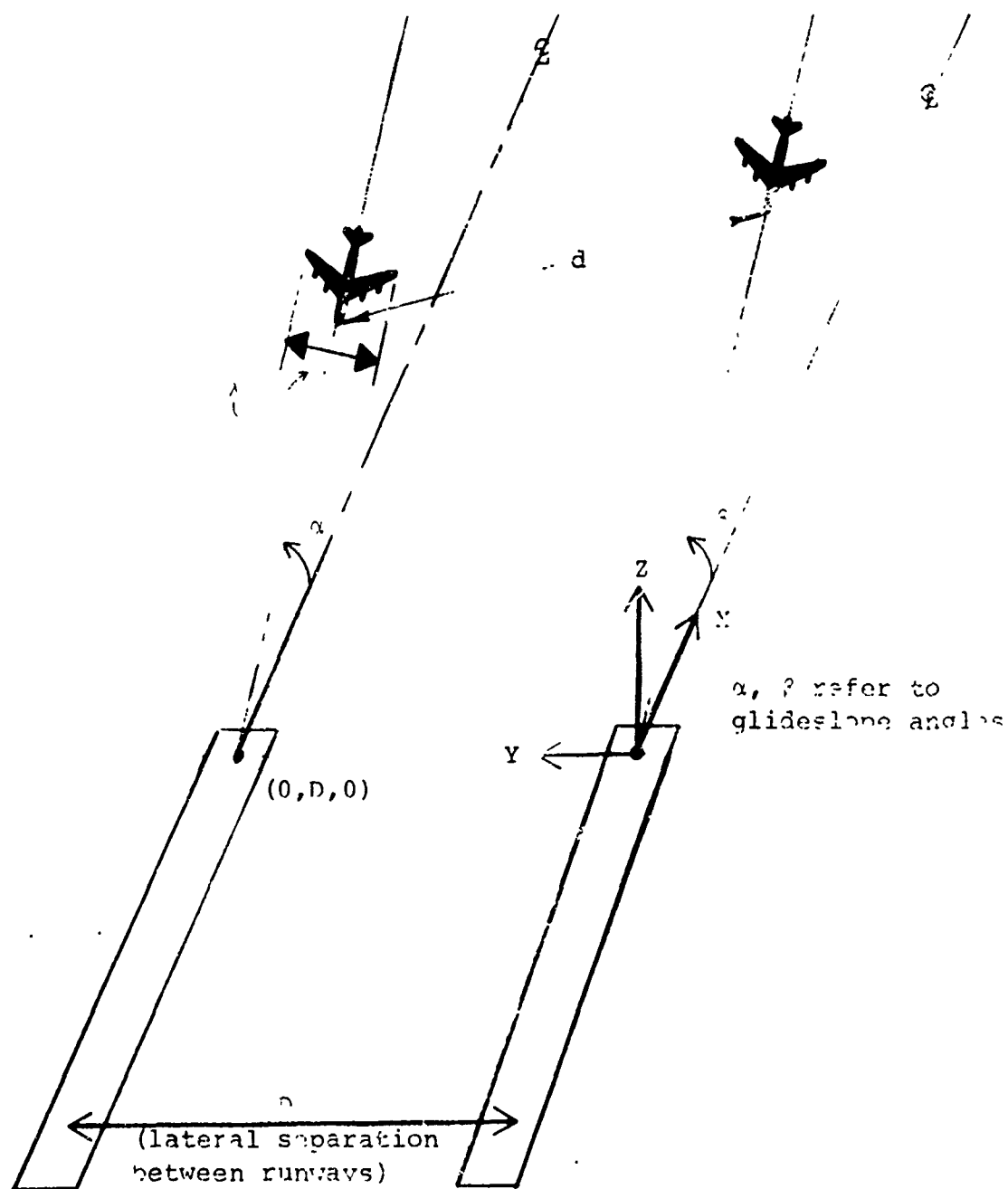
where

λ represents the wing span of the particular aircraft in question

and

f_d represents the probability density function of the random variable d .

The evaluation of Equation 2.6.1-1 appears to be simple if the density function f_d is known or can be analytically determined. However, the assumptions employed in developing Equation 2.6.1-1



Probability of Collision between Aircraft

$$\equiv P[i \leq \lambda] \equiv \int_{-\infty}^{\lambda} f_d(\xi) d\xi$$

Figure 2.6.1-1 Probability of Collision

vary for each of the four cases mentioned in Section 2.6. Therefore, the analytical development of Equation 2.6.1-1 for each case is discussed independently in the remaining four subsections to this section. Assumptions for each individual case always imply a worst case situation; i.e., the probability of collision model developed for a particular case represents the most conservative model for aircraft operating under normal conditions.

2.6.1.1 STOL/STOL Independent

This section considers the analytical development for probability of collision between two STOL aircraft flying independent parallel approaches. As illustrated in Figure 2.6.1-2, the runways are parallel and separated by D feet.

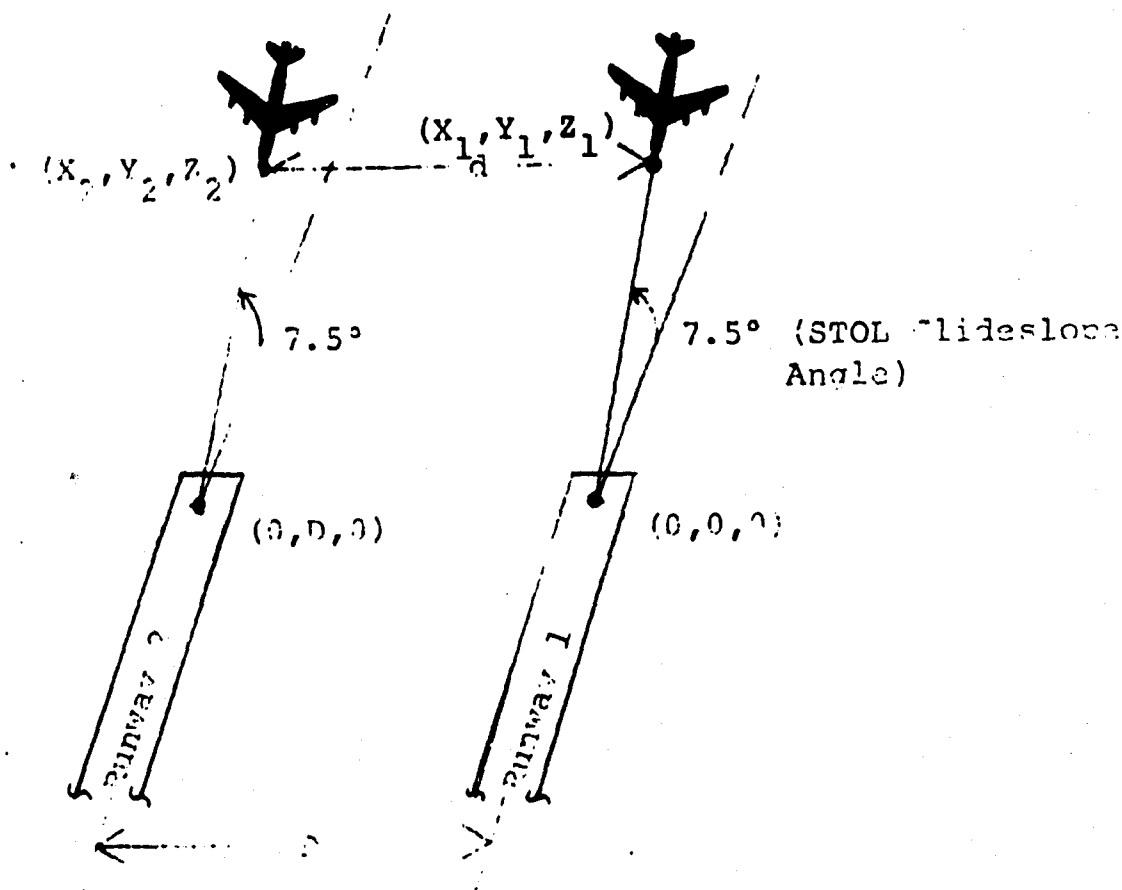


Figure 2.6.1-2

Probability of Collision Geometry for
STOL/STOL Independent Operations

The coordinate system is defined as in Figure 2.6.1-1; thus,

$X_i \equiv \text{aircraft}_i \text{ longitudinal position}$

$Y_i \equiv \text{aircraft}_i \text{ lateral position}$

$Z_i \equiv \text{aircraft}_i \text{ vertical position} \quad i = 1, 2.$

The analytical development presented in the remainder of this section utilizes the following assumptions for STOL/STOL independent operations:

- (i) longitudinal coincidence is maintained between aircraft approaching adjacent runways, i.e., $X_1 = X_2$;
- (ii) vertical coincidence is maintained between aircraft approaching adjacent runways, i.e., $Z_1 = Z_2$; and
- (iii) Y_1 and Y_2 are independent and normally distributed random variables, $N(\mu_1, \sigma_1^2)$ and $N(\mu_2, \sigma_2^2)$, respectively (Section 2.5).

For STOL/STOL independent operations, the primary dimension of interest is lateral; therefore, a lateral distribution is utilized in the determination of the probability of collision. To assure a worst case condition, longitudinal and vertical coincidence is assumed; thus, no statistics are associated with these dimensions.

Referring to Figure 2.6.1-2, the probability of collision for independent STOL/STOL approaches is defined as:

$$\begin{aligned}
 P[d \leq \lambda] &= P[d^2 \leq \lambda^2], \quad \lambda < 1 \\
 &= P[(X_1 - X_2)^2 + (Y_1 - Y_2)^2 + (Z_1 - Z_2)^2 \leq \lambda^2] \\
 &= P[(Y_1 - Y_2)^2 \leq \lambda^2] \\
 &= P[-\lambda \leq Y_1 - Y_2 \leq \lambda] \quad (2.6.1-2)
 \end{aligned}$$

where

λ is a constant (wing span) such that a collision occurs if $d \leq \lambda$.

Now, $Y_1 - Y_2$ is distributed $N(\mu_1 - \mu_2, \sigma_1^2 + \sigma_2^2)$, so that Equation 2.6.1-2 becomes:

$$P[d \leq \lambda] = \Phi \left\{ \frac{\lambda - \mu_1 + \mu_2}{\sigma_1^2 + \sigma_2^2} \right\} - \bar{\Phi} \left\{ \frac{-\lambda - \mu_1 + \mu_2}{\sigma_1^2 + \sigma_2^2} \right\} \quad (2.6.1-3)$$

where

Φ is the standard normal distribution function defined by

$$\Phi(\xi) = \frac{1}{2\pi} \int_{-\infty}^{\xi} \exp\left(-\frac{\alpha^2}{2}\right) d\alpha$$

Equation 2.6.1-3 then represents the analytical expression for determining probability of collision for STOL/STOL independent operations.

It was found that the standard normal distribution, denoted by $\Phi(\xi)$ in Equation 2.6.1-3, could only be evaluated for $|\xi| < 6$ using standard available routines. Since it was necessary to evaluate this expression for $|\xi| \geq 5$, a method was required to supplement the standard procedure. Therefore, a table of values for $Q(\xi) = 1 - \Phi(\xi)$ from E. S. Pearson and H. O. Hartley (Reference 1) was used to evaluate $\Phi(\xi)$ for $|\xi| \geq 6$. A portion of this table is shown in Table 2.6.1-1. Since the only values of ξ given in the tables are integers, values of $-\log_{10} Q(\xi)$ for non-integer values of ξ were obtained by quadratic interpolation; e.g., the value of $-\log_{10} Q(\xi)$ for $\xi = \xi_0$ (non-integer) is obtained as follows:

$$-\log_{10} Q(\xi_0) \approx A_1 \xi_0^2 + A_2 \xi_0 + A_3$$

where

$$A_1 = \frac{1}{2} [y(Jx+2) - 2y(Jx+1) + y(Jx)]$$

$$A_2 = y(Jx+1) - A_1(Jx+1)^2 - y(Jx) + A_1(Jx)^2$$

$$A_3 = y(Jx) - A_1(Jx)^2 - A_2(Jx)$$

$$Jx = \text{largest integer} \leq \xi_0$$

and

$y(Jx) = -\log_{10} Q(Jx)$ as indicated in Table 2.6.1-1. Therefore, if $-\log_{10} Q(\xi_0) = y_0$, then $P(X \geq \xi_0) \approx 10^{-y_0}$

Table 2.6.1-1

Sample Table of the Normal Probability
Function for Large Arguments

ξ	$-\log_{10} Q(\xi)$
5	6.542
6	9.006
7	11.893
8	15.206
.	
.	
.	

$$Q(\xi) = 1 - \Phi(\xi)$$

$$= P(X \geq \xi)$$

$$\text{and } y(\xi) = -\log_{10} Q(\xi)$$

and a close approximation to $\phi(\xi_0)$ is given by

$$\phi(\xi_0) \approx 1 - 10^{-Y_0}$$

2.6.1.2 CTOL/CTOL Independent

The analytical expression used in determining the probability of collision for CTOL/CTOL independent operations is developed in this section. The geometry on which the analysis in this section is based is presented in Figure 2.6.1-3.

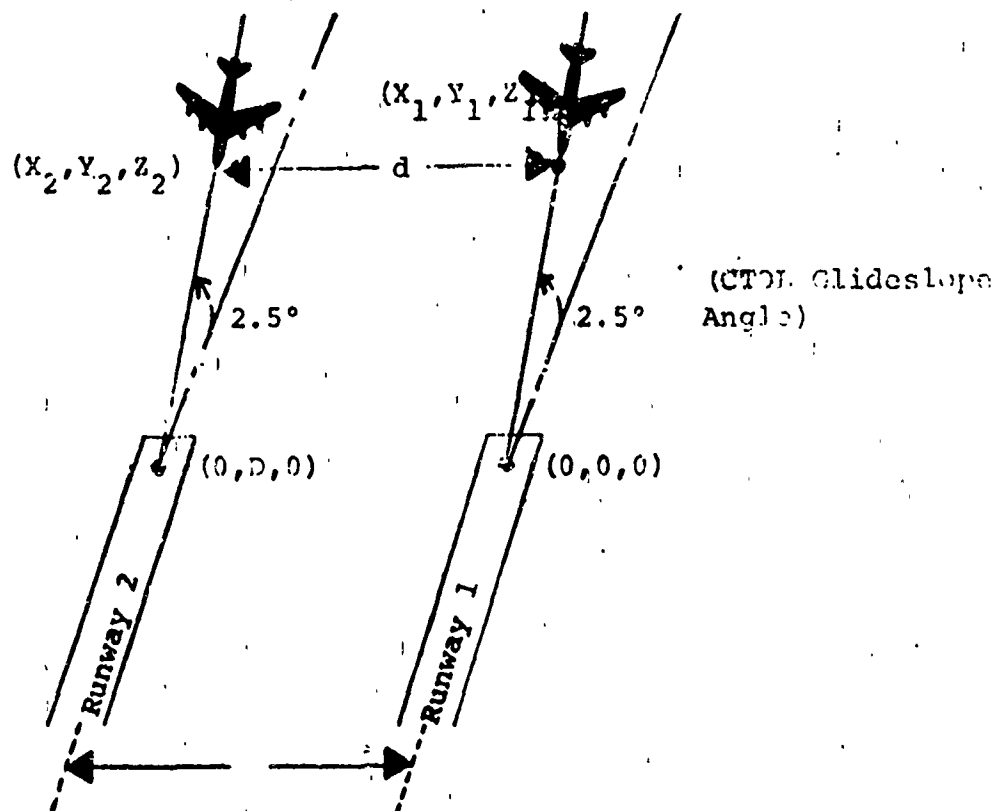


Figure 2.6.1-3

Probability of Collision Geometry for CTOL/CTOL Independent Operations

The analysis for CTOL/CTOL independent operations for parallel runways utilizes the following assumptions:

- (i) longitudinal coincidence exists between aircraft approaching adjacent runways, i.e., $X_1 = X_2$;

- (ii) vertical coincidence exists between aircraft approaching adjacent runways, i.e., $Z_1 = Z_2$; and
- (iii) Y_1 and Y_2 are independent random variables distributed according to the PDF's obtained from Appendix H for VOR-CTOL (Lateral), BC-ILS-I-CTOL (Lateral), and FC-ILS-I-CTOL (Lateral).

As stated in Section 2.6.1, assumptions (i) and (ii) represent worst case conditions upon which the probability of collision model developed in the remainder of this section is based.

Since $X_1 = X_2$ and $Z_1 = Z_2$, the probability of collision is defined as:

$$P[d \leq \lambda] = P[-\lambda \leq Y_1 - Y_2 \leq \lambda] \quad (2.6.1-4)$$

In order to evaluate Equation 2.6.1-4, information concerning the probability density function of the random variable $S = Y_1 - Y_2$ is required. Since the analytical forms of the densities of Y_1 and Y_2 are not available, the density of S , say $f_S(s)$, was obtained as the convolution of density outputs for Y_1 and Y_2 as defined in Appendix H for the particular approach systems discussed in assumption (iii). The remainder of this sub-section describes how $f_S(s)$ is determined using the convolution approach, and the subsequent evaluation of Equation 2.6.1-4.

The density $f_S(s)$ can be expressed as the convolution of Y_1 and Y_2 :

$$f_S(s) = \int_{-\infty}^{\infty} g_{Y_1}(s-\tau) g_{Y_2}(\tau) d\tau \quad (2.6.1-5)$$

where $g_{Y_1}(\cdot)$ and $g_{Y_2}(\cdot)$ denote the densities of Y_1 and Y_2 , respectively. Since g_{Y_1} and g_{Y_2} are solutions to the Fokker-Planck equation, these densities are defined by a finite number of points representing the respective densities. The integral in Equation 2.6.1-5 is then evaluated using the following procedure. For each value of s , $f_S(s)$ is obtained by

- (a) determining the smallest value of τ_1 , such that $s-\tau_1$ and τ_1 lie in the domains of g_{Y_1} and g_{Y_2} , respectively;

(b) determining the largest value of τ , say τ_2 , such that $s-\tau_2$ and τ_2 lie in the domains of g_{Y_1} and g_{Y_2} , respectively; and

(c) performing a trapezoidal integration as illustrated in Figure 2.6.1-4 to determine:

$$f_S(s) \approx \int_{\tau_1}^{\tau_2} g_{Y_1}(s-\tau) g_{Y_2}(-\tau) d\tau \quad (2.6.1-6)$$

Equation 2.6.1-4 can be written as:

$$P[d \leq \lambda] = \int_{-\lambda}^{\lambda} f_S(s) ds \quad (2.6.1-7)$$

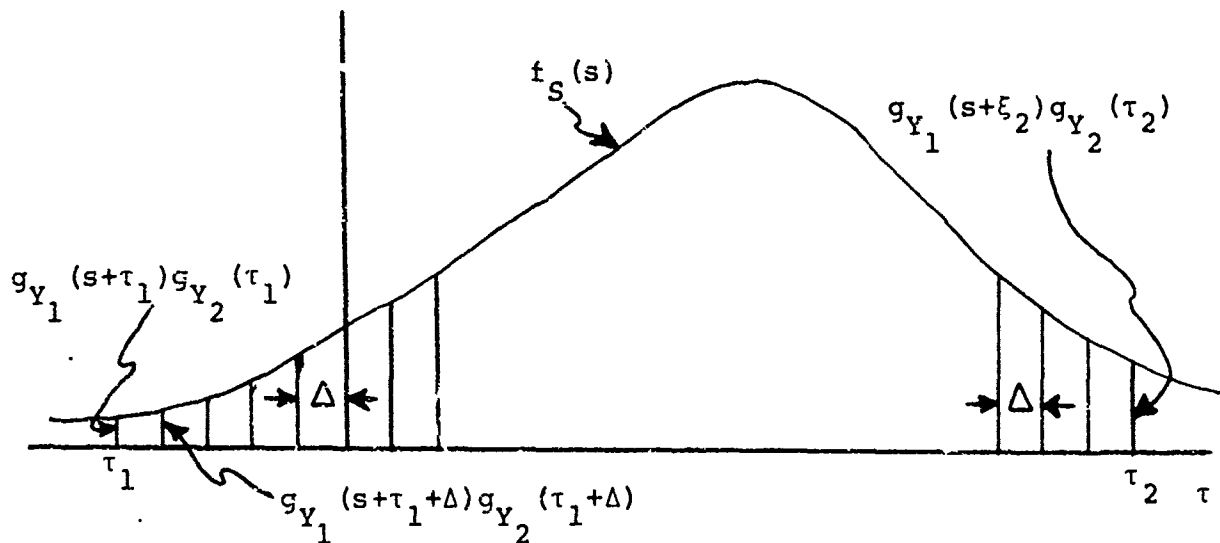


Figure 2.6.1-4 Graphical Illustration of Convolution Method

Combining Equations 2.6.1-6 and 2.6.1-7, the following equation is obtained:

$$P[d \leq \lambda] = \int_{-\lambda}^{\lambda} \int_{\tau_1}^{\tau_2} g_{Y_1}(s-\tau) g_{Y_2}(-\tau) d\tau ds \quad (2.6.1-8)$$

Equation 2.6.1-8 then provides the complete analytical expression used in determining the probability of collision for CTOL/CTOL independent operations.

2.6.1.3 CTOL/CTOL Dependent

The probability of collision for CTOL/CTOL dependent operations is developed in this section. Figure 2.6.1-5 represents the geometry associated with CTOL/CTOL dependent operations. It should be noted that, unlike preceding cases, the coordinate system on which the analysis in this section is based assumes that longitudinal position is measured along the glideslope plane and not along a horizontal extension of the runway centerline. Therefore, vertical position is measured perpendicular to the glideslope plane; i.e., positive or negative vertical errors imply that the aircraft is above or below the glideslope plane, respectively. The lateral or Y' -axis is orthogonal to the $X'Z'$ -plane with the origin of the coordinate system located at the touchdown point of runway 1.

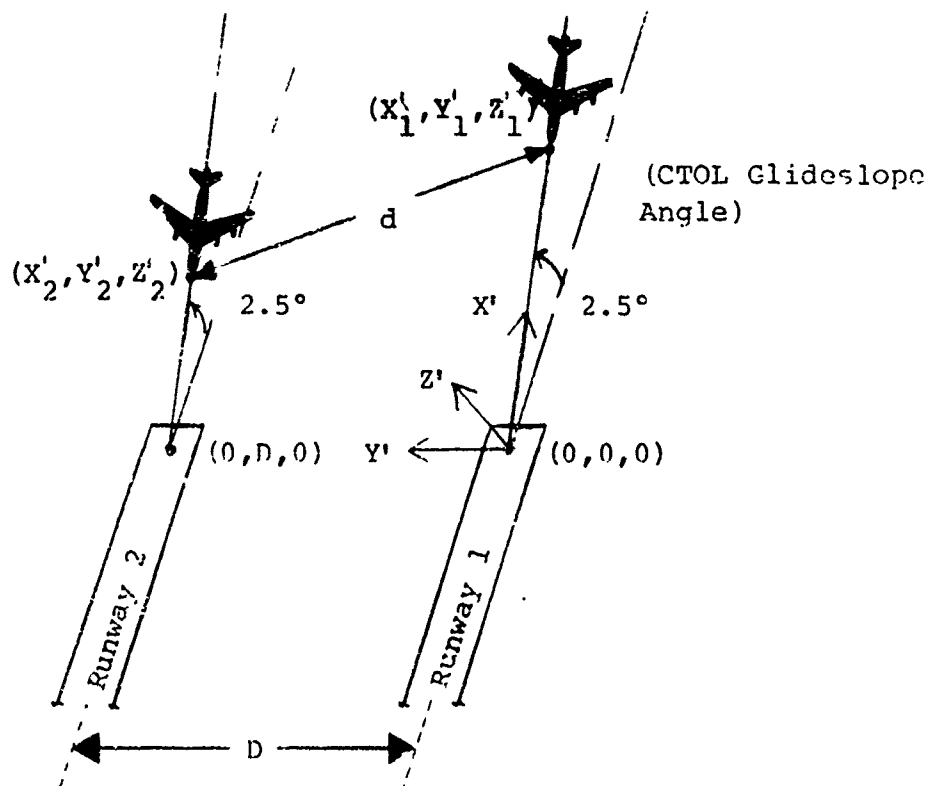


Figure 2.6.1-5

Probability of Collision Geometry for
CTOL/CTOL Dependent Operations

The following assumptions regarding CTOL/CTOL dependent operations are made for the purpose of the analysis presented in this section:

- (i) approaching aircraft are assumed to be in the glideslope plane, i.e., $z'_1 = z'_2 = 0$;
- (ii) velocities of aircraft 1 and 2 are assumed to be normally distributed, $N(\mu_1, \sigma_1^2)$ and $N(\mu_2, \sigma_2^2)$, respectively (from Section 2.3); and
- (iii) y'_1 and y'_2 are assumed to be independent random variables governed by the respective densities output as solutions to the Fokker-Planck equation (from Section 2.5).

For CTOL/CTOL dependent operations, the primary dimensions of interest are lateral and longitudinal; therefore, lateral and longitudinal distributions are utilized to determine the probability of collision. To assure a worst case condition, the aircraft are assumed to remain in the glideslope plane ($z'_1 = z'_2 = 0$); thus, no statistics are associated with the vertical dimension. Since the aircraft velocity is assumed to be normally distributed, it follows from the analysis in Section 2.3 that the longitudinal position, x'_1 , of the aircraft is normal, say $N(\mu_{\ell_1}, \sigma_{\ell_1}^2)$ and $N(\mu_{\ell_2}, \sigma_{\ell_2}^2)$.

The probability of collision as defined in the Lateral Separation Study for CTOL/CTOL dependent operations is given as:

$$P\{d \leq \lambda\} = P\left\{\left[(x'_1 - x'_2)^2 + (y'_1 - y'_2)^2\right] \leq \lambda^2\right\} \quad (2.6.1-9)$$

In order to evaluate the right-hand side of Equation 2.6.1-9, new random variables S_1 and S_2 are introduced

where

$$S_1 = x'_1 - x'_2,$$

$$S_2 = y'_1 - y'_2 \quad (2.6.1-10)$$

Now since $\lambda > 0$, the region R of the $s_1 s_2$ -plane defined by

$$s_1^2 + s_2^2 \leq \lambda^2$$

is a circle (Figure 2.6.1-6) with radius λ ; therefore, $P[d \leq \lambda]$ equals the probability mass in the circle (Reference 2);

$$P[d \leq \lambda] = \iint_{s_1^2 + s_2^2 \leq \lambda^2} f_{s_1 s_2}(s_1, s_2) ds_1 ds_2 \quad (2.6.1-11)$$

where

$f_{s_1 s_2}(s_1, s_2)$ is the joint probability density of s_1 and s_2 .

If s_1 and s_2 are assumed to be independent, then

$f_{s_1 s_2}(s_1, s_2)$ can be written as $f_{s_1 s_2}(s_1, s_2) = f_{s_1}(s_1) \cdot f_{s_2}(s_2)$

and Equation 2.6.1-11 then becomes:

$$P[d \leq \lambda] = \iint_{s_1^2 + s_2^2 \leq \lambda^2} f_{s_1}(s_1) f_{s_2}(s_2) ds_1 ds_2. \quad (2.6.1-12)$$

As illustrated in Figure 2.6.1-6, an upper bound which provides a close approximation to Equation 2.6.1-12 is the region R; i.e.

$$P[d \leq \lambda] \approx \iint_{R'} f_{s_1}(s_1) f_{s_2}(s_2) ds_1 ds_2 \quad (2.6.1-13)$$

where

$$R' = \{(s_1, s_2): -\lambda \leq s_1 \leq \lambda, -\lambda \leq s_2 \leq \lambda\}.$$

The right-hand side of Equation 2.6.1-13 then provides the expression upon which the probability of collision for the CTOL/CTOL dependent case is based. This upper bound can be written as:

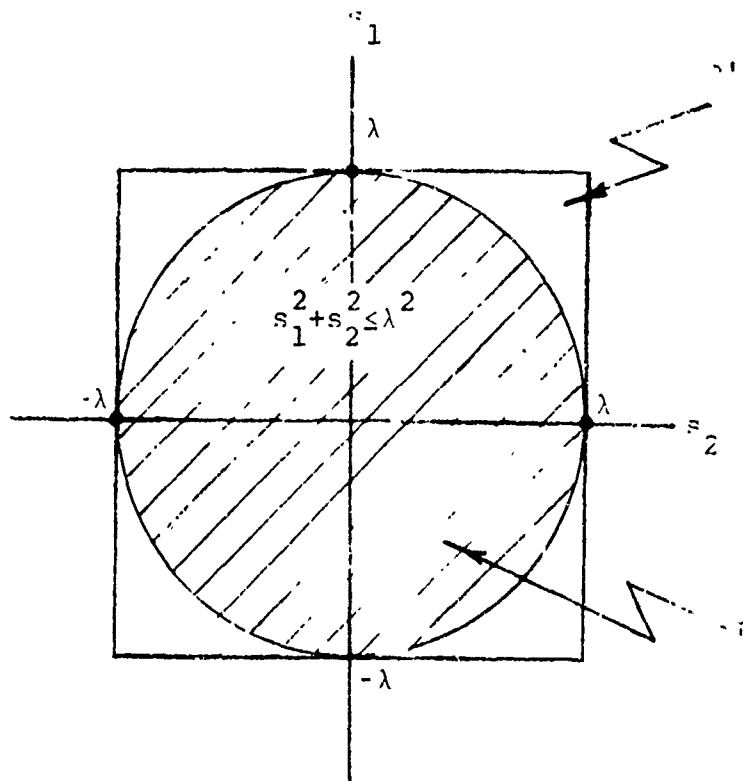


Figure 2.6.1-6

Region of $s_1 s_2$ -plane for which
Probability of Collision is Defined

$$\begin{aligned}
 P[d \leq \lambda] &\approx \iint_{R'} f_{s_1}(s_1) f_{s_2}(s_2) ds_1 ds_2 \\
 &= \int_{-\lambda}^{\lambda} f_{s_1}(s_1) ds_1 \int_{-\lambda}^{\lambda} f_{s_2}(s_2) ds_2 \\
 &= [\Phi(t_1) - \Phi(t_2)] \int_{-\lambda}^{\lambda} f_{s_2}(s_2) ds_2
 \end{aligned} \tag{2.6.1-14}$$

where

$$t_1 = \frac{\lambda - \mu_{s_1} + \mu_{s_2}}{\sigma_{s_1}^2 + \sigma_{s_2}^2}$$

$$t_2 = \frac{-\lambda - \mu_{\ell_1} + \mu_{\ell_2}}{\sigma_{\ell_1}^2 + \sigma_{\ell_2}^2}$$

ϕ = standard normal distribution

Since the densities of v_1' and Y_2' are the output of the Fokker-Planck equation, the integral on the right-hand side in Equation 2.6.1-14 is evaluated using the convolution method described by Equations 2.6.1-5, 6, and 7 in Section 2.6.1.2.

2.6.1.4 CTOL/STOL Independent

The geometry associated with the CTOL/STOL independent operations is identical to the CTOL/CTOL independent operation, with one exception - the glideslope angle for the STOL approach is 7.5 degrees as indicated in Figure 2.6.1-7.

Since the approach is an independent operation, longitudinal coincidence ($X_1 = X_2$) is assumed to assure a worst case condition as in the independent approach cases analyzed in Sections 2.6.1.1 and 2.6.1.2. Other assumptions utilized in the analysis given in this section are:

- (i) Vertical positions, Z_1 and Z_2 , of aircraft 1 and 2 are normally distributed, $N(\mu_1, \sigma_1^2)$ and $N(\mu_2, \sigma_2^2)$, respectively (Section 2.5);
- (ii) Y_2 is a random variable distributed according to the density output as a solution to the Fokker-Planck equation (Section 2.5); and
- (iii) Y_1 is distributed $N(\mu_{Y_1}, \sigma_{Y_1}^2)$ (Section 2.5).

The primary dimensions of interest for CTOL/STOL independent operations are lateral and vertical; therefore, lateral and vertical distributions are utilized in the determination of probability of collision.

Using the preceding assumptions, the probability of collision for CTOL/STOL independent approaches is defined as

$$P[\Delta \leq \lambda] = P \left\{ \left| (Y_1 - Y_2)^2 + (Z_1 - Z_2)^2 \right| \leq \lambda^2 \right\}. \quad (2.6.1-15)$$

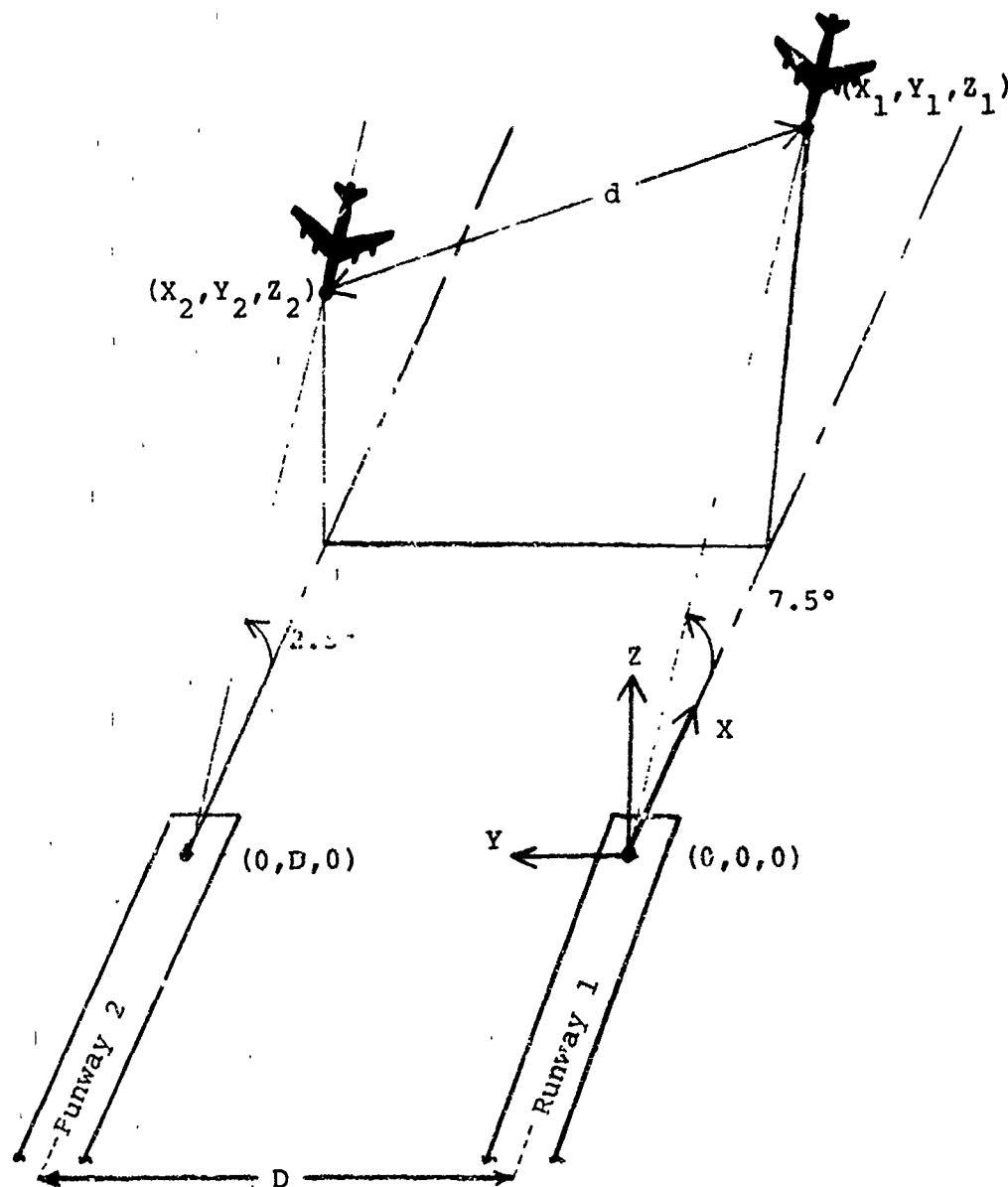


Figure 2.6.1-7

Probability of Collision Geometry for CTOL/STOL Independent Operations

The analysis involved in developing an analytical expression for the right-hand side of Equation 2.6.1-15 is identical to the analysis in the preceding section except that the random variables S_1 and S_2 defined in Equation 2.6.1-10 are now defined as:

$$S_1 = z_1 - z_2$$

$$S_2 = y_1 - y_2$$

Employing the analytical approach outlined by Equations 2.6.1-11 through 2.6.1-13, the formal expression for the probability of collision for CTOL/STOL independent operations is given as:

$$P[d \leq \lambda] = [\Phi(t_1) - \Phi(t_2)] \int_{-\lambda}^{\lambda} f_{s_2}(s_2) ds_2 \quad (2.6.1-16)$$

where

$$t_1 = \frac{\lambda - \mu_1 + \mu_2}{\sigma_1^2 + \sigma_2^2}$$

$$t_2 = \frac{-\lambda - \mu_1 + \mu_2}{\sigma_1^2 + \sigma_2^2}$$

Φ = standard normal distribution.

2.6.2 PROBABILITY OF COLLISION DATA GENERATION

As stated in Section 2.6, the probability of collision between approaching aircraft is used in considering the reduction of the present lateral spacing criteria between parallel runways. Analytical forms of the probability of collision models for the STOL/STOL independent operations, CTOL/CTOL independent operations, CTOL/CTOL dependent operations, and CTOL/STOL independent operations are given in Equations 2.6.1-3, 8, 14, and 16, respectively. This section describes all the combinations of aircraft and runway configurations, operations, and approach systems for which probability of collision data was generated in the Lateral Separation Study.

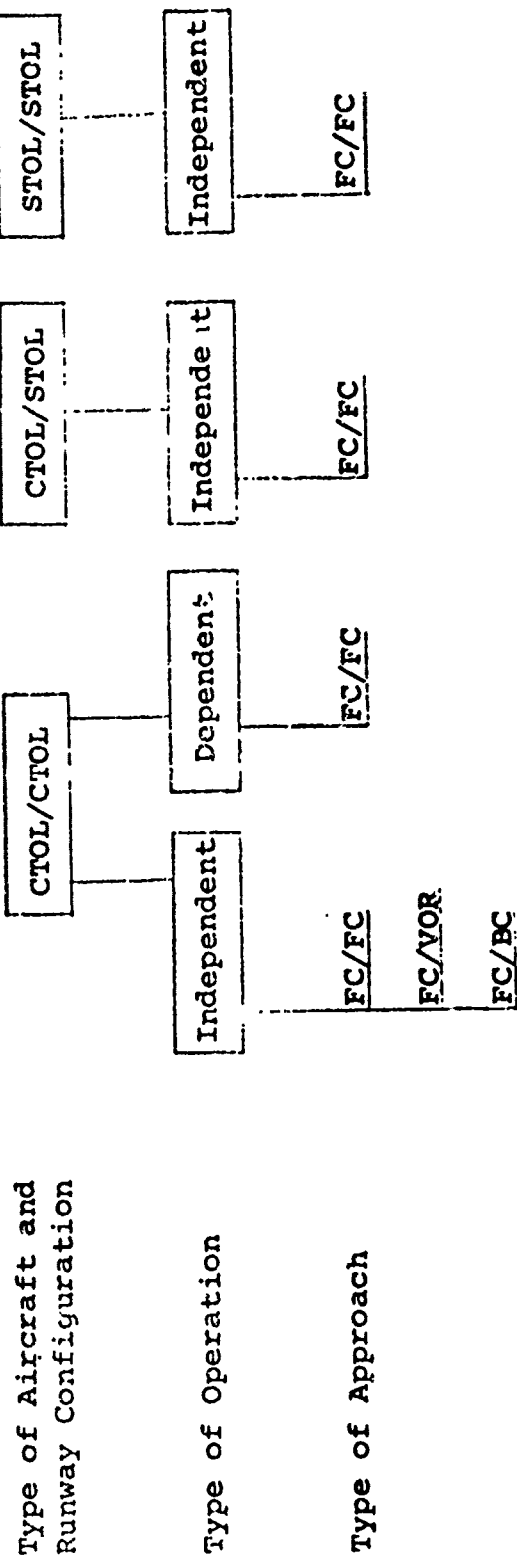
Specific combinations for CTOL/CTOL, CTOL/STOL, and STOL/STOL aircraft and runway configurations are described in detail in Sections 2.5.2.1, 2, and 3 along with a discussion of the probability of collision data generated for each combination. Results based on the combinations described in these sections are included in Appendix I in tabular form and are discussed in Section 3.5. An explanation of the tabular organization of results is also furnished in Section 3.5. Figure 2.6.2-1

represents a classification of all cases considered in the probability of collision data generation for the CTOL/CTOL, CTOL/STOL, and STOL/STOL aircraft and runway configurations.

For the purpose of clarity, an explanation of acronyms and nomenclature shown in Figure 2.6.2-1 will now be given since these terms are used throughout the remainder of this discussion.

- FC - Acronym referring to "front course" Category I ILS approach system.
- BC - Acronym referring to "back course" Category I ILS approach system.
- VOR - Acronym for an approach on a VOR/DME (VHF Omnidirectional Range/Distance Measuring Equipment) approach system. This is assumed to be conducted inbound "to" the station.
- FC/FC - Symbol referring to two Category I aircraft approaching parallel runways via FC approach systems.
- FC/BC - Refers to two Category I aircraft approaching parallel runways - one aircraft using a FC approach, and the other using a BC approach.
- FC/VOR - Refers to two Category I aircraft approaching parallel runways - one aircraft using a FC approach and the other using a VOR approach.

The maximum range at which probabilities of collision for CTOL/CTOL independent and dependent operations are calculated is the turn-on range. The turn-on range was selected because it is assumed to represent the worst case condition. At ranges greater than this range, vertical separation between parallel approaches increases; therefore, the vertical coincidence assumption is no longer valid. At ranges less than this range, the lateral distribution standard deviation decreases, resulting in lower probabilities of collision. Based upon the measured distribution data from Appendix H, the apparent turn-on range for independent operations for FC, BC, and VOR approaches was 6, 5, and 6 NMi, respectively. Probabilities of



NOTE: The notation used above is X/Y $\begin{matrix} \nearrow \\ \nwarrow \end{matrix}$ Runway 1
Runway 2

Figure 2.5.2-1

Cases Considered in Probability of Collision Analysis

collision were also evaluated at intermediate ranges of four and two miles.

Probabilities were calculated at these ranges for a fixed lateral spacing between runways. The lateral spacings considered were 5000, 4300, 3500, 3000, 2500, 2000, and 1500 feet. The 5000 feet lateral spacing case was selected since it is the current minimum spacing criteria between parallel runways for independent IFR operations. The lateral spacing of 4300 feet was selected as another case since this number represents the present lateral spacing between runways at several airports. The remainder of the lateral spacings considered were chosen so as to represent typical spacings between 3500 and 1500 feet.

Probabilities of collision for CTOL/STOL and STOL/STOL cases were considered at a maximum range from the STOL touchdown of 12,000 feet. The 12,000 foot range was chosen since it is the maximum range from the touchdown for which measured STOL distribution data was available; thus, it represents the apparent turn-on range for the STOL aircraft. Probabilities of collision were calculated for the same lateral spacings as considered for the CTOL/CTOL case.

The parameter representing aircraft wing span, λ , was assumed to be 200 feet for all probability of collision calculations. This parameter represents a worst case condition since it is approximately the wing span of the largest class of aircraft considered (Boeing 747) in this study (Reference 3). All distribution data required for a probability of collision calculation of the cases at the previously described ranges is contained in Appendix H. The means of these distributions were assumed to define an "ideal" track, i.e., on an extension of the runway centerline, in the glideslope plane and traveling at the nominal approach speed.

2.6.2.1 CTOL/CTOL - Probability of Collision Data Generation

Specific combinations of approach systems for the CTOL/CTOL aircraft and runway configuration for which probability of collision data were generated include:

- (a) FC/FC - Independent
- (b) FC/VOR - Independent
- (c) FC/BC - Independent
- (d) FC/FC - Dependent

The model used for generating probability of collision data for combinations in (a), (b), and (c) is given by Equation 2.6.1-8. Equation 2.6.1-14 represents the model used to generate data for combination (d).

The evaluation of Equation 2.6.1-8 for case (a) above was accomplished by:

- (1) evaluating the expression for g_{y_1} and g_{y_2}

where g_{y_1} is the probability density function

(PDF) at the initial range for the FC-ILS-I-CTOL (Lateral) system from Appendix H, and

g_{y_2} is identical to g_{y_1} but has a mean equal

to the lateral spacing between the runways
(D)

- (2) repeating step (1) with the lateral error PDF's for the ranges of four miles and two miles; and

- (3) repeating the two preceding steps for lateral spacings of 1500, 2000, 2500, 3000, 3500, and 4300 feet.

These three steps are the same for evaluating probabilities of collision for cases (b) and (c) except that g_{y_2} represents the

PDF's for VOR-CTOL (Lateral), and FC-ILS-I-CTOL (Lateral), from Appendix H for the respective cases. A detailed description of these PDF's is furnished in Appendix H.

Figure 2.6.2-2 illustrates the conditions for which probabilities of collision were generated for FC/FC dependent operations (case (d)). As indicated in the figure, probability of collision data generation was divided into four main cases. The primary difference between the cases is that each represents a different nominal longitudinal spacing between approaching aircraft.

As stated previously, for dependent operations, it is assumed that at some range greater than the outer marker, the controller has established the desired longitudinal spacing between the two aircraft and the nominal approach speeds for the two aircraft. This range is assumed to be 9 nmi (54720 feet), which corresponds to the approximate range at which the 1000 foot vertical separation is lost. It is further assumed that the nominal approach speeds for the two aircraft are equal. Based upon the preceding assumptions and the nominal longitudinal spacings noted in Figure 2.6.2-2, the FC-ILS-I-CTOL (Longitudinal) PDF's for the two aircraft were selected from Appendix H at the appropriate ranges.

	Case I	Case II	Case III	Case IV
Longitudinal spacing between adjacent aircraft, NMi	3	2	1	.25
Ranges* from threshold for which P_C was calculated, NMi	3 2 1	4 3 2 1	5 4 3 2 1	5 4 3 2 1

All cases calculated for lateral separations of 1500, 2000, 2500, 3000, 3500, 4300, and 5000 feet.

*NOTE: Range is measured from touchdown point to the closest aircraft.

Figure 2.6.2-2

Cases Considered in Probability of Collision for
CTOL/CTOL Dependent Operations

Equation 2.6.1-14 represents the model used in generating the probability of collision for all four cases. The lateral PDF's used are those for the FC-ILS-I-CTOL (Lateral) system (Appendix H) at the appropriate ranges.

2.6.2.2 CTOL/STOL - Probability of Collision Data Generation

The range interval over which the probability of collision for a CTOL/STOL - FC/FC - independent operation is calculated is shown in Figure 2.6.2-3. The maximum range (12,000 feet) is determined as being the range at which the 1000 foot vertical separation is lost and the minimum range (5000 feet) corresponds to that range where the CTOL aircraft "go visual", i.e., 200 feet altitude for Category I operating conditions.

Figure 2.6.2-4 illustrates the runway configurations and corresponding ranges from the touchdown at which probabilities of collision were calculated.

The distributions used for the STOL FC-ILS approach are those for the FC-ILS-I-STOL (Lateral and Vertical) systems defined in Appendix H (both are gaussian), and the CTOL-FC-ILS distributions are those defined in Appendix H for the FC-ILS-I-CTOL (Lateral and Vertical) systems at the ranges indicated in Figure 2.6.2-4.

The CTOL/STOL runway configuration indicated in Figure 2.6.2-5 was eliminated since the point at which vertical separation was one thousand feet occurred after the CTOL aircraft have gone VFR.

2.6.2.3 STOL/STOL - Probability of Collision Data Generation

Probability of collision data for STOL/STOL-FC/FC-independent approaches was generated at ranges from the touchdown of 12,000, 7,000, and 1,000 feet. The lateral error PDF's (gaussian) are given in Appendix H for the FC-ILS-I-STOL (Lateral) system at the appropriate ranges. The analytical model used in generation of probability of collision data for STOL/STOL approaches is given by Equation 2.6.1-3. Results are discussed in Section 3.5 and presented in Appendix I.

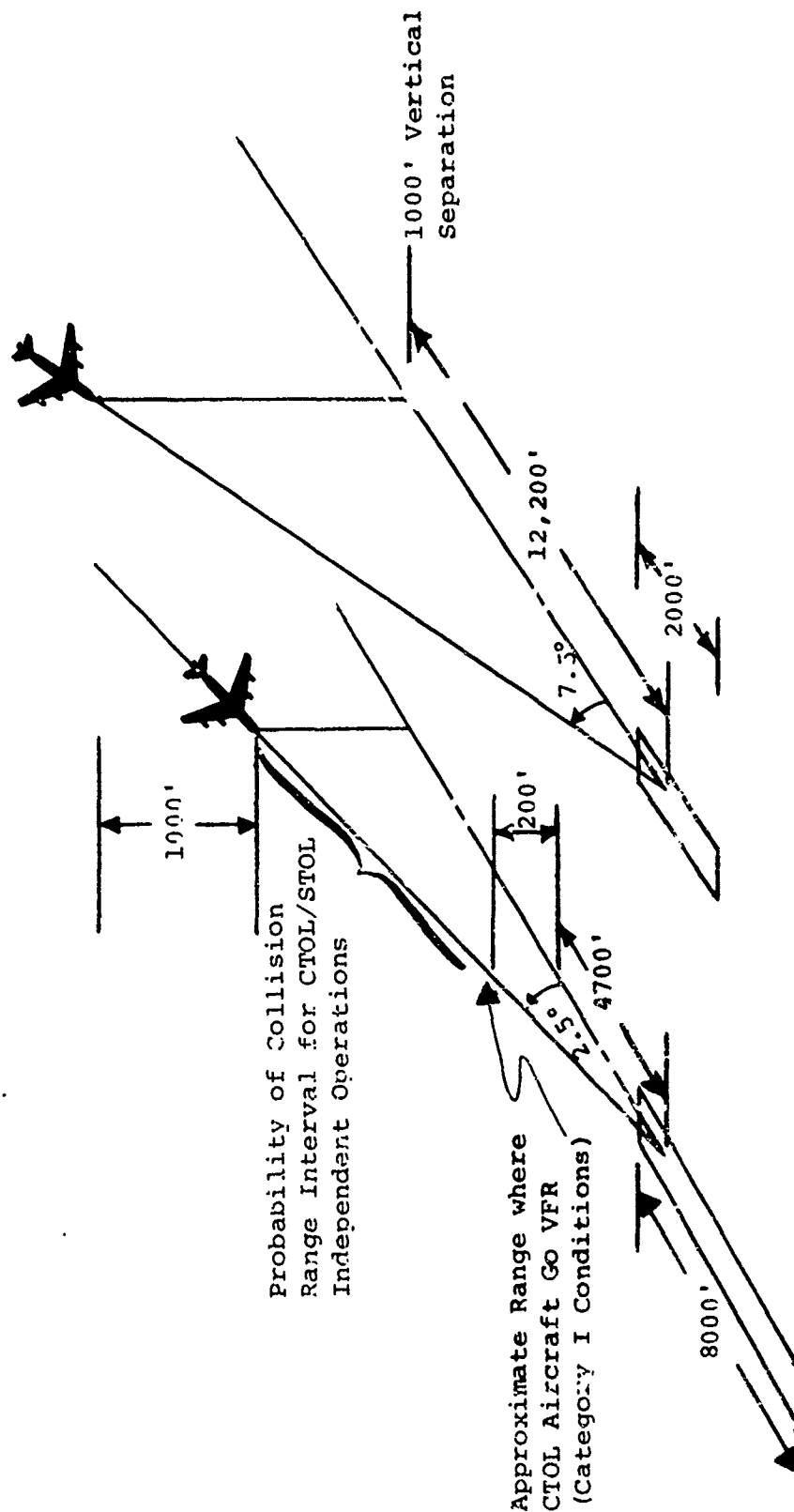


Figure 2.6.2-3 Probability of Collision Geometry for CTOL/STOL Independent Operations

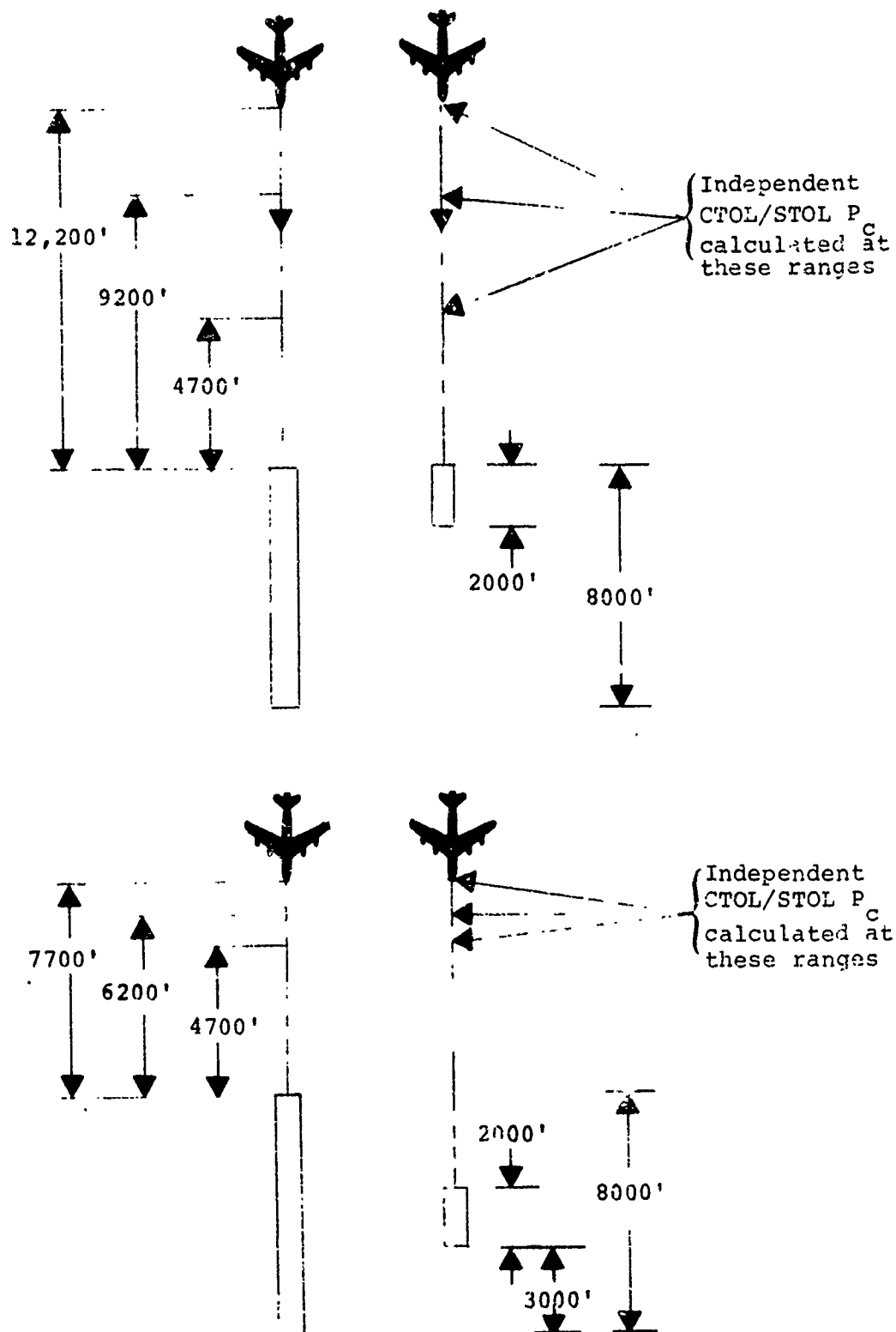


Figure 2.6.2-4 Runway Configurations Considered for CTOL/STOL Independent Operations

CTOL Aircraft
Go VFR

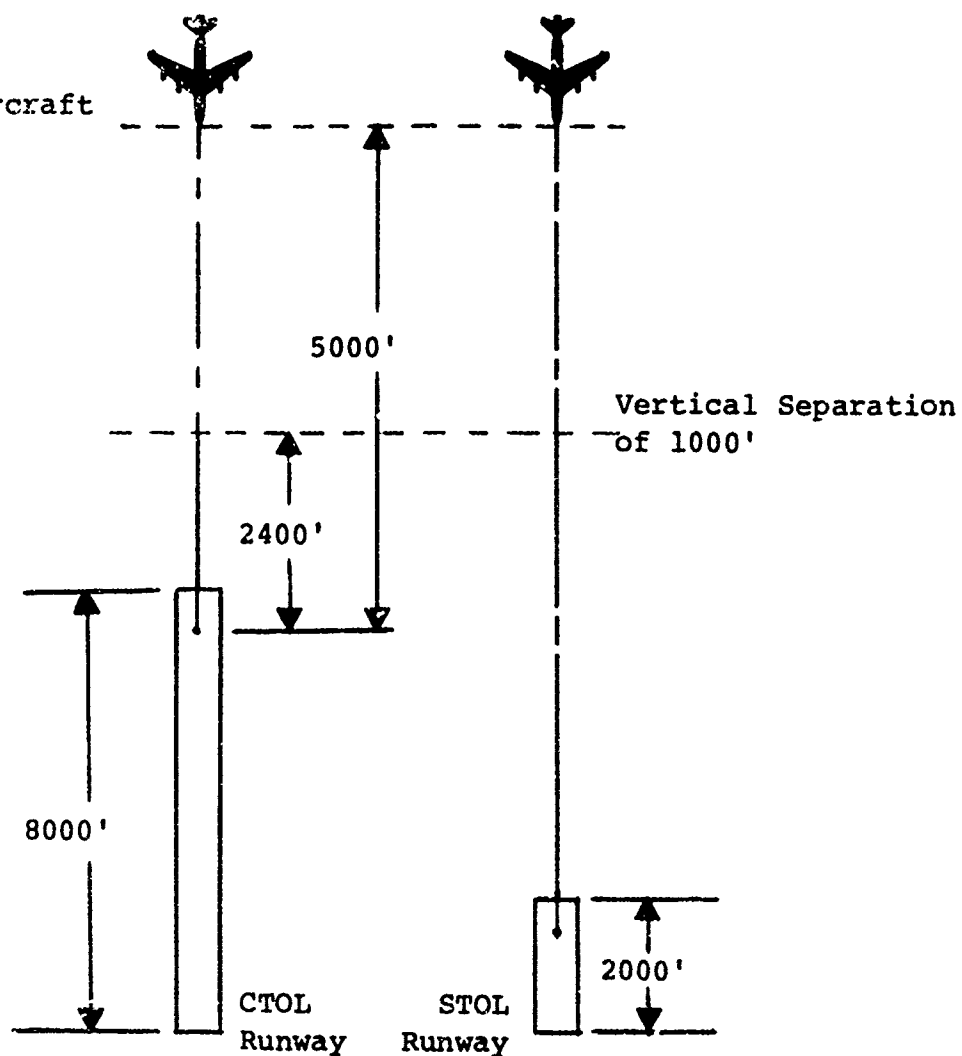


Figure 2.6.2-5

CTOL/STOL Threshold Displacement for which
Probability of Collision Was Not Considered

REFERENCES

1. Pearson, E. S., and h. O. Hartley, Biometrika, Volume I, Cambridge University Press, Cambridge, England, 1954.
2. Papoulis, A., Probability, Random Variables, and Stochastic Processes, McGraw-Hill, New York, 1965.
3. Hockaday, S.L.M., A Model to Investigate the Separation of Landing Aircraft, with Special Reference to Collision Risk, PhD Dissertation in Engineering, Graduate Division of the University of California, Berkeley.

SECTION 2.7

BLUNDER ANALYSIS

This portion of the Lateral Separation Final Report is an investigation of the airspace required for recovery from abnormal operations, blunders. This airspace is defined as the total lateral extension of the normal operating zone (NOZ) required to bring a blundered aircraft to a course parallel with either the runway centerline or parallel to the course of the aircraft in the adjacent parallel approach path.

There are two basic types of blunder situations that are considered in the evaluation of the runway separation requirements. Type 1 blunders occur when an aircraft that is on a track which intercepts the approach course at 10° , 20° , or 30° passes through the normal operating zone and proceeds toward the adjacent track. Type 1 blunders would typically occur during curved approach operations as the aircraft turns from the base leg onto the final leg. Due to large intercept angles between the base leg and final leg, overshoots could easily occur causing a type 1 blunder. Type 2 blunders occur when an aircraft which is established on the final approach course (within the normal operating zone) makes a turn toward the adjacent course at 15° , 30° , or 45° . Type 2 blunders would typically be caused by a system malfunction - either equipment or pilot.

The remainder of this section is divided into subsections which analyze recovery operations for single aircraft maneuvers and recovery operations for dual aircraft maneuvers. The parameters used in both analyses are contained in Table 2.7-1.

In the following blunder analyses, the quantity being sought is the recovery airspace required, measured from the action point (assumed to occur at NOZ). The blunder analyses are not dependent upon the "cause" of the blunder; therefore, type 1 and type 2 blunders are analyzed identically.

The action point is defined as the initial point at which the controller should identify a blunder. For this analysis it is assumed that the blunder is identified by a "position only" measurement technique; therefore, the action point is coincident with the NOZ boundary. If the measurement technique could sense heading and velocity, the action point would occur sooner, i.e., some place within the NOZ, and the required blunder recovery airspace would be reduced.

Table 2.7-1 Blundered Aircraft Parameter Values

Parameters	Values	Units
Departure Angles		
Type 1 Blunder	10, 20, and 30	degrees
Type 2 Blunder	15, 30, and 45	degrees
DAS Range Accuracy (ϵ_R)	1.5, 1.0, .5, and .2	percentages of range
DAS Azimuth Accuracy (ϵ_A)	1.5, 1.0, and .5	degrees
DAS Update Delays	4, 2, 1, .5, .1, and .01	seconds
Aircraft Velocities	60, 80, 100, 120, 140, and 160	knots
Aircraft Bank Angles	10, 20, 30, and 40	degrees
Pilot/Aircraft Reaction Times	1.5, 5, and 8	seconds
Communication Times	1 to 10	seconds

2.7.1 SINGLE AIRCRAFT ANALYSIS

2.7.1.1 Introduction

The purpose of the single aircraft analysis is to evaluate the cross-track distance (blunder recovery airspace) required for an aircraft to recover from the type 1 and type 2 blunders. The blunder recovery maneuver is assumed to be a coordinated turn in the glideslope plane performed by the blundering aircraft. It is necessary to establish a set of ground rules and assumptions to serve as a guideline throughout the single aircraft analysis. These ground rules and assumptions are presented and explained in the following section.

2.7.1.2 Approach

The blunder recovery airspace required for a single aircraft to recover from either of the two types of blunder situations is evaluated by considering the geometry of the situation. In the type 2 blunder, the requirement for a corrective command from the controller is not known until the controller's presentation of the aircraft position reaches the defined normal operating zone limit. In normal operating circumstances, aircraft entering at large intercept angles are

advised of their proximity to the extended runway centerline; however, depending on the pilot reaction and other factors, the type 1 blunder may not be alleviated. In the worst case, the controller does not detect the violation of the decision boundary until the aircraft has moved a cross-track distance equal to its cross-track velocity times the Data Acquisition System (DAS) update time and the DAS system error. See Figure 2.7.1-1 for a pictorial representation of this situation. The controller then transmits a correction maneuver command to the pilot. Because of the requirement for addresses in the command, the action information is not actually available to the pilot for a period of a few seconds. In this time and the time it takes for the pilot and aircraft to react, the aircraft continues along its deviated flight path. If at this point the aircraft starts a corrective maneuver, the aircraft is fully corrected, in terms of heading, within a distance proportional to the amount of heading change. The total of all these contributions constitute the blunder recovery airspace.

The equations used for the single aircraft analysis are derived from the geometric representation shown in Figure 2.7.1-1. Since the normal operating zone boundary is the action point to start the single aircraft blunder analysis, both type 1 and type 2 boundaries are analyzed through the same techniques and equations. The nomenclature for the single aircraft analysis equations is as follows:

T_1 = Summed Delays = Data Acquisition System Update
Delay + Communication Time + Pilot/Aircraft
Reaction Time

β = Departure Angle

V = Aircraft Velocity

ϕ = Bank Angle

$\dot{\psi}$ = Turn Rate ($d\psi/dt$)

EDAS = Data Acquisition System Error

The distance traveled by the blundered aircraft during the delays of the data update time, communication time, and pilot/aircraft reaction time is given by

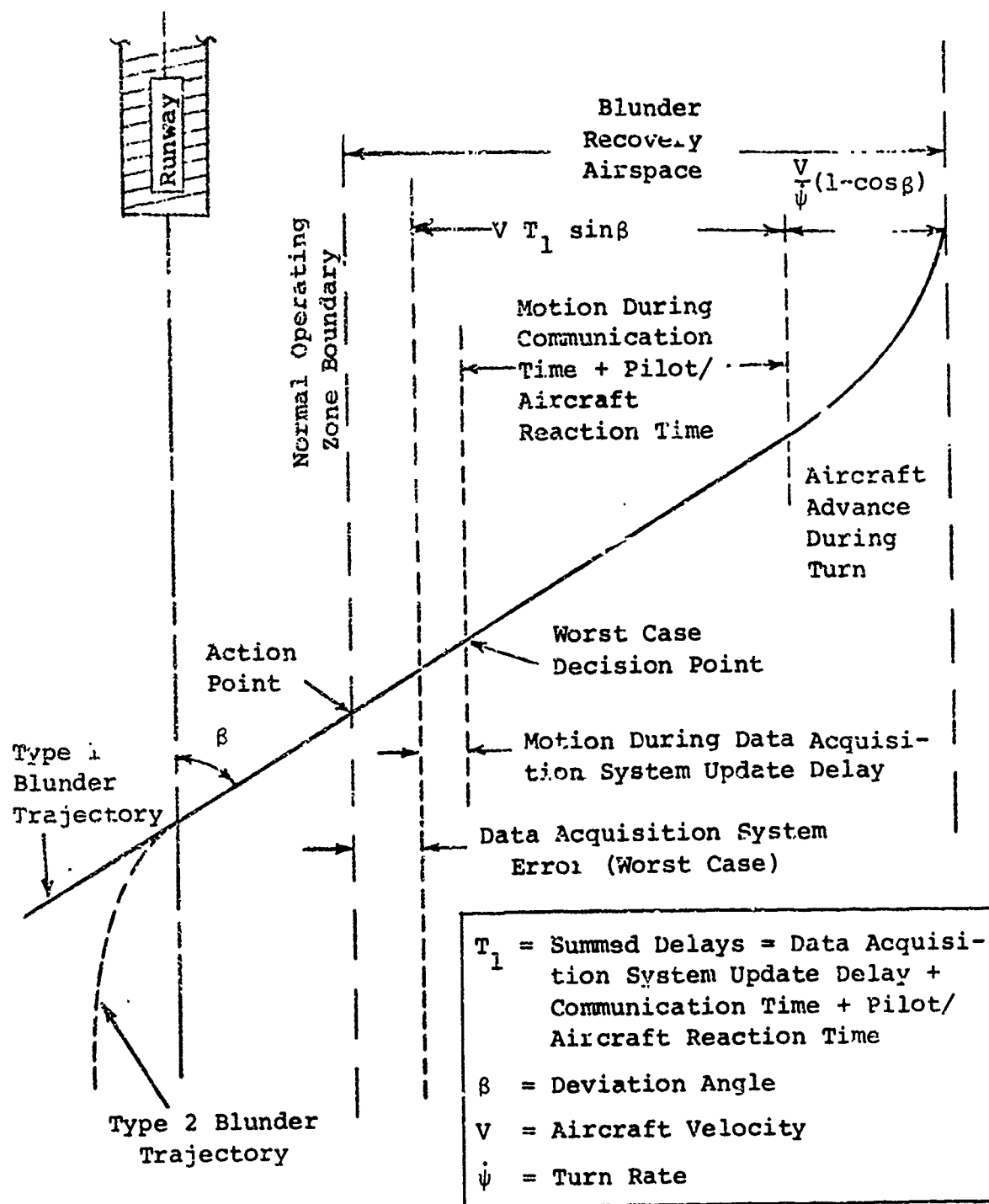


Figure 2.7.1-1

Single Aircraft Geometric Analysis of the Two Types of Blunders

$$D_{\text{DELAYS}} = VT_1 \sin\beta$$

and is derived from the geometric representation. This geometric analysis generally follows that developed by Blake and Smith (Reference 1).

The distance traveled during the recovery maneuver (perpendicular to the NOZ boundary) must also be defined. This distance is determined from Figure 2.7.1-2 as

$$D_{\text{TURN}} = R(1 - \cos\beta)$$

where R is the radius of turn, and

$$R = \frac{V}{\dot{\psi}}$$

$$\text{Therefore, } D_{\text{TURN}} = \frac{V}{\dot{\psi}}(1 - \cos\beta),$$

where the turn rate $\dot{\psi}$ is determined from

$$\dot{\psi} = \frac{32.2 \tan \phi}{V} \quad (2.7.1-1)$$

This equation was derived in Appendix A.

There is also a lateral distance due to the worst case errors of the DAS that can be considered. However, this distance is dependent upon the location of the DAS, which is dependent on the specific airport configuration; therefore, the DAS error, EDAS, is evaluated separately. However, EDAS will continue to be included throughout the blunder analysis due to its effect on the total recovery area.

The procedure for estimating EDAS for a specific configuration is discussed below. The EDAS considered is only that component which contributes to the lateral recovery airspace for a given blunder correction. Two DAS error sources are considered in this analysis - range error (ϵ_R) and azimuth error (ϵ_A). DAS lateral position errors are primarily affected by these errors.

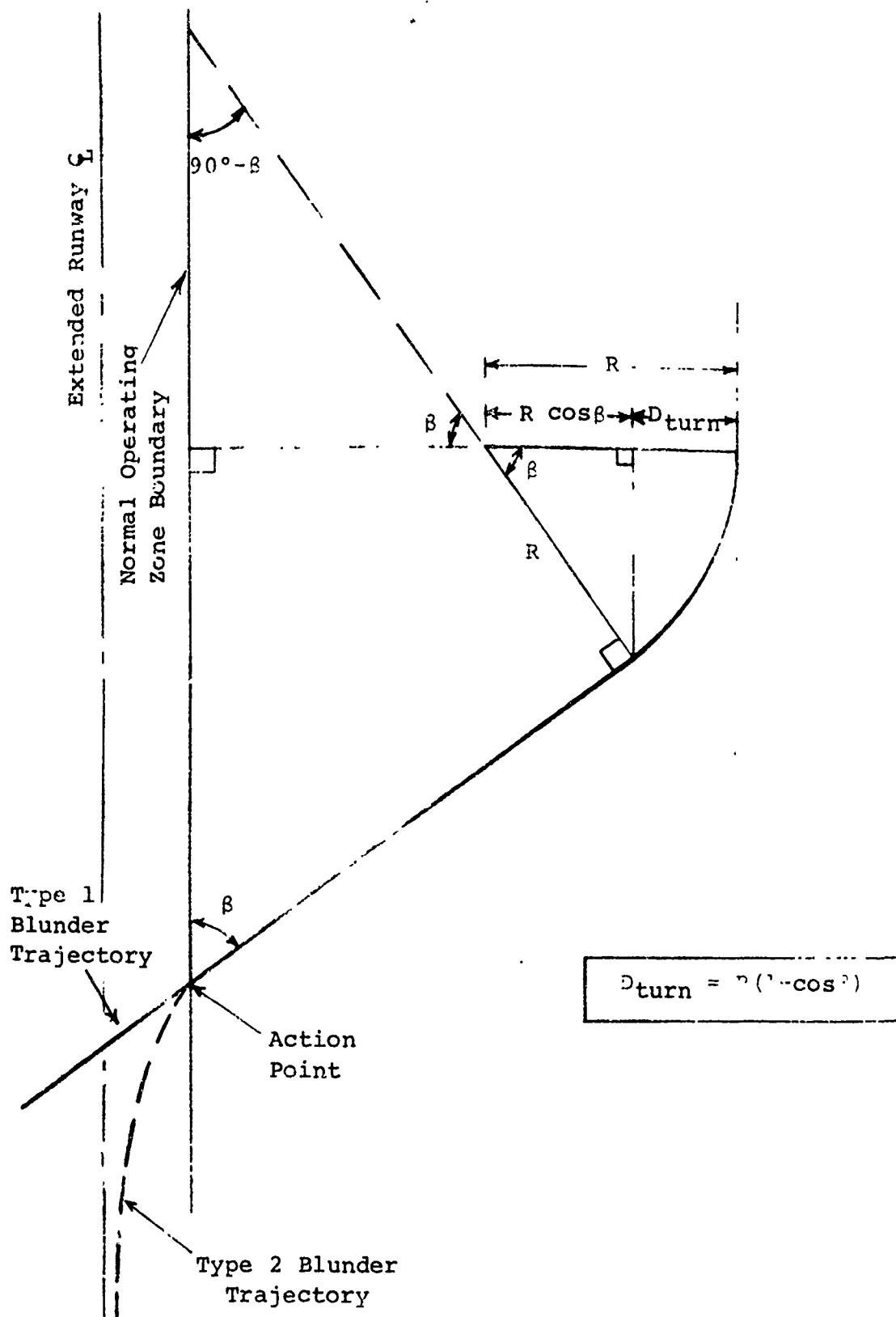


Figure 2.7.1-2 Single Aircraft Recovery Geometr

In order to estimate the EDAS, it is necessary to know the location of both the DAS antenna as well as the blundered aircraft. These locations are specified as follows:

$X_{A/C}$ - Aircraft ground range to touchdown, ft.

$Y_{A/C}$ - Aircraft lateral location from the runway centerline, ft.

$Z_{A/C}$ - Aircraft altitude, ft.

X_{DAS} - DAS antenna ground range from touchdown, ft.

Y_{DAS} - DAS antenna lateral location from the runway centerline, ft.

Z_{DAS} - DAS antenna altitude, ft.

Figure 2.7.1-3 illustrates a possible DAS location configuration. Determination of the lateral component of the DAS positional error (EDAS) due to range error and azimuth error is illustrated in Figure 2.7.1-3 and shown below.

$$EDAS = E_A \cos \rho + E_R \sin \rho \quad (2.7.1-2)$$

where

$$E_A = R \tan \epsilon_A \quad (2.7.1-3)$$

$$E_R = \frac{\epsilon_R R}{100} \quad (2.7.1-4)$$

$$R = \sqrt{(X_{DAS} - X_{A/C})^2 + (Y_{DAS} - Y_{A/C})^2 + (Z_{DAS} - Z_{A/C})^2} \quad (2.7.1-5)$$

$$\rho = \tan^{-1} \left| \frac{Y_{DAS} - Y_{A/C}}{X_{DAS} - X_{A/C}} \right| \quad (2.7.1-6)$$

Possible values to consider for ϵ_A and ϵ_R are listed in Table 2.7-1. The resulting value of EDAS for a specific DAS

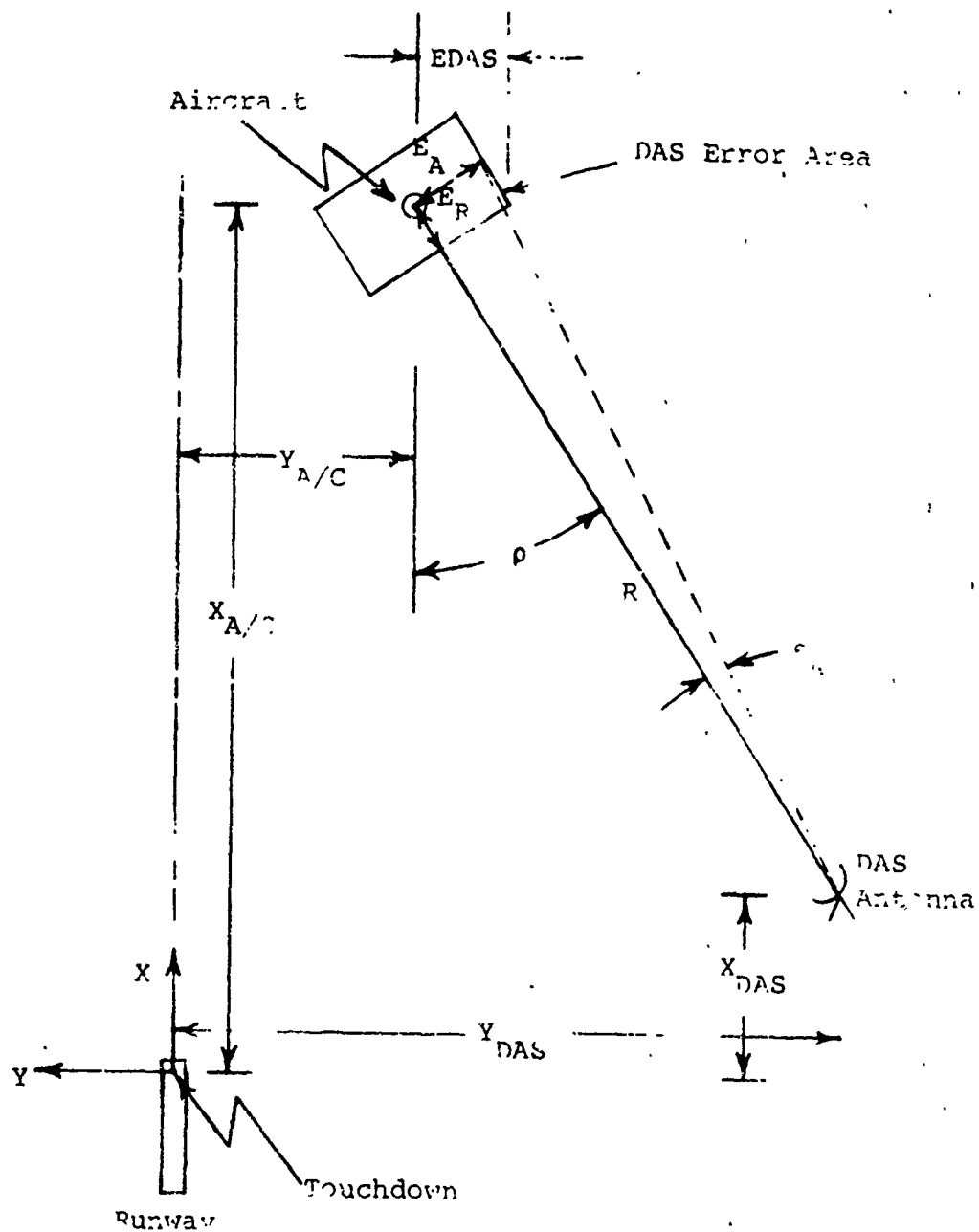


Figure 2.7.1-3 DAS Configuration

location configuration should be added to the blunder recovery airspace data as discussed in the following sections.

The final equation for the total distance traveled by a single blundered aircraft in a recovery maneuver is

$$D_{TOTAL} = VT_1 \sin\beta + EDAS + \frac{V}{\dot{\psi}} (1 - \cos\beta) \quad (2.7.1-7)$$

2.7.1.3 Results

The single aircraft analysis is used to determine the minimum airspace required for an aircraft to recover from either of the two types of blunder situations. Equations 2.7.1-1 and 2.7.1-7 were used to define the blunder recovery airspace. These equations were solved for combinations of the parameter values listed in Table 2.7-1. EDAS was set to zero in the equations. The lateral recovery airspace required for parameter combinations for the single aircraft blunder analysis is presented in tabular form in Appendix J. Values for EDAS should be added to these data when the position of the DAS antenna with respect to the blundered aircraft is known or can be approximated (Equations 2.7.1-2 through 6).

Typical output data from the single aircraft analysis is contained in Table 2.7.1-1. This table is a selected sample of the data in Appendix J, and the column headings are explained as follows:

Departure Angle (deg.) - the angle at which a blundered aircraft heads toward the adjacent approach course measured from the extended runway centerline.

Velocity (knots) - the velocity of the blundered aircraft.

Bank Angle (deg.) - the bank angle that the blundered aircraft uses to make the corrective maneuver.

Summed Delays (sec.) - a total of all the delays of the blundered aircraft, including DAS Update Delay, Communication Time, and Pilot/Aircraft Reaction Time.

Blunder Recovery Airspace (ft.) - the lateral recovery airspace, excluding EDAS, required for a blundered aircraft to recover from the type 1 and type 2 blunders, measured from the action point and perpendicular to the extended runway centerline.

Table 2.7.1-1 Single Aircraft Blunder Data

DEPARTURE ANGLE (DEG.)	VELOCITY (KNOTS)	BANK ANGLE (DEG.)	SUMMED DELAYS (SEC.)	BLUNDER RECOVERY AIRSPACE (T.)
30.00	100.00	40.00	2.50	352.25
30.00	100.00	40.00	9.00	900.77
30.00	100.00	40.00	16.00	1491.50
30.00	100.00	40.00	22.00	1997.84
30.00	100.00	30.00	2.50	416.27
30.00	100.00	30.00	9.00	964.60
30.00	100.00	30.00	16.00	1555.54
30.00	100.00	30.00	22.00	2061.88
30.00	100.00	20.00	2.50	536.62
30.00	100.00	20.00	9.00	1065.16
30.00	100.00	20.00	16.00	1675.00
30.00	100.00	20.00	22.00	2182.25
30.00	100.00	10.00	2.50	383.17
30.00	100.00	10.00	9.00	1431.70
30.00	100.00	10.00	16.00	2022.45
30.00	100.00	10.00	22.00	2528.70
30.00	120.00	40.00	2.50	436.58
30.00	120.00	40.00	9.00	1114.82
30.00	120.00	40.00	16.00	1823.70
30.00	120.00	40.00	22.00	2431.31
30.00	120.00	30.00	2.50	548.74
30.00	120.00	30.00	9.00	1207.04
30.00	120.00	30.00	16.00	1915.91
30.00	120.00	30.00	22.00	2523.57
30.00	120.00	20.00	2.50	722.19
30.00	120.00	20.00	9.00	1500.34
30.00	120.00	20.00	16.00	2089.22
30.00	120.00	20.00	22.00	2698.05
30.00	120.00	10.00	2.50	1221.13
30.00	120.00	10.00	9.00	1879.37
30.00	120.00	10.00	16.00	2528.25
30.00	120.00	10.00	22.00	3195.80

Reproduced from
best available copy.

Table 2.7.1-2 illustrates a reference blunder case and shows the changes of the blunder recovery airspace with respect to the variations of each parameter. The reference blunder case is shown in Figure 2.7.1-4 to illustrate the meaning of each parameter. Table 2.7.1-2 also shows the best case blunder conditions and the worst case blunder conditions for the parameter set considered.

The reference blunder case illustrated in Table 2.7.1-2 was also used to determine the sensitivity coefficients of the parameters used in the lateral recovery airspace solution. As shown in Table 2.7-1-2, these parameters were the departure angle (β), summed delays (T_1), velocity (V), and bank angle (ϕ). Each parameter was varied, and its sensitivity coefficient was calculated by

$$S_P^D = \frac{\Delta D}{\Delta P}$$

where ΔD is the change in the lateral recovery airspace due to a change of ΔP , and ΔP is the change in the selected parameter. The coefficients were found to be

$$S_{\beta}^D = 34.34 \text{ ft./deg.}$$

$$S_{T_1}^D = 57.73 \text{ ft./sec.}$$

$$S_V^D = 7.14 \text{ ft./knot}$$

$$S_{\phi}^D = -4.10 \text{ ft./deg.}$$

Figure 2.7.1-5 illustrates how the blunder sensitivity was calculated. From these sensitivity coefficients, it can be seen that the "summed delays" parameter, T_1 , is the major contributor to the lateral recovery airspace; whereas, the aircraft bank angle, ϕ , contributes the least to the recovery airspace.

The output of the single aircraft blunder analysis was verified by the use of the system model and by manually checking randomly selected cases.

Table 2.1.1-2 Single Aircraft Data Trends
(Excluding DAS Error)

	Departure Angle (deg.)	Velocity (knots)	Bank Angle (deg.)	Summed Delays (sec.)	Blunder Recovery Airspace (ft.)
Reference Case	20	100	30	9	611.95
Summed Delays Variation	20	100	30	16	1016.03
	20	100	30	22	1362.39
Bank Angle Variation	20	100	20	9	666.12
	20	100	10	9	822.12
Velocity Variation	20	120	30	9	756.51
	20	140	30	9	908.48
Departure Angle Variation	30	100	30	9	964.80
	45	100	30	9	1522.92
Best Case	10	60	40	2.5	49.73
Worst Case	45	160	10	22	7962.98

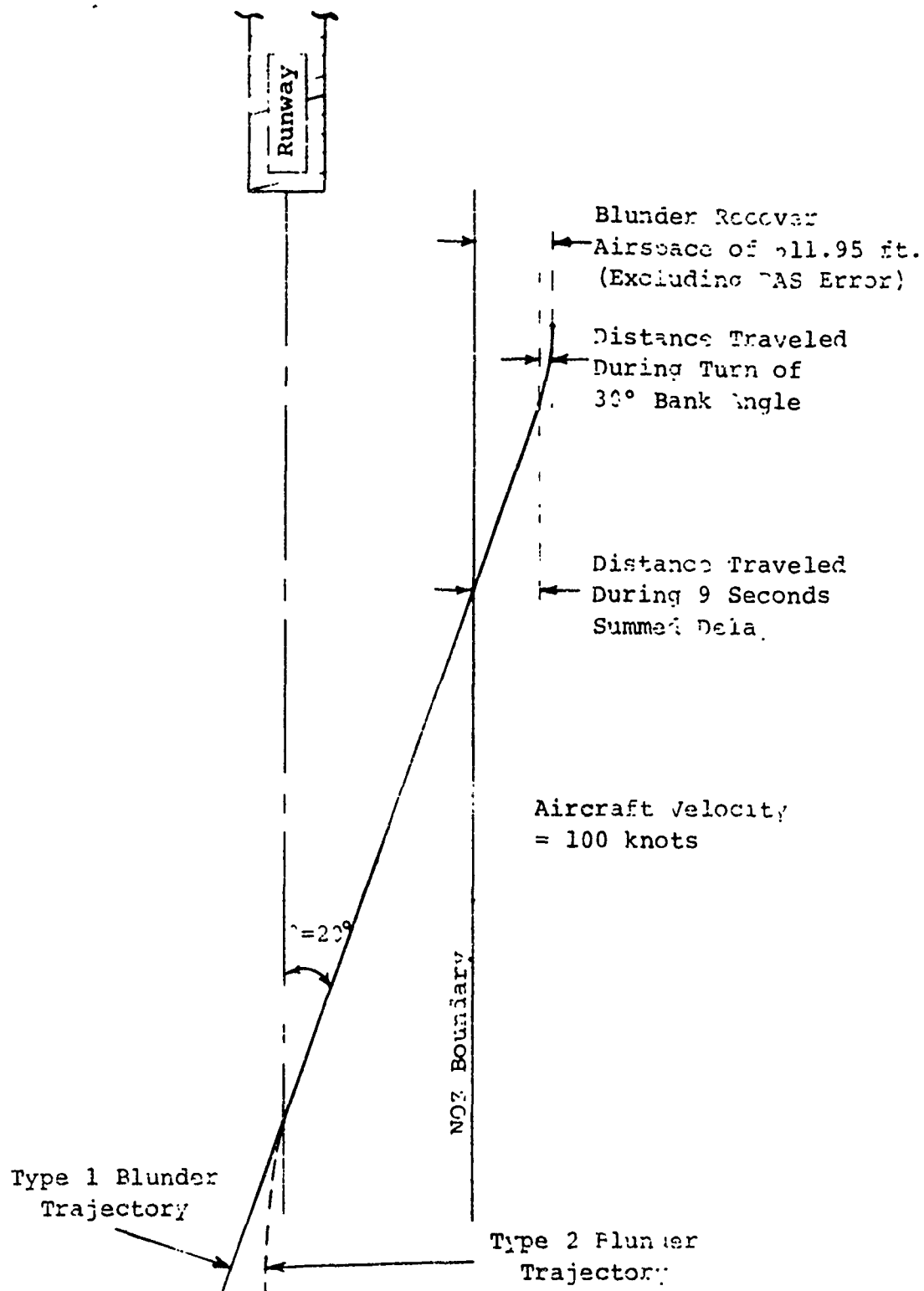


Figure 2.7.1-4 Reference Blunder Case for Single Aircraft

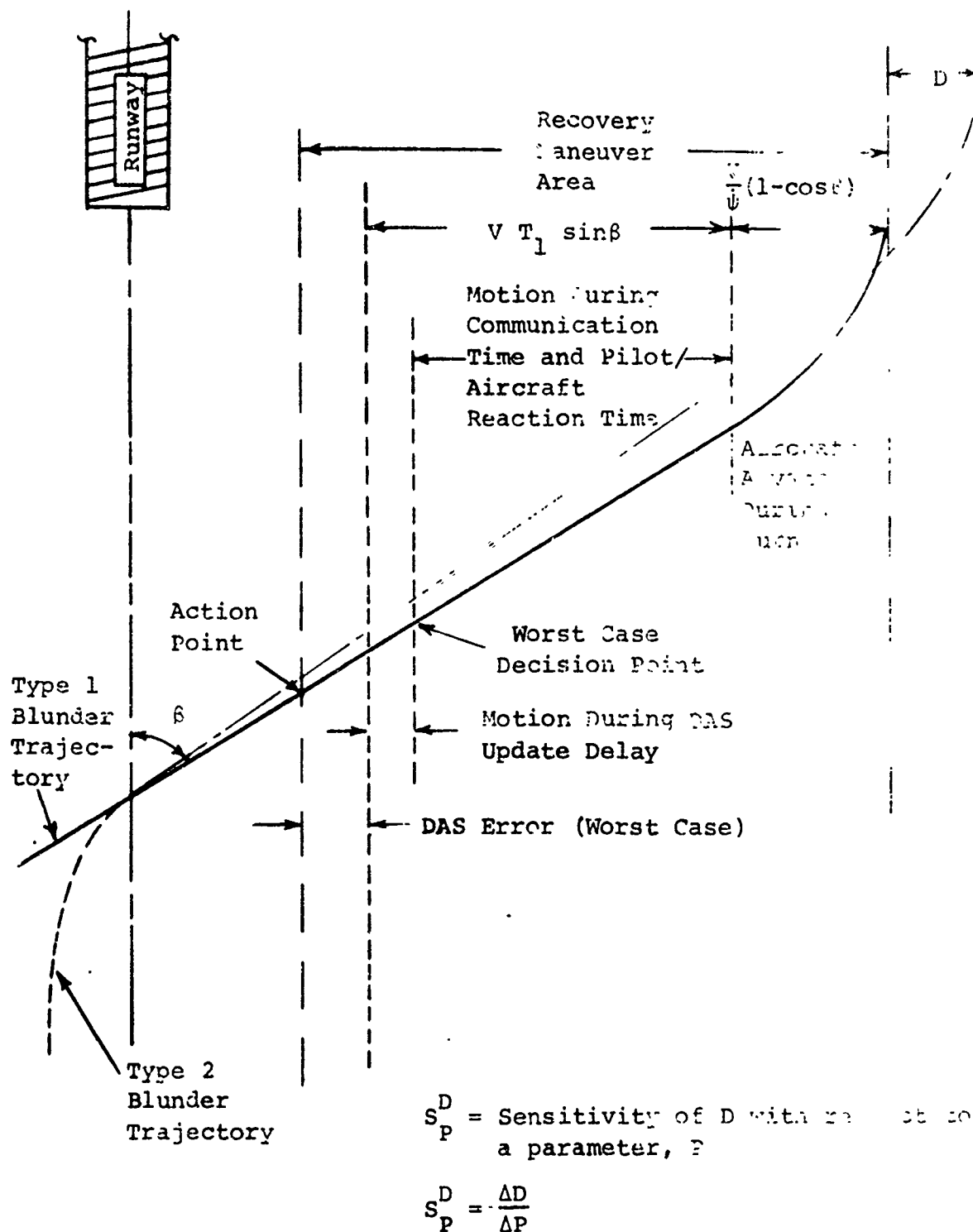


Figure 2.7.1-5 Blunder Sensitivity

2.7.2 DUAL AIRCRAFT ANALYSIS

2.7.2.1 Introduction

The purpose of the dual aircraft analysis is to evaluate the blunder recovery airspace required for a blundered aircraft to recover from the type 1 and type 2 blunders. The dual aircraft analysis assumes that the blundered aircraft does not respond to controller warnings; therefore, it is necessary for the controller to command an avoidance maneuver for the adjacent aircraft approaching the adjacent runway. The recovery of the blundered aircraft is considered complete when the heading of the blundered aircraft is the same as the heading of the aircraft on the adjacent approach course, meaning that both aircraft are flying parallel courses at that instant. Therefore, this analysis technique not only requires maneuvering the blundered aircraft but also requires maneuvering the aircraft on the adjacent course. The same set of ground rules, assumptions, and parameters used for the single aircraft analysis are used, along with other assumptions, to serve as a guideline throughout the dual aircraft analysis.

2.7.2.2 Approach

The geometry of the situation is again used in the evaluation of the required blunder recovery airspace. Figure 2.7.2-1 is a pictorial representation of the dual aircraft maneuver situation. In both types of blunders, the requirement for a corrective command from the controller is not known until the controller's presentation of the blundered aircraft position reaches the defined NOZ limit. However, the controller does not detect the violation of the decision boundary until the blundered aircraft has moved a cross-track distance equal to its cross-track velocity times the DAS update delay and the DAS system error. The controller then transmits a correction maneuver to the pilot of the blundered aircraft. After allowing time for the blundered aircraft to respond to the corrective maneuver issued, the controller alerts the controller of the aircraft on the adjacent approach course. The blundered aircraft now has traveled an additional cross-track distance due to the delays of the controller's communication time. While the blundered aircraft is traveling an even farther cross-track distance due to the delays of the pilot and the aircraft, the controller of the adjacent aircraft is responding to the situation and transmitting a message to his aircraft to maneuver. At this point in time, the blundered

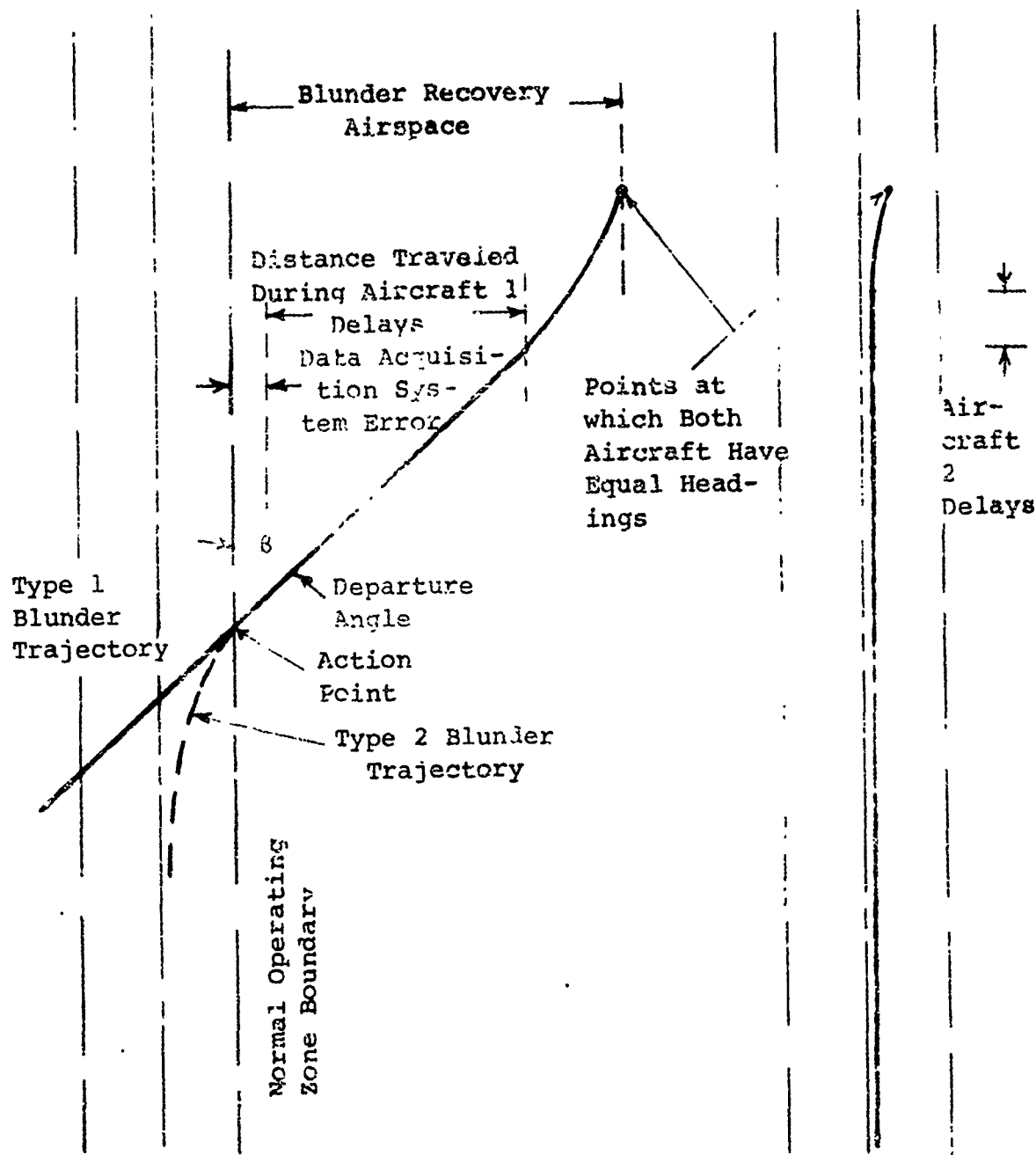


Figure 2.7.2-1 Dual Aircraft Geometric Analysis

aircraft has started its correction maneuver, and the adjacent aircraft starts its maneuver after the pilot and aircraft delays. When the heading of the adjacent aircraft becomes equal to that of the blundered aircraft, the blunder condition is considered to be corrected. Knowing these conditions and delays, it is possible to determine the cross-track distance traveled by the blundered aircraft before the blunder condition was corrected.

The procedure described above is best defined as a sequence of delays which directly affects the cross-track distance traveled by a blundered aircraft. This sequence is illustrated in Table 2.7.2-1 and is used to derive equations for cross-track distance evaluation of the blundered aircraft. It should be noted that the DAS error is evaluated separately, as explained in Section 2.7.1.2.

The nomenclature for the dual aircraft analysis equations is as follows:

β = Departure Angle of the Blundered Aircraft

V_1 = Velocity of Blundered Aircraft

T_1 = Blundered Aircraft Summed Delays = DAS Update Delay + Controller₁ Communication Time + Pilot₁/Aircraft₁ Reaction Time

ϕ_1 = Bank Angle of Blundered Aircraft

$\dot{\psi}_1$ = Turn Rate of Blundered Aircraft

EDAS = DAS Error

T_2 = Adjacent Aircraft Summed Delays = Controller₁ to Controller₂ Delay + Controller₂ Communication Time + Pilot₂/Aircraft₂ Reaction Time

$\dot{\psi}_2$ = Turn Rate of Adjacent Aircraft

The blundered aircraft parameters considered in this analysis are listed in Table 2.7-1 and the adjacent aircraft parameters are

T_2 = 1, 4, 7, 10 seconds

$\dot{\psi}_2$ = ~3 deg./sec.

Table 2.7.2-1

Dual Aircraft Blunder Analysis
Sequence of Delays

Blundered Aircraft	Adjacent Aircraft
(1) DAS update delay	
(2) Controller ₁ communication time	
(3) Pilot ₁ reaction time	
(4) Aircraft ₁ response time	(4) Controller ₁ to Controller ₂ delay
(5) Aircraft ₁ turn time	(5) Controller ₂ communication time
	(6) Pilot ₂ reaction time
	(7) Aircraft ₂ response time
	(8) Aircraft ₂ turn time

The total cross-track distance traveled by the blundered aircraft is

$$D_{\text{TOTAL}} = d_1 + d_2 + \text{EDAS}, \quad (2.7.2-1)$$

where d_1 is the lateral distance the blundered aircraft travels during the blunder summed delays, T_1

$$d_1 = V_1 T_1 \sin \beta, \quad (2.7.2-2)$$

$$\text{EDAS} = \text{DAS Error}. \quad (2.7.2-3)$$

EDAS is evaluated for a specific DAS antenna location as explained in Section 2.7.1.2 (Equations 2.7.1-2 through 6). Therefore, it is necessary to find d_2 , the distance traveled by the blundered aircraft during the turn maneuver.

To determine the distance d_2 , it is first necessary to determine the time required for the blundered aircraft to perform the turn maneuver, $T_{\text{turn } 1}$, shown in Figure 2.7.2-2. The time at which the blunder has been corrected, T_F , is determined from Figure 2.7.2-2. After determining T_F , $T_{\text{turn } 1}$ is determined. The graph indicates heading angle versus time for both the blundered aircraft and the adjacent aircraft. The blundered aircraft is flying at a heading, ψ_1 , of $180^\circ - \beta$ and the adjacent aircraft is flying at a heading, ψ_2 , of 180° , where 180° is assumed for computational convenience to be a course parallel to the runway centerline. As shown, the blundered aircraft first initiates its bank angle at T_1 causing its heading to change at an assumed constant turn rate. This rate is

$$\dot{\psi}_1 = \frac{32.2 \tan \phi_1}{V_1}. \quad (2.7.2-4)$$

At a later point in time, T_2 , the adjacent aircraft initiates its bank angle maneuver, causing its heading to also change at a turn rate assumed to be constant. This rate is defined to be

$$\dot{\psi}_2 = -3^\circ/\text{sec}. \quad (2.7.2-5)$$

Initiating these constant rates of turn causes the heading angles of both aircraft to change at slopes equal to $\dot{\psi}_1$ and $\dot{\psi}_2$. The point at which the heading angles of each aircraft are equal,

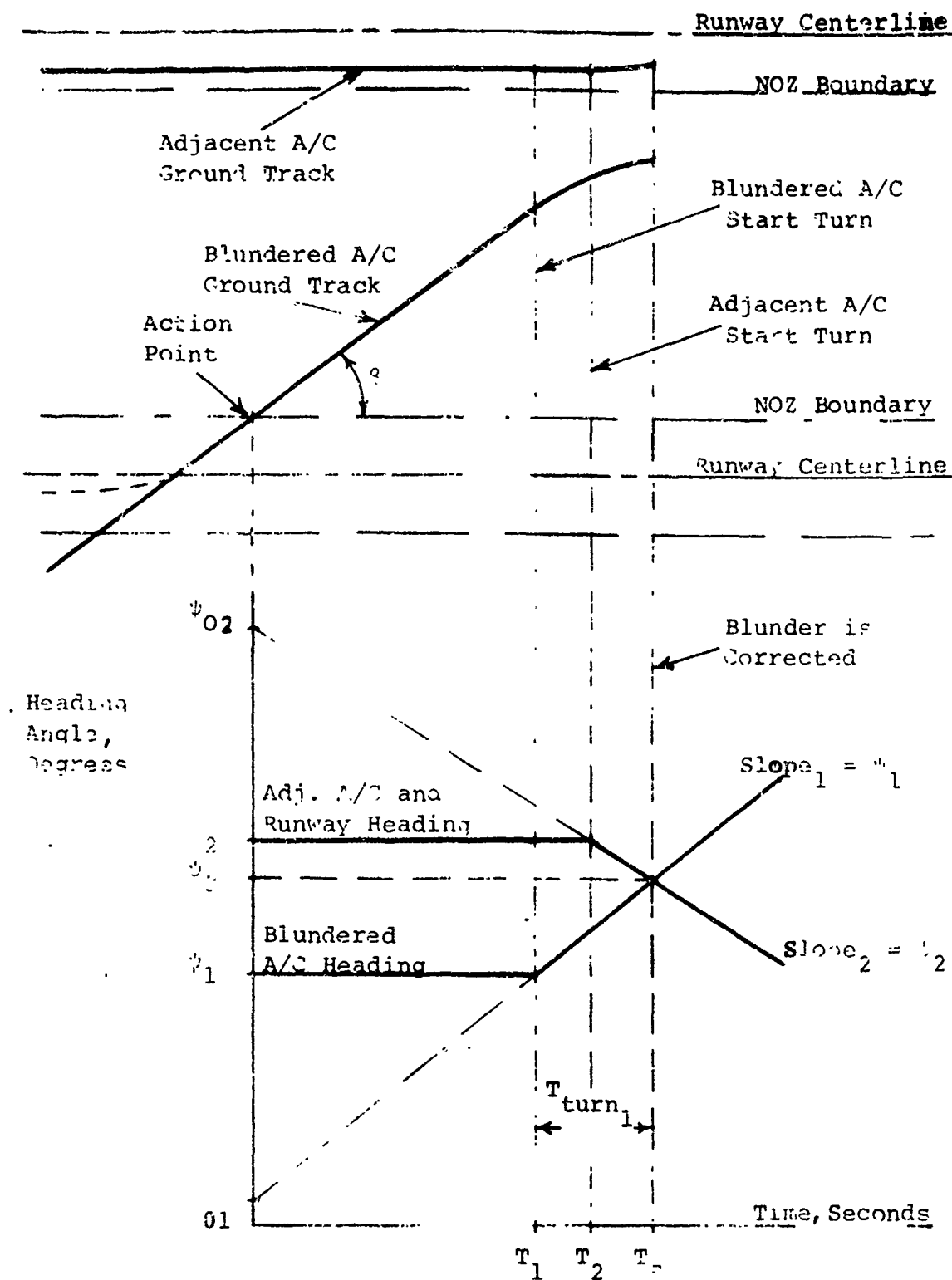


Figure 2.7.2-2 Dual Aircraft Blunder Analysis Illustration

ψ_3 , determines the time at which both aircraft are on parallel courses (T_F); i.e., the blunder has been resolved. For the blundered aircraft,

$$\psi_3 = \dot{\psi}_1 T_F + \psi_{01} \quad (2.7.2-6)$$

where

$$\psi_{01} = \psi_1 - \dot{\psi}_1 T_1, \quad (2.7.2-7)$$

and for the adjacent aircraft,

$$\psi_3 = \dot{\psi}_2 T_F + \psi_{02} \quad (2.7.2-8)$$

$$\psi_{02} = \psi_2 - \dot{\psi}_2 T_2. \quad (2.7.2-9)$$

Equating Equations 2.7.2-6 and 2.7.2-8 and solving for T_F yields

$$T_F = \frac{\psi_{02} - \psi_{01}}{\dot{\psi}_1 - \dot{\psi}_2}; \text{ for } \psi_3 < 180^\circ. \quad (2.7.2-10)$$

At this point, it should be noted that if the delays of the adjacent aircraft are too large, it is possible for the blundered aircraft to correct the blunder by achieving a course parallel with its own approach course before the adjacent aircraft can start its maneuver. In this case, $\psi_3 = 180^\circ$ and T_F is determined from Equation 2.7.2-6 as

$$T_F = \frac{180^\circ - \psi_{01}}{\dot{\psi}_1}. \quad (2.7.2-11)$$

Having determined T_F , the time required for the turn is found from Figure 2.7.2-2 as

$$T_{\text{turn } 1} = T_F - T_1. \quad (2.7.2-12)$$

After finding $T_{\text{turn } 1}$, the cross-track distance, d_2 , traveled by the blundered aircraft during its turn is found

using the geometry shown in Figure 2.7.2-3. This figure illustrates the geometry of only the blundered aircraft. From Figure 2.7.2-3 and the equation for tangential velocity for a constant turn rate, the radius of turn for the blundered aircraft is determined.

$$r = \frac{V_1}{\dot{\psi}_1} \quad (2.7.2-13)$$

Also, the angle, θ_1 , turned by the blundered aircraft during its correction is found as

$$\theta_1 = \dot{\psi}_1 T_{\text{turn } 1}. \quad (2.7.2-14)$$

Knowing r and θ_1 , the cross-track distance traveled during the turn, d_2 , can be determined from Figure 2.7.2-3 and the equations below:

$$\theta_2 = \beta - \theta_1 \quad (2.7.2-15)$$

$$d_2 = r \cos \theta_2 - r \cos \beta$$

Having found d_2 , the total cross-track distance traveled by the blundered aircraft during the blunder condition is stated as

$$\begin{aligned} D_{\text{TOTAL}} &= d_1 + d_2 + \text{EDAS}, \\ &= V_1 T_1 \sin \beta + r (\cos \theta_2 - \cos \beta) + \text{EDAS}. \end{aligned} \quad (2.7.2-16)$$

2.7.2.3 Results

The dual aircraft analysis is used to evaluate the blunder recovery airspace required for a blundered aircraft to recover from the two types of blunder conditions. By maneuvering both the blundered aircraft and the aircraft on the adjacent approach course, the blunder condition is considered resolved when the headings of both aircraft are equal. The equations derived in the dual aircraft analysis (Equations 2.7.2-3 through 2.7.2-16) were used to determine the lateral recovery airspace for all combinations of the parameter values (excluding EDAS), and the results are presented in



tabular form in Appendix K. Values for EDAS should be included when the position of the DAS antenna is known for a particular system, as described in Section 2.7.1.2 (Equations 2.7.1-2 through 2.7.1-6). Also, as stated in Section 2.7.2.2, ψ_2 is set equal to -3.0 degrees per second, and ψ_2 is assumed to be equal to 180 degrees (or equal to the assumed runway heading).

Appendix K contains the lateral recovery airspace required for all parameter combinations for the dual aircraft analysis. Table 2.7.2-2 contains typical output data from the dual aircraft analysis and represents an overview of the data contained in Appendix K. The column headings for Table 2.7.2-2 and Appendix K are explained as follows:

Blundered Departure Angle (deg.) - the angle at which a blundered aircraft heads toward the adjacent approach course measured from the extended runway centerline.

Blundered Velocity (knots) - the velocity of the blundered aircraft.

Blundered Bank Angle (deg.) - the bank angle that the blundered aircraft uses to make the corrective maneuver.

Blundered Summed Delays (sec.) - a total of all the delays of the blundered aircraft, including DAS Update Delay, Communication Time, and Pilot/Aircraft Reaction Time.

Adjacent Summed Delays (sec.) - a total of all the delays of the adjacent aircraft, including the Communication Time and Pilot/Aircraft Reaction Time measured after the Blundered Summed Delays.

Corrected Parallel Headings (deg.) - the heading angle of both the blundered and adjacent aircraft at the point in time when they are flying parallel courses (i.e., the blunder is corrected). For this analysis, the approach heading was assumed to be 180°.

Blunder Correction Time (sec.) - the total time required for a blundered aircraft to attain a flight course parallel with that of the aircraft on the adjacent course (total blunder recovery time measured from the time the blundered aircraft reaches the action point until the blunder is corrected).

Blunder Recovery Airspace (ft.) - the lateral recovery airspace, excluding EDAS, required for a blundered aircraft to recover to

Table 2.7.2-2 Dual Aircraft Blunder Data

BLUNDERED DEPARTURE ANGLE (DEG.)	BLUNDERED VELOCITY (KNOTS)	BLUNDERED BANK ANGLE (DEG.)	BLUNDERED SUMMED DELAYS (SEC.)	ADJACENT SUMMED DELAYS (SEC.)	CORRECTED PARALLEL HEADINGS (DEG.)	BLUNDER CORRECTION TIME (SEC.)	BLUNDER RECOVERY AIRSPACE (FT.)
30.00	100.00	40.00	2.50	1.00	174.87	5.21	342.00
30.00	100.00	40.00	2.50	4.00	180.00	5.77	352.23
30.00	100.00	40.00	2.50	7.00	180.00	5.77	352.23
30.00	100.00	40.00	2.50	10.00	180.00	5.77	352.23
30.00	100.00	40.00	9.00	1.00	174.87	11.71	896.54
30.00	100.00	40.00	9.00	4.00	180.00	12.27	900.77
30.00	100.00	40.00	9.00	7.00	180.00	12.27	900.77
30.00	100.00	40.00	9.00	10.00	180.00	12.27	900.77
30.00	100.00	40.00	10.00	1.00	174.87	18.71	1487.27
30.00	100.00	40.00	10.00	4.00	180.00	19.27	1491.50
30.00	100.00	40.00	10.00	7.00	180.00	19.27	1491.50
30.00	100.00	40.00	10.00	10.00	180.00	19.27	1491.50
30.00	100.00	40.00	22.00	1.00	174.87	24.71	1993.61
30.00	100.00	40.00	22.00	4.00	180.00	25.27	1997.84
30.00	100.00	40.00	22.00	7.00	180.00	25.27	1997.84
30.00	100.00	40.00	22.00	10.00	180.00	25.27	1997.84
30.00	100.00	30.00	2.50	1.00	172.37	6.04	402.69
30.00	100.00	30.00	2.50	4.00	178.47	7.01	415.72
30.00	100.00	30.00	2.50	7.00	180.00	7.25	416.27
30.00	100.00	30.00	2.50	10.00	180.00	7.25	416.27
30.00	100.00	30.00	9.00	1.00	172.37	12.54	951.23
30.00	100.00	30.00	9.00	4.00	178.47	13.51	964.26
30.00	100.00	30.00	9.00	7.00	180.00	13.75	964.26
30.00	100.00	30.00	9.00	10.00	180.00	13.75	964.26
30.00	100.00	30.00	16.00	1.00	172.37	19.54	1541.96
30.00	100.00	30.00	16.00	4.00	178.47	20.51	1554.99
30.00	100.00	30.00	16.00	7.00	180.00	20.75	1555.54
30.00	100.00	30.00	16.00	10.00	180.00	20.75	1555.54
30.00	100.00	30.00	22.00	1.00	172.37	25.54	2046.30
30.00	100.00	30.00	22.00	4.00	178.47	26.01	2061.33
30.00	100.00	30.00	22.00	7.00	180.00	26.75	2061.33
30.00	100.00	30.00	22.00	10.00	180.00	26.75	2061.33

a course parallel with that of the adjacent aircraft. The blunder recovery airspace is measured from the action point perpendicular to the extended runway centerline.

Some examples of the output data are shown in Table 2.7.2-3. This table illustrates a reference blunder case and shows the changes of the blunder recovery airspace with respect to the variations of each parameter. An illustration of the reference case is shown in Figure 2.7.2-4. Also, the best case blunder conditions and the worst case blunder conditions for the dual aircraft analysis for the given parameter set are shown in Table 2.7.2-3. It should be noted that the blunder recovery airspace does not always vary with a change of the adjacent summed delays. This condition is due to the blundered aircraft correcting its heading error before the adjacent aircraft has time to start a maneuver.

Table 2.7.2-3 Dual Aircraft Data Trends
(Excluding DAS Error)

	Blundered Departure Angle (deg.)	Blundered Velocity (knots)	Blundered Bank Angle (deg.)	Blundered Summed Delays (sec.)	Adjacent Summed Delays (sec.)	Blunder Recovery Airspace (ft.)
Reference Case	20	100	30	9	1	607.41
(Adjacent)						
Summed Delays	20	100	30	9	4	611.95
Variation	20	100	30	9	7	611.95
(Blundered)						
Summed Delays	20	100	30	16	1	1011.49
Variation	20	100	30	22	1	1357.85
(Blundered)						
Bank Angle	20	100	20	9	1	648.58
Variation	20	100	10	9	1	729.88
(Blundered)						
Velocity	20	120	30	9	1	746.89
Variation	20	140	30	9	1	890.96
(Blundered)						
Departure	30	100	30	9	1	951.23
Angle	45	100	30	9	1	1486.80
Variation						
Best Case	10	60	40	2.5	1	49.73
Worst Case	45	160	10	22	10	6896.57

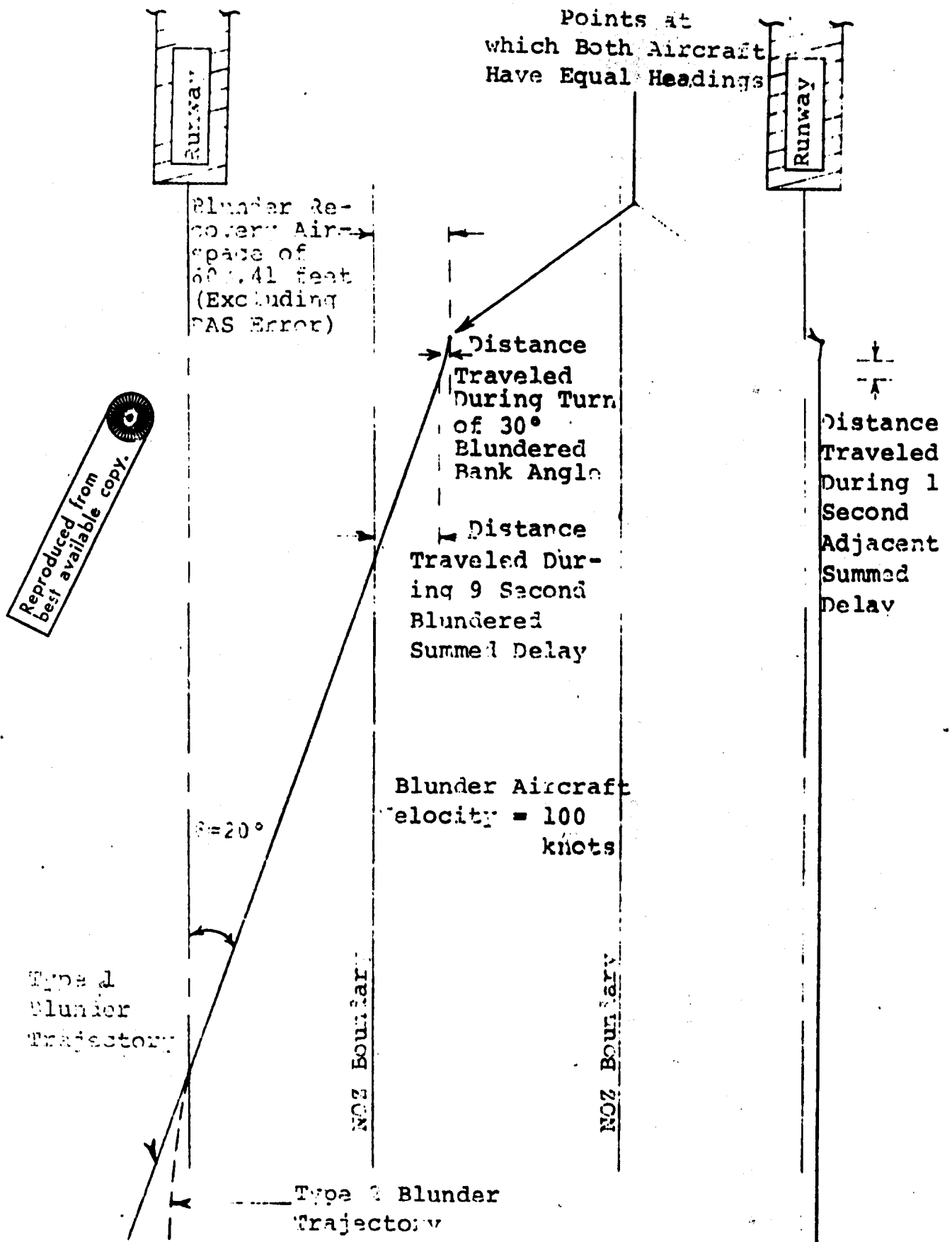


Figure 2.7.2-4 Dual Aircraft Reference Blunder Case

REFERENCES

1. Blake, N. A. and E. E. Smith, "Data Acquisition System Design Considerations", Report of Department of Transportation Air Traffic Control Advisory Committee, U.S. Government Printing Office, Washington, D.C., December 1969.

SECTION 3

STUDY OUTPUTS

The results necessary to solve the problem defined in Section 1.1 are discussed in this section and listed in Table 3-1. A detailed discussion of the development and generation of each of these results is contained in the subsections of Section 2 as noted in Table 3-1. The section which contains a discussion of the output data and the appendix which presents the data for each of the study outputs are also shown in Table 3-1.

The measured distribution data which was compiled to verify the system models, to provide initial lateral error distributions for the Fokker-Planck equation, and to provide vertical error distributions for the probability of collision determination is discussed in Section 3.1.

Approach system models developed in Sections 2.1, 2.4, and 2.5 are presented and discussed in Section 3.2. The models are divided into two categories:

- (1) models developed for use in the generation of lateral error probability density functions for the following approach system.
 - (a) FC-ILS-I-CTOL
 - (b) FC-ILS-II-CTOL
 - (c) BC-ILS-I-CTOL
 - (d) VOR-CTOL
 - (e) FC-ILS-I-STOL
- (2) models developed to be used as analysis tools including:
 - (a) Curved Path Model
 - (b) Multiple Aircraft/Runway Model

Section 3.3 discusses the sensitivity data which was generated to identify the dominant approach system parameters and errors, as well as to aid in the development of the approach system models.

The probability density function data which was generated for use in the probability of collision determination as well as in the normal operating zone determination is discussed in Section 3.4. Also discussed in this section is the resulting normal operating zone data which is ultimately to be used in the determination of minimum runway spacings as discussed in Volume I of this report (Section 4).

Section 3.5 discusses the probability of collision data for the various required aircraft and runway configurations,

Table 3-1 Study Outputs

Output	Development Section	Discussion Section	Presentation Appendix
Measured Distribution Data	2.3	3.1	F
System Models	2.1, 2.4, 2.5	3.2	G
Sensitivity Data	2.4	3.3	F
Probability Density Functions	2.5	3.4	H
Normal Operating Zones	2.5	3.4	H
Probability of Collision Data	2.6	3.5	I
Blunder Data	2.7	3.6	J, K

approach types, and operations. The probability of collision data is utilized as a relative "safety" measure in the determination of minimum runway spacing.

The data generated in the blunder analysis, which is an investigation of the airspace required for an aircraft to recover from abnormal operations or blunders, is discussed in Section 3.6. The blunder analysis was performed for two types of blunder recovery maneuvers:

- (1) the recovery maneuver is performed by the blundered aircraft only, and
- (2) the recovery maneuver is performed by both the blundered aircraft and the aircraft on the adjacent approach path.

The blunder data is to be utilized in the determination of the minimum runway spacings as described in Volume I (Section 4).

SECTION 3.1

MEASURED DISTRIBUTION DATA

Measured distribution data, as referred to in this report, consists of trajectory data for a finite sample of aircraft flying IFR approaches. Data is included for distributions in three dimensions - lateral, vertical, and longitudinal. The lateral data consists of distributions about the extended runway centerline; the vertical data consists of distributions about the glideslope plane; and the longitudinal data consists of distributions about a nominal longitudinal location.

The measured distribution data was utilized in this study for three purposes:

1. to verify that the models, as formulated, are good representations of the actual systems (Sections 2.4 and 2.5),
2. to provide initial distributions for the various techniques utilized to generate the probability density functions (Section 2.5), and
3. to provide vertical error distributions for use in the probability of collision determination (Section 2.6).

The purpose of this section is to present the measured distribution data for the systems listed in Table 3.1-1. The methods and sources utilized in the derivation of this data are discussed in Section 2.3. The distribution data for each of these systems is discussed in Section 3.1.1 and included, in its entirety, in Appendix E. Problem areas pertinent to the data's validity are examined in Section 3.1.2.

Table 3.1-1 Required Measured Distributions

Distribution	System
Lateral	FC-ILS-I-CTOL
	FC-ILS-II-CTOL
	BC-ILS-I-CTOL
	VOR-CTOL
	FC-ILS-I-STOL
Vertical	FC-ILS-I-CTOL
	FC-ILS-I-STOL
Longitudinal	FC-ILS-I-CTOL

3.1.1 DISTRIBUTION DATA PRESENTATION

As discussed in Section 2.3, the measured distribution data used in the Lateral Separation project was divided into three classes depending upon the characteristics of the data. The classes characterize:

1. systems for which field data has been collected and the distribution is presented in a tabular form of a three dimensional histogram and/or a mean and standard deviation table,
2. systems for which field data has been collected and the distribution has been assumed gaussian, and
3. systems for which no field data has been collected.

These classes are briefly discussed in the paragraphs which follow.

Tabular Distribution Data

A common form used in presenting distribution data is a tabular form of histogram data and/or mean and standard deviation data. The systems in Table 3.1-1 which fall into this class are shown below:

1. FC-ILS-I-CTOL (Lateral)
2. FC-ILS-I-CTOL (Lateral)
3. BC-ILS-I-CTOL (Lateral)
4. VOR-CTOL (Lateral)
5. FC-ILS-I-CTOL (Vertical)

Data for these systems are presented in two forms. One form is the sample mean and standard deviation at each of several specified ranges; the other form is a tabulation of histogram data for the observed data. An example of the mean and standard deviation data is given in Table 3.1.1-1 for the FC-ILS-I-CTOL (Lateral) system. An example of the tabular histogram data presentation is given in Table 3.1.1-2. The complete data set for each of the above systems is given in Appendix E.

Histogram data is presented at the same specific ranges as the mean and standard deviation data. The range to touchdown is given in meters across the top of the page. The lateral deviation partitions are given in multiples of the partition interval along the vertical axis. The partition intervals are five or ten meters as noted in the Table. The numbers in the body of the table represent how many aircraft are observed in partition at the indicated range.

Table 3.1.1-1

Mean and Standard Deviation Versus Range for
PC-ILS-I-CTOL - Lateral*

Range, meters	Number of Samples	Mean, meters	Standard Deviation, meters
600	513	-.0161	11.8945
1200	618	-3.0435	22.0739
1800	633	-5.2973	26.4976
2400	642	-6.7594	31.9235
3000	644	-2.8728	35.8871
3600	638	1.6535	37.7171
4200	622	8.9878	43.6031
4800	631	8.3098	46.9545
5400	630	8.4069	53.4121
6000	631	6.9212	61.9021
6600	629	2.9729	68.5195
7500	513	14.46	75.30
8100	500	11.83	83.99
8700	490	7.67	90.20
9300	468	6.31	93.60
9900	447	4.83	97.60
10500	423	12.93	92.45
11100	387	16.36	91.98
11700	342	17.42	94.11
12300	324	21.30	100.43
12900	307	26.29	96.41
13500	283	28.54	102.12
14100	245	28.99	103.63
14700	224	33.03	103.14
15300	181	27.42	97.75
15900	134	25.53	113.84

*Charleston data is included in the range interval from 1200 meters to 6600 meters, inclusive, but not elsewhere, since the data collection ranges were not coincident elsewhere.

Table 3.1.1-2 Distribution of Lateral Displacements for
FC-ILS-I-CTOL - Lateral**

Partition Interval	Range, hundreds of meters										
	6*	12*	18*	24	30	36	42	48	54	60	66
-20 to -79	0.	1.	4.	0.	2.	1.	2.	2.	2.	4.	5.
-19	1.	0.	1.	1.	0.	1.	1.	0.	0.	0.	2.
-18	0.	0.	0.	0.	0.	0.	0.	0.	1.	1.	3.
-17	0.	1.	1.	0.	1.	0.	1.	0.	0.	1.	2.
-16	0.	0.	1.	2.	0.	0.	0.	0.	1.	4.	1.
-15	0.	0.	1.	1.	1.	1.	0.	1.	1.	1.	2.
-14	0.	2.	1.	0.	0.	0.	0.	0.	1.	1.	0.
-13	0.	3.	1.	1.	0.	1.	1.	2.	3.	2.	2.
-12	0.	3.	6.	2.	3.	2.	1.	1.	2.	3.	2.
-11	0.	1.	3.	1.	1.	3.	2.	6.	2.	3.	7.
-10	0.	2.	4.	0.	0.	1.	1.	0.	2.	3.	3.
-9	1.	3.	6.	3.	7.	3.	3.	6.	4.	13.	5.
-8	1.	4.	6.	4.	2.	1.	4.	9.	11.	8.	7.
-7	2.	2.	14.	3.	8.	6.	5.	7.	8.	6.	20.
-6	3.	17.	24.	9.	3.	7.	17.	14.	15.	15.	15.
-5	1.	16.	39.	13.	18.	21.	14.	24.	18.	23.	32.
-4	15.	47.	37.	35.	23.	36.	28.	20.	31.	32.	22.
-3	25.	56.	57.	49.	54.	45.	42.	32.	27.	41.	32.
-2	93.	90.	86.	75.	78.	74.	51.	42.	48.	40.	47.
-1	112.	76.	54.	110.	98.	55.	47.	52.	57.	45.	53.
0	120.	98.	73.	115.	93.	86.	76.	73.	70.	75.	54.
1	64.	83.	61.	89.	94.	74.	71.	70.	67.	48.	50.
2	28.	40.	41.	50.	61.	68.	70.	84.	62.	47.	45.
3	13.	21.	32.	39.	31.	49.	50.	49.	50.	43.	40.
4	9.	20.	20.	15.	23.	36.	44.	44.	24.	36.	38.
5	2.	10.	12.	6.	18.	19.	24.	26.	33.	29.	33.
6	0.	8.	11.	8.	11.	12.	22.	18.	22.	29.	21.
7	0.	2.	6.	1.	4.	7.	9.	11.	16.	24.	22.
8	0.	4.	6.	2.	2.	4.	11.	11.	17.	13.	7.
9	0.	2.	7.	2.	0.	4.	7.	9.	6.	5.	18.
10	1.	1.	3.	2.	2.	6.	6.	4.	6.	10.	10.
11	0.	0.	1.	1.	1.	2.	5.	1.	4.	2.	6.
12	0.	1.	4.	1.	1.	1.	1.	2.	3.	4.	3.
13	1.	2.	3.	1.	2.	1.	2.	3.	4.	0.	2.
14	1.	0.	3.	1.	1.	0.	1.	5.	2.	2.	2.
15	0.	0.	1.	0.	0.	0.	1.	1.	1.	4.	3.
16	0.	0.	1.	0.	1.	1.	1.	0.	1.	1.	3.
17	0.	0.	0.	0.	0.	0.	1.	0.	1.	2.	1.
18	0.	0.	0.	0.	0.	0.	0.	0.	0.	1.	1.
19	0.	0.	0.	0.	0.	0.	0.	0.	2.	2.	0.
20 to 56	0.	2.	2.	0.	0.	0.	0.	2.	5.	8.	8.

*At these ranges, the partitions are at five meter intervals; elsewhere, the partitions are at ten meter intervals.

**Charleston data is included in the range interval from 1200 meters to 6600 meters, inclusive, but not elsewhere, since the data collection ranges were not coincident elsewhere.

Gaussian Distributed Data

Where the processing of the published data has presumed gaussian distributions, these assumptions are maintained. Specifically, the systems of Table 3.1-1 for which gaussian distributions have been assumed are the following:

1. FC-ILS-I-STOL (Lateral)
2. FC-ILS-I-STOL (Vertical)

When the data is presumed to be distributed according to the gaussian distribution laws, the entire distribution is completely described by the mean and variance. Generally, the reported means of the data have been small. A representative example of the lateral deviation standard deviation is given in Figure 3.1.1-1 for a FC-ILS-I-STOL (Lateral). The distribution data for both of the above systems is presented in Appendix E.

Systems with No Collected Data

In the consideration of dependent parallel IFR operations for CTOL aircraft, it was necessary to determine the longitudinal spacing distribution about a nominal longitudinal location. Since no measured data of this type was available, it was necessary to make certain assumptions concerning the data for the FC-ILS-I-CTOL (longitudinal) system. It was assumed that the aircraft velocity was normally distributed about a nominal mean approach velocity, \bar{V} , with a standard deviation, σ_V .

$$V = N(\bar{V}, \sigma_V^2)$$

The resulting longitudinal distribution is shown to be gaussian and is presented below.

$$X' = N(\bar{X}', \sigma_{X'}^2)$$

$$\bar{X}' = X_0' - \bar{V}t$$

$$\sigma_{X'} = \frac{\sigma_V t}{\sqrt{2}}$$

where

X' ~ longitudinal location, feet

\bar{X}' ~ mean longitudinal location, feet

$\sigma_{X'}$ ~ longitudinal location standard deviation, feet

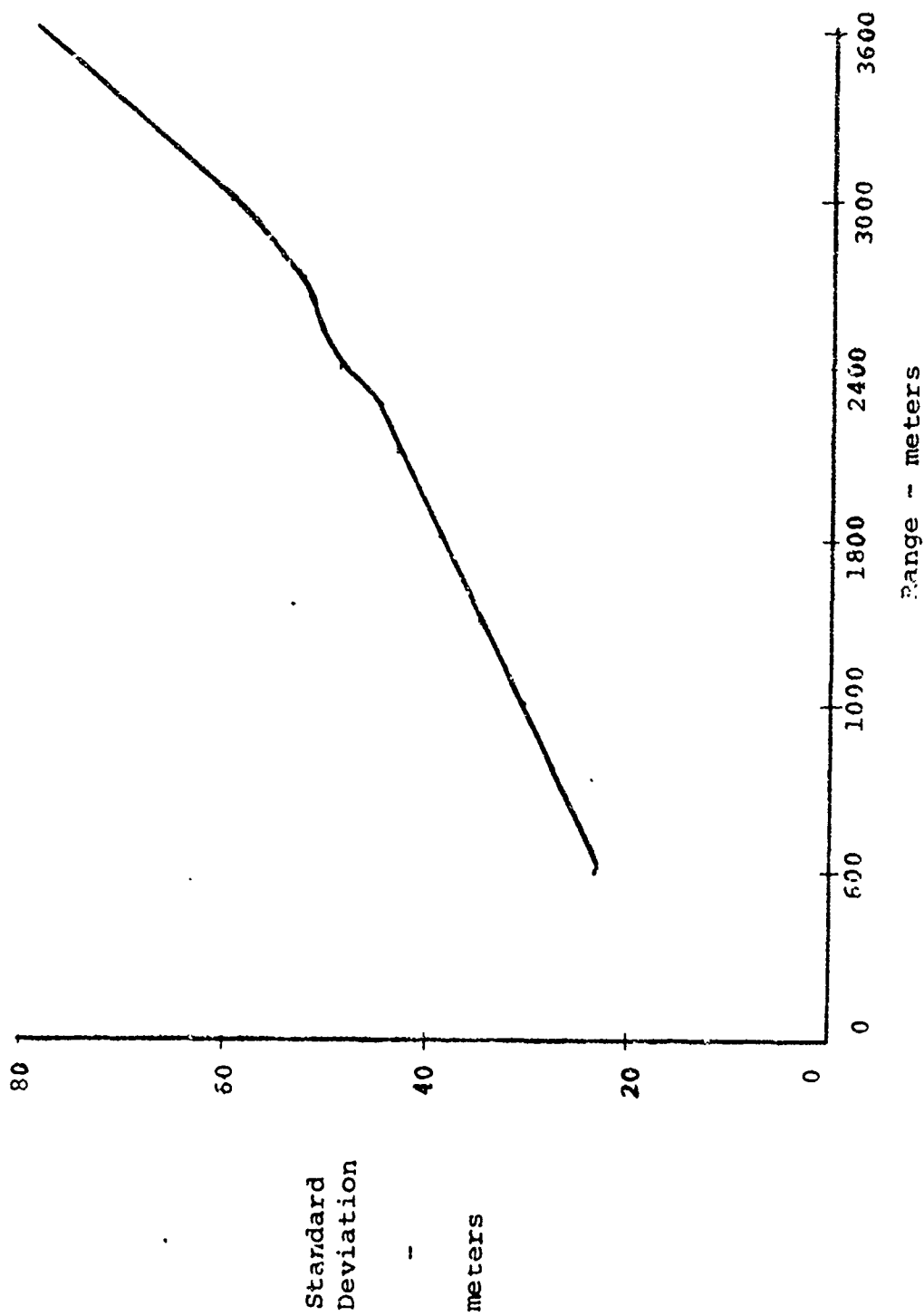


Figure 3.1.1-1 Standard Deviation Versus Range for FC-ILS-1-STOL (Lateral)

X'_0 ~ initial longitudinal location, feet

\bar{V} ~ aircraft mean velocity, feet/second

σ_V ~ velocity distribution standard deviation, feet/second

t ~ time from the point where the aircraft velocity control is initiated, seconds

3.1.2 MEASURED DISTRIBUTION DATA VALIDITY OBSERVATIONS

The resulting data set representing each system in Table 3.1-1 must be checked carefully to verify that the data represents that system. Possible problem areas which might affect the validity of the data are discussed in the paragraphs which follow.

Turn-on Range

To be able to combine data collected at various airports or to obtain meaningful comparisons between various approach systems, the collected data should be taken from sources having comparable turn-on ranges. Furthermore, the turn-on range for each set of data needs to be identified in order to exclude that data associated with the "delivery" technique before turn-on.

The turn-on range is governed, in part, by the traffic rate. If the traffic rate is high, there is a tendency to have the aircraft "in trail" at longer ranges, sometimes as much as 20 to 25 miles. This gives the pilot considerably greater time to establish a better track on the ILS (or VOR) beam and, therefore, a finer definition of the required wind correction angle. Under these circumstances, the distribution at the outer marker will be much narrower than the distribution for those aircraft that turn-on within one or two miles of the outer marker.

Turn-on ranges were not available for any of the data other than that collected at Charleston; however, the turn-on ranges can be inferred from the relative number of aircraft in the data set as range decreases. Table 3.1.2-1 indicates the apparent turn-on ranges of the various lateral systems.

Turn-on Direction and Overshoot

At some airports with parallel runways, the standard

Table 3.1.2-1

Summary of the Percent of Aircraft at Various Ranges

Lateral Approach System	Percent of A/C which Have Turned- On Prior to This Range					Apparent Turn-on Range, NMi
	5.02 NMi	5.98 NMi	6.96 NMi	7.93 NMi	8.58 NMi	
FC-ILS-I-CTOL	63	55	45	30	20	6
FC-ILS-II-CTOL	84	70	47	31	18	6
BC-ILS-I-CTOL	49	37	22	5	1	5
VOR-CTOL	89	77	41	31	31	6

traffic patterns are prescribed so that the turn-on to the final approach to a right-hand runway of a pair of parallel runways will normally require a right turn (as viewed by the pilot). Conversely, the left runway normally requires a left turn. Presently, procedures state that the turn-on to the final approach to each of the parallel independent runways shall occur with a minimum of 1000 feet vertical separation between the two aircraft. This procedure minimizes the effects of overshoots which occur at turn-on. However, if in the future the procedures are changed such that the 1000 feet vertical separation requirement is eliminated or reduced, it will be necessary to consider the effects of overshoots. For this reason, an analysis was conducted on the front course and back course data collected at Charleston, S. C., in order to determine the amount of overshoot at turn-on and the direction of turn-on.

Overshoot as used in this analysis is defined as the distance that an aircraft travels beyond the extended runway centerline measured on the opposite side from the turn-on direction.

Analysis of the front course ILS data revealed that 37 percent turned-on from the left, 17 percent turned-on from the right, and the remainder had turned-on to the final approach prior to the range at which the data collection started. The maximum overshoot observed was 919 feet with an average overshoot of 287 feet.

A similar analysis of back course data revealed that 30 percent turned on from the left, 23 percent turned on

from the right, and the remainder had turned on previously. The average overshoot observed was 408 feet with a maximum of 2112 feet*.

Sample Size

When collecting data for the purpose of determining the error distribution, it is necessary to collect sufficient data to assure an adequate sample. When the class of distributions cannot be predetermined, but must be derived, the usual method of determining an adequate sample size is by the method of convergence. In this method, the data collection activity is continued until the mean, variance, or any other required distribution parameters converge to a constant value and the parameters do not change with the addition of new data.

Since most of the data was obtained in a reduced form from previous data collection efforts, it was not possible to use convergence techniques to determine the existence of an adequate sample size. However, by comparing the trend of the standard deviations of the data at various ranges and the number of data points available at those ranges, it is possible to make some general observations concerning the sample size.

Table 3.1.2-2 is a summary of the maximum number of samples collected in the previous and current collection efforts for the various approach systems and the number of samples at the turn-on range. As shown in the table, there is a large variation in the number of samples for the various systems. A larger sample size usually results in more accurate distribution parameters.

The tables in Appendix E for the distributions listed in Table 3.1.2-2 indicate the number of samples upon which each mean and standard deviation at the discrete ranges along the approach are based. Often, erratic changes in the standard deviation correspond directly to an insufficient sample size or indicate a region such as that beyond the turn-on range where the distribution is poorly defined.

Ground Proximity

Operational problems at short ranges include an acute awareness by the pilot of the ground proximity and the effects on the pilot at breakout into VFR conditions.

Data such as the FC-ILS-I-CTOL (Vertical) data, Figure 3.1.2-1, must be examined with these considerations in mind.

*This occurred at a range of 7.5 NMi.

Table 3.1.2-2 System Sample Size

	Maximum Sample Size	Sample Size at Turn-on	Sample Size at Minimum Range
Lateral			
FC-ILS-I-CTOL	644	387	633
FC-ILS-II-CTOL	232	161	225
BC-ILS-I-CTOL	109	40	67
VOR-CTOL	88	78	44
FC-II S-I-STOL	*	*	*
Vertical			
FC-ILS-I-CTOL	519	363	508
FC-ILS-I-STOL	*	*	*

*Number of samples on STOL data not available.

The dip in standard deviation at the 3700 meter range could be attributed to a response to visual clues. Due to these vertical operational problems, a larger sample size is required to define the vertical error distributions at small ranges.

Simulated Versus Actual IFR Conditions

Some of the data collected at Charleston [FC-ILS-I-CTOL (Lateral), BC-ILS-I-CTOL (Lateral) and VOR-CTOL (Lateral)] and all of the data collected at NAPEC [FC-ILS-I-STOL (Lateral), FC-ILS-I-STOL (Vertical), and VOR-CTOL (Lateral)] were collected under simulated IFR conditions. Although simulated conditions (blocking possible visual references) create the same visual and physical illusions as actual IFR conditions, the pilot's attitude could be different for the two situations. The attitude differences could be attributed to the fact that the pilot knows that conversion to VFR can be made at his option, regardless of the aircraft's position on the approach, simply by removing the hooding device. Under actual IFR, the break-out altitude is governed by prevailing weather and the pilot must reach the weather ceiling before conversion to VFR can occur.

Assumed Distributions

No data has been collected on the distribution of aircraft about the nominal longitudinal position. The distribution for FC-ILS-I-CTOL (Longitudinal) was derived from the

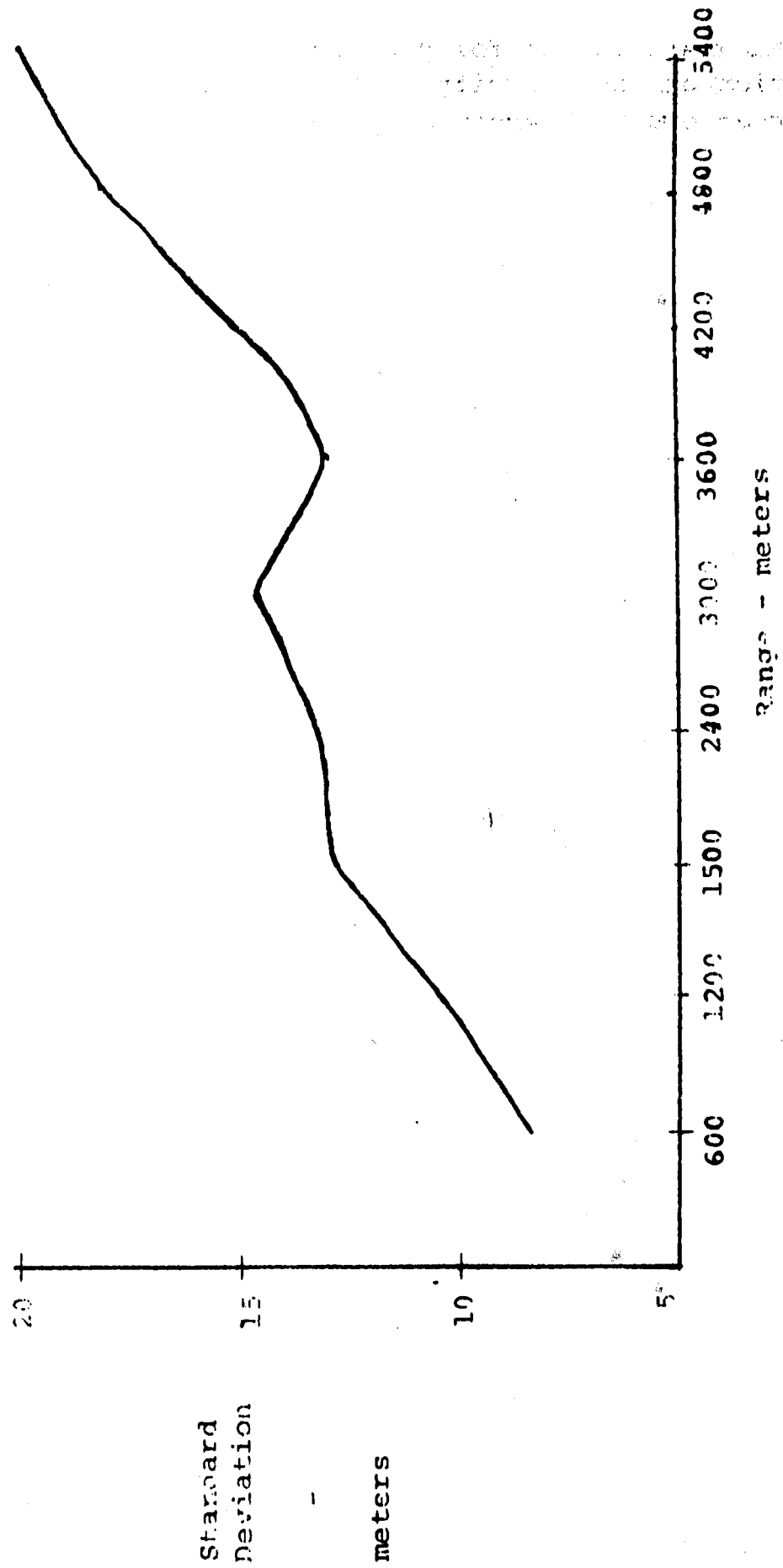


Figure 3.1.2-1 PC-ILS-I-CTOI, (Vertical) Standard Deviation Versus Range

assumed distribution for velocity errors. The mean and standard deviation of the velocity distribution were assumed based on conversations with experienced pilots.

SECTION 3.2

SYSTEM MODELS

As stated in the problem definition (Section 1.1), the first specific problem area was the development of system models which describe the required approach systems. The model development task, described in Section 2.1, was broken into two parts:

- (1) the development of models to be used in the generation of lateral deviation probability density functions, and
- (2) the development of models to be used as analysis tools to study approach systems.

The models included in (1) are

1. FC-ILS-I-CTOL
2. FC-ILS-II-CTOL
3. BC-ILS-I-CTOL
4. VOR-CTOL
5. FC-ILS-I-STOL

and the models included in (2) are

1. Curved Path Model
2. Multiple Aircraft/Runway Model

Three coordinate systems are used in the models. These systems are a runway system, a glideslope system, and an aircraft body centered system. The three systems and their relationships to one another are shown in Figure 3.2-1*.

Due to similarities in all of the required models, a nominal system model was developed in Section 2.1.2 from which all required expanded models were developed as discussed in Section 2.1.3. The nominal model represents a composite set of CTOL aircraft approaching a CTOL runway on the front course of an ILS Category I approach system. Three versions of the nominal model were developed for use in the various required analyses:

- (1) Nominal System Model (Figure 3.2-2)
- (2) Nonlinear Simulated Delay Nominal Model (Figure 3.2-3)
- (3) Linear Simulated Delay Nominal Model (Figure 3.2-4)

The nominal model parameter values and initial state distributions are contained in Tables 3.2-1 and 3.2-2, respectively.

Based upon the model concepts defined in Section 2.1.1, it was necessary to expand the nominal model to encompass

*All figures and tables are included at the end of this section.

various operational procedures and runway configurations. The first effort was the expansion of the nominal model to include the approach systems discussed in Section 2.1.3.1.

1. FC-ILS-I-CTOL
2. FC-ILS-II-CTOL
3. BC-ILS-I-CTOL
4. VOR-CTOL
5. FC-ILS-I-STOL

The resulting model for each of these approach systems is given in Appendix G. The nominal model block diagrams (Figures 3.2-2, 3, and 4) are representative of all of the above models. The above models were developed for use in the generation of the required lateral deviation probability density functions. Combinations of CTOL/STOL aircraft approaching CTOL/STOL runways for ILS (front course or back course)/VOR guidance equipment operating under Category I/Category II conditions may be simulated. The specific combination simulated by each of the above models corresponds to the above listed approach systems. Since the development of each of the above models was based upon fitting the model to a specific set of measured distribution data, the model is only as accurate as the measured distribution data to which it was fit.

In addition to the above models, it was necessary to develop two models to be used as analysis tools to study approach systems:

- (1) Curved Path Model
- (2) Multiple Aircraft/Runway Model

Both of these models were developed by expanding the nominal model to include the necessary operations and runway configurations as discussed in Section 2.1.3.2. These models may be used in the prediction of distribution data for systems in which no measured field data exists. Certain system characteristics which are difficult to observe in the actual approach system (such as multiple aircraft relative velocities and locations, aircraft bank angle and heading angle, curved path characteristics, etc.) may be obtained from these system models.

Both the curved path model and the multiple aircraft/runway model have been programmed in FORTRAN IV computer programs. The computer programs, including source listings, flow charts, and operating instructions, are described in detail in the User's Manual. The model parameter values and initial conditions are inputs into the programs and must be determined by the user depending upon the specific approach system to be modeled. Possible sources for determining the model parameter

values and initial conditions for a particular approach system to be modeled are Tables 3.2-1, 3.2-2, 3.2-3, and 3.2-4.

The curved path system model is capable of simulating IFR operations for CTOL or STOL aircraft operating on CTOL or STOL runways with either an ILS (Category I or Category II) or a VOR guidance system. Arrivals can be simulated on either straight-in approach paths or three-dimension general curved paths. Departures and missed approaches may also be simulated, but only on straight paths. The curved path model may be used as an analysis tool for studying curved approaches, departures, and missed approaches.

The curved path model consists basically of three separate models which are valid in different regions of the curved approach geometry as illustrated in Figure 3.2-5. When the aircraft is operating in the base leg region of the curved approach path, then the base leg model shown in Figure 3.2-6 is used. From the time the aircraft's range to the way point becomes equal to R_{turn} until T_{turn} seconds later, the turning model shown in Figure 3.2-7 is valid. After the aircraft has completed the turn, the nominal model shown in Figure 3.2-2 is valid.

The multiple aircraft/runway model may be used to study the effects of longitudinal separation on lateral safety requirements for parallel/non-parallel, CTOL/STOL, and independent/dependent final approaches as well as other analyses. This model can simulate up to four aircraft flying independent or dependent final approaches or departures to or from two parallel or skewed CTOL and/or STOL runways. Both CTOL and STOL type aircraft may be simulated approaching or departing either of the two runways.

The model is illustrated by the block diagram in Figure 3.2-8 and the configuration shown in Figure 3.2-9. Each of the four aircraft shown in the figure is simulated by the nominal model block diagram (Figure 3.2-2). The possible runway configurations which may be simulated with the multiple aircraft/runway model are shown in Figures 3.2-10 and 3.2-11.

To summarize, the system models developed in the model development task include:

- (1) a nominal model to aid in the development of the various required models listed below,
- (2) five approach system models:
 1. FC-ILS-I-CTOL
 2. FC-ILS-II-CTOL
 3. BC-ILS-I-CTOL
 4. VOR-CTOL

5. FC-ILS-I-STOL

for use in the generation of lateral deviation probability density functions, and

(3) two expanded models:

1. Curved Path Model

2. Multiple Aircraft/Runway Model

for use as analysis tools to study approach systems.

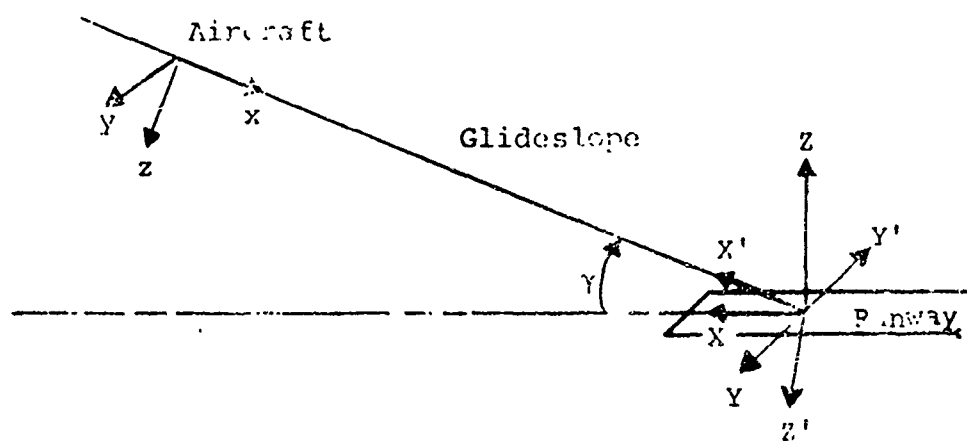


Figure 3.2-1. Coordinate Systems

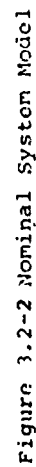




Figure 3.2-3 Nonlinear, Simulated Delay Nominal Model



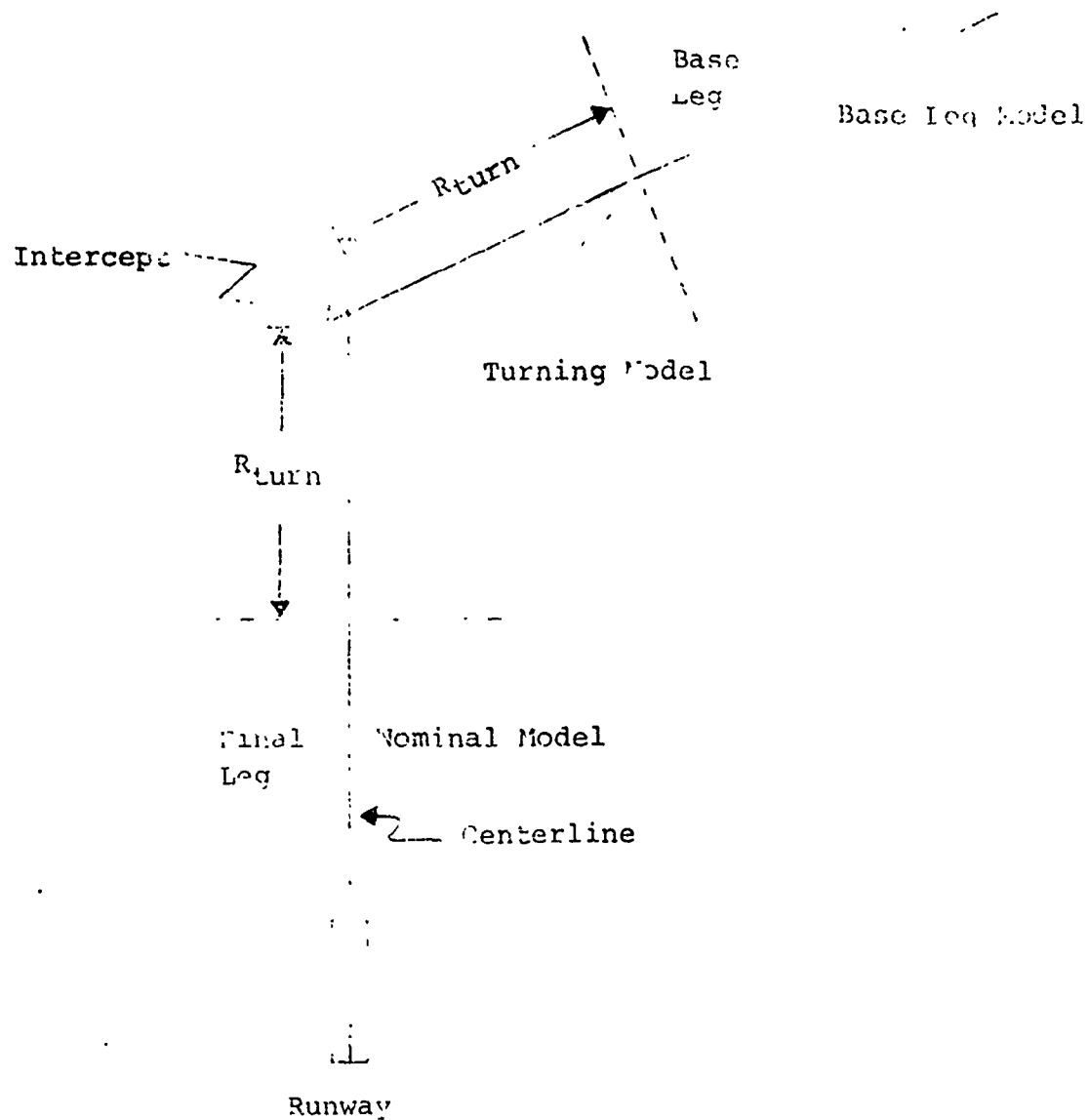
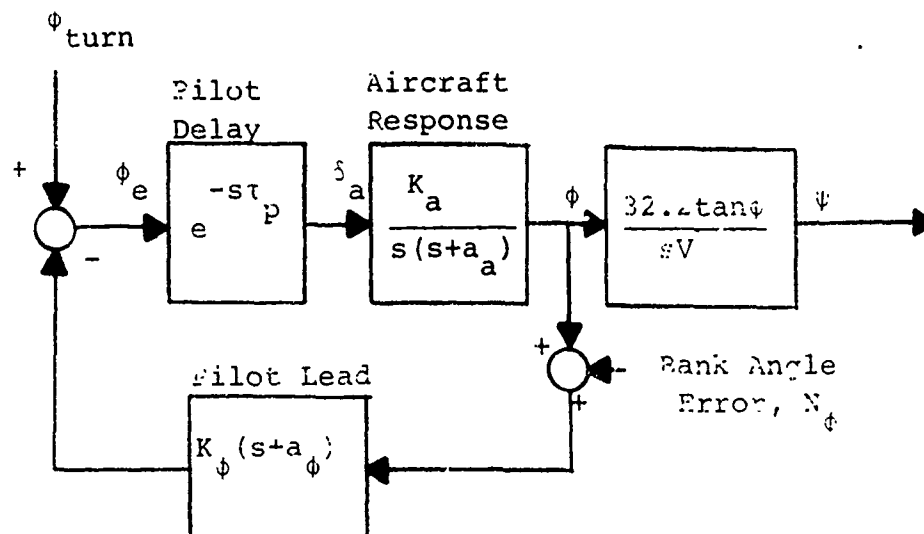


Figure 3.2-5 Curved Model Regions of Validity



$$R_{turn} = \frac{V}{\dot{\psi}_{tr}} \tan \left| \frac{\beta}{2} \right| + V \tau_c$$

$$T_{turn} = \left| \frac{\beta}{\dot{\psi}_{tr}} \right|$$

$$\phi_{turn} = - \tan^{-1} \left[\frac{(\dot{\psi}_{tr} + N_{tr})V}{32.2} \right]$$

Limits

$$\phi \leq \phi_{LI''}$$

$$\dot{\phi} \leq \dot{\phi}_{LI''}$$

Figure 3.2-7 Turning System Model

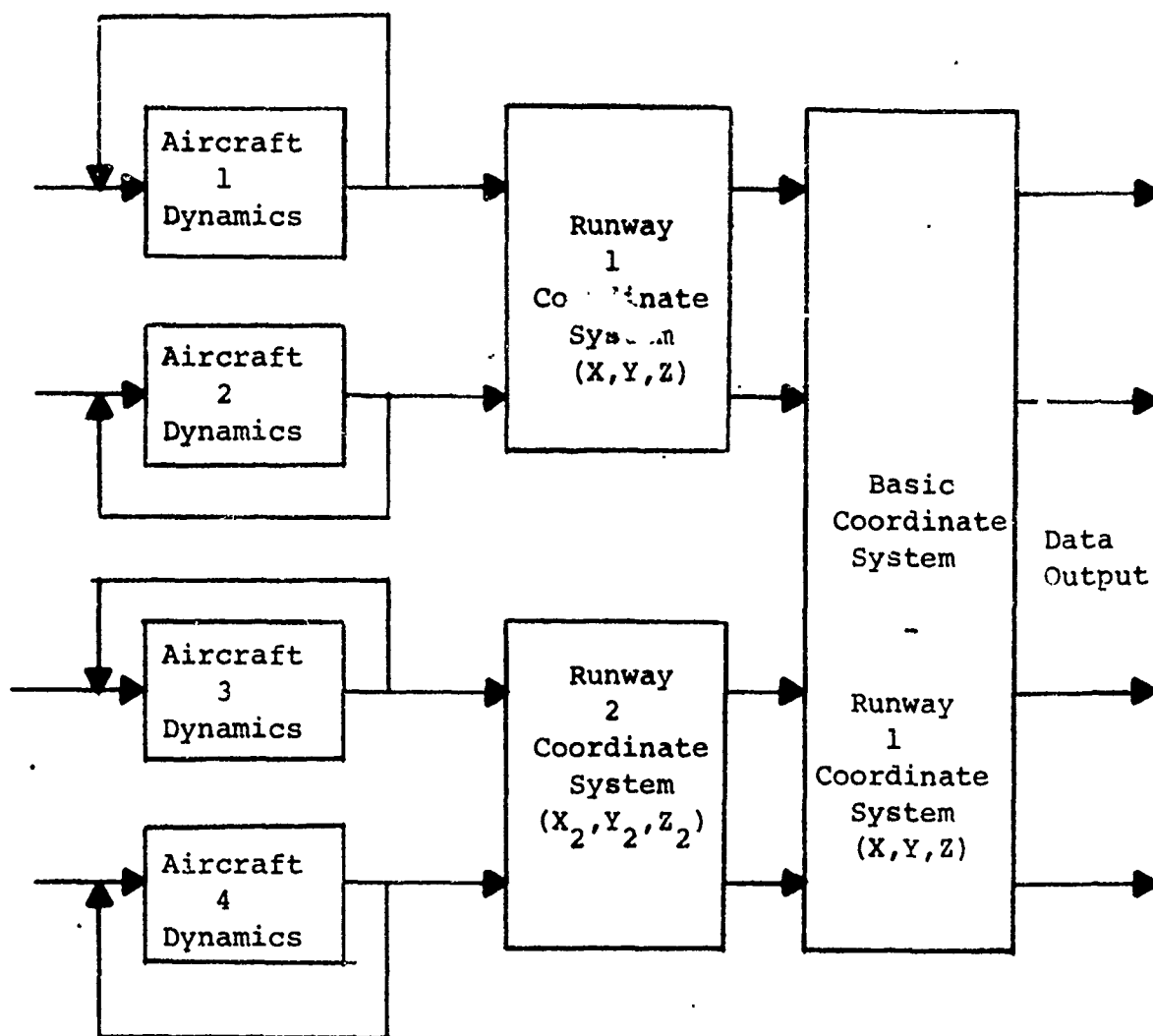


Figure 3.2-8 Multiple Aircraft/Runway Model Block Diagram

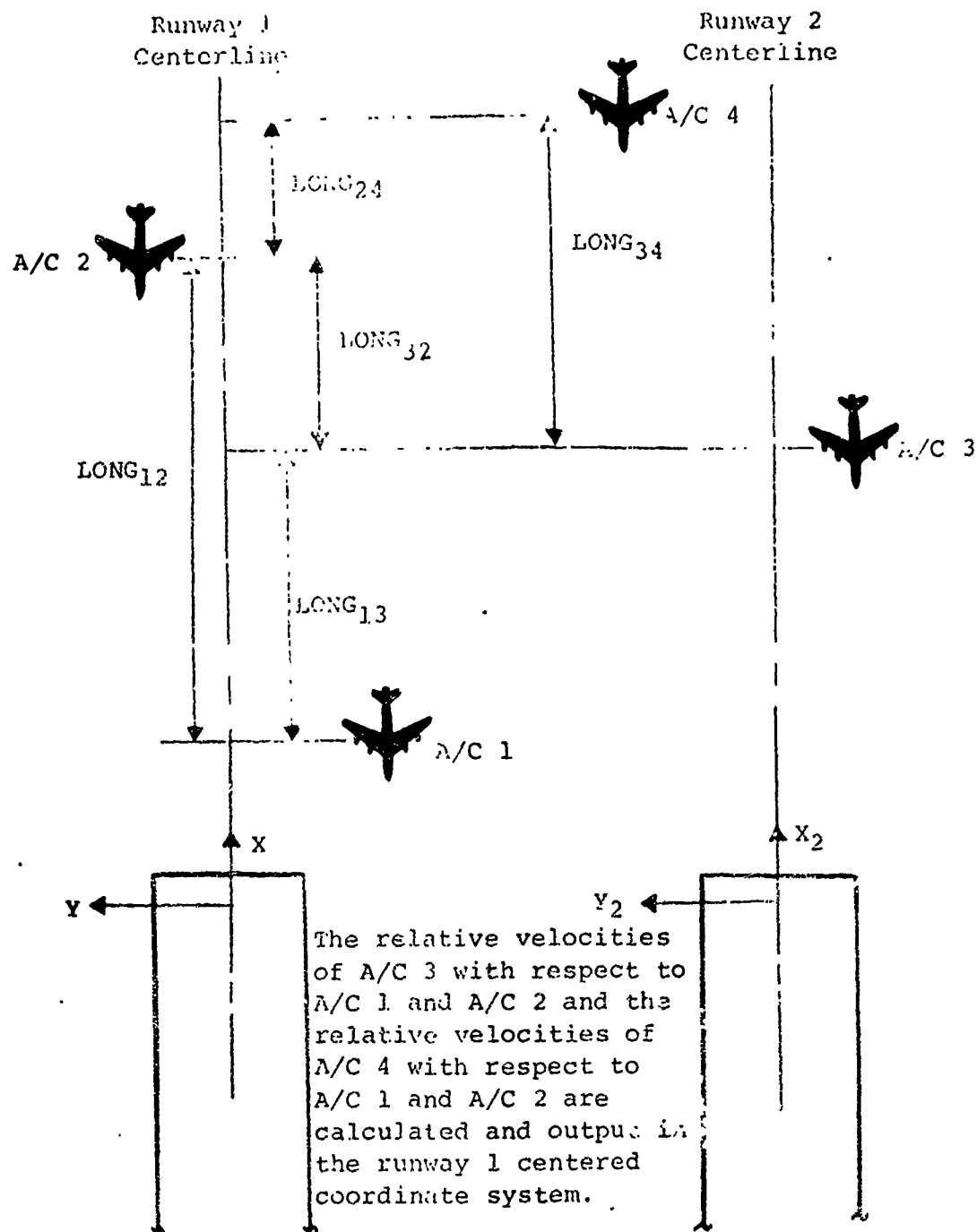


Figure 3.2-9
Possible Configuration for
Multiple Aircraft/Runway Model

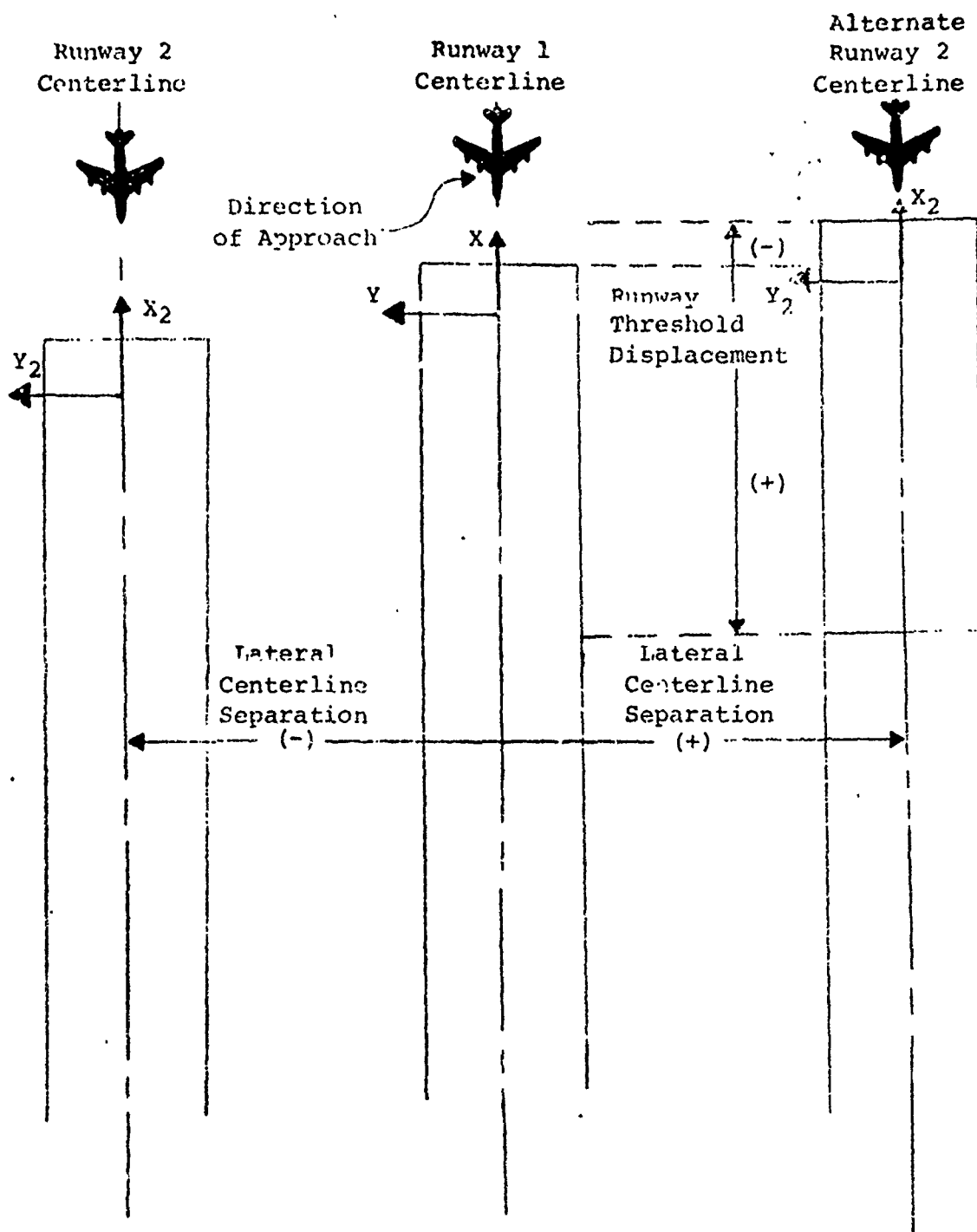
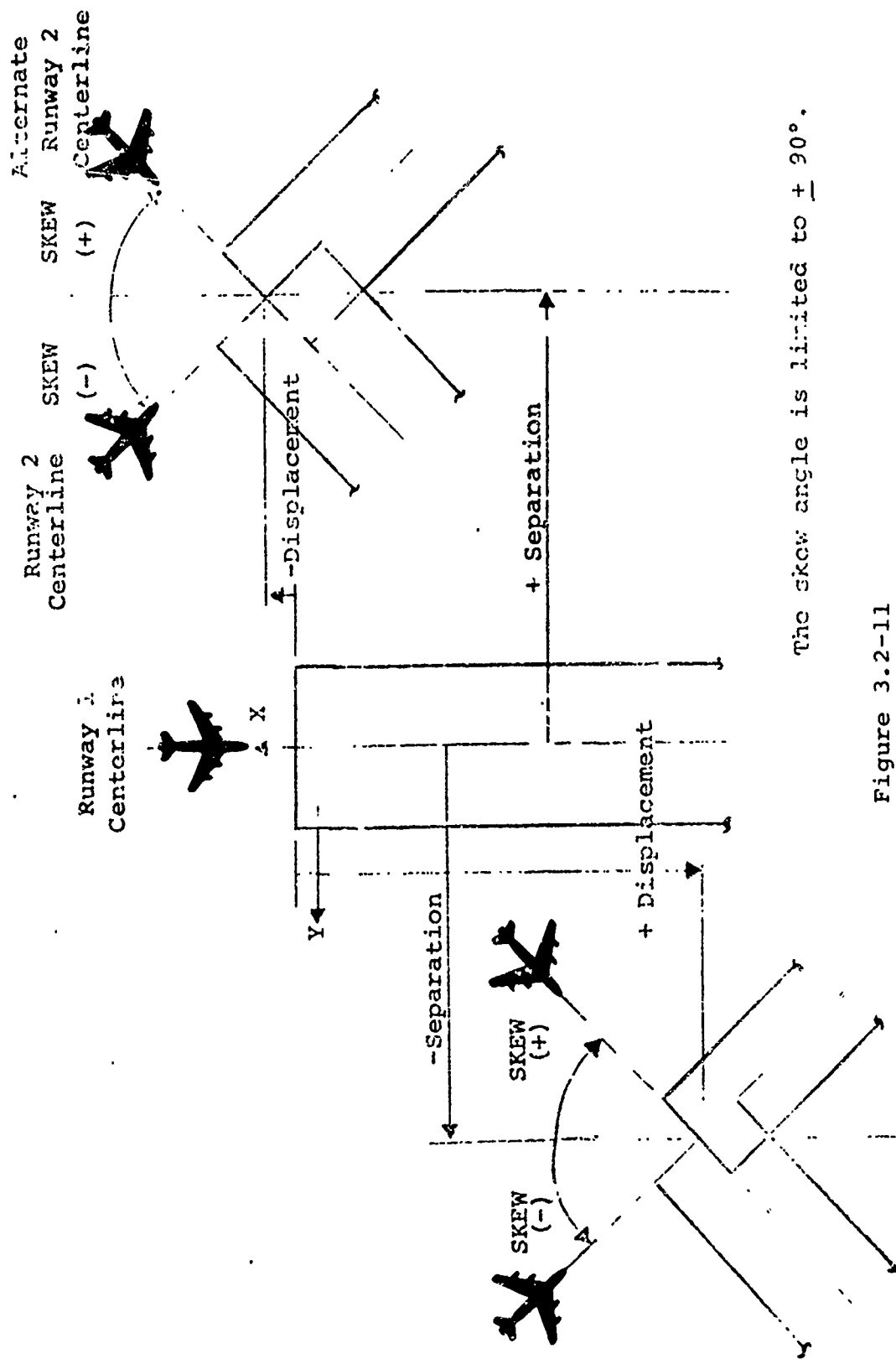


Figure 3.2-10
Multiple Aircraft/Runway Model
Possible Parallel Runway Configurations



The skew angle is limited to $\pm 90^\circ$.

Figure 3.2-11

Multiple Aircraft/Runway Model

Possible Skewed Runway Configurations

Table 3.2-1 Nominal Model Parameter Values

Symbol	Value	Units	Reference	Comments
a_a	1.0	sec^{-1}	4	CTOL aircraft
a_{p1}	.04	-	2	Simulated delay models (Equation 2.1.2-2)
a_{p2}	-.35	-	2	Simulated delay models (Equation 2.1.2-3)
a_{p3}	.04	-	2	Simulated delay models (Equation 2.1.2-4)
a_{p4}	.35	-	2	Simulated delay models (Equation 2.1.2-5)
a_{p5}	.007	-	2	Simulated delay models (Equation 2.1.2-1)
a_ϕ	1.5	sec^{-1}	1	
K_a	1.0	sec^{-2}	-	Assumed
K_p	1.0	-	-	Simulated delay models
$K_{\epsilon e}$	4.8	-	-	Nonlinear models, deter- mined in Section 2.4.3
$K'_{\epsilon e}$.000075 at 9 N. Mi to .000354 at .75 N. Mi.	$\frac{\text{rad}}{\text{ft}}$	-	Linear model (Equation 2.1.2-7)
K_ϕ	1.33	sec	1	
K_ψ	1.9	-	1	
$K_{\psi e}$	1.0	-	1	
L	9000.	feet	-	FC-ILS Approach

Table 3.2-1 Nominal Model Parameter Values (Continued)

Symbol	Value	Units	Reference	Comments
N_R	$\pm .00048$	rad	6, 7	1 σ value, determined in Section 2.1.4 (ILS _R)
N_T	$\pm .001497$	rad	15	1 σ value, determined in Section 2.1.4 (ILS _T for Category I/Category II)
N_E	$\pm .00349$	rad	-	1 σ value, determined in Section 2.1.4
N_ϕ	$\pm .1047$ at 9 N. Mi. $\pm .0436$ at 0 N. Mi.	rad	-	1 σ value, determined in Section 2.4.3 (Varies linearly with range)
N_ψ	$\pm .01745$	rad	-	1 σ value, determined in Section 2.1.4
V	236.4	ft/sec	-	Assumed (140 knots for CTOL aircraft)
γ	2.5	deg	-	CTOL runway
θ_0	0.	rad	-	Assumed
τ_p	.7	sec	-	Assumed
ϕ_{LIM}	.367	rad	-	Equation 2.1.2-6
$\dot{\phi}_{LIM}$.1745	rad/sec	-	Assumed (10 deg/sec)
$\dot{\psi}_{LIM}$.0524	rad/sec	-	Assumed (3 deg/sec)
ψ_R	3.1416	rad	-	Same as run-in heading. Assumed to be 180° for an approach.

Table 3.2-2
Nominal Model Initial State Distributions (at $x'_0 = 9\text{NMi}$)

State	Symbol	σ^*	Units
x_{10}	y'_0	198	feet
x_{20}	ψ_0	.02	radians
x_{30}	ϕ_0	.01	radians
x_{40}	IS	.12	
x_{50}	IS	.26	
x_{60}	IS	.54	

*Assumed Gaussian with mean = 0 and variance = σ^2

Table 3.2-3 Expanded Model Parameter Values

Item	Symbol	Value	Units	Comments
CTOL Aircraft	a_a	1	sec ⁻¹	References 4 and 21
	K_a	1	sec ⁻²	Assumed
	V	236.4	ft/sec	Assumed (140 knots)
	ϕ_{LIM}	.367	rad	Equation 2.1.2-6
	$\dot{\phi}_{LIM}$.1745	rad	Assumed (10 deg/sec)
	$\dot{\psi}_{LIM}$.0524	rad	Assumed (3 deg/sec)
STOL Aircraft	a_a	.6	sec ⁻¹	References 20 and 21
	K_a	1.667	sec ⁻²	Assumed
	V	108.1	ft/sec	Assumed (64 knots)
	ϕ_{LIM}	.1742	rad	Equation 2.1.2-6
	$\dot{\phi}_{LIM}$.1745	rad	Assumed (10 deg/sec)
	$\dot{\psi}_{LIM}$.0524	rad	Assumed (3 deg/sec)
CTOL Runway	γ	2.5	deg	Reference 22
FC-ILS	L	9000	ft	Assumed
BC-ILS	L	-1000	ft	Assumed
VOR	L	4000	ft	Assumed
STOL Runway	γ	7.5	deg	Reference 23
FC-ILS	L	9000	ft	Value is consistent with the measured field data

Table 3.2-3 Expanded Model Parameter Values (Continued)

Item	Symbol	Value	Units	Comments
Pilot	a_{p1}	.04	-	Simulated delay models (Equation 2.1.2-2)
	a_{p2}	-.35	-	Simulated delay models (Equation 2.1.2-3)
	a_{p3}	.04	-	Simulated delay models (Equation 2.1.2-4)
	a_{p4}	.35	-	Simulated delay models (Equation 2.1.2-5)
	a_{p5}	.007	-	Simulated delay models (Equation 2.1.2-1)
	a_{ϕ}	1.5	sec ⁻¹	Reference 1
	K_p	1.0	-	Simulated delay models
	K_{ϵ_e}	-	-	Determined in Section 2.5 by fitting measured distribution data (Nonlinear models)
	K'_{ϵ_e}	-	$\frac{\text{rad}}{\text{ft}}$	Equation 2.1.2-7 (Linear model)
	K_{ϕ}	1.33	sec	Reference 1
	K_{ψ}	1.9	-	Reference 1

Table 3.2-2 Expanded Model Parameter Values (Continued)

Item	Symbol	Value	Units	Comments
Lateral Guidance Equipment ILS-I	K_{ψ_e}	1.0	-	Reference 1
	N_c	.00349	rad	Determined in Section 2.1.4 (1 σ value)
	N_ϕ	-	rad	Determined in Section 2.5 by fitting measured distribution data (1 σ value)
	N_ψ	$\pm .01745$	rad	Determined in Section 2.1.4 (1 σ value)
	τ_p	.7	sec	Assumed
	N_R	$\pm .00048$	rad	Determined in Section 2.1.4 (1 σ value)
	N_T	$\pm .001715$	rad	Determined in Section 2.1.4 (1 σ value)
	ILS-II			
	N_R	$\pm .00048$	rad	Determined in Section 2.1.4 (1 σ value)
	N_T	$\pm .001749$	rad	Determined in Section 2.1.4 (1 σ value)
VOR	N_R	$\pm .02155$	rad	Determined in Section 2.1.4 (1 σ value)

Table 3.2-3 Expanded Model Parameter Values (Continued)

Item	Symbol	Value	Units	Comments
VOR 'Cont'd)	N_T	$\pm .0218$	rad	Determined from Section 2.1.4 (1 σ value)

Table 3.2-4 Error Summary

Item	Value [*] 1σ, deg**	Reference	Remarks
VOR _R	<u>±</u> 1.235	-	Value for models - average of values from references below
	<u>±</u> .25	6, 7	Collins VOR/ILS 51RV-2B; Collins VOR/LOC 51R-7A,-8A
	<u>±</u> .5	14	Collins VOR/ILS 51RV-1
	<u>±</u> 1.25	9, 12	General/Industrial Aviation Usage: FAA, NECAP 1964 program
	<u>±</u> 2.25	11	General/Industrial Aviation Usage
	<u>±</u> 2.3	8	FAA, NECAP II, General Aviation Usage
VOR _T	<u>±</u> 1.25	-	Value for models - average of values from references below
	<u>±</u> 1.0	9, 11	General/Industrial Aviation Usage
	<u>±</u> 1.5	10	General/Industrial Aviation Usage (assumed)
ILS _R	<u>±</u> .0275	-	Value for models - average of values from references below
	<u>±</u> .021	7	Collins 51R-7A,-8A (assumed)
	<u>±</u> .0335	6	Collins 51RV-2B
ILS _T	<u>±</u> .1	15	Category I (assumed)
ILS _T	<u>±</u> .0715	-	Category II (assumed)

Table 3.2-4 Error Summary (Continued)

Item	Value* deg**	Reference	Remarks
ASF	$\pm .5$	-	Value for models - average of values from references below
	$\pm .5$	13	NAFEC ASR-2
	$\pm .5$	13	NAFEC ASR-5
Heading Angle, N_h	$\pm 1.$	-	Assumed
Bank Angle, N_b	$\pm .5$	-	Assumed
CBI, N_c	$\pm .2$	-	Assumed
Turn Rate, N_{tr}	$\pm .2^{***}$	-	Assumed

Reproduced from
best available copy.

More accurate estimates of these pilot errors are made for the nominal approach system model in Section 2.4

* All random errors are assumed to be white gaussian noise sources with the mean equal to zero and standard deviation equal to 10.

** All angular errors are implemented in the models in radians.

*** Units are deg/sec; implemented in rad/sec.

SECTION 3.3

SENSITIVITY DATA

The purpose of the sensitivity analysis is to identify the effects of selected pertinent model parameters and model errors on the lateral distribution of the approach system. The sensitivity analysis was performed by utilizing the nominal system model defined in Section 2.1.2, with specific initial conditions, as the reference condition. Each of the pertinent parameters and errors of the nominal system model was varied about its nominal value, and the resulting sensitivity coefficient of the lateral deviation or lateral distribution standard deviation was calculated at various points in range. A sensitivity coefficient, S_p^X , identifies the amount that the variable, X , changes from the reference condition due to a small change in the parameter, P .

The sensitivity coefficients for each parameter and error were calculated and plotted at common points in range. The resulting parameter and error sensitivity curves are presented in Appendix F.

The parameter sensitivity curves illustrate the sensitivity of the lateral deviation to each of the pertinent parameters (Table 3.3-1) as a function of range and time. The reference condition is defined by the nominal model with all initial conditions equal to zero except as follows:

$$Y_0' = 500 \text{ ft.}$$

$$X_0' = 13.53 \text{ NMi.}$$

$$\psi_0' = 3.14159 \text{ rad. (runway azimuth arbitrarily chosen to be equal to } 180^\circ)$$

A typical example from the parameter sensitivity curves of Appendix F is shown in Figure 3.3-1. This example illustrates the sensitivity of the lateral deviation to the pilot gain on heading angle error, K_{ψ_e} , as a function of range and time,

about the given reference condition. A small change in K_{ψ_e} from its reference value causes the lateral deviation response to vary from the reference response as shown in Figure 3.3-1.

Table 3.3-1 Sensitivity Analysis Parameters

Symbol	Reference Value	Units	Description
V	236.4444	ft/sec	Aircraft airspeed
K_{ϵ_e} (angular)	1.5	rad/rad	Pilot tracking gain on the angular localizer error
K_{ψ_e}	1.0	rad/rad	Pilot gain on heading angle error
K_{ψ}	1.9	rad/rad	Pilot gain on heading angle feedback
K_{ϕ}	1.333	sec	Pilot gain on the bank angle divided by a_{ϕ}
K_a	1.0	1/sec ²	Aircraft bank rate to aileron response gain multiplied by a_a
a_a	1.0	1/sec	Inverse of the aircraft bank rate to aileron response time constant
a_{ϕ}	1.5	1/sec	Inverse of the pilot lead time constant on bank angle feedback
τ_p	0.7	sec	Pilot/control delay
L	9000.0	ft	-X coordinate of the lateral guidance transmitting antenna

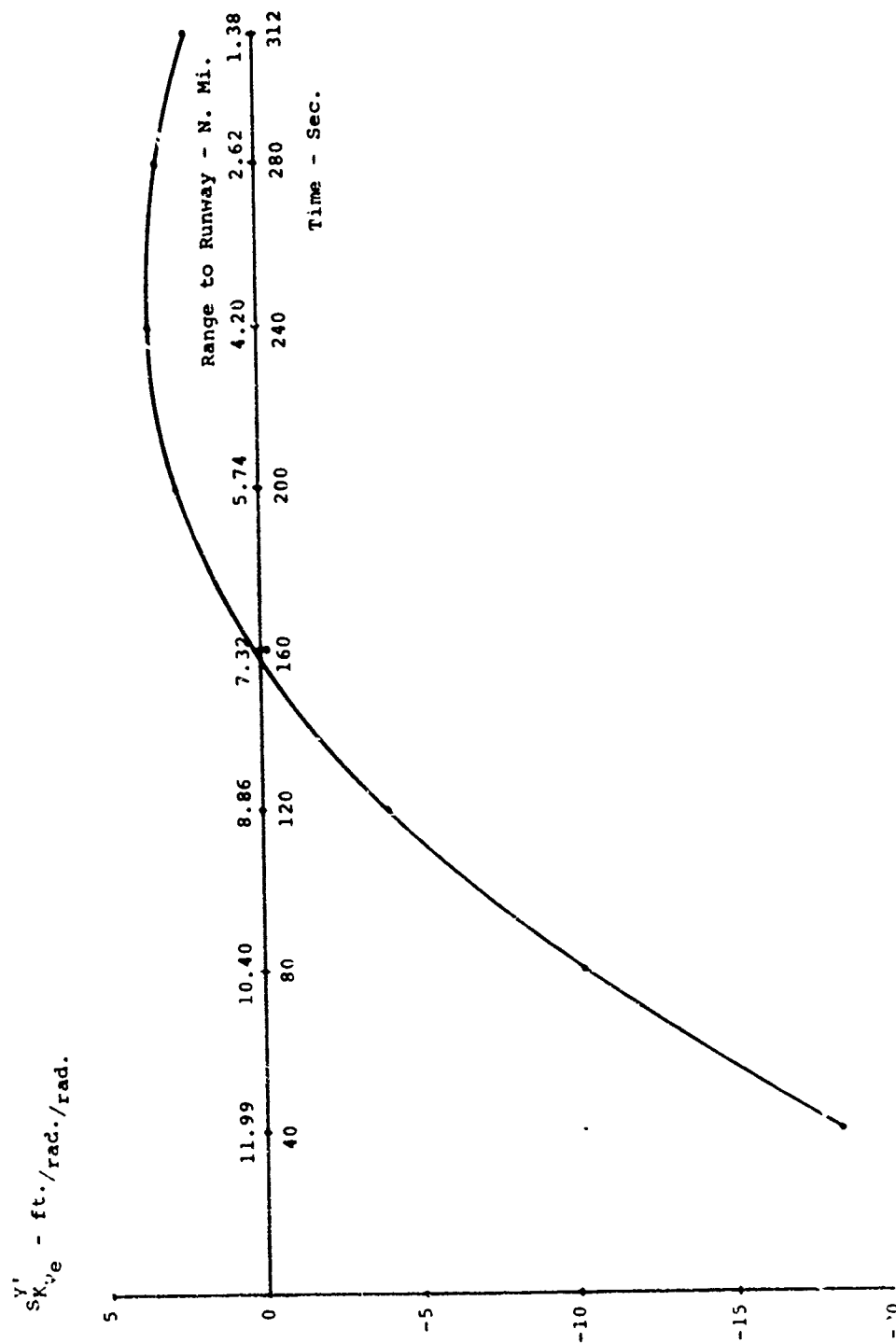


Figure 3.3-1 Lateral Deviation Sensitivity Coefficients with Respect to K_{ψ_e}

For illustration, consider a small positive change in the gain, and note that Figure 3.3-1 shows that the lateral deviation response will be less than the reference response for ranges greater than 7.32 nautical miles and greater than the reference response for ranges less than this range.

The error sensitivity curves illustrate the sensitivity of the lateral distribution standard deviation to the standard deviation changes to each of the pertinent system errors (Table 3.3-2) as a function of range and time. The reference condition is defined by the nominal model with the initial state distributions given in Table 2.4.3-1. A typical example from the error sensitivity curves in Appendix F is shown in Figure 3.3-2. This example illustrates the sensitivity of the lateral deviation distribution (standard deviation, σ_y) to the initial heading angle distribution (standard deviation, σ_{ψ_0}) about the given reference condition. A small change in σ_{ψ_0} from its reference value causes the σ_y response to vary from the reference response as shown in Figure 3.3-2. For illustration purposes, consider a small positive change in σ_{ψ_0} . Note that the σ_y response will be greater than the reference response, and this variation decreases with range.

Table 2.3-2 Sensitivity Analysis Errors

Symbol	Reference Value (Rad.)	Description
$\sigma_{N_{\psi}}$.01745	Pilot heading angle error distribution standard deviation
$\sigma_{N_{\phi}}$.1047 @ 9Nmi .0456 @ 0Nmi	Pilot bank angle error distribution standard deviation
σ_{ILS_R}	.00048	ILS equipment receiver error distribution standard deviation
σ_{ILS_T}	.001497	ILS equipment transmitter error distribution standard deviation
$\sigma_{N_{\epsilon}}$.00349	Pilot localizer tracking error (final leg) distribution standard deviation
σ_{ψ_0}	.02	Initial condition on heading state distribution standard deviation

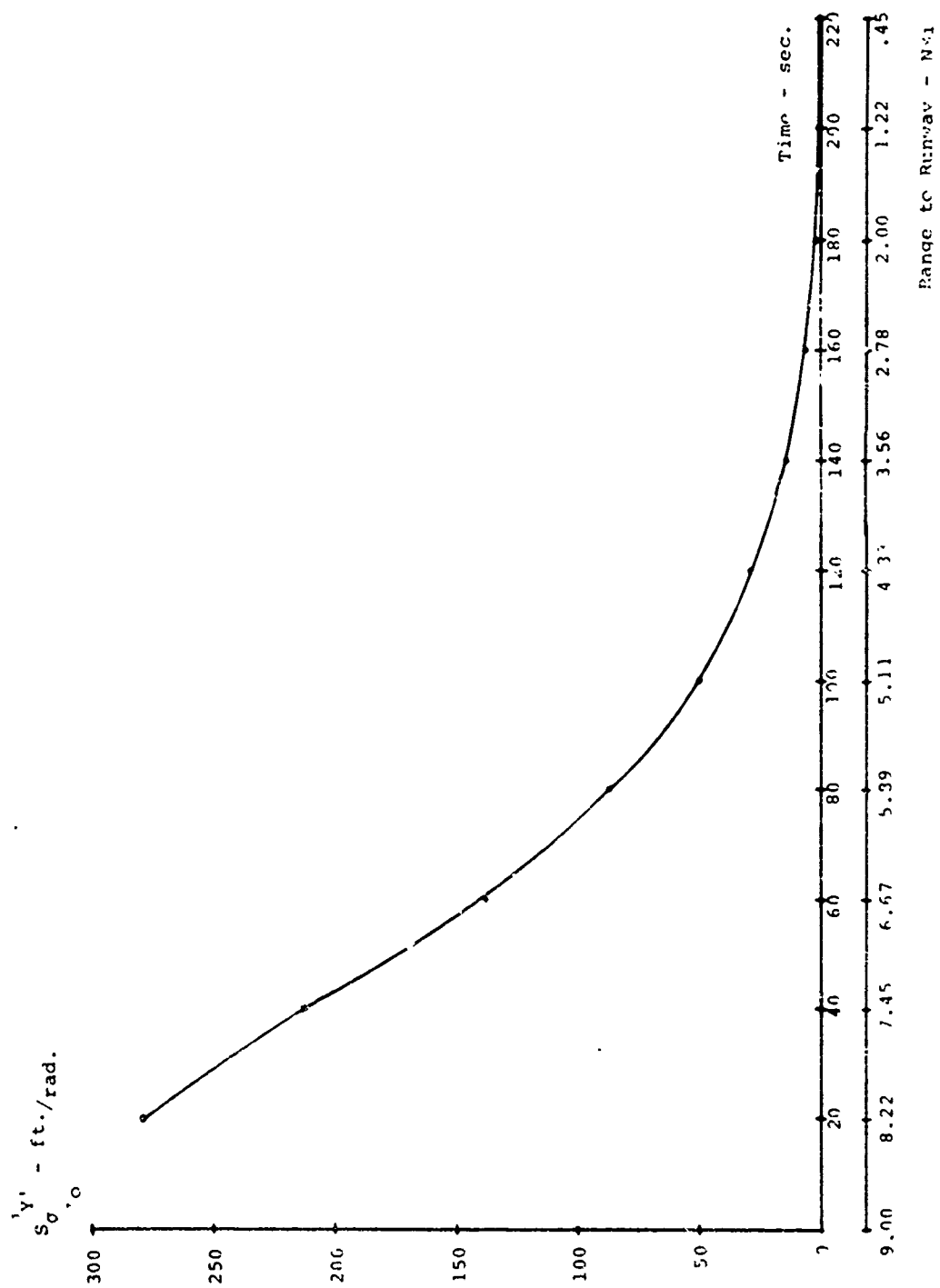


Figure 3.3-2 Lateral Distribution Sensitivity Coefficients $\sigma_{y'}$ with Respect to σ_{ψ_0}

SECTION 3.4

PROBABILITY DENSITY FUNCTION DATA

The importance of the error PDF's in the lateral, vertical, and longitudinal dimensions is indicated by the fact that two of the three data sets required for minimum runway spacing determination, probability of collision data and NOZ data, are based on the PDF's. The generation of probability of collision data is based on the error statistics or probability density functions for each of the three dimensions. The NOZ data requires specific knowledge of only the lateral PDF. Therefore, the generation of these PDF's, especially the lateral PDF's, requires accurate descriptions of both the body of the distribution as well as the tails of the distribution.

Using the techniques described in Section 2.5, the PDF's are generated for each of the approach systems listed in Table 3.4-1. For each system, the PDF type and method of determination are indicated. The PDF data is discussed in Section 3.4.1 and presented in Appendix H. Also, for each of the lateral approach systems, a NOZ is calculated as described in Section 2.5.3.1, and for CTOL/STOL skewed operations, a NOZ is determined as described in Section 2.5.3.2. The NOZ data is discussed in Section 3.4.2 and presented in Appendix H.

3.4.1 ERROR DISTRIBUTION DATA

The resultant error distributions for each of the dimensions are determined using either the Fokker-Planck equation, the measured error data directly, or by using certain assumptions as to the physics of the problem. Due to the importance of the lateral dimension to the probability of collision calculations and NOZ calculations, the Fokker-Planck equation is used to develop the range-ordered set of lateral PDF's. The vertical PDF's are based on a gaussian fit to the range-ordered vertical measured distribution data. The longitudinal PDF's required to calculate the probability of collision for the dependent CTOL/CTOL case are determined by using an assumed gaussian distributed velocity error.

Lateral PDF's

The lateral PDF's are generated using the verified approach system models and the Fokker-Planck equation as discussed in Section 2.5. The corresponding models utilized for each of the lateral systems listed in Table 3.4.1-1 are

Table 3.4-1

Probability Density Functions

Dimension	Approach System	PDF Type	Method of Determination
<u>Lateral</u>	FC-ILS-I-CTOL	Fokker-Planck Output	Fokker-Planck
	FC-ILS-II-CTOL	Fokker-Planck Output	Fokker-Planck
	BC-ILS-I-CTOL	Fokker-Planck Output	Fokker-Planck
	VOR-CTOL	Fokker-Planck Output	Fokker-Planck
	FC-ILS-I-STOL	Fokker-Planck Output	Fokker-Planck
<u>Vertical</u>	FC-ILS-I-CTOL	Gaussian	Measured Distribution Data
	FC-ILS-I-STOL	Gaussian	Measured Distribution Data
<u>Longitudinal</u>	FC-ILS-I-CTOL	Gaussian	Assumed Velocity Distribution

included in Appendix G. The Fokker-Planck equation for each of the first four cases is initialized using the modified Bergerhout distribution fit to the measured distribution data at the range indicated in Table 3.4.1-1. The modified Bergerhout distribution is used to initialize the CTOL lateral cases in an effort to better describe the measured distribution data, which had a large number of data points in the tails of the distribution. The initial distribution used for the STOL case is the gaussian distribution (Reference 1). The resultant PDF's for all five cases are determined quite accurately at 23.6 feet increments in range using the Fokker-Planck equation. This accuracy is due to the fact that the Fokker-Planck equation utilizes the dynamics of the system to generate the resulting PDF's. The PDF's for all five cases at selected ranges are presented in Appendix H.

Table 3.4.1-1

Lateral PDF's

Lateral Approach System	PDF Initial Range, NMi.
FC-ILS-I-CTOL	6
FC-ILS-II-CTOL	6
BC-ILS-I-CTOL	5
VOR-CTOL	6
FC-ILS-I-STOL	2

Vertical PDF's

The vertical PDF's are determined using the FC-ILS-I-CTOL and STOL measured distribution for the corresponding cases. The STOL gaussian vertical data is selected based on the study results in Reference 1. The gaussian distribution fit to the CTOL measured data is selected due to two reasons. First, there is insufficient data to accurately model the truncation of the lower end of the tails of the CTOL vertical distribution at ranges close to the runway. Second, the CTOL vertical distribution data is required only to calculate the CTOL/STOL probability of collision data. Thus, the upper half of the CTOL vertical distribution is the portion of the PDF which is important and data in this region tends to support a gaussian fit. The CTOL and STOL vertical PDF data is required at the following five ranges:

2 nmi, 1.5 nmi, 1.25 nmi, 1 nmi, and .75 nmi. The gaussian distributions corresponding to selected ranges for both the STOL and the CTOL cases are included in Appendix H.

Longitudinal PDF's

The longitudinal PDF is essential to the determination of the probability of collision data for the dependent CTOL/CTOL case. Since there is no measured data available for the longitudinal errors on the final approach, an assumption concerning this distribution is made as discussed in Section 2.5. The longitudinal PDF was derived based upon the velocity error distribution which was assumed normally distributed with a mean equal to the approach speed and a standard deviation of 5 knots. The resulting longitudinal PDF's at selected ranges are included in Appendix H.

3.4.2 NOZ DATA

Besides being used in the probability of collision data generation, the PDF's for the lateral dimension were used to calculate the NOZ's. The only exception to this is the CTOL/STOL skewed runway NOZ in which the analytical approach discussed in Section 2.5.3 was used. The NOZ is defined as being that zone which includes either 68% or 95% of the operations. The NOZ is symmetric about the extended runway centerline since the means of the lateral error PDF's are assumed to be zero. The selection of the 68% or 95% NOZ is based on the traffic rate and controller communication workload. The NOZ data discussion is subdivided into two parts. The first section deals with NOZ's for approach systems in general, and the second section discusses the CTOL/STOL skewed runway case.

NOZ Data for Approach Systems

The 68% and 95% NOZ's are determined from a direct integration of the lateral PDF's for each of the five cases listed in Table 3.4-1. The NOZ is divided into three regions: approach, runway, and departure. The approach region begins at the turn-on range and ends at either 5000 feet or 1500 feet from touchdown for CTOL and STOL aircraft, respectively. This range corresponds to the minimum range at which the aircraft should be VFR. The second region is the region over the runway itself which consists of two parallel lines spaced according to the value of the NOZ of the VFR range. The departure region is a mirror image of the approach region. The three regions are pictured in Figure 3.4.2-1. The locus of

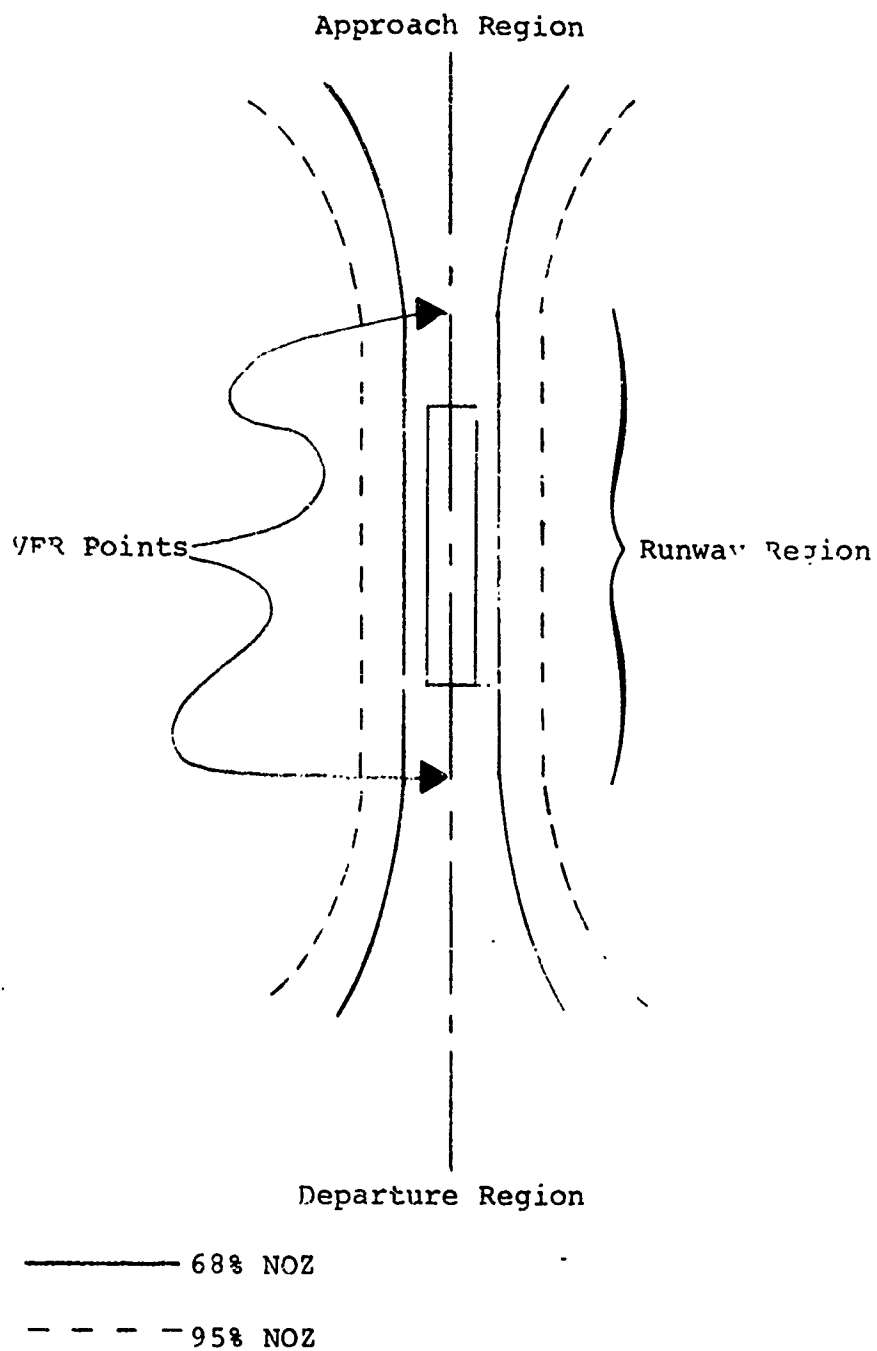


Figure 3.4.2-1 NOZ Regions

NOZ points is plotted in Appendix H for each of the five systems.

NOZ Data for CTOL/STOL Skewed Runways

Due to the lack of measured distribution data for STOL aircraft on curved departures, the method of NOZ determination for this case is different from the previous case. The 68% and 95% NOZ's for the STOL system in the CTOL/STOL configuration were determined using the techniques described in Section 2.5.3.2. The NOZ for runway spacing is required only at the point of minimum spacing between the CTOL runway and the STOL departure path. The 68% and 95% NOZ's for skew angles from ten to ninety degrees in ten degree increments at the CTOL runway - STOL departure path minimum spacing point are tabulated in Appendix H.

REFERENCE

1. -, "STOL Steep Approaches in the Breguet 941", Memorandum Report - Attachment 1, DOT-FAA, FS-640, November 1969.

SECTION 3.5

PROBABILITY OF COLLISION DATA

Probability of collision results obtained in the Lateral Separation Study are discussed in this section and presented in tabular form in Appendix I. These results represent a primary output of the Lateral Separation Study, and constitute a portion of the information necessary to determine a minimum allowable spacing between parallel runways for aircraft operating under IFR conditions. All cases categorized under CTOL/CTOL, CTOL/STOL, and STOL/STOL for which probability of collision data was generated are shown in Figure 3.5-1*

The objective of this analysis is to provide a relative measure of safety for minimum runway spacing considerations; the objective is not to provide an absolute measure of probability of collision. For this reason, worst case conditions are employed in all probability of collision calculations. The definition of the worst case condition for each specific system considered is dependent upon which dimensions are the primary dimensions of interest. In each case, the primary dimensions of interest are the only dimensions in which statistics are used; in the other dimensions, the absolute worst condition is assumed as illustrated in Table 3.5-1.

For the above reasons, the probability of collision data discussed in this section should be utilized as a "relative" measure of safety as opposed to an "absolute" measure.

Probability of collision data for CTOL/CTOL independent, CTOL/CTOL dependent, CTOL/STOL, and STOL/STOL are not directly comparable; e.g., data obtained for CTOL/CTOL independent operations should not be compared with data obtained for CTOL/STOL independent operations. The reason the different cases cited cannot be compared in terms of the probability of collision data generated for each case is that some cases employ statistics in only one dimension; whereas, other cases employ statistics in two dimensions. Specific dimensions in which statistics were utilized for each case is shown in Table 3.5-1. The type of distribution used for a specific dimension in each case is also shown. Cases in Table 3.5-1 which employ statistics in two dimensions produce probability of collision data smaller in magnitude than data generated for one dimensional cases.

*All figures and tables are included at the end of this section.

CTOL/CTOL probability of collision data are contained in Appendix I, Tables I-2 through I-8. Probability of collision data for CTOL/STOL and STOL/STOL approaches are contained in Tables I-9 and 10 and Table I-11, respectively. A table guide to all cases which are categorized under CTOL/CTOL, CTOL/STOL, and STOL/STOL approaches is also furnished in Appendix I. A discussion of the data along with examples illustrating how to use the tables and interpret the data is given in the following sections.

3.5.1 CTOL/CTOL PROBABILITY OF COLLISION DATA

Probability of collision data for the CTOL/CTOL aircraft and runway configuration was generated for both independent and dependent operations where independent and dependent operations are defined as in Section 2.6. For the purpose of clarity, discussions of the data generated for these two types of operations are presented separately.

CTOL/CTOL Independent Operations

Tables I-2 through I-4 in Appendix I contain probability of collision data for all CTOL/CTOL independent operations considered. The type of approach, type of operation, and the type of aircraft and runway configuration are specified in the captions of the respective tables.

As indicated in Figure 3.5.1-1, probabilities of collision contained in each of these three tables are calculated at the turn-on range and at four and two miles from the runway threshold for a fixed lateral spacing between runways. The data were generated at the above ranges for lateral spacings of 1500, 3000, 2500, 3000, 3500, 4300, and 5000 feet between runways.

Data contained in Tables I-2, I-3, and I-4 are for FC/FC, FC/VOR, and FC/BC approach systems, respectively.

CTOL/CTOL Dependent Operations

Probability of collision data generated for CTOL/CTOL dependent operations is contained in Tables I-5 through I-8 of Appendix I. The only approach system considered for dependent operations was FC/FC. Each of the tables corresponds to a different longitudinal spacing between approaching aircraft; i.e., Tables I-5, I-6, I-7, and I-8 were generated assuming longitudinal spacings of three, two, one, and one-fourth miles, respectively. Figure 3.5.1-2 illustrates the ranges of the leading aircraft from the runway threshold for which probability of collision was calculated for each of the

longitudinal spacings above. For a given longitudinal spacing and the above range values, the probability of collision was calculated for lateral spacings of 1500, 2000, 2500, 3000, 3500, 4300, and 5000 feet.

3.5.2 CTOL/STOL INDEPENDENT OPERATIONS

Tables I-9 and I-10 contain probability of collision data generated for CTOL/STOL approaches. The primary difference between data in the two tables is that data in Table I-9 is based on the runway configuration depicted in Figure 3.5.2-1a, and data contained in Table I-10 is based on the runway configuration in Figure 3.5.2-1b.

As indicated in Table I-9, probability of collision data was calculated at ranges from the threshold of 12,200, 9,200, and 4,700 feet for a fixed lateral spacing. Probability collision data in Table I-10 was calculated at ranges from the CTOL runway touchdown point of 7,700, 6,200, and 4,700 feet for a fixed lateral spacing. Probability of collision data in each of these tables was generated at each of the specified ranges for lateral separations of 1500, 2000, 2500, 3000, 3500, 4300, and 5000 feet.

3.5.3 STOL/STOL INDEPENDENT OPERATIONS

Table I-11 in Appendix I contains probability of collision data generated for STOL/STOL - FC/FC - independent operations. Data was generated at ranges of 12,000, 7,000, and 1,000 feet from the touchdown point for lateral spacings between runways of 1500, 2000, 2500, 3000, 3500, 4300, and 5000 feet.

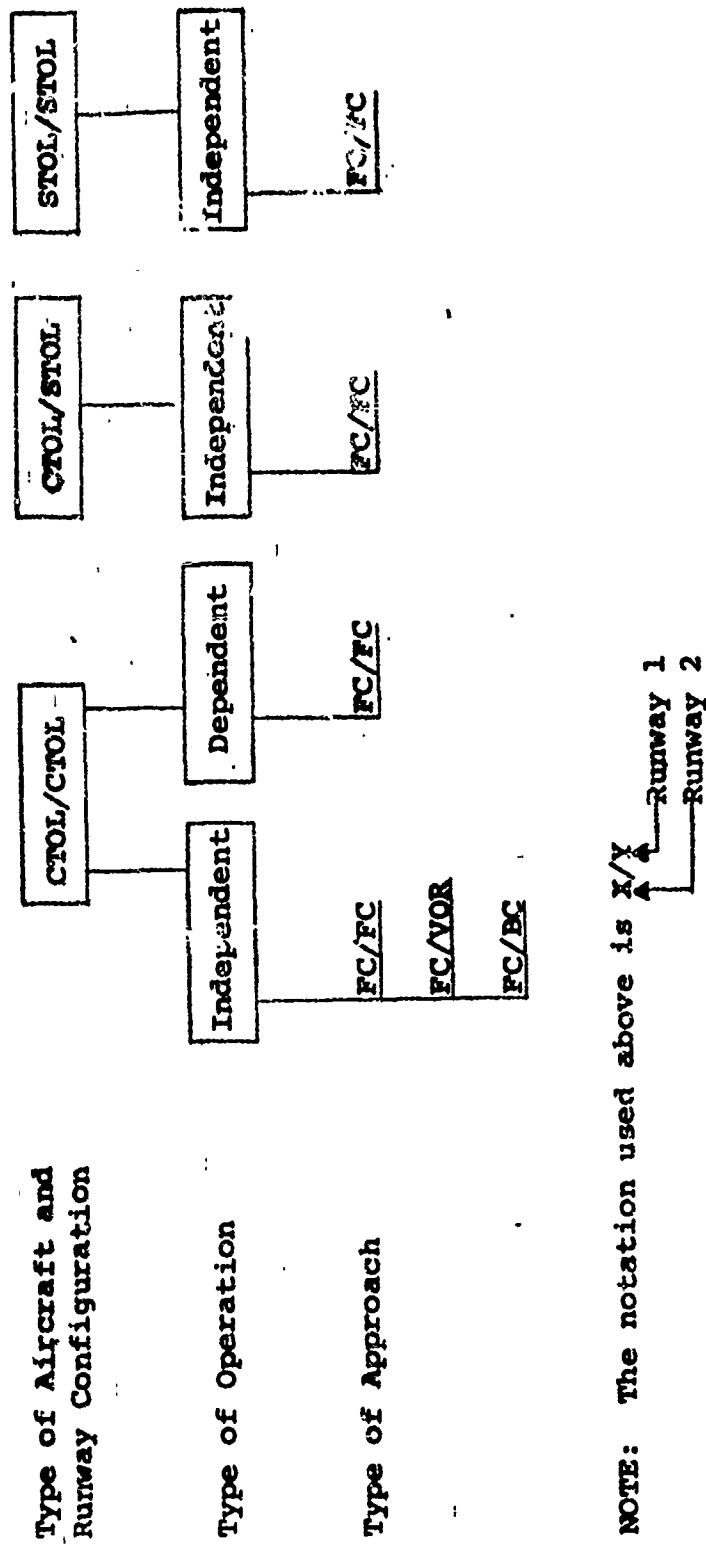


Figure 3.5-1

Cases Considered in Probability of Collision Analysis

Table 3.5-1
Distributions for Lateral, Vertical, and
Longitudinal Dimensions for the Approach Systems

Type of Aircraft - Runway Configuration and Operation	Primary Dimensions of Interest	Type of Distribution Assumed*	Worst Case Condition
CTOL/CTOL Independent	Lateral	FP Output/FP Output	Longitudinal and Vertical Coincidence
CTOL/CTOL Dependent	Lateral Longitudinal	FP Output/FP Output Gaussian/Gaussian	Vertical Coincidence
CTOL/STOL Independent	Lateral Vertical	FP Output/Gaussian Gaussian/Gaussian	Longitudinal Coincidence
STOL/STOL Independent	Lateral	Gaussian/Gaussian	Longitudinal and Vertical Coincidence

*FP - Fokker-Planck

Aircraft and Runway Configuration

Table I-1

CTOL/CTOL* Probability of Collision Data for FC/FC** Independent Operations***

Lateral Separation Feet	Range from Threshold, N. Miles	Probability of Collision
1500	6	
	4	
	2	
2000	6	
	4	
	2	
3000	6	
	4	

*Specifies Type of Approach

**Specifies Type of Approach

***Specifies Type of Operation

Figure 3.5.1-1

Explanation of Heading Information for Probability of Collision Tables

Longitudinal spacing
between adjacent
aircraft, NMI

Ranges* from threshold
for which PC was
calculated, NMI

Case I	Case II	Case III	Case IV
3	2	1	.25
3	4	5	5
2	3	4	4
1	2	3	3
	1	2	2
		1	1

All cases calculated for lateral separations of 1500,
2000, 2500, 3000, 3500, 4300, and 5000 feet.

*NOTE: Range is measured from touchdown point to the closest aircraft.

Figure 3.5.1-2

Cases Considered in Probability of Collision for
CTOL/CTOL Dependent Operations

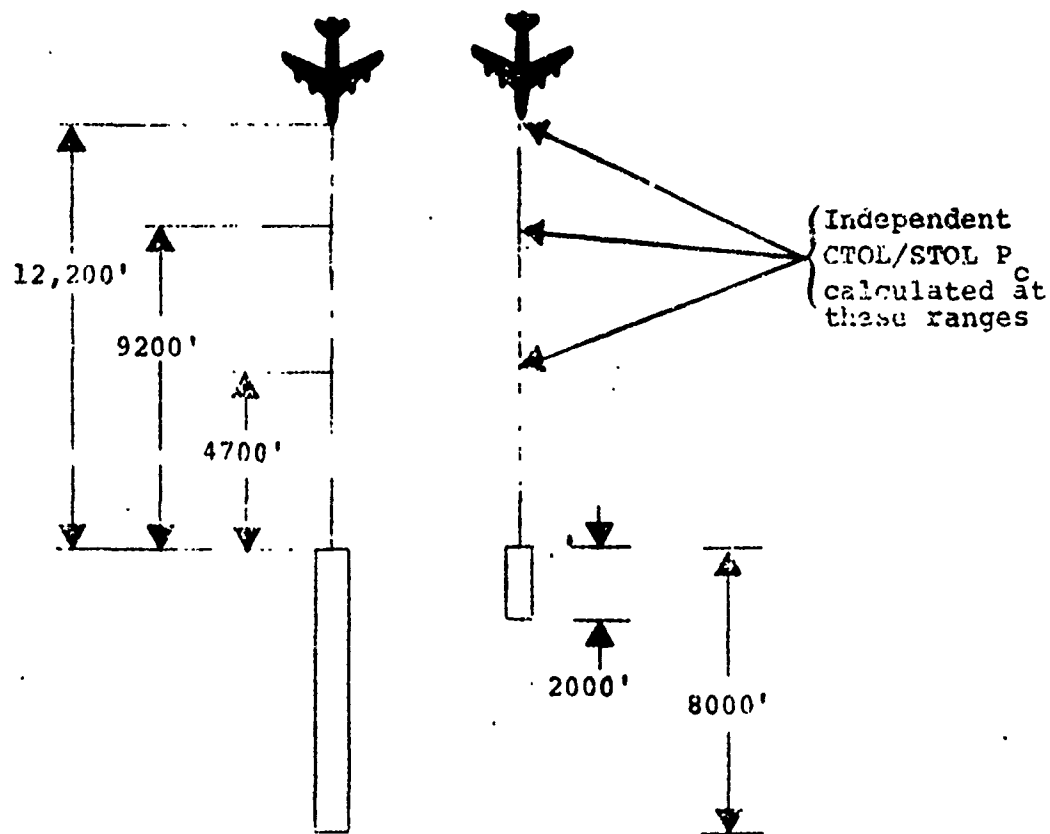


Figure 3.5.2-1a Runway Configuration for CTOL/STOL Independent Operations with No Threshold Displacement

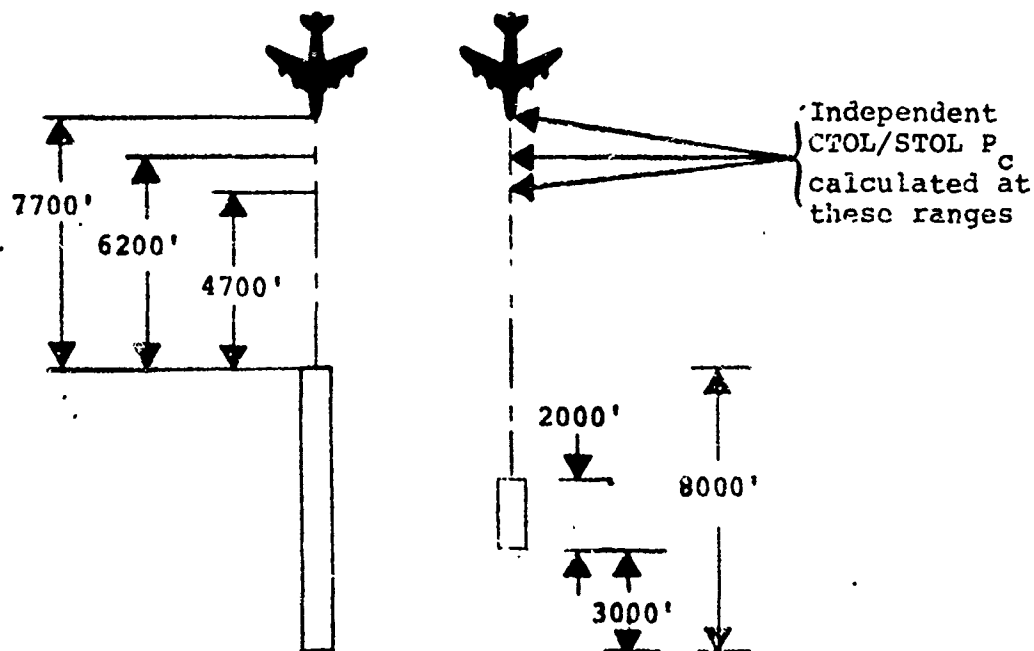


Figure 3.5.2-1b Runway Configuration for CTOL/STOL Independent Operations with 3000' Threshold Displacement

SECTION 3.6

BLUNDER DATA

The blunder analysis is an investigation of the airspace required for an aircraft to recover from abnormal operations or blunders. This airspace is identified as the total lateral extension of the normal operating zone (NOZ) required to bring a blundered aircraft to a course parallel with either the runway centerline or parallel to the course of the aircraft in the adjacent parallel approach path. A thorough description of the blunder analysis is presented in Section 2.7.

There are two basic types of blunder situations that were considered in the evaluation of the runway separation requirements. Type 1 blunders occur when an aircraft that is on a track which intercepts the approach course at 10° , 20° , and 30° , passes through the normal operating zone, and proceeds toward the adjacent track. Type 2 blunders occur when an aircraft which is established on the final approach course within the NOZ makes a turn toward the adjacent course at 15° , 30° , and 45° .

The blunder analysis was divided into two areas which analyze recovery operations for single aircraft recovery maneuvers and recovery operations for dual aircraft maneuvers. Since the blunder analyses are not dependent upon the "cause" of the blunder, type 1 and type 2 blunders are analyzed identically.

The blunder recovery airspace required for a single aircraft recovery maneuver for either of the two types of blunder situations was evaluated by considering the geometry of the situation as shown in Figure 3.6-1.

The parameters used in the single aircraft analysis are those specified in Table 3.6-1. The blunder recovery area, for all possible combinations of these parameter values, can be obtained from the results of the analysis. The blunder data, excluding the DAS error, for the single aircraft analysis is presented in tabular form in Appendix J. Typical output data from the single aircraft analysis is contained in Table 3.6-2, where the column headings are explained as follows:

Departure Angle (deg.) - the angle at which a blundered aircraft heads toward the adjacent approach course measured from the extended runway centerline.

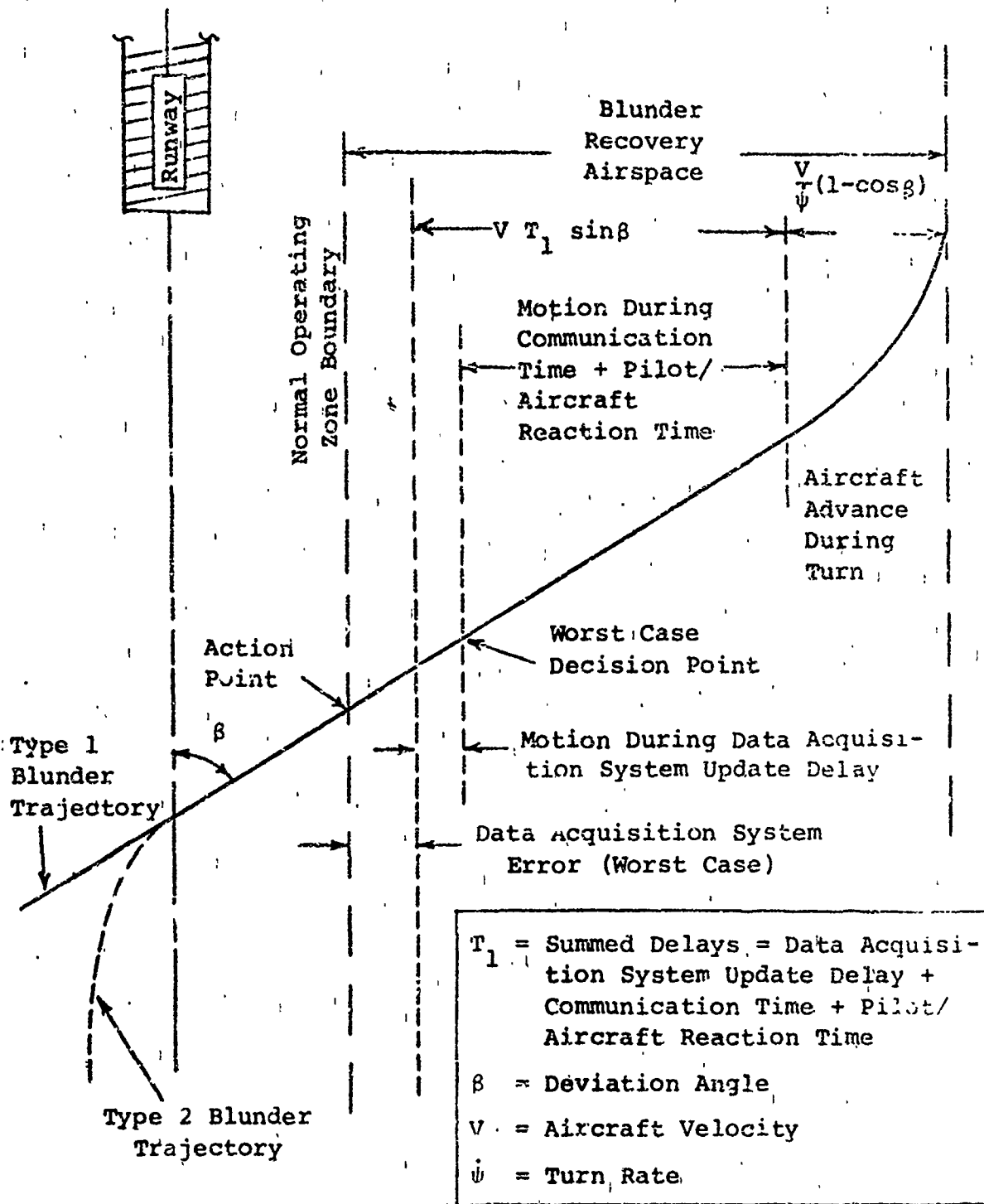


Figure 3.6-1

Single Aircraft Geometric Analysis of the Two Types of Blunders

Table 3.6-1 Blundered Aircraft Parameter Values

Parameters	Values	Units
Departure Angles		
Type 1	10, 20, and 30	degrees
Type 2	15, 30, and 45	degrees
DAS Range Accuracy (ϵ_R)	1.5, 1.0, .5, and .2	percentages of range
DAS Azimuth Accuracy (ϵ_A)	1.5, 1.0, and .5	degrees
DAS Update Delays	4, 2, 1, .5, .1, and .01	seconds
Aircraft Velocities	60, 80, 100, 120, 140, and 160	knots
Aircraft Bank Angles	10, 20, 30, and 40	degrees
Pilot/Aircraft Reaction Times	1.5, 5, and 8	seconds
Communication Times	1 to 10	seconds

Table 3.6-2 Single Aircraft Blunder Data

DEPARTURE ANGLE (DEG.)	VELOCITY (KNOTS)	BACK ANGLE (DEG.)	SUMMED DELAYS (SEC.)	FLUNDER RECOVERY AIRSPACE (F.T.)
30.00	100.00	40.00	2.50	352.23
30.00	100.00	40.00	9.00	900.77
30.00	100.00	40.00	16.00	1491.50
30.00	100.00	40.00	22.00	1997.84
30.00	100.00	30.00	2.50	416.27
30.00	100.00	30.00	9.00	964.80
30.00	100.00	30.00	16.00	1555.54
30.00	100.00	30.00	22.00	2061.88
30.00	100.00	20.00	2.50	536.62
30.00	100.00	20.00	9.00	1005.16
30.00	100.00	20.00	16.00	1675.65
30.00	100.00	20.00	22.00	2102.23
30.00	100.00	10.00	2.50	483.17
30.00	100.00	10.00	9.00	1431.70
30.00	100.00	10.00	16.00	2022.43
30.00	100.00	10.00	22.00	2528.73
30.00	120.00	40.00	2.50	456.58
30.00	120.00	40.00	9.00	1114.82
30.00	120.00	40.00	16.00	1823.70
30.00	120.00	40.00	22.00	2431.31
30.00	120.00	30.00	2.50	548.79
30.00	120.00	30.00	9.00	1207.04
30.00	120.00	30.00	16.00	1915.91
30.00	120.00	30.00	22.00	2523.52
30.00	120.00	20.00	2.50	722.10
30.00	120.00	20.00	9.00	1380.34
30.00	120.00	20.00	16.00	2009.22
30.00	120.00	20.00	22.00	2696.63
30.00	120.00	10.00	2.50	1221.13
30.00	120.00	10.00	9.00	1879.37
30.00	120.00	10.00	16.00	2531.25
30.00	120.00	10.00	22.00	3195.86

Velocity (knots) - the velocity of the blundered aircraft.

Bank Angle (deg.) - the bank angle that the blundered aircraft uses to make the corrective maneuver.

Summed Delays (sec.) - a total of all the delays of the blundered aircraft, including DAS Update Delay, Communication Time, and Pilot/Aircraft Reaction Time.

Blunder Recovery Airspace (ft.) - the lateral recovery airspace excluding EDAS, required for a blundered aircraft to recover from the type 1 and type 2 blunders, measured from the action point and perpendicular to the extended runway centerline.

To utilize the single aircraft analysis data contained in Appendix J, the desired set of parameter values to be studied must first be selected from Table 3.6-1. For the purpose of illustration, assume values for the parameters as follows:

Departure Angle	- 30 degrees
DAS Range Accuracy (ϵ_R)	- .5 percent of range
DAS Azimuth Accuracy (ϵ_A)	- 1.0 degrees
DAS Update Delay	- 1 second
Aircraft Velocity	- 100 knots
Aircraft Bank Angle	- 30 degrees
Pilot/Aircraft Reaction Time	- 5 seconds
Communication Time	- 4 seconds

First, find the departure angle (30 degrees) in the blunder data table (Table 3.6-2). The aircraft velocity (100 knots) and the aircraft bank angle (30 degrees) can now be found in the appropriate columns. Sum the DAS update delay (1 second), the pilot/aircraft reaction time (5 seconds), and the communication time (4 seconds) to yield the summed delay (10 seconds). The desired Blunder Recovery Airspace (1,049.15 feet), excluding DAS error, can be found by linear interpolation between the two recovery airspaces, (964.80 feet and 1,555.54 feet) for the appropriate two closest summed delay values (9 seconds and 16 seconds).

It should be noted that the Blunder Recovery Airspace of Appendix J does not include the Data Acquisition System error (EDAS). The value of EDAS may be calculated using the desired values of ϵ_R (.5 percent of range) and ϵ_A (1 degree) and the procedure discussed below.

In order to determine the EDAS, it is necessary to know the location of the DAS antenna as well as the blundered aircraft. These locations are specified as follows:

$X_{A/C}$ - Aircraft ground range to touchdown, ft.

$Y_{A/C}$ - Aircraft lateral location from the runway centerline, ft.

$Z_{A/C}$ - Aircraft altitude, ft.

X_{DAS} - DAS antenna ground range from touchdown, ft.

Y_{DAS} - DAS antenna lateral location from the runway centerline, ft.

Z_{DAS} - DAS antenna altitude, ft.

Figure 3.6-2 illustrates a possible DAS location configuration. Determination of the lateral component of the EDAS due to range error and azimuth error is illustrated in Figure 3.6-2 and shown below.

$$EDAS = E_A \cos \rho + E_R \sin \rho$$

where

$$E_A = R \tan \epsilon_A$$

$$E_R = \frac{\epsilon_R R}{100}$$

$$R = \sqrt{(X_{DAS} - X_{A/C})^2 + (Y_{DAS} - Y_{A/C})^2 + (Z_{DAS} - Z_{A/C})^2}$$

$$\rho = \tan^{-1} \left| \frac{Y_{DAS} - Y_{A/C}}{X_{DAS} - X_{A/C}} \right|$$

Assuming values of the EDAS location parameters as follows:

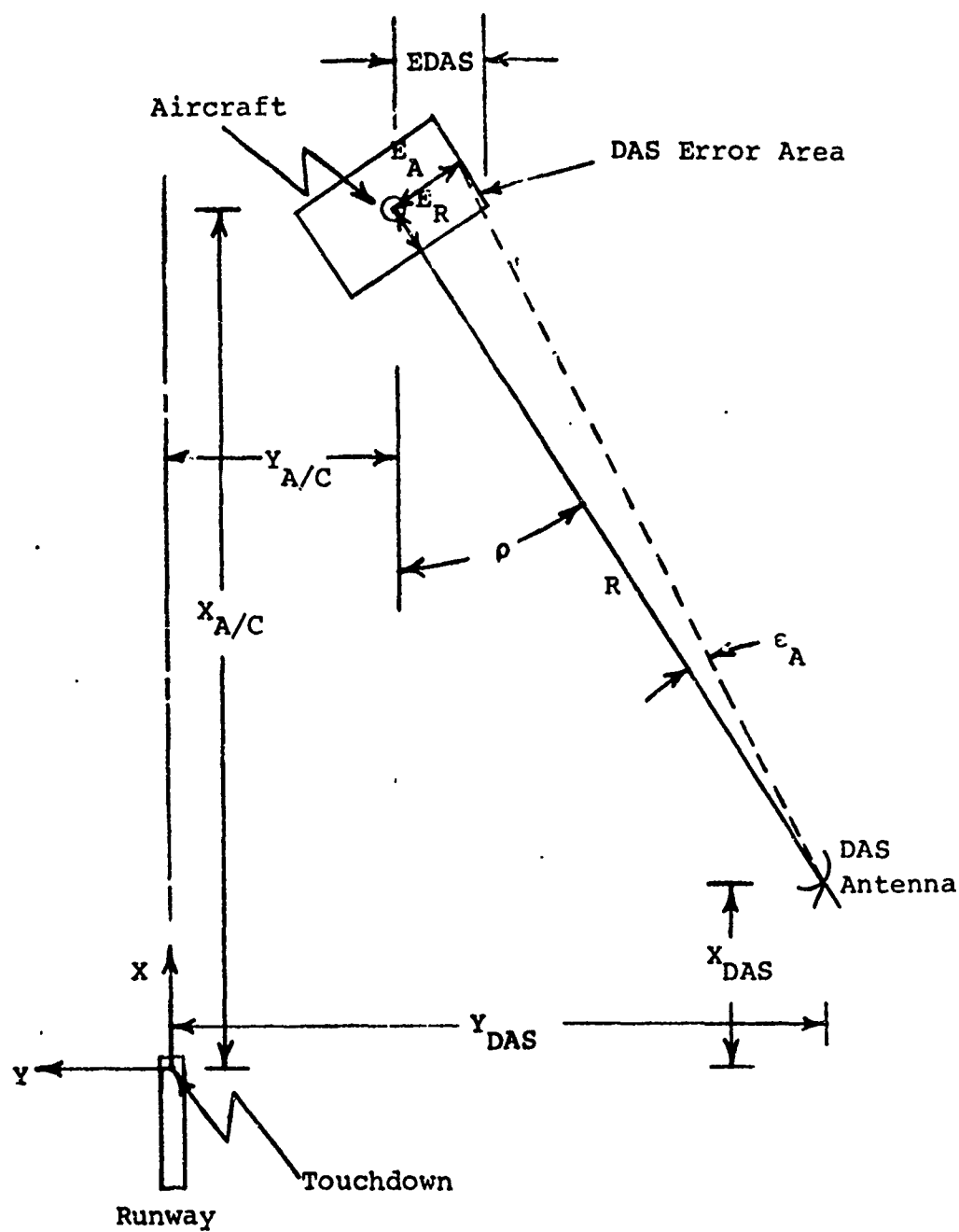


Figure 3.6-2 DAS Configuration

$$\begin{aligned}
 X_{A/C} &= 6,000 \text{ ft.} \\
 Y_{A/C} &= -1,500 \text{ ft.} \\
 Z_{A/C} &= 300 \text{ ft.} \\
 X_{DAS} &= 500 \text{ ft.} \\
 Y_{DAS} &= -2,500 \text{ ft.} \\
 Z_{DAS} &= 0 \text{ ft.}
 \end{aligned}$$

EDAS is calculated to be 101.17 feet. The value of EDAS (101.17 feet) is added to the blunder recovery airspace (1,049.15 feet) to find the total airspace required (1,150.32 feet) for an aircraft to recover from the defined blunder condition.

The dual aircraft analysis was used to evaluate the blunder recovery airspace required for a blundered aircraft to recover from the type 1 and type 2 blunders, assuming that the blundered aircraft failed to respond to the controller's warnings. The failure to respond makes it necessary for the controller to command an avoidance maneuver for the adjacent aircraft approaching the adjacent runway. The recovery of the blundered aircraft was considered complete when the heading of the blundered aircraft was the same as the heading of the aircraft on the adjacent approach course, meaning that both aircraft were flying parallel courses at that instant.

The geometry of the situation, as shown in Figure 3.6-3, was used to evaluate the required blunder recovery airspace for a blundered aircraft to recover to a course parallel with that of the adjacent aircraft. The parameter combinations used in the dual aircraft analysis for the blundered aircraft are those specified in Table 3.6-1. The parameter values used for the adjacent aircraft are 1, 4, 7, and 10 seconds for the Adjacent Summed Delays, and 3 degrees per second for the corrective maneuver turn rate. The blunder recovery area for all possible combinations of these parameter values can be obtained from the results of the analysis.

The blunder data, excluding the DAS error, for the dual aircraft analysis is presented in tabular form in Appendix K, and typical output data from the dual aircraft analysis is contained in Table 3.6-3, where the column headings are explained as follows:

Blundered Departure Angle (deg.) - the angle at which a blundered aircraft heads toward the adjacent approach course measured from the extended runway centerline.

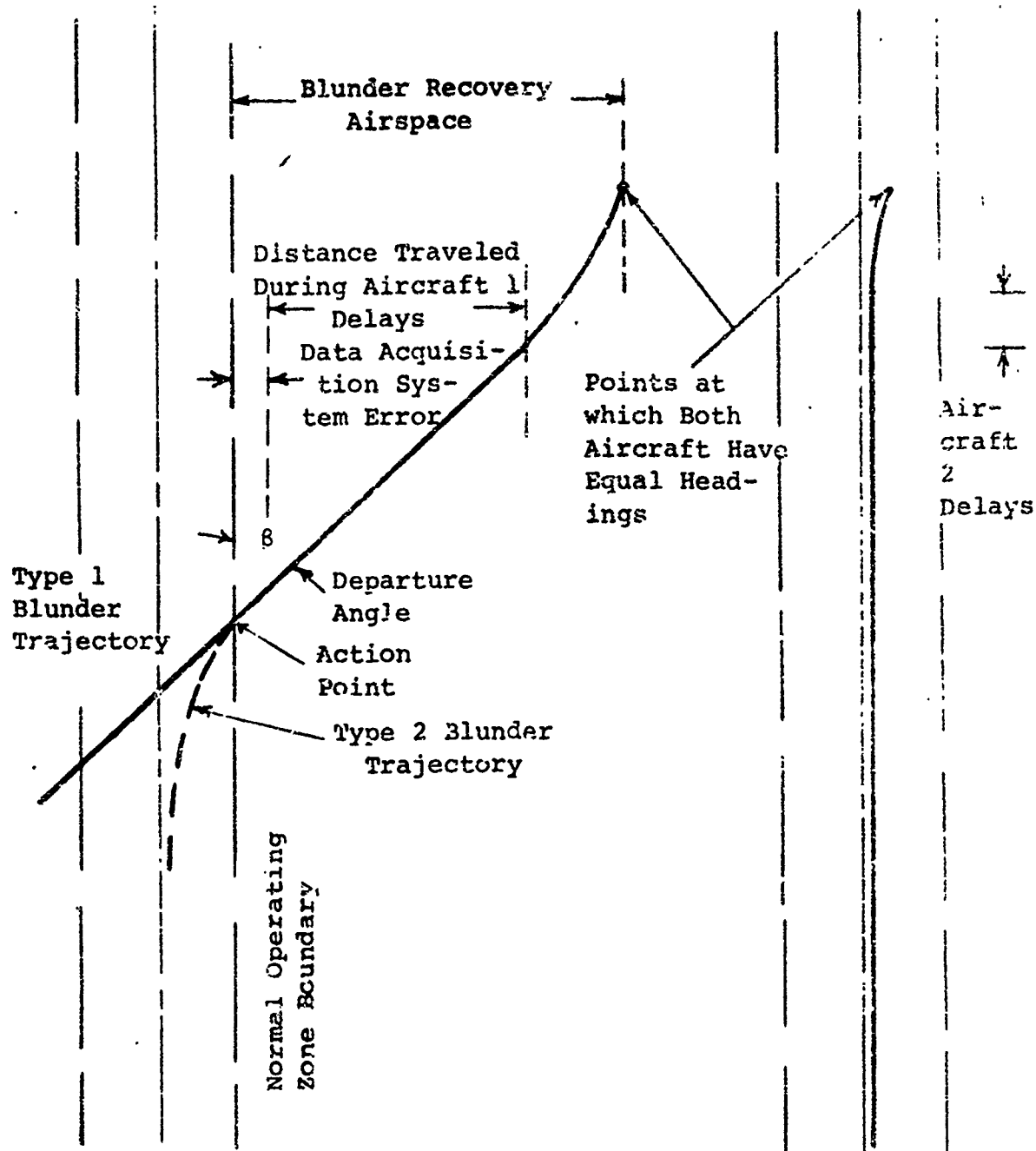


Figure 3.6-3 Dual Aircraft Geometric Analysis

Table 3.6-3 Dual Aircraft Blunder Data

BLUNDERED DEPARTURE ANGLE (DEG.)	BLUNDERED VELOCITY (KNOTS)	BLUNDERED DATA ANGLE (DEG.)	BLUNDERED SUMMED DELAYS (SEC.)	ADJACENT SUMMED DELAYS (SEC.)	CORRECTED PARALLEL HEADINGS (DEG.)	BLUNDER CORRECTION TIME (SEC.)	BLUNDER RECOVERY AIRSPACE (FT.)
30.00	100.00	40.00	2.50	1.00	174.87	5.21	342.00
30.00	100.00	40.00	2.50	4.00	180.00	5.77	352.23
30.00	100.00	40.00	2.50	7.00	180.00	5.77	352.23
30.00	100.00	40.00	2.50	10.00	160.00	5.77	352.23
30.00	100.00	40.00	4.00	1.00	174.87	11.71	896.54
30.00	100.00	40.00	9.00	4.00	180.00	12.27	900.77
30.00	100.00	40.00	9.00	7.00	160.00	12.27	900.77
30.00	100.00	40.00	9.00	10.00	160.00	12.27	900.77
30.00	100.00	40.00	10.00	1.00	174.87	18.71	1487.27
30.00	100.00	40.00	10.00	4.00	160.00	19.27	1491.50
30.00	100.00	40.00	10.00	7.00	160.00	19.27	1491.50
30.00	100.00	40.00	10.00	10.00	160.00	19.27	1491.50
30.00	100.00	40.00	22.00	1.00	174.87	24.71	1993.61
30.00	100.00	40.00	22.00	4.00	160.00	25.27	1997.84
30.00	100.00	40.00	22.00	7.00	160.00	25.27	1997.84
30.00	100.00	40.00	22.00	10.00	160.00	25.27	1997.84
30.00	100.00	30.00	2.50	1.00	172.57	6.04	402.64
30.00	100.00	30.00	2.50	4.00	173.47	7.01	415.72
30.00	100.00	30.00	2.50	7.00	180.00	7.25	416.27
30.00	100.00	30.00	2.50	10.00	180.00	7.25	416.27
30.00	100.00	30.00	9.00	1.00	172.57	12.54	951.23
30.00	100.00	30.00	9.00	4.00	178.47	13.51	964.26
30.00	100.00	30.00	9.00	7.00	160.00	13.75	964.26
30.00	100.00	30.00	9.00	10.00	160.00	13.75	964.26
30.00	100.00	30.00	16.00	1.00	172.57	19.54	1541.06
30.00	100.00	30.00	16.00	4.00	178.47	20.51	1554.09
30.00	100.00	30.00	16.00	7.00	160.00	20.75	1555.54
30.00	100.00	30.00	16.00	10.00	160.00	20.75	1555.54
30.00	100.00	30.00	22.00	1.00	172.57	25.54	2046.10
30.00	100.00	30.00	22.00	4.00	178.47	26.51	2061.35
30.00	100.00	30.00	22.00	7.00	160.00	26.75	2061.08
30.00	100.00	30.00	22.00	10.00	160.00	26.75	2061.08

Blundered Velocity (knots) - the velocity of the blundered aircraft.

Blundered Bank Angle (deg.) - the bank angle that the blundered aircraft uses to make the corrective maneuver.

Blundered Summed Delays (sec.) - a total of all the delays of the blundered aircraft, including DAS Update Delay, Communication Time, and Pilot/Aircraft Reaction Time.

Adjacent Summed Delays (sec.) - a total of all the delays of the adjacent aircraft, including Communication Time and Pilot/Aircraft Reaction Time measured after the Blundered Summed Delays.

Corrected Parallel Headings (deg.) - the heading angle of both the blundered and adjacent aircraft at the point in time when they are flying parallel courses (i.e., the blunder is corrected).

Blunder Correction Time (sec.) - the total time required for a blundered aircraft to attain a flight course parallel with that of the aircraft on the adjacent course (total blunder recovery time measured from the time the blundered aircraft reaches the action point until the blunder is corrected).

Blunder Recovery Airspace (ft.) - the lateral recovery airspace, excluding EDAS, required for a blundered aircraft to recover to a course parallel with that of the adjacent aircraft. The blunder recovery airspace is measured from the action point perpendicular to the extended runway centerline.

To utilize the dual aircraft analysis data contained in Appendix K, the desired set of blundered aircraft parameter values to be studied must first be selected from Table 3.6-1. For the purpose of illustration, assume the desired set of values to be as follows:

Departure Angle	- 30 degrees
DAS Range Accuracy (ϵ_R)	- .5 percent of range
DAS Azimuth Accuracy (ϵ_A)	- 1.0 degrees
DAS Update Delay	- 1 second
Aircraft Velocity	- 100 knots
Aircraft Bank Angle	- 30 degrees
Pilot/Aircraft Reaction Time	- 5 seconds

Communication Time

- 4 seconds

Also, assume the Adjacent Summed Delays to be 2 seconds.

First, find the departure angle (30 degrees) in the dual aircraft blunder data table (Table 3.6-3). The aircraft velocity (100 knots) and the aircraft bank angle (30 degrees) can now be found in the appropriate columns. Sum the DAS update delay (1 second), the pilot/aircraft reaction time (5 seconds), and the communication time (4 seconds) to yield the blunder summed delay (10 seconds). This summed delay value falls between two values (9 seconds and 16 seconds) in the Blundered Summed Delay output column. Since the delays of the adjacent aircraft (2 seconds) falls between two values (1 second and 4 seconds) in the Adjacent Summed Delays output column, the desired blunder recovery airspace (1,039.96 feet) can be found by a double linear interpolation, between the two sets of recovery airspaces (951.23 feet and 964.26 feet) and (1,541.96 feet and 1,554.99 feet).

It should be noted that the blunder recovery airspace of Appendix K does not include the Data Acquisition System error (EDAS). However, the value of EDAS may be calculated by using the identical technique explained previously for the single aircraft blunder analysis. By using the desired values of ϵ_R (.5 percent of range) and ϵ_A (1 degree) and by using the same assumed EDAS location parameter as used in the illustrative example for the single aircraft blunder analysis, the value of EDAS is 101.17 feet.

Upon finding the value of EDAS (101.17 feet), it may be added to the blunder recovery airspace (1,039.96 feet) to find the total airspace required (1,141.13 feet) for an aircraft to recover from the defined blunder condition.

SECTION 4

SUMMARY

The Lateral Separation Study provides a method for determining the minimum lateral spacing between runways and measuring the relative safety for a given runway spacing. A detailed procedural description of this method is contained in Volume I of this report. The basic objectives of Volume II are to present the data essential to the determination of minimum runway spacings and to describe the development of the techniques used to generate this data.

A presentation of the list of data essential to the determination of minimum runway spacings and a brief description of the problems associated with the generation of this data were contained in Section 1.1. Briefly, this data includes: probability of collision data, normal operating zone data, and blunder recovery data. The problems associated with the generation of the data were subdivided into four specific problem areas:

- (1) developing system models,
- (2) determining NOZ data,
- (3) determining probability of collision data, and
- (4) determining blunder recovery airspace data.

Once the solutions to the previous four problems are obtained, the problem of determining minimum spacing between runways can be solved (Volume 1). This minimum spacing based on an associated collision probability value determined by solving (3), a normal operating zone determined by solving (2), a blunder recovery area determined by solving (4), and a no transgression zone. A procedure for determining minimum runway spacings was determined for:

1. Parallel runways and independent operations for:
 - FC-ILS-CTOL/FC-ILS-CTOL
 - FC-ILS-CTOL/BC-ILS-CTOL
 - FC-ILS-CTOL/(VOR/DME)-CTOL
 - FC-ILS-CTOL/FC-ILS-STOL (different runway threshold locations)
 - FC-ILS-STOL/FC-ILS-STOL
2. Parallel runways and dependent operations for:
 - FC-ILS-CTOL/FC-ILS-CTOL
3. Skewed runways and independent operations for:
 - FC-ILS-CTOL/FC-ILS-STOL with due consideration for approaches, departures, and missed approaches.

Section 2 provided a detailed description of the development of techniques used to generate the required data. The basic method of approach is illustrated in Figure 4-1. Statistical descriptions of the location errors (probability density functions) of aircraft operating under IFR conditions were used directly to compute the probability of collision data and normal operating zone data. A deterministic analysis which included a parametric variation of the pertinent system parameters was used to generate the blunder recovery data.

The results of the various analyses described in Section 2 are discussed in Section 3 and presented in the appendices. In addition to the probability of collision data, normal operating zone data and blunder recovery data, several other study results were presented including: measured distribution data, approach system models, sensitivity data, and probability density function data.

The purpose of this section is to summarize the approach taken to generate the required data and to discuss the resulting data. A summary of the major tasks shown in Figure 4-1 and a brief discussion pertaining to the data generated by each task is contained in the following sections:

- (1) system models,
- (2) probability density functions,
- (3) normal operating zones,
- (4) probability of collision, and
- (5) blunder recovery airspace.

System Models

As shown in Figure 4-1, the first effort undertaken was the development of system models which describe the required approach systems. The system models represent the lateral dynamics of a composite set of aircraft operating under IFR conditions. The model development task, described in Section 2.1, was divided into two parts:

- (1) the development of models to be used in the generation of lateral deviation probability density functions:
 1. FC-ILS-I-CTOL,
 2. FC-ILS-II-CTOL,
 3. BC-ILS-I-CTOL ,
 4. VOR-CTOL,
 5. FC-ILS-I-STOL, and
- (2) the development of models to be used as analysis tools to study approach systems:

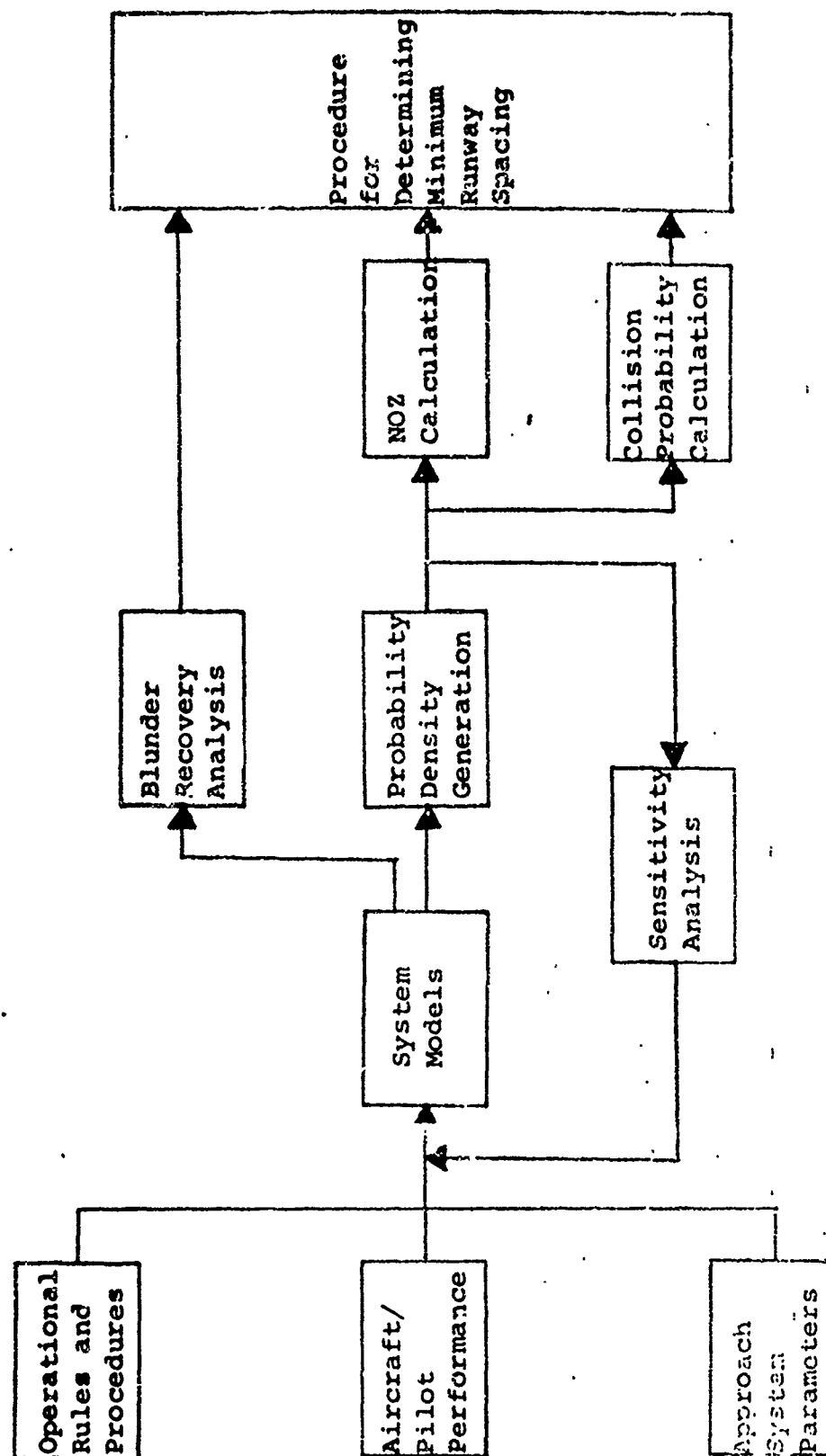


Figure 4-1 Method of Solution

1. Curved Path Model and
2. Multiple Aircraft/Runway Model

Due to similarities in all of the required models, a nominal system model was developed in Section 2.1.2 from which all required expanded models were developed as discussed in Section 2.1.3. The nominal model represents a composite set of CTOL aircraft approaching a CTOL runway on the front course of an ILS Category I approach system. Three versions of the nominal model were developed for use in the various required analyses:

- (1) Nominal System Model,
- (2) Nonlinear, Simulated Delay Nominal Model, and
- (3) Linear Simulated Delay Nominal Model

Verification of the nominal model was accomplished in Section 2.4 by performing three analyses: time response analysis, frequency response analysis, and statistical response analysis. By comparing the nominal model predicted lateral distribution to measured distribution data, the nominal model was shown to accurately describe the FC-ILS-INOM-CTOL approach system.

In an effort to determine the dominant system parameters, errors, and initial conditions, a sensitivity analysis was performed on the nominal model using both a deterministic and a statistical approach. The sensitivity analysis yielded an effective means of determining dominant elements in the approach system and can, in turn, be used to adapt system models to measured distribution data or new system requirements. The system parameters which appear to have the largest effect upon the lateral deviation are those associated with the pilot. The aircraft and runway associated parameters appear to have a small effect in comparison to the pilot parameters. The system errors which appear to have the largest effect upon the lateral error distribution are those due to pilot attitude. Also, the effect due to system equipment errors tends to increase with decreasing range, while the effect due to initial condition errors, such as heading angle, tend to decrease as range decreases.

The verified nominal model was used to develop the models needed for the generation of the lateral error probability density functions. These models simulate a composite set of aircraft flying the final leg of an instrument approach under IFR conditions. The nominal model was adapted to the measured distribution data (Section 2.3 and 3.1) for each of the approach system models as described in Section 2.5. This process utilized the sensitivity data to determine the changes in the model

parameters and/or errors necessary to adapt the nominal model such that the model-predicted distribution accurately approximated the measured distribution data. This process yielded five approach system models which accurately described the lateral dynamics of the following approach systems:

- FC-ILS-I-CTOL
- FC-ILS-II-CTOL
- BC-ILS-I-CTOL
- VOR-CTOL
- FC-ILS-I-STOL

The nominal model could be modified in a similar manner to simulate other approach systems, aircraft, pilots, procedures, etc. Additionally, the evaluation of new concepts and future systems can be accomplished by modifying the nominal model.

In addition to the above models, it was necessary to develop two models to be used as analysis tools to study approach systems:

- (1) Curved Path Model
- (2) Multiple Aircraft/Runway Model

Both of these models were developed by expanding the nominal model to include the necessary operations and runway configurations as discussed in Section 2.1.3.2. These models may be used in the prediction of distribution data for systems in which no measured field data exists as well as for departures and missed approaches. Certain system characteristics which are difficult to observe in the actual approach system (such as multiple aircraft relative velocities and locations, aircraft bank angle and heading angle, curved path characteristics, etc.) may be obtained from these system models.

Both the curved path model and the multiple aircraft/runway model have been programmed in FORTRAN IV computer programs. The computer programs, including source listings, flow charts, and operating instructions, are described in detail in the User's Manual.

Probability Density Functions

A positional error probability density function, as utilized in this study, is a statistical description of the errors about an "ideal track". It is defined for a composite set of aircraft flying the final leg of an instrument approach under IFR conditions. A complete three dimensional statistical description of these errors is required to aid in the generation of data necessary to determine minimum runway spacings (NOZ

and probability of collision data). For this reason, the positional error probability density space consists of three dimensions (lateral, vertical, and longitudinal).

The primary dimension utilized in the lateral separation criteria determination is the lateral dimension. For this reason, lateral approach system models were developed which, when included in the Fokker-Planck equation, accurately generate the lateral PDF for the required approach systems. The basic approach for generating the required lateral PDF's includes four steps:

1. Determine the lateral error PDF to be used to initialize the Fokker-Planck equation.
2. Incorporate the approach system model into nonlinear state equations.
3. Reduce the nonlinear state equations to a set of linear second order state equations.
4. Incorporate the reduced state equations into the Fokker-Planck equation and generate the PDF with the initial distribution from step 1.

Using the above approach, lateral PDF's were generated for the systems listed below:

1. FC-ILS-I-CTOL
2. FC-ILS-II-CTOL
3. BC-ILS-I-CTOL
4. VOR-CTOL
5. FC-ILS-I-STOL

The reduced system model state equations that were used in the Fokker-Planck equation, resulted in accurate approximations to the original models over the ranges considered.

The measured distribution data (Section 2.3), used in the initialization of the Fokker-Planck equation, was collected from various sources. The resulting data was obtained by combining the data from the various sources into one data set representing each of the required approach systems. The Fokker-Planck equation for each of the first four cases is initialized at the turn-on range using the modified Burgerhout distribution fit to the measured distribution data. The modified Burgerhout distribution is used to initialize the CTOL lateral cases in an effort to better describe the measured distribution data, which had a large number of data points in the tails of the distribution. The initial distribution used for the STOL case is the gaussian distribution.

The PDF's for all five cases are determined quite accurately using the Fokker-Planck equation. This accuracy is due to the fact that the Fokker-Planck equation utilizes the

dynamics of the system to generate the resulting PDF's. The increments used in the Fokker-Planck calculation were 23.6 feet in range and 174 feet laterally.

The resulting lateral PDF's for all cases are symmetric with a mean on the extended runway centerline and a standard deviation which decreases monotonically from the turn-on range to the final range. The VOR and BC-ILS lateral errors are much larger than the FC-ILS lateral errors.

The description, implementation, and verification of the Fokker-Planck equation as applied to this study is contained in Sections 2.2 and 2.5. The Fokker-Planck equation yields an effective and accurate method for predicting probability density functions. New or different approach systems in which no measured distribution data is available could also be studied using the Fokker-Planck equation.

For the collision probability determination, the composite CTOL/STOL operations required vertical dimension error PDF's for FC-ILS-I-CTOL and FC-ILS-I-STOL. This results from the fact the CTOL operation has a different glideslope (2.5°) than the STOL (7.5°) operation; and, therefore, the worst case assumption of vertical coincidence is not valid. A gaussian vertical error PDF was selected for both of the approach systems. The gaussian distributions were determined by using the measured error distribution data as the vertical error PDF. The measured data standard deviations were linearly interpolated to arrive at vertical distributions at the required range points for the two vertical systems. The means for both the CTOL and STOL vertical PDF's were set to the glideslope value to reduce the problem of including system biases that were peculiar to the measured data collection sites. No attempt was made to include the non-symmetrical distribution effect which occurs near touchdown for either of the two systems.

The need for a longitudinal error density function was predicated by the requirement to determine probability of collision data for dependent operations. Thus, a longitudinal error density function was required for the FC-ILS-I-CTOL approach system. Using a gaussian velocity error distribution with a constant standard deviation and a mean equal to the nominal approach speed, the longitudinal error probability density function was generated as discussed in Section 2.3.2.3.

Normal Operating Zones

The PDF's for the lateral dimension were used to calculate the NOZ's for the following approach systems:

1. FC-ILS-I-CTOL
2. FC-ILS-II-CTOL
3. BC-ILS-I-CTOL
4. VOR-CTOL
5. FC-ILS-I-STOL

The NOZ is defined as being that zone which includes either 68% or 95% of the operations. The NOZ is symmetric about the extended runway centerline since the means of the lateral error PDF's are assumed to be zero. A direct integration of the lateral PDF's for each of the five cases was used to determine the resulting NOZ's. The NOZ's followed the same trend as the lateral PDF standard deviations, as expected.

Due to the lack of measured distribution data for STOL aircraft on curved departures, the method of NOZ determination for the CTOL/STOL skewed runway is different from the previous case. The 68% and 95% NOZ's for the STOL system in the CTOL/STOL configuration were determined using a Monte Carlo simulation of the STOL curved departure. The NOZ for minimum spacing determination is required only at the point of minimum spacing between the CTOL runway and the STOL departure path.

Probability of Collision

In order to determine the minimum lateral spacing between two parallel runways, a means of measuring the relative safety of two aircraft attempting to land on parallel runways is needed. This relative safety is defined to be the probability of collision in the Lateral Separation Study.

The objective of this analysis is to provide a relative measure of safety, rather than an absolute measure of collision probability. For this reason, worst case conditions are employed in all probability of collision calculations. The definition of the worst case condition for each specific system considered is dependent upon which dimensions are the primary dimensions of interest. In each case, the primary dimensions of interest are the only dimensions in which statistics are used; in the other dimensions, the absolute worst condition is assumed as illustrated in Table 4-1. For the above reasons, the probability of collision data discussed in this section should be utilized as a "relative" measure of safety as opposed to an "absolute" measure.

It is assumed throughout this analysis that the airspace requirements for a departure are no greater than for an approach; therefore, probability of collision models are based on approaches, and all subsequent results obtained are assumed to be equally valid for both departures and approaches.

Table 4-1
Distributions for Lateral, Vertical, and
Longitudinal Dimensions for Probability of Collision Calculations

Type of Aircraft - Runway Configuration and Operation	Primary Dimensions of Interest	Type of Distributor Assumed*	Worst Case Condition
CTOL/CTOL Independent	Lateral	FP Output/FP Output	Longitudinal and Vertical Coincidence
CTOL/CTOL Dependent	Lateral Longitudinal	FP Output/FP Output Gaussian/Gaussian	Vertical Coincidence
CTOL/STOL Independent	Lateral Vertical	FP Output/Gaussian Gaussian/Gaussian	Longitudinal Coincidence
STOL/STOL Independent	Lateral	Gaussian/Gaussian	Longitudinal and Vertical Coincidence

*FP - Fokker-Planck

The probability of collision between two aircraft approaching parallel runways is considered in Section 2.6 for the following cases:

- (a) CTOL/CTOL independent operations
- (b) STOL/STOL independent operations
- (c) CTOL/CTOL dependent operations
- (d) CTOL/STOL independent operations.

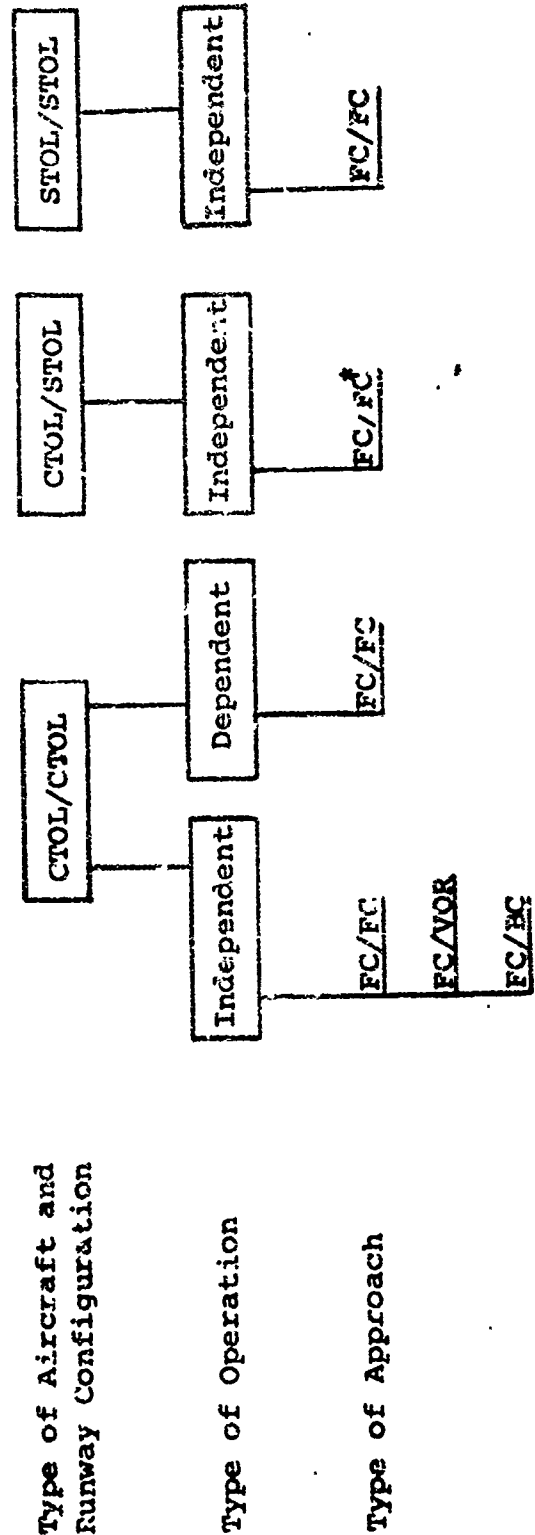
The aircraft lateral, vertical, and longitudinal error probability density functions are used in the generation of the required probabilities of collision, as discussed in Section 2.6.2. The specific cases for which probability of collision data were generated are illustrated in Figure 4-2.

The probability of collision data for CTOL/CTOL independent operations indicates that the probability of collision is smallest for FC/FC approach configurations. The probabilities of collision for FC/BC and FC/VOR approaches are approximately the same magnitude, but both are larger than FC/FC approaches. Probability of collision for STOL/STOL independent operations are extremely small in comparison with CTOL/CTOL independent approaches. The effect of a gaussian longitudinal PDF yields very small probability of collision values for large longitudinal separations for CTOL/CTOL dependent operations. The probability of collision values for CTOL/STOL operations with a 3000 foot threshold displacement are considerably larger than for those operations with no threshold displacement.

Blunder Recovery Airspace

The blunder analysis is an investigation of the airspace required for an aircraft to recover from abnormal operations or blunders. This airspace is identified as the total lateral extension of the normal operating zone required to bring a blundered aircraft to a course parallel with either the runway centerline or parallel to the course of the aircraft in the adjacent parallel approach path. A thorough description of the blunder analysis is presented in Section 2.7. The blunder analysis was divided into two areas which analyze recovery operations for single aircraft recovery maneuvers and recovery operations for dual aircraft maneuvers.

A deterministic approach was used in this analysis which considered a parametric variation of the blunder parameter values. These parameter values bound all reasonable operating conditions, equipment accuracies, system delays, aircraft/pilot dynamics, and communication times. The resulting blunder recovery airspace was determined from the geometry of



NOTE: The notation used above is X/Y
 ↑ Runway 1
 ↑ Runway 2

*Different runway threshold locations were considered.

Figure 4.2

Cases Considered in Probability of Collision Analysis

the blunder recovery operations.

The blunder recovery airspace required for corrective maneuvers by both the blundered aircraft and the adjacent aircraft was generally less than that required for corrective maneuvers by the blundered aircraft only. As indicated in Section 2.7, the dominant contributors to blunder recovery airspace are the system delays followed by departure angle, aircraft velocity, and aircraft bank angle in order of decreasing dominance.

APPENDIX A

AIRCRAFT MODEL

This appendix describes an aircraft model and includes a complete set of equations for defining the trajectory of an aircraft maneuvering in pitch and yaw simultaneously. This model will be used to generate the state equations for the analytical solution.

The coordinate systems used in this derivation are shown in Figure A-1. The body axis system is identified by the x, y, z axes and has its origin at the aircraft center-of-gravity. The x axis is defined positive forward along the aircraft fuselage centerline; the z axis is positive along the earth's gravitational vector toward the center of the earth; and the y axis completes the system. The earth's axis system is identified by the X', Y', Z' axes and has its origin on the earth's surface. The Z' axis is positive along the earth's gravitational vector toward the center of the earth.

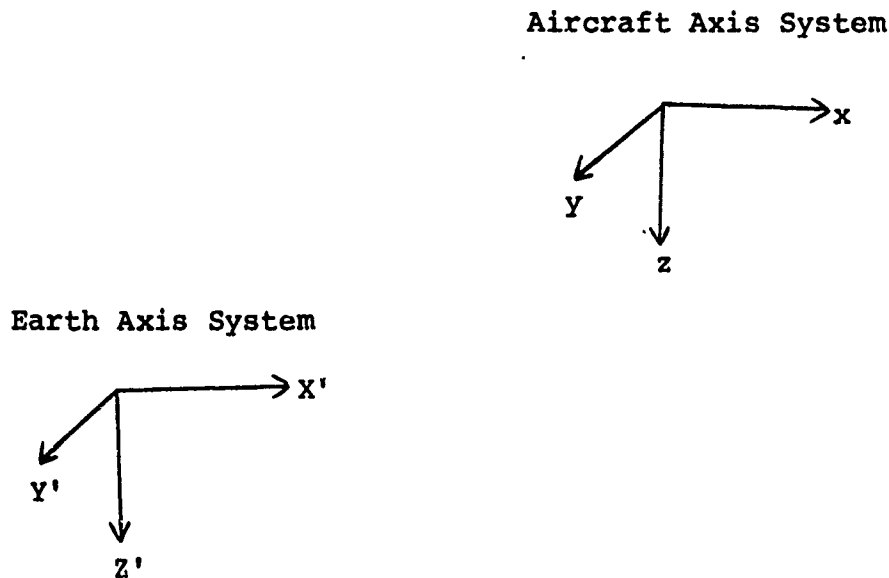


Figure A-1 Coordinate Systems

The aircraft is assumed to maneuver at a constant airspeed and with no sideslip or angle of attack. Further, only normal acceleration is considered to be acting on the aircraft. Using the aircraft body axes as a reference, the acceleration is expressed as, $\bar{a} = \bar{\omega} \times \bar{v}$, where \bar{a} is the inertial acceleration vector of the aircraft, $\bar{\omega}$ is the rotation rate vector of the aircraft body axes and \bar{v} is the aircraft velocity vector.

The inertial acceleration is composed of the total acceleration of the aircraft ($\bar{a}_z = \text{Lift/Mass}$) and the gravitational acceleration (\bar{g}).

$$\bar{a} = 32.2(\bar{a}_z + \bar{g}) = 32.2(a_{13} \bar{x} + a_{23} \bar{y} + (a_{33} + a_z) \bar{z})$$

In this equation, a_{ij} is defined as the direction cosine of the i th row and the j th column of the Earth to vehicle direction cosine matrix, a_z is the total normal acceleration (positive downward along the positive z axis) and \bar{x} , \bar{y} , \bar{z} are unit vectors along the x , y , and z body axes respectively.

The rotation rate of the aircraft body axes may be written in terms of the rotational rates (p, q, r) about the x, y , and z body axes.

$$\bar{\omega} = p \bar{x} + q \bar{y} + r \bar{z}$$

This equation may be rewritten by making use of the following Euler rate equations,

$$p = \dot{\psi} a_{13} + \dot{\phi}$$

$$q = \dot{\psi} a_{23} + \dot{\theta} \cos \phi$$

$$r = \dot{\psi} a_{33} - \dot{\theta} \sin \phi$$

$$\omega = (\dot{\psi} a_{13} + \dot{\phi}) \bar{x} + (\dot{\psi} a_{23} + \dot{\theta} \cos \phi) \bar{y} + (\dot{\psi} a_{33} - \dot{\theta} \sin \phi) \bar{z}$$

where ψ , θ , ϕ are the Euler angles which define aircraft body axis orientation with respect to the Earth axis system. The Euler angle rates, $\dot{\psi}$, $\dot{\theta}$, and $\dot{\phi}$, correspond to a yaw (ψ), pitch (θ), bank (ϕ) sequence in transforming from earth axes to body axes.

The velocity vector (\bar{V}) lies along the aircraft x body axis due to the assumption of zero sideslip and angle of attack; i.e. $\bar{V} = V \bar{x}$. The cross product, $\bar{a} = \bar{\omega} \times \bar{V}$, gives the following result.

$$\begin{aligned} 32.2(a_{13} \bar{x} + a_{23} \bar{y} + (a_{33} + a_z) \bar{z}) \\ = V(\dot{\psi} a_{33} - \dot{\theta} \sin \phi) \bar{y} - V(\dot{\psi} a_{23} + \dot{\theta} \cos \phi) \bar{z} \end{aligned}$$

$$a_{13} = 0$$

$$a_{23} = \frac{V}{32.2} (\dot{\psi} a_{33} - \dot{\theta} \sin \phi)$$

$$a_{33} + a_z = \frac{-V}{32.2} (\dot{\psi} a_{23} + \dot{\theta} \cos \phi)$$

The equality, $a_{13} \bar{x} = 0$, indicates that the acceleration along the x body axis must be zero which agrees with the assumption of constant velocity. The second and third equalities may be solved simultaneously to produce the following equations for the Euler angle rates.

$$\dot{\psi} = \frac{+32.2(a_{23} \cos \phi - (a_{33} + a_z) \sin \phi)}{V(a_{33} \cos \phi + a_{23} \sin \phi)} = \frac{-32.2 a_z \sin \phi}{V \cos \theta}$$

$$\dot{\theta} = \frac{-32.2(a_{23}^2 + (a_{33} + a_z) a_{33})}{V(a_{33} \cos \phi + a_{23} \sin \phi)} = \frac{-32.2(\cos \theta + \cos \phi a_z)}{V}$$

Therefore, if the aircraft bank angle (ϕ) and total normal acceleration (a_z) are known as functions of time, the above equations may be integrated to determine the Euler angles (radians) for Earth axes to airplane body axes. These Euler angles may be used to define the direction cosine matrix (A) between Earth and body axes.

$$(A) = \begin{bmatrix} a_{11} & a_{12} & a_{13} \\ a_{21} & a_{22} & a_{23} \\ a_{31} & a_{32} & a_{33} \end{bmatrix}$$

For the specified ψ , θ , ϕ sequence the elements are defined as follows.

$$a_{11} = \cos \theta \cos \psi$$

$$a_{12} = \cos \theta \sin \psi$$

$$a_{13} = -\sin \theta$$

$$a_{21} = \sin \phi \sin \theta \cos \psi - \cos \phi \sin \psi$$

$$a_{22} = \sin \phi \sin \theta \sin \psi + \cos \phi \cos \psi$$

$$a_{23} = \sin \phi \cos \theta$$

$$a_{31} = \cos \phi \sin \theta \cos \psi + \sin \phi \sin \psi$$

$$a_{32} = \cos \phi \sin \theta \sin \psi - \sin \phi \cos \psi$$

$$a_{33} = \cos \phi \cos \theta$$

It is normally required to define the aircraft velocity rates on the earth axes ($V_{X'}$, $V_{Y'}$, $V_{Z'}$). This may be accomplished by using the transpose of the matrix $(A)^T$.

$$\begin{bmatrix} V_{X'} \\ V_{Y'} \\ V_{Z'} \end{bmatrix} = (A)^T \begin{bmatrix} V \\ 0 \\ 0 \end{bmatrix}$$

$$V_{X'} = V \cos \theta \cos \psi$$

$$V_{Y'} = V \cos \theta \sin \psi$$

$$V_{Z'} = -V \sin \theta$$

In addition, the location of the aircraft on the Earth axis (X' , Y' , Z') may be found by integrating the velocities.

If a level, coordinated turn is to be performed, the maneuver is defined by the following equations.

$$\theta = 0$$

$$a_z = \frac{-1}{\cos \phi}$$

These produce the following results which agree with the standard rate equations.

$$\dot{\theta} = 0$$

$$\dot{\psi} = \frac{32.2 \tan \phi}{V}$$

If a pitch acceleration maneuver is to be performed, it is defined by the following equations.

$$\phi = 0$$

$$a_z = f(t)$$

These produce the following results which agree with the standard pitch rate equation.

$$\dot{\psi} = 0$$

$$\dot{\theta} = \frac{-32.2 (\cos \theta + a_z)}{V}$$

The complete aircraft model equations and coordinate system are defined below:

Input - $\phi = f(t)$, radians

Initial Conditions - x_0', y_0', z_0' , ft

V , ft/sec

ψ_0, θ_0, ϕ_0 , radians

Equations of Motion - $\dot{\psi} = \frac{32.2 \tan \phi}{V}$

$$\dot{\theta} = 0$$

$$\psi = \psi_0 + \int \dot{\psi} dt$$

$$\theta = \theta_0$$

Equations of Motion -
(Continued)

$$v_x' = v \cos\theta_0 \cos\psi$$

$$v_y' = v \cos\theta_0 \sin\psi$$

$$v_z' = -v \sin\theta_0$$

$$x' = x_0' + \int v_x' dt$$

$$y' = y_0' + \int v_y' dt$$

$$z' = z_0' + \int v_z' dt$$

APPENDIX B

A MATHEMATICAL DESCRIPTION OF DAVISON'S METHOD

The linear model to be reduced is of the form

$$\underline{x} = A\underline{x} + b$$

where A is a real NxN matrix, and b is a real Nx1 vector.
The solution to this system as given by Davison is

$$\underline{x} = SDS^{-1}b$$

where S is an NxN matrix of normalized eigenvectors of A
(each eigenvector is a column of S) and D is an NxN diagonal
matrix with the i-th diagonal element equal to

$$\lambda_i^{-1} [-1 + \exp(\lambda_i t)]$$

where λ_i is the i-th eigenvalue of A and $t > 0$ denotes time (in
seconds for this application). This solution can be written
in the form

$$\underline{x} = \begin{bmatrix} x_1 \\ x_2 \\ \vdots \\ x_n \end{bmatrix} = \sum_{i=1}^n \left\{ \frac{-1 + \exp(\lambda_i t)}{\lambda_i} \begin{bmatrix} s_{1i} \\ \vdots \\ s_{ni} \end{bmatrix} [s_{i1}b_1 + \dots + s_{in}b_n] \right\}$$

where

$$S = (s_{ij}; i=1, \dots, n; j=1, \dots, n)$$

$$S^{-1} = (s^{ij}; i=1, \dots, n; j=1, \dots, n)$$

$$b = \begin{bmatrix} b_1 \\ b_2 \\ . \\ . \\ . \\ b_n \end{bmatrix}$$

and $\sum_{i=1}^n s_{ij}^2 = 1$ for $j = 1, 2, \dots, n$.

Let x_1 be the state to be examined, in this case lateral deviation, then

$$x_1(t) = \left\{ \sum_{i=1}^n \frac{-1 + \exp(\lambda_i t)}{\lambda_i} \sum_{j=1}^n s_{1i} s^{ij} b_j \right\} \quad (1)$$

To reduce this system, Davison assumes the λ_i 's are sorted in the order of increasing modulus, i.e.,

$$\lambda_1 \leq \lambda_2 \leq \dots \leq \lambda_n.$$

If the reduced system is to contain L states ($L < n$), then it is assumed the \underline{x} vector (also the A and b matrices) is organized such that states x_1, \dots, x_L are retained and x_{L+1}, \dots, x_n are deleted. Consequently, if L states are to be retained, then they will be the first L states of the \underline{x} vector.

Partition the A and S matrices as shown below:

$$A = \begin{pmatrix} A_0 & A_1 \\ \hline & \end{pmatrix} \begin{matrix} L \\ n-L \end{matrix}$$

L n-L

$$S = \begin{pmatrix} S_0 & \\ \hline S_1 & \end{pmatrix} \begin{matrix} L \\ n-L \end{matrix}$$

L n-L

The reduced system is of the form

$$\underline{x} = A^* \underline{x} + b^*$$

where

- (i) $A^* = A_0 + A_1 S_1^{-1} S_0^{-1}$
- (ii) $b^* = S_0 \begin{bmatrix} S^{-1} b \end{bmatrix}$
- (iii) $\begin{bmatrix} S^{-1} b \end{bmatrix}$ = first L rows of $S^{-1} b$.

Using this method, the eigenvalues of A^* are $\lambda_1, \lambda_2, \dots, \lambda_L$.

The new state equation for lateral separation (x_1) is of the same form as in (1), namely,

$$x_1(t) = \sum_{i=1}^L \frac{-1 + \exp(\lambda_i t)}{\lambda_i} \sum_{j=1}^L y_{1i} y^{ij} b_j^*$$

where

- (i) $Y = (Y_{ij}) = L \times L$ matrix of eigenvectors of A^*
(ii) $Y^{-1} = (Y^{ij})$

$$(iii) b^* = \begin{bmatrix} b_1^* \\ \cdot \\ \cdot \\ \cdot \\ b_L^* \end{bmatrix}$$

APPENDIX C

SOLUTIONS OF PARTIAL DIFFERENTIAL EQUATIONS BY THE USE OF FINITE DIFFERENCES

When using a finite-difference technique to solve a second order partial differential equation (plus associated boundary and initial conditions), a network of grid points is first established throughout the region of interest occupied by the independent variables. The general form of the partial differential equation is represented by $U = U(x_1, x_2, t)$ where the explicit form of U contains no derivatives beyond second-order. Let the two space coordinates, x_1 and x_2 , and time, t , be the independent variables. The respective grid spacings are Δx_1 , Δx_2 , and Δt . Subscripts i , j , and n may then be used to denote that space point having coordinates $(i\Delta x_1, j\Delta x_2, n\Delta t)$, also called the grid-point (i, j, n) . Let the exact solution to the partial differential equation be $u = u(x_1, x_2, t)$ and let its approximation, to be determined at each grid point by the method of finite differences, be $V_{i,j,n}$.

The partial derivatives of the original partial differential equation are then approximated by suitable finite-difference expressions involving Δx_1 , Δx_2 , Δt , and $V_{i,j,n}$. This procedure leads to a set of algebraic equations in the $V_{i,j,n}$, whose values may then be determined. By making the grid spacings sufficiently small, it is hoped that $V_{i,j,n}$ will become a sufficiently close approximation to $u_{i,j,n}$ at any grid point (i, j, n) .

Suppose for simplicity that $u = u(x_1, x_2, t)$. Assuming that u possesses a sufficient number of partial derivatives, the values of u at the two points (x_1, x_2, t) and $(x_1+h, x_2+k, t+s)$ are related by the Taylor expansion:

$$\begin{aligned} u(x_1+h, x_2+k, t+s) = & u(x_1, x_2, t) + \left(h \frac{\partial}{\partial x_1} + k \frac{\partial}{\partial x_2} + s \frac{\partial}{\partial t} \right) u(x_1, x_2, t) \\ & + \frac{1}{2!} \left(h \frac{\partial}{\partial x_1} + k \frac{\partial}{\partial x_2} + s \frac{\partial}{\partial t} \right)^2 u(x_1, x_2, t) + \dots \\ & + \frac{1}{(n-1)!} \left(h \frac{\partial}{\partial x_1} + k \frac{\partial}{\partial x_2} + s \frac{\partial}{\partial t} \right)^{n-1} u(x_1, x_2, t) + R_n \end{aligned}$$

where the remainder term is given by

$$R_n = \frac{1}{n!} \left(h \frac{\partial}{\partial x_1} + k \frac{\partial}{\partial x_2} + s \frac{\partial}{\partial t} \right)^n u(x_1 + \xi h, x_2 + \xi k, t + \xi s),$$

$$0 < \xi < 1.$$

That is,

$$R_n = F |h| + |k| + |s|)^n,$$

which means there exists a positive constant M such that

$$|R_n| \leq M |h| + |k| + |s|)^n \text{ as } h, k, \text{ and } s \text{ tend to zero.}$$

The space point $(i\Delta x_1, j\Delta x_2, n\Delta t)$ is surrounded by neighboring grid points. Expanding in Taylor's series form for $u_{i-1,j,n}$ about the central value $u_{i,j,n}$, the following is obtained:

$$u_{i-1,j,n} = u_{i,j,n} - \Delta x_1 u_{x_1} + \frac{(\Delta x_1)^2}{2!} u_{x_1 x_1} - \frac{(\Delta x_1)^3}{3!} u_{x_1 x_1 x_1} + \frac{(\Delta x_1)^4}{4!} u_{x_1 x_1 x_1 x_1}$$

$$u_{i+1,j,n} = u_{i,j,n} + \Delta x_1 u_{x_1} + \frac{(\Delta x_1)^2}{2!} u_{x_1 x_1} + \frac{(\Delta x_1)^3}{3!} u_{x_1 x_1 x_1} + \frac{(\Delta x_1)^4}{4!} u_{x_1 x_1 x_1 x_1}$$

Here, $u_{x_1} = \frac{\partial u}{\partial x_1}$, $u_{x_1 x_1} = \frac{\partial^2 u}{\partial x_1^2}$, etc., and all derivatives are eval-

uated at the grid point (i, j, n) . By taking these equations singly, and by subtracting one from the other, the following finite-difference formulas for the first and second-order derivatives at (i, j, n) are obtained:

$$\frac{\partial u}{\partial x_1} = \frac{u_{i+1,j,n} - u_{i,j,n}}{\Delta x_1} + F(\Delta x_1),$$

$$\frac{\partial u}{\partial x_1} = \frac{u_{i,j,n} - u_{i-1,j,n}}{\Delta x_1} + F(\Delta x_1),$$

$$\frac{\partial u}{\partial x_1} = \frac{u_{i+1,j,n} - u_{i-1,j,n}}{2\Delta x_1} + F(\Delta x_1),$$

$$\frac{\partial^2 u}{\partial x_1^2} = \frac{u_{i-1,j,n} - 2u_{i,j,n} + u_{i+1,j,n}}{(\Delta x_1)^2} + F[(\Delta x_1)^2].$$

The first three of these four formulas are known respectively as the forward, backward, and central difference forms. Similar

forms exist for $\frac{\partial u}{\partial x_2}$, $\frac{\partial^2 u}{\partial x_2^2}$, $\frac{\partial u}{\partial t}$, and $\frac{\partial^2 u}{\partial t^2}$. It may also be shown that

$$\frac{\partial^2 u}{\partial x_1 \partial x_2} = \frac{u_{i+1,j+1} - u_{i-1,j+1} - u_{i+1,j-1} + u_{i-1,j-1}}{4\Delta x_1 \Delta x_2} + F[(\Delta x_1 + \Delta x_2)^2].$$

APPENDIX D

VARIANCE PROPAGATION OF A LINEAR SYSTEM

This appendix develops a vector equation which describes the behavior of the output variance of a linear system having a gaussian input.

For gaussian distributions the mean and variance of the response of a linear system give a complete statistical description of the process. It can be shown¹ that the results of any linear operation on a gaussian distribution is another gaussian distribution. Thus, if the input to the system is gaussian, and if the transformation of mean and variance can be determined, then the output distribution of the system is completely defined.

Considering a continuous dynamic transformation, the first-order time-varying vector differential equation is

$$\dot{\underline{x}}(t) = A(t)\underline{x}(t) + B(t)\underline{u}(t) \quad (1)$$

A priori knowledge of the mean and variance of $\underline{x}(t_0)$ and $\underline{u}(t)$ is assumed and these quantities are denoted as follows:

$$\begin{aligned} \underline{\mu}_x(t_0) &= E[\underline{x}(t_0)] & V_x(t_0) &= \text{Var}[\underline{x}(t_0)] \\ \underline{\mu}_u(t) &= E[\underline{u}(t)] & V_u(t_1, t_2) &= \text{Cov}[\underline{u}(t_1), \underline{u}(t_2)] \end{aligned}$$

The equations that determine the mean and variance of $\underline{x}(t)$, $\underline{\mu}_x(t)$ and $V_x(t_1, t_2)$, are derived as follows. Applying the definition of expectation to Equation (1), the mean is given as $\dot{\underline{\mu}}_x(t) = A(t)\underline{\mu}_x(t) + B(t)\underline{\mu}_u(t)$ (2)

Differentiation of the definition of variance yields

$$\begin{aligned} \dot{V}_x(t) &= \frac{d}{dt} \left(E[\underline{x}(t)\underline{x}^T(t)] \right) \\ &= E[\dot{\underline{x}}(t)\underline{x}^T(t) + \underline{x}(t)\dot{\underline{x}}^T(t)] \end{aligned}$$

¹ Sage, A.P. and Melsa, J.L., Estimation Theory with Applications to Communications and Control, McGraw-Hill, New York, 1971.

where $\underline{\mu}_x(t) = 0$. Substituting Equation (1) in the above expression gives

$$\begin{aligned}\dot{\hat{V}}_x(t) &= E[A(t)\underline{x}(t)\underline{x}^T(t) + B(t)\underline{u}(t)\underline{x}^T(t)] \\ &\quad + E[\underline{x}(t)\underline{x}^T(t)A^T(t) + \underline{x}(t)\underline{u}^T(t)B^T(t)] \\ &= A(t)V_x(t) + V_x(t)A^T(t) + B(t)V_{ux}(t) + V_{xu}(t)B^T(t)\end{aligned}\quad (3)$$

Assuming $\underline{u}(t)$ to be white noise, but not limiting it to being a stationary random process, it can be shown that for $t_1 = t_2 = t$,

$$V_{xu}(t) \doteq V_{xu}(t, t) = \frac{B(t) \psi_u(t)}{2}$$

and

$$V_{ux}(t) \doteq V_{xu}^T(t) = \frac{\psi_u^T(t) B^T(t)}{2}$$

$$\psi_u(t) = \psi_u^T(t)$$

Therefore Equation (3) becomes

$$\dot{\hat{V}}_x(t) = A(t)V_x(t) + V_x(t)A^T(t) + B(t)\psi_u(t)B^T(t)\quad (4)$$

Equations (2) and (4) are the mean and variance, respectively, of the linear system and were evaluated numerically using trapezoidal and Runge-Kutta techniques of integration.

APPENDIX E

MEASURED DISTRIBUTION DATA

Lateral deviations of aircraft have been measured at various airports by several organizations including the FAA and Resalab. Though the data was collected with different techniques, it has been processed to remove all known errors and is presented in a form such that it can be combined with other collected data.

The data used by Resalab in the lateral separation project is presented in this appendix. Distribution data is presented for the systems shown in Table E-1.

Table E-1 Required Measured Distributions

System*	Table Number	Comments
Lateral Distribution FC-ILS-INOM-CTOL	E-2	Nominal Measured Distribution Data
FC-ILS-I-CTOL	E-3,E-4	Histogram Data,Mean and Standard Deviation Table
FC-ILS-II-CTOL	E-5,E-6	Histogram Data,Mean and Standard Deviation Table
BC-ILS-I-CTOL	E-7,E-8	Histogram Data,Mean and Standard Deviation Table
VOR-CTOL	E-9	Mean and Standard Deviation Table
FC-ILS-I-STOL	E-10	Assumed Gaussian
Vertical Distribution FC-ILS-I-CTOL	E-11	Mean and Standard Deviation Table
FC-ILS-I-STOL	E-12	Assumed Gaussian

Table E-1 Required Measured Distributions (Continued)

System*	Table Number	Comments
Longitudinal Distribution FC-ILS-I-CTOL	E-13	Assumed Gaussian

*Representative example - FC-ILS-I-CTOL where

FC ~ front course
 ILS ~ Instrument Landing System
 I ~ Category I aircraft on Category I beams
 CTOL ~ CTOL aircraft on CTOL runways

The histogram data is presented at the same specific ranges as the mean and variance data. The range to touchdown is given in meters across the top of the page. The lateral deviations are given in multiples of the partition intervals on the vertical axis. The partition intervals are five or ten meters as noted on the tables. The numbers in the body of the table represent the number of aircraft observed in the indicated partition at the indicated range.

Table E-2

Nominal Measured Distribution Data
(FC-ILS-INOM-CTOL-Lateral) *

Range, meters	Number of Samples	Mean, meters	Standard Deviation, meters
600	273	0.2525	8.7127
1200	282	1.9240	14.0975
1800	282	3.8906	17.3632
2400	285	2.5271	23.1017
3000	288	3.5440	23.7841
3600	288	3.7867	23.3097
4200	290	5.4440	27.2086
4800	289	6.2429	27.8675
5400	286	6.3073	31.8867
6000	287	6.1269	31.3588
6600	281	8.22	37.15
7500	274	8.93	41.22
8100	264	7.48	43.69
8700	257	9.34	47.83
9300	248	9.00	47.51
9900	242	9.02	48.76
10500	231	8.02	50.56
11100	211	8.64	55.59
11700	189	8.79	52.66
12300	172	10.79	51.10
12900	152	10.39	57.35
13500	136	12.59	51.77
14100	127	12.76	58.14
14700	109	13.01	56.92
15300	84	14.49	55.25
15900	63	16.68	60.12

*-, Data Collected for "Revalidation of the Data Base Used in Establishing the Criteria for Simultaneous ILS Approaches to Parallel Runways", DOT-FAA-SRDS - Subprogram No. 150-502, May 1970.

Table E-3 Distribution of Lateral Displacements for
FC-ILS-I-CTOL - Lateral**

Partition Interval	Range, hundreds of meters										
	6*	12*	18*	24	30	36	42	48	54	60	66
-20 to -79	0.	1.	4.	0.	2.	1.	2.	2.	2.	4.	5.
-19	1.	0.	1.	1.	0.	1.	1.	0.	0.	0.	2.
-18	0.	0.	0.	0.	0.	0.	0.	0.	1.	1.	3.
-17	0.	1.	1.	0.	1.	0.	1.	0.	0.	1.	2.
-16	0.	0.	1.	2.	0.	0.	0.	0.	1.	4.	1.
-15	0.	0.	1.	1.	1.	1.	0.	1.	1.	1.	2.
-14	0.	2.	1.	0.	0.	0.	0.	0.	1.	1.	0.
-13	0.	3.	1.	1.	0.	1.	1.	2.	3.	2.	2.
-12	0.	3.	6.	2.	3.	2.	1.	1.	2.	3.	2.
-11	0.	1.	3.	1.	1.	3.	2.	6.	2.	3.	7.
-10	0.	2.	4.	0.	0.	1.	1.	0.	2.	3.	3.
-9	1.	3.	6.	3.	7.	3.	3.	6.	4.	13.	5.
-8	2.	4.	6.	4.	2.	1.	4.	9.	11.	8.	7.
-7	2.	2.	14.	3.	8.	6.	5.	7.	8.	6.	20.
-6	3.	17.	24.	9.	3.	7.	17.	14.	15.	15.	15.
-5	2.	16.	39.	13.	18.	21.	14.	24.	18.	23.	32.
-4	15.	47.	37.	35.	23.	36.	28.	20.	31.	32.	22.
-3	25.	56.	57.	49.	54.	45.	42.	32.	27.	41.	32.
-2	93.	90.	86.	75.	78.	74.	51.	42.	48.	40.	47.
-1	112.	76.	54.	110.	98.	65.	47.	52.	57.	45.	53.
0	128.	98.	73.	115.	93.	86.	76.	73.	70.	75.	54.
1	64.	93.	61.	89.	94.	74.	71.	70.	67.	48.	50.
2	25.	40.	41.	50.	61.	68.	70.	84.	62.	47.	45.
3	13.	21.	32.	39.	31.	49.	50.	49.	50.	43.	40.
4	9.	20.	20.	15.	23.	36.	44.	44.	24.	36.	38.
5	2.	10.	12.	6.	18.	19.	24.	26.	33.	29.	33.
6	0.	8.	11.	8.	11.	12.	22.	18.	22.	29.	21.
7	0.	2.	6.	1.	4.	7.	9.	11.	16.	24.	22.
8	0.	4.	6.	2.	2.	4.	11.	11.	17.	13.	7.
9	3.	2.	7.	2.	0.	4.	7.	9.	6.	5.	18.
10	1.	1.	3.	2.	2.	6.	6.	4.	6.	10.	10.
11	0.	0.	1.	1.	1.	2.	5.	1.	4.	2.	6.
12	0.	1.	4.	1.	1.	1.	1.	2.	3.	4.	3.
13	1.	2.	3.	1.	2.	1.	2.	3.	4.	0.	2.
14	1.	0.	3.	1.	1.	0.	1.	5.	2.	2.	2.
15	0.	0.	1.	0.	0.	0.	1.	1.	1.	4.	3.
16	0.	0.	1.	0.	1.	1.	1.	0.	1.	1.	3.
17	0.	0.	0.	0.	0.	0.	1.	0.	1.	2.	1.
18	0.	0.	0.	0.	0.	0.	0.	0.	0.	1.	1.
19	0.	0.	0.	0.	0.	0.	0.	0.	2.	2.	0.
20 to 56	0.	2.	2.	0.	0.	0.	0.	2.	5.	8.	8.

*At these ranges, the partitions are at five meter intervals; elsewhere, the partitions are at ten meter intervals.

**Charleston data is included in the range interval from 1200 meters to 6600 meters, inclusive, but not elsewhere, since the data collection ranges were not coincident elsewhere.

Table E-3 Distribution of Lateral Displacements for
FC-ILS-I-CTOL - Lateral (Continued)

Partition Interval	Range, hundreds of meters										
	75	81	87	93	99	105	111	117	123	129	135
-20 to -79	5.	7.	8.	14.	16.	10.	9.	5.	5.	7.	9.
-19	2.	2.	2.	0.	1.	4.	0.	2.	0.	0.	0.
-18	1.	1.	1.	2.	2.	3.	2.	2.	2.	3.	3.
-17	0.	2.	1.	2.	3.	0.	2.	1.	2.	2.	1.
-16	1.	0.	2.	3.	1.	3.	2.	3.	1.	3.	3.
-15	1.	4.	6.	1.	2.	4.	4.	2.	2.	2.	0.
-14	1.	2.	8.	6.	2.	4.	5.	3.	4.	1.	1.
-13	2.	2.	10.	3.	5.	2.	0.	7.	2.	3.	1.
-12	5.	10.	8.	6.	2.	7.	4.	1.	4.	2.	3.
-11	4.	7.	3.	5.	1.	5.	6.	4.	4.	2.	1.
-10	7.	4.	6.	6.	2.	0.	1.	5.	4.	4.	3.
-9	6.	6.	10.	4.	5.	9.	4.	9.	4.	7.	7.
-8	11.	14.	8.	6.	5.	10.	5.	8.	11.	5.	5.
-7	10.	9.	8.	8.	8.	9.	7.	11.	4.	5.	6.
-6	11.	13.	12.	14.	7.	14.	15.	6.	10.	7.	8.
-5	26.	32.	15.	22.	16.	13.	12.	11.	8.	10.	2.
-4	24.	16.	26.	20.	24.	13.	12.	8.	12.	11.	8.
-3	22.	28.	22.	21.	26.	20.	11.	10.	11.	10.	12.
-2	23.	26.	24.	18.	24.	18.	23.	16.	14.	18.	12.
-1	27.	29.	26.	26.	17.	19.	11.	12.	13.	9.	10.
0	40.	32.	31.	32.	22.	25.	24.	17.	16.	10.	11.
1	30.	40.	46.	30.	18.	25.	24.	17.	14.	19.	15.
2	45.	38.	21.	33.	21.	23.	27.	16.	12.	10.	12.
3	34.	31.	26.	34.	28.	27.	20.	22.	14.	12.	10.
4	39.	32.	27.	23.	30.	21.	23.	18.	24.	12.	16.
5	25.	26.	25.	23.	22.	18.	22.	21.	20.	15.	15.
6	27.	20.	26.	17.	19.	25.	17.	24.	16.	16.	15.
7	13.	17.	17.	18.	19.	11.	18.	15.	15.	15.	11.
8	14.	6.	11.	10.	12.	18.	15.	9.	17.	16.	13.
9	8.	12.	7.	11.	12.	10.	12.	14.	9.	8.	8.
10	7.	3.	8.	6.	10.	11.	9.	12.	6.	7.	5.
11	7.	9.	8.	5.	6.	7.	3.	5.	9.	6.	7.
12	3.	4.	2.	4.	3.	7.	7.	2.	5.	9.	7.
13	6.	1.	3.	6.	4.	6.	2.	3.	3.	7.	9.
14	1.	2.	1.	6.	4.	1.	4.	3.	2.	7.	7.
15	0.	2.	2.	1.	1.	4.	4.	7.	2.	2.	4.
16	1.	0.	2.	2.	3.	1.	4.	3.	1.	5.	3.
17	2.	2.	2.	2.	0.	4.	0.	1.	2.	2.	3.
18	2.	0.	3.	0.	2.	2.	4.	1.	0.	3.	1.
19	0.	3.	1.	2.	1.	1.	2.	1.	2.	1.	3.
20 to 56	10.	10.	11.	9.	9.	9.	9.	8.	11.	9.	10.

Table E-3 Distribution of Lateral Displacements for
FC-ILS-I-CTOL - Lateral (Continued)

Partition Interval	Range, hundreds of meters			
	141	147	153	159
-20 to -79	8.	9.	6.	5.
-19	1.	0.	1.	1
-18	1.	0.	0.	0
-17	1.	1.	0.	0
-16	3.	0.	1.	0
-15	2.	2.	1.	1
-14	1.	1.	0.	0
-13	1.	1.	1.	0
-12	0.	2.	0.	1
-11	2.	1.	0.	0
-10	1.	1.	4.	4
-9	3.	3.	2.	3
-8	2.	2.	3.	1
-7	5.	3.	3.	4
-6	5.	2.	5.	1
-5	5.	7.	5.	3
-4	3.	8.	6.	2
-3	12.	6.	2.	3
-2	14.	8.	4.	3
-1	9.	4.	4.	5
0	11.	5.	13.	1
1	10.	5.	12.	5
2	5.	14.	10.	8
3	14.	10.	13.	9
4	11.	11.	14.	7
5	17.	15.	6.	13
6	11.	11.	8.	8
7	10.	16.	10.	4
8	10.	10.	10.	6
9	11.	5.	10.	4
10	9.	11.	9.	6
11	12.	8.	2.	5
12	8.	5.	1.	1
13	3.	4.	2.	0
14	1.	1.	3.	3
15	2.	3.	2.	2
16	5.	0.	0.	1
17	0.	5.	2.	0
18	0.	1.	0.	1
19	4.	1.	1.	0
20 to 56	7.	7.	4.	4.

Table E-4

Mean and Standard Deviation Versus Range for
FC-ILS-I-CTOL - Lateral*

Range, meters	Number of Samples	Mean, meters	Standard Deviation, meters
600	513	-.0161	11.8943
1200	618	-3.0435	22.0739
1800	633	-5.2973	26.4976
2400	642	-6.7594	31.9236
3000	644	-2.8728	35.8871
3600	638	1.6535	37.7171
4200	622	8.9878	43.6031
4800	631	8.3098	46.9545
5400	630	8.4069	53.4125
6000	631	6.9212	61.9026
6600	629	2.9729	68.5199
7500	513	14.46	75.30
8100	500	11.83	83.99
8700	490	7.67	90.20
9300	468	6.37	93.00
9900	447	4.83	97.60
10500	423	12.93	92.45
11100	387	16.36	91.98
11700	342	17.42	94.11
12300	324	21.30	100.43
12900	307	26.29	96.41
13500	283	28.54	102.12
14100	245	28.99	103.63
14700	224	33.03	103.14
15300	181	27.42	97.75
15900	134	25.53	113.84

*Charleston data is included in the range interval from 1200 meters to 6600 meters, inclusive, but not elsewhere, since the data collection ranges were not coincident elsewhere.

Table E-5 Distribution of Lateral Displacements for FC-ILS-II-
CTOL - Lateral**

Partition Interval	Range, hundreds of meters										
	6*	12*	18*	24	30	36	42	48	54	60	66
-21 to -27	0	0.	0.	1.	0.	0.	0.	0.	0.	0.	0.
-20	0	0.	0.	0.	0.	0.	0.	0.	0.	0.	0.
-19	0	0.	0.	0.	1.	0.	0.	0.	0.	0.	0.
-18	0	0.	0.	0.	0.	0.	0.	0.	0.	0.	0.
-17	0	0.	0.	0.	0.	0.	0.	0.	0.	0.	0.
-16	0	0.	0.	0.	0.	0.	0.	0.	0.	0.	0.
-15	0	0.	0.	0.	0.	0.	0.	0.	1.	0.	0.
-14	0	2.	0.	0.	0.	0.	0.	0.	0.	0.	0.
-13	0	0.	1.	0.	0.	0.	0.	1.	0.	0.	0.
-12	0	0.	0.	0.	0.	0.	0.	0.	0.	0.	0.
-11	0	0.	0.	0.	0.	0.	0.	1.	1.	0.	1.
-10	0	0.	0.	0.	0.	0.	0.	0.	0.	0.	3.
-9	0	0.	0.	0.	0.	0.	1.	0.	0.	0.	0.
-8	2	0.	1.	0.	0.	2.	1.	0.	0.	2.	1.
-7	0	1.	3.	1.	2.	1.	0.	1.	1.	2.	3.
-6	1	1.	1.	1.	1.	0.	1.	2.	1.	6.	6.
-5	1	6.	4.	3.	2.	1.	2.	1.	4.	4.	3.
-4	8	8.	13.	6.	4.	5.	4.	8.	5.	10.	6.
-3	12	15.	15.	12.	15.	17.	19.	17.	24.	21.	22.
-2	31	42.	36.	27.	32.	35.	30.	37.	34.	23.	23.
-1	61	37.	39.	60.	55.	56.	56.	37.	42.	41.	36.
0	41	39.	28.	50.	53.	51.	48.	54.	47.	50.	39.
1	36	25.	35.	37.	37.	33.	40.	36.	32.	38.	35.
2	21	22.	25.	18.	17.	15.	10.	21.	13.	16.	14.
3	6	17.	12.	7.	6.	5.	9.	8.	13.	12.	16.
4	1	5.	6.	2.	3.	4.	5.	1.	4.	3.	4.
5	0	2.	2.	0.	0.	2.	3.	4.	1.	0.	5.
6	0	3.	0.	0.	0.	2.	2.	2.	3.	1.	2.
7	0	0.	2.	0.	0.	0.	0.	0.	2.	2.	1.
8	0	0.	0.	0.	0.	0.	0.	0.	0.	1.	0.
9	0	0.	0.	0.	0.	0.	0.	1.	0.	0.	3.
10	0	0.	0.	0.	1.	0.	0.	0.	0.	1.	0.
11	0	1.	1.	1.	0.	0.	0.	0.	0.	0.	0.
12	0	0.	0.	0.	0.	0.	0.	0.	0.	0.	0.
13	0	0.	0.	0.	0.	0.	0.	0.	0.	0.	1.
14	0	0.	0.	0.	0.	0.	0.	0.	0.	0.	0.
15	0	0.	0.	0.	0.	0.	0.	0.	0.	0.	0.
17	0	0.	0.	0.	0.	0.	1.	0.	0.	0.	0.
18	0	0.	0.	0.	0.	0.	0.	0.	0.	0.	0.
20	0	0.	1.	0.	0.	0.	0.	0.	0.	0.	0.
21 to 23	0	0.	0.	0.	0.	0.	0.	0.	0.	0.	0.

*At these ranges the partitions are at five meter intervals; elsewhere, the partitions are at ten meter intervals.

**-, Data Collected for "Revalidation of the Data Base Used in Establishing the Criteria for Simultaneous ILS Approaches to Parallel Runways", DOT-FAA-SRDS - Subprogram No. 150-502, May '70.

Table E-5 Distribution of Lateral Displacements for FC-ILS-II-CTOL - Lateral (Continued)

Partition	Range, hundreds of meters										
Interval	75	81	87	93	99	105	111	117	123	129	135
-21 to -27	0.	0.	0.	0.	0.	0.	1.	0.	0.	1.	0.
-20	0.	0.	0.	0.	0.	0.	0.	0.	1.	0.	1.
-19	0.	0.	0.	1.	0.	0.	0.	1.	0.	0.	0.
-18	1.	0.	0.	0.	1.	0.	0.	0.	0.	0.	0.
-17	0.	0.	0.	0.	0.	0.	0.	0.	0.	0.	0.
-16	0.	1.	2.	0.	0.	0.	0.	1.	3.	0.	0.
-15	0.	0.	0.	0.	0.	1.	1.	0.	0.	0.	0.
-14	0.	0.	0.	1.	0.	0.	0.	0.	0.	0.	0.
-13	0.	0.	0.	0.	0.	1.	1.	0.	1.	0.	0.
-12	0.	1.	0.	0.	0.	0.	2.	0.	0.	0.	0.
-11	1.	2.	1.	1.	2.	2.	1.	2.	0.	1.	2.
-10	0.	1.	0.	1.	1.	1.	4.	0.	1.	2.	1.
-9	1.	1.	1.	2.	2.	4.	1.	0.	2.	1.	0.
-8	1.	0.	6.	1.	3.	2.	2.	3.	0.	1.	1.
-7	2.	3.	2.	2.	4.	6.	1.	2.	3.	2.	0.
-6	5.	5.	10.	9.	7.	4.	2.	9.	1.	5.	1.
-5	9.	5.	5.	9.	9.	4.	11.	7.	9.	3.	4.
-4	11.	13.	15.	9.	8.	14.	9.	10.	8.	7.	5.
-3	23.	19.	9.	20.	12.	10.	5.	4.	11.	7.	8.
-2	19.	26.	25.	15.	15.	10.	13.	10.	5.	9.	10.
-1	30.	27.	22.	20.	22.	24.	17.	15.	16.	14.	14.
0	29.	33.	33.	29.	26.	18.	16.	14.	10.	15.	14.
1	34.	24.	20.	19.	25.	22.	23.	16.	20.	16.	12.
2	19.	17.	14.	17.	15.	14.	12.	17.	14.	5.	6.
3	9.	10.	9.	11.	14.	17.	15.	11.	8.	12.	7.
4	9.	9.	11.	8.	6.	10.	9.	11.	9.	4.	3.
5	5.	0.	5.	8.	4.	6.	4.	3.	5.	0.	2.
6	6.	7.	5.	4.	6.	4.	3.	1.	0.	1.	0.
7	2.	1.	3.	5.	2.	0.	4.	3.	1.	1.	1.
8	1.	1.	1.	2.	2.	4.	1.	2.	0.	1.	0.
9	0.	1.	1.	1.	2.	0.	1.	1.	1.	0.	0.
10	0.	0.	0.	0.	0.	0.	0.	0.	0.	0.	1.
11	0.	0.	1.	0.	0.	1.	0.	0.	1.	0.	1.
12	0.	0.	0.	0.	1.	0.	1.	0.	1.	0.	0.
13	0.	0.	0.	0.	0.	0.	0.	0.	0.	0.	0.
14	0.	1.	0.	0.	0.	0.	0.	0.	0.	0.	0.
15	1.	1.	0.	0.	0.	0.	0.	0.	0.	1.	1.
17	0.	0.	1.	0.	0.	0.	0.	0.	0.	0.	0.
18	0.	0.	0.	0.	0.	0.	1.	0.	0.	0.	0.
20	0.	0.	0.	0.	0.	0.	0.	0.	0.	0.	0.
21 to 23	0.	0.	0.	0.	0.	0.	0.	0.	0.	1.	0.

Table E-5 Distribution of Lateral Displacements for FC-ILS-II-CTOL - Lateral (Continued)

Partition Interval	Range, hundreds of meters			
	141	147	153	159
-21 to -27	0.	0.	0.	0
-20	0.	0.	0.	0
-19	0.	0.	0.	0
-18	1.	0.	0.	0
-17	1.	0.	1.	0
-16	0.	0.	0.	0
-15	0.	0.	0.	0
-14	0.	1.	0.	0
-13	0.	0.	0.	1
-12	0.	1.	0.	0
-11	0.	1.	1.	1
-10	0.	0.	0.	0
-9	0.	1.	1.	1
-8	0.	0.	0.	0
-7	2.	1.	0.	0
-6	4.	2.	3.	0
-5	3.	2.	3.	2
-4	5.	1.	4.	2
-3	8.	9.	5.	3
-2	10.	8.	4.	7
-1	7.	6.	6.	1
0	9.	10.	3.	5
1	15.	3.	11.	6
2	10.	5.	2.	2
3	6.	9.	2.	4
4	1.	7.	4.	0
5	0.	2.	3.	2
6	1.	0.	1.	1
7	2.	0.	1.	0
8	0.	0.	0.	1
9	0.	1.	0.	0
10	0.	1.	0.	0
11	0.	0.	1.	0
12	1.	0.	1.	0
13	0.	0.	0.	0
14	0.	0.	0.	0
15	0.	0.	0.	1
17	0.	0.	0.	0
18	0.	0.	0.	0
20	0.	0.	0.	0
21 to 23	1.	0.	0.	0

Table E-6

Mean and Standard Deviation Versus Range for
FC-ILS-II-CTOL - Lateral*

Range, meters	Number of Samples	Mean, meters	Standard Deviation, meters
600	221	-0.0491	8.8117
1200	226	0.5283	13.4814
1800	225	0.9456	15.0610
2400	226	-0.0800	22.9214
3000	229	0.0066	22.3851
3600	229	0.0801	19.5490
4200	232	1.6891	23.5641
4800	231	1.4297	22.6955
5400	228	-0.1319	25.0692
6000	231	0.0309	25.5990
6600	224	1.20	31.65
7500	218	1.47	34.53
8100	209	-0.60	36.99
8700	202	-0.24	40.78
9300	195	-0.09	39.98
9900	189	0.16	40.98
10500	179	-0.34	41.90
11100	161	-0.10	50.39
11700	143	-0.48	43.47
12300	128	0.36	42.77
12900	110	-2.06	51.03
13500	95	-0.82	44.00
14100	87	-0.16	48.24
14700	71	0.35	42.80
15300	57	-0.04	48.46
15900	41	2.82	48.74

*-, Data Collected for "Revalidation of the Data Base Used in Establishing the Criteria for Simultaneous ILS Approaches to Parallel Runways", DOT-FAA-SRDS - Subprogram No. 150-502, May 1970.

Table E-7

Distribution of Lateral Displacements for
BC-ILS-I-CTOL - Lateral

Partition Interval	Range, hundreds of meters												
	12*	18*	24	30	36	42	48	54	60	66	72	78	84
-20 to -75	1.	1.	0.	0.	1.	2.	2.	3.	4.	5.	4.	4.	4.
-19	0.	0.	0.	0.	0.	0.	0.	0.	0.	1.	0.	0.	1.
-18	1.	1.	0.	0.	1.	0.	0.	0.	0.	0.	1.	1.	0.
-17	0.	0.	0.	1.	1.	0.	0.	0.	0.	0.	2.	0.	1.
-16	0.	0.	0.	0.	0.	0.	0.	1.	1.	0.	0.	1.	1.
-15	0.	0.	0.	0.	0.	0.	1.	0.	0.	0.	1.	2.	1.
-14	0.	0.	0.	0.	0.	0.	0.	0.	0.	0.	0.	0.	0.
-13	1.	0.	0.	1.	1.	1.	0.	0.	1.	0.	2.	1.	4.
-12	0.	1.	0.	1.	1.	1.	1.	1.	0.	1.	3.	2.	2.
-11	0.	1.	1.	1.	0.	0.	1.	0.	0.	2.	1.	3.	2.
-10	0.	0.	3.	1.	0.	0.	1.	0.	0.	3.	1.	1.	6.
-9	1.	1.	0.	0.	0.	2.	0.	2.	1.	3.	3.	5.	2.
-8	0.	0.	1.	3.	1.	0.	2.	2.	0.	1.	2.	2.	4.
-7	1.	0.	1.	1.	1.	0.	1.	1.	5.	1.	2.	2.	1.
-6	0.	1.	0.	1.	0.	2.	3.	1.	2.	2.	2.	1.	3.
-5	2.	0.	1.	2.	2.	2.	1.	1.	3.	3.	2.	0.	0.
-4	1.	4.	5.	2.	1.	3.	2.	1.	3.	3.	2.	1.	0.
-3	3.	2.	0.	5.	8.	7.	5.	3.	5.	2.	0.	4.	0.
-2	9.	6.	0.	4.	9.	5.	1.	7.	3.	7.	1.	3.	1.
-1	14.	9.	9.	5.	10.	4.	6.	6.	4.	1.	3.	3.	0.
0	9.	6.	13.	11.	7.	8.	9.	7.	6.	1.	6.	4.	1.
1	13.	7.	7.	11.	9.	9.	6.	7.	7.	4.	4.	3.	3.
2	3.	9.	15.	9.	8.	7.	6.	4.	5.	3.	4.	1.	2.
3	2.	10.	6.	6.	5.	6.	3.	3.	3.	4.	5.	2.	1.
4	1.	2.	3.	1.	1.	1.	5.	5.	3.	4.	1.	2.	1.
5	0.	0.	4.	4.	1.	2.	3.	1.	0.	1.	2.	1.	2.
6	1.	0.	0.	0.	1.	2.	3.	2.	2.	9.	0.	0.	4.
7	1.	1.	2.	1.	0.	3.	2.	2.	0.	1.	0.	1.	0.
8	1.	2.	0.	1.	0.	2.	2.	3.	3.	0.	0.	1.	1.
9	0.	1.	1.	0.	2.	0.	1.	1.	1.	0.	3.	1.	1.
10	1.	0.	0.	1.	1.	1.	0.	2.	2.	1.	2.	1.	2.
11	0.	1.	0.	0.	1.	0.	0.	2.	1.	0.	2.	1.	2.
12	0.	3.	0.	0.	0.	0.	0.	3.	3.	0.	1.	1.	1.
13	0.	0.	1.	0.	0.	2.	0.	0.	0.	1.	1.	1.	1.
14	1.	0.	0.	0.	0.	0.	1.	0.	1.	1.	1.	1.	0.
15	0.	0.	0.	0.	0.	0.	2.	0.	0.	1.	1.	0.	0.
16	0.	0.	0.	0.	0.	0.	0.	0.	0.	0.	0.	0.	1.
17	0.	0.	1.	0.	0.	0.	0.	0.	0.	0.	0.	1.	0.
18	0.	0.	0.	0.	0.	0.	0.	0.	0.	0.	0.	0.	1.
19	0.	1.	0.	0.	0.	1.	0.	0.	0.	0.	0.	0.	0.
20 to 50	0.	0.	0.	1.	1.	0.	0.	0.	0.	0.	0.	2.	1.

*At these ranges, the partitions are at five meter intervals; elsewhere, the partitions are at ten meter intervals.

Table E-7 Distribution of Lateral Displacements for BC-ILS-I-CTOL - Lateral (Continued)

Partition Interval	Range, hundreds of meters												
	90	96	102	108	114	120	126	132	138	144	150	156	162
-20 to -75	6.	11.	8.	9.	6.	5.	5.	5.	4.	3.	1.	.	0.
-19	0.	0.	3.	0.	1.	0.	0.	0.	0.	0.	0.	0.	0.
-18	3.	0.	1.	0.	0.	0.	0.	0.	0.	0.	0.	0.	0.
-17	2.	2.	0.	0.	0.	0.	1.	0.	1.	0.	0.	0.	0.
-16	1.	1.	1.	1.	0.	0.	0.	0.	0.	0.	0.	0.	0.
-15	2.	1.	0.	0.	1.	0.	0.	0.	0.	0.	1.	0.	0.
-14	2.	1.	3.	1.	0.	1.	0.	0.	0.	0.	0.	1.	0.
-13	0.	1.	0.	3.	0.	1.	1.	1.	0.	0.	0.	0.	0.
-12	1.	2.	0.	1.	0.	0.	0.	0.	0.	0.	0.	0.	0.
-11	4.	0.	0.	0.	2.	1.	1.	0.	0.	0.	0.	0.	0.
-10	1.	0.	0.	0.	0.	1.	0.	0.	0.	0.	0.	0.	0.
-9	0.	1.	0.	2.	1.	1.	0.	0.	0.	0.	0.	0.	0.
-8	1.	1.	1.	0.	0.	1.	1.	0.	0.	0.	0.	0.	0.
-7	1.	3.	2.	0.	1.	1.	1.	0.	0.	0.	0.	0.	0.
-6	2.	1.	0.	0.	1.	0.	0.	0.	0.	0.	0.	0.	0.
-5	0.	1.	2.	2.	0.	0.	0.	0.	0.	0.	0.	1.	0.
-4	1.	2.	0.	0.	0.	0.	2.	0.	0.	0.	0.	0.	0.
-3	0.	0.	1.	2.	2.	0.	0.	0.	0.	0.	0.	0.	0.
-2	0.	2.	2.	0.	0.	0.	0.	0.	0.	0.	1.	1.	0.
-1	1.	2.	0.	0.	1.	0.	1.	0.	0.	0.	0.	0.	1.
0	2.	1.	3.	2.	0.	0.	0.	0.	1.	0.	0.	0.	0.
1	3.	1.	3.	0.	1.	1.	1.	0.	0.	1.	2.	0.	0.
2	1.	1.	0.	0.	0.	1.	0.	1.	0.	0.	0.	0.	0.
3	0.	1.	0.	2.	1.	0.	0.	0.	0.	1.	0.	0.	0.
4	1.	1.	1.	1.	1.	0.	0.	0.	0.	1.	0.	0.	0.
5	5.	3.	1.	1.	2.	0.	0.	2.	0.	0.	0.	0.	0.
6	1.	0.	2.	1.	0.	1.	0.	0.	1.	0.	0.	0.	0.
7	1.	0.	0.	1.	0.	1.	0.	1.	1.	1.	0.	0.	0.
8	1.	1.	1.	1.	1.	1.	2.	1.	0.	0.	0.	0.	0.
9	0.	1.	0.	1.	2.	1.	0.	0.	1.	1.	0.	0.	0.
10	2.	0.	2.	1.	0.	1.	2.	1.	0.	1.	0.	0.	0.
11	2.	1.	1.	0.	2.	0.	0.	0.	1.	0.	0.	0.	0.
12	1.	1.	0.	1.	0.	1.	0.	0.	1.	0.	0.	0.	0.
13	0.	0.	2.	1.	1.	1.	1.	1.	0.	0.	0.	0.	0.
14	1.	1.	0.	1.	1.	2.	1.	0.	0.	0.	0.	0.	0.
15	1.	1.	0.	0.	0.	0.	0.	0.	0.	0.	0.	0.	0.
16	0.	0.	1.	0.	0.	1.	0.	0.	0.	0.	0.	0.	0.
17	0.	0.	0.	0.	0.	0.	0.	0.	0.	0.	0.	0.	0.
18	1.	2.	0.	1.	0.	0.	1.	0.	0.	0.	0.	0.	0.
19	0.	0.	1.	0.	0.	0.	0.	0.	0.	0.	0.	0.	0.
20 to 50	2.	4.	3.	4.	4.	3.	3.	2.	0.	0.	0.	0.	0.

Table E-8

Mean and Standard Deviation Versus Range For
BC-ILS-I-CTOL - Lateral

Range, meters	Number of Samples	Mean, meters	Standard Deviation, meters
1200	67	-6.096	24.795
1800	72	-0.305	31.733
2400	74	1.829	45.583
3000	90	-6.706	53.419
3600	99	-7.925	55.513
4200	104	-3.048	54.319
4800	109	-2.438	63.889
5400	108	-7.620	74.582
6000	105	-16.459	90.459
6600	68	-33.528	127.553
7200	64	-46.330	140.525
7800	61	-45.720	149.057
8400	58	-51.207	153.766
9000	53	-51.207	166.192
9600	52	-49.073	171.310
10200	45	-46.939	181.969
10800	40	-46.025	187.788
11400	32	-23.470	187.053
12000	27	-17.678	204.177
12600	24	-33.223	220.563
13200	15	-56.998	248.233
13800	11	-115.215	247.142
14400	9	-83.820	214.080
15000	5	-85.344	117.117
15600	3	-74.981	62.179
16200	1	-10.058	-

Table E-9

Mean* and Standard Deviation Versus Range for VOR-CTOL - Lateral

Range, meters	Number of Samples	Standard Deviation, meters
3000	44	51.408
3600	59	69.309
4200	87	71.220
4800	88	78.925
5400	88	85.960
6000	88	93.400
6600	87	83.336
7200	86	93.412
7800	78	103.730
8400	78	111.417
9000	78	117.696
9600	76	124.331
10200	73	130.631
10800	68	138.889
11400	63	153.812
12000	38	170.402
12600	37	190.436
13200	36	204.329
13800	34	211.745
14400	34	225.897
15000	27	259.081
15600	27	260.745
16200	27	312.198

*Mean = 0 for all range intervals.

Table E-10

Mean and Standard Deviation Versus Range for
FC-ILS-I-STOL - Lateral*

Range, meters	Mean, meters	Standard Deviation, meters
600	-4.5720	23.4696
900	-6.0960	26.5177
1200	-7.6200	30.1753
1500	-10.6680	34.4425
1800	-12.1920	38.4049
2100	-13.7160	43.2817
2400	-16.7641	48.7681
2700	-19.8121	52.1209
3000	-16.7641	59.4361
3600	3.0480	78.6386

*-, "STOL Steep Approaches in the Breguet 941", Memorandum
Report - Attachment 1, DOT-FAA, FS-640, November 1969.

Table E-11

Mean and Standard Deviation Versus Range for
FC-ILS-I-CTOL - Vertical*

Range, meters	Number of Samples	Mean, meters	Standard Deviation, meters
600	409	-3.4855	8.4295
1200	458	-1.6974	10.4520
1800	508	-0.4770	12.8971
2400	519	-0.1967	13.0635
3000	515	-0.6443	14.5217
3600	507	-1.6859	12.9151

*-, Data Collected for "Revalidation of the Data Base Used in Establishing the Criteria for Simultaneous ILS Approaches to Parallel Runways", DOT-FAA-SPDS - Subprogram No. 150-502, May 1970.

Table E-12

Mean and Standard Deviation Versus Range for
FC-ILS-I-STOL - Vertical*

Range, meters	Mean, meters	Standard Deviation, meters
600	-6.0960	8.5344
900	-6.0960	10.0584
1200	-6.0960	12.1920
1500	-6.0960	14.3256
1800	-6.0960	17.6784
2100	-6.0960	20.4216
2400	-9.1440	22.8600
2700	-10.6680	26.8225
3000	-13.7160	27.4321
3600	-22.0041	28.3465

* -, "Ground Noise Measurements During Landing and Take-off Operations of a McDonnell-Douglas 188 (Breguet 941) STOL Airplane", Langley Working Paper, LWP-741, 18 April 1969.

Table E-13

FC-ILS-I-CTOL - Longitudinal

Assumed gaussian:

$$X' = N(\bar{X}', \sigma_{X'}^2)$$

$$\bar{X}' = X_0' - Vt$$

$$\sigma_{X'} = \frac{\sigma_V t}{\sqrt{2}}$$

where

X' ~ longitudinal location, feet

\bar{X}' ~ mean longitudinal location, feet

$\sigma_{X'}$ ~ longitudinal location standard deviation, feet

X_0' ~ initial longitudinal location, feet

V ~ aircraft mean velocity, feet/second (assumed to be 236.444 feet/second for CTOL aircraft)

σ_V ~ velocity distribution standard deviation, feet/second (assumed to be 8.444 feet/second)

t ~ time from the point where the aircraft velocity control is initiated, seconds

APPENDIX F

SENSITIVITY ANALYSIS

The purpose of the sensitivity analysis is to identify the effects of selected pertinent model parameters and model errors on the lateral distribution of the approach system. The sensitivity analysis was performed by utilizing the nominal approach system model defined in the Lateral Separation Study, with specific initial conditions, as the reference condition. Each of the pertinent parameters and errors of the nominal system model was varied about its reference value, and the resulting sensitivity coefficient of the lateral deviation or lateral distribution standard deviation was calculated at various points in range. A sensitivity coefficient, S_P^X , identifies the amount that the variable, X, changes from the reference condition due to a small change in the parameter, P.

$$S_P^X = \frac{\Delta X}{\Delta P}$$

The sensitivity coefficients for each parameter and error were calculated and plotted at common points in range. The resulting parameter and error sensitivity curves are presented in this appendix. It should be noted that the sensitivity data is only valid for small variations about the reference condition.

The parameter sensitivity curves (Figures F-1 through F-10) illustrate the sensitivity of the lateral deviation to each of the pertinent parameters (Table F-1) as a function of range and time. The reference condition is defined by the nominal model with all initial conditions equal to zero except as follows:

$$Y'_0 = 500 \text{ ft. (arbitrary initial lateral deviation)}$$

$$X'_0 = 13.53 \text{ NMi (arbitrary initial range)}$$

$$\psi_0 = 3.14159 \text{ rad. (runway arbitrarily chosen to be equal to } 180^\circ)$$

The error sensitivity curves (Figures F-11 through F-14) illustrate the sensitivity of the lateral distribution

standard deviation to the standard deviation changes to each of the pertinent system errors (Table F-2) as a function of range and time. The reference condition is defined by the nominal model with the initial state distributions given in Table F-3.

Table F-1 Sensitivity Analysis Parameters

Symbol	Reference Value	Units	Description
V	236.4444	ft/sec	Aircraft airspeed
K_{ϵ_e} (angular)	4.8	rad/rad	Pilot tracking gain on the angular localizer error
K_{ψ_e}	1.0	rad/rad	Pilot gain on heading angle error
K_{ψ}	1.9	rad/rad	Pilot gain on heading angle feedback
K_{ϕ}	1.333	sec	Pilot gain on the bank angle divided by a_{ϕ}
K_a	1.0	1/sec ²	Aircraft bank rate to aileron response gain multiplied by a_a
a_a	1.0	1/sec	Inverse of the aircraft bank rate to aileron response time constant
a_{ϕ}	1.5	1/sec	Inverse of the pilot lead time constant on bank angle feedback
τ_p	0.7	sec	Pilot/control delay
L	9000.0	ft	-X coordinate of the lateral guidance transmitting antenna

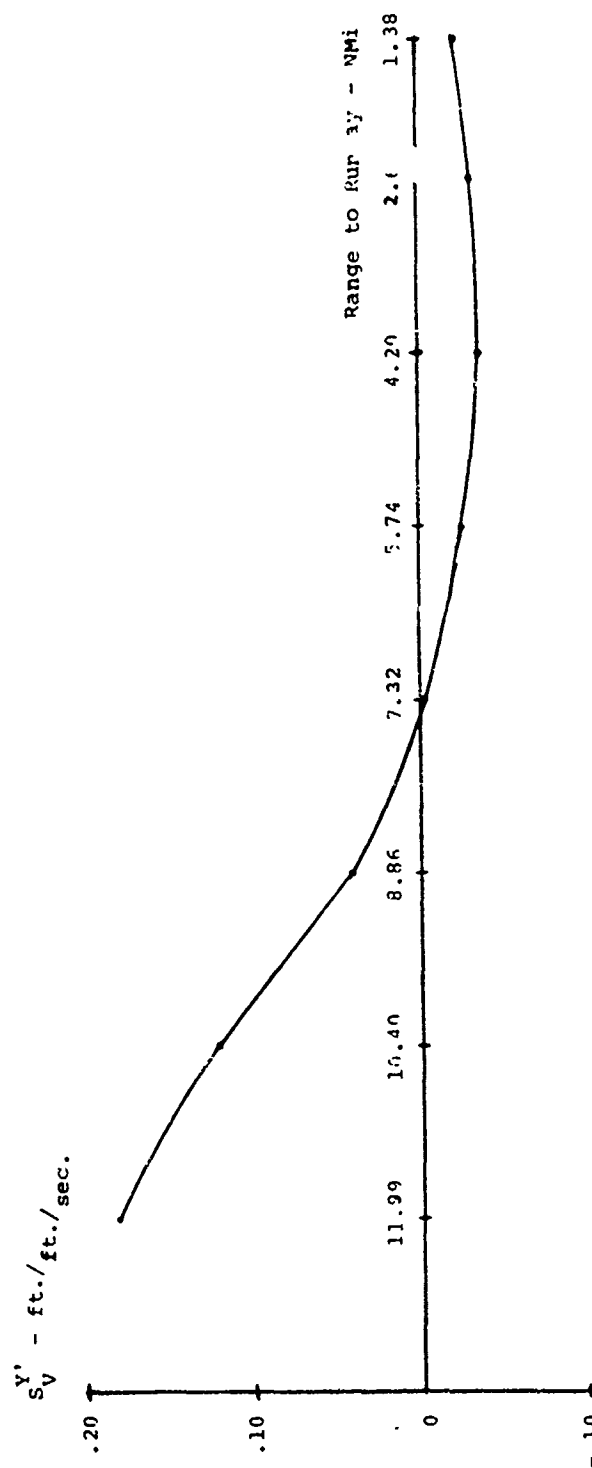
Table F-2 Sensitivity Analysis Errors

Symbol	Reference Value (Rad.)	Description
$\sigma_{N\psi}$.01745	Pilot heading angle error distribution standard deviation
$\sigma_{N\phi}$.1047 @ 9NMi .0436 @ 0NMi	Pilot bank angle error distribution standard deviation
σ_{ILS_R}	.00048	ILS equipment receiver error distribution standard deviation
σ_{ILS_T}	.001497	ILS equipment transmitter error distribution standard deviation
$\sigma_{N\epsilon}$.00349	Pilot localizer tracking error (final leg) distribution standard deviation
σ_{ψ_0}	.02	Initial condition on heading state distribution standard deviation

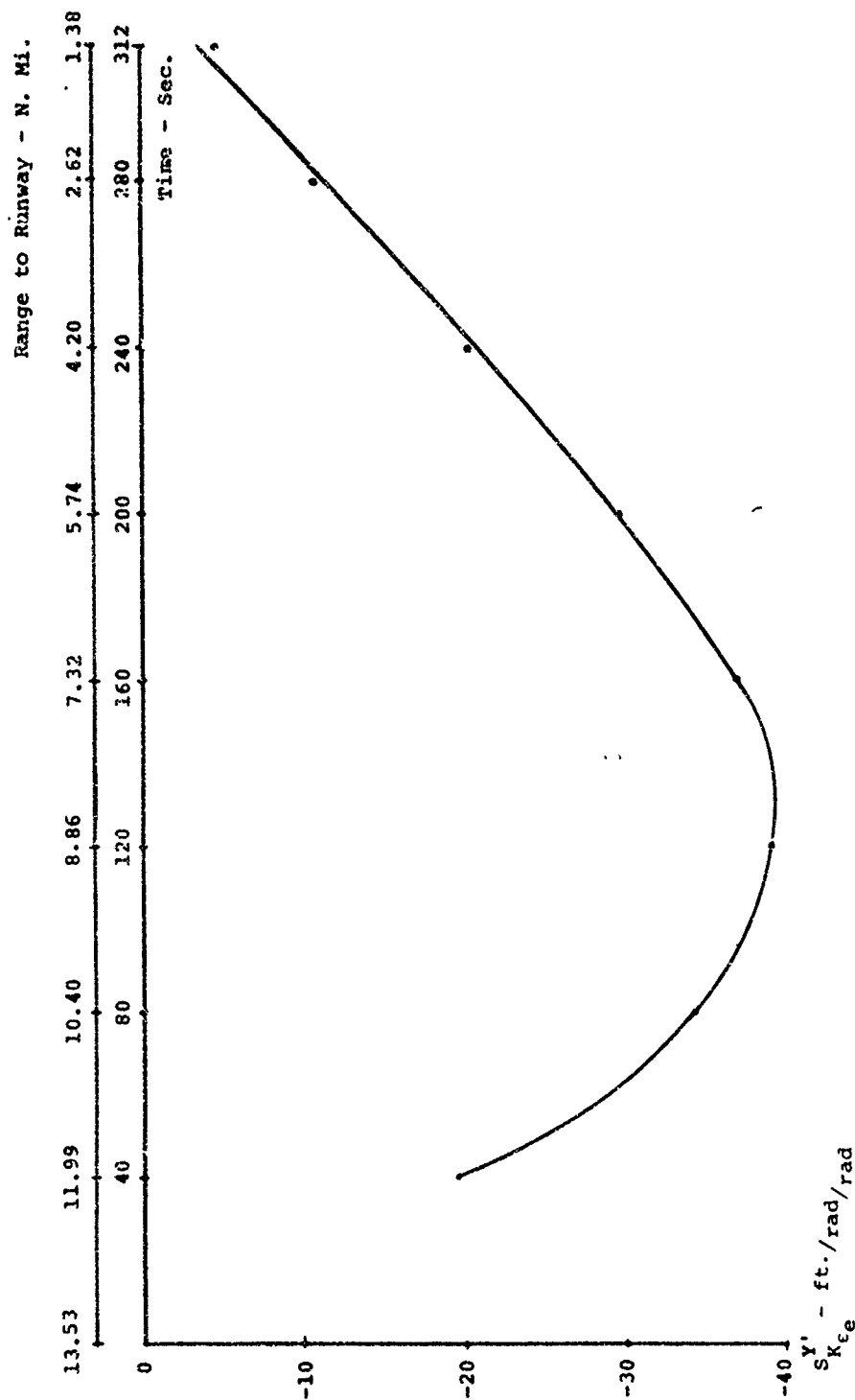
Table F-3
Nominal Model Initial State Distributions (at $X'_0 = 9\text{NMi}$)

State	Symbol	σ^*	Units	Comments
X_{1_0}	Y'_0	198	feet	Lateral Deviation
X_{2_0}	ψ_0	.02	radians	Heading Angle
X_{3_0}	ϕ_0	.01	radians	Bank Angle
X_{4_0}	IS	.12		Intermediate State
X_{5_0}	IS	.26		Intermediate State
X_{6_0}	IS	.54		Intermediate State

*Assumed Gaussian with mean = 0, variance = σ^2



F-1 LATERAL DEVIATION SENSITIVITY COEFFICIENTS (with respect to V)



S-2 LATERAL POINT ON SENSITIVITY COEFFICIENTS (with respect to K_{ϵ_e})

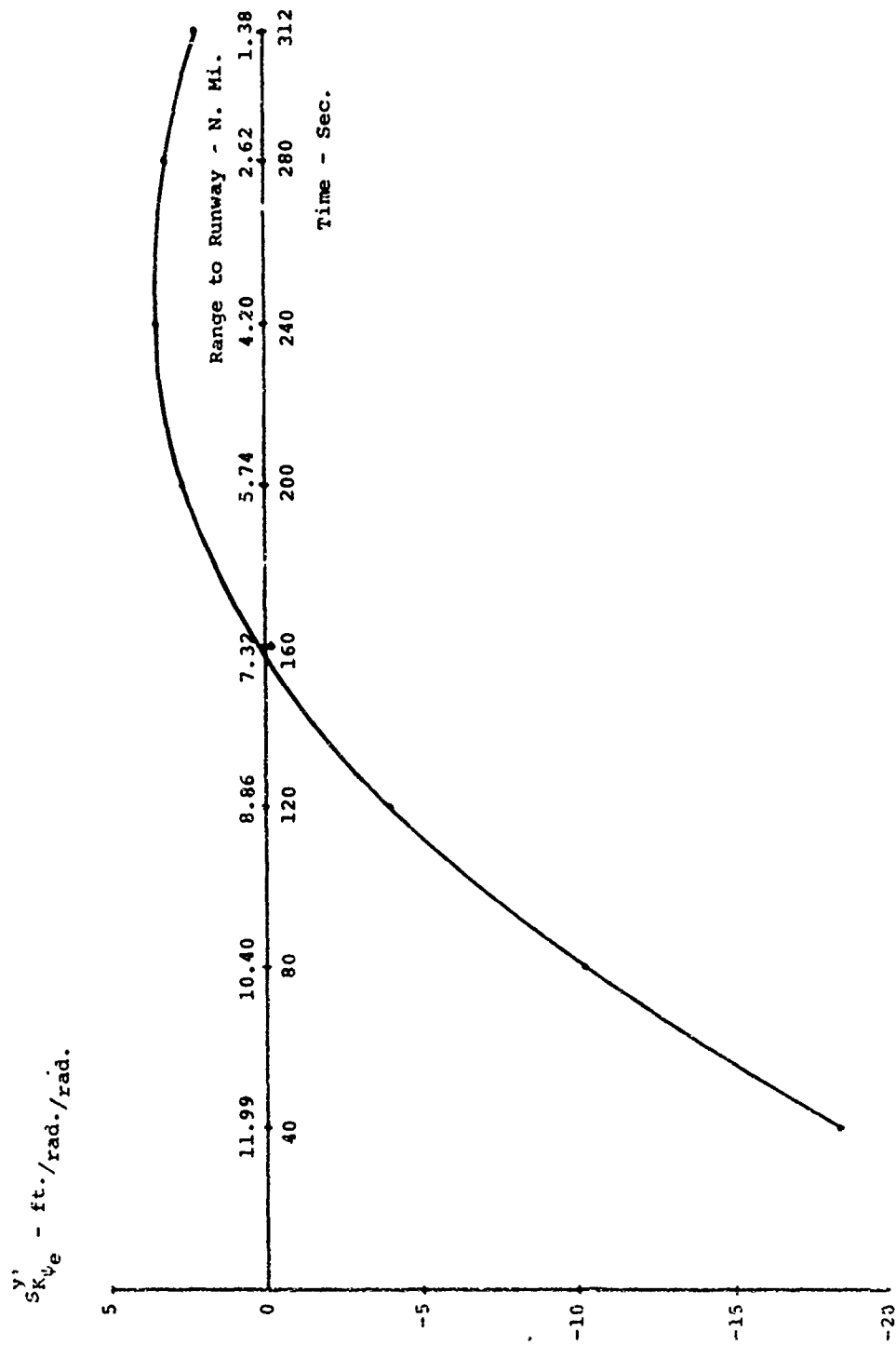
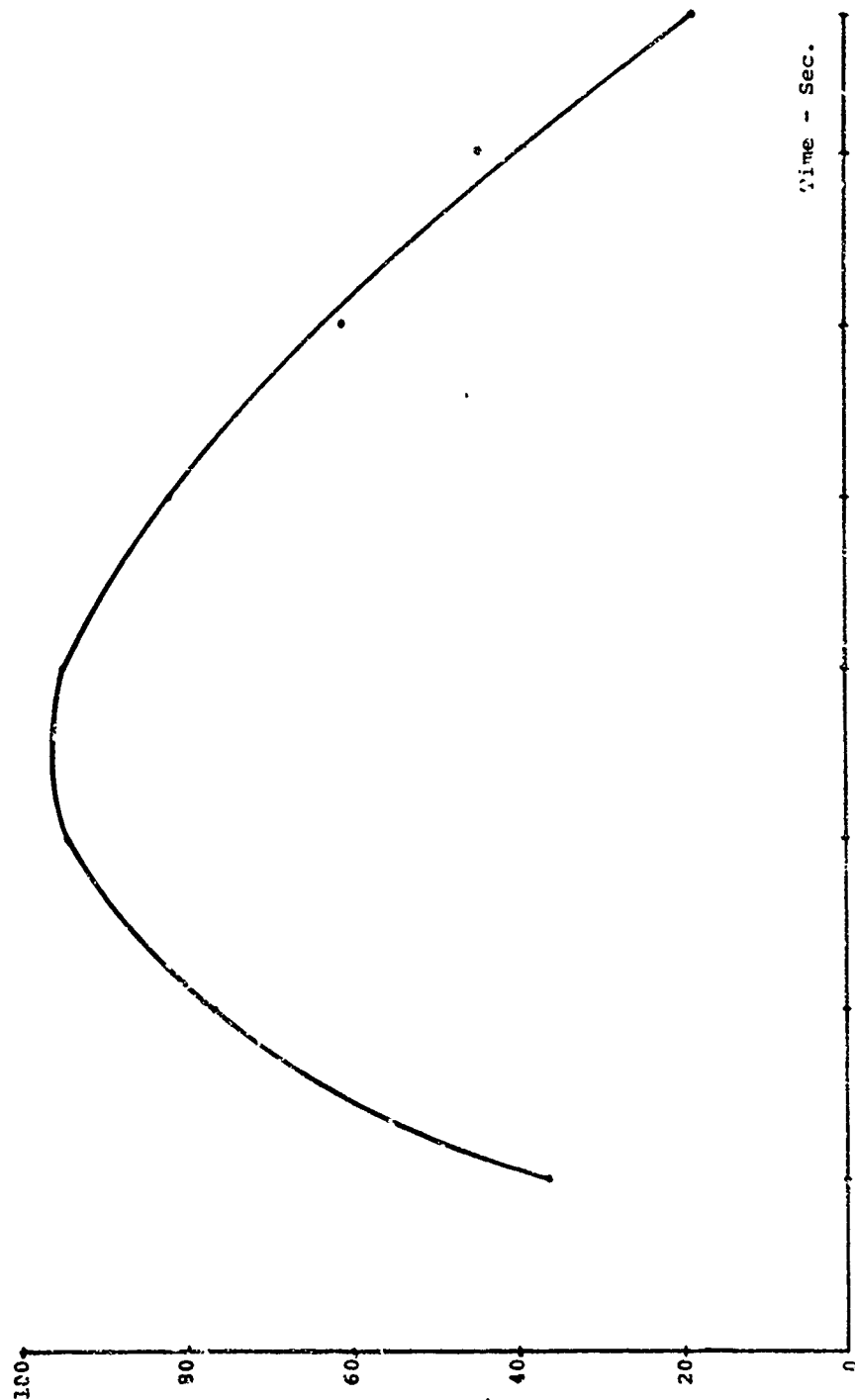


FIGURE 3 LATERAL DEVIATION SENSITIVITY COEFFICIENTS (with respect to K_{y_e})

$S' - f_c / \text{rad.} / \text{rad.}$
 K_ψ

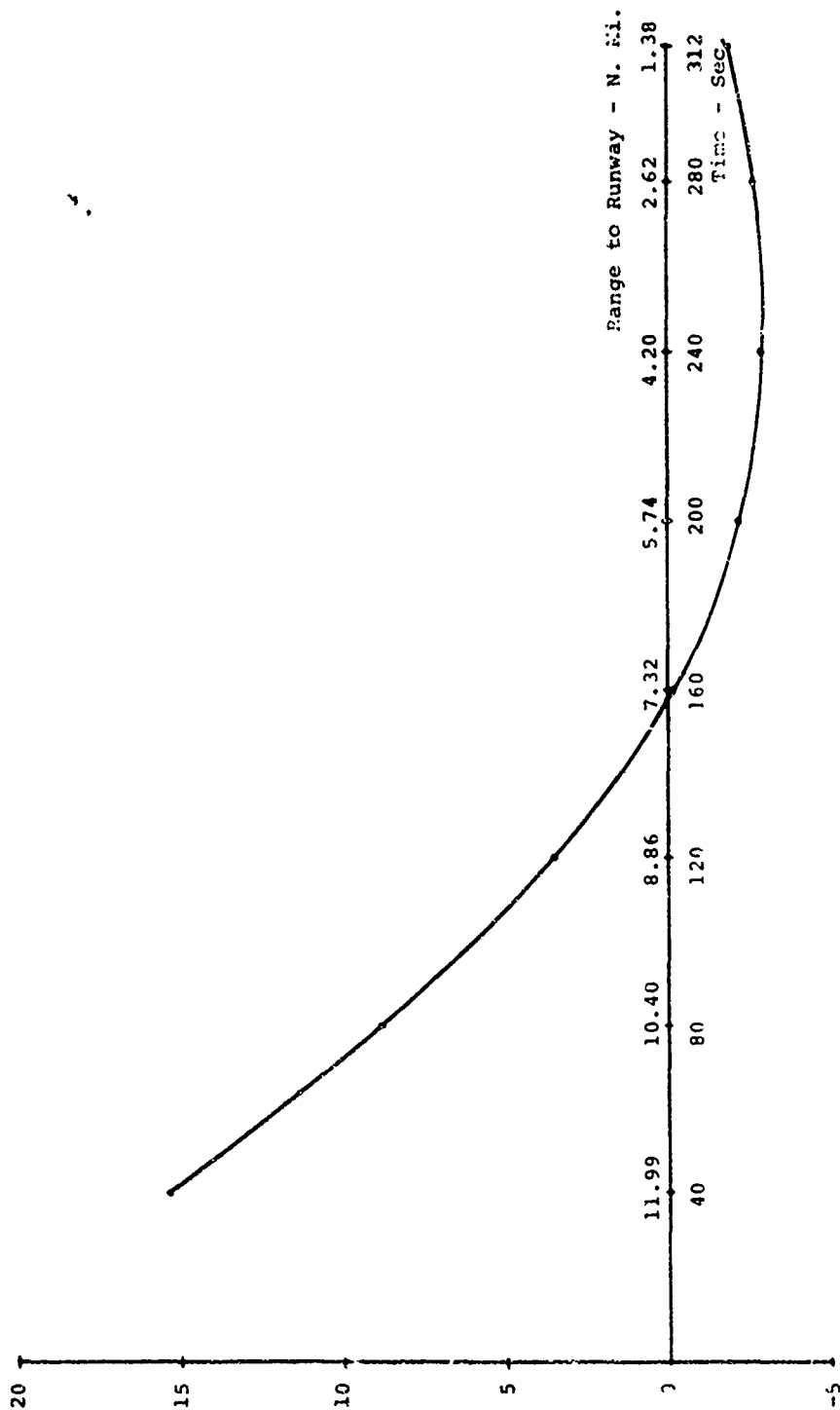


Time - Sec.

Time - Sec.	Range to Norway - N. W.
40	11.59
80	10.40
120	8.86
160	7.20
200	5.74
240	4.20
280	2.62
320	1.28

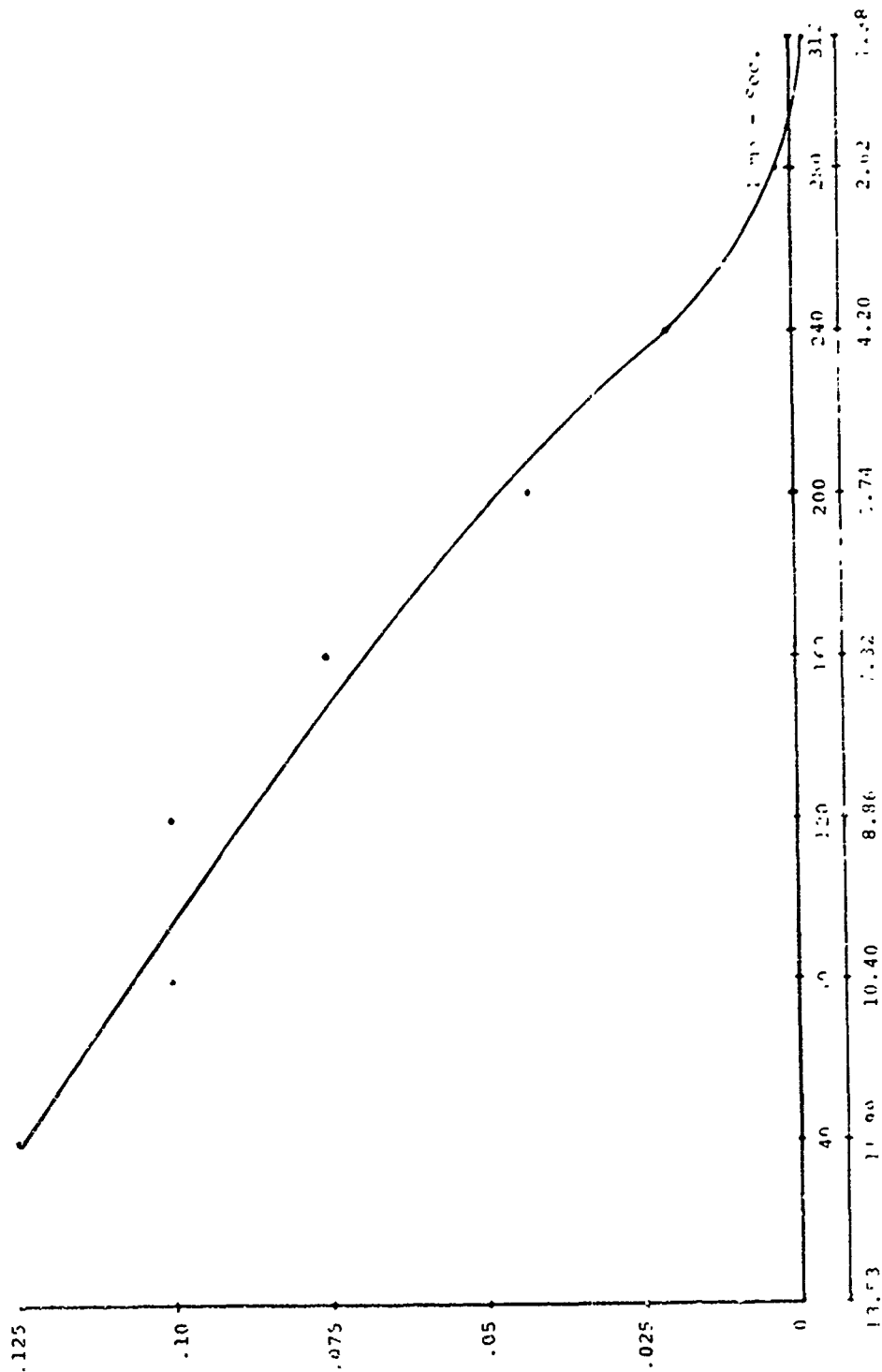
P-4 LATE-ON DEVIANT SENSITIVE (with respect to K_ψ)

$y' - \text{ft./sec.}$
 S_{K_ϕ}



--5 ATERAL DEVIATION SENSITIVITY COEFFICIENTS (with respect to K_ϕ)

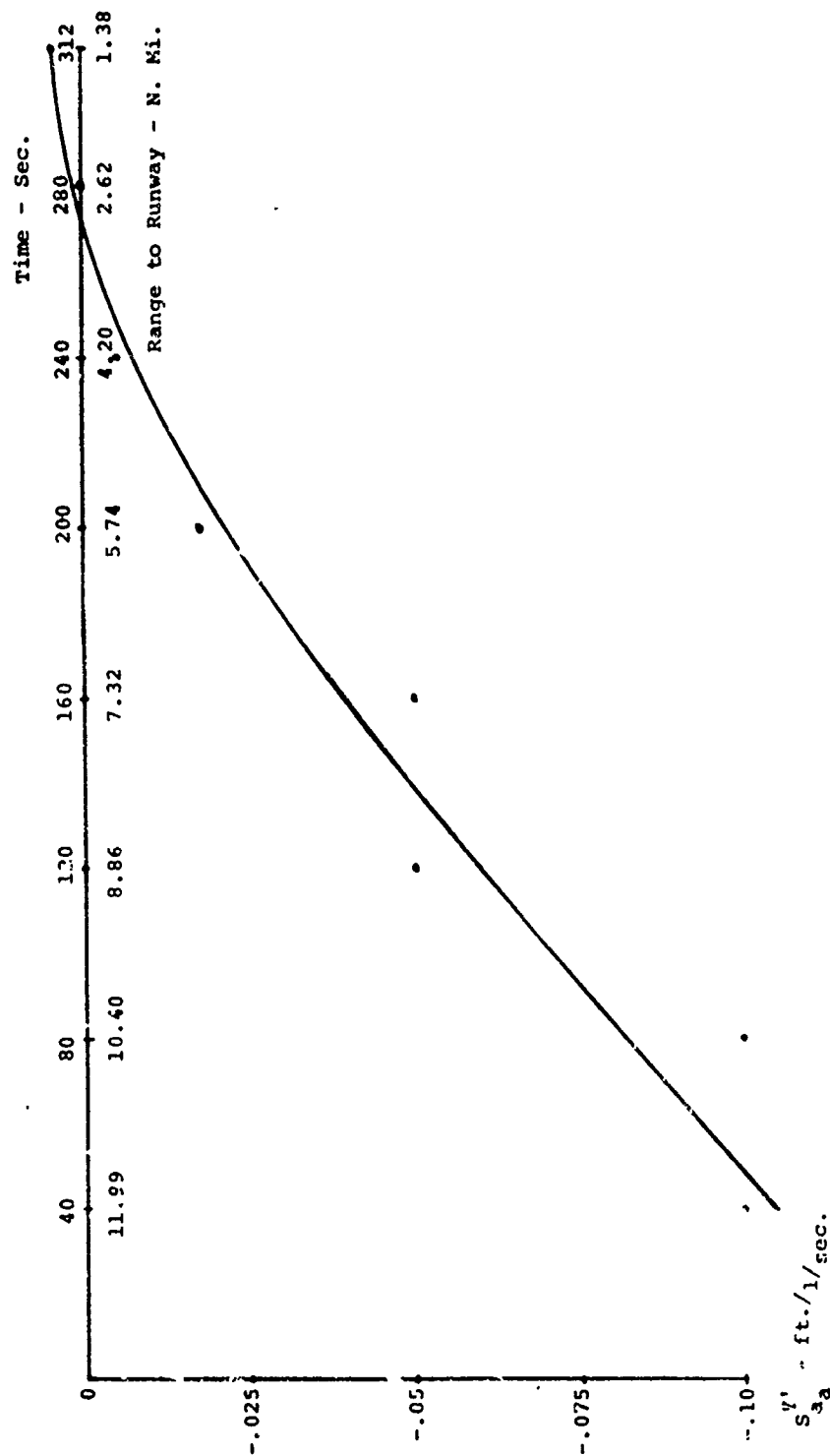
$\zeta_{K_a} = \text{ft.}/\text{sec.}^2$



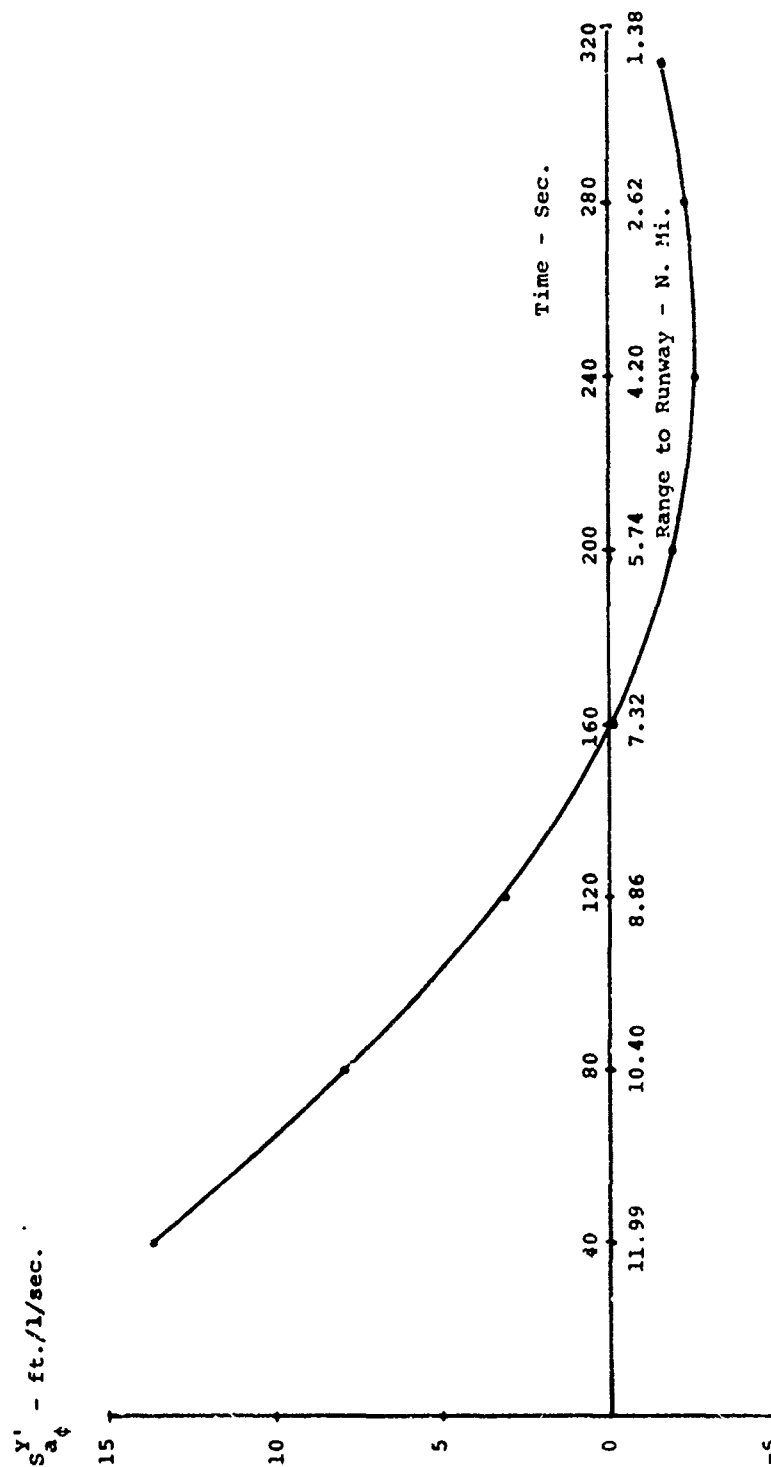
F-6 LIFT ALLOCATION SENSITIVITY OF P-11'S

Range to Radar - 1.58

4.20 2.02 1.58

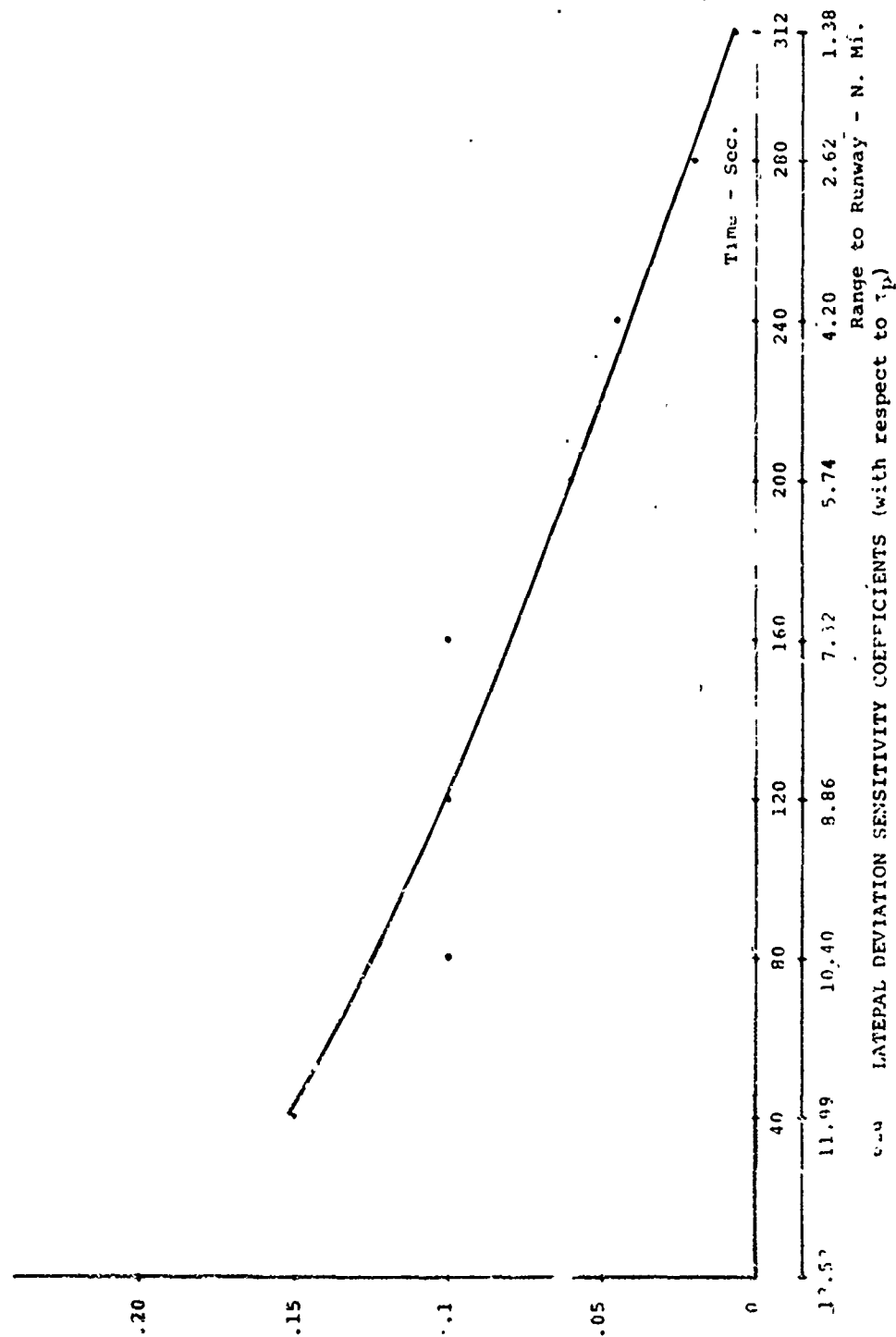


F-7 LATERAL DEVIATION SENSITIVITY COEFFICIENTS (with respect to a_a)

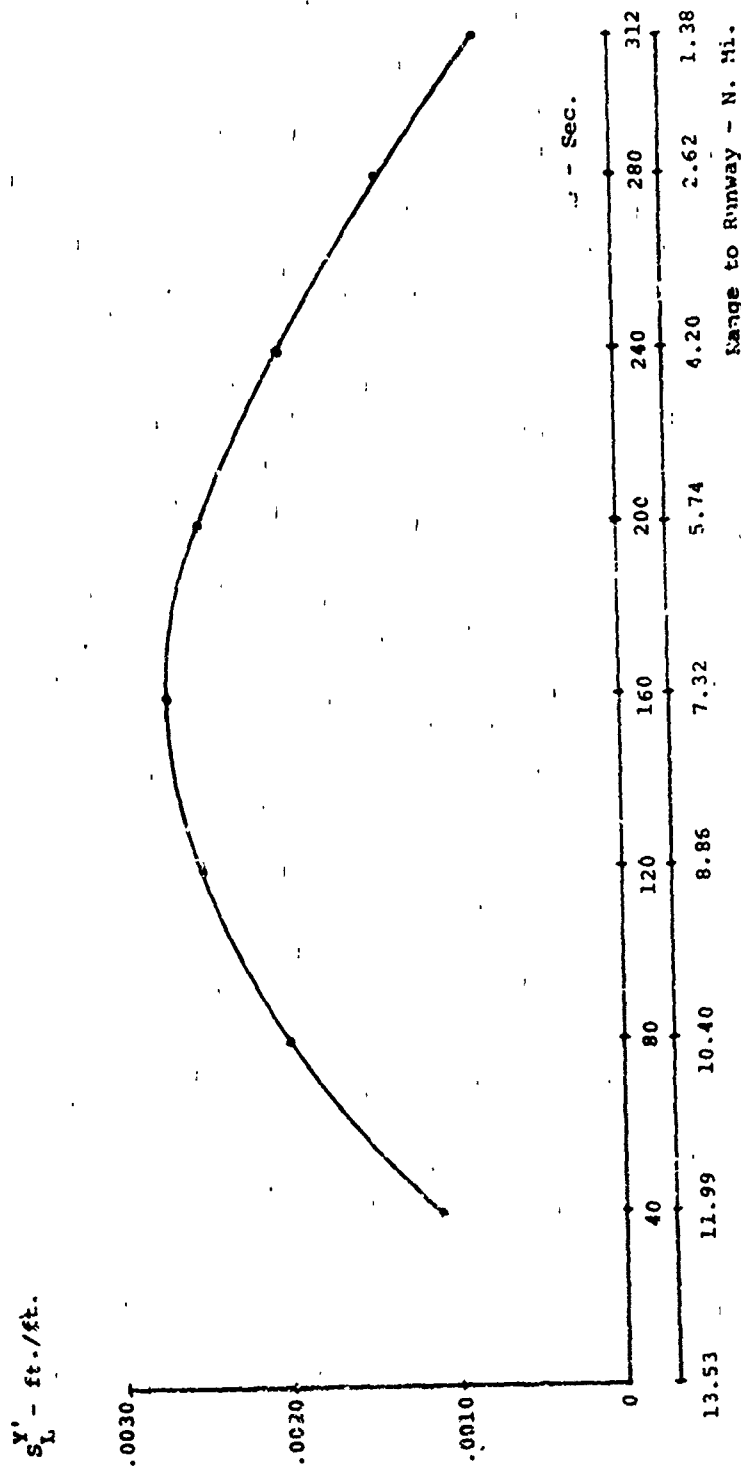


F-12 LATERAL DEVIATION SENSITIVITY COEFFICIENTS (with respect to a_4)

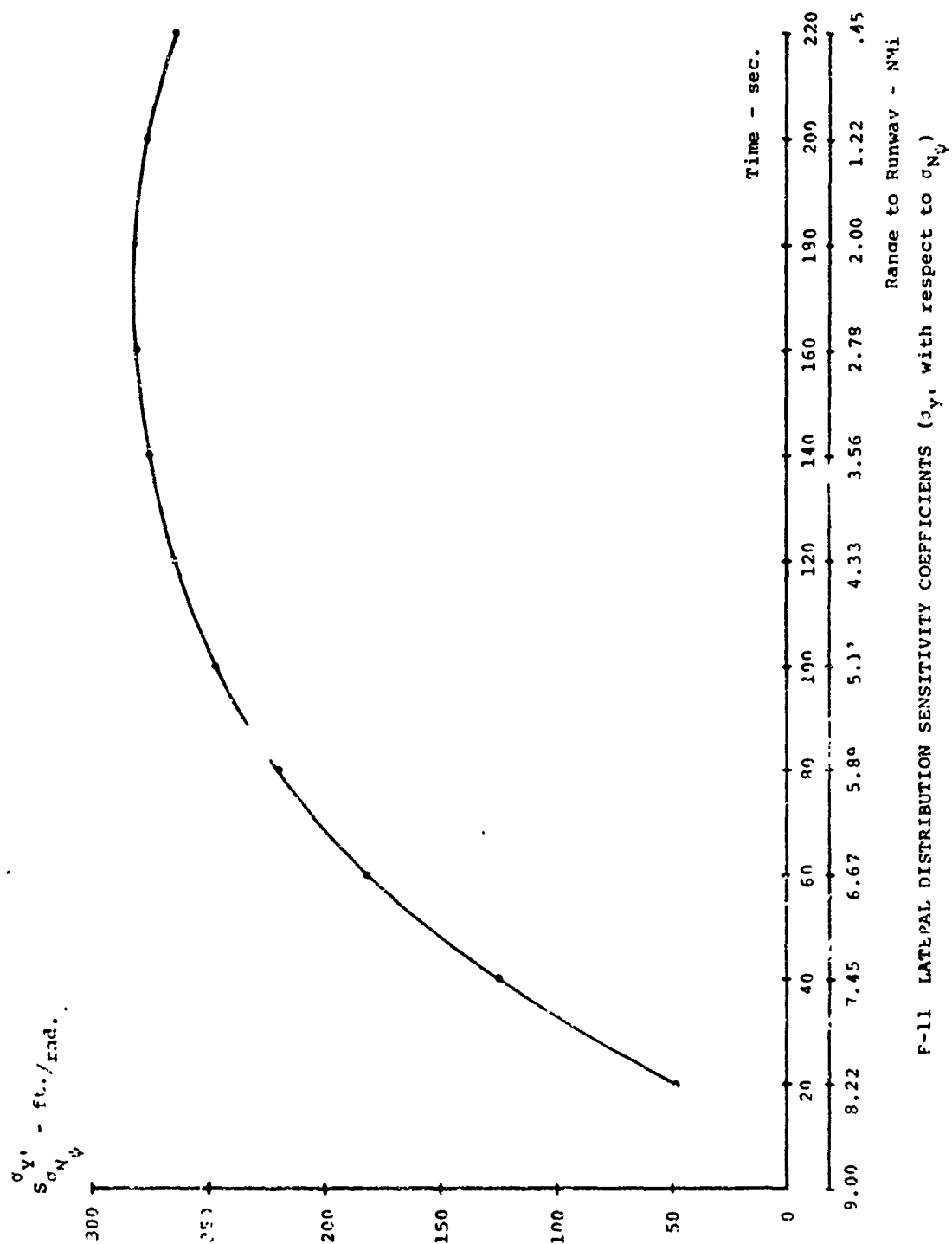
s'_{tp} - ft./sec.



6-3 LATEPAL DEVIATION SENSITIVITY COEFFICIENTS (with respect to t_p)



F-10 LATERAL DEVIATION SENSITIVITY COEFFICIENTS (with respect to L)

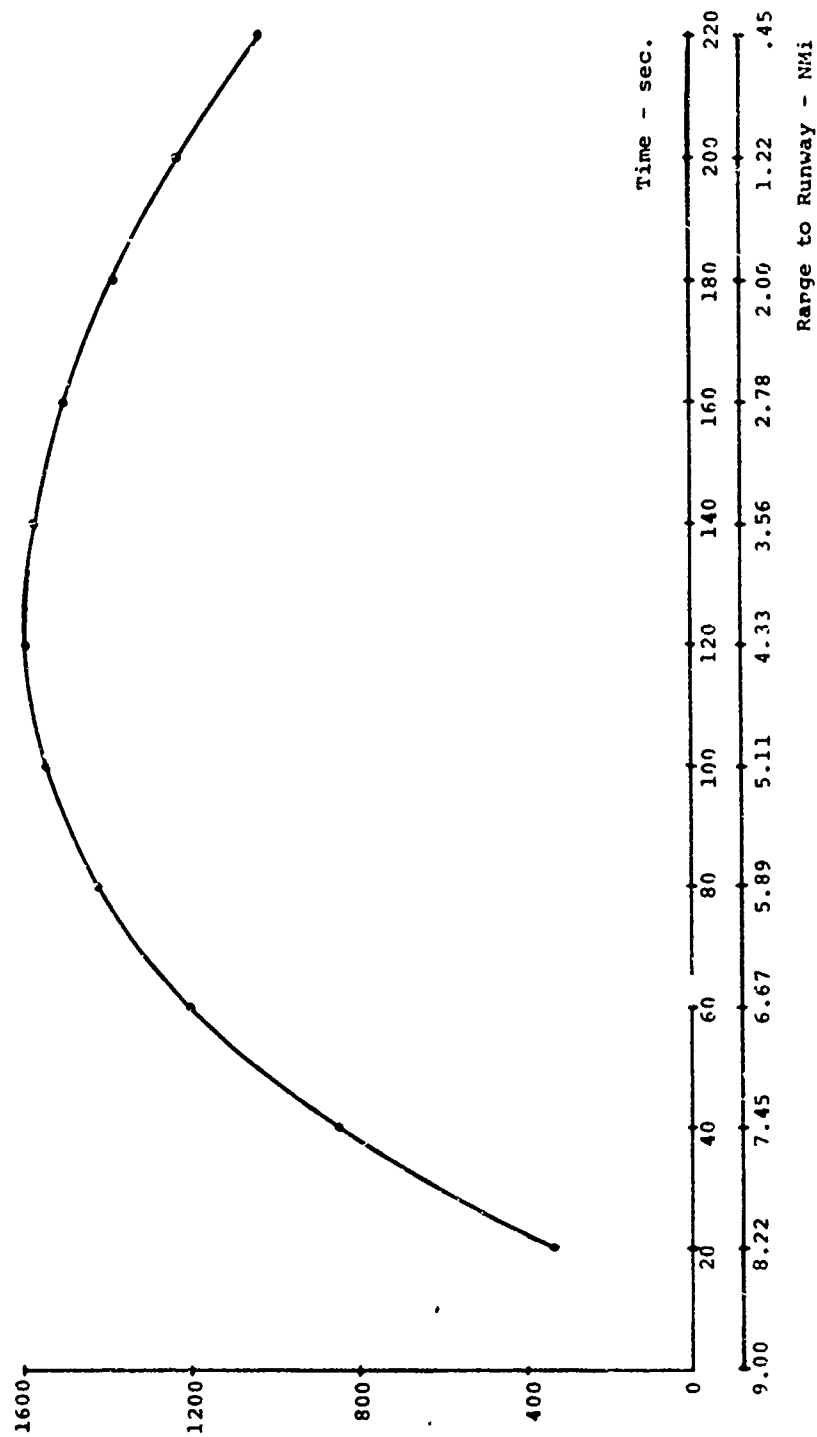


F-15

F-11 LATERAL DISTRIBUTION SENSITIVITY COEFFICIENTS (σ_y , with respect to σ_{N_y})

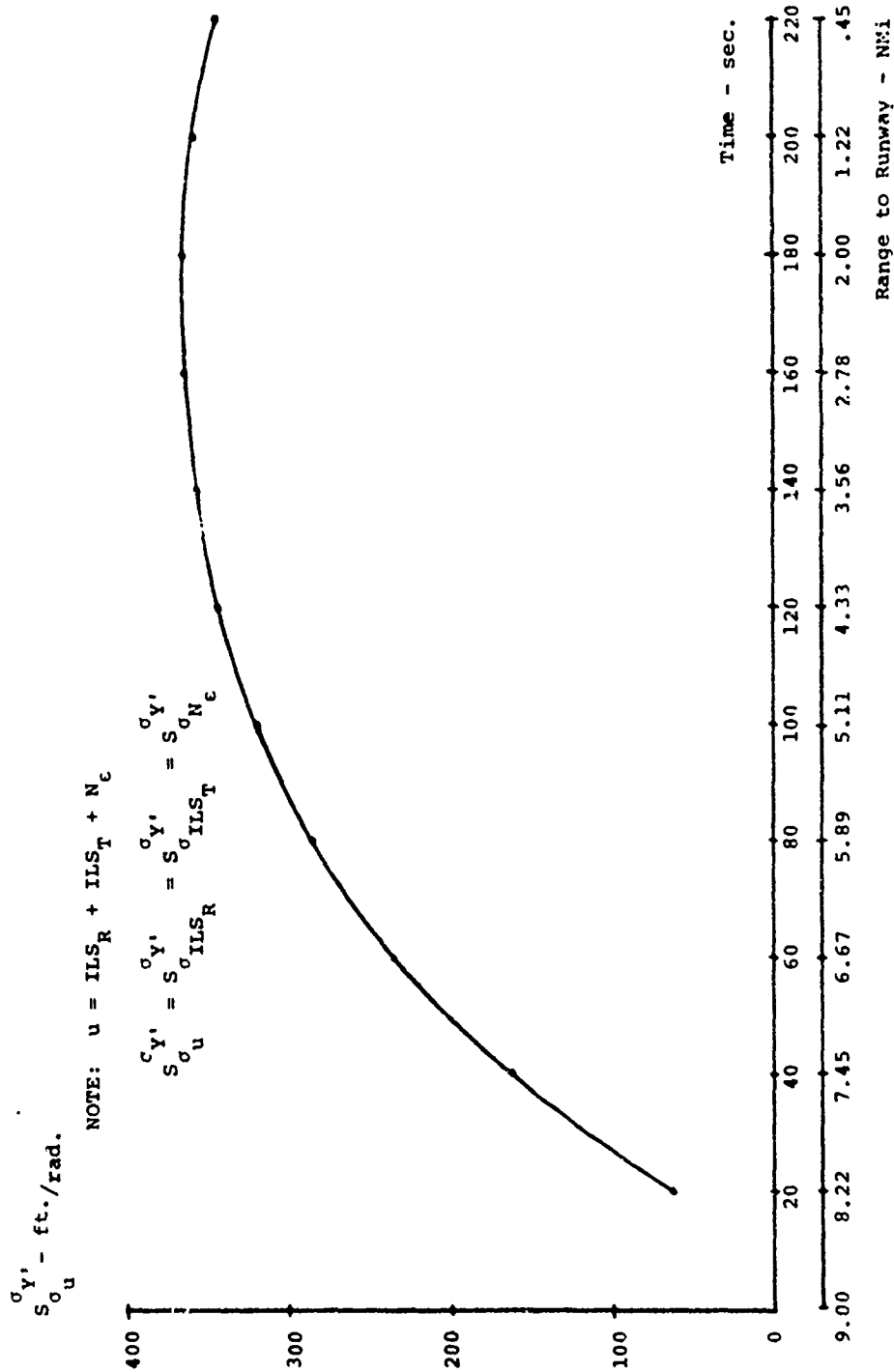
Range to Runway - NMi

σ_{N_t} - ft./rad.

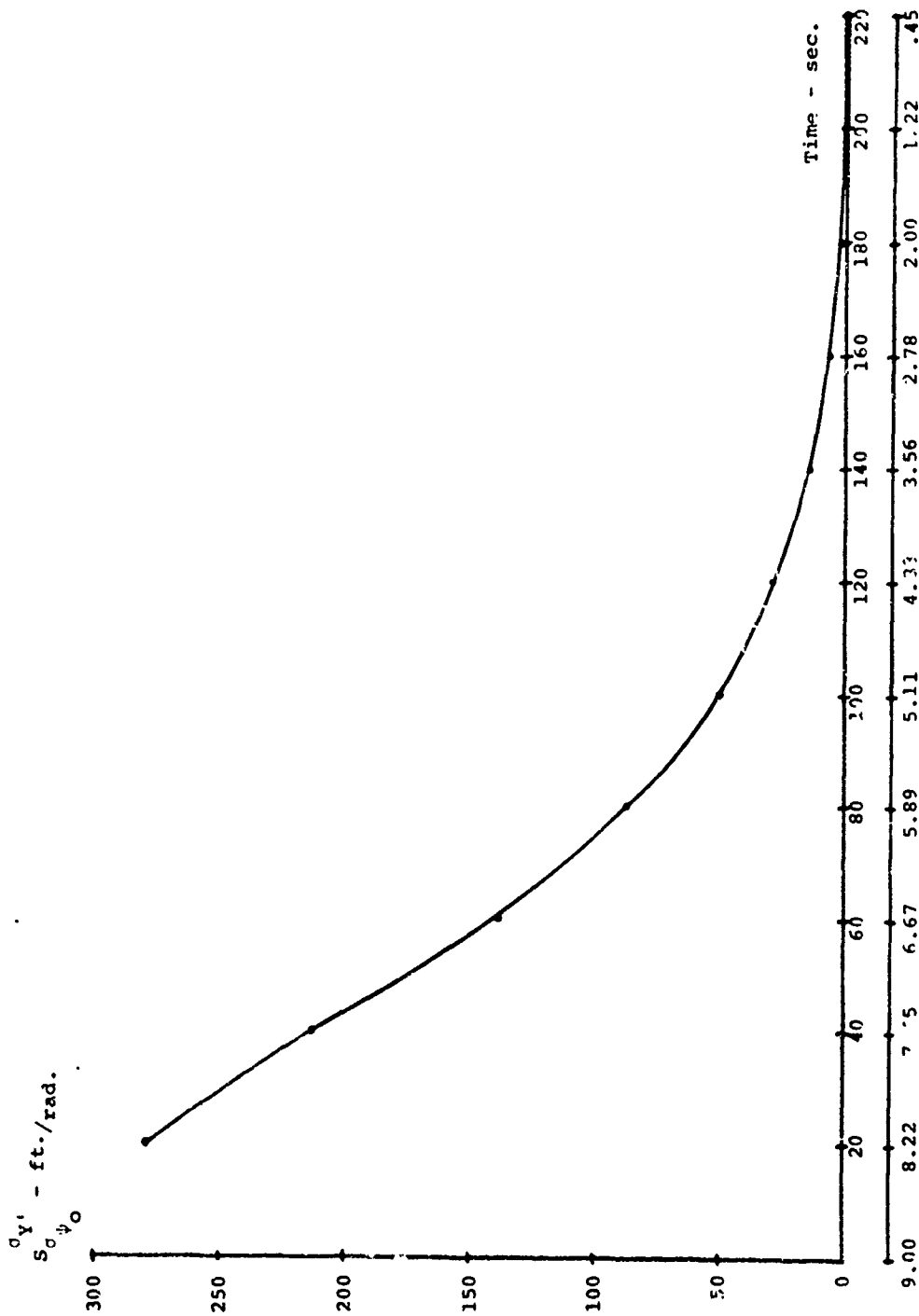


F-12 LATERAL DISTRIBUTION SENSITIVITY COEFFICIENTS (σ_y , with respect to σ_{N_t})

Range to Runway - NMi



F-13 LATERAL DISTRIBUTION SENSITIVITY COEFFICIENTS (σ_y , with respect to σ_u)



Range to Runway - 14.1

F-14 LATERAL DISTRIBUTION SENSITIVITY COEFFICIENTS (σ_y , with respect to σ_{y0})

APPENDIX G

APPROACH SYSTEM MODELS

The approach system models, shown in this appendix, were developed in the runway lateral separation study to aid in the determination of minimum runway spacing criteria. This appendix contains models for the approach systems listed in Table G-1. The models represent a composite set of aircraft flying the final leg of an instrument approach under IFR conditions.

General System Model

Figure G-1 contains the major components in the model structure: pilot, course deviation indicator, and ground controller.

List of Symbols

All symbols used in the various models, their units, and a brief description of each are listed in Table G-2. The dot notation over a variable indicates the time derivative of that variable. A zero subscript indicates the initial condition.

Assumptions

Runway lateral separation requirements, as defined in this study, are based upon the following assumptions:

- 1) the system's lateral and vertical tracking dynamics are independent, and
- 2) the aircraft remains in the glideslope plane.

These assumptions result in a study reflecting the "worst case" possibility. Thus, the system models simulate lateral control only.

The aircraft are assumed to perform coordinated turns in the glideslope plane in order to nullify any lateral displacement error. This assumption simplifies the aircraft dynamics equations.

Coordinate Systems

Three coordinate systems are used in the models. These systems are a runway system, a glideslope system, and an aircraft body centered system. The three systems and their relationships to one another are shown in Figure G-2.

The runway system is identified by the X, Y, Z axes. The axes have their origin at the touchdown point for approaches

and the liftoff point for departures. The touchdown point for an approach is defined as the point on the runway at which an aircraft on an ideal track would first touch the runway (i.e., for FC-ILS, it would be the glideslope intercept point). For a departure, the liftoff point is defined as the point an aircraft would lift off the runway for an ideal departure. The X axis is defined positive out along the runway centerline, the Z axis is positive up along the earth's gravitational vector, and the Y axis completes the right-handed system.

The glideslope system is identified by the X', Y', and Z' axes. The axes also have their origin at the touchdown or liftoff point. The X' axis is defined positive out along an ideal track. For a FC-ILS approach, the X' axis is defined as being along the intersection of the ILS localizer and glideslope beams. For a FC-ILS departure, the X' axis is defined similarly, assuming a glideslope equivalent beam exists with its intercept point coincident with the liftoff point and extending along the departure path. The Y' axis is coincident with the -Y axis, and the Z' axis completes the right-handed system.

The body centered system is identified by the x, y, and z axes and has its origin at the aircraft center-of-gravity. The x axis is defined positive forward along the aircraft fuselage centerline, the y axis is positive out along the starboard wing, and the z axis completes the right-handed system.

Approach System Model Block Diagrams, Parameter Values and Initial Distributions

The models for the approach systems in Table G-1 are represented by the following block diagrams:

- 1) Approach System Model (Figure G-3)
- 2) Nonlinear Simulated Delay Approach System Model (Figure G-4)
- 3) Linear Simulated Delay Approach System Model (Figure G-5)

These three block diagrams were developed for use in the various analyses required in the lateral separation study. The simulated delay included in (2) and (3) above is implemented with the following equations.

$$\tau_p = \text{actual delay, seconds}$$

$$a_{p_5} = \frac{\tau_p}{100}$$

$$a_{p_1} = \left(\frac{\tau_p - a_{p_5}}{2\sqrt{3}} \right)^2$$

$$a_{p_2} = -\frac{1}{2} (\tau_p - a_{p_5})$$

$$a_{p_3} = \left(\frac{\tau_p - a_{p_5}}{2\sqrt{3}} \right)^2$$

$$a_{p_4} = \frac{1}{2} (\tau_p - a_{p_5})$$

The model parameter values and initial distributions for each of the approach systems are presented in Tables G-3 through G-14.

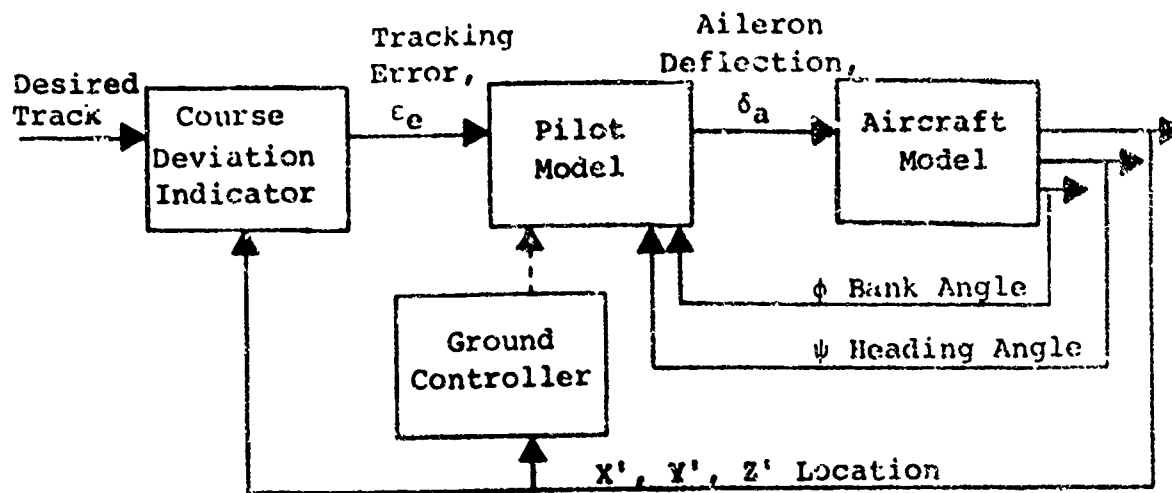


Figure G-1 General Approach System Model

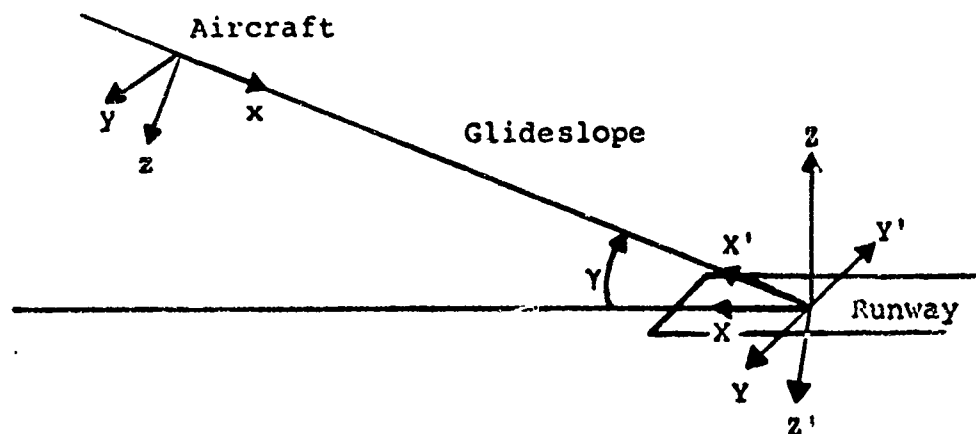


Figure G-2 Coordinate Systems

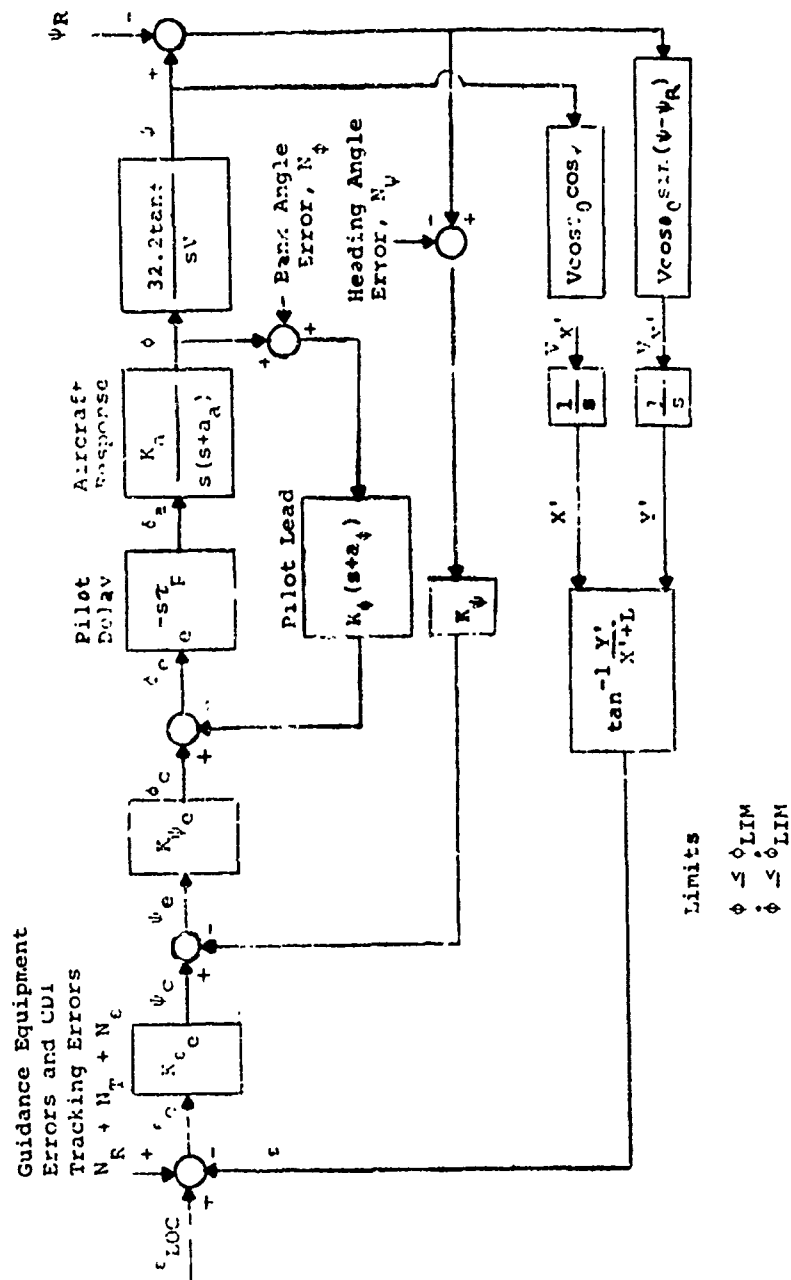


Figure G-3 Approach System Model



Figure G-4 Nonlinear, Simulated Delay Approach System Model

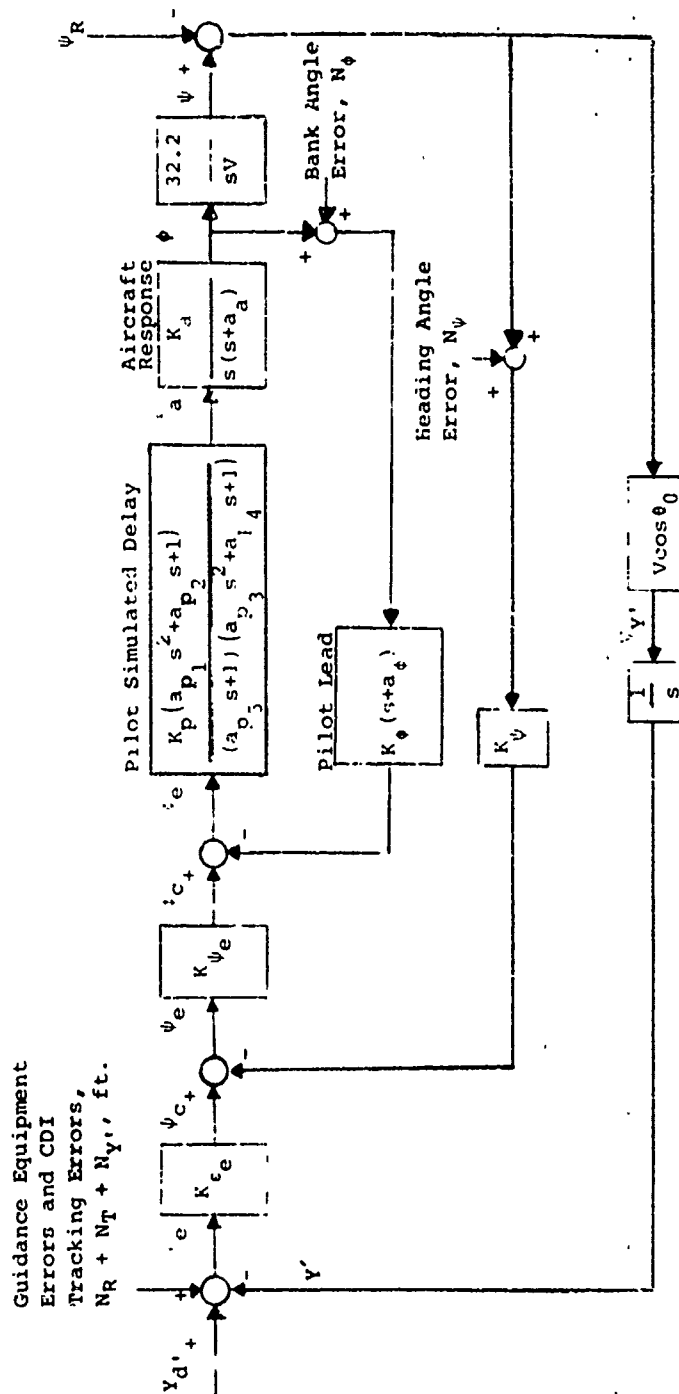


Figure G-5 Linear, Simulated Delay Approach System Model

Table G-1 Approach Systems

Designation	Primary User Class	Runway Type	Approach Guidance System
FC-ILS-INOM-CTOL	CTOL Category I	CTOL	Front Course, ILS Category I
FC-ILS-I-CTOL	CTOL Category I	CTOL	Front Course, ILS Category I
FC-ILS-II-CTOL	CTOL Category II	CTOL	Front Course, ILS, Category II
BC-ILS-I-CTOL	CTOL Category I	CTOL	Back Course, ILS, Category I
VOR-CTOL	CTOL Category I	CTOL	VOR (tracking in- bound to a station within the airport boundary)
FC-ILS-I-STOL	STOL Category I	STOL	Front Course, ILS, Category I

Table G-2 List of Symbols

Symbol	Units	Description
a_a	1/sec	Inverse of the aircraft bank rate to aileron response time constant
$\left. \begin{array}{l} a_{p1} \\ a_{p2} \\ a_{p3} \\ a_{p4} \\ a_{p5} \end{array} \right\}$		Coefficients used in the simulated pilot/control delay
a_ϕ	1/sec	Inverse of the pilot lead time constant on bank angle feedback
K_a	1/sec ²	Aircraft bank rate to aileron response gain multiplied by a_a
K_p	rad/rad	Pilot gain on simulated delay
K_{ϵ_e} (angular)	rad/rad	Pilot tracking gain on the angular localizer error
K'_{ϵ_e} (displacement)	rad/ft	Pilot tracking gain on the displacement error from the localizer beam
K_ϕ	sec	Pilot gain on the bank angle divided by a_ϕ
K_ψ	rad/rad	Pilot gain on heading angle feedback
K_{ψ_e}	rad/rad	Pilot gain on heading angle error
L	ft	-X coordinate of the lateral guidance transmitting antenna
N_R	rad	Lateral guidance equipment receiver noise
N_T	rad	Lateral guidance equipment transmitter noise

Table G-2 List of Symbols (Continued)

Symbol	Units	Description
$N_{Y'}$	ft	Pilot lateral tracking error (base leg)
N_{ϵ}	rad	Pilot localizer tracking error (final leg)
N_{ϕ}	rad	Pilot bank angle error
N_{ψ}	rad	Pilot heading angle error
V	ft./sec	Aircraft airspeed
$V_{X'}$	ft/sec	Aircraft velocity along the glideslope coordinate system
$V_{Y'}$		
$V_{Z'}$		
$\begin{Bmatrix} x \\ \dot{y} \\ z \end{Bmatrix}$	ft	Aircraft body centered coordinate system
$\begin{Bmatrix} X \\ Y \\ Z \end{Bmatrix}$	ft	Runway coordinate system
$\begin{Bmatrix} X' \\ Y' \\ Z' \end{Bmatrix}$	ft	Glideslope coordinate system
Y'_d	ft	Desired location of the aircraft in the glideslope axis system

Table G-2 List of Symbols (Continued)

Symbol	Units	Description
γ	rad	Glideslope angle
δ_a	rad	Aileron deflection
ϵ	rad	Angular position of the aircraft in the glideslope axis system
ϵ_e	rad	Angular error of the aircraft position in the glideslope axis system
ϵ_{LOC}	rad	Desired angular position of the aircraft
θ_o	rad	Pitch angle in glideslope axis system
τ_p	sec	Pilot/control delay
ϕ_c	rad	Command bank angle
ϕ_e	rad	Error between commanded and anticipated bank angle
ϕ_{LIM}	rad	Bank angle limit
$\dot{\phi}_{LIM}$	rad/sec	Bank rate limit
ψ θ ϕ	rad	Heading, pitch and bank angles of the aircraft attitude in the glideslope axis system, respectively
ψ_c	rad	Commanded heading angle

Table G-2 List of Symbols (Continued)

Symbol	Units	Description
ψ_e	rad	Heading error defined in glideslope axis system
$\dot{\psi}_{LIM}$	rad/sec	Turn rate limit
ψ_R	rad	Reference heading angle in the glideslope axis system (zero error condition) arbitrarily assigned the value of 180°.

Table G-3 Model Parameter Values for FC-ILS-INOM-CTOL

Symbol	Value	Units	Comments
a_a	1.0	sec^{-1}	
a_{p_1}	.04	-	Simulated delay models
a_{p_2}	-.35	-	Simulated delay models
a_{p_3}	.04	-	Simulated delay models
a_{p_4}	.35	-	Simulated delay models
a_{p_5}	.007	-	Simulated delay models
a_{γ}	1.5	sec^{-1}	
K_a	1.0	sec^{-2}	
K_p	1.0	-	Simulated delay models
K_{ϵ_e}	4.8	-	Nonlinear models
K'_{ϵ_e}	.000075 at 9 NMi to .000354 at .75 NMi	$\frac{\text{rad}}{\text{ft}}$	Linear model $K'_{\epsilon_e} = \frac{K_{\epsilon_e}}{X' + L}$
K_{ϕ}	1.33	sec	
K_{ψ}	1.9	-	
K_{ψ_e}	1.0	-	

Table G-3 Model Parameter Values for FC-ILS-INOM-CTOL (Continued)

Symbol	Value	Units	Comments
L	9000.	feet	
N_R	$\pm .00048$	rad	White gaussian noise 1 σ value
N_T	$\pm .001497$	rad	White gaussian noise 1 σ value
N_ϵ	$\pm .00349$	rad	White gaussian noise 1 σ value
N_ϕ	$\pm .1047$ at 9 NMI; $\pm .0436$ at 0 NMI	rad	White gaussian noise 1 σ value (Varies linearly with range)
N_ψ	$\pm .01745$	rad	White gaussian noise 1 σ value
V	236.4	ft/sec	140 knots
γ	2.5	deg	
θ_o	0.	rad	Assumed
τ_p	.7	sec	
ϕ_{LIM}	.367	rad	
$\dot{\phi}_{LIM}$.1745	rad/sec	10 deg/sec
$\dot{\psi}_{LIM}$.0524	rad/sec	3 deg/sec
ψ_R	3.1416	rad	Arbitrary heading for an approach

Table G-4

Initial Distributions for FC-ILS-INOM-CTOL (at $X'_0 = 9\text{Nmi}$)

Symbol	Distribution	σ	Units
Y'_0	Gaussian	198	feet
ψ_0	Gaussian	.02	radians
χ_0	Gaussian	.01	radians

Mean = 0

Table G-5 Model Parameter Values for FC-ILS-I-CTOL

Symbol	Value	Units	Comments
a_a	1.0	sec^{-1}	
a_{p_1}	.04	-	Simulated delay models
a_{p_2}	-.35	-	Simulated delay models
a_{p_3}	.04	-	Simulated delay models
a_{p_4}	.35	-	Simulated delay models
a_{p_5}	.007	-	Simulated delay models
a_ϕ	1.5	sec^{-1}	
K_u	1.0	sec^{-2}	Simulated delay models
K_p	1.0	-	Simulated delay models
K_{ϵ_e}	3.0	-	Nonlinear models
K'_{ϵ_e}	.000047 at 9 NMi to .000221 at .75 NMi	$\frac{\text{rad}}{\text{ft}}$	Linear model $K'_{\epsilon_e} = \frac{K_{\epsilon_e}}{X'+L}$
K_ϕ	1.33	sec	
K_ψ	1.9	-	
K_{ψ_e}	1.0	-	

Table G-5 Model Parameter Values for FC-ILS-I-STOL (Continued)

Symbol	Value	Units	Comments
L	9000.	feet	
N_R	± 0.00048	rad	White gaussian noise 1 σ value
N_T	± 0.001745	rad	White gaussian noise 1 σ value
N_ϵ	± 0.00349	rad	White gaussian noise 1 σ value
N_ϕ	± 0.1169 at 9 Nmi; ± 0.0218 at 0 Nmi	rad	White gaussian noise 1 σ value (Varies linearly with range)
N_ψ	± 0.01745	rad	White gaussian noise 1 σ value
V	236.4	ft/sec	140 knots
γ	2.5	deg	
θ_o	0.	rad	Assumed
τ_p	.7	sec	
ϕ_{LIM}	.367	rad	
$\dot{\phi}_{LIM}$.1745	rad/sec	10 deg/sec
$\dot{\psi}_{LIM}$.0524	rad/sec	3 deg/sec
ψ_R	3.1416	rad	Arbitrary heading for an approach

Table G-6

Initial Distributions for FC-ILS-I-CTOL (at $X'_0 = 6\text{Nmi}$)

Symbol	Distribution	σ	Units
Y'_0	Modified Burgerhout	348.	feet
ψ_0	Gaussian	.02	radians
ϕ_0	Gaussian	.01	radians

Mean = 0

Table G-7 Model Parameter Values for FC-ILS-II-CTOL

Symbol	Value	Units	Comments
a_a	1.0	sec^{-1}	
a_{p_1}	.04	-	Simulated delay models
a_{p_2}	-.35	-	Simulated delay models
a_{p_3}	.04	-	Simulated delay models
a_{p_4}	.35	-	Simulated delay models
a_{p_5}	.007	-	Simulated delay models
a	1.5	sec^{-1}	
a	1.0	sec^{-2}	Simulated delay models
K_p	1.0	-	Simulated delay models
F_e	4.5	-	Nonlinear models
k_e	.000075 at 9 N/mi to .000354 at .75 N/mi	$\frac{\text{rad}}{\text{ft}}$	Linear model $k'_e = \frac{k_e}{X'+L}$
τ	1.33	sec	
K_d	1.9	-	
K	1.0	-	

Table G-7 Model Parameter Values for FC-ILS-II-CTOL (Continued)

Symbol	Value	Units	Comments
L	9000.	feet	
N_R	$\pm .00048$	rad	White gaussian noise 1 σ value
N_T	$\pm .001248$	rad	White gaussian noise 1 σ value
N_ϵ	$\pm .00349$	rad	White gaussian noise 1 σ value
N_ϕ	$\pm .1034$ at 9 NMi; $\pm .0286$ at 0 NMi	rad	White gaussian noise 1 σ value (Varies linearly with range)
N_ψ	$\pm .01745$	rad	White gaussian noise 1 σ value
V	236.4	ft/sec	140 knots
γ	2.5	deg	
θ_o	0.	rad	Assumed
τ_p	.7	sec	
ϕ_{LIM}	.367	rad	
$\dot{\phi}_{LIM}$.1745	rad/sec	10 deg/sec
$\dot{\psi}_{LIM}$.0524	rad/sec	3 deg/sec
ψ_R	3.1416	rad	Arbitrary heading for an approach

Table G-8

Initial Distributions for FC-ILS-II-CTOL (at $X'_0 = 5.34\text{NMi}$)

Symbol	Distribution	σ	Units
Y'_0	Modified Burgerhout	135.	feet
ψ_0	Gaussian	.02	radians
ϕ_0	Gaussian	.01	radians

Mean = 0

Table G-9 Model Parameter Values for BC-ILS-I-CTOL

Symbol	Value	Units	Comments
a_a	1.0	sec^{-1}	
a_{p_1}	.04	-	Simulated delay models
a_{p_2}	-.35	-	Simulated delay models
a_{p_3}	.04	-	Simulated delay models
a_{p_4}	.35	-	Simulated delay models
a_{p_5}	.007	-	Simulated delay models
a_ϕ	1.5	sec	
K_a	1.0	sec^{-2}	
K_p	1.0	-	Simulated delay models
K_{ϵ_e}	3.0	-	Nonlinear models
K'_{ϵ_e}	.000047 at 9 NMi to .000221 at .75 NMi	$\frac{\text{rad}}{\text{ft}}$	Linear model $K'_{\epsilon_e} = \frac{K_{\epsilon_e}}{X' + L}$
K_ϕ	1.33	sec	
K_ψ	1.9	-	
K_{ψ_e}	1.0	-	

Table G-9 Model Parameter Values for BC-ILS-I-CTOL (Continued)

Symbol	Value	Units	Comments
L	-1000.	feet	
N_R	± 0.00048	rad	White gaussian noise 1 σ value
N_T	± 0.001745	rad	White gaussian noise 1 σ value
N_E	± 0.00349	rad	White gaussian noise 1 σ value
N_ϕ	$\pm 0.1034; 9 \text{ NMi}$ $\pm 0.0279; 0 \text{ NMi}$	rad	White gaussian noise 1 σ value (Varies linearly with range)
N_ψ	± 0.01745	rad	White gaussian noise 1 σ value
V	236.4	ft/sec	140 knots
γ	2.5	deg	
θ_o	0.	rad	Assumed
τ_p	.7	sec	
ϕ_{LIM}	.367	rad	
$\dot{\phi}_{LIM}$.1745	rad/sec	10 deg/sec
$\dot{\psi}_{LIM}$.0524	rad/sec	3 deg/sec
ψ_R	3.1416	rad	Arbitrary heading for an approach

Table G-10

Initial Distributions for BC-ILS-I-CTOL (at $X'_0 = 5.18771$)

Symbol	Distribution	σ	Units
Y'_0	Modified Burgerhout	562.	feet
ψ_0	Gaussian	.02	radians
ϕ_0	Gaussian	.01	radians

Mean = 0

Table G-11 Model Parameter Values for VOR-CTOL

Symbol	Value	Units	Comments
a_a	1.0	sec^{-1}	
a_{p_1}	.04	-	Simulated delay models
a_{p_2}	-.35	-	Simulated delay models
a_{p_3}	.04	-	Simulated delay models
a_{p_4}	.35	-	Simulated delay models
a_{p_5}	.007	-	Simulated delay models
a_ϕ	1.5	sec^{-1}	
K_a	1.0	sec^{-2}	
K_p	1.0	-	Simulated delay models
$K_{\epsilon e}$	3.0	-	Nonlinear models
$K'_{\epsilon e}$.000047 at 9NMi to .000221 at .75NMi	$\frac{\text{rad}}{\text{ft}}$	Linear model $K'_{\epsilon e} = \frac{K_{\epsilon e}}{X' + L}$
K_ϕ	1.33	sec	
K_ψ	1.9	-	
$K_{\psi e}$	1.0	-	

Table G-11 Model Parameter Values for VOR-CTOL (Continued)

Symbol	Value	Units	Comments
L	4000.	feet	
N_R	$\pm .02155$	rad	White gaussian noise 1 σ value
N_T	$\pm .02182$	rad	White gaussian noise 1 σ value
N_ϵ	$\pm .00349$	rad	White gaussian noise 1 σ value
N_ϕ	$\pm .1034$ at 9 NMI to .0279 at 0 NMI	rad	White gaussian noise 1 σ value (Varies linearly with range)
N_ψ	$\pm .01745$	rad	White gaussian noise 1 σ value
V	236.4	ft/sec	140 knots
γ	2.5	deg	
θ_o	0.	rad	Assumed
τ_p	.7	sec	
ϕ_{LIM}	.367	rad	
$\dot{\phi}_{LIM}$.1745	rad/sec	10 deg/sec
$\dot{\psi}_{LIM}$.0524	rad/sec	3 deg/sec
ψ_R	3.1416	rad	Arbitrary heading for an approach

Table G-12

Initial Distributions for VOR-CTOL (at $X'_0 = 6\text{Nmi}$)

Symbol	Distribution	σ	Units
γ'_0	Modified Burgerhout	546.	feet
ψ_0	Gaussian	.02	radians
ϕ_0	Gaussian	.01	radians

Mean = 0

Table G-13 Model Parameter Values for FC-ILS-I-STOL

Symbol	Value	Units	Comments
a_a	1.667	sec^{-1}	
a_{p_1}	.04	-	Simulated delay models
a_{p_2}	-.35	-	Simulated delay models
a_{p_3}	.04	-	Simulated delay models
a_{p_4}	.35	-	Simulated delay models
a_{p_5}	.007	-	Simulated delay models
a_ϕ	1.5	sec^{-1}	
K_a	1.667	sec^{-2}	
K_p	1.0	-	Simulated delay models
K_{ϵ_e}	4.8	-	Nonlinear models
K'_{ϵ_e}	.000075 at 0 Nmi to .000354 at .75 Nmi	$\frac{\text{rad}}{\text{ft}}$	Linear model $K'_{\epsilon_e} = \frac{K_{\epsilon_e}}{X'+L}$
K_ϕ	1.33	sec	
K_ψ	1.9	-	
K_{ψ_e}	1.0	-	

Table G-13 Model Parameter Values for FC-ILS-I-STOL (Continued)

Symbol	Value	Units	Comments
L	9000.	feet	
N_R	± 0.00048	rad	White gaussian noise 1 σ value
N_T	± 0.001745	rad	White gaussian noise 1 σ value
N_E	± 0.00349	rad	White gaussian noise 1 σ value
N_ϕ	± 0.1047 at 2 Nmi; ± 0.07625 at 0 Nmi	rad	White gaussian noise 1 σ value (Varies linearly with range)
N_ψ	± 0.01745	rad	White gaussian noise 1 σ value
V	108.089	ft/sec	64 knots
γ	7.5	deg	
θ_o	0.	rad	Assumed
τ_p	.7	sec	
ϕ_{LIM}	.367	rad	
$\dot{\phi}_{LIM}$.1745	rad/sec	10 deg/sec
$\dot{\psi}_{LIM}$.0524	rad/sec	3 deg/sec
ψ_R	3.1416	rad	Arbitrary heading for an approach

Table G-14

Initial Distributions for EC-ILS-I-STOL (at $X'_0 = 2NM11$)

Symbol	Distribution	σ	Units
Y'_0	Gaussian	260.	feet
ψ_0	Gaussian	.1	radians
ϕ_0	Gaussian	.02	radians

Mean = 0

APPENDIX H

PROBABILITY DENSITY FUNCTION DATA AND NORMAL OPERATING ZONE DATA

Probability density functions obtained using the techniques described in the Lateral Separation Study are presented in this appendix for the systems listed in Table H-1. The PDF's are used for determining the probability of collision data necessary in the determination of minimum runway spacings. Table H-1 indicates the figure numbers for the PDF's selectable by dimension, approach system, and range. The lateral PDF's are generated by the Fokker-Planck equation and the vertical, and longitudinal PDF's are gaussian fits to the measured and assumed distribution data, respectively. The axes for all the figures were made as compatible as possible so that direct comparisons of the relative shape of the PDF'S could be made.

Normal operating zone data is provided for the approach systems listed in Table H-1 and for STOL runways skewed with respect to the adjacent CTOL runway. Figures H-25 through H-29 present the NOZ's for the five lateral approach systems listed in Table H-1. The five NOZ's are to scale and, therefore, may be compared directly. Table H-2 is a list of the NOZ's at the minimum distance between the CTOL runway and the STOL departure path for skew angles between 10° and 90° in 10° increments.

Table H-1 PDF Cases

Approach Systems	Ranges - nmi	Figure Numbers
<u>Lateral</u>		
FC-ILS-I-CTOL	6, 4, 2	H-1, H-2, H-3
FC-ILS-II-CTOL	, 4, 2	H-4, H-5, H-6
BC-ILS-I-CTOL	5, 4, 2	H-7, H-8, H-9
VOR-CTOL	6, 4, 2	H-10, H-11, H-12
FC-ILS-I-STOL	2, 1.5, .75	H-13, H-14, H-15
<u>Vertical</u>		
FC-ILS-I-CTOL	2, 1.5, .75	H-16, H-17, H-18
FC-ILS-I-STOL	2, 1.5, .75	H-19, H-20, H-21
<u>Longitudinal</u>		
FC-ILS-I-CTOL	6, 4, 2	H-22, H-23, H-24

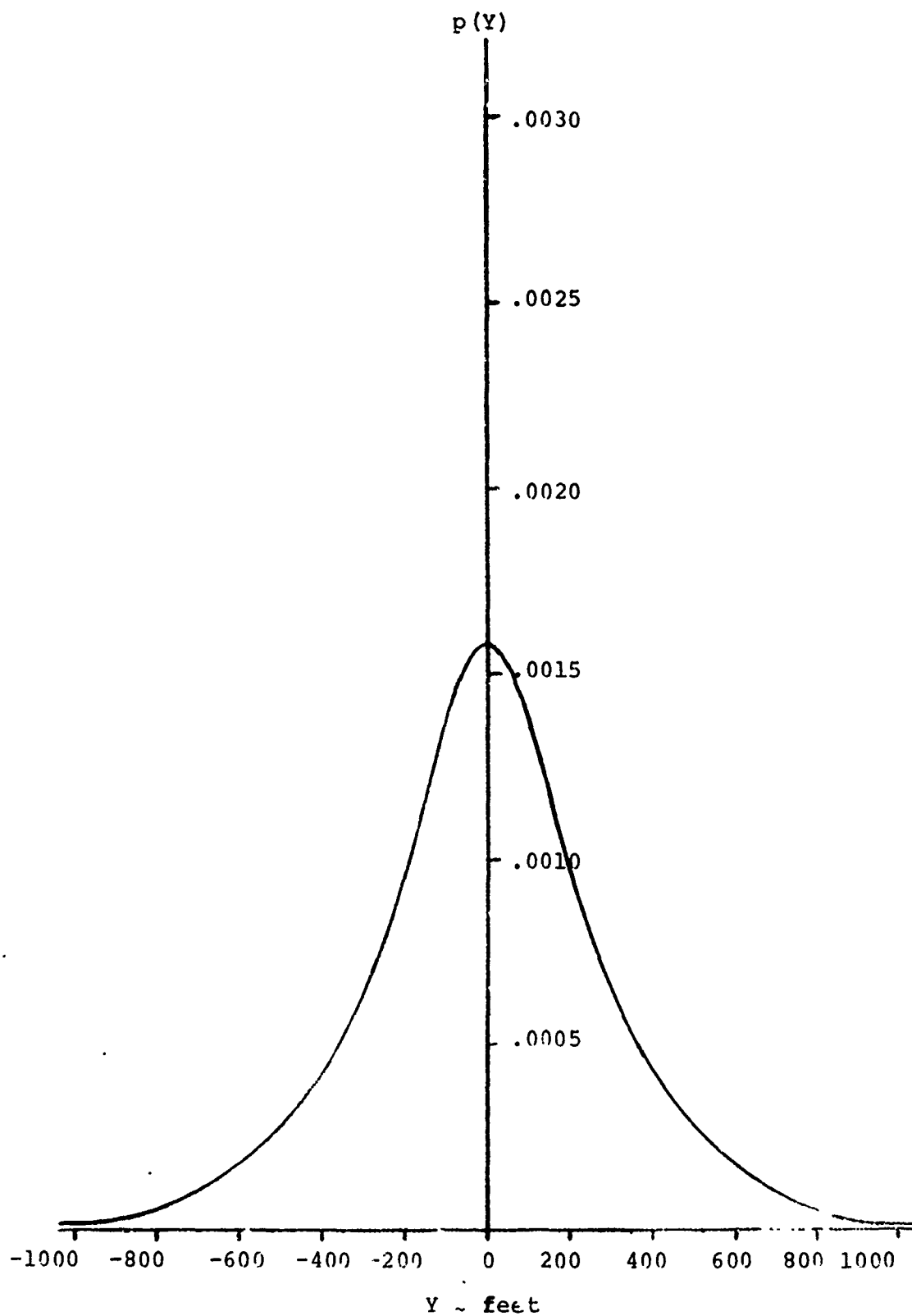


Figure H-1 Lateral PDF for FC-ILS-I-CTOL at Six NM from Touchdown

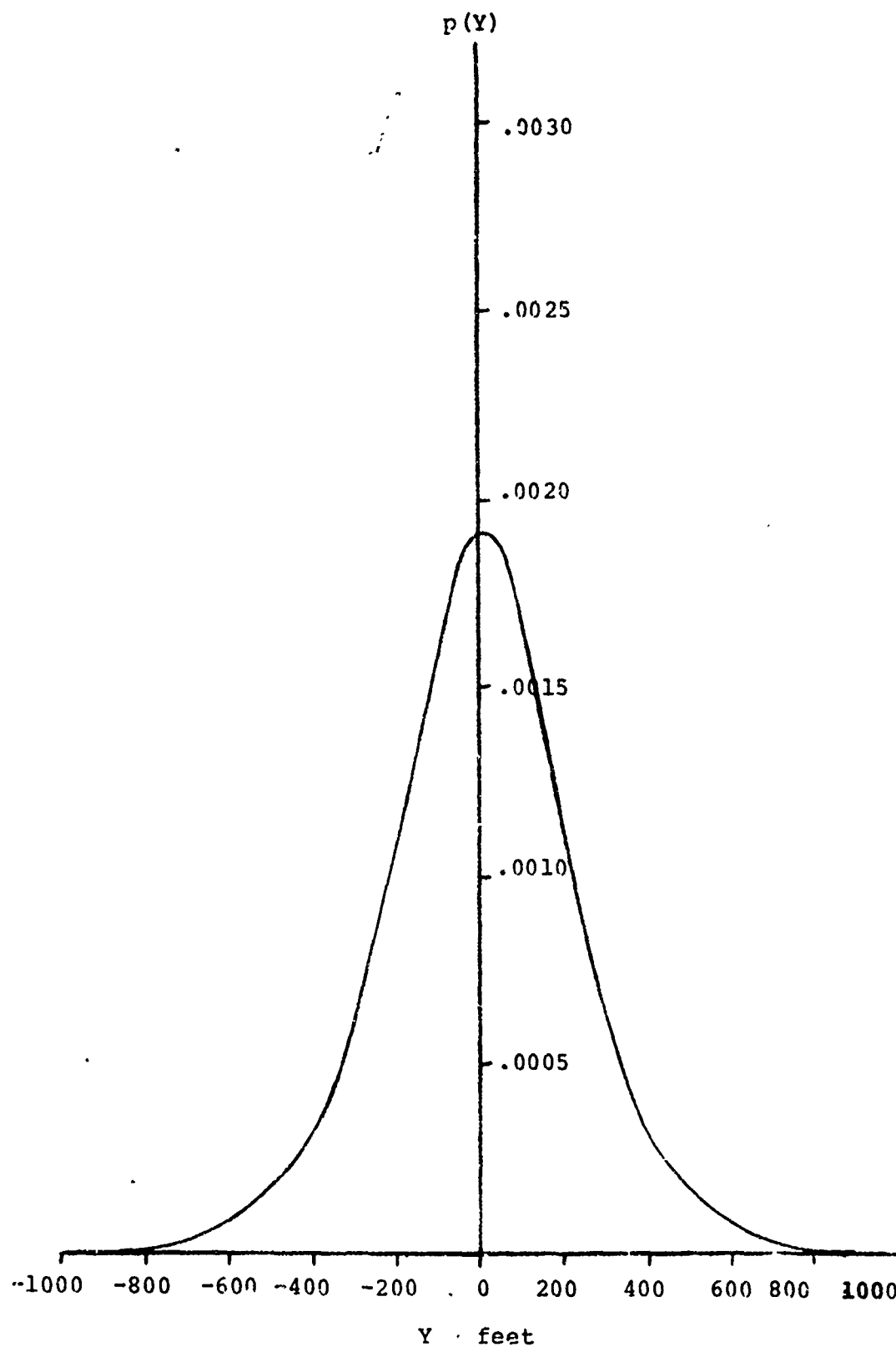


Figure H-2 Lateral PDF for FC-ILS-I-CTOL at Four NMi from Touchdown

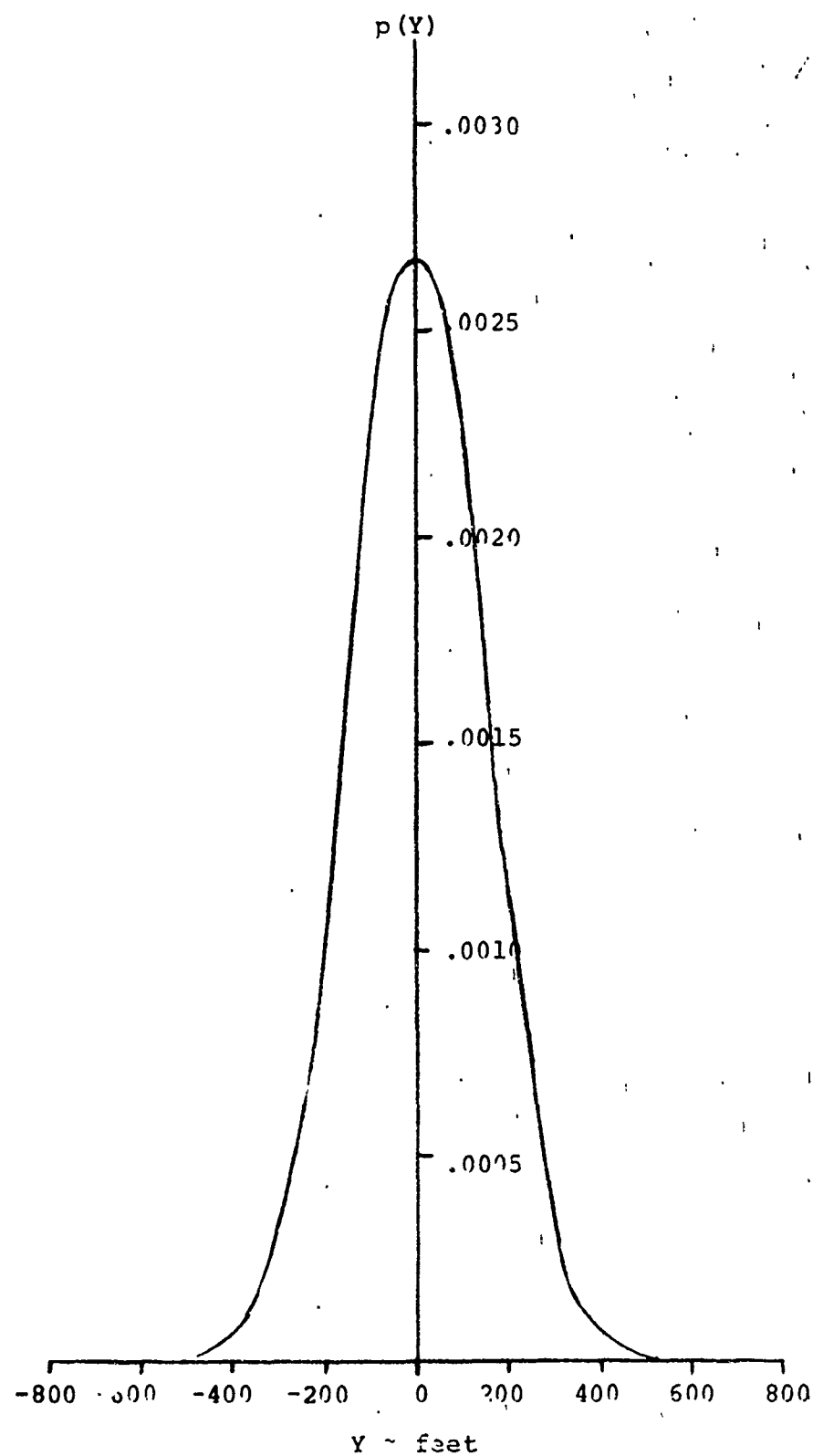


Figure H-3 Lateral PDF for EC-ILS-I-CTOL at Two NMi from Touchdown

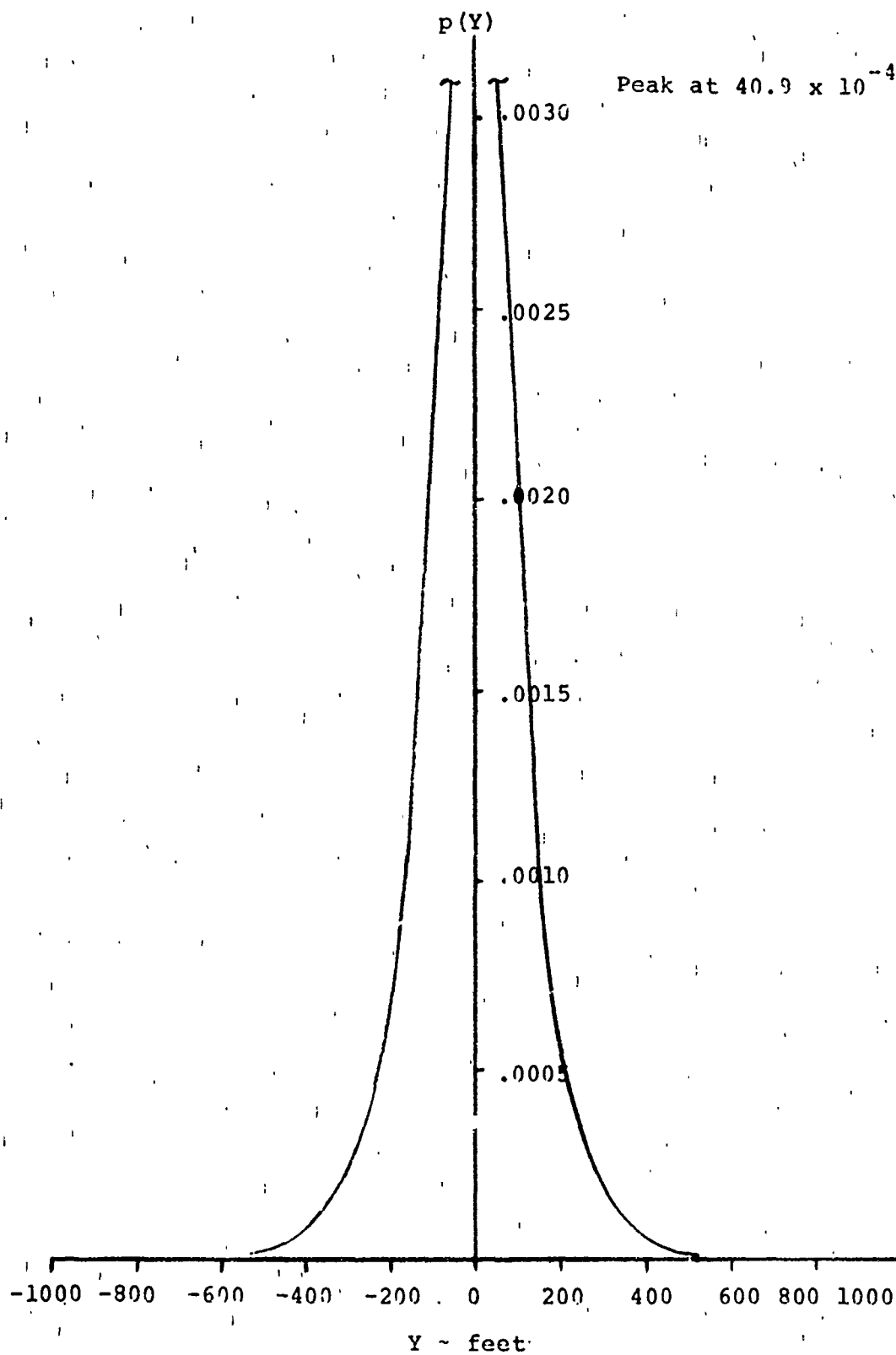


Figure H-4 Lateral PDF for FC-ILS-II-CTOL at Five NMi from Touchdown

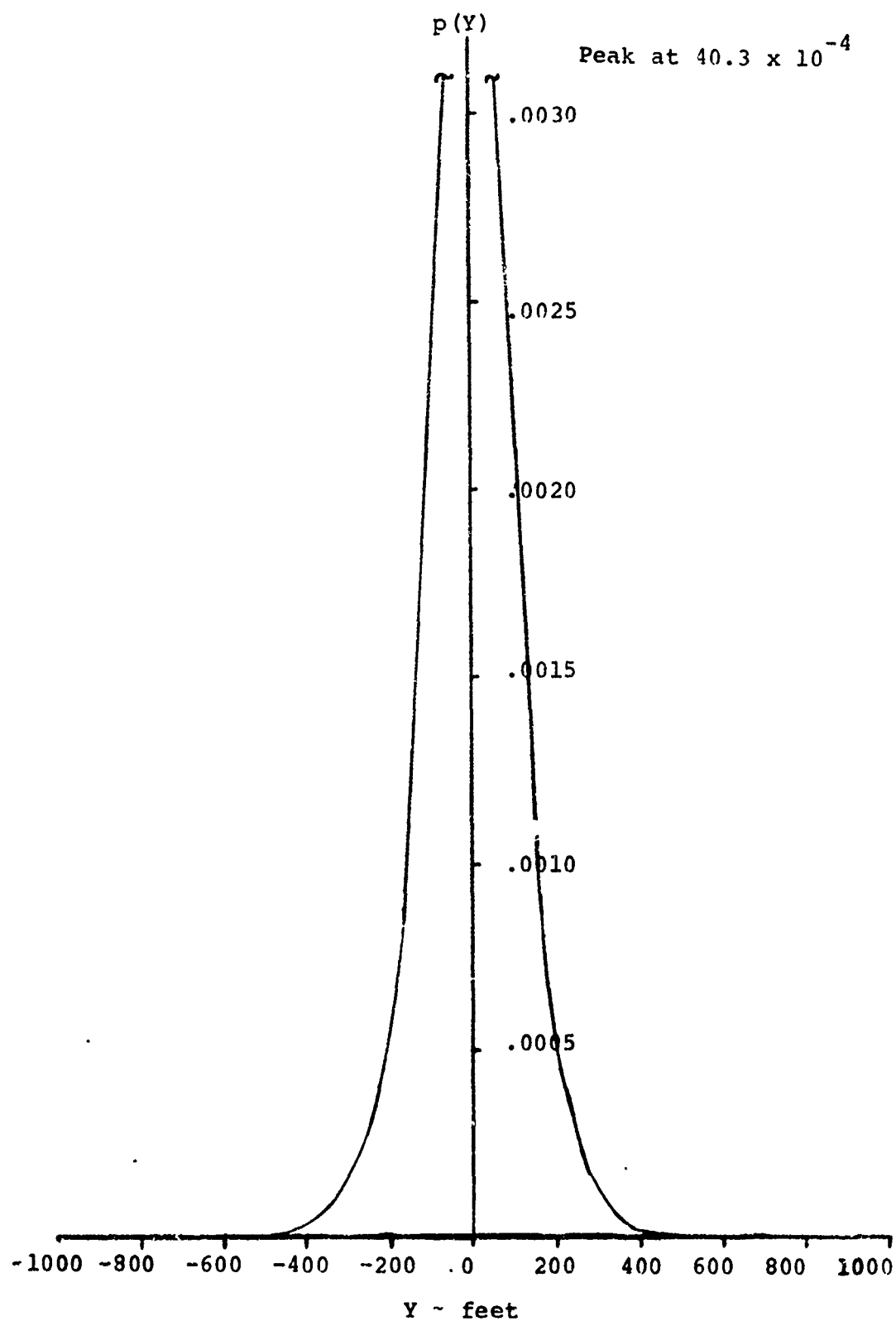


Figure H-5 Lateral PDF for FG-ILS-II-CTOL at Four NMi from Touchdown

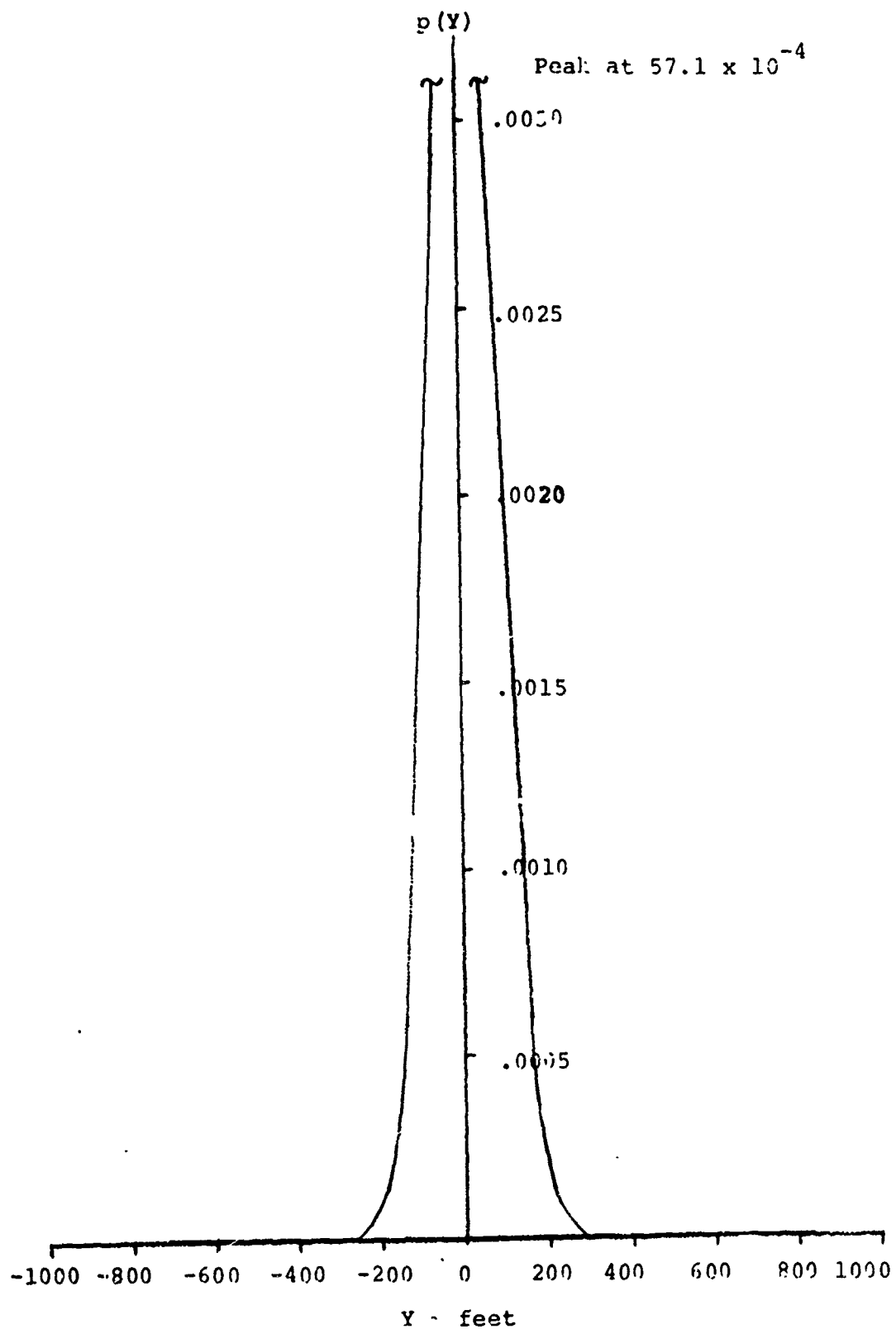


Figure H-6 Lateral PDF for FC-ILS-II-CTOL at Two NMi from Touchdown

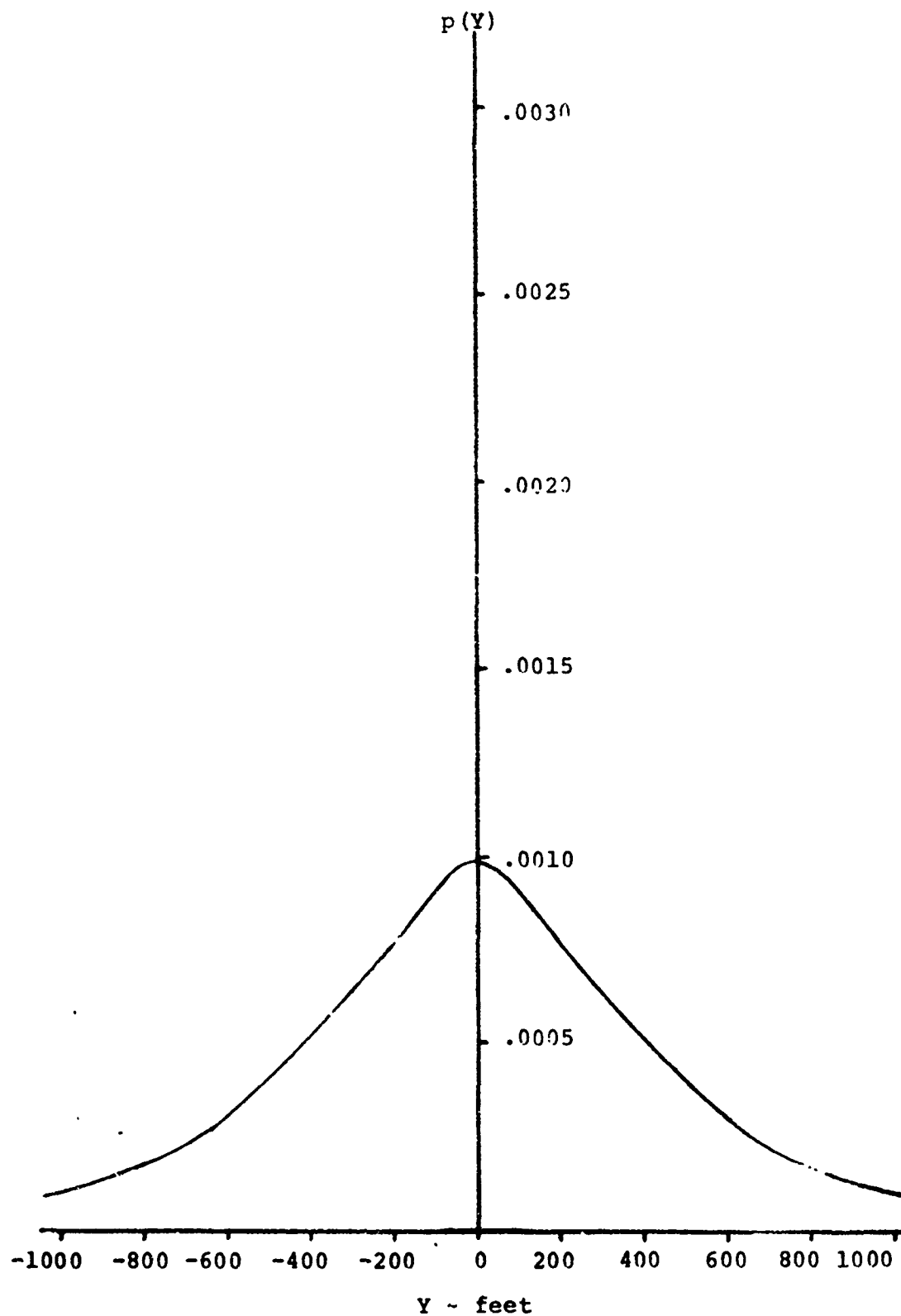


Figure H-7 Lateral PDF for BC-ILS-I-CTOL at Five NMi from Touchdown.

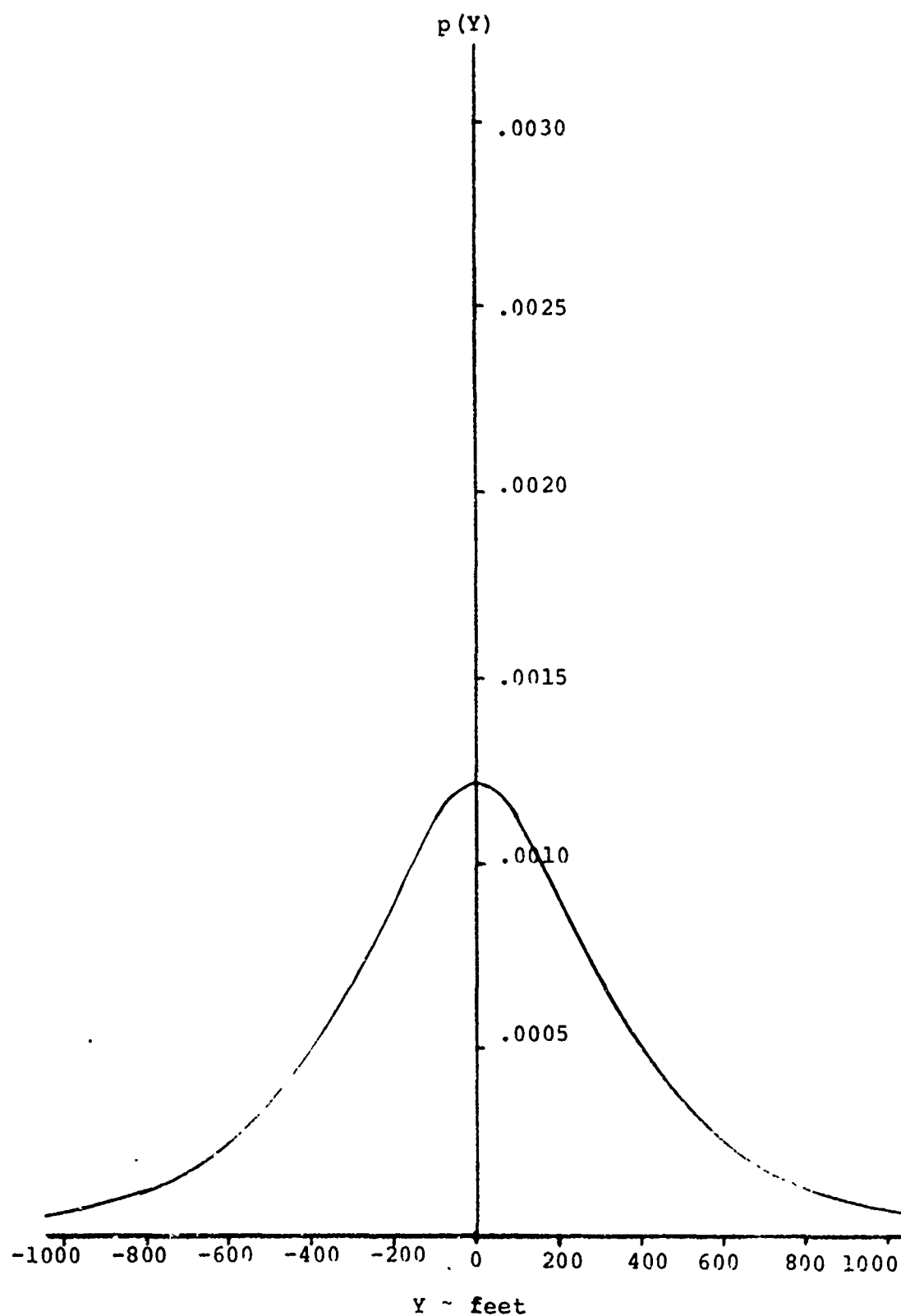


Figure H-8 Lateral PDF for BC-ILS-I-CTOL at Four NMi from Touchdown

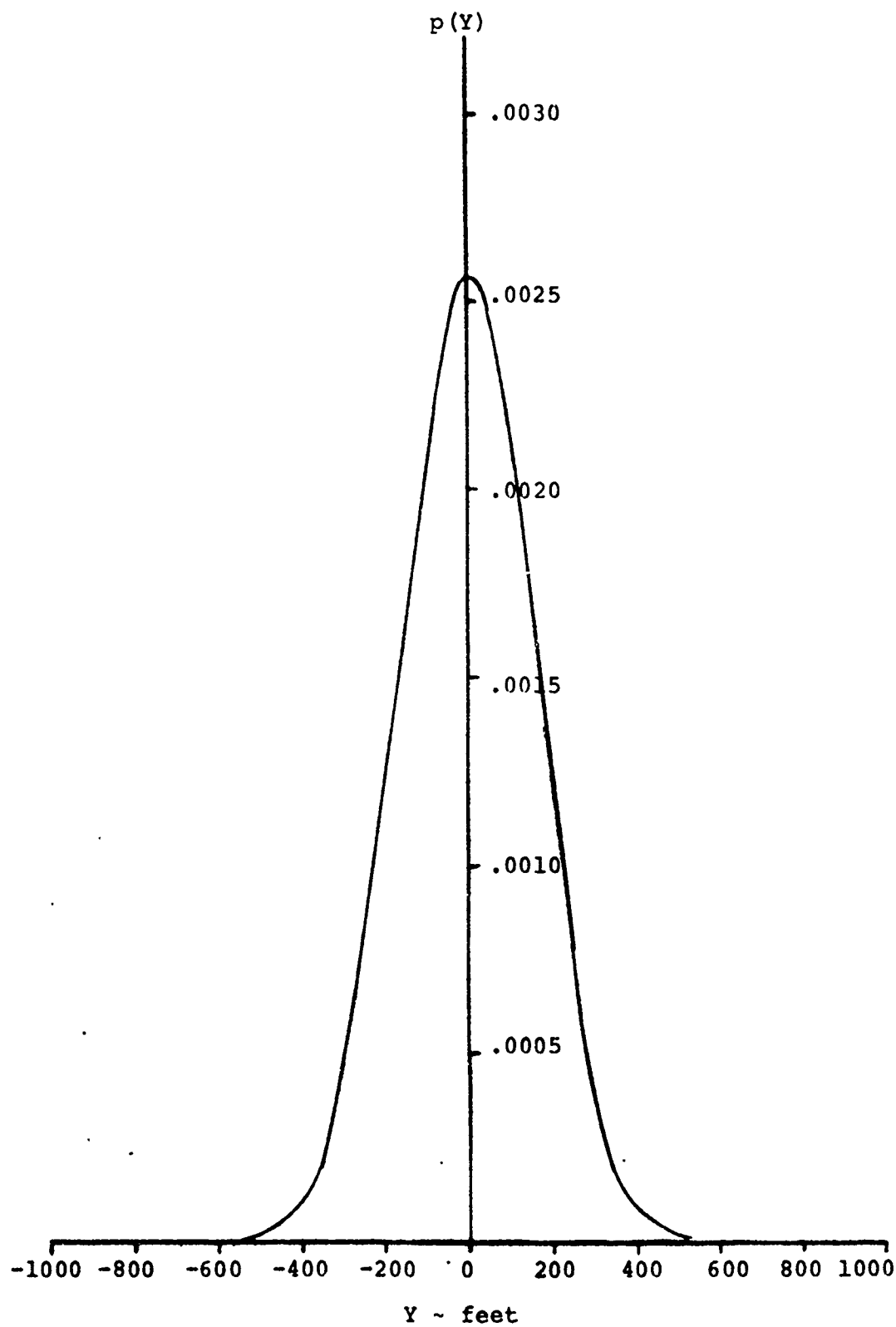


Figure H-9 Lateral PDF for BC-ILS-I-CTOL at Two NMi from Touchdown

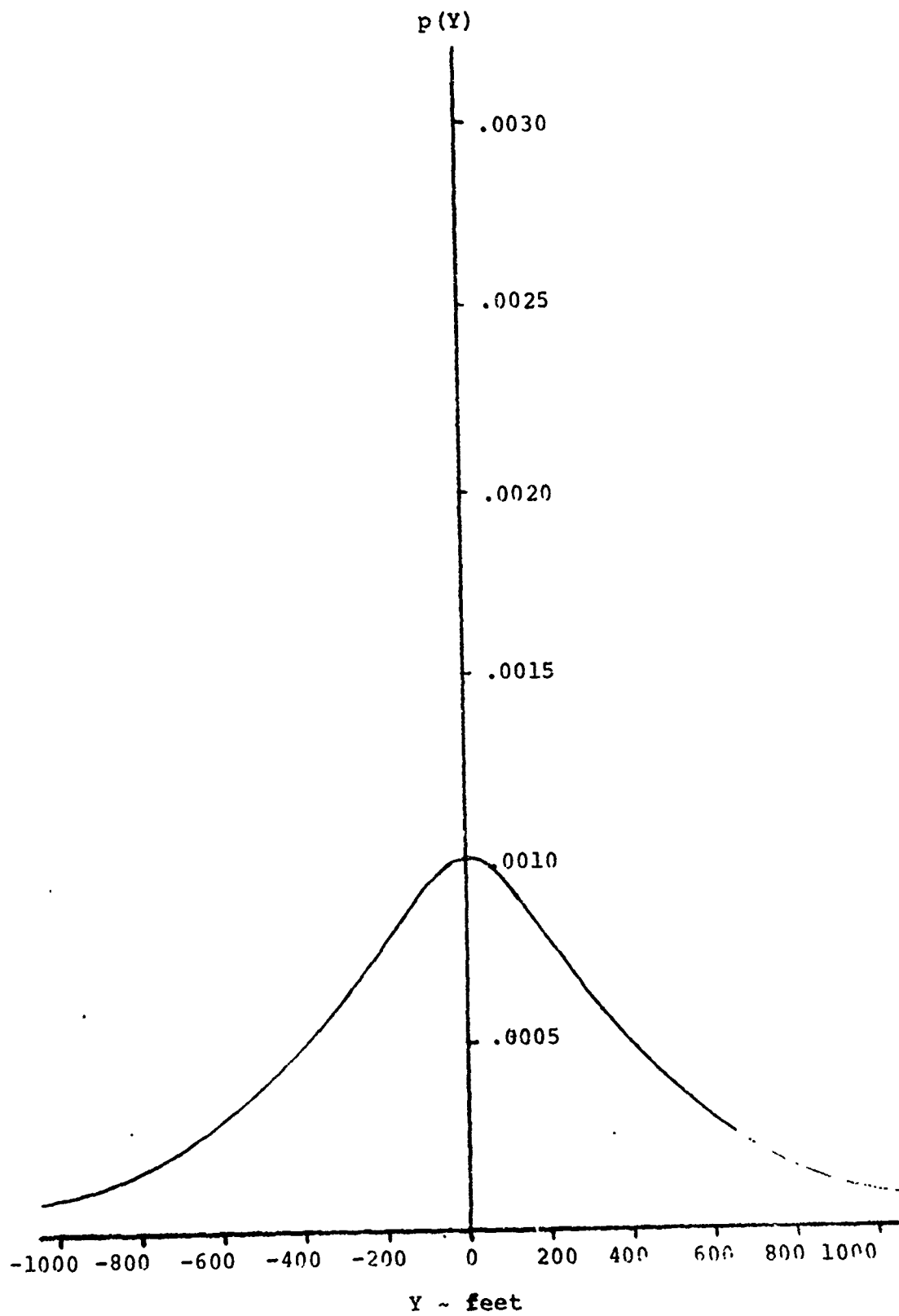


Figure H-10 Lateral PDF for VOR-CTOL at Six NMi from Touchdown

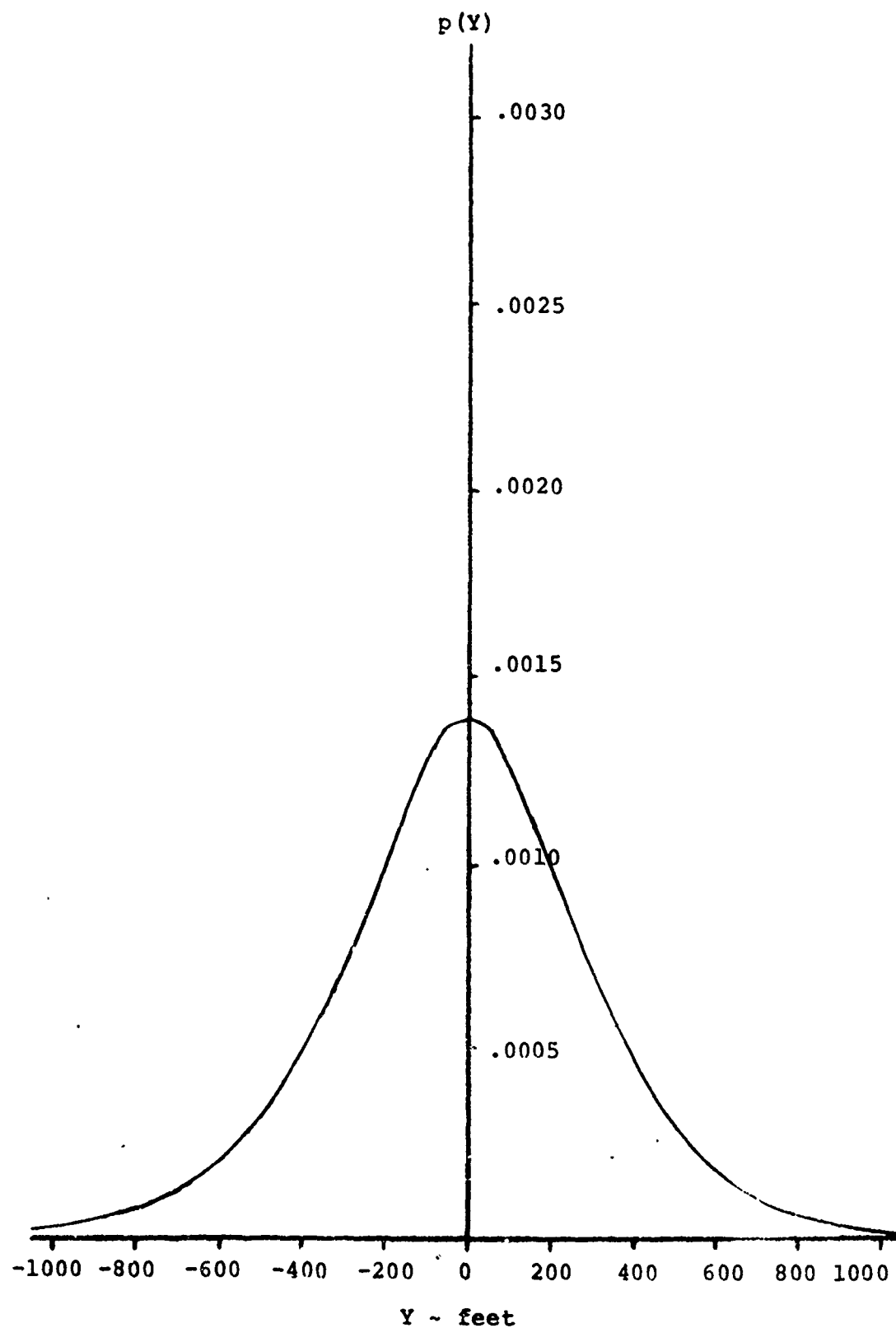


Figure H-11 Lateral PDF for VOR-CTOL at Four NMi from Touchdown

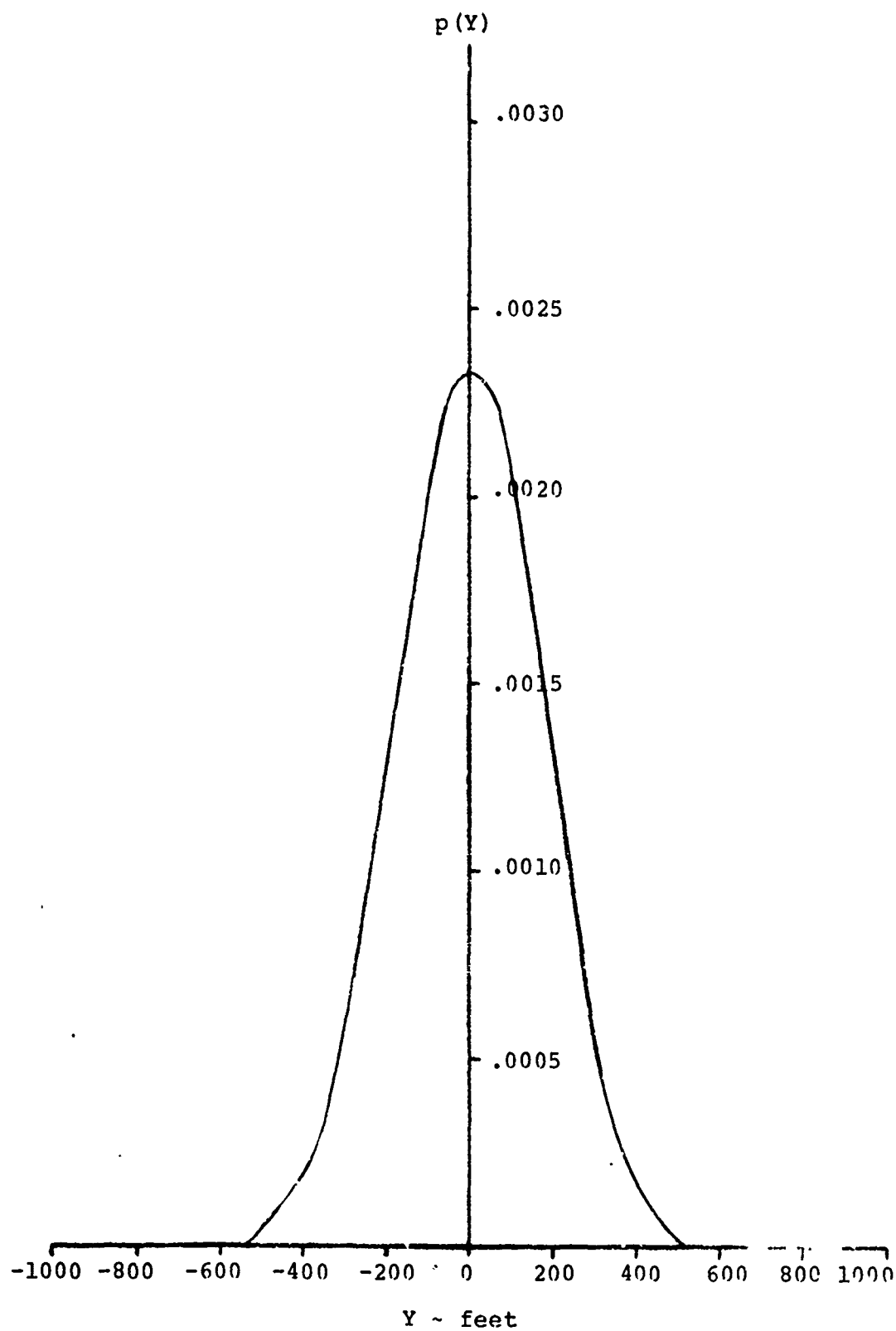


Figure H-12 Lateral PDF for VOR-CTOL at Two NMI from Touchdown

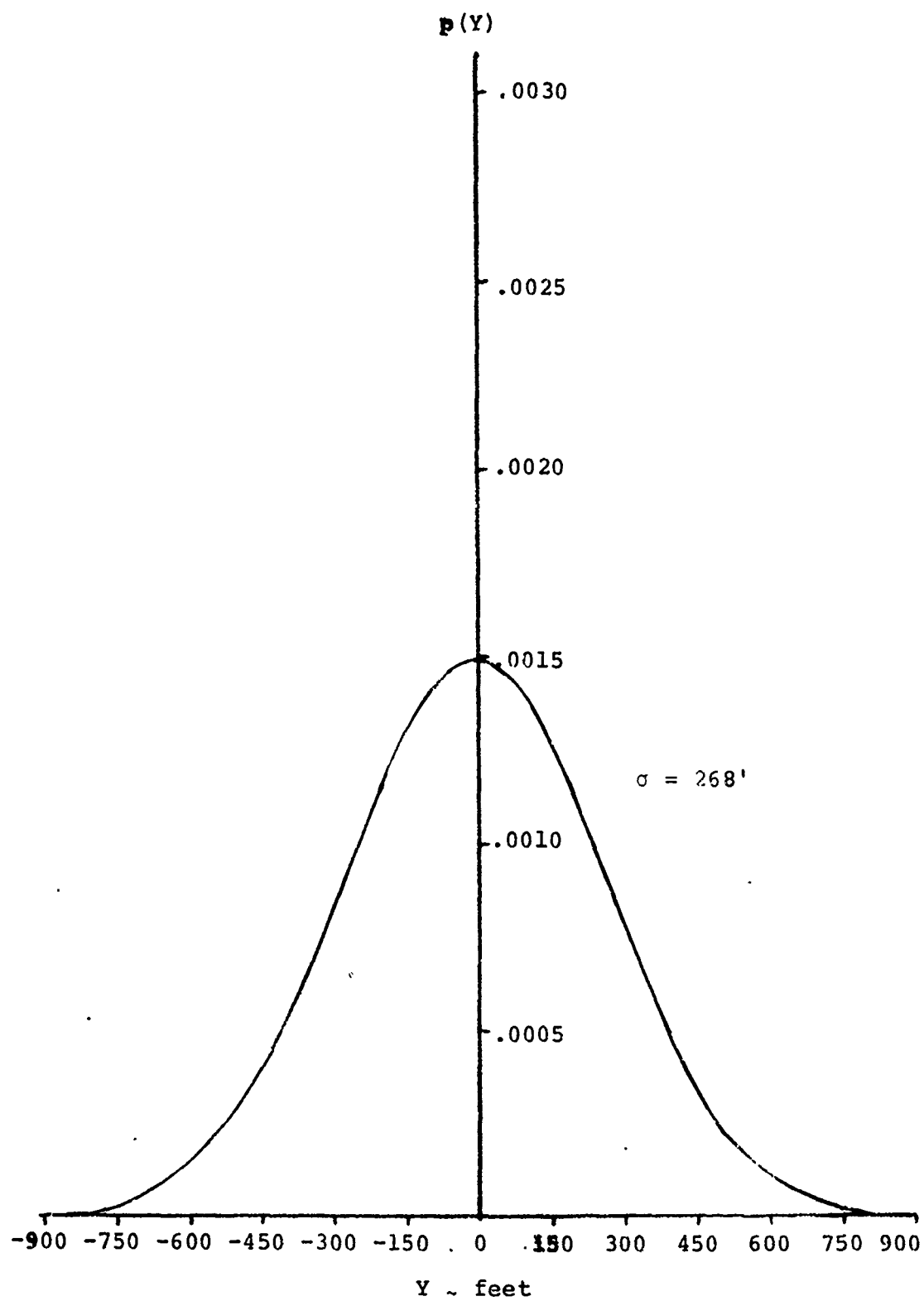


Figure H-13 Lateral PDF for FC-ILS-I-STOL at 2 NMi from Touchdown

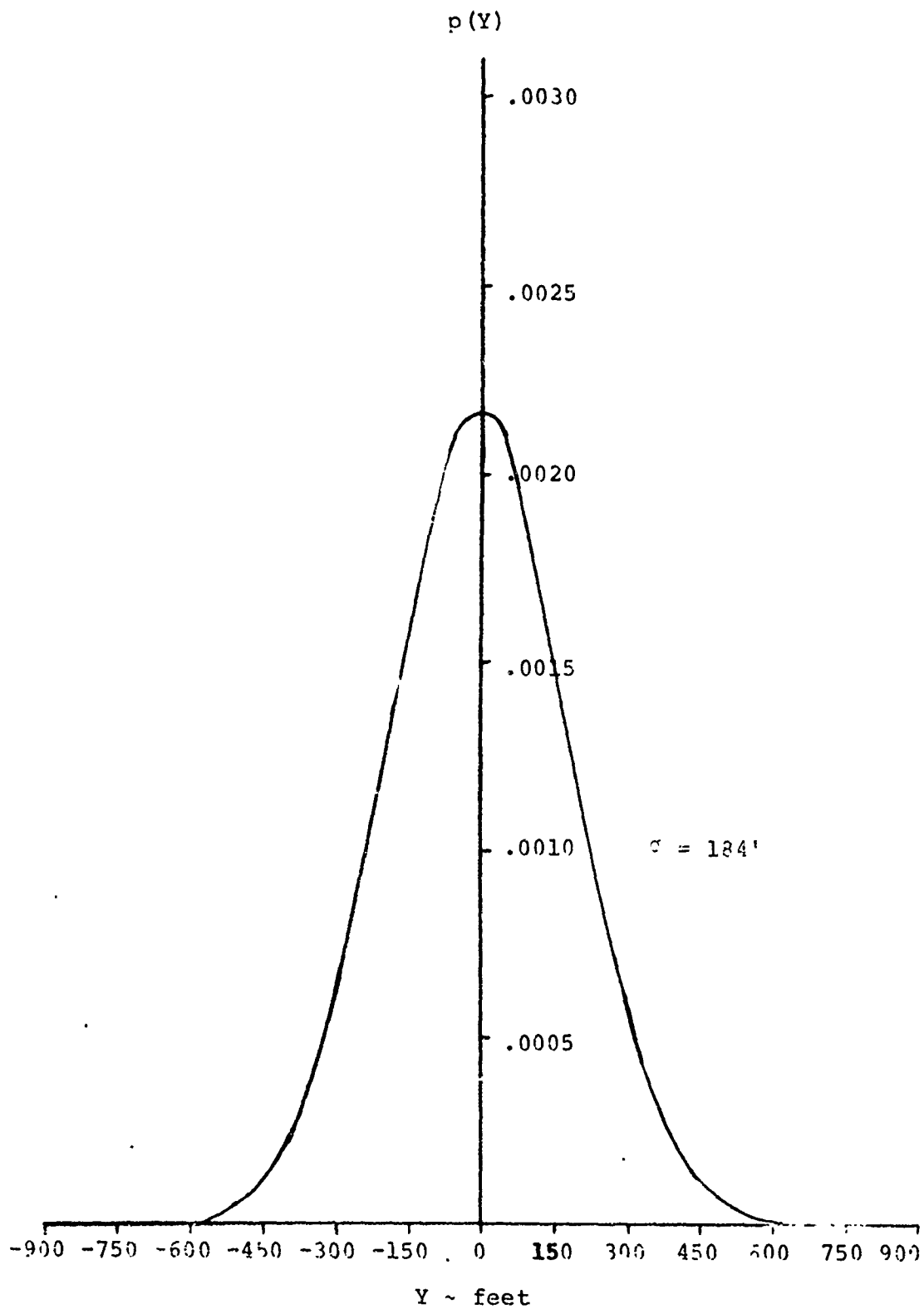


Figure H-14 Lateral PDF for FC-ILS-I-STOL at 1.5 NMi from Touchdown

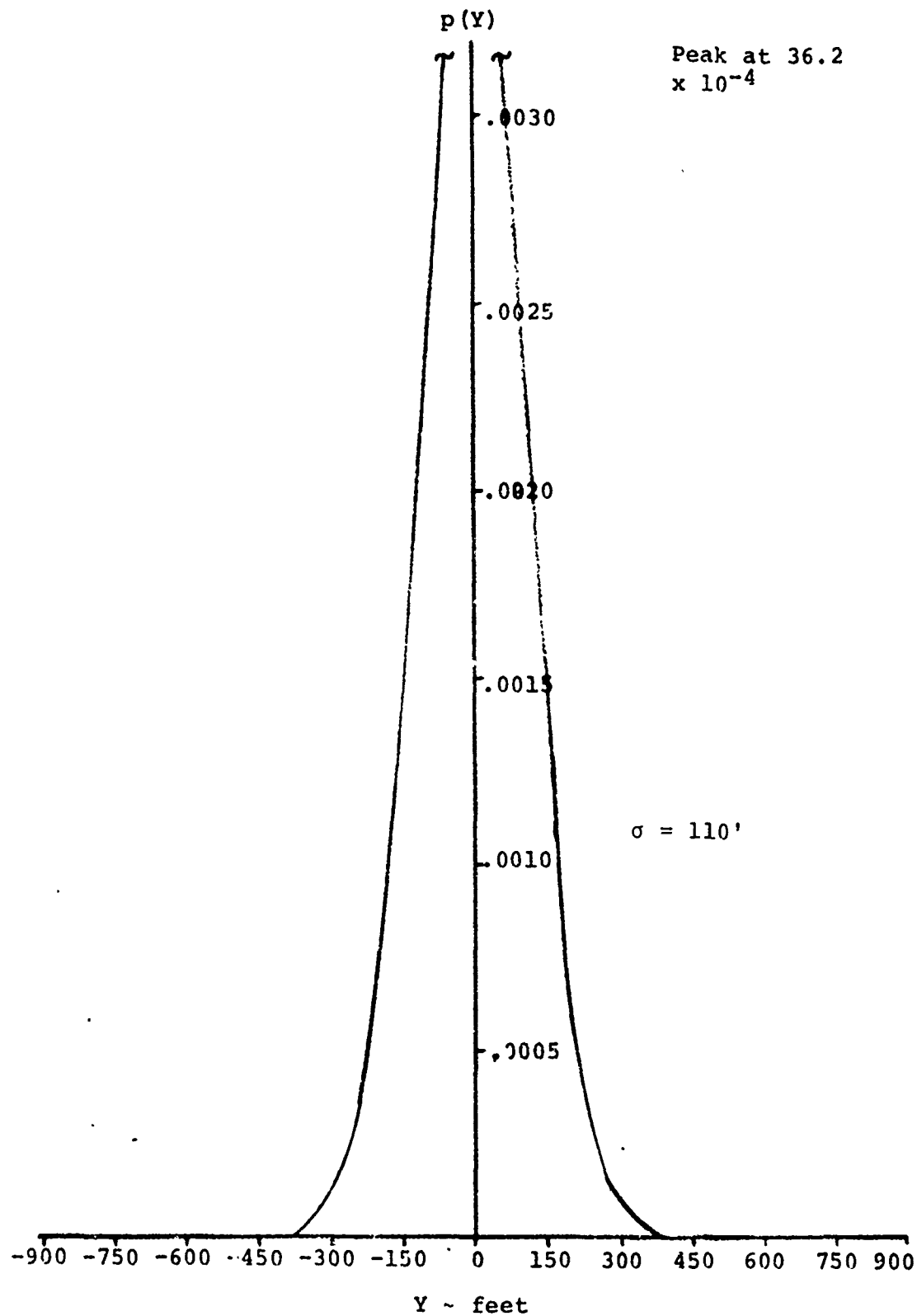


Figure H-15 Lateral PDF for PC-ILS-I-STOL at 75 NMi from Touchdown

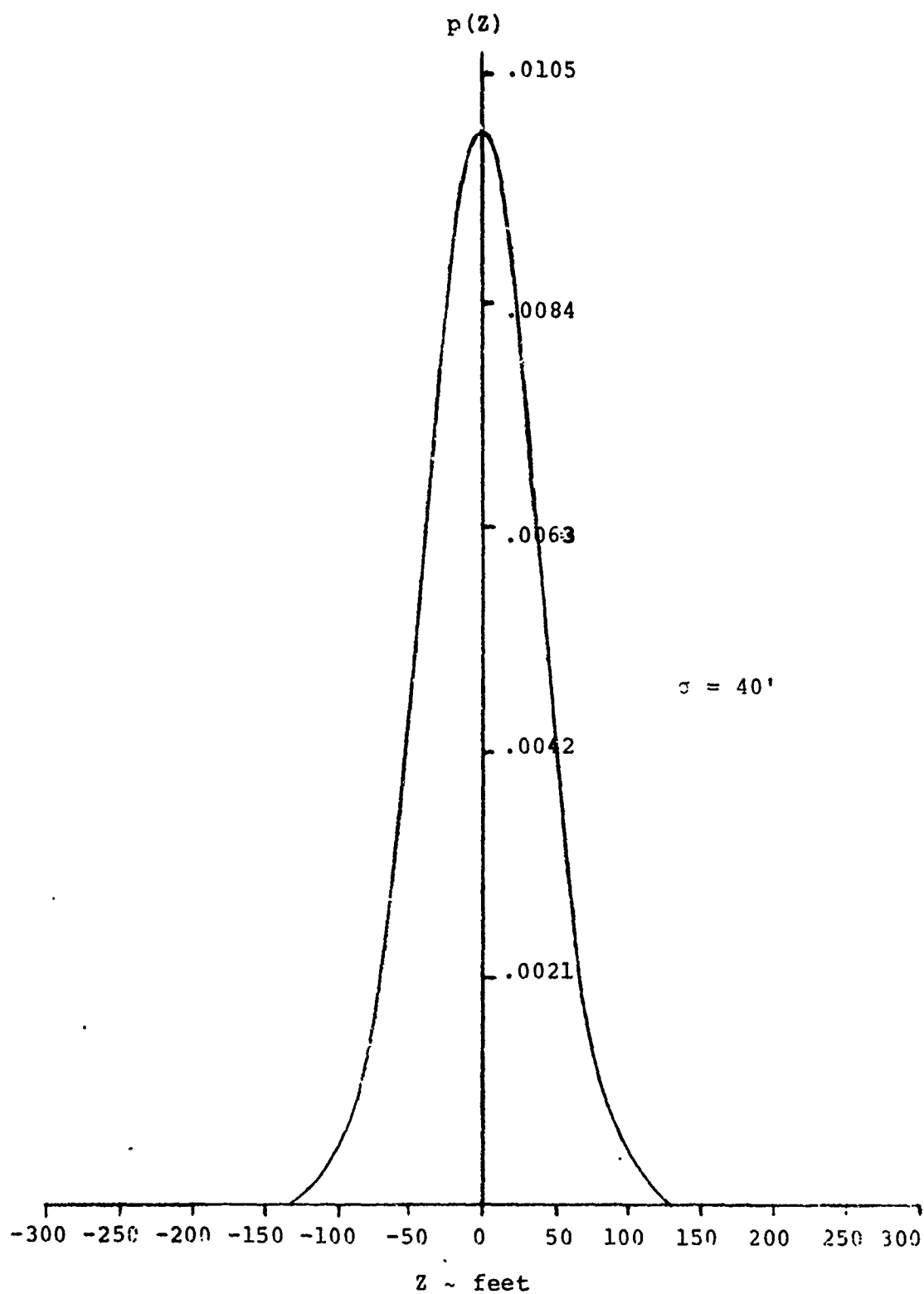


Figure H-16 Vertical PDF for FC-ILS-I-CTOL at 2 NMi from Touchdown

H-

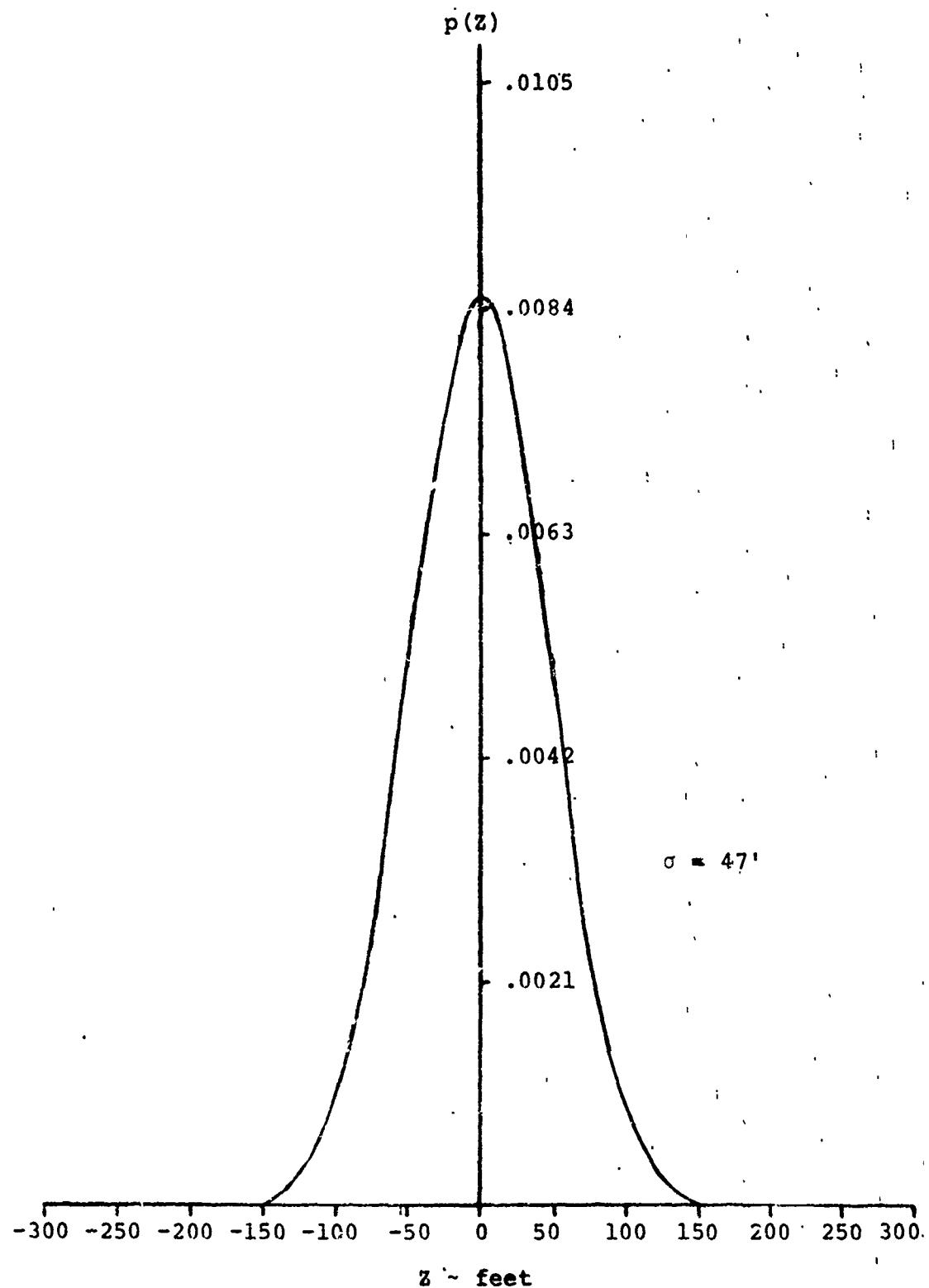


Figure H-17 Vertical PDF for FC-ILS-I-CTOL at 1.5 NMi from Touchdown

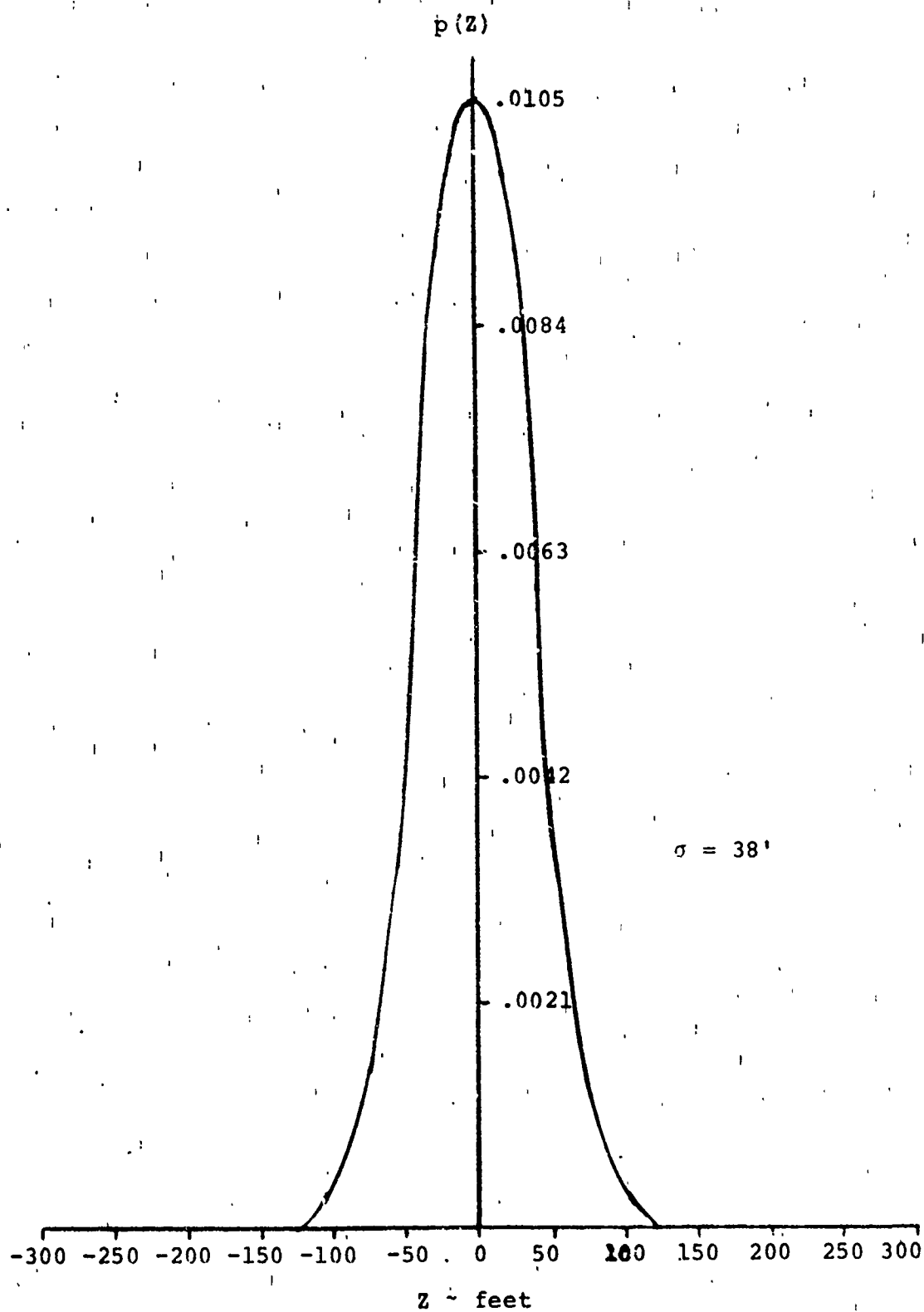


Figure H-18 Vertical PDF for FC-ILS-I-CTOL at .75 NMi from Touchdown

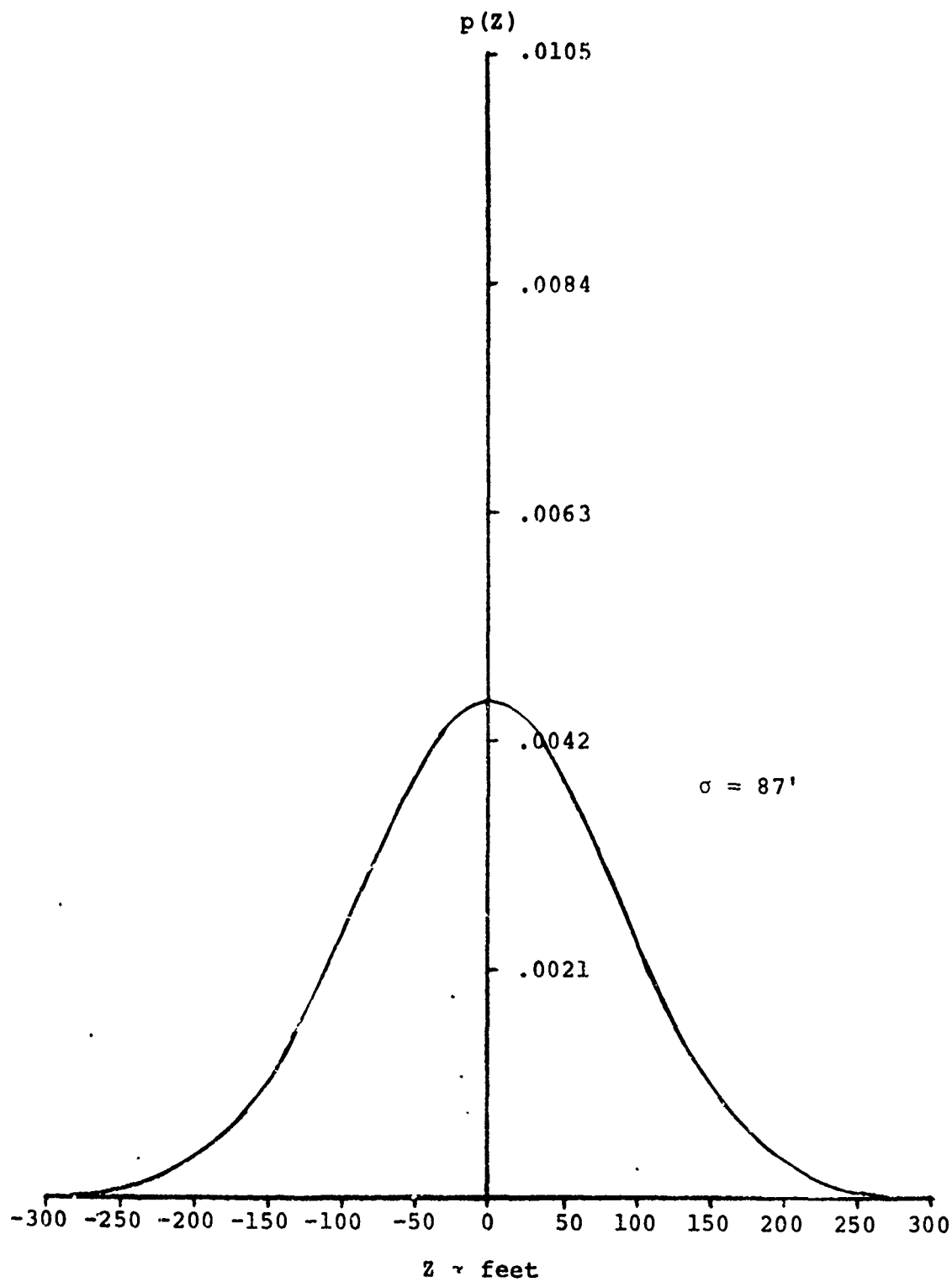


Figure H-19 Vertical PDF for FC-ILS-I-STOL at Two NMi from Touchdown

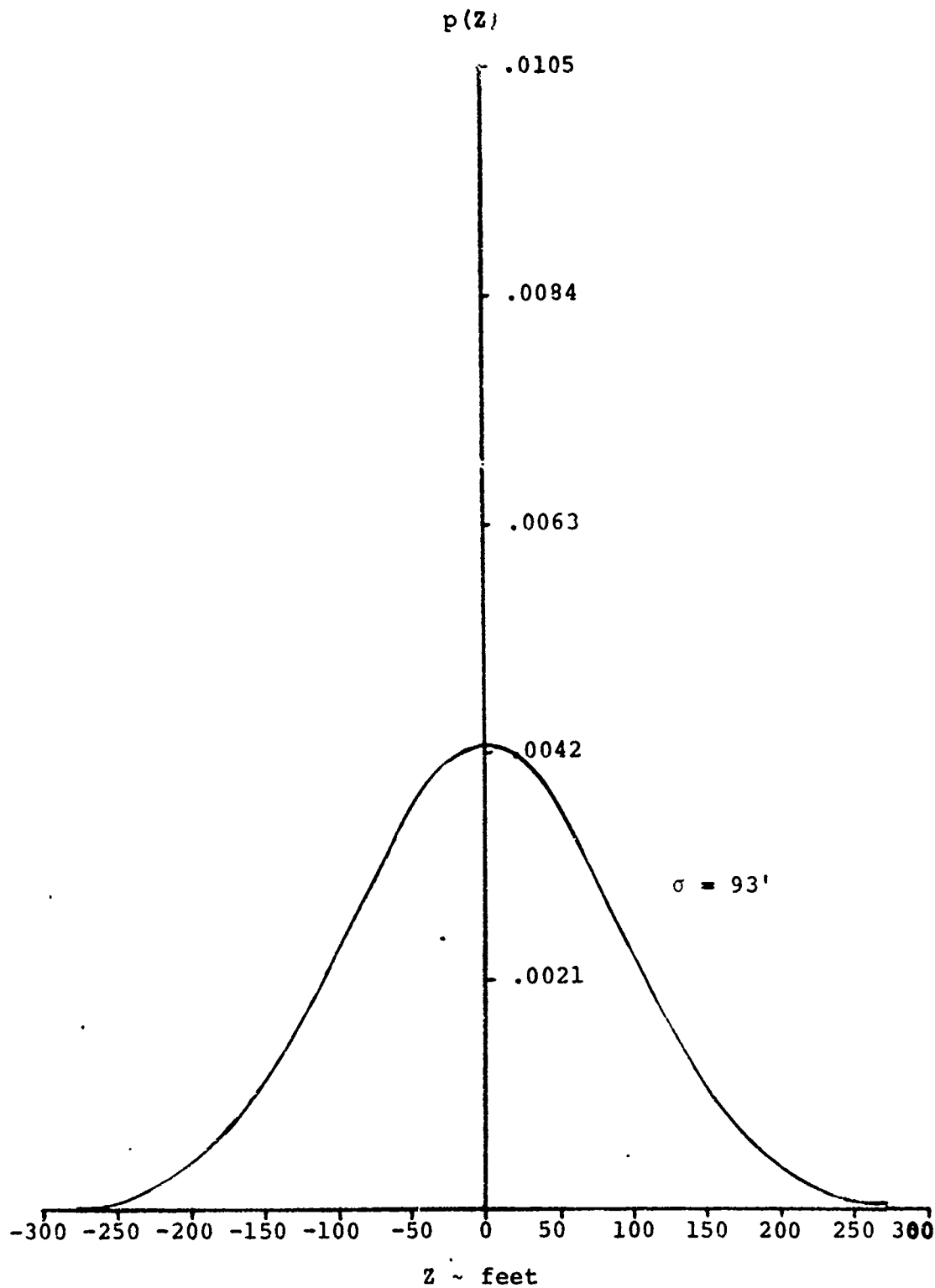


Figure H-20 Vertical PDF for FC-ILS-I-STOL at 1.5 NM from Touchdown

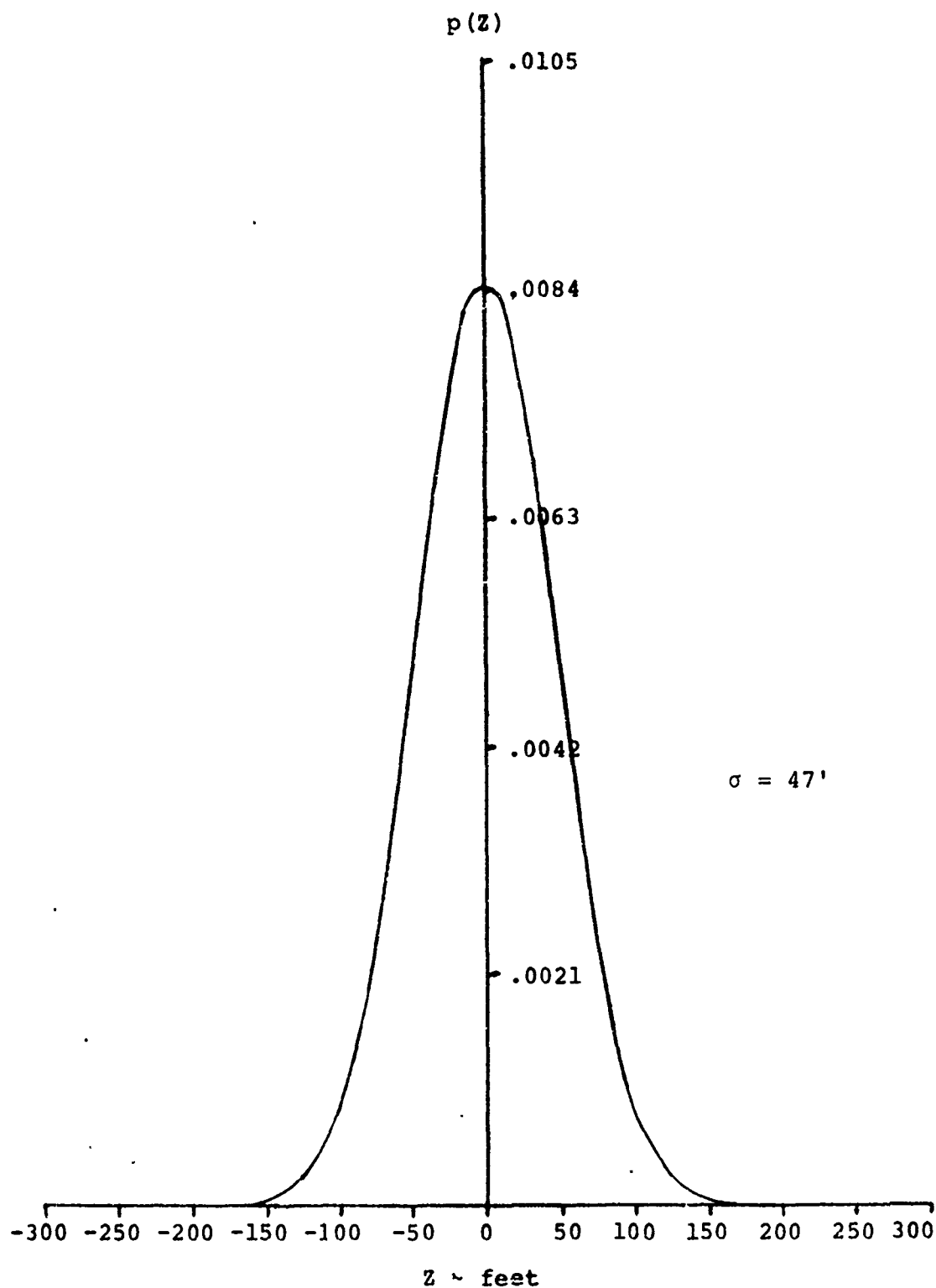


Figure H-21 Vertical PDF for FC-ILS-I-STOL at .75 NMi
from Touchdown

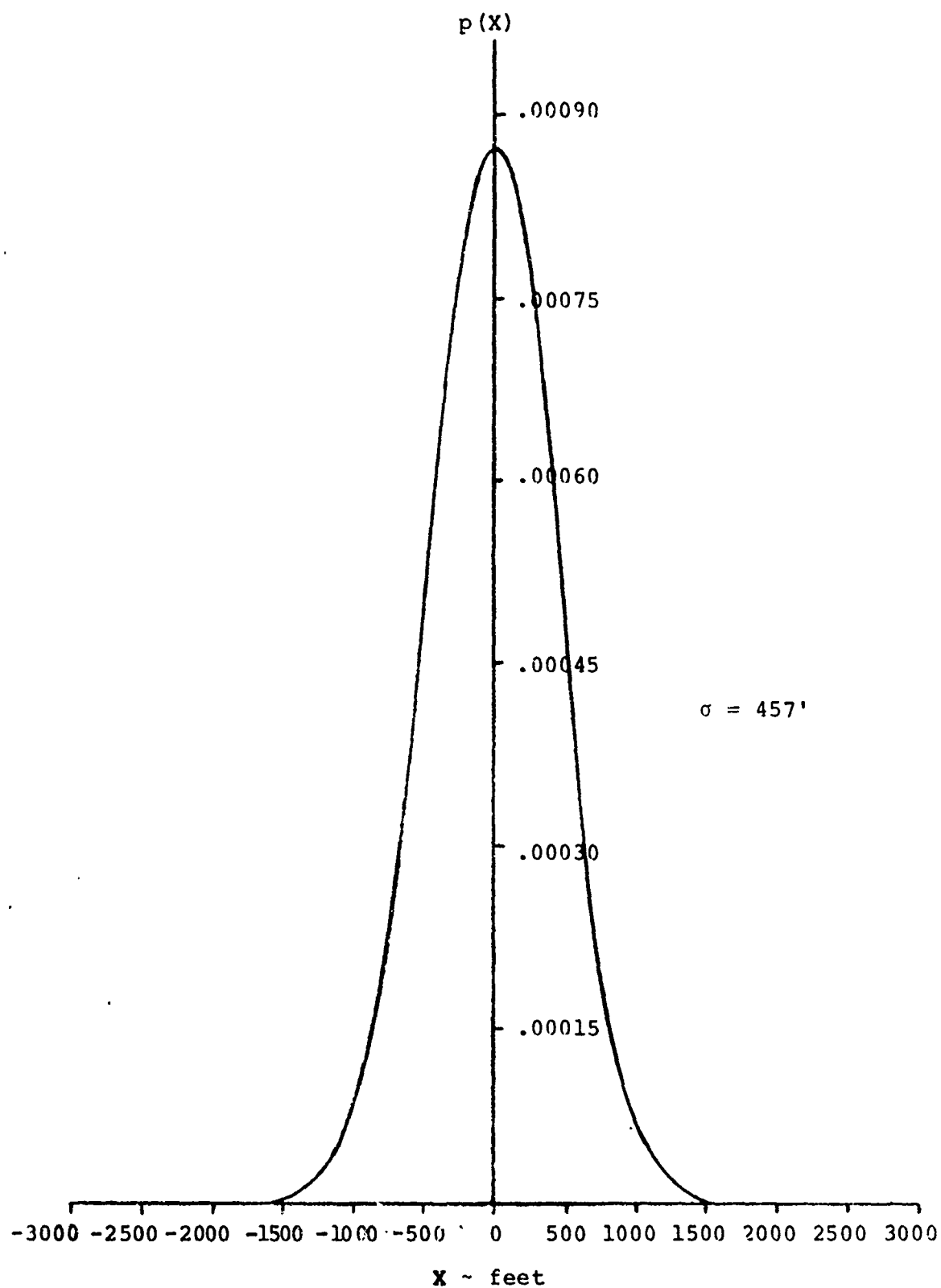


Figure H-22 Longitudinal PDF for FC-ILS-I-CTOL at Six NMi from Touchdown

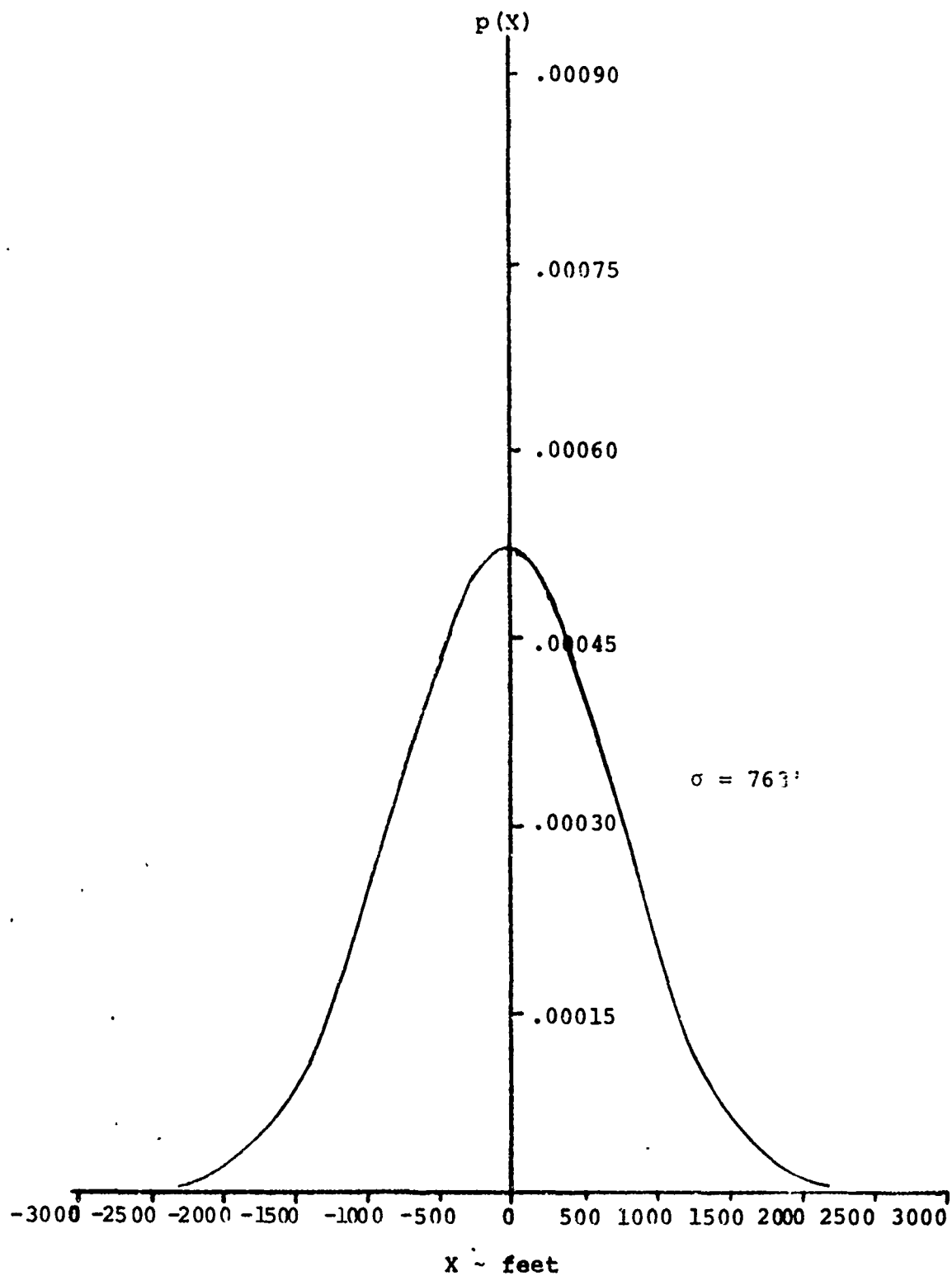


Figure H-23 Longitudinal PDF for FC-ILS-I-CTOL at Four NMi from Touchdown

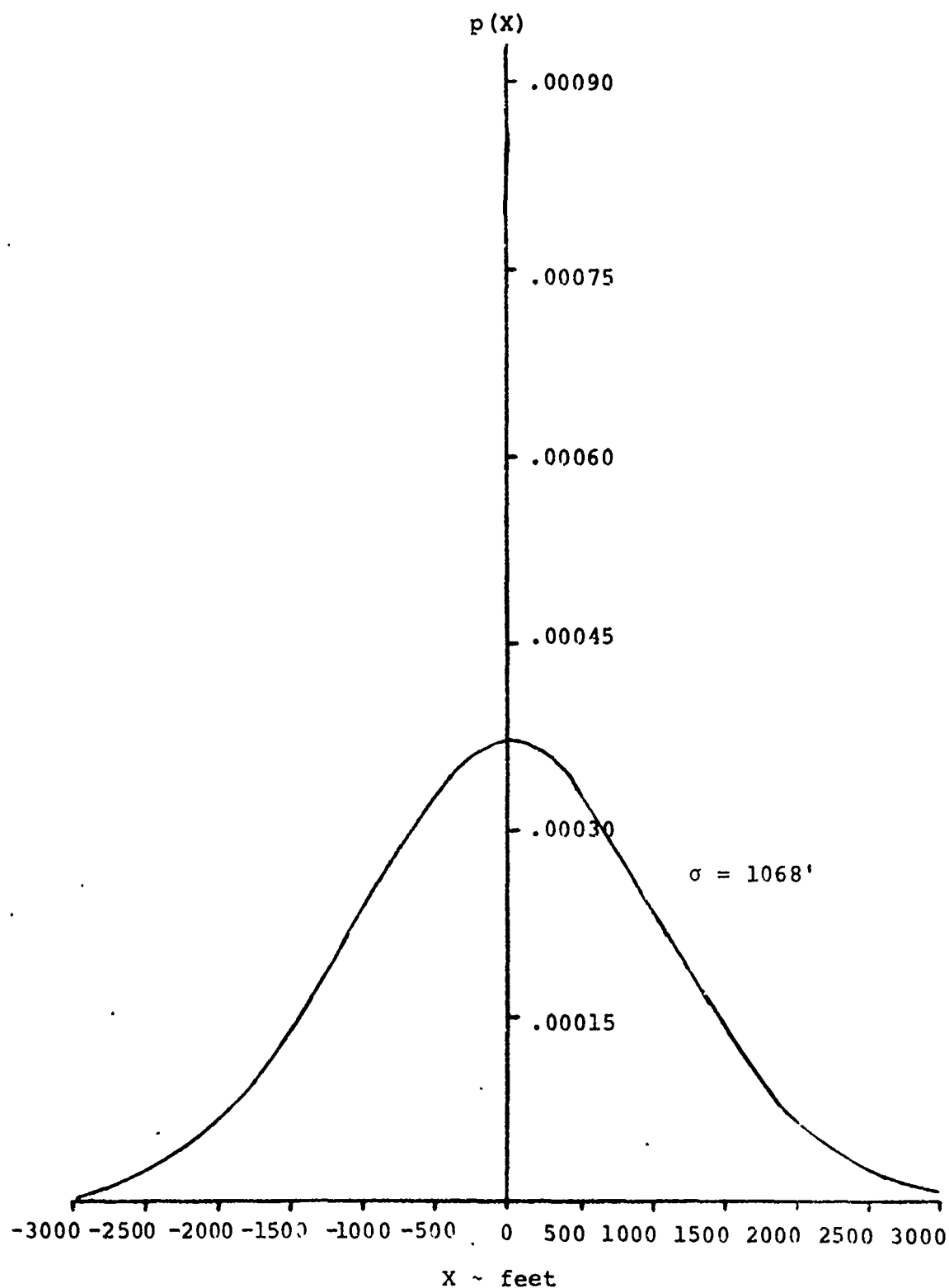


Figure H-24 Longitudinal PDF for FC-ILS-I-CTOL at Two NMi from Touchdown

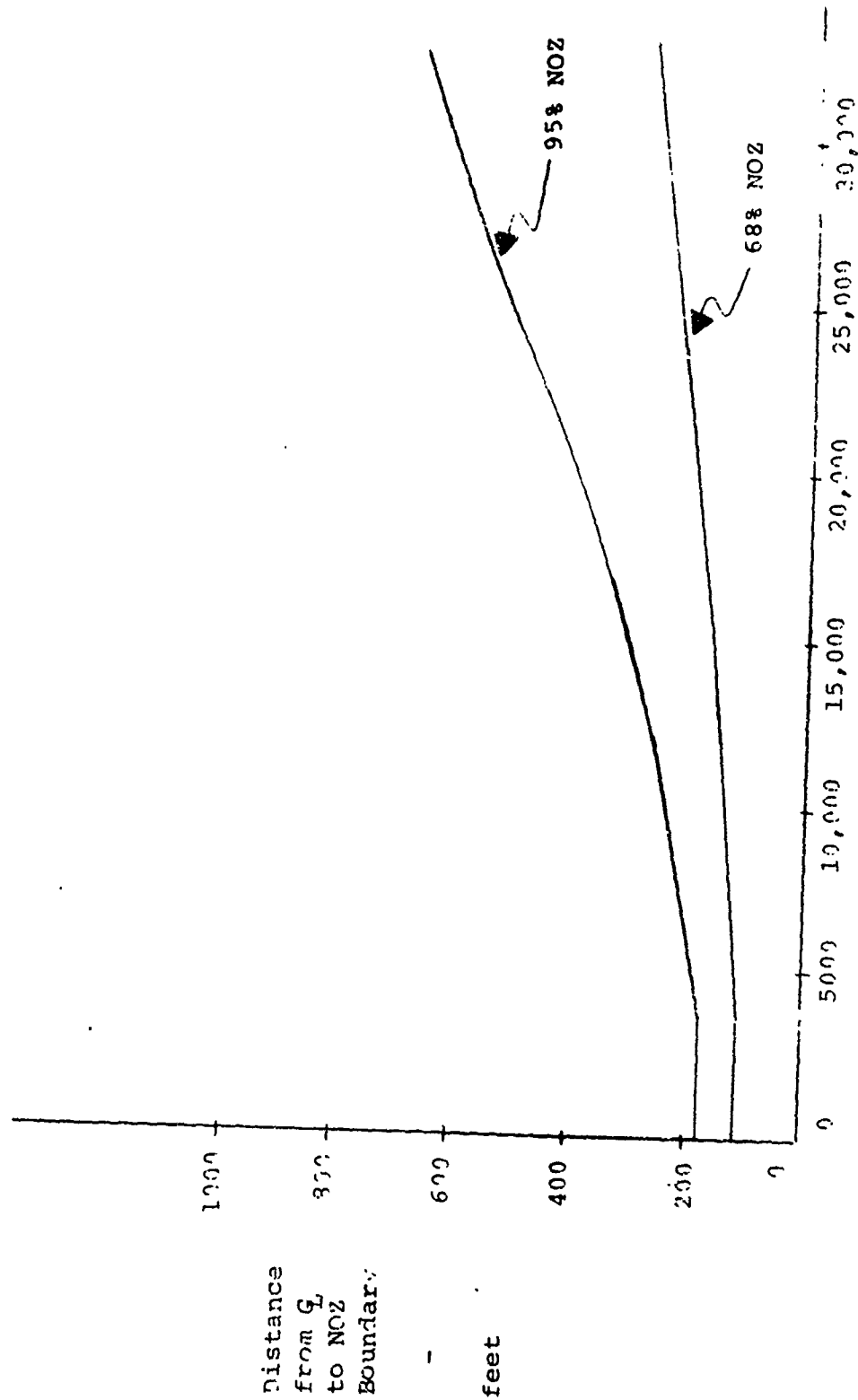


Figure H-25 NO₂ Boundaries for ILS-I-CTOL

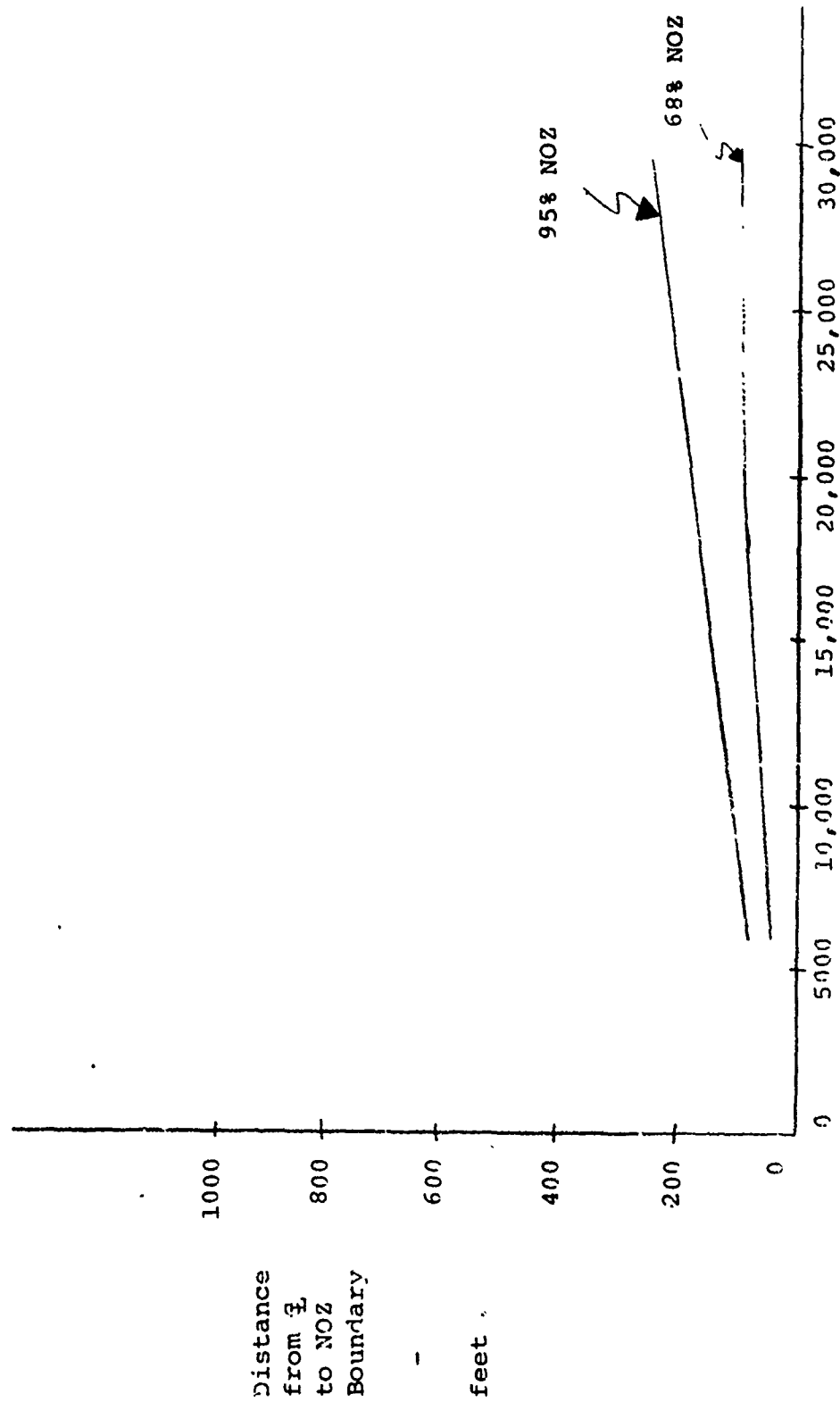


Figure H-26 NOZ Boundaries for F-111-II-CTOL

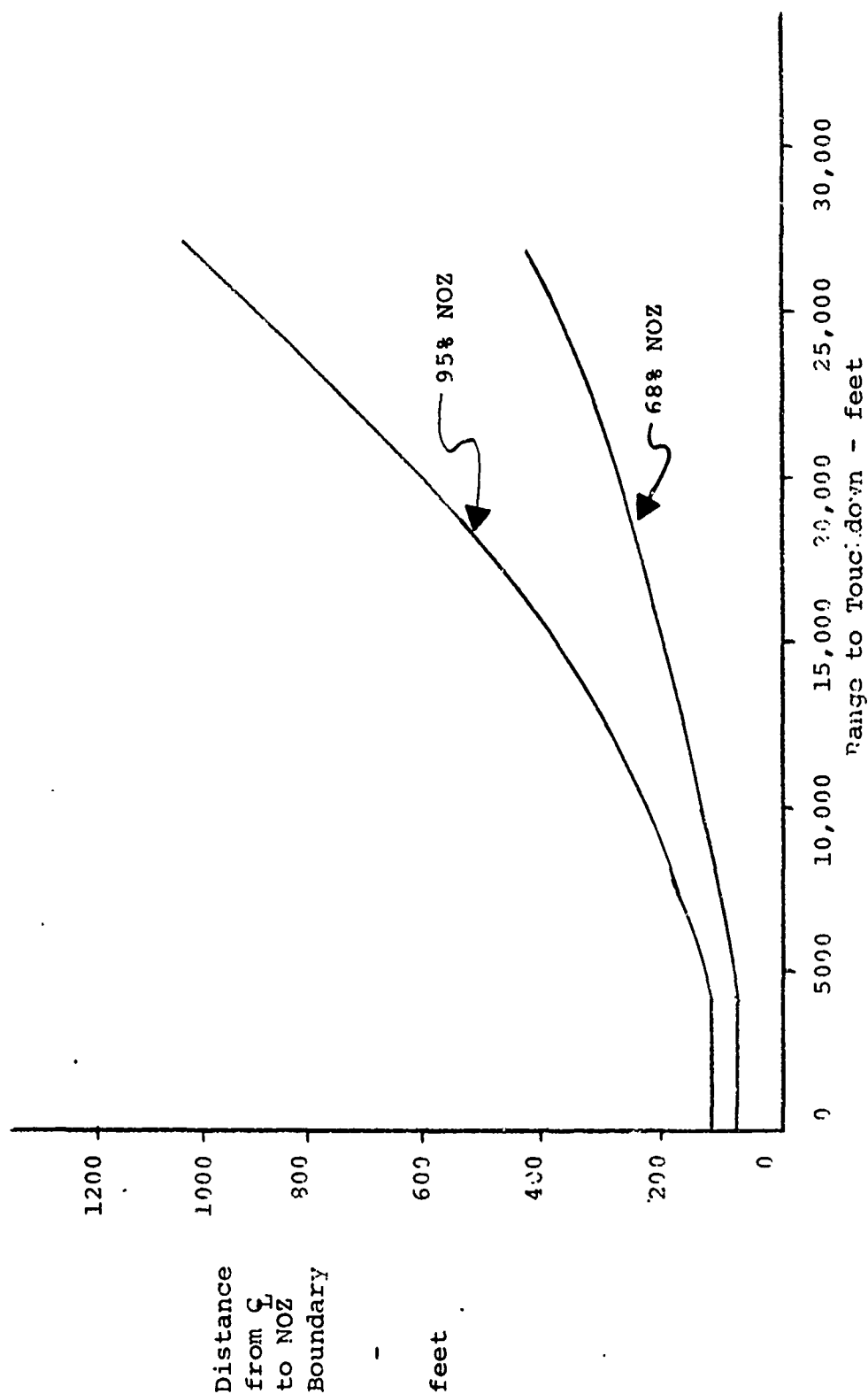


Figure H-27 NOZ Boundaries for BC-ILS-I-CTOL

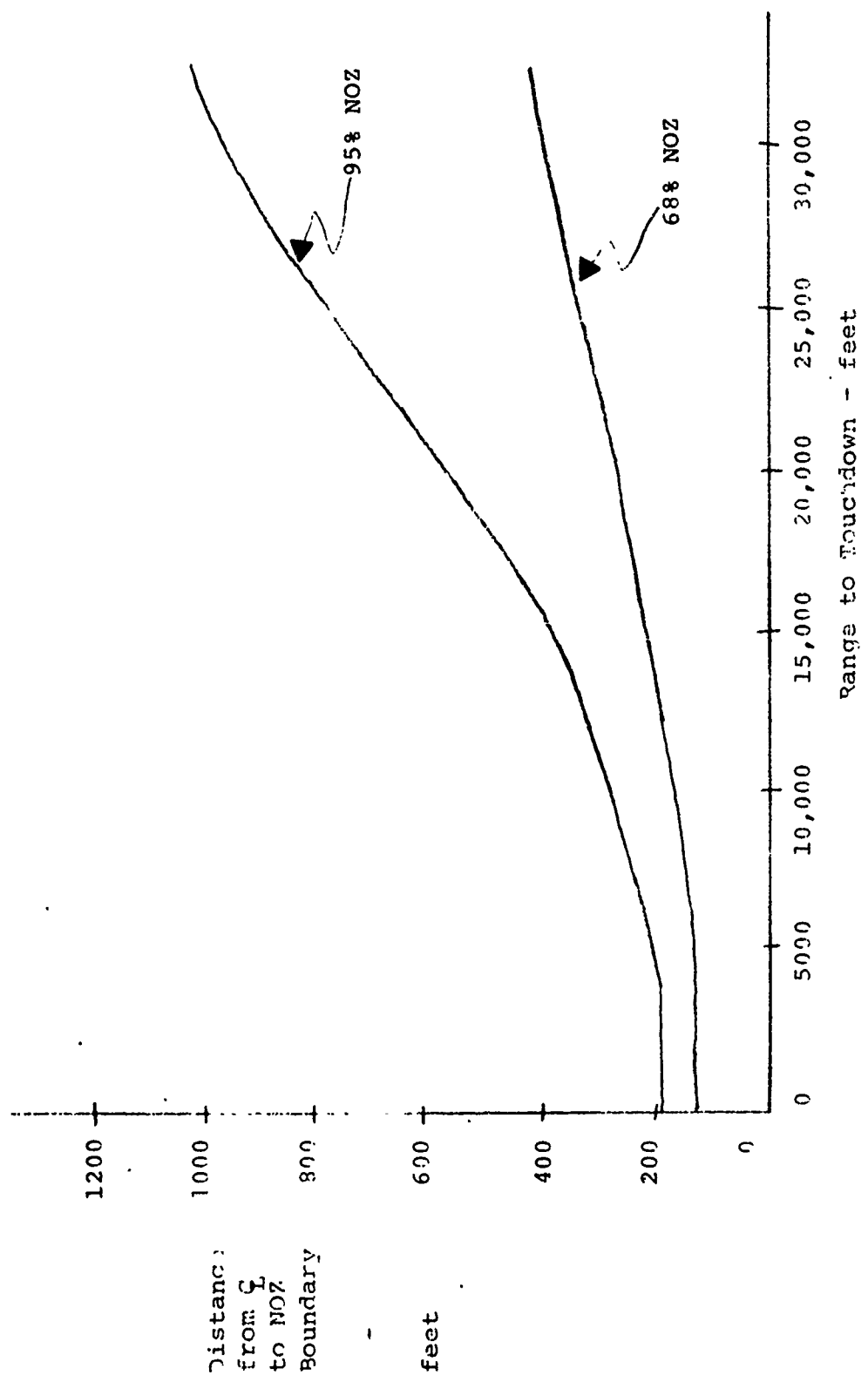


Figure H-25 NOZ Boundaries for VOR-CTOL

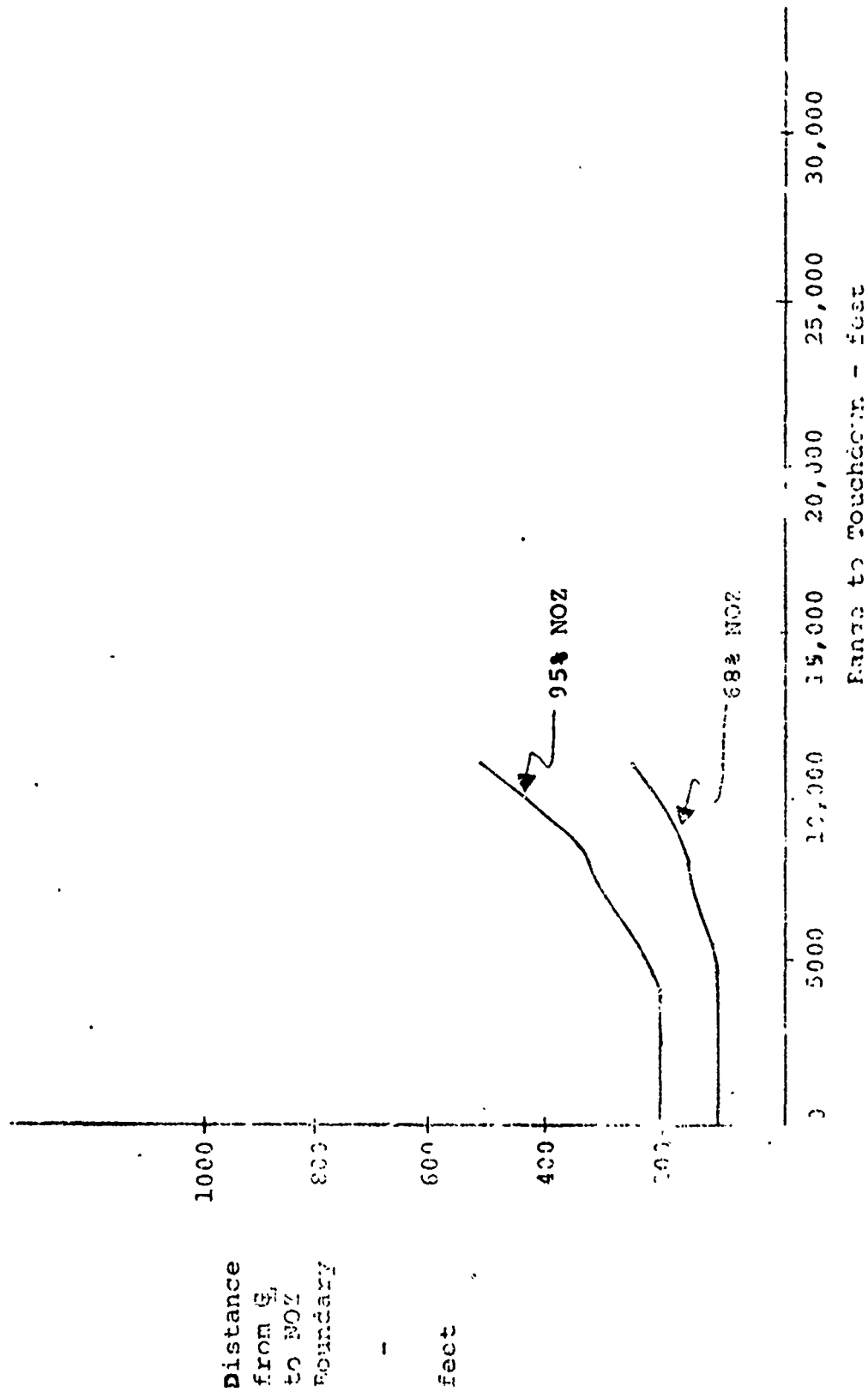


Figure H-29 NOZ Boundaries for PC-ILS-I-STOL

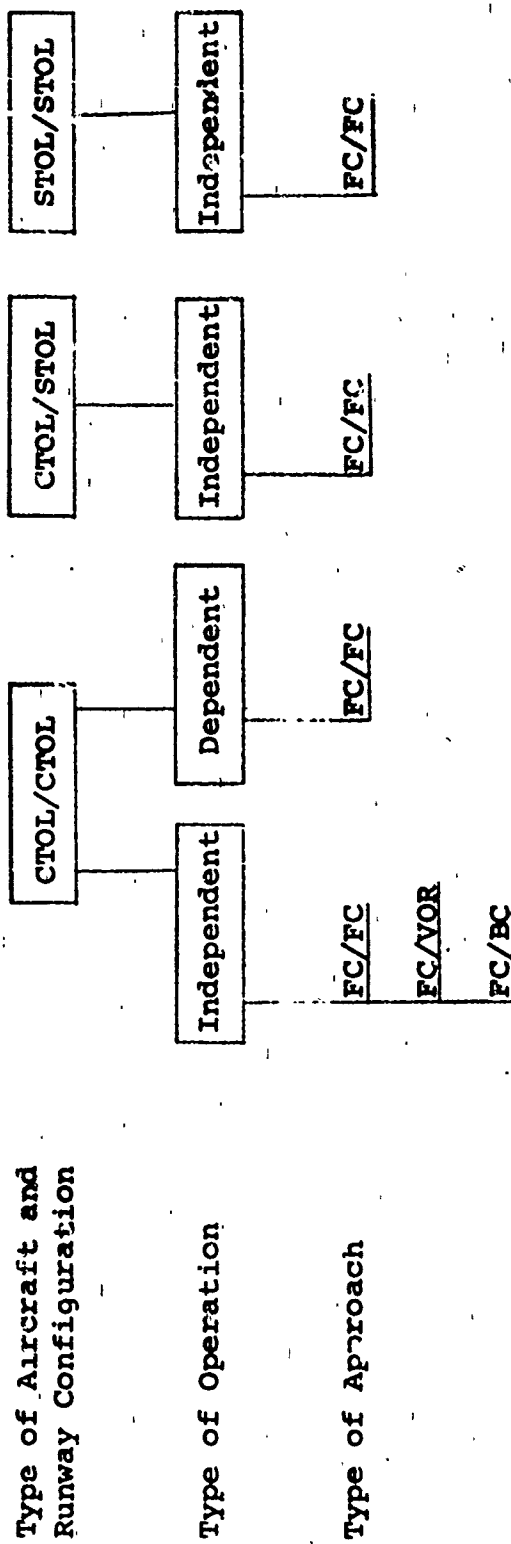
Table H-2 CTOL/STOL Skewed NOZ Results

Skew Angle, degrees	$\sigma_{R'}$ NOZ (68%), feet	$2\sigma_{R'}$ NOZ (95%), feet
10	91.35	182.70
20	89.24	178.48
30	93.04	186.08
40	110.55	221.10
50	144.24	288.48
60	191.33	382.66
70	248.07	496.14
80	311.33	622.66
90	378.46	756.92

APPENDIX I

PROBABILITY OF COLLISION DATA

Probability of collision results obtained in the Lateral Separation Study are presented in tabular form in this appendix. These results represent a primary output of the Lateral Separation Study and constitute a portion of the information necessary to determine a minimum allowable spacing between parallel runways for aircraft operating under IFR condition. Probability of collision data for CTOL/CTOL, CTOL/STOL, and STOL/STOL aircraft and runway configurations are presented in tabular form and include probability of collision results obtained in the Lateral Separation Study for all cases cited in Figure I-1. Table I-1 is a guide to the probability of collision tables contained in this appendix. Zero values shown in the tables for each particular case denote probability of collision values which were smaller than the computational errors associated with a digital computer.



NOTE: The notation used above is X/Y

Runway 1

Runway 2

Figure I-1

Cases Considered in Probability of Collision Analysis

Table I-1 Guide to Probability of Collision Tables

Aircraft and Runway Configuration	Operation	Approach	Table	Comments
CTOL/CTOL	Independent	FC/FC	I-2	
		FC/VOR	I-3	
	Dependent	FC/BC	I-4	
		FC/FC	I-5	Longitudinal Spacing of Three NMi
			I-6	Longitudinal Spacing of Two NMi
			I-7	Longitudinal Spacing of One NMi
			I-8	Longitudinal Spacing of One-Fourth NMi
CTOL/STOL	Independent	FC/FC	I-9	No Threshold Displacement
			I-10	3000 foot Threshold Displacement
STOL/STOL	Independent	FC/FC	I-11	

Table I-2

CTOL/CTOL Probability of Collision Data for
FC/FC Independent Operations

Runway Separation, feet	Range from Threshold, nmi.	Probability of Collision
1500	6	.68 10^{-2}
	4	.75 10^{-3}
	2	.50 10^{-5}
2000	6	.11 10^{-2}
	4	.54 10^{-4}
	2	.16 10^{-7}
2500	6	.17 10^{-5}
	4	.28 10^{-5}
	2	.38 10^{-10}
3000	6	.22 10^{-4}
	4	.95 10^{-7}
	2	.30 10^{-13}
3500	6	.23 10^{-5}
	4	.37 10^{-8}
	2	.13 10^{-16}
4300	6	.57 10^{-7}
	4	.65 10^{-11}
	2	.16 10^{-22}
5000	6	.17 10^{-8}
	4	.16 10^{-13}
	2	.20 10^{-28}

Table I-3

CTOL/CTOL Probability of Collision Data for
FC/VOR Independent Operations

Runway Separation, feet	Range from Threshold, nmi.	Probability of Collision
1500	6	.18 10^{-1}
	4	.29 10^{-2}
	2	.16 10^{-4}
2000	6	.49 10^{-2}
	4	.27 10^{-3}
	2	.82 10^{-7}
2500	6	.14 10^{-2}
	4	.39 10^{-4}
	2	.31 10^{-9}
3000	6	.38 10^{-3}
	4	.35 10^{-5}
	2	.66 10^{-12}
3500	6	.67 10^{-4}
	4	.14 10^{-6}
	2	.92 10^{-15}
4300	6	.23 10^{-5}
	4	.14 10^{-8}
	2	.90 10^{-20}
5000	6	.12 10^{-6}
	4	.98 10^{-11}
	2	.12 10^{-24}

Table I-4

CTOL/CTOL Probability of Collision Data for
FC/BC Independent Operations

Runway Separation, feet	Range from Threshold, nmi.	Probability of Collision
1500	5	.17 10^{-1}
	4	.61 10^{-2}
	2	.38 10^{-5}
2000	5	.45 10^{-2}
	4	.52 10^{-3}
	2	.11 10^{-7}
2500	5	.13 10^{-2}
	4	.97 10^{-4}
	2	.15 10^{-10}
3000	5	.36 10^{-3}
	4	.29 10^{-4}
	2	.63 10^{-14}
3500	5	.57 10^{-4}
	4	.28 10^{-5}
	2	.15 10^{-17}
4300	5	.10 10^{-5}
	4	.16 10^{-7}
	2	.55 10^{-24}
5000	5	.28 10^{-7}
	4	.40 10^{-9}
	2	.28 10^{-30}

Table I-5

CTOL/CTOL Probability of Collision Data for FC/FC Dependent Operations and Longitudinal Spacing of Three Miles

Runway Separation, feet	Range from Threshold, nmi.	Probability of Collision
1500	3	10^{-71}
	2	10^{-51}
	1	10^{-39}
2000	3	10^{-72}
	2	10^{-52}
	1	10^{-40}
2500	3	10^{-73}
	2	10^{-53}
	1	10^{-42}
3000	3	10^{-74}
	2	10^{-55}
	1	10^{-44}
3500	3	10^{-76}
	2	10^{-56}
	1	10^{-46}
4300	3	10^{-78}
	2	10^{-60}
	1	10^{-53}
5000	3	10^{-81}
	2	10^{-64}
	1	10^{-63}

Table I-6

CTOL/CTOL Probability of Collision Data for FC/FC Dependent Operations and Longitudinal Spacing of Two Miles

Runway Separation, feet	Range from Threshold, nmi.	Probability of Collision
1500	4	10^{-43}
	3	10^{-29}
	2	10^{-22}
	1	10^{-19}
2000	4	10^{-44}
	3	10^{-31}
	2	10^{-24}
	1	10^{-21}
2500	4	10^{-44}
	3	10^{-32}
	2	10^{-26}
	1	10^{-24}
3000	4	10^{-46}
	3	10^{-33}
	2	10^{-28}
	1	10^{-26}
3500	4	10^{-47}
	3	10^{-35}
	2	10^{-30}
	1	10^{-29}
4300	4	10^{-49}
	3	10^{-38}
	2	10^{-33}
	1	10^{-36}

Table I-6 CTOL/CTOL Probability of Collision Data for FC/FC
Dependent Operations and Longitudinal Spacing of Two
Miles (Continued)

Runway Separation, feet	Range from Threshold, nmi.	Probability of Collision
5000	4	10^{-51}
	3	10^{-41}
	2	10^{-38}
	1	10^{-46}

Table I-7

CTOL/CTOL Probability of Collision Data for FC/FC Dependent Operations and Longitudinal Spacing of One Mile

Runway Separation, feet	Range from Threshold, nmi.	Probability of Collision
1500	5	10^{-16}
	4	10^{-11}
	3	10^{-9}
	2	10^{-9}
	1	10^{-10}
2000	5	10^{-17}
	4	10^{-12}
	3	10^{-11}
	2	10^{-11}
	1	10^{-13}
2500	5	10^{-18}
	4	10^{-13}
	3	10^{-12}
	2	10^{-13}
	1	10^{-17}
3000	5	10^{-19}
	4	10^{-15}
	3	10^{-14}
	2	10^{-16}
	1	10^{-21}
3500	5	10^{-20}
	4	10^{-16}

Table I-7 CTOL/CTOL Probability of Collision Data for FC/FC
Dependent Operations and Longitudinal Spacing of One
Mile (Continued)

Runway Separation, feet	Range from Threshold, nmi.	Probability of Collision
3500	3	10^{-16}
	2	10^{-18}
	1	10^{-25}
4300	5	10^{-22}
	4	10^{-18}
	3	10^{-19}
	2	10^{-23}
	1	10^{-35}
5000	5	10^{-23}
	4	10^{-21}
	3	10^{-22}
	2	10^{-27}
	1	$<10^{-120}$

Table I-8

CTOL/CTOL Probability of Collision Data for FC/FC Dependent Operations and Longitudinal Spacing of .25 Miles

Runway Separation, feet	Range from Threshold, nmi.	Probability of Collision
1500	5	.14 10^{-3}
	4	.53 10^{-4}
	3	.76 10^{-5}
	2	.46 10^{-6}
	1	.68 10^{-10}
2000	5	.17 10^{-4}
	4	.41 10^{-5}
	3	.28 10^{-6}
	2	.16 10^{-8}
	1	.17 10^{-14}
2500	5	.17 10^{-5}
	4	.23 10^{-6}
	3	.28 10^{-8}
	2	.57 10^{-11}
	1	.11 10^{-19}
3000	5	.13 10^{-6}
	4	.87 10^{-8}
	3	.84 10^{-10}
	2	.60 10^{-14}
	1	.75 10^{-26}

Table I-8 CTOL/CTOL Probability of Collision Data for FC/FC
Dependent Operations and Longitudinal Spacing of .25
Miles (Continued)

Runway Separation feet	Range from Threshold, nmi.	Probability of Collision
3500	5	.90 10^{-8}
	4	.38 10^{-9}
	3	.70 10^{-12}
	2	.40 10^{-17}
	1	.14 10^{-33}
4300	5	.10 10^{-9}
	4	.12 10^{-11}
	3	.10 10^{-15}
	2	.10 10^{-22}
	1	$<10^{-120}$
5000	5	.12 10^{-11}
	4	.31 10^{-14}
	3	.22 10^{-19}
	2	.29 10^{-28}
	1	$<10^{-120}$

Table I-9

CTOL/STOL Probability of Collision Data for FC/FC Independent Operations and No Threshold Displacement

Runway Separation, feet	Range from Threshold, feet	Probability of Collision
1500	12700	10^{-23}
	9200	10^{-14}
	4700	10^{-16}
2000	12200	10^{-26}
	9200	10^{-17}
	4700	10^{-23}
2500	12200	10^{-29}
	9200	10^{-21}
	4700	10^{-35}
3000	12200	10^{-32}
	9200	10^{-25}
	4700	10^{-40}
3500	12200	10^{-36}
	9200	10^{-30}
	4700	10^{-40}
4300	12200	10^{-42}
	9200	10^{-40}
	4700	10^{-40}
5000	12200	10^{-50}
	9200	10^{-45}
	4700	10^{-40}

Table I-10

CTOL/STOL Probability of Collision Data for FC/FC Independent
Operations with Threshold Displacement of 3000 Feet

Runway Separation, feet	Range from Threshold, feet	Probability of Collision
1500	7700	10^{-12}
	6200	10^{-11}
	4700	10^{-12}
2000	7700	10^{-16}
	6200	10^{-16}
	4700	10^{-19}
2500	7700	10^{-21}
	6200	10^{-22}
	4700	10^{-26}
3000	7700	10^{-26}
	6200	10^{-30}
	4700	10^{-39}
3500	7700	10^{-33}
	6200	10^{-40}
	4700	10^{-39}
4300	7700	10^{-42}
	6200	10^{-40}
	4700	10^{-39}
5000	7700	10^{-42}
	6200	10^{-40}
	4700	10^{-39}

Table I-11

STOL/STOL Probability of Collision Data for
FC/FC Independent Operations

Runway Separation, feet	Range from Threshold, feet	Probability of Collision
1500	12000	10^{-2}
	7000	10^{-9}
	1000	10^{-41}
2000	12000	10^{-5}
	7000	10^{-18}
	1000	10^{-73}
2500	12000	10^{-9}
	7000	10^{-28}
	1000	10^{-118}
3000	12000	10^{-13}
	7000	10^{-41}
	1000	$<10^{-120}$
3500	12000	10^{-17}
	7000	10^{-57}
	1000	$<10^{-120}$
4300	12000	10^{-26}
	7000	10^{-88}
	1000	$<10^{-120}$
5000	12000	10^{-36}
	7000	10^{-120}
	1000	$<10^{-120}$

APPENDIX J

SINGLE AIRCRAFT BLUNDER ANALYSIS DATA

This appendix contains the output data for the single aircraft blunder analysis performed in the Lateral Separation study. The purpose of this analysis is to evaluate the cross-track distance (blunder recovery airspace) required for an aircraft to recover from the type 1 and type 2 blunders. Type 1 blunders occur when an aircraft that is on a track which intercepts the approach course at 10°, 20°, or 30° passes through the normal operating zone and proceeds toward the adjacent track. Type 2 blunders occur when an aircraft which is established on the final approach course (within the normal operating zone) makes a turn toward the adjacent course at 15°, 30°, or 45°. The blunder recovery maneuver is assumed to be a coordinated turn in the glideslope plane performed by the blundering aircraft. The geometry of the single aircraft analysis is shown in Figure J-1.

The single aircraft analysis utilized combinations of the blunder parameter values listed in Table J-1 excluding the data acquisition system (DAS) accuracies (ϵ_R and ϵ_A). The lateral recovery airspace required for parameter combinations for the single aircraft blunder analysis is presented in tabular form in Table J-2. Values for DAS errors (EDAS) should be added to these data when the position of the DAS antenna with respect to the blundered aircraft is known.

EDAS is evaluated using the following equations:

$$EDAS = E_A \cos \rho + \sin \rho$$

where,

$$E_A = R \tan \epsilon_A$$

$$E_R = \frac{\epsilon_R R}{100}$$

$$R = \sqrt{(X_{DAS} - X_{A/C})^2 + (Y_{DAS} - Y_{A/C})^2 + (Z_{DAS} - Z_{A/C})^2}$$

$$\rho = \tan^{-1} \left| \frac{Y_{DAS} - Y_{A/C}}{X_{DAS} - X_{A/C}} \right|$$

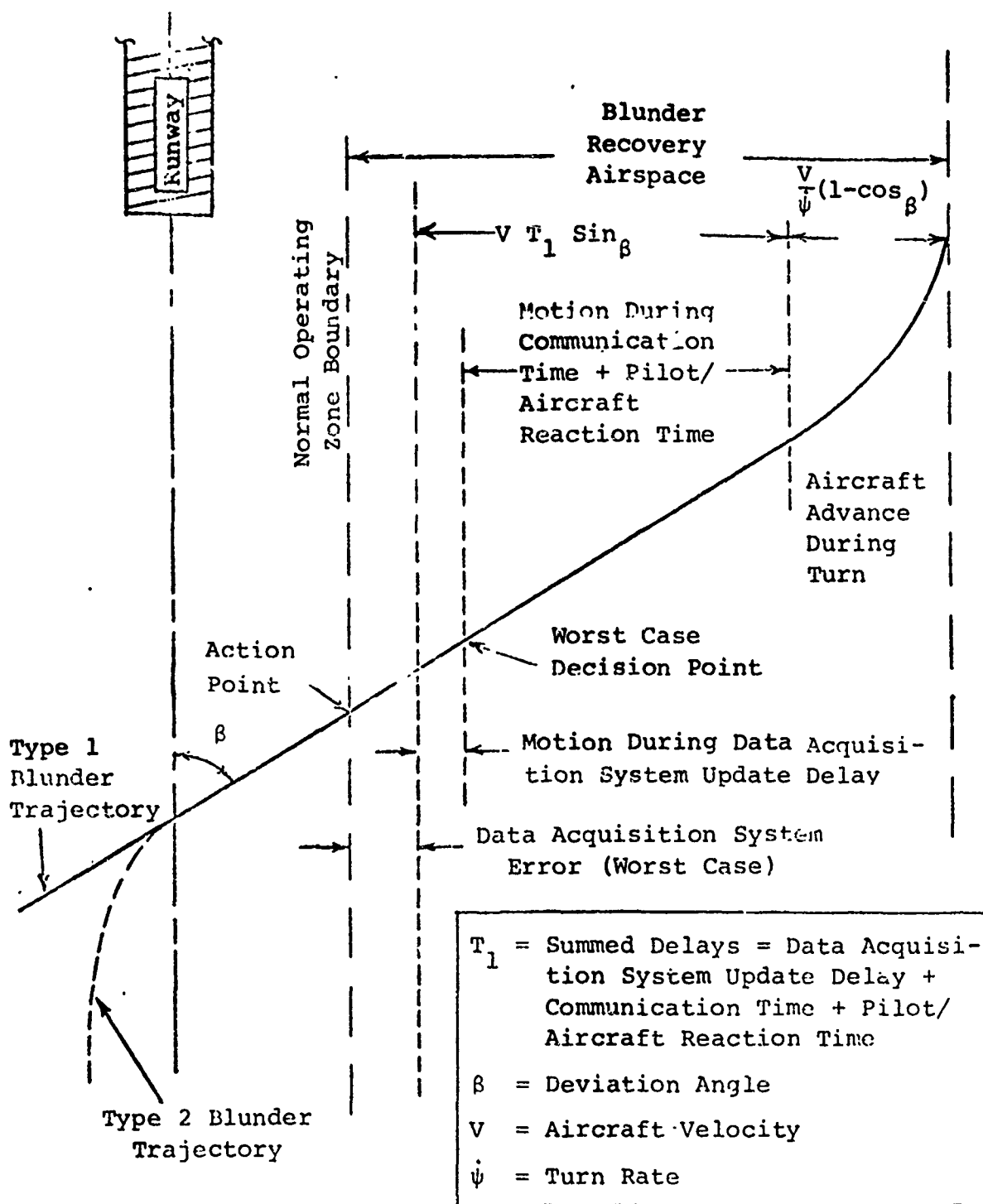


Figure J-1

Single Aircraft Geometric Analysis of the Two Types of Blunders

Table J-1 Blundered Aircraft Parameter Values

Parameters	Values	Units
Departure Angles		
Type 1 Blunder	10, 20, and 30	degrees
Type 2 Blunder	15, 30, and 45	degrees
DAS Range Accuracy (ϵ_R)	1.5, 1.0, .5, and .2	percentages of range
DAS Azimuth Accuracy (ϵ_A)	1.5, 1.0, and .5	degrees
DAS Update Delays	4, 2, 1, .5, .1, and .01	seconds
Aircraft Velocities	60, 80, 100, 120, 140, and 160	knots
Aircraft Bank Angles	10, 20, 30, and 40	degrees
Pilot/Aircraft Reaction Times	1.5, 5, and 8	seconds
Communication Times	1 to 10	seconds

with,

$X_{A/C}$ - Aircraft ground range to touchdown, ft.

$Y_{A/C}$ - Aircraft lateral location from the runway centerline, ft.

$Z_{A/C}$ - Aircraft altitude, ft.

X_{DAS} - DAS antenna ground range from touchdown, ft.

Y_{DAS} - DAS antenna lateral location from the runway centerline, ft.

Z_{DAS} - DAS antenna altitude, ft.

The above equations were derived by using the geometry illustrated in Figure J-2.

The column headings for Table J-2 are explained as follows.

Departure Angle (deg.) - the angle at which a blundered aircraft heads toward the adjacent approach course measured from the extended runway centerline.

Velocity (knots) - the velocity of the blundered aircraft.

Bank Angle (deg.) - the bank angle that the blundered aircraft uses to make the corrective maneuver.

Summed Delays (sec.) - a total of all the delays of the blundered aircraft, including DAS Update Delay, Communication Time, and Pilot/Aircraft Reaction Time.

Blunder Recovery Airspace (ft.) - the lateral recovery airspace, excluding EDAS, required for a blundered aircraft to recover from the type 1 or type 2 blunders, measured from the action point and perpendicular to the extended runway centerline.

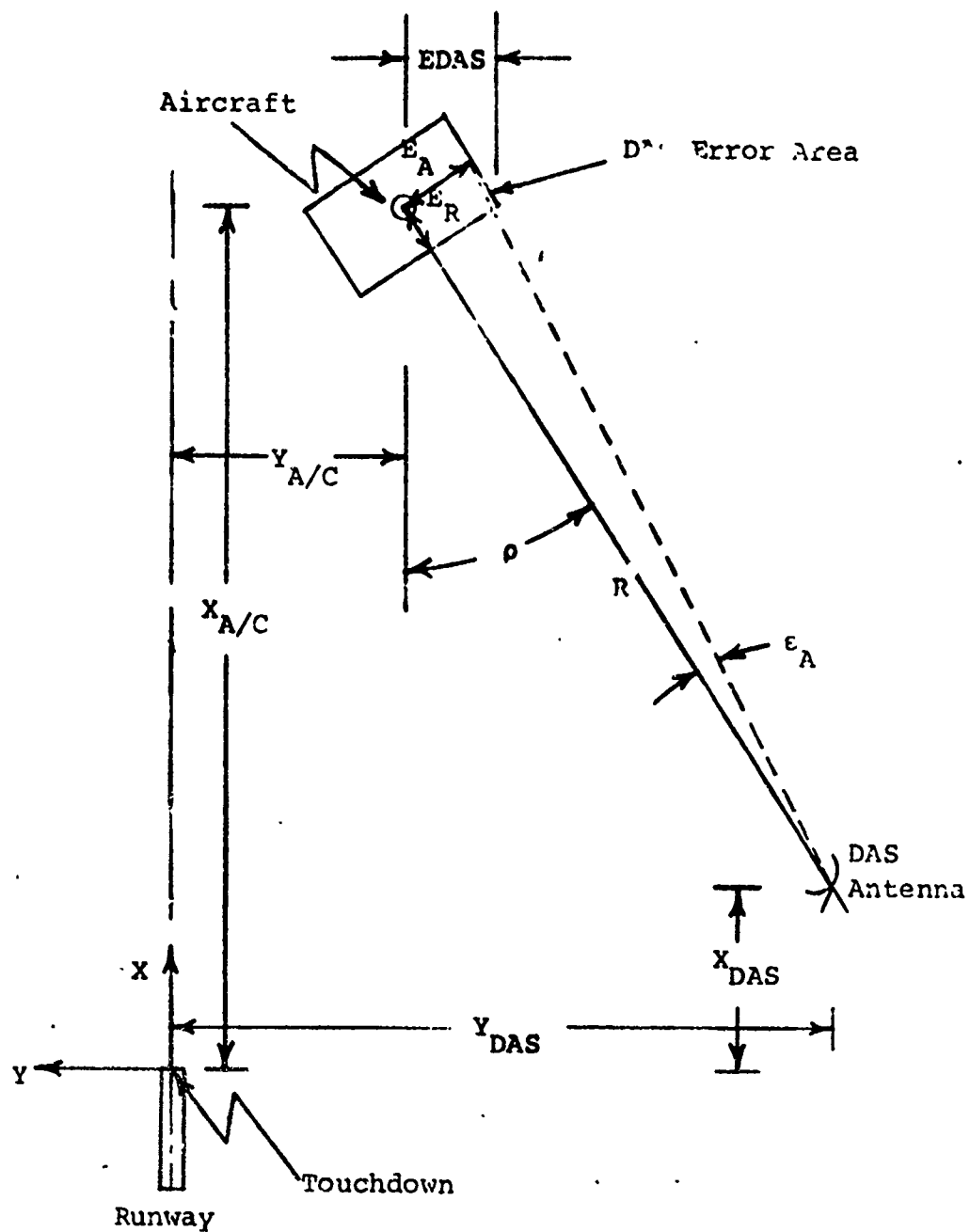


Figure J-2 DAS Configuration

Table J-2

Single Aircraft Blunder Analysis Output

PAGE = 1

BLUNDER
RECOVERY
AIRSPACE (FT.)

BLUNDER ANALYSIS

SUMMED
DELAYS (SEC.)

VELOCITY
(KNOTS)

DEPARTURE
ANGLE (DEG.)

PANK
ANGLE (DEG.)

10.00	60.00	40.00	2.50	49.73
10.00	60.00	40.00	9.00	164.03
10.00	60.00	40.00	16.00	287.13
10.00	60.00	40.00	22.00	392.64
10.00	60.00	30.00	2.50	52.34
10.00	60.00	30.00	9.00	166.65
10.00	60.00	30.00	16.00	289.74
10.00	60.00	30.00	22.00	395.25
10.00	60.00	20.00	2.50	57.26
10.00	60.00	20.00	9.00	171.56
10.00	60.00	20.00	16.00	294.65
10.00	60.00	20.00	22.00	400.16
10.00	60.00	10.00	2.50	71.40
10.00	60.00	10.00	9.00	185.71
10.00	60.00	10.00	16.00	306.80
10.00	60.00	10.00	22.00	414.31
10.00	80.00	40.00	2.50	68.87
10.00	80.00	40.00	9.00	221.27
10.00	80.00	40.00	16.00	385.40
10.00	80.00	40.00	22.00	526.08
10.00	80.00	30.00	2.50	73.52
10.00	80.00	30.00	9.00	225.92
10.00	80.00	30.00	16.00	390.05
10.00	80.00	30.00	22.00	530.73
10.00	80.00	20.00	2.50	82.25
10.00	80.00	20.00	9.00	234.65
10.00	80.00	20.00	16.00	398.78
10.00	80.00	20.00	22.00	539.46
10.00	80.00	10.00	2.50	107.40
10.00	80.00	10.00	9.00	259.80
10.00	80.00	10.00	16.00	423.93
10.00	80.00	10.00	22.00	564.61

DEPARTURE ANGLE(DEG.)	VELOCITY (KNOTS)	BLUNDER ANALYSIS	SUMMED DELAYS(SEC.)	BLUNDER RECOVERY "IRSPACE"(FT.)
10.00	100.00	40.00	2.50	69.29
10.00	100.00	40.00	9.00	279.79
10.00	100.00	40.00	16.00	484.95
10.00	100.00	40.00	22.00	650.80
10.00	100.00	30.00	2.50	96.55
10.00	100.00	30.00	9.00	287.06
10.00	100.00	30.00	16.00	492.21
10.00	100.00	30.00	22.00	666.06
10.00	100.00	20.00	2.50	110.20
10.00	100.00	20.00	9.00	300.70
10.00	100.00	20.00	16.00	505.80
10.00	100.00	20.00	22.00	681.71
10.00	100.00	10.00	2.50	149.50
10.00	100.00	10.00	9.00	340.00
10.00	100.00	10.00	16.00	545.16
10.00	100.00	10.00	22.00	721.01
10.00	120.00	40.00	2.50	110.99
10.00	120.00	40.00	9.00	339.60
10.00	120.00	40.00	16.00	585.79
10.00	120.00	40.00	22.00	796.81
10.00	120.00	30.00	2.50	121.45
10.00	120.00	30.00	9.00	350.05
10.00	120.00	30.00	16.00	596.24
10.00	120.00	30.00	22.00	807.26
10.00	120.00	20.00	2.50	141.10
10.00	120.00	20.00	9.00	369.71
10.00	120.00	20.00	16.00	615.90
10.00	120.00	20.00	22.00	826.92
10.00	120.00	10.00	2.50	197.69
10.00	120.00	10.00	9.00	426.29
10.00	120.00	10.00	16.00	672.48
10.00	120.00	10.00	22.00	863.50

LUNDER
 RECOVERY
 SPACE (FT.)

DEPARTURE ANGLE (DEG.)	VELOCITY (KNOTS)	BLINDS ANALYSIS	MARK ANGLE (DEG.)	SUMMED DELAYS (SEC.)	SPACE (FT.)
10.00	140.00		40.00	2.50	153.97
10.00	140.00		40.00	9.00	400.68
10.00	140.00		40.00	16.00	687.90
10.00	140.00		40.00	22.00	934.09
10.00	140.00		50.00	2.50	148.21
10.00	140.00		50.00	9.00	414.31
10.00	140.00		50.00	16.00	702.14
10.00	140.00		50.00	22.00	946.33
10.00	140.00		25.00	2.50	174.96
10.00	140.00		25.00	9.00	441.60
10.00	140.00		25.00	16.00	726.89
10.00	140.00		25.00	22.00	975.06
10.00	140.00		10.00	2.50	251.98
10.00	140.00		10.00	9.00	518.69
10.00	140.00		10.00	16.00	805.91
10.00	140.00		10.00	22.00	1052.10
10.00	160.00		40.00	2.50	158.24
10.00	160.00		40.00	9.00	463.05
10.00	160.00		40.00	16.00	791.30
10.00	160.00		40.00	22.00	1072.60
10.00	160.00		50.00	2.50	170.83
10.00	160.00		50.00	9.00	481.64
10.00	160.00		50.00	16.00	809.89
10.00	160.00		50.00	22.00	1091.25
10.00	160.00		20.00	2.50	211.77
10.00	160.00		20.00	9.00	516.57
10.00	160.00		20.00	16.00	844.83
10.00	160.00		20.00	22.00	1120.19
10.00	160.00		10.00	2.50	312.37
10.00	160.00		10.00	9.00	617.17
10.00	160.00		10.00	16.00	945.43
10.00	160.00		10.00	22.00	1220.79

 Reproduced from
 best available copy.


UNDER
RECOVERY
FIRSTAGE (FT.)

VELOCITY (K IN/LS)	ANALYSIS	SUMMED DELAYS (SEC.)
15.00	40.00	2.50
15.00	40.00	9.00
15.00	40.00	16.00
15.00	40.00	22.00
15.00	50.00	2.50
15.00	50.00	9.00
15.00	50.00	16.00
15.00	50.00	22.00
15.00	60.00	2.50
15.00	60.00	9.00
15.00	60.00	16.00
15.00	60.00	22.00
15.00	70.00	2.50
15.00	70.00	9.00
15.00	70.00	16.00
15.00	70.00	22.00
15.00	80.00	2.50
15.00	80.00	9.00
15.00	80.00	16.00
15.00	80.00	22.00
15.00	90.00	2.50
15.00	90.00	9.00
15.00	90.00	16.00
15.00	90.00	22.00
15.00	100.00	2.50
15.00	100.00	9.00
15.00	100.00	16.00
15.00	100.00	22.00

Reproduced from
best available copy.

***** BLUNDER ANALYSIS *****

DEPARTURE ANGLE (DEG.)	VELOCITY (KNOTS)	BACK ANGLE (DEG.)	SIMPLE DELAYS (SEC.)	BLUNDER RECOVERY SPACE (FT.)
15.00	100.00	35.00	2.50	145.13
15.00	100.00	40.00	9.00	429.08
15.00	100.00	40.00	16.00	734.80
15.00	100.00	40.00	22.00	996.90
15.00	100.00	30.00	2.50	161.42
15.00	100.00	30.00	9.00	445.36
15.00	100.00	30.00	16.00	751.15
15.00	100.00	30.00	22.00	1013.25
15.00	100.00	20.00	2.50	192.03
15.00	100.00	20.00	9.00	475.97
15.00	100.00	20.00	16.00	761.70
15.00	100.00	20.00	22.00	1043.80
15.00	100.00	10.00	2.50	280.17
15.00	100.00	10.00	9.00	564.11
15.00	100.00	10.00	16.00	869.90
15.00	100.00	10.00	22.00	1132.00
15.00	120.00	40.00	2.50	162.78
15.00	120.00	40.00	9.00	523.52
15.00	120.00	40.00	16.00	890.40
15.00	120.00	40.00	22.00	1204.93
15.00	120.00	30.00	2.50	206.24
15.00	120.00	30.00	9.00	546.97
15.00	120.00	30.00	16.00	913.91
15.00	120.00	30.00	22.00	1228.43
15.00	120.00	20.00	2.50	250.32
15.00	120.00	20.00	9.00	591.05
15.00	120.00	20.00	16.00	957.99
15.00	120.00	20.00	22.00	1272.51
15.00	120.00	10.00	2.50	377.25
15.00	120.00	10.00	9.00	717.97
15.00	120.00	10.00	16.00	1084.91
15.00	120.00	10.00	22.00	1399.43

LUNDER
RECOVERY
AIRSPACE (FT.)

223.31
620.83
1048.93
1415.87
255.23
652.75
1060.85
1447.79
315.22
712.75
1140.84
1507.79
467.96
885.50
1313.59
1680.54
266.70
721.01
1210.27
1629.63
308.40
762.71
1251.96
1671.33
356.76
641.07
1356.33
1749.69
612.39
1066.70
1555.96
1975.32

Reproduced from
best available copy.



DEPARTURE ANGLE (DEG.)	VELOCITY (KNOTS)	ALT (FEET)	TIME (SECS)	*****
15.00	140.00	40.00	2.50	
15.00	140.00	40.00	9.00	
15.00	140.00	40.00	16.00	
15.00	140.00	40.00	22.00	
15.00	140.00	40.00	2.50	
15.00	140.00	40.00	9.00	
15.00	140.00	40.00	16.00	
15.00	140.00	40.00	22.00	
15.00	140.00	40.00	2.50	
15.00	140.00	40.00	9.00	
15.00	140.00	40.00	16.00	
15.00	140.00	40.00	22.00	
15.00	140.00	40.00	2.50	
15.00	140.00	40.00	9.00	
15.00	140.00	40.00	16.00	
15.00	140.00	40.00	22.00	
15.00	140.00	40.00	2.50	
15.00	140.00	40.00	9.00	
15.00	140.00	40.00	16.00	
15.00	140.00	40.00	22.00	
15.00	140.00	40.00	2.50	
15.00	140.00	40.00	9.00	
15.00	140.00	40.00	16.00	
15.00	140.00	40.00	22.00	

BLUJOL ANALYSIS

DEPARTURE ANGLE (DEG.)	VELOCITY (KNOTS)	LAUNCH ANGLE (DEG.)	SUMMED DELAYS (SEC.)	LINEAR RECOVERY SPACE (FT.)
20.00	60.00	40.00	2.50	169.48
20.00	60.00	40.00	9.00	334.61
20.00	60.00	40.00	16.00	577.00
20.00	60.00	40.00	22.00	784.88
20.00	60.00	50.00	2.50	119.86
20.00	60.00	50.00	9.00	344.99
20.00	60.00	50.00	16.00	587.44
20.00	60.00	50.00	22.00	795.25
20.00	60.00	20.00	2.50	139.36
20.00	60.00	20.00	9.00	304.49
20.00	60.00	20.00	16.00	606.94
20.00	60.00	20.00	22.00	814.75
20.00	60.00	10.00	2.50	195.52
20.00	60.00	10.00	9.00	420.65
20.00	60.00	10.00	16.00	663.10
20.00	60.00	10.00	22.00	870.92
20.00	80.00	40.00	2.50	156.15
20.00	80.00	40.00	9.00	456.32
20.00	80.00	40.00	16.00	779.59
20.00	80.00	40.00	22.00	1056.68
20.00	80.00	50.00	2.50	174.60
20.00	80.00	50.00	9.00	474.77
20.00	80.00	50.00	16.00	798.04
20.00	80.00	50.00	22.00	1075.13
20.00	80.00	20.00	2.50	209.27
20.00	80.00	20.00	9.00	509.44
20.00	80.00	20.00	16.00	832.71
20.00	80.00	20.00	22.00	1109.80
20.00	80.00	10.00	2.50	309.10
20.00	80.00	10.00	9.00	609.28
20.00	80.00	10.00	16.00	932.55
20.00	80.00	10.00	22.00	1209.63

HEADING ANALYSIS

 (LUNDER
RECOVERY
AIRSPACE (FT.))

 SUMMED
DELAYS (SEC.)

 VELOCITY
(KNOTS)

 DEPARTURE
ANGLE (DEG.)

 P-4K
ANGLE (DEG.)

20.00	100.00	40.00	2.50	207.90
20.00	100.00	40.00	9.00	583.12
20.00	100.00	40.00	16.00	987.20
20.00	100.00	40.00	22.00	1333.56
20.00	100.00	30.00	2.50	236.73
20.00	100.00	30.00	9.00	611.95
20.00	100.00	30.00	16.00	1016.03
20.00	100.00	30.00	22.00	1362.39
20.00	100.00	20.00	2.50	290.90
20.00	100.00	20.00	9.00	666.12
20.00	100.00	20.00	16.00	1070.21
20.00	100.00	20.00	22.00	1416.55
20.00	100.00	10.00	2.50	446.90
20.00	100.00	10.00	9.00	822.12
20.00	100.00	10.00	16.00	1226.20
20.00	100.00	10.00	22.00	1572.56
20.00	120.00	40.00	2.50	264.74
20.00	120.00	40.00	9.00	715.00
20.00	120.00	40.00	16.00	1199.91
20.00	120.00	40.00	22.00	1615.53
20.00	120.00	30.00	2.50	340.55
20.00	120.00	30.00	9.00	720.31
20.00	120.00	30.00	16.00	1241.42
20.00	120.00	30.00	22.00	1577.04
20.00	120.00	20.00	2.50	384.26
20.00	120.00	20.00	9.00	834.53
20.00	120.00	20.00	16.00	1319.43
20.00	120.00	20.00	22.00	1735.06
20.00	120.00	10.00	2.50	608.90
20.00	120.00	10.00	9.00	1059.16
20.00	120.00	10.00	16.00	1544.06
20.00	120.00	10.00	22.00	1959.69

BULLALF ANALYSIS

DEPARTURE ANGLE (DEG.)	VELOCITY (KNOTS)	RAPIR ANGLE (DEG.)	SUMMED DELAYS (SEC.)	UNDER RECOVERY AIRSPACE (FT.)
20.00	140.00	40.00	2.50	326.67
20.00	140.00	40.00	9.00	851.98
20.00	140.00	40.00	16.00	1417.69
20.00	140.00	40.00	22.00	1902.59
20.00	140.00	50.00	2.50	383.17
20.00	140.00	50.00	9.00	908.48
20.00	140.00	50.00	16.00	1474.19
20.00	140.00	50.00	22.00	1959.09
20.00	140.00	20.00	2.50	469.35
20.00	140.00	20.00	9.00	1014.66
20.00	140.00	20.00	16.00	1560.38
20.00	140.00	0.00	22.00	2065.28
20.00	140.00	10.00	2.50	795.10
20.00	140.00	10.00	9.00	1320.41
20.00	140.00	10.00	16.00	1886.13
20.00	140.00	10.00	22.00	2371.03
20.00	160.00	40.00	2.50	393.68
20.00	160.00	40.00	9.00	994.03
20.00	160.00	40.00	16.00	1640.57
20.00	160.00	40.00	22.00	2194.74
20.00	160.00	50.00	2.50	467.48
20.00	160.00	50.00	9.00	1067.83
20.00	160.00	50.00	16.00	1714.36
20.00	160.00	50.00	22.00	2268.54
20.00	160.00	20.00	2.50	606.17
20.00	160.00	20.00	9.00	1206.52
20.00	160.00	20.00	16.00	1853.05
20.00	160.00	20.00	22.00	2497.23
20.00	160.00	10.00	2.50	1005.51
20.00	160.00	10.00	9.00	1605.86
20.00	160.00	10.00	16.00	2252.40
20.00	160.00	10.00	22.00	2806.57

PAGE = 10

***** HULLER ANALYSIS *****

DEPARTURE ANGLE (DEG.)	VELOCITY (KNOTS)	DOWN ANGLE (DEG.)	SHOWN DELAYS (SEC.)	LUNDER RECOVERY AIRSPACE (FT.)
30.00	60.00	40.00	2.50	177.44
30.00	60.00	40.00	9.00	506.56
30.00	60.00	40.00	16.00	861.00
30.00	60.00	40.00	22.00	1164.80
30.00	60.00	50.00	2.50	200.49
30.00	50.00	50.00	9.00	529.61
30.00	60.00	50.00	16.00	864.05
30.00	60.00	50.00	22.00	1187.86
30.00	60.00	40.00	2.50	243.82
30.00	60.00	20.00	9.00	572.94
30.00	60.00	20.00	16.00	927.38
30.00	60.00	20.00	22.00	1231.18
30.00	60.00	10.00	2.50	368.57
30.00	60.00	10.00	9.00	697.70
30.00	60.00	10.00	16.00	1052.13
30.00	60.00	10.00	22.00	1355.94
30.00	80.00	40.00	2.50	259.18
30.00	80.00	40.00	9.00	698.01
30.00	80.00	40.00	16.00	1170.60
30.00	80.00	40.00	22.00	1575.67
30.00	80.00	50.00	2.50	300.17
30.00	80.00	50.00	9.00	739.00
30.00	80.00	50.00	16.00	1211.58
30.00	80.00	50.00	22.00	1616.65
30.00	80.00	20.00	2.50	377.19
30.00	80.00	20.00	9.00	816.02
30.00	80.00	20.00	16.00	1288.61
30.00	80.00	20.00	22.00	1693.68
30.00	80.00	10.00	2.50	598.98
30.00	80.00	10.00	9.00	1037.81
30.00	80.00	10.00	16.00	1510.40
30.00	80.00	10.00	22.00	1915.47

UNDER
RECOVERY
AIRSPACE (T.)

BLUNDER ANALYSIS

SUMMED
DELAYS (SEC.)

VELOCITY
(KNOTS)

WIND
ANGLE (DEG.)

WIND
ANGLE (DEG.)

30.00	100.00	40.00	2.50	352.23
30.00	100.00	40.00	9.00	900.77
30.00	100.00	40.00	16.00	1491.50
30.00	100.00	40.00	22.00	1997.84
30.00	100.00	30.00	2.50	416.27
30.00	100.00	30.00	9.00	964.60
30.00	100.00	30.00	16.00	1555.54
30.00	100.00	30.00	22.00	2061.88
30.00	100.00	20.00	2.50	536.62
30.00	100.00	20.00	9.00	1065.16
30.00	100.00	20.00	16.00	1675.89
30.00	100.00	20.00	22.00	2182.23
30.00	100.00	10.00	2.50	883.17
30.00	100.00	10.00	9.00	1431.70
30.00	100.00	10.00	16.00	2022.43
30.00	100.00	10.00	22.00	2528.78
30.00	120.00	40.00	2.50	456.58
30.00	120.00	40.00	9.00	1114.82
30.00	120.00	40.00	16.00	1823.70
30.00	120.00	40.00	22.00	2431.31
30.00	120.00	30.00	2.50	548.79
30.00	120.00	30.00	9.00	1207.04
30.00	120.00	30.00	16.00	1915.91
30.00	120.00	30.00	22.00	2523.52
30.00	120.00	20.00	2.50	722.10
30.00	120.00	20.00	9.00	1380.34
30.00	120.00	20.00	16.00	2069.22
30.00	120.00	20.00	22.00	2796.83
30.00	120.00	10.00	2.50	1221.13
30.00	120.00	10.00	9.00	1879.37
30.00	120.00	10.00	16.00	2531.25
30.00	120.00	10.00	22.00	3195.86

***** BLUNDER ANALYSIS *****				*****	
DEPARTURE ANGLE (DEG.)	VELOCITY (KNOTS)	HANK ANGLE (DEG.)	SUMMED DELAYS (SEC.)	LUNDEP RECOVERY AIRSPACE (FT.)	
30.00	140.00	40.00	2.50	572.22	
30.00	140.00	40.00	9.00	1340.17	
30.00	140.00	40.00	16.00	2167.20	
30.00	140.00	40.00	22.00	2876.07	
30.00	140.00	30.00	2.50	697.74	
30.00	140.00	30.00	9.00	1465.69	
30.00	140.00	30.00	16.00	2292.71	
30.00	140.00	30.00	22.00	3001.59	
30.00	140.00	20.00	2.50	933.63	
30.00	140.00	20.00	9.00	1701.58	
30.00	140.00	20.00	16.00	2528.61	
30.00	140.00	20.00	22.00	3237.48	
30.00	140.00	10.00	2.50	1612.86	
30.00	140.00	10.00	9.00	2380.81	
30.00	140.00	10.00	16.00	3207.84	
30.00	140.00	10.00	22.00	3916.71	
30.00	160.00	40.00	2.50	699.17	
30.00	160.00	40.00	9.00	1576.83	
30.00	160.00	40.00	16.00	2522.00	
30.00	160.00	40.00	22.00	3332.14	
30.00	160.00	30.00	2.50	803.11	
30.00	160.00	30.00	9.00	1740.77	
30.00	160.00	30.00	16.00	2685.94	
30.00	160.00	30.00	22.00	3496.08	
30.00	160.00	20.00	2.50	1171.22	
30.00	160.00	20.00	9.00	2048.87	
30.00	160.00	20.00	16.00	2994.04	
30.00	160.00	20.00	22.00	3804.19	
30.00	160.00	10.00	2.50	2058.37	
30.00	160.00	10.00	9.00	2930.03	
30.00	160.00	10.00	16.00	3881.20	
30.00	160.00	10.00	22.00	4691.35	

***** BLUNDER ANALYSIS *****					*****	
DEPARTURE ANGLE (DEG.)	VELOCITY (KNOTS)	BANK ANGLE (DEG.)	SUNMED DELAYS (SEC.)		BLUNDER RECOVERY AIRSPACE (FT.)	
45.00	60.00	40.00	2.50		290.19	
45.00	60.00	40.00	9.00		755.64	
45.00	60.00	40.00	16.00		1256.89	
45.00	60.00	40.00	22.00		1686.53	
45.00	60.00	30.00	2.50		340.59	
45.00	60.00	30.00	9.00		806.04	
45.00	60.00	30.00	16.00		1307.29	
45.00	60.00	30.00	22.00		1736.94	
45.00	60.00	20.00	2.50		435.31	
45.00	60.00	20.00	9.00		900.70	
45.00	60.00	20.00	16.00		1402.01	
45.00	60.00	20.00	22.00		1831.66	
45.00	60.00	10.00	2.50		708.05	
45.00	60.00	10.00	9.00		1173.50	
45.00	60.00	10.00	16.00		1674.75	
45.00	60.00	10.00	22.00		2104.40	
45.00	80.00	40.00	2.50		436.33	
45.00	80.00	40.00	9.00		1056.93	
45.00	80.00	40.00	16.00		1725.26	
45.00	80.00	40.00	22.00		2298.12	
45.00	80.00	30.00	2.50		525.93	
45.00	80.00	30.00	9.00		1146.53	
45.00	80.00	30.00	16.00		1814.86	
45.00	80.00	30.00	22.00		2387.72	
45.00	80.00	20.00	2.50		694.32	
45.00	80.00	20.00	9.00		1314.92	
45.00	80.00	20.00	16.00		1983.20	
45.00	80.00	20.00	22.00		2556.12	
45.00	80.00	10.00	2.50		1179.19	
45.00	80.00	10.00	9.00		1799.79	
45.00	80.00	10.00	16.00		2468.13	
45.00	80.00	10.00	22.00		3040.99	

***** BLUNDER ANALYSIS *****

DEPARTURE ANGLE(DEG.)	VELOCITY (KNOTS)	BANK ANGLE(DEG.)	SUMMED DELAYS(SEC.)	LUNDER RECOVERY AIRSPACE(FT.)
45.00	100.00	40.00	2.50	607.17
45.00	100.00	40.00	9.00	1382.92
45.00	100.00	40.00	16.00	2218.34
45.00	100.00	40.00	22.00	2934.41
45.00	100.00	30.00	2.50	747.17
45.00	100.00	30.00	9.00	1522.92
45.00	100.00	30.00	16.00	2358.34
45.00	100.00	30.00	22.00	3074.42
45.00	100.00	20.00	2.50	1010.29
45.00	100.00	20.00	9.00	1786.04
45.00	100.00	20.00	16.00	2621.46
45.00	100.00	20.00	22.00	3337.53
45.00	100.00	10.00	2.50	1767.90
45.00	100.00	10.00	9.00	2543.65
45.00	100.00	10.00	16.00	3379.07
45.00	100.00	10.00	22.00	4095.14
45.00	120.00	40.00	2.50	802.72
45.00	120.00	40.00	9.00	1733.62
45.00	120.00	40.00	16.00	2736.12
45.00	120.00	40.00	22.00	3595.41
45.00	120.00	30.00	2.50	1004.32
45.00	120.00	30.00	9.00	1935.22
45.00	120.00	30.00	16.00	2937.72
45.00	120.00	30.00	22.00	3797.01
45.00	120.00	20.00	2.50	1363.21
45.00	120.00	20.00	9.00	2314.10
45.00	120.00	20.00	16.00	3316.61
45.00	120.00	20.00	22.00	4175.90
45.00	120.00	10.00	2.50	2474.17
45.00	120.00	10.00	9.00	3405.07
45.00	120.00	10.00	16.00	4407.57
45.00	120.00	10.00	22.00	5266.86

***** BLUNDER ANALYSIS *****

DEPARTURE ANGLE (DEG.)	VELOCITY (KNOTS)	BANK ANGLE (DEG.)	SUMMED DELAYS (SEC.)	BLUNDER RECOVERY AIRSPACE (FT.)
45.00	140.00	40.00	2.50	1022.97
45.00	140.00	40.00	9.00	2109.02
45.00	140.00	40.00	16.00	3278.61
45.00	140.00	40.00	22.00	4281.11
45.00	140.00	30.00	2.50	1297.37
45.00	140.00	30.00	9.00	2383.42
45.00	140.00	30.00	16.00	3553.01
45.00	140.00	30.00	22.00	4555.51
45.00	140.00	20.00	2.50	1813.08
45.00	140.00	20.00	9.00	2899.13
45.00	140.00	20.00	16.00	4068.72
45.00	140.00	20.00	22.00	5071.22
45.00	140.00	10.00	2.50	3298.00
45.00	140.00	10.00	9.00	4384.05
45.00	140.00	10.00	16.00	5553.64
45.00	140.00	10.00	22.00	6556.14
45.00	160.00	40.00	2.50	1267.93
45.00	160.00	40.00	9.00	2509.12
45.00	160.00	40.00	16.00	3845.80
45.00	160.00	40.00	22.00	4991.52
45.00	160.00	30.00	2.50	1626.33
45.00	160.00	30.00	9.00	2867.53
45.00	160.00	30.00	16.00	4204.20
45.00	160.00	30.00	22.00	5349.92
45.00	160.00	20.00	2.50	2299.91
45.00	160.00	20.00	9.00	3541.10
45.00	160.00	20.00	16.00	4877.78
45.00	160.00	20.00	22.00	6023.50
45.00	160.00	10.00	2.50	4239.39
45.00	160.00	10.00	9.00	5480.59
45.00	160.00	10.00	16.00	6817.26
45.00	160.00	10.00	22.00	7962.98

APPENDIX K

DUAL AIRCRAFT BLUNDER ANALYSIS DATA

This appendix contains the output data for the dual aircraft blunder analysis performed in the Lateral Separation study. The purpose of the dual aircraft analysis is to evaluate the blunder recovery airspace required for a blundered aircraft to recover from the type 1 and type 2 blunders, assuming that the blundered aircraft does not immediately respond to controller warnings. Type 1 blunders occur when an aircraft that is on a track which intercepts the approach course at 10°, 20°, or 30° passes through the normal operating zone and proceeds toward the adjacent track. Type 2 blunders occur when an aircraft which is established on the final approach course (within the normal operating zone) makes a turn toward the adjacent course at 15°, 30°, or 45°. The failure of the aircraft to respond makes it necessary for the controller to command an avoidance maneuver for the adjacent aircraft approaching the adjacent runway. The recovery of the blundered aircraft is considered complete when the heading of the blundered aircraft is the same as the heading of the aircraft on the adjacent approach course, meaning that both aircraft are flying parallel courses at that instant. Therefore, this analysis technique not only requires maneuvering the blundered aircraft but also requires maneuvering the aircraft on the adjacent course. The recovery maneuvers are assumed to be coordinated turns in the glideslope plane. The dual aircraft blunder analysis is based upon the assumed sequence of events shown in Table K-1 and the geometry shown in Figure K-1.

The dual aircraft analysis was used to determine the lateral recovery airspace for all combinations of the parameter values in Table K-2, excluding the data acquisition system (DAS) accuracies (ϵ_R and ϵ_A), and the results are presented in tabular form in Table K-3. Values for DAS errors (EDAS) should be added to these data when the position of the DAS antenna and the blundered aircraft can be approximated.

EDAS is evaluated by using the following equations:

$$EDAS = E_A \cos \phi + \sin \phi$$

Table K-1

Dual Aircraft Blunder Analysis
Sequence of Delays

Blundered Aircraft	Adjacent Aircraft
(1) DAS update delay	
(2) Controller ₁ communication time	
(3) Pilot ₁ reaction time	
(4) Aircraft ₁ response time	(4) Controller ₁ to Controller ₂ delay
(5) Aircraft ₁ turn time	(5) Controller ₂ communication time
	(6) Pilot ₂ reaction time
	(7) Aircraft ₂ response time
	(8) Aircraft ₂ turn time

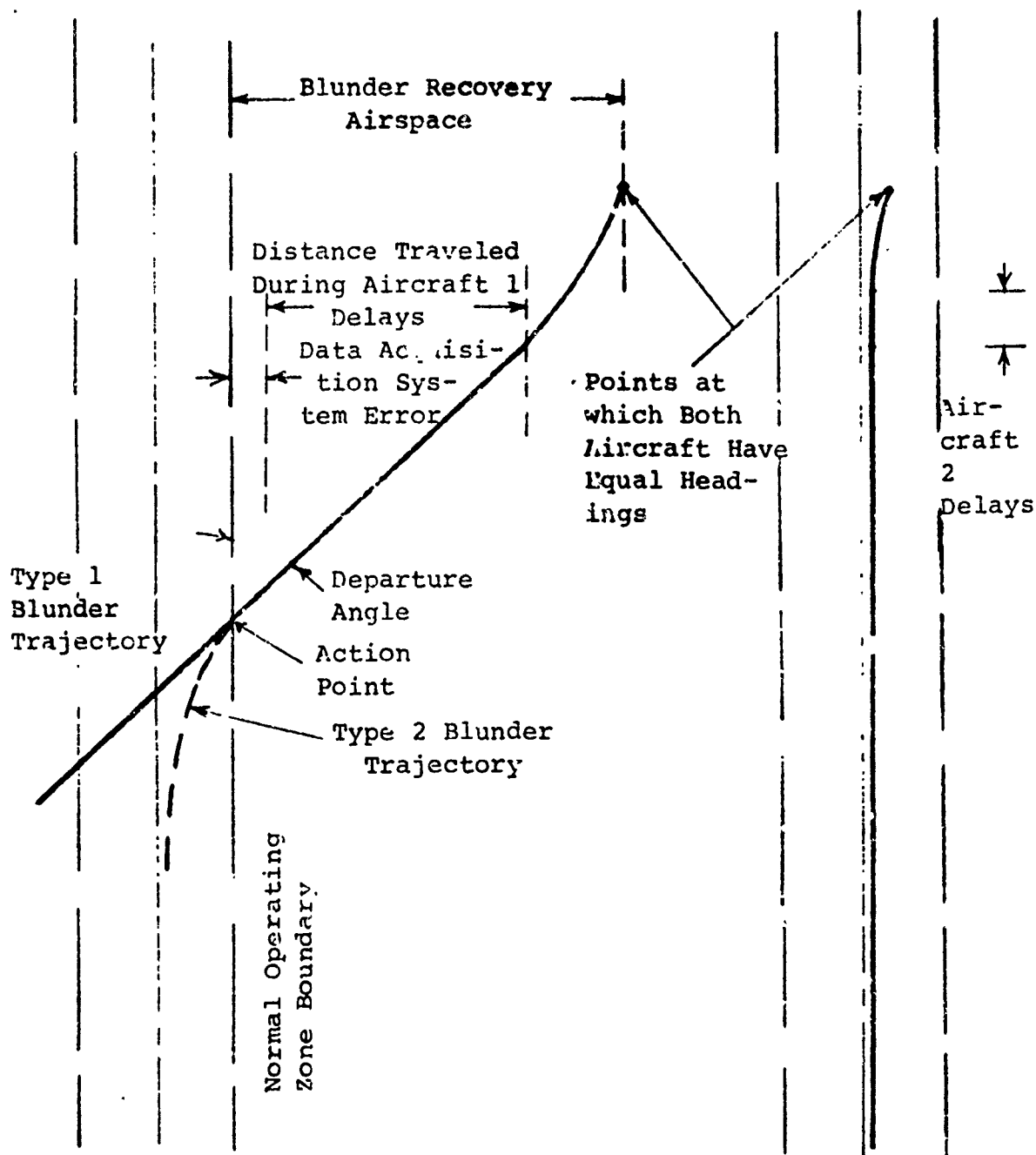


Figure K-1 Dual Aircraft Geometric Analysis

Table K-2 Blundered Aircraft Parameter Values

Parameters	Values	Units
Departure Angles		
Type 1 Blunder	10, 20, and 30	degrees
Type 2 Blunder	15, 30, and 45	degrees
DAS Range Accuracy (ϵ_R)	1.5, 1.0, .5, and .2	percentages of range
DAS Azimuth Accuracy (ϵ_A)	1.5, 1.0, and .5	degrees
DAS Update Delays	4, 2, 1, .5, .1, and .01	seconds
Aircraft Velocities	60, 80, 100, 120, 140, and 160	knots
Aircraft Bank Angles	10, 20, 30, and 40	degrees
Pilot/Aircraft Reaction Times	1.5, 5, and 8	seconds
Communication Times	1 to 10	seconds

where,

$$E_A = R \tan \epsilon_A$$

$$E_R = \frac{\epsilon_R R}{100}$$

$$R = \sqrt{(X_{DAS} - X_{A/C})^2 + (Y_{DAS} - Y_{A/C})^2 + (Z_{DAS} - Z_{A/C})^2}$$

$$\rho = \tan^{-1} \left| \frac{Y_{DAS} - Y_{A/C}}{X_{DAS} - X_{A/C}} \right|$$

with,

$X_{A/C}$ - Aircraft ground range to touchdown, ft.

$Y_{A/C}$ - Aircraft lateral location from the runway centerline, ft.

$Z_{A/C}$ - Aircraft altitude, ft.

X_{DAS} - DAS antenna ground range from touchdown, ft.

Y_{DAS} - DAS antenna lateral location from the runway centerline, ft.

Z_{DAS} - DAS antenna altitude, ft.

The above equations were derived by using the geometry illustrated in Figure K-2.

The column headings for Table K-3 are explained as follows:

Blundered Departure Angle (deg.) - the angle at which a blundered aircraft heads toward the adjacent approach course measured from the extended runway centerline.

Blundered Velocity (knots) - the velocity of the blundered aircraft.

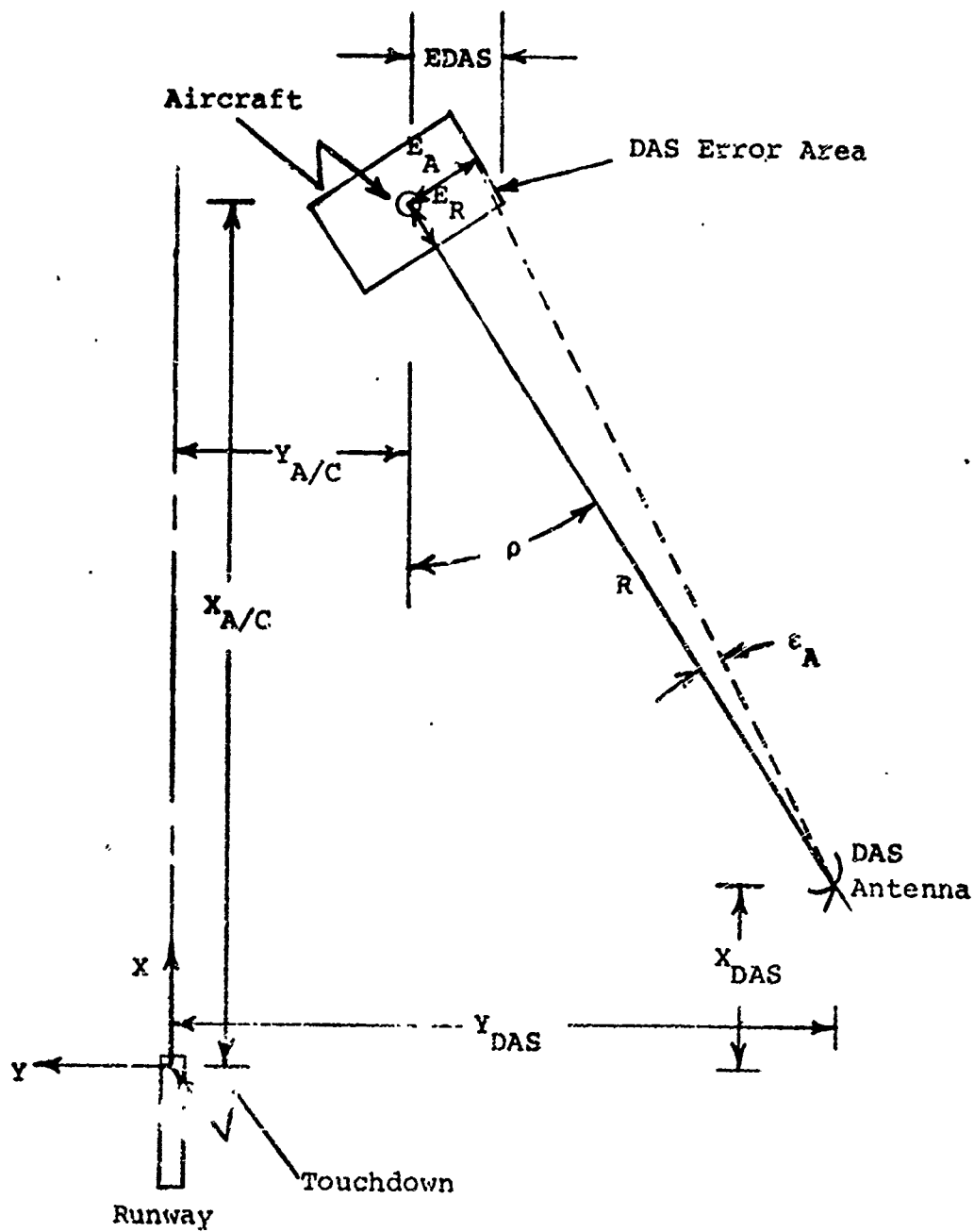


Figure K-2 DAS Configuration

Blundered Bank Angle (deg.) - the bank angle that the blundered aircraft uses to make the corrective maneuver.

Blundered Summed Delays (sec.) - a total of all the delays of the blundered aircraft, including DAS Update Delay, Communication Time, and Pilot/Aircraft Reaction Time.

Adjacent Summed Delays (sec.) - a total of all the delays of the adjacent aircraft, including the Communication Time and Pilot/Aircraft Reaction Time measured from the time controller₁ communicates to controller₂. This occurs at the end of the Blundered Summed Delays.

Corrected Parallel Headings (deg.) - the heading angle of both the blundered and adjacent aircraft at the point in time when they are flying parallel courses (i.e., the blunder is corrected).

Blunder Correction Time (sec.) - the total time required for a blundered aircraft to attain a flight course parallel with that of the aircraft on the adjacent course (total blunder recovery time measured from the time the blundered aircraft reaches the action point until the blunder is corrected).

Blunder Recovery Airspace (ft.) - the lateral recovery airspace, excluding EDAS, required for a blundered aircraft to recover to a course parallel with that of the adjacent aircraft. The blunder recovery airspace is measured from the action point perpendicular to the extended runway centerline.

The dual aircraft analysis assumed that the heading of the adjacent aircraft was equal to 180 degrees (the assumed runway heading) and that the turn rate of the adjacent aircraft was equal to -3.0 degrees per second. It should be noted that the blunder recovery airspace does not always vary with a change of the adjacent summed delays. This condition is due to the blundered aircraft correcting its heading error before the adjacent aircraft has time to start a maneuver.

Table K-3

Dual Aircraft Blunder Analysis Output

***** BLUNDER ANALYSIS - DUAL AIRCRAFT MANEUVER ***** PAGE = 1

BLUNDERED DEPARTURE ANGLE (DEG.)	BLUNDERED VELOCITY (KNOTS)	BLUNDERED BANK ANGLE (DEG.)	BLUNDERED SUMMED DELAYS (SEC.)	ADJACENT SUMMED DELAYS (SEC.)	CORRECTED PARALLEL HEADINGS (DEG.)	BLUNDER CORRECTION TIME (SEC.)	BLUNDER RECOVERY AIRSPACE (FT.)
10.00	60.00	40.00	2.50	1.00	180.00	3.15	49.73
10.00	60.00	40.00	2.50	4.00	180.00	3.15	49.73
10.00	60.00	40.00	2.50	7.00	180.00	3.15	49.73
10.00	60.00	40.00	2.50	10.00	180.00	3.15	49.73
10.00	60.00	40.00	9.00	1.00	180.00	9.65	164.03
10.00	60.00	40.00	9.00	4.00	180.00	9.65	164.03
10.00	60.00	40.00	9.00	7.00	180.00	9.65	164.03
10.00	60.00	40.00	9.00	10.00	180.00	9.65	164.03
10.00	60.00	40.00	16.00	1.00	180.00	16.65	287.13
10.00	60.00	40.00	16.00	4.00	180.00	16.65	287.13
10.00	60.00	40.00	16.00	7.00	180.00	16.65	287.13
10.00	60.00	40.00	16.00	10.00	180.00	16.65	287.13
10.00	60.00	40.00	22.00	1.00	180.00	22.65	392.64
10.00	60.00	40.00	22.00	4.00	180.00	22.65	392.64
10.00	60.00	40.00	22.00	7.00	180.00	22.65	392.64
10.00	60.00	40.00	22.00	10.00	180.00	22.65	392.64
10.00	60.00	30.00	2.50	1.00	180.00	3.45	52.34
10.00	60.00	30.00	2.50	4.00	180.00	3.45	52.34
10.00	60.00	30.00	2.50	7.00	180.00	3.45	52.34
10.00	60.00	30.00	2.50	10.00	180.00	3.45	52.34
10.00	60.00	30.00	9.00	1.00	180.00	9.95	166.65
10.00	60.00	30.00	9.00	4.00	180.00	9.95	166.65
10.00	60.00	30.00	9.00	7.00	180.00	9.95	166.65
10.00	60.00	30.00	9.00	10.00	180.00	9.95	166.65
10.00	60.00	30.00	16.00	1.00	180.00	16.95	289.74
10.00	60.00	30.00	16.00	4.00	180.00	16.95	289.74
10.00	60.00	30.00	16.00	7.00	180.00	16.95	289.74
10.00	60.00	30.00	16.00	10.00	180.00	16.95	289.74
10.00	60.00	30.00	22.00	1.00	180.00	22.95	395.25
10.00	60.00	30.00	22.00	4.00	180.00	22.95	395.25
10.00	60.00	30.00	22.00	7.00	180.00	22.95	395.25
10.00	60.00	30.00	22.00	10.00	180.00	22.95	395.25

***** BLUNDER ANALYSIS - DATA, AIRCRAFT MANEUVER ***** PAGE = 2

BLUNDERED DEPARTURE ANGLE (DEG.)	BLUNDERED VELOCITY (KNOTS)	BLUNDERED BANK ANGLE (DEG.)	BLUNDERED SUMMED DELAYS (SEC.)	ADJACENT SUMMED DELAYS (SEC.)	CORRECTED PARALLEL HEADINGS (DEG.)	LUNDER CORRECTION TIME (SEC.)	BLUNDER RECOVERY AIRSPACE (FT.)
10.00	60.00	20.00	2.50	1.00	178.95	3.85	57.11
10.00	60.00	20.00	2.50	4.00	180.00	4.01	57.26
10.00	60.00	20.00	2.50	7.00	180.00	4.01	57.26
10.00	60.00	20.00	2.50	10.00	180.00	4.01	57.26
10.00	60.00	20.00	9.00	1.00	178.95	10.35	171.41
10.00	60.00	20.00	9.00	4.00	180.00	10.51	171.56
10.00	60.00	20.00	9.00	7.00	180.00	10.51	171.56
10.00	60.00	20.00	9.00	10.00	180.00	10.51	171.56
10.00	60.00	20.00	16.00	1.00	178.95	17.35	294.51
10.00	60.00	20.00	16.00	4.00	180.00	17.51	294.65
10.00	60.00	20.00	16.00	7.00	180.00	17.51	294.65
10.00	60.00	20.00	16.00	10.00	180.00	17.51	294.65
10.00	60.00	20.00	22.00	1.00	178.95	23.35	400.02
10.00	60.00	20.00	22.00	4.00	180.00	23.51	400.16
10.00	60.00	20.00	22.00	7.00	180.00	23.51	400.16
10.00	60.00	20.00	22.00	10.00	180.00	23.51	400.16
10.00	60.00	10.00	2.50	1.00	176.72	4.59	60.45
10.00	60.00	10.00	2.50	4.00	180.00	5.61	71.40
10.00	60.00	10.00	2.50	7.00	180.00	5.61	71.40
10.00	60.00	10.00	2.50	10.00	180.00	5.61	71.40
10.00	60.00	10.00	9.00	1.00	176.72	11.09	102.75
10.00	60.00	10.00	9.00	4.00	180.00	12.11	105.71
10.00	60.00	10.00	9.00	7.00	180.00	12.11	105.71
10.00	60.00	10.00	9.00	10.00	180.00	12.11	105.71
10.00	60.00	10.00	16.00	1.00	176.72	18.09	305.85
10.00	60.00	10.00	16.00	4.00	180.00	19.11	308.80
10.00	60.00	10.00	16.00	7.00	180.00	19.11	308.80
10.00	60.00	10.00	16.00	10.00	180.00	19.11	308.80
10.00	60.00	10.00	22.00	1.00	176.72	24.09	411.36
10.00	60.00	10.00	22.00	4.00	180.00	25.11	414.31
10.00	60.00	10.00	22.00	7.00	180.00	25.11	414.31
10.00	60.00	10.00	22.00	10.00	180.00	25.11	414.31

***** BLUNDER ANALYSIS - JUAL AIRCRAFT MANEUVER ***** PAGE = 3

BLUNDERED DEPARTURE ANGLE (DEG.)	BLUNDERED VELOCITY (KNOTS)	BLUNDERED BANK ANGLE (DEG.)	BLUNDERED SUMMIT DELAYS (SEC.)	ADJACENT SUMMIT DELAYS (SEC.)	CORRECTED PARALLEL HEADINGS (DEG.)	BLUNDER CORRECTION TIME (SEC.)	BLUNDER RECOVERY AIRSPACE (FT.)
10.00	80.00	40.00	2.50	1.00	180.00	3.37	68.87
10.00	80.00	40.00	2.50	4.00	180.00	3.37	68.87
10.00	80.00	40.00	2.50	7.00	180.00	3.37	68.87
10.00	80.00	40.00	2.50	10.00	180.00	3.37	68.87
10.00	80.00	40.00	9.00	1.00	180.00	9.87	221.27
10.00	80.00	40.00	9.00	4.00	180.00	9.87	221.27
10.00	80.00	40.00	9.00	7.00	180.00	9.87	221.27
10.00	80.00	40.00	1.00	10.00	180.00	9.87	221.27
10.00	80.00	40.00	16.00	1.00	180.00	16.87	385.40
10.00	80.00	40.00	16.00	4.00	180.00	16.87	385.40
10.00	80.00	40.00	16.00	7.00	180.00	16.87	385.40
10.00	80.00	40.00	16.00	10.00	180.00	16.87	385.40
10.00	80.00	40.00	22.00	1.00	180.00	22.87	526.08
10.00	80.00	40.00	22.00	4.00	180.00	22.87	526.08
10.00	80.00	40.00	22.00	7.00	180.00	22.87	526.08
10.00	80.00	40.00	22.00	10.00	180.00	22.87	526.08
10.00	80.00	30.00	2.50	1.00	179.42	3.69	73.47
10.00	80.00	30.00	2.50	4.00	180.00	3.77	73.52
10.00	80.00	30.00	2.50	7.00	180.00	3.77	73.52
10.00	80.00	30.00	2.50	10.00	180.00	3.77	73.52
10.00	80.00	30.00	9.00	1.00	179.42	10.19	225.87
10.00	80.00	30.00	9.00	4.00	180.00	10.27	225.92
10.00	80.00	30.00	9.00	7.00	180.00	10.27	225.92
10.00	80.00	30.00	9.00	10.00	180.00	10.27	225.92
10.00	80.00	30.00	16.00	1.00	179.42	17.19	390.00
10.00	80.00	30.00	16.00	4.00	180.00	17.27	390.05
10.00	80.00	30.00	16.00	7.00	180.00	17.27	390.05
10.00	80.00	30.00	16.00	10.00	180.00	17.27	390.05
10.00	80.00	30.00	22.00	1.00	179.42	23.19	530.68
10.00	80.00	30.00	22.00	4.00	180.00	23.27	530.73
10.00	80.00	30.00	22.00	7.00	180.00	23.27	530.73
10.00	80.00	30.00	22.00	10.00	180.00	23.27	530.73

***** FLUNDER ANALYSIS - DUAL AIRCRAFT NAME JVE *****

BLUNDERED DEPARTURE ANGLE (DEG.)	BLUNDERED VELOCITY (KNOTS)	BLUNDERED BANK ANGLE (DEG.)	BLUNDERED SUMMED DELAYS (SEC.)	ADJACENT SUMMED DELAYS (SEC.)	BLUNDERED CORRECTION TIME (SEC.)	BLUNDER RECOVERY AIRSPACE (FT.)
10.00	80.00	20.00	2.50	1.00	4.15	81.40
10.00	80.00	20.00	2.50	4.00	4.51	82.25
10.00	80.00	20.00	2.50	7.00	4.51	82.25
10.00	80.00	20.00	2.50	10.00	4.51	82.25
10.00	80.00	20.00	9.00	1.00	10.63	233.81
10.00	80.00	20.00	9.00	4.00	11.01	234.65
10.00	80.00	20.00	9.00	7.00	11.01	234.65
10.00	80.00	20.00	9.00	10.00	11.01	234.65
10.00	80.00	20.00	16.00	1.00	17.63	397.93
10.00	80.00	20.00	16.00	4.00	18.01	398.78
10.00	80.00	20.00	16.00	7.00	18.01	398.78
10.00	80.00	20.00	16.00	10.00	18.01	398.78
10.00	80.00	20.00	22.00	1.00	23.63	538.61
10.00	80.00	20.00	22.00	4.00	24.01	539.46
10.00	80.00	20.00	22.00	7.00	24.01	539.46
10.00	80.00	20.00	22.00	10.00	24.01	539.46
10.00	80.00	10.00	2.50	1.00	4.90	98.71
10.00	80.00	10.00	2.50	4.00	6.57	107.38
10.00	80.00	10.00	2.50	7.00	6.65	107.40
10.00	80.00	10.00	2.50	10.00	6.65	107.40
10.00	80.00	10.00	9.00	1.00	11.40	251.14
10.00	80.00	10.00	9.00	4.00	13.07	259.78
10.00	80.00	10.00	9.00	7.00	13.15	259.80
10.00	80.00	10.00	9.00	10.00	13.15	259.80
10.00	80.00	10.00	16.00	1.00	18.40	415.27
10.00	80.00	10.00	16.00	4.00	20.07	423.91
10.00	80.00	10.00	16.00	7.00	20.15	423.93
10.00	80.00	10.00	16.00	10.00	20.15	423.93
10.00	80.00	10.00	22.00	1.00	24.40	555.95
10.00	80.00	10.00	22.00	4.00	26.07	564.59
10.00	80.00	10.00	22.00	7.00	26.15	564.61
10.00	80.00	10.00	22.00	10.00	26.15	564.61

Reproduced from
best available copy.



***** BLUNDER ANALYSIS - DUAL AIRCRAFT - MANEUVER ***** PAGE = 5

BLUNDERED DEPARTURE ANGLE (DEG.)	BLUNDERED VELOCITY (KNOTS)	BLUNDERED BANK ANGLE (DEG.)	BLUNDERED SUMMED DELAYS (SEC.)	ADJACENT SUMMED DELAYS (SEC.)	CORRECTED PARALLEL HEADINGS (DEG.)	BLUNDER CORRECTION TIME (SEC.)	BLUNDER RECOVERY AIRSPACE (FT.)
10.00	100.00	40.00	2.50	1.00	179.80	3.57	279.28
10.00	100.00	40.00	2.50	4.00	180.00	3.59	279.29
10.00	100.00	40.00	2.50	7.00	180.00	3.59	89.29
10.00	100.00	40.00	2.50	10.00	180.00	3.59	89.29
10.00	100.00	40.00	9.00	1.00	179.80	10.07	279.73
10.00	100.00	40.00	9.00	4.00	180.00	10.09	279.73
10.00	100.00	40.00	9.00	7.00	180.00	10.09	279.79
10.00	100.00	40.00	9.00	10.00	180.00	10.09	279.79
10.00	100.00	40.00	16.00	1.00	179.80	17.07	484.95
10.00	100.00	40.00	16.00	4.00	180.00	17.09	484.95
10.00	100.00	40.00	16.00	7.00	180.00	17.09	484.95
10.00	100.00	40.00	16.00	10.00	180.00	17.09	484.95
10.00	100.00	40.00	22.00	1.00	179.80	23.07	660.80
10.00	100.00	40.00	22.00	4.00	180.00	23.09	660.80
10.00	100.00	40.00	22.00	7.00	180.00	23.09	660.80
10.00	100.00	40.00	22.00	10.00	180.00	23.09	660.80
10.00	100.00	30.00	2.50	1.00	178.81	3.90	96.22
10.00	100.00	30.00	2.50	4.00	180.00	4.08	96.55
10.00	100.00	30.00	2.50	7.00	180.00	4.08	96.55
10.00	100.00	30.00	2.50	10.00	180.00	4.08	96.55
10.00	100.00	30.00	9.00	1.00	178.81	10.40	286.73
10.00	100.00	30.00	9.00	4.00	180.00	10.58	287.06
10.00	100.00	30.00	9.00	7.00	180.00	10.58	287.06
10.00	100.00	30.00	9.00	10.00	180.00	10.58	287.06
10.00	100.00	30.00	16.00	1.00	178.81	17.40	491.88
10.00	100.00	30.00	16.00	4.00	180.00	17.58	492.21
10.00	100.00	30.00	16.00	7.00	180.00	17.58	492.21
10.00	100.00	30.00	16.00	10.00	180.00	17.58	492.21
10.00	100.00	30.00	22.00	1.00	178.81	23.40	667.73
10.00	100.00	30.00	22.00	4.00	180.00	23.58	668.06
10.00	100.00	30.00	22.00	7.00	180.00	23.58	668.06
10.00	100.00	30.00	22.00	10.00	180.00	23.58	668.06

***** BLUNDER ANALYSIS - DUAL AIRCRAFT NAIEUVR *****

BLUNDERED DEPARTURE ANGLE (DEG.)	BLUNDERED VELOCITY (KNOTS)	BLUNDERED BANK ANGLE (DEG.)	BLUNDERED SUMMED DELAYS (SEC.)	ADJACENT SUMMED DELAYS (SEC.)	CORRECTED PARALLEL HEADINGS (DEG.)	BLUNDER CORRECTION TIME (SEC.)	BLUNDER RECOVERY AIRSPACE (FT.)
10.00	100.00	20.00	2.50	1.00	177.41	4.36	107.72
10.00	100.00	20.00	2.50	4.00	180.00	5.01	110.20
10.00	100.00	20.00	2.50	7.00	180.00	5.01	110.20
10.00	100.00	20.00	2.50	10.00	180.00	5.01	110.20
10.00	100.00	20.00	9.00	1.00	177.41	10.86	298.22
10.00	100.00	20.00	9.00	4.00	180.00	11.51	300.70
10.00	100.00	20.00	9.00	7.00	180.00	11.51	300.70
10.00	100.00	20.00	9.00	10.00	180.00	11.51	300.70
10.00	100.00	20.00	16.00	1.00	177.41	17.86	503.38
10.00	100.00	20.00	16.00	4.00	180.00	18.51	505.86
10.00	100.00	20.00	16.00	7.00	180.00	18.51	505.86
10.00	100.00	20.00	16.00	10.00	180.00	18.51	505.86
10.00	100.00	20.00	22.00	1.00	177.41	23.86	679.23
10.00	100.00	20.00	22.00	4.00	180.00	24.51	681.71
10.00	100.00	20.00	22.00	7.00	180.00	24.51	681.71
10.00	100.00	20.00	22.00	10.00	180.00	24.51	681.71
10.00	100.00	10.00	2.50	1.00	175.09	5.14	131.05
10.00	100.00	10.00	2.50	4.00	178.61	6.96	148.01
10.00	100.00	10.00	2.50	7.00	180.00	7.69	149.50
10.00	100.00	10.00	2.50	10.00	180.00	7.69	149.50
10.00	100.00	10.00	9.00	1.00	175.09	11.64	321.55
10.00	100.00	10.00	9.00	4.00	178.61	13.46	338.51
10.00	100.00	10.00	9.00	7.00	180.00	14.19	340.00
10.00	100.00	10.00	9.00	10.00	180.00	14.19	340.00
10.00	100.00	10.00	16.00	1.00	175.09	18.64	526.71
10.00	100.00	10.00	16.00	4.00	178.61	20.46	543.67
10.00	100.00	10.00	16.00	7.00	180.00	21.19	545.16
10.00	100.00	10.00	16.00	10.00	180.00	21.19	545.16
10.00	100.00	10.00	22.00	1.00	175.09	24.64	702.56
10.00	100.00	10.00	22.00	4.00	178.61	26.46	719.52
10.00	100.00	10.00	22.00	7.00	180.00	27.19	721.01
10.00	100.00	10.00	22.00	10.00	180.00	27.19	721.01

***** BLUNDER ANALYSIS - DUAL AIRCRAFT MANEUVER *****

BLUNDERED DEPARTURE ANGLE (DEG.)	BLUNDERED VELOCITY (KNOTS)	BLUNDERED BANK ANGLE (DEG.)	BLUNDERED SUMMED DELAYS (SEC.)	ADJACENT SUMMED DELAYS (SEC.)	CORRECTED PARALLEL HEADINGS (DEG.)	BLUNDER CORRECTION TIME (SEC.)	BLUNDER RECOVERY AIRSPACE (FT.)
10.00	120.00	40.00	2.50	1.00	179.34	3.72	110.89
10.00	120.00	40.00	2.50	4.00	180.00	3.81	110.99
10.00	120.00	40.00	2.50	7.00	180.00	3.81	110.99
10.00	120.00	40.00	2.50	10.00	180.00	3.81	110.99
10.00	120.00	40.00	9.00	1.00	179.34	10.22	339.49
10.00	120.00	40.00	9.00	4.00	180.00	10.31	339.60
10.00	120.00	40.00	9.00	7.00	180.00	10.31	339.60
10.00	120.00	40.00	9.00	10.00	180.00	10.31	339.60
10.00	120.00	40.00	16.00	1.00	179.34	17.22	585.60
10.00	120.00	40.00	16.00	4.00	180.00	17.31	585.79
10.00	120.00	40.00	16.00	7.00	180.00	17.31	585.79
10.00	120.00	40.00	16.00	10.00	180.00	17.31	585.79
10.00	120.00	40.00	22.00	1.00	179.34	23.22	796.71
10.00	120.00	40.00	22.00	4.00	180.00	23.31	796.81
10.00	120.00	40.00	22.00	7.00	180.00	23.31	796.81
10.00	120.00	40.00	22.00	10.00	180.00	23.31	796.81
10.00	120.00	30.00	2.50	1.00	178.28	4.07	120.45
10.00	120.00	30.00	2.50	4.00	180.00	4.40	121.45
10.00	120.00	30.00	2.50	7.00	180.00	4.40	121.45
10.00	120.00	30.00	2.50	10.00	180.00	4.40	121.45
10.00	120.00	30.00	9.00	1.00	178.28	10.57	349.06
10.00	120.00	30.00	9.00	4.00	180.00	10.90	350.05
10.00	120.00	30.00	9.00	7.00	180.00	10.90	350.05
10.00	120.00	30.00	9.00	10.00	180.00	10.90	350.05
10.00	120.00	30.00	16.00	1.00	178.28	17.57	595.25
10.00	120.00	30.00	16.00	4.00	180.00	17.90	596.24
10.00	120.00	30.00	16.00	7.00	180.00	17.90	596.24
10.00	120.00	30.00	16.00	10.00	180.00	17.90	596.24
10.00	120.00	30.00	22.00	1.00	178.28	23.57	806.27
10.00	120.00	30.00	22.00	4.00	180.00	23.90	807.26
10.00	120.00	30.00	22.00	7.00	180.00	23.90	807.26
10.00	120.00	30.00	22.00	10.00	180.00	23.90	807.26

***** BLUNDER ANALYSIS - DUAL AIRCRAFT *****										P, G, L = A	
BLUNDERED DEPARTURE ANGLE (DEG.)	BLUNDERED VELOCITY (KNOTS)	BLUNDERED BANK ANGLE (DEG.)	BLUNDERED SUMMED DELAYS (SEC.)	ADJACENT SUMMED DELAYS (SEC.)	CORRECTED PARALLEL HEADINGS (DEG.)	BLUNDER CORRECTION TIME (SEC.)	BLUNDER RECOVERY AIRSPACE (FT.)				
10.00	120.00	20.00	2.50	1.00	176.82	4.56	135.73				
10.00	120.00	20.00	2.50	4.00	180.00	5.52	141.10				
10.00	120.00	20.00	2.50	7.00	180.00	5.52	141.10				
10.00	120.00	20.00	2.50	10.00	180.00	5.52	141.10				
10.00	120.00	20.00	9.00	1.00	176.82	11.06	364.33				
10.00	120.00	20.00	9.00	4.00	180.00	12.02	369.71				
10.00	120.00	20.00	9.00	7.00	180.00	12.02	369.71				
10.00	120.00	20.00	9.00	10.00	180.00	12.02	369.71				
10.00	120.00	20.00	16.00	1.00	176.82	18.06	610.52				
10.00	120.00	20.00	16.00	4.00	180.00	19.02	615.90				
10.00	120.00	20.00	16.00	7.00	180.00	19.02	615.90				
10.00	120.00	20.00	16.00	10.00	180.00	19.02	615.90				
10.00	120.00	20.00	22.00	1.00	176.82	24.06	821.54				
10.00	120.00	20.00	22.00	4.00	180.00	25.02	826.92				
10.00	120.00	20.00	22.00	7.00	180.00	25.02	826.92				
10.00	120.00	20.00	22.00	10.00	180.00	25.02	826.92				
10.00	120.00	10.00	2.50	1.00	174.53	5.32	164.82				
10.00	120.00	10.00	2.50	4.00	177.67	7.28	191.72				
10.00	120.00	10.00	2.50	7.00	180.00	8.73	197.69				
10.00	120.00	10.00	2.50	10.00	180.00	8.73	197.69				
10.00	120.00	10.00	9.00	1.00	174.53	11.82	393.43				
10.00	120.00	10.00	9.00	4.00	177.67	13.78	420.33				
10.00	120.00	10.00	9.00	7.00	180.00	15.23	426.29				
10.00	120.00	10.00	9.00	10.00	180.00	15.23	426.29				
10.00	120.00	10.00	16.00	1.00	174.53	18.82	639.62				
10.00	120.00	10.00	16.00	4.00	177.67	20.78	666.52				
10.00	120.00	10.00	16.00	7.00	180.00	22.23	672.48				
10.00	120.00	10.00	16.00	10.00	180.00	22.23	672.48				
10.00	120.00	10.00	22.00	1.00	174.53	24.82	850.64				
10.00	120.00	10.00	22.00	4.00	177.67	26.78	877.54				
10.00	120.00	10.00	22.00	7.00	180.00	28.23	883.50				
10.00	120.00	10.00	22.00	10.00	180.00	28.23	883.50				

***** BLUNDER ANALYSIS - DUAL AIRCRAFT MANEUVER ***** PAGE = 9

BLUNDERED DEPARTURE ANGLE (DEG.)	BLUNDERED VELOCITY (KNOTS)	BLUNDERED BANK ANGLE (DEG.)	BLUNDERED SUMMEL DELAYS (SEC.)	ADJACENT SUMMEL DELAYS (SEC.)	CORRECTED PARALLEL HEADINGS (DEG.)	BLUNDER CORRECTION TIME (SEC.)	BLUNDER RECOVERY AIRSPACE (FT.)
10.00	140.00	40.00	2.50	1.00	178.92	3.86	133.60
10.00	140.00	40.00	2.50	4.00	180.00	4.03	133.97
10.00	140.00	40.00	2.50	7.00	180.00	4.03	133.97
10.00	140.00	40.00	2.50	10.00	180.00	4.03	133.97
10.00	140.00	40.00	9.00	1.00	178.92	10.36	400.31
10.00	140.00	40.00	9.00	4.00	180.00	10.53	400.68
10.00	140.00	40.00	9.00	7.00	180.00	10.53	400.68
10.00	140.00	40.00	9.00	10.00	180.00	10.53	400.68
10.00	140.00	40.00	16.00	1.00	178.92	17.36	687.53
10.00	140.00	40.00	16.00	4.00	180.00	17.53	687.90
10.00	140.00	40.00	16.00	7.00	180.00	17.53	687.90
10.00	140.00	40.00	16.00	10.00	180.00	17.53	687.90
10.00	140.00	40.00	22.00	1.00	178.92	23.36	933.72
10.00	140.00	40.00	22.00	4.00	180.00	23.53	934.09
10.00	140.00	40.00	22.00	7.00	180.00	23.53	934.09
10.00	140.00	40.00	22.00	10.00	180.00	23.53	934.09
10.00	140.00	30.00	2.50	1.00	177.81	4.23	146.00
10.00	140.00	30.00	2.50	4.00	180.00	4.72	143.21
10.00	140.00	30.00	2.50	7.00	180.00	4.72	148.21
10.00	140.00	30.00	2.50	10.00	180.00	4.72	148.21
10.00	140.00	30.00	9.00	1.00	177.81	10.73	412.71
10.00	140.00	30.00	9.00	4.00	180.00	11.22	414.91
10.00	140.00	30.00	9.00	7.00	180.00	11.22	414.91
10.00	140.00	30.00	9.00	10.00	180.00	11.22	414.91
10.00	140.00	30.00	16.00	1.00	177.81	17.73	699.93
10.00	140.00	30.00	16.00	4.00	180.00	18.22	702.14
10.00	140.00	30.00	16.00	7.00	180.00	18.22	702.14
10.00	140.00	30.00	16.00	10.00	180.00	18.22	702.14
10.00	140.00	30.00	22.00	1.00	177.81	23.73	946.12
10.00	140.00	30.00	22.00	4.00	180.00	24.22	948.33
10.00	140.00	30.00	22.00	7.00	180.00	24.22	948.33
10.00	140.00	30.00	22.00	10.00	180.00	24.22	948.33

***** BLUNDER ANALYSIS - DUAL AIRCRAFT ***** PAGE = 10

BLUNDER DEPARTURE ANGLE (DEG.)	BLUNDERED VELOCITY (KNOTS)	BLUNDERED BANK ANGLE (DEG.)	BLUNDERED SUMMED DELAYS (SEC.)	ADJACENT SUMMED DELAYS (SEC.)	CORRECTED PARALLEL HEADINGS (DEG.)	BLUNDER CORRECTION TIME (SEC.)	BLUNDER RECOVERY AIRSPACE (FT.)
10.00	140.00	20.00	2.50	1.00	176.32	4.73	165.15
10.00	140.00	20.00	2.50	4.00	180.00	6.02	174.96
10.00	140.00	20.00	2.50	7.00	180.00	6.02	174.96
10.00	140.00	20.00	2.50	10.00	180.00	6.02	174.96
10.00	140.00	20.00	9.00	1.00	176.32	11.23	431.86
10.00	140.00	20.00	9.00	4.00	180.00	12.52	441.66
10.00	140.00	20.00	9.00	7.00	180.00	12.52	441.66
10.00	140.00	20.00	9.00	10.00	180.00	12.52	441.66
10.00	140.00	20.00	16.00	1.00	176.32	18.23	719.08
10.00	140.00	20.00	16.00	4.00	180.00	19.52	728.89
10.00	140.00	20.00	16.00	7.00	180.00	19.52	728.89
10.00	140.00	20.00	16.00	10.00	180.00	19.52	728.89
10.00	140.00	20.00	22.00	1.00	176.32	24.23	965.27
10.00	140.00	20.00	22.00	4.00	180.00	25.52	975.08
10.00	140.00	20.00	22.00	7.00	180.00	25.52	975.08
10.00	140.00	20.00	22.00	10.00	180.00	25.52	975.08
10.00	140.00	10.00	2.50	1.00	174.09	5.47	199.70
10.00	140.00	10.00	2.50	4.00	176.92	7.53	237.78
10.00	140.00	10.00	2.50	7.00	179.75	9.58	251.89
10.00	140.00	10.00	2.50	10.00	180.00	9.76	251.98
10.00	140.00	10.00	9.00	1.00	174.09	11.97	466.40
10.00	140.00	10.00	9.00	4.00	176.92	14.03	504.48
10.00	140.00	10.00	9.00	7.00	179.75	16.08	518.59
10.00	140.00	10.00	9.00	10.00	180.00	16.26	518.69
10.00	140.00	10.00	16.00	1.00	174.09	18.97	753.63
10.00	140.00	10.00	16.00	4.00	176.92	21.03	791.70
10.00	140.00	10.00	16.00	7.00	179.75	23.08	805.81
10.00	140.00	10.00	16.00	10.00	180.00	23.26	805.91
10.00	140.00	10.00	22.00	1.00	174.09	24.97	993.82
10.00	140.00	10.00	22.00	4.00	176.92	27.03	1037.99
10.00	140.00	10.00	22.00	7.00	179.75	29.08	1052.01
10.00	140.00	10.00	22.00	10.00	180.00	29.26	1052.10

MANEUVER

DUAL AIRCRAFT

BLUNDER ANALYSIS

BLUNDERED

VELOCITY

(KNOTS)

BLUNDERED

BLUNDERED DEPARTURE ANGLE (DEG.)	BLUNDERED VELOCITY (KNOTS)	BLUNDERED BANK ANGLE (DEG.)	BLUNDERED SUMMED DELAYS (SEC.)	ADJACENT SUMMED DELAYS (SEC.)	CORRECTED PARALLEL HEADINGS (DEG.)	BLUNDER CORRECTION TIME (SEC.)	BLUNDER RECOVERY AIRSPACE (FT.)
10.00	160.00	40.00	2.50	1.00	178.53	3.99	157.36
10.00	160.00	40.00	2.50	4.00	180.00	4.24	158.24
10.00	160.00	40.00	2.50	7.00	180.00	4.24	158.24
10.00	160.00	40.00	2.50	10.00	180.00	4.24	158.24
10.00	160.00	40.00	9.00	1.00	178.53	10.49	462.16
10.00	160.00	40.00	9.00	4.00	180.00	10.74	463.05
10.00	160.00	40.00	9.00	7.00	180.00	10.74	463.05
10.00	160.00	40.00	9.00	10.00	180.00	10.74	463.05
10.00	160.00	40.00	16.00	1.00	178.53	17.49	790.42
10.00	160.00	40.00	16.00	4.00	180.00	17.74	791.30
10.00	160.00	40.00	16.00	7.00	180.00	17.74	791.30
10.00	160.00	40.00	16.00	10.00	180.00	17.74	791.30
10.00	160.00	40.00	22.00	1.00	178.53	23.49	1071.78
10.00	160.00	40.00	22.00	4.00	180.00	23.74	1072.66
10.00	160.00	40.00	22.00	7.00	180.00	23.74	1072.66
10.00	160.00	40.00	22.00	10.00	180.00	23.74	1072.66
10.00	160.00	30.00	2.50	1.00	177.38	4.37	172.74
10.00	160.00	30.00	2.50	4.00	180.00	5.04	176.83
10.00	160.00	30.00	2.50	7.00	180.00	5.04	176.83
10.00	160.00	30.00	2.50	10.00	180.00	5.04	176.83
10.00	160.00	30.00	9.00	1.00	177.38	10.87	477.55
10.00	160.00	30.00	9.00	4.00	180.00	11.54	481.64
10.00	160.00	30.00	9.00	7.00	180.00	11.54	481.64
10.00	160.00	30.00	9.00	10.00	180.00	11.54	481.64
10.00	160.00	30.00	16.00	1.00	177.38	17.87	805.80
10.00	160.00	30.00	16.00	4.00	180.00	18.54	809.89
10.00	160.00	30.00	16.00	7.00	180.00	18.54	809.89
10.00	160.00	30.00	16.00	10.00	180.00	18.54	809.89
10.00	160.00	30.00	22.00	1.00	177.38	23.87	1087.16
10.00	160.00	30.00	22.00	4.00	180.00	24.54	1091.25
10.00	160.00	30.00	22.00	7.00	180.00	24.54	1091.25
10.00	160.00	30.00	22.00	10.00	180.00	24.54	1091.25

***** BLUNDER ANALYSIS - DUAL AIRCRAFT *****

BLUNDERED DEPARTURE ANGLE (DEG.)	BLUNDERED VELOCITY (KNOTS)	BLUNDERED BANK ANGLE (DEG.)	BLUNDERED SUMMED DELAYS (SEC.)	ADJACENT SUMMED DELAYS (SEC.)	CORRECTED PARALLEL HEADINGS (DEG.)	BLUNDER CORRECTION TIME (SEC.)	PL RECEIVED AIR PACE (F)
10.00	160.00	20.00	2.50	1.00	175.89	4.87	191.78
10.00	160.00	20.00	2.50	4.00	179.97	6.51	211.77
10.00	160.00	20.00	2.50	7.00	180.00	6.52	211.77
10.00	160.00	20.00	2.50	10.00	180.00	6.52	211.77
10.00	160.00	20.00	9.00	1.00	175.89	11.37	500.59
10.00	160.00	20.00	9.00	4.00	179.97	13.01	516.57
10.00	160.00	20.00	9.00	7.00	180.00	13.02	516.57
10.00	160.00	20.00	9.00	10.00	180.00	13.02	516.57
10.00	160.00	20.00	16.00	1.00	175.89	18.37	828.84
10.00	160.00	20.00	16.00	4.00	179.97	20.01	844.83
10.00	160.00	20.00	16.00	7.00	180.00	20.02	844.83
10.00	160.00	20.00	16.00	10.00	180.00	20.02	844.83
10.00	160.00	20.00	22.00	1.00	175.89	24.37	1110.20
10.00	160.00	20.00	22.00	4.00	179.97	26.01	1126.19
10.00	160.00	20.00	22.00	7.00	180.00	26.02	1126.19
10.00	160.00	20.00	22.00	10.00	180.00	26.02	1126.19
10.00	160.00	10.00	2.50	1.00	173.72	5.59	235.40
10.00	160.00	10.00	2.50	4.00	176.30	7.73	285.64
10.00	160.00	10.00	2.50	7.00	176.88	9.87	309.92
10.00	160.00	10.00	2.50	10.00	180.00	10.80	312.37
10.00	160.00	10.00	9.00	1.00	173.72	12.09	540.21
10.00	160.00	10.00	9.00	4.00	176.30	14.23	590.45
10.00	160.00	10.00	9.00	7.00	178.98	16.37	614.73
10.00	160.00	10.00	9.00	10.00	180.00	17.30	617.17
10.00	160.00	10.00	16.00	1.00	173.72	19.09	868.46
10.00	160.00	10.00	16.00	4.00	176.30	21.23	918.70
10.00	160.00	10.00	16.00	7.00	178.88	23.37	942.98
10.00	160.00	10.00	16.00	10.00	180.00	24.30	945.43
10.00	160.00	10.00	22.00	1.00	173.72	25.09	1149.82
10.00	160.00	10.00	22.00	4.00	176.30	27.23	1200.06
10.00	160.00	10.00	22.00	7.00	178.88	29.37	1224.34
10.00	160.00	10.00	22.00	10.00	180.00	30.30	1226.79

***** BLUNDER ANALYSIS - DUAL AIRCRAFT MANEUVER ***** PAGE = 13

BLUNDERED DEPARTURE ANGLE (DEG.)	BLUNDERED VELOCITY (KNOTS)	BLUNDERED BANK ANGLE (DEG.)	BLUNDERED SUMMED DELAYS (SEC.)	ADJACENT SUMMED DELAYS (SEC.)	CORRECTED PARALLEL HEADINGS (DEG.)	BLUNDER CORRECTION TIME (SEC.)	BLUNDER RECOVERY AIRSPACE (FT.)
15.00	60.00	40.00	2.50	1.00	180.00	3.48	78.46
15.00	60.00	40.00	2.50	4.00	180.00	3.48	78.46
15.00	60.00	40.00	2.50	7.00	180.00	3.48	78.46
15.00	60.00	40.00	2.50	10.00	180.00	3.48	78.46
15.00	60.00	40.00	9.00	1.00	180.00	9.98	248.82
15.00	60.00	40.00	9.00	4.00	180.00	9.98	248.82
15.00	60.00	40.00	9.00	7.00	180.00	9.98	248.82
15.00	60.00	40.00	9.00	10.00	180.00	9.98	248.82
15.00	60.00	40.00	16.00	1.00	180.00	16.98	432.30
15.00	60.00	40.00	16.00	4.00	180.00	16.98	432.30
15.00	60.00	40.00	16.00	7.00	180.00	16.98	432.30
15.00	60.00	40.00	16.00	10.00	180.00	16.98	432.30
15.00	60.00	40.00	22.00	1.00	180.00	22.98	589.56
15.00	60.00	40.00	22.00	4.00	180.00	22.98	589.56
15.00	60.00	40.00	22.00	7.00	180.00	22.98	589.56
15.00	60.00	40.00	22.00	10.00	180.00	22.98	589.56
15.00	60.00	30.00	2.50	1.00	179.01	3.83	84.32
15.00	60.00	30.00	2.50	4.00	180.00	3.93	84.32
15.00	60.00	30.00	2.50	7.00	180.00	3.93	84.32
15.00	60.00	30.00	2.50	10.00	180.00	3.93	84.32
15.00	60.00	30.00	9.00	1.00	179.01	10.33	254.60
15.00	60.00	30.00	9.00	4.00	180.00	10.43	254.69
15.00	60.00	30.00	9.00	7.00	180.00	10.43	254.69
15.00	60.00	30.00	9.00	10.00	180.00	10.43	254.69
15.00	60.00	30.00	16.00	1.00	179.01	17.33	438.08
15.00	60.00	30.00	16.00	4.00	180.00	17.43	438.16
15.00	60.00	30.00	16.00	7.00	180.00	17.43	438.16
15.00	60.00	30.00	16.00	10.00	180.00	17.43	438.16
15.00	60.00	30.00	22.00	1.00	179.01	23.33	595.34
15.00	60.00	30.00	22.00	4.00	180.00	23.43	595.42
15.00	60.00	30.00	22.00	7.00	180.00	23.43	595.42
15.00	60.00	30.00	22.00	10.00	180.00	23.43	595.42

***** BLUNDER ANALYSIS - DUAL AIRCRAFT MANUEVER ***** PAGE = 14

BLUNDERED DEPARTURE ANGLE (DEG.)	BLUNDERED VELOCITY (KNOTS)	BLUNDERED BANK ANGLE (DEG.)	BLUNDERED SUMMED DELAYS (SEC.)	ADJACENT SUMMED DELAYS (SEC.)	CORRECTED PARALLEL HEADINGS (DEG.)	BLUNDER CORRECTION TIME (SEC.)	BLUNDER RECOVERY AIRSPACE (FT.)
15.00	60.00	20.00	2.50	1.00	177.39	4.37	94.44
15.00	60.00	20.00	2.50	4.00	180.00	4.76	95.34
15.00	60.00	20.00	2.50	7.00	180.00	4.76	95.34
15.00	60.00	20.00	2.50	10.00	180.00	4.76	95.34
15.00	60.00	20.00	9.00	1.00	177.39	10.37	264.80
15.00	60.00	20.00	9.00	4.00	180.00	11.26	265.71
15.00	60.00	20.00	9.00	7.00	180.00	11.26	265.71
15.00	60.00	20.00	9.00	10.00	180.00	11.26	265.71
15.00	60.00	20.00	16.00	1.00	177.39	17.87	448.27
15.00	60.00	20.00	16.00	4.00	180.00	18.26	449.18
15.00	60.00	20.00	16.00	7.00	180.00	18.26	449.18
15.00	60.00	20.00	16.00	10.00	180.00	18.26	449.18
15.00	60.00	20.00	22.00	1.00	177.39	23.87	605.53
15.00	60.00	20.00	22.00	4.00	180.00	24.26	606.44
15.00	60.00	20.00	22.00	7.00	180.00	24.26	606.44
15.00	60.00	20.00	22.00	10.00	180.00	24.26	606.44
15.00	60.00	10.00	2.50	1.00	174.31	5.40	118.16
15.00	60.00	10.00	2.50	4.00	178.96	6.85	126.77
15.00	60.00	10.00	2.50	7.00	180.00	7.17	127.07
15.00	60.00	10.00	2.50	10.00	180.00	7.17	127.07
15.00	60.00	10.00	9.00	1.00	174.31	11.90	288.53
15.00	60.00	10.00	9.00	4.00	178.96	13.35	297.14
15.00	60.00	10.00	9.00	7.00	180.00	13.67	297.44
15.00	60.00	10.00	9.00	10.00	180.00	13.67	297.44
15.00	60.00	10.00	16.00	1.00	174.31	18.90	472.00
15.00	60.00	10.00	16.00	4.00	178.96	20.35	480.61
15.00	60.00	10.00	16.00	7.00	180.00	20.67	480.91
15.00	60.00	10.00	16.00	10.00	180.00	20.67	480.91
15.00	60.00	10.00	22.00	1.00	174.31	24.90	629.25
15.00	60.00	10.00	22.00	4.00	178.96	26.35	637.67
15.00	60.00	10.00	22.00	7.00	180.00	26.67	638.17
15.00	60.00	10.00	22.00	10.00	180.00	26.67	638.17

***** BLUNDER ANALYSIS - DUAL AIRCRAFT ***** PAGE = 15

BLUNDERED DEPARTURE ANGLE (DEG.)	BLUNDERED VELOCITY (KNOTS)	BLUNDERED BANK ANGLE (DEG.)	BLUNDERED SUMMED DELAYS (SEC.)	ADJACENT SUMMED DELAYS (SEC.)	CORRECTED PARALLEL HEADINGS (DEG.)	BLUNDER CORRECTION TIME (SEC.)	BLUNDER RECOVERY AIRSPACE (FT.)
15.00	80.00	40.00	2.50	1.00	179.27	3.74	110.30
15.00	80.00	40.00	2.50	4.00	180.00	3.81	110.36
15.00	80.00	40.00	2.50	7.00	180.00	3.81	110.36
15.00	80.00	40.00	2.50	10.00	180.00	3.81	110.36
15.00	80.00	40.00	4.00	1.00	179.27	10.24	337.46
15.00	80.00	40.00	9.00	4.00	180.00	10.31	337.51
15.00	80.00	40.00	9.00	7.00	180.00	10.31	337.51
15.00	80.00	40.00	9.00	10.00	180.00	10.31	337.51
15.00	80.00	40.00	16.00	1.00	179.27	17.24	582.09
15.00	80.00	40.00	16.00	4.00	180.00	17.31	582.14
15.00	80.00	40.00	16.00	7.00	180.00	17.31	582.14
15.00	80.00	40.00	16.00	10.00	180.00	17.31	582.14
15.00	80.00	40.00	22.00	1.00	179.27	23.24	791.77
15.00	80.00	40.00	22.00	4.00	180.00	23.31	791.82
15.00	80.00	40.00	22.00	7.00	180.00	23.31	791.82
15.00	80.00	40.00	22.00	10.00	180.00	23.31	791.82
15.00	80.00	30.00	2.50	1.00	178.04	4.15	120.21
15.00	80.00	30.00	2.50	4.00	180.00	4.40	120.78
15.00	80.00	30.00	2.50	7.00	180.00	4.40	120.78
15.00	80.00	30.00	2.50	10.00	180.00	4.40	120.78
15.00	80.00	30.00	9.00	1.00	178.04	10.65	347.36
15.00	80.00	30.00	9.00	4.00	180.00	10.90	347.94
15.00	80.00	30.00	9.00	7.00	180.00	10.90	347.94
15.00	80.00	30.00	9.00	10.00	180.00	10.90	347.94
15.00	80.00	30.00	16.00	1.00	178.04	17.65	591.99
15.00	80.00	30.00	16.00	4.00	180.00	17.90	592.57
15.00	80.00	30.00	16.00	7.00	180.00	17.90	592.57
15.00	80.00	30.00	16.00	10.00	180.00	17.90	592.57
15.00	80.00	30.00	22.00	1.00	178.04	23.65	801.67
15.00	80.00	30.00	22.00	4.00	180.00	23.90	802.25
15.00	80.00	30.00	22.00	7.00	180.00	23.90	802.25
15.00	80.00	30.00	22.00	10.00	180.00	23.90	802.25

***** BLUNDER ANALYSIS - DUAL AIRCRAFT ***** PAGE = 16

BLUNDERED DEPARTURE ANGLE (DEG.)	BLUNDERED VELOCITY (KNOTS)	BLUNDERED BANK ANGLE (DEG.)	BLUNDERED SUMMED DELAYS (SEC.)	ADJACENT SUMMED DELAYS (SEC.)	CORRECTED PARALLEL HEADINGS (DEG.)	BLUNDER CORRECTION TIME (SEC.)	BLUNDER RECOVERY AIRSPACE (FT.)
15.00	80.00	20.00	2.50	1.00	176.23	4.76	137.00
15.00	80.00	20.00	2.50	4.00	180.00	5.52	140.37
15.00	80.00	20.00	2.50	7.00	180.00	5.52	140.37
15.00	80.00	20.00	2.50	10.00	180.00	5.52	140.37
15.00	80.00	20.00	9.00	1.00	176.23	11.26	364.16
15.00	80.00	20.00	9.00	4.00	180.00	12.02	367.53
15.00	80.00	20.00	9.00	7.00	180.00	12.02	367.53
15.00	80.00	20.00	9.00	10.00	180.00	12.02	367.53
15.00	80.00	20.00	16.00	1.00	176.23	18.26	608.78
15.00	80.00	20.00	16.00	4.00	180.00	19.02	612.16
15.00	80.00	20.00	16.00	7.00	180.00	19.02	612.16
15.00	80.00	20.00	16.00	10.00	180.00	19.02	612.16
15.00	80.00	20.00	22.00	1.00	176.23	24.26	816.47
15.00	80.00	20.00	22.00	4.00	180.00	25.02	821.84
15.00	80.00	20.00	22.00	7.00	180.00	25.02	821.84
15.00	80.00	20.00	22.00	10.00	180.00	25.02	821.84
15.00	80.00	10.00	2.50	1.00	173.02	5.83	172.96
15.00	80.00	10.00	2.50	4.00	177.03	7.49	192.46
15.00	80.00	10.00	2.50	7.00	180.00	8.73	156.78
15.00	80.00	10.00	2.50	10.00	180.00	8.73	196.78
15.00	80.00	10.00	9.00	1.00	173.02	12.33	400.12
15.00	80.00	10.00	9.00	4.00	177.03	13.99	419.61
15.00	80.00	10.00	9.00	7.00	180.00	15.23	423.94
15.00	80.00	10.00	9.00	10.00	180.00	15.23	423.94
15.00	80.00	10.00	16.00	1.00	173.02	19.33	644.75
15.00	80.00	10.00	16.00	4.00	177.03	20.99	664.24
15.00	80.00	10.00	16.00	7.00	180.00	22.23	668.56
15.00	80.00	10.00	16.00	10.00	180.00	22.23	668.56
15.00	80.00	10.00	22.00	1.00	173.02	25.33	854.43
15.00	80.00	10.00	22.00	4.00	177.03	26.99	873.92
15.00	80.00	10.00	22.00	7.00	180.00	28.23	878.25
15.00	80.00	10.00	22.00	10.00	180.00	28.23	878.25

***** BLUNDER ANALYSIS - DUAL AIRCRAFT ***** PAGE = 17

BLUNDERED DEPARTURE ANGLE (DEG.)	BLUNDERED VELOCITY (KNOTS)	BLUNDERED BANK ANGLE (DEG.)	BLUNDERED SUMMED DELAYS (SEC.)	ADJACENT SUMMED DELAYS (SEC.)	CORRECTED PARALLEL HEADINGS (DEG.)	BLUNDER CORRECTION TIME (SEC.)	BLUNDER RECOVERY AIRSPACE (FT.)
15.00	100.00	40.00	2.50	1.00	178.56	3.98	144.80
15.00	100.00	40.00	2.50	4.00	180.00	4.14	145.13
15.00	100.00	40.00	2.50	7.00	180.00	4.14	145.13
15.00	100.00	40.00	2.50	10.00	180.00	4.14	145.13
15.00	100.00	40.00	9.00	1.00	178.56	10.48	428.75
15.00	100.00	40.00	9.00	4.00	180.00	10.64	429.08
15.00	100.00	40.00	9.00	7.00	180.00	10.64	429.08
15.00	100.00	40.00	9.00	10.00	180.00	10.64	429.08
15.00	100.00	40.00	16.00	1.00	178.56	17.48	734.53
15.00	100.00	40.00	16.00	4.00	180.00	17.64	734.86
15.00	100.00	40.00	16.00	7.00	180.00	17.64	734.86
15.00	100.00	40.00	16.00	10.00	180.00	17.64	734.86
15.00	100.00	40.00	22.00	1.00	178.56	23.48	996.63
15.00	100.00	40.00	22.00	4.00	180.00	23.64	996.96
15.00	100.00	40.00	22.00	7.00	180.00	23.64	996.96
15.00	100.00	40.00	22.00	10.00	180.00	23.64	996.96
15.00	100.00	30.00	2.50	1.00	177.20	4.43	159.59
15.00	100.00	30.00	2.50	4.00	180.00	4.88	161.42
15.00	100.00	30.00	2.50	7.00	180.00	4.88	161.42
15.00	100.00	30.00	2.50	10.00	180.00	4.88	161.42
15.00	100.00	30.00	9.00	1.00	177.20	10.93	443.54
15.00	100.00	30.00	9.00	4.00	180.00	11.38	445.36
15.00	100.00	30.00	9.00	7.00	180.00	11.38	445.36
15.00	100.00	30.00	9.00	10.00	180.00	11.38	445.36
15.00	100.00	30.00	16.00	1.00	177.20	17.93	749.32
15.00	100.00	30.00	16.00	4.00	180.00	18.38	751.15
15.00	100.00	30.00	16.00	7.00	180.00	18.38	751.15
15.00	100.00	30.00	16.00	10.00	180.00	18.38	751.15
15.00	100.00	30.00	22.00	1.00	177.20	23.93	1011.42
15.00	100.00	30.00	22.00	4.00	180.00	24.38	1013.25
15.00	100.00	30.00	22.00	7.00	180.00	24.38	1013.25
15.00	100.00	30.00	22.00	10.00	180.00	24.38	1013.25

***** BLUNDER ANALYSIS - DUAL AIRCRAFT MANEUVER ***** PAGE = 18

BLUNDERED DEPARTURE ANGLE (DEG.)	BLUNDERED VELOCITY (KNOTS)	BLUNDERED BANK ANGLE (DEG.)	BLUNDERED SUMMED DELAYS (SEC.)	ADJACENT SUMMED DELAYS (SEC.)	CORRECTED PARALLEL HEADINGS (LEG.)	BLUNDER CORRECTION TIME (SEC.)	BLUNDER RECOVERY AIRSPACE (FT.)
15.00	100.00	20.00	2.50	1.00	175.26	5.08	183.73
15.00	100.00	20.00	2.50	4.00	180.00	6.27	192.03
15.00	100.00	20.00	2.50	7.00	180.00	6.27	192.03
15.00	100.00	20.00	2.50	10.00	180.00	6.27	192.03
15.00	100.00	20.00	9.00	1.00	175.26	11.58	467.67
15.00	100.00	20.00	9.00	4.00	180.00	12.77	475.97
15.00	100.00	20.00	9.00	7.00	180.00	12.77	475.97
15.00	100.00	20.00	9.00	10.00	180.00	12.77	475.97
15.00	100.00	20.00	16.00	1.00	175.26	18.58	773.45
15.00	100.00	20.00	16.00	4.00	180.00	19.77	781.76
15.00	100.00	20.00	16.00	7.00	180.00	19.77	781.76
15.00	100.00	20.00	16.00	10.00	180.00	19.77	781.76
15.00	100.00	20.00	22.00	1.00	175.26	24.58	1035.56
15.00	100.00	20.00	22.00	4.00	180.00	25.77	1043.86
15.00	100.00	20.00	22.00	7.00	180.00	25.77	1043.86
15.00	100.00	20.00	22.00	10.00	180.00	25.77	1043.86
15.00	100.00	10.00	2.50	1.00	172.04	6.15	231.84
15.00	100.00	10.00	2.50	4.00	175.56	7.98	265.12
15.00	100.00	10.00	2.50	7.00	179.08	9.81	279.53
15.00	100.00	10.00	2.50	10.00	180.00	10.28	280.17
15.00	100.00	10.00	9.00	1.00	172.04	12.65	515.78
15.00	100.00	10.00	9.00	4.00	175.56	14.48	549.06
15.00	100.00	10.00	9.00	7.00	179.08	16.31	563.47
15.00	100.00	10.00	9.00	10.00	180.00	16.78	564.11
15.00	100.00	10.00	16.00	1.00	172.04	19.65	821.57
15.00	100.00	10.00	16.00	4.00	175.56	21.48	854.85
15.00	100.00	10.00	16.00	7.00	179.08	23.31	869.25
15.00	100.00	10.00	16.00	10.00	180.00	23.78	869.90
15.00	100.00	10.00	22.00	1.00	172.04	25.65	1093.67
15.00	100.00	10.00	22.00	4.00	175.56	27.48	1116.95
15.00	100.00	10.00	22.00	7.00	179.08	29.31	1131.35
15.00	100.00	10.00	22.00	10.00	180.00	29.78	1132.00

***** BLUNDER ANALYSIS - DUAL AIRCRAFT MANEUVER *****										PAGE = 19
BLUNDERED DEPARTURE ANGLE (DEG.)	BLUNDERED VELOCITY (KNOTS)	BLUNDERED BANK ANGLE (DEG.)	BLUNDERED SUMMED DELAYS (SEC.)	ADJACENT SUMMED DELAYS (SEC.)	CORRECTED PARALLEL HEADINGS (DEG.)	BLUNDER CORRECTION TIME (SEC.)	BLUNDER RECOVERY AIRSPACE (FT.)			
15.00	120.00	40.00	2.50	1.00	177.93	4.13	181.79			
15.00	120.00	40.00	2.50	4.00	160.00	4.46	182.78			
15.00	120.00	40.00	2.50	7.00	160.00	4.46	182.78			
15.00	120.00	40.00	2.50	10.00	180.00	4.46	182.78			
15.00	120.00	40.00	9.00	1.00	177.93	10.69	522.52			
15.00	120.00	40.00	9.00	4.00	160.00	10.96	523.52			
15.00	120.00	40.00	9.00	7.00	180.00	10.96	523.52			
15.00	120.00	40.00	9.00	10.00	160.00	10.96	523.52			
15.00	120.00	40.00	16.00	1.00	177.93	17.69	889.45			
15.00	120.00	40.00	16.00	4.00	180.00	17.96	890.46			
15.00	120.00	40.00	16.00	7.00	180.00	17.96	890.46			
15.00	120.00	40.00	16.00	10.00	180.00	17.96	890.46			
15.00	120.00	40.00	22.00	1.00	177.93	23.69	1203.98			
15.00	120.00	40.00	22.00	4.00	180.00	23.96	1204.98			
15.00	120.00	40.00	22.00	7.00	180.00	23.96	1204.98			
15.00	120.00	40.00	22.00	10.00	180.00	23.96	1204.98			
15.00	120.00	30.00	2.50	1.00	176.46	4.68	202.03			
15.00	120.00	30.00	2.50	4.00	180.00	5.35	206.24			
15.00	120.00	30.00	2.50	7.00	180.00	5.35	206.24			
15.00	120.00	30.00	2.50	10.00	180.00	5.35	206.24			
15.00	120.00	30.00	9.00	1.00	176.46	11.18	542.76			
15.00	120.00	30.00	9.00	4.00	180.00	11.85	546.97			
15.00	120.00	30.00	9.00	7.00	180.00	11.85	546.97			
15.00	120.00	30.00	9.00	10.00	180.00	11.85	546.97			
15.00	120.00	30.00	16.00	1.00	176.46	18.18	909.70			
15.00	120.00	30.00	16.00	4.00	180.00	18.85	913.91			
15.00	120.00	30.00	16.00	7.00	180.00	18.85	913.91			
15.00	120.00	30.00	16.00	10.00	180.00	18.85	913.91			
15.00	120.00	30.00	22.00	1.00	176.46	24.18	1224.23			
15.00	120.00	30.00	22.00	4.00	180.00	24.85	1228.43			
15.00	120.00	30.00	22.00	7.00	180.00	24.85	1228.43			
15.00	120.00	30.00	22.00	10.00	180.00	24.85	1228.43			

***** BLUNDER ANALYSIS - DUAL AIRCRAFT NAMEUVER ***** PAGE = 20

BLUNDERED DEPARTURE ANGLE (DEG.)	BLUNDERED VELOCITY (KNOTS)	BLUNDERED BANK ANGLE (DEG.)	BLUNDERED SUMMED DELAYS (SEC.)	ADJACENT SUMMED DELAYS (SEC.)	CORRECTED PARALLEL HEADINGS (DEG.)	BLUNDER CORRECTION TIME (SEC.)	BLUNDER RECOVERY AIRSPACE (FT.)
15.00	120.00	20.00	2.50	1.00	174.45	5.35	233.90
15.00	120.00	20.00	2.50	4.00	179.17	6.78	249.95
15.00	120.00	20.00	2.50	7.00	180.00	7.02	250.32
15.00	120.00	20.00	2.50	10.00	180.00	7.02	250.32
15.00	120.00	20.00	9.00	1.00	174.45	11.65	574.64
15.00	120.00	20.00	9.00	4.00	179.17	13.28	590.68
15.00	120.00	20.00	9.00	7.00	180.00	13.52	591.05
15.00	120.00	20.00	9.00	10.00	180.00	13.52	591.05
15.00	120.00	20.00	16.00	1.00	174.45	18.85	941.58
15.00	120.00	20.00	16.00	4.00	179.17	20.28	957.63
15.00	120.00	20.00	16.00	7.00	180.00	20.52	957.99
15.00	120.00	20.00	16.00	10.00	180.00	20.52	957.99
15.00	120.00	20.00	22.00	1.00	174.45	24.85	1256.10
15.00	120.00	20.00	22.00	4.00	179.17	26.28	1272.15
15.00	120.00	20.00	22.00	7.00	180.00	26.52	1272.51
15.00	120.00	20.00	22.00	10.00	180.00	26.52	1272.51
15.00	120.00	10.00	2.50	1.00	171.28	6.41	293.66
15.00	120.00	10.00	2.50	4.00	174.41	8.36	342.94
15.00	120.00	10.00	2.50	7.00	177.55	10.32	370.65
15.00	120.00	10.00	2.50	10.00	180.00	11.84	377.23
15.00	120.00	10.00	9.00	1.00	171.28	12.91	634.39
15.00	120.00	10.00	9.00	4.00	174.41	14.86	683.67
15.00	120.00	10.00	9.00	7.00	177.55	16.82	711.38
15.00	120.00	10.00	9.00	10.00	180.00	18.34	717.97
15.00	120.00	10.00	16.00	1.00	171.28	19.91	1001.33
15.00	120.00	10.00	16.00	4.00	174.41	21.86	1050.61
15.00	120.00	10.00	16.00	7.00	177.55	23.82	1078.32
15.00	120.00	10.00	16.00	10.00	180.00	25.34	1084.91
15.00	120.00	10.00	22.00	1.00	171.28	25.91	1315.85
15.00	120.00	10.00	22.00	4.00	174.41	27.86	1365.13
15.00	120.00	10.00	22.00	7.00	177.55	29.82	1392.64
15.00	120.00	10.00	22.00	10.00	180.00	31.34	1399.43

***** BLUNDER ANALYSIS - DUAL AIRCRAFT MANEUVER ***** PAGE = 21

BLUNDERED DEPARTURE ANGLE (DEG.)	BLUNDERED VELOCITY (KNOTS)	BLUNDERED BANK ANGLE (DEG.)	BLUNDERED SUMMED DELAYS (SEC.)	ADJACENT SUB- DELAYS (SEC.)	CORRECTED PARALLEL HEADINGS (DEG.)	BLUNDER CORRECTION TIME (SEC.)	BLUNDER RECOVERY AIRSPACE (FT.)
15.00	140.00	40.00	2.50	1.00	177.35	4.38	221.09
15.00	140.00	40.00	2.50	4.00	180.00	4.79	223.31
15.00	140.00	40.00	2.50	7.00	180.00	4.79	223.31
15.00	140.00	40.00	2.50	10.00	180.00	4.79	223.31
15.00	140.00	40.00	9.00	1.00	177.35	10.88	618.61
15.00	140.00	40.00	9.00	4.00	180.00	11.29	620.83
15.00	140.00	40.00	9.00	7.00	180.00	11.29	620.83
15.00	140.00	40.00	9.00	10.00	180.00	11.29	620.83
15.00	140.00	40.00	16.00	1.00	177.35	17.88	1046.71
15.00	140.00	40.00	16.00	4.00	180.00	18.29	1048.93
15.00	140.00	40.00	16.00	7.00	180.00	18.29	1048.93
15.00	140.00	40.00	16.00	10.00	180.00	18.29	1048.93
15.00	140.00	40.00	22.00	1.00	177.35	23.88	1413.65
15.00	140.00	40.00	22.00	4.00	180.00	24.29	1415.87
15.00	140.00	40.00	22.00	7.00	180.00	24.29	1415.87
15.00	140.00	40.00	22.00	10.00	180.00	24.29	1415.87
15.00	140.00	30.00	2.50	1.00	175.81	4.90	247.19
15.00	140.00	30.00	2.50	4.00	180.00	5.83	255.23
15.00	140.00	30.00	2.50	7.00	180.00	5.83	255.23
15.00	140.00	30.00	2.50	10.00	180.00	5.83	255.23
15.00	140.00	30.00	9.00	1.00	175.81	11.40	644.71
15.00	140.00	30.00	9.00	4.00	180.00	12.33	652.75
15.00	140.00	30.00	9.00	7.00	180.00	12.33	652.75
15.00	140.00	30.00	9.00	10.00	180.00	12.33	652.75
15.00	140.00	30.00	16.00	1.00	175.81	18.40	1072.81
15.00	140.00	30.00	16.00	4.00	180.00	19.33	1080.85
15.00	140.00	30.00	16.00	7.00	180.00	19.33	1080.85
15.00	140.00	30.00	16.00	10.00	180.00	19.33	1080.85
15.00	140.00	30.00	22.00	1.00	175.81	24.40	1439.75
15.00	140.00	30.00	22.00	4.00	180.00	25.33	1447.79
15.00	140.00	30.00	22.00	7.00	180.00	25.33	1447.79
15.00	140.00	30.00	22.00	10.00	180.00	25.33	1447.79

***** BLUNDER ANALYSIS - DUAL AIRCRAFT MANEUVER ***** PAGE = 22

BLUNDERED DEPARTURE ANGLE (DEG.)	BLUNDERED VELOCITY (KNOTS)	BLUNDERED BANK ANGLE (DEG.)	BLUNDERED SUMMED DELAYS (SEC.)	ADJACENT SUMMED DELAYS (SEC.)	CORRECTED PARALLEL HEADINGS (DEG.)	BLUNDER CORRECTION TIME (SEC.)	BLUNDER RECOVERY AIRSPACE (FT.)
15.00	140.00	20.00	2.50	1.00	173.76	5.58	286.97
15.00	140.00	20.00	2.50	4.00	178.13	7.12	312.70
15.00	140.00	20.00	2.50	7.00	180.00	7.78	315.22
15.00	140.00	20.00	2.50	10.00	180.00	7.78	315.22
15.00	140.00	20.00	9.00	1.00	173.76	12.08	684.49
15.00	140.00	20.00	9.00	4.00	178.13	13.62	710.22
15.00	140.00	20.00	9.00	7.00	180.00	14.28	712.75
15.00	140.00	20.00	9.00	10.00	180.00	14.28	712.75
15.00	140.00	20.00	16.00	1.00	173.76	19.08	1112.58
15.00	140.00	20.00	16.00	4.00	178.13	20.62	1138.32
15.00	140.00	20.00	16.00	7.00	180.00	21.28	1140.84
15.00	140.00	20.00	16.00	10.00	180.00	21.28	1140.84
15.00	140.00	20.00	22.00	1.00	173.76	25.08	1479.53
15.00	140.00	20.00	22.00	4.00	178.13	26.62	1505.26
15.00	140.00	20.00	22.00	7.00	180.00	27.28	1507.79
15.00	140.00	20.00	22.00	10.00	180.00	27.28	1507.79
15.00	140.00	10.00	2.50	1.00	170.66	6.61	357.66
15.00	140.00	10.00	2.50	4.00	173.49	8.67	424.63
15.00	140.00	10.00	2.50	7.00	176.32	10.73	467.74
15.00	140.00	10.00	2.50	10.00	179.15	12.78	486.91
15.00	140.00	10.00	9.00	1.00	170.66	13.11	755.18
15.00	140.00	10.00	9.00	4.00	173.49	15.17	822.15
15.00	140.00	10.00	9.00	7.00	176.32	17.23	865.25
15.00	140.00	10.00	9.00	10.00	179.15	19.28	884.43
15.00	140.00	10.00	16.00	1.00	170.66	20.11	1183.28
15.00	140.00	10.00	16.00	4.00	173.49	22.17	1250.24
15.00	140.00	10.00	16.00	7.00	176.32	24.23	1293.36
15.00	140.00	10.00	16.00	10.00	179.15	26.28	1312.53
15.00	140.00	10.00	22.00	1.00	170.66	26.11	1550.22
15.00	140.00	10.00	22.00	4.00	173.49	28.17	1617.19
15.00	140.00	10.00	22.00	7.00	176.32	30.23	1660.30
15.00	140.00	10.00	22.00	10.00	179.15	32.28	1679.47

***** BLUNDER ANALYSIS - DUAL AIRCRAFT ***** PAGE = 23

BLUNDERED DEPARTURE ANGLE (DEG.)	BLUNDERED VELOCITY (KNOTS)	BLUNDERED BANK ANGLE (DEG.)	BLUNDERED SUMMED DELAYS (SEC.)	ADJACENT SUMMED DELAYS (SEC.)	CORRECTED PARALLEL HEADINGS (DEG.)	BLUNDER CORRECTION TIME (SEC.)	BLUNDER RECOVERY AIRSPACE (FT.)
15.00	160.00	40.00	2.50	1.00	176.82	4.56	262.54
15.00	160.00	40.00	2.50	4.00	180.00	5.12	266.70
15.00	160.00	40.00	2.50	7.00	160.00	5.12	266.70
15.00	160.00	40.00	2.50	10.00	180.00	5.12	266.70
15.00	160.00	40.00	9.00	1.00	176.82	11.06	716.85
15.00	160.00	40.00	9.00	4.00	160.00	11.62	721.01
15.00	160.00	40.00	9.00	7.00	180.00	11.62	721.01
15.00	160.00	40.00	9.00	10.00	180.00	11.62	721.01
15.00	160.00	40.00	16.00	1.00	176.82	18.06	1206.10
15.00	160.00	40.00	16.00	4.00	180.00	18.62	1210.27
15.00	160.00	40.00	16.00	7.00	180.00	18.62	1210.27
15.00	160.00	40.00	16.00	10.00	180.00	18.62	1210.27
15.00	160.00	40.00	22.00	1.00	176.82	24.06	1625.46
15.00	160.00	40.00	22.00	4.00	180.00	24.62	1629.63
15.00	160.00	40.00	22.00	7.00	180.00	24.62	1629.63
15.00	160.00	40.00	22.00	10.00	180.00	24.62	1629.63
15.00	160.00	30.00	2.50	1.00	175.22	5.09	294.78
15.00	160.00	30.00	2.50	4.00	180.00	6.30	308.40
15.00	160.00	30.00	2.50	7.00	180.00	6.30	308.40
15.00	160.00	30.00	2.50	10.00	180.00	6.30	308.40
15.00	160.00	30.00	9.00	1.00	175.22	11.59	749.09
15.00	160.00	30.00	9.00	4.00	180.00	12.80	762.71
15.00	160.00	30.00	9.00	7.00	180.00	12.80	762.71
15.00	160.00	30.00	9.00	10.00	180.00	12.80	762.71
15.00	160.00	30.00	16.00	1.00	175.22	18.59	1238.34
15.00	160.00	30.00	16.00	4.00	180.00	19.80	1251.96
15.00	160.00	30.00	16.00	7.00	180.00	19.80	1251.96
15.00	160.00	30.00	16.00	10.00	180.00	19.80	1251.96
15.00	160.00	30.00	22.00	1.00	175.22	24.59	1657.70
15.00	160.00	30.00	22.00	4.00	180.00	25.80	1671.33
15.00	160.00	30.00	22.00	7.00	180.00	25.80	1671.33
15.00	160.00	30.00	22.00	10.00	180.00	25.80	1671.33

***** BLUNDER AIRCRAFT - DUAL AIRCRAFT ***** PAGE = 24

BLUNDERED DEPARTURE ANGLE (DEG.)	BLUNDERED VELOCITY (KNOTS)	BLUNDERED BANK ANGLE (DEG.)	BLUNDERED SUMMED DELAYS (SEC.)	ADJACENT SUMMED DELAYS (SEC.)	CORRECTED PARALLEL HEADINGS (DEG.)	BLUNDER CORRECTION TIME (SEC.)	BLUNDER RECOVERY AIRSPACE (FT.)
15.00	160.00	20.00	2.50	1.00	173.16	5.78	342.44
15.00	160.00	20.00	2.50	4.00	177.24	7.42	379.52
15.00	160.00	20.00	2.50	7.00	180.00	8.53	386.76
15.00	160.00	20.00	2.50	10.00	180.00	8.53	386.76
15.00	160.00	20.00	9.00	1.00	173.16	12.28	796.75
15.00	160.00	20.00	9.00	4.00	177.24	13.92	833.93
15.00	160.00	20.00	9.00	7.00	180.00	15.03	841.07
15.00	160.00	20.00	9.00	10.00	180.00	15.03	841.07
15.00	160.00	20.00	16.00	1.00	173.16	19.28	1286.01
15.00	160.00	20.00	16.00	4.00	177.24	20.92	1323.09
15.00	160.00	20.00	16.00	7.00	180.00	22.03	1330.33
15.00	160.00	20.00	16.00	10.00	180.00	22.03	1330.33
15.00	160.00	20.00	22.00	1.00	173.16	25.28	1705.37
15.00	160.00	20.00	22.00	4.00	177.24	26.92	1742.45
15.00	160.00	20.00	22.00	7.00	180.00	28.03	1749.69
15.00	160.00	20.00	22.00	10.00	180.00	28.03	1749.69
15.00	160.00	10.00	2.50	1.00	173.16	6.78	423.32
15.00	160.00	10.00	2.50	4.00	172.74	8.92	509.29
15.00	160.00	10.00	2.50	7.00	175.31	11.06	569.46
15.00	160.00	10.00	2.50	10.00	177.89	13.20	605.71
15.00	160.00	10.00	9.00	1.00	170.16	13.28	877.63
15.00	160.00	10.00	9.00	4.00	172.74	15.42	963.60
15.00	160.00	10.00	9.00	7.00	175.31	17.56	1023.77
15.00	160.00	10.00	9.00	10.00	177.89	19.70	1058.01
15.00	160.00	10.00	16.00	1.00	173.16	20.28	1366.89
15.00	160.00	10.00	16.00	4.00	172.74	22.42	1452.86
15.00	160.00	10.00	16.00	7.00	175.31	24.56	1513.03
15.00	160.00	10.00	16.00	10.00	177.89	26.70	1547.27
15.00	160.00	10.00	22.00	1.00	170.16	26.28	1786.25
15.00	160.00	10.00	22.00	4.00	172.74	28.42	1872.22
15.00	160.00	10.00	22.00	7.00	175.31	30.56	1932.39
15.00	160.00	10.00	22.00	10.00	177.89	32.70	1966.63

***** RILUNDER ANALYSIS - DUAL AIRCRAFT MAP OVER *****

BLUNDERED DEPARTURE ANGLE (DEG.)	BLUNDERED VELOCITY (KNOTS)	BLUNDERED DIAK ANGLE (DEG.)	BLUNDERED SUMMED DELAYS (SEC.)	ADJACENT SUMMED DELAYS (SEC.)	CORRECTED PARALLEL HEADINGS (DEG.)	LUNDER CONNECTION TIME (SEC.)	BLUNDER RECOVERY AIRSPACE (FT.)
20.00	60.00	40.00	2.50	1.00	179.23	3.76	109.45
20.00	60.00	40.00	2.50	4.00	180.00	3.81	109.48
20.00	60.00	40.00	2.50	7.00	180.00	3.81	109.48
20.00	60.00	40.00	2.50	10.00	180.00	3.81	109.48
20.00	60.00	40.00	9.00	1.00	179.23	10.26	334.58
20.00	60.00	40.00	9.00	4.00	180.00	10.31	334.61
20.00	60.00	40.00	9.00	7.00	180.00	10.31	334.61
20.00	60.00	40.00	9.00	10.00	180.00	10.31	334.61
20.00	60.00	40.00	16.00	1.00	179.23	17.26	577.03
20.00	60.00	40.00	16.00	4.00	180.00	17.31	577.06
20.00	60.00	40.00	16.00	7.00	180.00	17.31	577.06
20.00	60.00	40.00	16.00	10.00	180.00	17.31	577.06
20.00	60.00	40.00	22.00	1.00	179.23	23.26	784.88
20.00	60.00	40.00	22.00	4.00	180.00	23.31	784.88
20.00	60.00	40.00	22.00	7.00	180.00	23.31	784.88
20.00	60.00	40.00	22.00	10.00	180.00	23.31	784.88
20.00	60.00	30.00	2.50	1.00	177.90	4.20	119.49
20.00	60.00	30.00	2.50	4.00	180.00	4.40	119.86
20.00	60.00	30.00	2.50	7.00	180.00	4.40	119.86
20.00	60.00	30.00	2.50	10.00	180.00	4.40	119.86
20.00	60.00	30.00	9.00	1.00	177.90	10.70	344.62
20.00	60.00	30.00	9.00	4.00	180.00	10.90	344.99
20.00	60.00	30.00	9.00	7.00	180.00	10.90	344.99
20.00	60.00	30.00	9.00	10.00	180.00	10.90	344.99
20.00	60.00	30.00	16.00	1.00	177.90	17.70	587.07
20.00	60.00	30.00	16.00	4.00	180.00	17.90	587.44
20.00	60.00	30.00	16.00	7.00	180.00	17.90	587.44
20.00	60.00	30.00	16.00	10.00	180.00	17.90	587.44
20.00	60.00	30.00	22.00	1.00	177.90	23.70	794.88
20.00	60.00	30.00	22.00	4.00	180.00	23.90	795.25
20.00	60.00	30.00	22.00	7.00	180.00	23.90	795.25
20.00	60.00	30.00	22.00	10.00	180.00	23.90	795.25

***** FLUNDER ANALYSIS - JUAL AIRCRAFT FLUNDER ***** PAGE = 26

BLUNDERED DEPARTURE ANGLE (DEG.)	BLUNDERED VELOCITY (KNOTS)	BLUNDERED BANK ANGLE (DEG.)	BLUNDERED SUMMED DELAYS (SEC.)	ADJACENT SUMMED DELAYS (SEC.)	CORRECTED PARALLEL HEADINGS (DEG.)	FLUNDER CORRECTION TIME (SEC.)	FLUNDER RECOVERY AIRSPACE (FT.)
20.00	60.00	20.00	2.50	1.00	175.84	4.89	137.05
20.00	60.00	20.00	2.50	4.00	180.00	5.52	139.36
20.00	60.00	20.00	2.50	7.00	180.00	5.52	139.36
20.00	60.00	20.00	2.50	10.00	180.00	5.52	139.36
20.00	60.00	20.00	9.00	1.00	175.84	11.39	362.18
20.00	60.00	20.00	9.00	4.00	180.00	12.02	364.49
20.00	60.00	20.00	9.00	7.00	160.00	12.02	364.49
20.00	60.00	20.00	9.00	10.00	180.00	12.02	364.49
20.00	60.00	20.00	16.00	1.00	175.84	18.39	604.63
20.00	60.00	20.00	16.00	4.00	180.00	19.02	606.94
20.00	60.00	20.00	16.00	7.00	180.00	19.02	606.94
20.00	60.00	20.00	16.00	10.00	180.00	19.02	606.94
20.00	60.00	20.00	22.00	1.00	175.84	24.39	812.45
20.00	60.00	20.00	22.00	4.00	180.00	25.02	814.76
20.00	60.00	20.00	22.00	7.00	180.00	25.02	814.76
20.00	60.00	20.00	22.00	10.00	180.00	25.02	814.76
20.00	60.00	10.00	2.50	1.00	171.89	6.20	177.47
20.00	60.00	10.00	2.50	4.00	176.55	7.65	192.24
20.00	60.00	10.00	2.50	7.00	180.00	8.73	195.52
20.00	60.00	10.00	2.50	10.00	180.00	8.73	195.52
20.00	60.00	10.00	9.00	1.00	171.89	12.70	402.60
20.00	60.00	10.00	9.00	4.00	176.55	14.15	417.37
20.00	60.00	10.00	9.00	7.00	180.00	15.23	420.65
20.00	60.00	10.00	9.00	10.00	180.00	15.23	420.65
20.00	60.00	10.00	16.00	1.00	171.89	19.70	645.05
20.00	60.00	10.00	16.00	4.00	176.55	21.15	659.82
20.00	60.00	10.00	16.00	7.00	180.00	22.23	663.10
20.00	60.00	10.00	16.00	10.00	180.00	22.23	663.10
20.00	60.00	10.00	22.00	1.00	171.89	25.70	852.87
20.00	60.00	10.00	22.00	4.00	176.55	27.15	867.64
20.00	60.00	10.00	22.00	7.00	180.00	28.23	870.92
20.00	60.00	10.00	22.00	10.00	180.00	28.23	870.92

***** BLUNDER ANALYSIS - DUAL AIRCRAFT MANEUVER *****

BLUNDERED DEPARTURE ANGLE (DEG.)	BLUNDERED VELOCITY (KNOTS)	BLUNDERED BANK ANGLE (DEG.)	BLUNDERED SUMMED DELAYS (SEC.)	ADJACENT SUMMED DELAYS (SEC.)	CORRECTED PARALLEL HEADINGS (DEG.)	BLUNDER CORRECTION TIME (SEC.)	BLUNDER RECOVERY AIRSPACE (FT.)
20.00	80.00	40.00	2.50	1.00	178.23	4.09	155.82
20.00	80.00	40.00	2.50	4.00	180.00	4.24	156.15
20.00	80.00	40.00	2.50	7.00	180.00	4.24	156.15
20.00	80.00	40.00	2.50	10.00	180.00	4.24	156.15
20.00	80.00	40.00	9.00	1.00	178.23	10.59	456.00
20.00	80.00	40.00	9.00	4.00	180.00	10.74	456.32
20.00	80.00	40.00	9.00	7.00	180.00	10.74	456.32
20.00	80.00	40.00	9.00	10.00	180.00	10.74	456.32
20.00	80.00	40.00	16.00	1.00	178.23	17.59	779.27
20.00	80.00	40.00	16.00	4.00	180.00	17.74	779.59
20.00	80.00	40.00	16.00	7.00	180.00	17.74	779.59
20.00	80.00	40.00	16.00	10.00	180.00	17.74	779.59
20.00	80.00	40.00	22.00	1.00	178.23	23.59	1056.35
20.00	80.00	40.00	22.00	4.00	180.00	23.74	1056.68
20.00	80.00	40.00	22.00	7.00	180.00	23.74	1056.68
20.00	80.00	40.00	22.00	10.00	180.00	23.74	1056.68
20.00	80.00	30.00	2.50	1.00	176.66	4.61	172.93
20.00	80.00	30.00	2.50	4.00	180.00	5.04	174.60
20.00	80.00	30.00	2.50	7.00	180.00	5.04	174.60
20.00	80.00	30.00	2.50	10.00	180.00	5.04	174.60
20.00	80.00	30.00	9.00	1.00	176.66	11.11	473.11
20.00	80.00	30.00	9.00	4.00	180.00	11.54	474.77
20.00	80.00	30.00	9.00	7.00	180.00	11.54	474.77
20.00	80.00	30.00	9.00	10.00	180.00	11.54	474.77
20.00	80.00	30.00	16.00	1.00	176.66	18.11	796.38
20.00	80.00	30.00	16.00	4.00	180.00	18.54	798.04
20.00	80.00	30.00	16.00	7.00	180.00	18.54	798.04
20.00	80.00	30.00	16.00	10.00	180.00	18.54	798.04
20.00	80.00	30.00	22.00	1.00	176.66	24.11	1073.46
20.00	80.00	30.00	22.00	4.00	180.00	24.54	1075.13
20.00	80.00	30.00	22.00	7.00	180.00	24.54	1075.13
20.00	80.00	30.00	22.00	10.00	180.00	24.54	1075.13

Reproduced from
best available copy.

***** CLUTTER ANALYSIS - DUAL AIRCRAFT - AFTERVIEW ***** P 65 = 28

UNCLUTTERED DUAL AIRCRAFT ANGLE (DEG.)	CLUTTERED DUAL AIRCRAFT ANGLE (DEG.)	CLUTTERED SUMMED DELAYS (SEC.)	ADJACENT SUMMED DELAYS (SEC.)	CORRECTED PARALLEL HEADINGS (DEG.)	CLUTTER CORRECTION TIME (SEC.)	BLUNDER RECOVERY AIRSPACE (FT.)
20.00	20.00	2.50	1.00	174.35	5.38	201.70
20.00	20.00	2.50	4.00	179.96	5.51	209.27
20.00	20.00	2.50	7.00	180.00	6.52	209.27
20.00	20.00	2.50	10.00	180.00	6.52	209.27
20.00	20.00	9.00	1.00	174.35	11.88	501.88
20.00	20.00	9.00	4.00	179.96	13.01	509.44
20.00	20.00	9.00	7.00	180.00	13.02	509.44
20.00	20.00	9.00	10.00	180.00	13.02	509.44
20.00	20.00	16.00	1.00	174.35	18.88	825.14
20.00	20.00	16.00	4.00	179.96	20.01	832.71
20.00	20.00	16.00	7.00	180.00	20.02	832.71
20.00	20.00	16.00	10.00	180.00	20.02	832.71
20.00	20.00	22.00	1.00	174.35	24.88	1102.23
20.00	20.00	22.00	4.00	179.96	26.01	1109.80
20.00	20.00	22.00	7.00	180.00	26.02	1109.80
20.00	20.00	22.00	10.00	180.00	26.02	1109.80
20.00	20.00	2.50	1.00	170.24	6.75	262.67
20.00	20.00	2.50	4.00	174.25	8.42	292.96
20.00	20.00	2.50	7.00	178.26	10.08	307.63
20.00	20.00	2.50	10.00	180.00	10.80	309.10
20.00	20.00	9.00	1.00	170.24	13.25	562.64
20.00	20.00	9.00	4.00	174.25	14.92	593.14
20.00	20.00	9.00	7.00	178.26	16.58	607.80
20.00	20.00	9.00	10.00	180.00	17.30	609.28
20.00	20.00	16.00	1.00	170.24	20.25	886.11
20.00	20.00	16.00	4.00	174.25	21.92	916.41
20.00	20.00	16.00	7.00	178.26	23.58	931.07
20.00	20.00	16.00	10.00	180.00	24.30	932.55
20.00	20.00	22.00	1.00	170.24	26.25	1163.20
20.00	20.00	22.00	4.00	174.25	27.92	1193.49
20.00	20.00	22.00	7.00	178.26	29.58	1208.16
20.00	20.00	22.00	10.00	180.00	30.30	1209.63

***** BLUNDER ANALYSIS - JIAL AIRCRAFT ***** PAGE = 20

BLUNDER ANGLE (DEG.)	BLUNDER VELOCITY (KNOTS)	BLUNDER BANK ANGLE (DEG.)	BLUNDERED SUMMED DELAYS (SEC.)	ADJACENT SUMMED DELAYS (SEC.)	CORRECTED PARALLEL HEADINGS (DEG.)	LUNDER CORRECTION TIME (SEC.)	BLUNDER RECOVERY AIRSPACE (FT.)
20.00	10.00	40.00	2.50	1.00	177.33	4.39	206.76
20.00	10.00	40.00	2.50	4.00	180.00	4.68	207.90
20.00	10.00	40.00	2.50	7.00	180.00	4.68	207.90
20.00	10.00	40.00	2.50	10.00	180.00	4.68	207.90
20.00	10.00	40.00	4.00	1.00	177.33	10.89	581.98
20.00	10.00	40.00	9.00	4.00	180.00	11.18	583.12
20.00	10.00	40.00	9.00	7.00	180.00	11.18	583.12
20.00	10.00	40.00	9.00	10.00	180.00	11.18	583.12
20.00	10.00	40.00	16.00	1.00	177.33	17.89	986.06
20.00	10.00	40.00	16.00	4.00	180.00	18.18	987.20
20.00	10.00	40.00	16.00	7.00	180.00	18.18	987.20
20.00	10.00	40.00	16.00	10.00	180.00	18.18	987.20
20.00	10.00	40.00	22.00	1.00	177.33	23.89	1332.42
20.00	10.00	40.00	22.00	4.00	180.00	24.18	1333.56
20.00	10.00	40.00	22.00	7.00	180.00	24.18	1333.56
20.00	10.00	40.00	22.00	10.00	180.00	24.18	1333.56
20.00	10.00	30.00	2.50	1.00	175.59	4.97	232.19
20.00	10.00	30.00	2.50	4.00	180.00	5.67	236.73
20.00	10.00	30.00	2.50	7.00	180.00	5.67	236.73
20.00	10.00	30.00	2.50	10.00	180.00	5.67	236.73
20.00	10.00	30.00	9.00	1.00	175.59	11.47	607.41
20.00	10.00	30.00	9.00	4.00	180.00	12.17	611.95
20.00	10.00	30.00	9.00	7.00	180.00	12.17	611.95
20.00	10.00	30.00	9.00	10.00	180.00	12.17	611.95
20.00	10.00	30.00	16.00	1.00	175.59	18.47	1011.49
20.00	10.00	30.00	16.00	4.00	180.00	19.17	1016.03
20.00	10.00	30.00	16.00	7.00	180.00	19.17	1016.03
20.00	10.00	30.00	16.00	10.00	180.00	19.17	1016.03
20.00	10.00	30.00	22.00	1.00	175.59	24.47	1357.85
20.00	10.00	30.00	22.00	4.00	180.00	25.17	1362.39
20.00	10.00	30.00	22.00	7.00	180.00	25.17	1362.39
20.00	10.00	30.00	22.00	10.00	180.00	25.17	1362.39

***** BLUNDER ANALYSIS - DUAL AIRCRAFT ***** PAGE = 31

BLUNDERED DEPARTURE ANGLE (DEG.)	BLUNDERED VELOCITY (KNOTS)	BLUNDERED BANK ANGLE (DEG.)	BLUNDERED SUMEL DELAYS (SEC.)	ADJACENT SUMEL DELAYS (SEC.)	CORRECTED PARALLEL HEADINGS (DEG.)	BLUNDER CORRECTION TIME (SEC.)	BLUNDER RECOVERY AIRSPACE (FT.)
20.00	120.00	40.00	2.50	1.00	176.52	4.66	261.94
20.00	120.00	40.00	2.50	4.00	180.00	5.12	264.74
20.00	120.00	40.00	2.50	7.00	180.00	5.12	264.74
20.00	120.00	40.00	2.50	10.00	180.00	5.12	264.74
20.00	120.00	40.00	9.00	1.00	176.52	11.16	712.20
20.00	120.00	40.00	9.00	4.00	180.00	11.62	715.00
20.00	120.00	40.00	9.00	7.00	180.00	11.62	715.00
20.00	120.00	40.00	9.00	10.00	180.00	11.62	715.00
20.00	120.00	40.00	16.00	1.00	176.52	18.16	1197.10
20.00	120.00	40.00	16.00	4.00	180.00	18.62	1199.91
20.00	120.00	40.00	16.00	7.00	180.00	18.62	1199.91
20.00	120.00	40.00	16.00	10.00	180.00	18.62	1199.91
20.00	120.00	40.00	22.00	1.00	176.52	24.16	1612.73
20.00	120.00	40.00	22.00	4.00	180.00	24.62	1615.53
20.00	120.00	40.00	22.00	7.00	180.00	24.62	1615.53
20.00	120.00	40.00	22.00	10.00	180.00	24.62	1615.53
20.00	120.00	30.00	2.50	1.00	174.65	5.28	296.62
20.00	120.00	30.00	2.50	4.00	180.00	6.30	306.25
20.00	120.00	30.00	2.50	7.00	180.00	6.30	306.25
20.00	120.00	30.00	2.50	10.00	180.00	6.30	306.25
20.00	120.00	30.00	9.00	1.00	174.65	11.78	746.89
20.00	120.00	30.00	9.00	4.00	180.00	12.80	756.51
20.00	120.00	30.00	9.00	7.00	180.00	12.80	756.51
20.00	120.00	30.00	9.00	10.00	180.00	12.80	756.51
20.00	120.00	30.00	16.00	1.00	174.65	18.78	1231.79
20.00	120.00	30.00	16.00	4.00	180.00	19.80	1241.42
20.00	120.00	30.00	16.00	7.00	180.00	19.80	1241.42
20.00	120.00	30.00	16.00	10.00	180.00	19.80	1241.42
20.00	120.00	30.00	22.00	1.00	174.65	24.78	1647.42
20.00	120.00	30.00	22.00	4.00	180.00	25.80	1657.04
20.00	120.00	30.00	22.00	7.00	180.00	25.80	1657.04
20.00	120.00	30.00	22.00	10.00	180.00	25.80	1657.04

0.65 = 30

BLUNDERED DEPARTURE ANGLE (DEG.)	BLUNDERED VELOCITY (KNOTS)	BLUNDERED BANK ANGLE (DEG.)	BLUNDERED SURFED DELAYS (SEC.)	ADJACENT SURFED DELAYS (SEC.)	CORRECTED PARALLEL DELAYS (SEC.)	LUNDER CORRECTION TIME (SEC.)	LUNDER RECOVERY AIRSPACE (FT.)
20.00	120.00	20.00	2.50	1.00	172.07	6.14	350.83
20.00	120.00	20.00	2.50	4.00	176.80	7.57	378.30
20.00	120.00	20.00	2.50	7.00	180.00	8.53	384.26
20.00	120.00	20.00	2.50	10.00	180.00	8.53	384.26
20.00	120.00	20.00	9.00	1.00	172.07	12.64	801.09
20.00	120.00	20.00	9.00	4.00	176.80	14.07	829.07
20.00	120.00	20.00	9.00	7.00	180.00	15.03	834.53
20.00	120.00	20.00	9.00	10.00	180.00	15.03	834.53
20.00	120.00	20.00	10.00	1.00	172.07	19.64	1286.00
20.00	120.00	20.00	10.00	4.00	176.80	21.07	1313.97
20.00	120.00	20.00	10.00	7.00	180.00	22.03	1319.43
20.00	120.00	20.00	10.00	10.00	180.00	22.03	1319.43
20.00	120.00	20.00	22.00	1.00	172.07	25.64	1701.62
20.00	120.00	20.00	22.00	4.00	176.80	27.07	1729.60
20.00	120.00	20.00	22.00	7.00	180.00	28.03	1735.06
20.00	120.00	20.00	22.00	10.00	180.00	28.03	1735.06
20.00	120.00	10.00	2.50	1.00	168.02	7.49	451.54
20.00	120.00	10.00	2.50	4.00	171.16	9.45	523.04
20.00	120.00	10.00	2.50	7.00	174.30	11.40	573.13
20.00	120.00	10.00	2.50	10.00	177.44	13.35	601.66
20.00	120.00	10.00	9.00	1.00	168.02	13.99	901.30
20.00	120.00	10.00	9.00	4.00	171.16	15.95	973.31
20.00	120.00	10.00	9.00	7.00	174.30	17.90	1023.40
20.00	120.00	10.00	9.00	10.00	177.44	19.85	1051.92
20.00	120.00	10.00	16.00	1.00	168.02	20.99	1386.71
20.00	120.00	10.00	16.00	4.00	171.16	22.95	1458.21
20.00	120.00	10.00	16.00	7.00	174.30	24.90	1508.30
20.00	120.00	10.00	16.00	10.00	177.44	26.85	1536.82
20.00	120.00	10.00	22.00	1.00	168.02	26.99	1802.33
20.00	120.00	10.00	22.00	4.00	171.16	28.95	1873.64
20.00	120.00	10.00	22.00	7.00	174.30	30.90	1923.93
20.00	120.00	10.00	22.00	10.00	177.44	32.85	1952.45

Reproduced from
best available copy.



***** BLUNDER ANALYSIS - DUAL AIRCRAFT ANALYSIS ***** PAGE = 33

BLUNDER ANALYSIS (SEC.)	BLUNDER VELOCITY (KNOTS)	BLUNDER BACK ANGLE (DEG.)	BLUNDER SUMMED DELAYS (SEC.)	ADJACENT SUMMED DELAYS (SEC.)	CONNECTED PARALLEL HEADINGS (DEG.)	BLUNDER CORRECTION TIME (SEC.)	BLUNDER RECOVERY AIRSPACE (FT.)
20.00	141.00	40.00	2.50	1.00	175.78	4.91	321.05
20.00	141.00	40.00	2.50	4.00	180.00	5.55	326.67
20.00	141.00	40.00	2.50	7.00	180.00	5.55	326.67
20.00	141.00	40.00	2.50	10.00	180.00	5.55	326.67
20.00	141.00	40.00	4.00	1.00	175.78	11.41	846.36
20.00	141.00	40.00	9.00	4.00	180.00	12.05	851.98
20.00	141.00	40.00	9.00	7.00	180.00	12.05	851.98
20.00	141.00	40.00	9.00	10.00	180.00	12.05	851.98
20.00	141.00	40.00	16.00	1.00	175.78	18.41	1412.08
20.00	141.00	40.00	16.00	4.00	180.00	19.05	1417.69
20.00	141.00	40.00	16.00	7.00	180.00	19.05	1417.69
20.00	141.00	40.00	16.00	10.00	180.00	19.05	1417.69
20.00	141.00	40.00	22.00	1.00	175.78	24.41	1896.98
20.00	141.00	40.00	22.00	4.00	180.00	25.05	1902.59
20.00	141.00	40.00	22.00	7.00	180.00	25.05	1902.59
20.00	141.00	40.00	22.00	10.00	180.00	25.05	1902.59
20.00	141.00	30.00	2.50	1.00	173.81	5.56	365.65
20.00	141.00	30.00	2.50	4.00	179.21	6.76	382.88
20.00	141.00	30.00	2.50	7.00	180.00	6.94	383.17
20.00	141.00	30.00	2.50	10.00	180.00	6.94	383.17
20.00	141.00	30.00	9.00	1.00	173.81	12.06	890.96
20.00	141.00	30.00	9.00	4.00	179.21	13.26	908.19
20.00	141.00	30.00	9.00	7.00	180.00	13.44	908.48
20.00	141.00	30.00	9.00	10.00	180.00	13.44	908.48
20.00	141.00	30.00	16.00	1.00	173.81	19.06	1456.68
20.00	141.00	30.00	16.00	4.00	179.21	20.26	1473.91
20.00	141.00	30.00	16.00	7.00	180.00	20.44	1474.19
20.00	141.00	30.00	16.00	10.00	180.00	20.44	1474.19
20.00	141.00	30.00	22.00	1.00	173.81	25.06	1941.58
20.00	141.00	30.00	22.00	4.00	179.21	26.26	1958.81
20.00	141.00	30.00	22.00	7.00	180.00	26.44	1959.09
20.00	141.00	30.00	22.00	10.00	180.00	26.44	1959.09

K-41

Reproduced from
best available copy.

***** PLUNDER ANALYSIS - DUAL AIRCRAFT *****										PAGE = 34	
ALPHABETIC AIRCRAFT	ALTIMETER VELOCITY (KNOTS)	PLUNDERED DUAL ANGLE (DEG.)	PLUNDERED SUMMED RELAYS (SEC.)	ADJACENT SUMMED RELAYS (SEC.)	CONNECTED PARALLEL RELAYS (SEC.)	PLUNDER CORRECTION TIME (SEC.)	PLUNDER RECOVERY AIRSPACE (FT.)				
20.00	14.00	20.00	2.50	1.00	171.19	6.44	433.13				
20.00	14.00	20.00	2.50	4.00	175.57	7.98	475.10				
20.00	14.00	20.00	2.50	7.00	179.94	9.52	489.35				
20.00	14.00	20.00	2.50	10.00	180.00	9.54	489.35				
20.00	14.00	20.00	9.00	1.00	171.19	12.94	956.43				
20.00	14.00	20.00	9.00	4.00	175.57	14.48	1000.41				
20.00	14.00	20.00	9.00	7.00	179.94	16.02	1014.66				
20.00	14.00	20.00	9.00	10.00	180.00	15.04	1014.66				
20.00	14.00	20.00	16.00	1.00	171.19	19.94	1524.15				
20.00	14.00	20.00	16.00	4.00	175.57	21.48	1566.12				
20.00	14.00	20.00	16.00	7.00	179.94	23.02	1580.38				
20.00	14.00	20.00	16.00	10.00	180.00	23.04	1580.38				
20.00	14.00	20.00	22.00	1.00	171.19	25.94	2009.05				
20.00	14.00	20.00	22.00	4.00	175.57	27.48	2051.02				
20.00	14.00	20.00	22.00	7.00	179.94	29.02	2065.28				
20.00	14.00	20.00	22.00	10.00	180.00	29.04	2065.28				
20.00	14.00	10.00	2.50	1.00	167.23	7.76	552.04				
20.00	14.00	10.00	2.50	4.00	170.07	9.81	647.65				
20.00	14.00	10.00	2.50	7.00	172.90	11.87	719.62				
20.00	14.00	10.00	2.50	10.00	175.73	13.92	767.78				
20.00	14.00	10.00	9.00	1.00	167.23	14.26	1077.35				
20.00	14.00	10.00	9.00	4.00	170.07	16.31	1172.96				
20.00	14.00	10.00	9.00	7.00	172.90	18.37	1244.93				
20.00	14.00	10.00	9.00	10.00	175.73	20.42	1293.08				
20.00	14.00	10.00	16.00	1.00	167.23	21.26	1643.07				
20.00	14.00	10.00	16.00	4.00	170.07	23.31	1738.68				
20.00	14.00	10.00	16.00	7.00	172.90	25.37	1810.65				
20.00	14.00	10.00	16.00	10.00	175.73	27.42	1858.80				
20.00	14.00	10.00	22.00	1.00	167.23	27.26	2127.97				
20.00	14.00	10.00	22.00	4.00	170.07	29.31	2223.53				
20.00	14.00	10.00	22.00	7.00	172.90	31.37	2295.55				
20.00	14.00	10.00	22.00	10.00	175.73	33.42	2343.70				

***** BLUNDER ANALYSIS - DUAL AIRCRAFT ***** PAGE = 35

BLUNDERED DEPARTURE ANGLE (DEG.)	BLUNDERED VELOCITY (KNOTS)	BLUNDERED BANK ANGLE (DEG.)	BLUNDERED SUMMED DELAYS (SEC.)	ADJACENT SUMMED DELAYS (SEC.)	CORRECTED PARALLEL HEADINGS (DEG.)	BLUNDER CORRECTION TIME (SEC.)	BLUNDER RECOVERY AIRSPACE (FT.)
20.00	160.00	40.00	2.50	1.00	175.10	5.13	383.81
20.00	160.00	40.00	2.50	4.00	160.00	5.99	393.68
20.00	160.00	40.00	2.50	7.00	180.00	5.99	393.68
20.00	160.00	40.00	2.50	10.00	180.00	5.99	393.68
20.00	160.00	40.00	9.00	1.00	175.10	11.63	984.16
20.00	160.00	40.00	9.00	4.00	160.00	12.49	994.03
20.00	160.00	40.00	9.00	7.00	180.00	12.49	994.03
20.00	160.00	40.00	9.00	10.00	160.00	12.49	994.03
20.00	160.00	40.00	16.00	1.00	175.10	18.63	1630.70
20.00	160.00	40.00	16.00	4.00	180.00	19.49	1640.57
20.00	160.00	40.00	16.00	7.00	180.00	19.49	1640.57
20.00	160.00	40.00	16.00	10.00	180.00	19.49	1640.57
20.00	160.00	40.00	22.00	1.00	175.10	24.63	2184.87
20.00	160.00	40.00	22.00	4.00	180.00	25.49	2194.74
20.00	160.00	40.00	22.00	7.00	180.00	25.49	2194.74
20.00	160.00	40.00	22.00	10.00	180.00	25.49	2194.74
20.00	160.00	30.00	2.50	1.00	173.06	5.81	438.77
20.00	160.00	30.00	2.50	4.00	178.18	7.11	465.49
20.00	160.00	30.00	2.50	7.00	180.00	7.57	467.48
20.00	160.00	30.00	2.50	10.00	180.00	7.17	467.48
20.00	160.00	30.00	9.00	1.00	173.06	12.31	1039.12
20.00	160.00	30.00	9.00	4.00	178.18	13.61	1065.84
20.00	160.00	30.00	9.00	7.00	180.00	14.07	1067.83
20.00	160.00	30.00	9.00	10.00	180.00	14.07	1067.83
20.00	160.00	30.00	16.00	1.00	173.06	19.31	1685.65
20.00	160.00	30.00	16.00	4.00	178.18	20.61	1712.38
20.00	160.00	30.00	16.00	7.00	180.00	21.07	1714.36
20.00	160.00	30.00	16.00	10.00	180.00	21.07	1714.36
20.00	160.00	30.00	22.00	1.00	173.06	25.31	2239.83
20.00	160.00	30.00	22.00	4.00	178.18	26.61	2266.53
20.00	160.00	30.00	22.00	7.00	180.00	27.07	2266.54
20.00	160.00	30.00	22.00	10.00	180.00	27.07	2268.54

***** BLUNDER ANALYSIS - DUAL AIRCRAFT ***** PAGE = 36

BLUNDERED DEPARTURE ANGLE (DEG.)	BLUNDERED VELOCITY (KNOTS)	BLUNDERED DIP ANGLE (DEG.)	BLUNDERED SUMMED DELAYS (SEC.)	ADJACENT SUMMED DELAYS (SEC.)	CORRECTED PARALLEL HEADINGS (DEG.)	BLUNDER CORRECTIO. TIME (SEC.)	BLUNDER RECOVERY AIRSPACE (FT.)
20.00	160.00	20.00	2.50	1.00	170.42	6.69	519.46
20.00	160.00	20.00	2.50	4.00	174.50	8.33	577.55
20.00	160.00	20.00	2.50	7.00	178.58	9.97	604.26
20.00	160.00	20.00	2.50	10.00	180.00	10.54	606.17
20.00	160.00	20.00	9.00	1.00	170.42	13.19	1119.81
20.00	160.00	20.00	9.00	4.00	174.50	14.83	1177.90
20.00	160.00	20.00	9.00	7.00	178.58	16.47	1204.61
20.00	160.00	20.00	9.00	10.00	180.00	17.04	1206.52
20.00	160.00	20.00	16.00	1.00	170.42	20.19	1766.35
20.00	160.00	20.00	16.00	4.00	174.50	21.83	1924.44
20.00	160.00	20.00	16.00	7.00	178.58	23.47	1851.15
20.00	160.00	20.00	16.00	10.00	180.00	24.04	1853.05
20.00	160.00	20.00	22.00	1.00	170.42	26.19	2320.52
20.00	160.00	20.00	22.00	4.00	174.50	27.83	2378.61
20.00	160.00	20.00	22.00	7.00	178.58	29.47	2405.32
20.00	160.00	20.00	22.00	10.00	180.00	30.04	2407.23
20.00	160.00	10.00	2.50	1.00	166.59	7.97	655.29
20.00	160.00	10.00	2.50	4.00	169.17	10.11	776.66
20.00	160.00	10.00	2.50	7.00	171.75	12.25	872.48
20.00	160.00	10.00	2.50	10.00	174.33	14.39	942.56
20.00	160.00	10.00	9.00	1.00	166.59	14.47	1255.65
20.00	160.00	10.00	9.00	4.00	169.17	16.61	1377.01
20.00	160.00	10.00	9.00	7.00	171.75	18.75	1472.83
20.00	160.00	10.00	9.00	10.00	174.33	20.89	1542.91
20.00	160.00	10.00	16.00	1.00	166.59	21.47	1902.18
20.00	160.00	10.00	16.00	4.00	169.17	23.61	2023.55
20.00	160.00	10.00	16.00	7.00	171.75	25.75	2119.37
20.00	160.00	10.00	16.00	10.00	174.33	27.89	2189.45
20.00	160.00	10.00	22.00	1.00	166.59	27.47	2456.35
20.00	160.00	10.00	22.00	4.00	169.17	29.61	2577.72
20.00	160.00	10.00	22.00	7.00	171.75	31.75	2673.54
20.00	160.00	10.00	22.00	10.00	174.33	33.89	2743.62

***** BLUNDER ANALYSIS - JUAL AIRCRAFT MAP OVER ***** PAGE = 37

BLUNDERED DEPARTURE ANGLE (DEG.)	BLUNDERED VELOCITY (KNOTS)	BLUNDERED BANK ANGLE (DEG.)	BLUNDERED SUMMED DELAYS (SEC.)	ADJACENT SUMMED DELAYS (SEC.)	CORRECTED PARALLEL HEADINGS (DEG.)	BLUNDER CORRECTION TIME (SEC.)	BLUNDER RECOVERY AIRSPACE (FT.)
30.00	61.00	40.00	2.50	1.00	177.59	4.30	177.10
30.00	61.00	40.00	2.50	4.00	180.00	4.46	177.44
30.00	61.00	40.00	2.50	7.00	180.00	4.46	177.44
30.00	61.00	40.00	2.50	10.00	180.00	4.46	177.44
30.00	61.00	40.00	9.00	1.00	177.59	10.80	506.22
30.00	61.00	40.00	9.00	4.00	180.00	10.96	506.56
30.00	61.00	40.00	9.00	7.00	180.00	10.96	506.56
30.00	61.00	40.00	9.00	10.00	180.00	10.96	506.56
30.00	61.00	40.00	16.00	1.00	177.59	17.80	860.66
30.00	61.00	40.00	16.00	4.00	180.00	17.96	861.00
30.00	61.00	40.00	16.00	7.00	180.00	17.96	861.00
30.00	61.00	40.00	16.00	10.00	180.00	17.96	861.30
30.00	61.00	40.00	22.00	1.00	177.59	23.80	1164.46
30.00	61.00	40.00	22.00	4.00	180.00	23.96	1164.40
30.00	61.00	40.00	22.00	7.00	180.00	23.96	1164.80
30.00	61.00	40.00	22.00	10.00	180.00	23.96	1164.80
30.00	61.00	30.00	2.50	1.00	175.68	4.94	198.92
30.00	61.00	30.00	2.50	4.00	180.00	5.35	200.49
30.00	61.00	30.00	2.50	7.00	180.00	5.35	200.49
30.00	61.00	30.00	2.50	10.00	180.00	5.35	200.49
30.00	61.00	30.00	9.00	1.00	175.68	11.44	528.04
30.00	61.00	30.00	9.00	4.00	180.00	11.85	529.61
30.00	61.00	30.00	9.00	7.00	180.00	11.85	529.61
30.00	61.00	30.00	9.00	10.00	180.00	11.85	529.61
30.00	61.00	30.00	16.00	1.00	175.68	18.44	882.48
30.00	61.00	30.00	16.00	4.00	180.00	18.85	884.05
30.00	61.00	30.00	16.00	7.00	180.00	18.85	884.05
30.00	61.00	30.00	16.00	10.00	180.00	18.85	884.05
30.00	61.00	30.00	22.00	1.00	175.68	24.44	1166.29
30.00	61.00	30.00	22.00	4.00	180.00	24.85	1187.86
30.00	61.00	30.00	22.00	7.00	180.00	24.85	1187.86
30.00	61.00	30.00	22.00	10.00	180.00	24.85	1187.86

***** BLUNDER ANALYSIS - DUAL AIRCRAFT ***** PAGE = 34

BLUNDERED DEPARTURE ANGLE (DEG.)	BLUNDERED VELOCITY (KNOTS)	BLUNDERED BANK ANGLE (DEG.)	BLUNDERED SUMMED DELAYS (SEC.)	ADJACENT SUMMED DELAYS (SEC.)	CORRECTED PARALLEL HEADINGS (DEG.)	BLUNDER CORRECTION TIME (SEC.)	BLUNDER RECOVERY AIRSPACE (FT.)
30.00	60.00	20.00	2.50	1.00	172.72	5.93	236.77
30.00	60.00	20.00	2.50	4.00	178.92	6.86	243.66
30.00	60.00	20.00	2.50	7.00	180.00	7.02	243.82
30.00	60.00	20.00	2.50	10.00	180.00	7.02	243.82
30.00	60.00	20.00	9.00	1.00	172.72	12.43	565.89
30.00	60.00	20.00	9.00	4.00	178.92	13.36	572.78
30.00	60.00	20.00	9.00	7.00	180.00	13.52	572.94
30.00	60.00	20.00	9.00	10.00	180.00	13.52	572.94
30.00	60.00	20.00	16.00	1.00	172.72	19.43	920.33
30.00	60.00	20.00	16.00	4.00	178.92	20.36	927.22
30.00	60.00	20.00	16.00	7.00	180.00	20.52	927.38
30.00	60.00	20.00	16.00	10.00	180.00	20.52	927.38
30.00	60.00	20.00	22.00	1.00	172.72	25.43	1224.13
30.00	60.00	20.00	22.00	4.00	178.92	26.36	1231.03
30.00	60.00	20.00	22.00	7.00	180.00	26.52	1231.18
30.00	60.00	20.00	22.00	10.00	180.00	26.52	1231.18
30.00	60.00	10.00	2.50	1.00	167.36	7.81	322.73
30.00	60.00	10.00	2.50	4.00	171.72	9.26	349.74
30.00	60.00	10.00	2.50	7.00	176.37	10.71	364.95
30.00	60.00	10.00	2.50	10.00	180.00	11.84	368.57
30.00	60.00	10.00	9.00	1.00	167.06	14.31	651.86
30.00	60.00	10.00	9.00	4.00	171.72	15.76	678.86
30.00	60.00	10.00	9.00	7.00	176.37	17.21	694.00
30.00	60.00	10.00	9.00	10.00	180.00	18.34	697.70
30.00	60.00	10.00	16.00	1.00	167.06	21.31	1006.29
30.00	60.00	10.00	16.00	4.00	171.72	22.76	1033.30
30.00	60.00	10.00	16.00	7.00	176.37	24.21	1048.51
30.00	60.00	10.00	16.00	10.00	180.00	25.34	1052.13
30.00	60.00	10.00	22.00	1.00	167.36	27.31	1310.10
30.00	60.00	10.00	22.00	4.00	171.72	28.76	1337.10
30.00	60.00	10.00	22.00	7.00	176.37	30.21	1352.32
30.00	60.00	10.00	22.00	10.00	180.00	31.34	1355.94

***** BLUNDER ANALYSIS - DUAL AIRCRAFT *****

BLUNDERED DEPARTURE ANGLE (DEG.)	BLUNDERED VELOCITY (KNOTS)	BLUNDERED BANK ANGLE (DEG.)	BLUNDERED SUMMED DELAYS (SEC.)	ADJACENT SUMMED DELAYS (SEC.)	CORRECTED PARALLEL HEADINGS (DEG.)	BLUNDER CORRECTION TIME (SEC.)	BLUNDER RECOVERY AIRSPACE (FT.)
30.00	81.00	40.00	2.50	1.00	175.16	4.78	257.66
30.00	81.00	40.00	2.50	4.00	180.00	5.12	259.18
30.00	81.00	40.00	2.50	7.00	180.00	5.12	259.18
30.00	81.00	40.00	2.50	10.00	180.00	5.12	259.18
30.00	81.00	40.00	9.00	1.00	176.16	11.28	696.49
30.00	81.00	40.00	9.00	4.00	180.00	11.62	698.01
30.00	81.00	40.00	9.00	7.00	180.00	11.62	698.01
30.00	81.00	40.00	9.00	10.00	180.00	11.62	698.01
30.00	81.00	40.00	16.00	1.00	176.16	18.28	1169.08
30.00	81.00	40.00	16.00	4.00	180.00	18.62	1170.60
30.00	81.00	40.00	16.00	7.00	180.00	18.62	1170.60
30.00	81.00	40.00	16.00	10.00	180.00	18.62	1170.60
30.00	81.00	40.00	22.00	1.00	176.16	24.28	1574.15
30.00	81.00	40.00	22.00	4.00	180.00	24.62	1575.67
30.00	81.00	40.00	22.00	7.00	180.00	24.62	1575.67
30.00	81.00	40.00	22.00	10.00	180.00	24.62	1575.67
30.00	81.00	30.00	2.50	1.00	173.91	5.53	294.63
30.00	81.00	30.00	2.50	4.00	180.00	6.30	300.17
30.00	81.00	30.00	2.50	7.00	180.00	6.30	300.17
30.00	81.00	30.00	2.50	10.00	180.00	6.30	300.17
30.00	81.00	30.00	9.00	1.00	173.91	12.03	733.46
30.00	81.00	30.00	9.00	4.00	180.00	12.80	739.00
30.00	81.00	30.00	9.00	7.00	180.00	12.80	739.00
30.00	81.00	30.00	9.00	10.00	180.00	12.80	739.00
30.00	81.00	30.00	16.00	1.00	173.91	19.03	1206.04
30.00	81.00	30.00	16.00	4.00	180.00	19.80	1211.58
30.00	81.00	30.00	16.00	7.00	180.00	19.80	1211.58
30.00	81.00	30.00	16.00	10.00	180.00	19.80	1211.58
30.00	81.00	30.00	22.00	1.00	173.91	25.03	1611.12
30.00	81.00	30.00	22.00	4.00	180.00	25.80	1616.65
30.00	81.00	30.00	22.00	7.00	180.00	25.80	1616.65
30.00	81.00	30.00	22.00	10.00	180.00	25.80	1616.65

***** BLUNDER ANALYSIS - DUAL AIRCRAFT ***** PAGE = 40

BLUNDER DEPARTURE ANGLE (DEG.)	BLUNDERED VELOCITY (KNOTS)	BLUNDERED BANK ANGLE (DEG.)	BLUNDERED SUMMED DELAYS (SEC.)	ADJACENT SUMMED DELAYS (SEC.)	CORRECTED PARALLEL HEADINGS (DEG.)	BLUNDER CORRECTION TIME (SEC.)	BLUNDER RECOVERY AIRSPACE (FT.)
30.00	60.00	20.00	2.50	1.00	170.56	6.64	356.23
30.00	60.00	20.00	2.50	4.00	176.20	7.77	373.77
30.00	60.00	20.00	2.50	7.00	180.00	8.53	377.19
30.00	60.00	20.00	2.50	10.00	180.00	8.53	377.19
30.00	60.00	20.00	9.00	1.00	170.56	13.14	795.06
30.00	60.00	20.00	9.00	4.00	176.20	14.27	812.60
30.00	60.00	20.00	9.00	7.00	180.00	15.03	816.02
30.00	60.00	20.00	9.00	10.00	180.00	15.03	816.02
30.00	60.00	20.00	16.00	1.00	170.56	20.14	1267.65
30.00	60.00	20.00	16.00	4.00	176.20	21.27	1285.18
30.00	60.00	20.00	16.00	7.00	180.00	22.03	1288.61
30.00	60.00	20.00	16.00	10.00	180.00	22.03	1288.61
30.00	60.00	20.00	22.00	1.00	170.56	26.14	1672.72
30.00	60.00	20.00	22.00	4.00	176.20	27.27	1690.26
30.00	60.00	20.00	22.00	7.00	180.00	28.03	1693.68
30.00	60.00	20.00	22.00	10.00	180.00	28.03	1693.68
30.00	60.00	10.00	2.50	1.00	164.70	8.60	485.15
30.00	60.00	10.00	2.50	4.00	168.71	10.26	536.81
30.00	60.00	10.00	2.50	7.00	172.72	11.93	573.06
30.00	60.00	10.00	2.50	10.00	176.72	13.59	593.73
30.00	60.00	10.00	9.00	1.00	164.70	15.10	923.97
30.00	60.00	10.00	9.00	4.00	168.71	16.76	975.64
30.00	60.00	10.00	9.00	7.00	172.72	18.43	1011.89
30.00	60.00	10.00	9.00	10.00	176.72	20.09	1032.56
30.00	60.00	10.00	16.00	1.00	164.70	22.10	1396.56
30.00	60.00	10.00	16.00	4.00	168.71	23.76	1448.22
30.00	60.00	10.00	16.00	7.00	172.72	25.43	1484.48
30.00	60.00	10.00	16.00	10.00	176.72	27.09	1505.15
30.00	60.00	10.00	22.00	1.00	164.70	28.10	1801.63
30.00	60.00	10.00	22.00	4.00	168.71	29.76	1853.29
30.00	60.00	10.00	22.00	7.00	172.72	31.43	1889.55
30.00	60.00	10.00	22.00	10.00	176.72	33.09	1910.22

***** ROLLER ANALYSIS - DUAL AIRCRAFT MANEUVER ***** PAGE = 41

DEPARTURE ANGLE (DEG.)	ROLLER VELOCITY (KNOTS)	ROLLER BANK ANGLE (DEG.)	ROLLER SUMMED DELAYS (SEC.)	ADJACENT SUMMED DELAYS (SEC.)	CORRECTED PARALLEL HEADINGS (DEG.)	ROLLER CORRECTION TIME (SEC.)	ROLLER RECOVERY AIRSPACE (FT.)
30.00	100.00	40.00	2.50	1.00	174.87	5.21	340.00
30.00	100.00	40.00	2.50	4.00	180.00	5.77	352.23
30.00	100.00	40.00	2.50	7.00	180.00	5.77	352.23
30.00	100.00	40.00	2.50	10.00	180.00	5.77	352.23
30.00	100.00	40.00	9.00	1.00	174.87	11.71	896.54
30.00	100.00	40.00	9.00	4.00	180.00	12.27	900.77
30.00	100.00	40.00	9.00	7.00	180.00	12.27	900.77
30.00	100.00	40.00	9.00	10.00	180.00	12.27	900.77
30.00	100.00	40.00	16.00	1.00	174.87	18.71	1487.27
30.00	100.00	40.00	16.00	4.00	180.00	19.27	1491.50
30.00	100.00	40.00	16.00	7.00	180.00	19.27	1491.50
30.00	100.00	40.00	16.00	10.00	180.00	19.27	1491.50
30.00	100.00	40.00	22.00	1.00	174.87	24.71	1993.61
30.00	100.00	40.00	22.00	4.00	180.00	25.27	1997.84
30.00	100.00	40.00	22.00	7.00	180.00	25.27	1997.84
30.00	100.00	40.00	22.00	10.00	180.00	25.27	1997.84
30.00	100.00	30.00	2.50	1.00	172.37	6.04	402.09
30.00	100.00	30.00	2.50	4.00	178.47	7.01	415.72
30.00	100.00	30.00	2.50	7.00	180.00	7.25	416.27
30.00	100.00	30.00	2.50	10.00	180.00	7.25	416.27
30.00	100.00	30.00	9.00	1.00	172.37	12.54	951.23
30.00	100.00	30.00	9.00	4.00	178.47	13.51	964.26
30.00	100.00	30.00	9.00	7.00	180.00	13.75	964.26
30.00	100.00	30.00	9.00	10.00	180.00	13.75	964.26
30.00	100.00	30.00	16.00	1.00	172.37	19.54	1541.06
30.00	100.00	30.00	16.00	4.00	178.47	20.51	1554.89
30.00	100.00	30.00	16.00	7.00	180.00	20.75	1555.54
30.00	100.00	30.00	16.00	10.00	180.00	20.75	1555.54
30.00	100.00	30.00	22.00	1.00	172.37	25.54	2046.30
30.00	100.00	30.00	22.00	4.00	178.47	26.51	2061.33
30.00	100.00	30.00	22.00	7.00	180.00	26.75	2061.88
30.00	100.00	30.00	22.00	10.00	180.00	26.75	2061.88

***** LUNDEK ANALYSIS - DUAL AIRCRAFT ANALYSIS ***** PAGE = 42

BLUNDEK DEPARTURE ANGLE (DEG.)	BLUNDEK VELOCITY (KNOTS)	BLUNDEK MARK ANGLE (DEG.)	BLUNDEK SUMMED DELAYS (SEC.)	ADJACENT SUMMED DELAYS (SEC.)	CORRECTED PARALLEL HOLDINGS (DEG.)	LUNDEK CORRECTION TIME (SEC.)	BLUNDEK RECOVERY AIRSPACE (FT.)
30.00	10.00	20.00	2.50	1.00	108.01	7.23	490.44
30.00	10.00	20.00	2.50	4.00	173.94	8.52	523.06
30.00	10.00	20.00	2.50	7.00	179.06	9.81	536.31
30.00	10.00	20.00	2.50	10.00	180.00	10.04	536.62
30.00	10.00	20.00	9.00	1.00	168.81	13.73	1038.98
30.00	10.00	20.00	9.00	4.00	173.94	15.02	1071.60
30.00	10.00	20.00	9.00	7.00	179.08	16.31	1084.84
30.00	10.00	20.00	9.00	10.00	180.00	16.54	1085.16
30.00	10.00	20.00	16.00	1.00	168.81	20.73	1629.71
30.00	10.00	20.00	16.00	4.00	173.94	22.02	1662.33
30.00	10.00	20.00	16.00	7.00	179.08	23.31	1675.57
30.00	10.00	20.00	16.00	10.00	180.00	23.54	1675.89
30.00	10.00	20.00	22.00	1.00	168.81	26.73	2136.05
30.00	10.00	20.00	22.00	4.00	173.94	28.02	2168.67
30.00	10.00	20.00	22.00	7.00	179.08	29.31	2181.91
30.00	10.00	20.00	22.00	10.00	180.00	29.54	2182.23
30.00	10.00	10.00	2.50	1.00	162.91	9.20	661.58
30.00	10.00	10.00	2.50	4.00	163.43	11.02	743.08
30.00	10.00	10.00	2.50	7.00	169.95	12.85	806.17
30.00	10.00	10.00	2.50	10.00	173.47	14.68	850.61
30.00	10.00	10.00	9.00	1.00	162.91	15.70	1210.12
30.00	10.00	10.00	9.00	4.00	166.43	17.52	1291.61
30.00	10.00	10.00	9.00	7.00	169.95	19.35	1354.70
30.00	10.00	10.00	9.00	10.00	173.47	21.18	1399.15
30.00	10.00	10.00	16.00	1.00	162.91	22.70	1800.85
30.00	10.00	10.00	16.00	4.00	166.43	24.52	1882.35
30.00	10.00	10.00	16.00	7.00	169.95	26.35	1945.44
30.00	10.00	10.00	16.00	10.00	173.47	28.18	1989.88
30.00	10.00	10.00	22.00	1.00	162.91	28.70	2307.19
30.00	10.00	10.00	22.00	4.00	166.43	30.52	2388.69
30.00	10.00	10.00	22.00	7.00	169.95	32.35	2451.78
30.00	10.00	10.00	22.00	10.00	173.47	34.18	2496.22

K-50

Reproduced from
best available copy

***** PLUNDER ANALYSIS - DUAL AIRCRAFT CAPTURE ***** PAGE = 43

PLUNDERED VELOCITY (KNOTS)	PLUNDERED BANK ANGLE (DEG.)	PLUNDERED SUMMED DELAYS (SEC.)	ADJACENT SUMMED DELAYS (SEC.)	CORRECTED PARALLEL HEADINGS (DEG.)	PLUNDER CORRECTION TIME (SEC.)	PLUNDER RECOVERY AIRSPACE (FT.)
30.00	40.00	2.50	1.00	173.70	5.60	447.40
30.00	40.00	2.50	4.00	180.00	6.42	456.58
30.00	40.00	2.50	7.00	180.00	6.42	456.58
30.00	40.00	2.50	10.00	180.00	6.42	456.58
30.00	40.00	9.00	1.00	173.70	12.10	1105.65
30.00	40.00	9.00	4.00	180.00	12.92	1114.82
30.00	40.00	9.00	7.00	180.00	12.92	1114.82
30.00	40.00	9.00	10.00	180.00	12.92	1114.82
30.00	40.00	16.00	1.00	173.70	19.10	1814.52
30.00	40.00	16.00	4.00	180.00	19.92	1823.70
30.00	40.00	16.00	7.00	180.00	19.92	1823.70
30.00	40.00	16.00	10.00	180.00	19.92	1823.70
30.00	40.00	22.00	1.00	173.70	25.10	2422.13
30.00	40.00	22.00	4.00	180.00	25.92	2431.31
30.00	40.00	22.00	7.00	180.00	25.92	2431.31
30.00	40.00	22.00	10.00	180.00	25.92	2431.31
30.00	30.00	2.50	1.00	171.01	6.50	521.71
30.00	30.00	2.50	.00	176.74	7.59	545.23
30.00	30.00	2.50	7.00	180.00	8.20	548.79
30.00	30.00	2.50	10.00	180.00	8.20	548.79
30.00	30.00	9.00	1.00	171.01	13.00	1179.95
30.00	30.00	9.00	4.00	176.74	14.09	1203.47
30.00	30.00	9.00	7.00	180.00	14.70	1207.04
30.00	30.00	9.00	10.00	180.00	14.70	1207.04
30.00	30.00	16.00	1.00	171.01	20.00	1888.83
30.00	30.00	16.00	4.00	176.74	21.09	1912.35
30.00	30.00	16.00	7.00	180.00	21.70	1915.91
30.00	30.00	16.00	10.00	180.00	21.70	1915.91
30.00	30.00	22.00	1.00	171.01	26.00	2496.44
30.00	30.00	22.00	4.00	176.74	27.09	2519.96
30.00	30.00	22.00	7.00	180.00	27.70	2523.52
30.00	30.00	22.00	10.00	180.00	27.70	2523.52

Reproduced from
Best Available Copy.

***** LUNDER ANALYSIS - INITIAL AIRCRAFT ANALYSIS *****										PAGE = 44	
BLUNDER ANALYSIS (SEC.)	BLUNDER ANALYSIS (SEC.)	BLUNDER ANALYSIS (SEC.)	BLUNDER ANALYSIS (SEC.)	BLUNDER ANALYSIS (SEC.)	BLUNDER ANALYSIS (SEC.)	BLUNDER ANALYSIS (SEC.)	BLUNDER ANALYSIS (SEC.)	BLUNDER ANALYSIS (SEC.)	BLUNDER ANALYSIS (SEC.)	BLUNDER ANALYSIS (SEC.)	BLUNDER ANALYSIS (SEC.)
30.00	12.000	20.00	2.50	1.00	167.32	7.73	636.79				
30.00	12.000	20.00	2.50	4.00	172.05	9.15	688.45				
30.00	12.000	20.00	2.50	7.00	176.77	10.56	716.55				
30.00	12.000	20.00	2.50	10.00	180.00	11.55	722.10				
30.00	12.000	20.00	4.00	1.00	167.32	14.23	1295.04				
30.00	12.000	20.00	9.00	4.00	172.05	15.65	1346.70				
30.00	12.000	20.00	9.00	7.00	176.77	17.08	1374.80				
30.00	12.000	20.00	4.00	10.00	180.00	18.05	1380.34				
30.00	12.000	20.00	16.00	1.00	167.32	21.23	2003.91				
30.00	12.000	20.00	16.00	4.00	172.05	22.65	2055.57				
30.00	12.000	20.00	16.00	7.00	176.77	24.08	2083.67				
30.00	12.000	20.00	16.00	10.00	180.00	25.05	2089.22				
30.00	12.000	20.00	22.00	1.00	167.32	27.23	2611.52				
30.00	12.000	20.00	22.00	4.00	172.05	28.65	2663.18				
30.00	12.000	20.00	22.00	7.00	176.77	30.08	2691.28				
30.00	12.000	20.00	22.00	10.00	180.00	31.05	2696.83				
30.00	12.000	10.00	2.50	1.00	161.51	9.66	948.05				
30.00	12.000	10.00	2.50	4.00	164.65	11.62	963.24				
30.00	12.000	10.00	2.50	7.00	167.78	13.57	1057.52				
30.00	12.000	10.00	2.50	10.00	170.92	15.53	1130.63				
30.00	12.000	10.00	9.00	1.00	161.51	16.16	1506.30				
30.00	12.000	10.00	4.00	4.00	164.65	18.12	1621.48				
30.00	12.000	10.00	4.00	7.00	167.78	20.07	1715.77				
30.00	12.000	10.00	4.00	10.00	170.92	22.03	1788.87				
30.00	12.000	10.00	16.00	1.00	161.51	23.16	2215.17				
30.00	12.000	10.00	16.00	4.00	164.65	25.12	2330.36				
30.00	12.000	10.00	16.00	7.00	167.78	27.07	2424.65				
30.00	12.000	10.00	16.00	10.00	170.92	29.03	2497.75				
30.00	12.000	10.00	22.00	1.00	161.51	29.16	2622.78				
30.00	12.000	10.00	22.00	4.00	164.65	31.12	2937.97				
30.00	12.000	10.00	22.00	7.00	167.78	33.07	3032.25				
30.00	12.000	10.00	22.00	10.00	170.92	35.03	3105.36				

BLUNDERED DEPARTURE ANGLE (DEG.)	BLUNDERED VELOCITY (KNOTS)	BLUNDERED BANK ANGLE (DEG.)	BLUNDERED SUMMED DELAYS (SEC.)	ADJACENT SUMMED DELAYS (SEC.)	CORRECTED PARALLEL HEADINGS (DEG.)	BLUNDER CORRECTION TIME (SEC.)	BLUNDER RECOVERY AIRSPACE (FT.)
30.00	14.000	40.00	2.50	1.00	172.04	5.95	555.17
30.00	14.000	40.00	2.50	4.00	178.81	6.90	571.78
30.00	14.000	40.00	2.50	7.00	180.00	7.06	572.22
30.00	14.000	40.00	2.50	10.00	180.00	7.08	572.22
30.00	14.000	40.00	9.00	1.00	172.64	12.45	1323.12
30.00	14.000	40.00	9.00	4.00	178.81	13.40	1339.73
30.00	14.000	40.00	9.00	7.00	180.00	13.58	1340.17
30.00	14.000	40.00	9.00	10.00	180.00	13.58	1340.17
30.00	14.000	40.00	16.00	1.00	172.64	19.45	2150.15
30.00	14.000	40.00	16.00	4.00	173.81	20.40	2166.75
30.00	14.000	40.00	16.00	7.00	180.00	20.58	2167.20
30.00	14.000	40.00	16.00	10.00	180.00	20.58	2167.20
30.00	14.000	40.00	22.00	1.00	172.64	25.45	2859.03
30.00	14.000	40.00	22.00	4.00	178.81	26.40	2875.53
30.00	14.000	40.00	22.00	7.00	180.00	26.58	2876.07
30.00	14.000	40.00	22.00	10.00	180.00	26.58	2876.07
30.00	14.000	30.00	2.50	1.00	169.81	6.90	650.40
30.00	14.000	30.00	2.50	4.00	175.22	8.09	687.28
30.00	14.000	30.00	2.50	7.00	180.00	9.16	697.74
30.00	14.000	30.00	2.50	10.00	180.00	9.16	697.74
30.00	14.000	30.00	9.00	1.00	169.81	13.40	1418.35
30.00	14.000	30.00	9.00	4.00	175.22	14.59	1455.23
30.00	14.000	30.00	9.00	7.00	180.00	15.66	1465.69
30.00	14.000	30.00	9.00	10.00	180.00	15.66	1465.69
30.00	14.000	30.00	16.00	1.00	169.81	20.40	2245.37
30.00	14.000	30.00	16.00	4.00	175.22	21.59	2282.26
30.00	14.000	30.00	16.00	7.00	180.00	22.66	2292.71
30.00	14.000	30.00	16.00	10.00	180.00	22.66	2292.71
30.00	14.000	30.00	22.00	1.00	169.81	26.40	2954.25
30.00	14.000	30.00	22.00	4.00	175.22	27.59	3091.13
30.00	14.000	30.00	22.00	7.00	180.00	28.66	3001.59
30.00	14.000	30.00	22.00	10.00	180.00	28.66	3001.59

Reproduced from
best available copy.

Reproduced from
best available copy.

***** H-100 ANALYSIS - DUAL AIRCRAFT *****										PAGE = 47
BLUNDERED VELOCITY (KNOTS)	BLUNDERED DARK ANGLE (DEG.)	BLUNDERED SUMMED DELAYS (SEC.)	ADJUSTED SUMMED DELAYS (SEC.)	CORRECTED PARALLEL HEADINGS (DEG.)	LUNDER CORRECTION TIME (SEC.)	BLUNDER RECOVERY AIRSPACE (FT.)				
30.00	40.00	2.50	1.00	171.66	6.28	670.65				
30.00	40.00	2.50	4.00	177.57	7.31	896.75				
30.00	40.00	2.50	7.00	180.00	7.73	699.17				
30.00	40.00	2.50	10.00	180.00	7.73	699.17				
30.00	40.00	9.00	1.00	171.66	12.78	1548.31				
30.00	40.00	9.00	4.00	177.57	13.81	1574.40				
30.00	40.00	9.00	7.00	180.00	14.23	1576.83				
30.00	40.00	9.00	10.00	180.00	14.23	1576.83				
30.00	40.00	16.00	1.00	171.66	19.78	2493.48				
30.00	40.00	16.00	4.00	177.57	20.81	2519.57				
30.00	40.00	16.00	7.00	180.00	21.23	2522.00				
30.00	40.00	16.00	10.00	180.00	21.23	2522.00				
30.00	40.00	22.00	1.00	171.66	25.78	3303.62				
30.00	40.00	22.00	4.00	177.57	26.81	3329.72				
30.00	40.00	22.00	7.00	180.00	27.23	3332.14				
30.00	40.00	22.00	10.00	180.00	27.23	3332.14				
30.00	30.00	2.50	1.00	168.74	7.25	787.65				
30.00	30.00	2.50	4.00	173.86	8.55	840.58				
30.00	30.00	2.50	7.00	178.97	9.84	862.47				
30.00	30.00	2.50	10.00	180.00	10.11	863.11				
30.00	30.00	9.00	1.00	168.74	13.75	1665.31				
30.00	30.00	9.00	4.00	173.86	15.05	1718.23				
30.00	30.00	9.00	7.00	178.97	16.34	1740.13				
30.00	30.00	9.00	10.00	180.00	16.61	1740.77				
30.00	30.00	16.00	1.00	168.74	20.75	2610.48				
30.00	30.00	16.00	4.00	173.86	22.05	2663.40				
30.00	30.00	16.00	7.00	178.97	23.34	2685.30				
30.00	30.00	16.00	10.00	180.00	23.61	2685.94				
30.00	30.00	22.00	1.00	168.74	26.75	3420.63				
30.00	30.00	22.00	4.00	173.86	28.05	3473.55				
30.00	30.00	22.00	7.00	178.97	29.34	3495.45				
30.00	30.00	22.00	10.00	180.00	29.61	3496.08				

Reproduced from
unclassified source

***** BUNDER ANALYSIS - DUAL AIRCRAFT - AIR OVER ***** PAGE = 49

DEPARTURE ANGLE (DEG.)	BUNDER VELOCITY (KNOTS)	BUNDER DARK ANGLE (DEG.)	BUNDER SUMMIT DELAYS (SEC.)	ADJACENT SUMMIT DELAYS (SEC.)	CORRECTED PARALLEL HEADINGS (DEG.)	BUNDER CORRECTION TIME (SEC.)	BUNDER RECOVERY AIRSPACE (FT.)
45.00	6.000	40.00	2.50	1.00	175.13	5.12	288.82
45.00	6.000	40.00	2.50	4.00	180.00	5.44	290.19
45.00	6.000	40.00	2.50	7.00	180.00	5.44	290.19
45.00	6.000	40.00	2.50	10.00	180.00	5.44	290.19
45.00	6.000	40.00	9.00	1.00	175.13	11.62	754.26
45.00	6.000	40.00	3.00	4.00	180.00	11.94	755.64
45.00	6.000	40.00	9.00	7.00	180.00	11.94	755.64
45.00	6.000	40.00	9.00	10.00	180.00	11.94	755.64
45.00	6.000	40.00	16.00	1.00	175.13	18.62	1255.52
45.00	6.000	40.00	16.00	4.00	180.00	18.94	1256.89
45.00	6.000	40.00	16.00	7.00	180.00	18.94	1256.89
45.00	6.000	40.00	16.00	10.00	180.00	18.94	1256.89
45.00	6.000	40.00	22.00	1.00	175.13	24.62	1685.16
45.00	6.000	40.00	22.00	4.00	180.00	24.94	1686.53
45.00	6.000	40.00	22.00	7.00	180.00	24.94	1686.53
45.00	6.000	40.00	22.00	10.00	180.00	24.94	1686.53
45.00	6.000	30.00	2.50	1.00	172.35	6.05	335.68
45.00	6.000	30.00	2.50	4.00	179.35	6.72	340.55
45.00	6.000	30.00	2.50	7.00	180.00	6.78	340.59
45.00	6.000	30.00	2.50	10.00	180.00	6.78	340.59
45.00	6.000	30.00	9.00	1.00	172.35	12.55	801.13
45.00	6.000	30.00	9.00	4.00	179.35	13.22	806.00
45.00	6.000	30.00	9.00	7.00	180.00	13.28	806.04
45.00	6.000	30.00	9.00	10.00	180.00	13.28	806.04
45.00	6.000	30.00	16.00	1.00	172.35	19.55	1302.38
45.00	6.000	30.00	16.00	4.00	179.35	20.22	1307.25
45.00	6.000	30.00	16.00	7.00	180.00	20.28	1307.29
45.00	6.000	30.00	16.00	10.00	180.00	20.28	1307.29
45.00	6.000	30.00	22.00	1.00	172.35	25.55	1732.02
45.00	6.000	30.00	22.00	4.00	179.35	26.22	1736.90
45.00	6.000	30.00	22.00	7.00	180.00	26.28	1736.94
45.00	6.000	30.00	22.00	10.00	180.00	26.28	1736.94

Reproduced from
 available for
 use

***** BLOWER ANALYSIS - TUBAL AIRCRAFT *****										PAGE = 50	
BLUNDER	VELOCITY (KTS)	BLUNDER SINK ANGLE (DEG.)	BLUNDER SINK ANGLE (DEG.)	BLUNDER SINK ANGLE (DEG.)	BLUNDER SINK ANGLE (DEG.)	BLUNDER SINK ANGLE (DEG.)	BLUNDER SINK ANGLE (DEG.)	BLUNDER SINK ANGLE (DEG.)	BLUNDER SINK ANGLE (DEG.)	BLUNDER CORRECTION TIME (SEC.)	BLUNDER RECOVERY AIRSPACE (FT.)
43000	0.00	20.00	20.00	20.00	20.00	20.00	20.00	20.00	20.00	7.40	416.34
43000	0.00	20.00	20.00	20.00	20.00	20.00	20.00	20.00	20.00	8.42	430.90
43000	0.00	20.00	20.00	20.00	20.00	20.00	20.00	20.00	20.00	9.29	435.31
43000	0.00	20.00	20.00	20.00	20.00	20.00	20.00	20.00	20.00	9.29	435.31
43000	0.00	20.00	20.00	20.00	20.00	20.00	20.00	20.00	20.00	13.98	861.79
43000	0.00	20.00	20.00	20.00	20.00	20.00	20.00	20.00	20.00	14.92	896.35
43000	0.00	20.00	20.00	20.00	20.00	20.00	20.00	20.00	20.00	15.79	900.76
43000	0.00	20.00	20.00	20.00	20.00	20.00	20.00	20.00	20.00	15.79	900.76
43000	0.00	20.00	20.00	20.00	20.00	20.00	20.00	20.00	20.00	20.90	1383.04
43000	0.00	20.00	20.00	20.00	20.00	20.00	20.00	20.00	20.00	21.92	1397.60
43000	0.00	20.00	20.00	20.00	20.00	20.00	20.00	20.00	20.00	22.79	1402.01
43000	0.00	20.00	20.00	20.00	20.00	20.00	20.00	20.00	20.00	22.79	1402.01
43000	0.00	20.00	20.00	20.00	20.00	20.00	20.00	20.00	20.00	26.98	1812.69
43000	0.00	20.00	20.00	20.00	20.00	20.00	20.00	20.00	20.00	27.92	1827.25
43000	0.00	20.00	20.00	20.00	20.00	20.00	20.00	20.00	20.00	28.79	1831.66
43000	0.00	20.00	20.00	20.00	20.00	20.00	20.00	20.00	20.00	28.79	1831.66
43000	0.00	20.00	20.00	20.00	20.00	20.00	20.00	20.00	20.00	30.23	597.18
43000	0.00	20.00	20.00	20.00	20.00	20.00	20.00	20.00	20.00	31.68	642.14
43000	0.00	20.00	20.00	20.00	20.00	20.00	20.00	20.00	20.00	33.12	675.63
43000	0.00	20.00	20.00	20.00	20.00	20.00	20.00	20.00	20.00	34.57	697.42
43000	0.00	20.00	20.00	20.00	20.00	20.00	20.00	20.00	20.00	36.73	1062.63
43000	0.00	20.00	20.00	20.00	20.00	20.00	20.00	20.00	20.00	38.18	1107.59
43000	0.00	20.00	20.00	20.00	20.00	20.00	20.00	20.00	20.00	39.62	1141.08
43000	0.00	20.00	20.00	20.00	20.00	20.00	20.00	20.00	20.00	41.07	1162.87
43000	0.00	20.00	20.00	20.00	20.00	20.00	20.00	20.00	20.00	43.73	1563.88
43000	0.00	20.00	20.00	20.00	20.00	20.00	20.00	20.00	20.00	45.18	1608.84
43000	0.00	20.00	20.00	20.00	20.00	20.00	20.00	20.00	20.00	46.62	1642.33
43000	0.00	20.00	20.00	20.00	20.00	20.00	20.00	20.00	20.00	48.07	1664.13
43000	0.00	20.00	20.00	20.00	20.00	20.00	20.00	20.00	20.00	49.73	1993.52
43000	0.00	20.00	20.00	20.00	20.00	20.00	20.00	20.00	20.00	51.18	2038.49
43000	0.00	20.00	20.00	20.00	20.00	20.00	20.00	20.00	20.00	52.62	2071.98
43000	0.00	20.00	20.00	20.00	20.00	20.00	20.00	20.00	20.00	54.07	2093.77

***** BLUNDER ANALYSIS - DUAL AIRCRAFT ***** PAGE = 51

BLUNDER DEPARTMENT (CODE)	BLUNDER LOCALITY (K. DTS)	BLUNDERED BANK ANGLE (DEG.)	BLUNDERED SUMMED DELAYS (SEC.)	ADJACENT SUMMED DELAYS (SEC.)	CORRECTED PARALLEL HEADINGS (DEG.)	BLUNDER CORRECTION TIME (SEC.)	BLUNDER RECOVERY AIRSPACE (FT.)
43.00	00.00	40.00	2.50	1.00	173.05	5.82	431.36
43.00	00.00	40.00	2.50	4.00	180.00	6.42	436.33
43.00	00.00	40.00	2.50	7.00	180.00	6.42	436.33
43.00	00.00	40.00	2.50	10.00	180.00	6.42	436.33
43.00	00.00	40.00	9.00	1.00	173.05	12.32	1051.96
43.00	00.00	40.00	9.00	4.00	180.00	12.92	1056.93
43.00	00.00	40.00	9.00	7.00	180.00	12.92	1056.93
43.00	00.00	40.00	9.00	10.00	180.00	12.92	1056.93
43.00	00.00	40.00	10.00	1.00	173.05	19.32	1720.30
43.00	00.00	40.00	10.00	4.00	180.00	19.92	1725.26
43.00	00.00	40.00	10.00	7.00	180.00	19.92	1725.26
43.00	00.00	40.00	10.00	10.00	180.00	19.92	1725.26
43.00	00.00	40.00	22.00	1.00	173.05	25.32	2293.16
43.00	00.00	40.00	22.00	4.00	180.00	25.92	2298.12
43.00	00.00	40.00	22.00	7.00	180.00	25.92	2298.12
43.00	00.00	40.00	22.00	10.00	180.00	25.92	2298.12
43.00	00.00	30.00	2.50	1.00	169.78	6.91	510.35
43.00	00.00	30.00	2.50	4.00	176.30	7.73	523.88
43.00	00.00	30.00	2.50	7.00	180.00	8.20	525.93
43.00	00.00	30.00	2.50	10.00	180.00	8.20	525.93
43.00	00.00	30.00	9.00	1.00	169.78	13.41	1130.95
43.00	00.00	30.00	9.00	4.00	176.30	14.23	1144.48
43.00	00.00	30.00	9.00	7.00	180.00	14.70	1146.53
43.00	00.00	30.00	9.00	10.00	180.00	14.70	1146.53
43.00	00.00	30.00	16.00	1.00	169.78	20.41	1799.29
43.00	00.00	30.00	16.00	4.00	176.30	21.23	1812.81
43.00	00.00	30.00	16.00	7.00	180.00	21.70	1814.86
43.00	00.00	30.00	16.00	10.00	180.00	21.70	1814.86
43.00	00.00	30.00	22.00	1.00	169.78	26.41	2372.15
43.00	00.00	30.00	22.00	4.00	176.30	27.23	2385.67
43.00	00.00	30.00	22.00	7.00	180.00	27.70	2387.72
43.00	00.00	30.00	22.00	10.00	180.00	27.70	2387.72

K-59

Reprod. from
best available copy.

***** BLUNDER ANALYSIS - DUAL AIRCRAFT MANEUVER *****

BLUNDER ANGLE (DEG.)	BLUNDERED VELOCITY (KNOTS)	BLUNDERED HANK ANGLE (DEG.)	BLUNDERED SUMMED DELAYS (SEC.)	ADJACENT SUMMED DELAYS (SEC.)	CORRECTED PARALLEL HEADINGS (DEG.)	BLUNDER CORRECTION TIME (SEC.)	BLUNDER RECOVERY AIRSPACE (FT.)
45.00	60.00	20.00	2.50	1.00	164.94	8.52	640.89
45.00	60.00	20.00	2.50	4.00	170.55	9.65	673.22
45.00	80.00	20.00	2.50	7.00	176.17	10.78	690.84
45.00	80.00	20.00	2.50	10.00	180.00	11.55	694.32
45.00	60.00	20.00	9.00	1.00	164.94	13.02	1261.49
45.00	80.00	20.00	9.00	4.00	170.55	16.15	1293.82
45.00	80.00	20.00	9.00	7.00	176.17	17.28	1311.44
45.00	80.00	20.00	9.00	10.00	180.00	13.05	1314.92
45.00	60.00	20.00	16.00	1.00	164.94	22.02	1929.82
45.00	60.00	20.00	16.00	4.00	170.55	23.15	1962.16
45.00	80.00	20.00	16.00	7.00	176.17	24.28	1979.78
45.00	80.00	20.00	16.00	10.00	180.00	25.05	1983.26
45.00	60.00	20.00	22.00	1.00	164.94	28.02	2502.68
45.00	80.00	20.00	22.00	4.00	170.55	29.15	2535.02
45.00	80.00	20.00	22.00	7.00	176.17	30.28	2552.64
45.00	80.00	20.00	22.00	10.00	180.00	31.05	2556.12
45.00	60.00	10.00	2.50	1.00	156.38	11.37	910.16
45.00	60.00	10.00	2.50	4.00	160.39	13.04	992.90
45.00	80.00	10.00	2.50	7.00	164.40	14.70	1060.85
45.00	80.00	10.00	2.50	10.00	168.40	16.37	1113.66
45.00	60.00	10.00	9.00	1.00	156.38	17.87	1530.76
45.00	80.00	10.00	9.00	4.00	160.39	19.54	1613.50
45.00	80.00	10.00	9.00	7.00	164.40	21.20	1681.45
45.00	80.00	10.00	9.00	10.00	168.40	22.87	1734.26
45.00	60.00	10.00	16.00	1.00	156.38	24.87	2199.05
45.00	80.00	10.00	16.00	4.00	160.39	26.54	2281.84
45.00	80.00	10.00	16.00	7.00	164.40	28.20	2349.78
45.00	80.00	10.00	16.00	10.00	168.40	29.87	2402.60
45.00	60.00	10.00	22.00	1.00	156.38	30.87	2771.95
45.00	80.00	10.00	22.00	4.00	160.39	32.54	2854.70
45.00	80.00	10.00	22.00	7.00	164.40	34.20	2922.64
45.00	80.00	10.00	22.00	10.00	168.40	35.87	2975.46

Reproduced from
best available copy.

Reproduced from
best available copy.

***** BLUNDER ANALYSIS - DUAL AIRCRAFT *****										PAGE = 53	
BLUNDERED DEPARTURE ANGLE (DEG.)	BLUNDERED VELOCITY (KNOTS)	BLUNDERED BACK ANGLE (DEG.)	BLUNDERED SUMMED DELAYS (SEC.)	ADJACENT SUMMED DELAYS (SEC.)	CORRECTED PARALLEL HEADINGS (DEG.)	BLUNDER CORRECTION, TIME (SEC.)	BLUNDER RECOVERY AIRSPACE (FT.)				
45.00	100.00	40.00	2.50	1.00	171.17	6.44	594.67				
45.00	100.00	40.00	2.50	4.00	177.95	7.18	606.50				
45.00	100.00	40.00	2.50	7.00	180.00	7.41	607.17				
45.00	100.00	40.00	2.50	10.00	180.00	7.41	607.17				
45.00	100.00	40.00	9.00	1.00	171.17	12.94	1370.42				
45.00	100.00	40.00	9.00	4.00	177.95	13.68	1382.24				
45.00	100.00	40.00	9.00	7.00	180.00	13.91	1382.92				
45.00	100.00	40.00	9.00	10.00	180.00	13.91	1382.92				
45.00	100.00	40.00	16.00	1.00	171.17	19.77	2205.84				
45.00	100.00	40.00	16.00	4.00	177.95	20.68	2217.67				
45.00	100.00	40.00	16.00	7.00	180.00	20.91	2218.34				
45.00	100.00	40.00	16.00	10.00	180.00	20.91	2218.34				
45.00	100.00	40.00	22.00	1.00	171.17	25.94	2921.92				
45.00	100.00	40.00	22.00	4.00	177.95	26.68	2933.74				
45.00	100.00	40.00	22.00	7.00	180.00	26.91	2934.41				
45.00	100.00	40.00	22.00	10.00	180.00	26.91	2934.41				
45.00	100.00	50.00	2.50	1.00	167.53	7.66	711.05				
45.00	100.00	50.00	2.50	4.00	173.63	8.62	737.72				
45.00	100.00	50.00	2.50	7.00	179.73	9.59	747.16				
45.00	100.00	50.00	2.50	10.00	180.00	9.63	747.17				
45.00	100.00	50.00	9.00	1.00	167.53	14.16	1486.80				
45.00	100.00	50.00	9.00	4.00	173.63	15.12	1513.47				
45.00	100.00	50.00	9.00	7.00	179.73	16.09	1522.90				
45.00	100.00	50.00	9.00	10.00	180.00	16.13	1522.92				
45.00	100.00	50.00	16.00	1.00	167.53	21.16	2322.22				
45.00	100.00	50.00	16.00	4.00	173.63	22.12	2348.89				
45.00	100.00	50.00	16.00	7.00	179.73	23.09	2358.32				
45.00	100.00	50.00	16.00	10.00	180.00	23.13	2358.34				
45.00	100.00	50.00	22.00	1.00	167.53	27.16	3036.29				
45.00	100.00	50.00	22.00	4.00	173.63	28.12	3064.97				
45.00	100.00	50.00	22.00	7.00	179.73	29.09	3074.40				
45.00	100.00	50.00	22.00	10.00	180.00	29.13	3074.42				

Reproduced from
Best available copy

***** WILLOW AIRCRAFT ANALYSIS - DUAL AIRCRAFT *****										P GE = 54	
WILLOW AIRCRAFT (LBS.)	WILLOW VELOCITY (KNOTS)	WILLOW ANGLE (DEG.)	WILLOW SUMMED DELAYS (SEC.)	ADJACENT SUMMED DELAYS (SEC.)	CORRECTED PARALLEL READINGS (DEG.)	LUNDF CORRECTION TIME (SEC.)	WILLOW RECOVERY AIRSPACE (FT.)				
45.00	10.00	20.00	2.50	1.00	162.37	9.38	896.06				
45.00	10.00	20.00	2.50	4.00	167.50	10.67	952.64				
45.00	10.00	20.00	2.50	7.00	172.63	11.96	990.19				
45.00	10.00	20.00	2.50	10.00	177.76	13.25	1006.43				
45.00	10.00	20.00	9.00	1.00	162.37	15.88	1671.81				
45.00	10.00	20.00	9.00	4.00	167.50	17.17	1728.38				
45.00	10.00	20.00	9.00	7.00	172.63	18.46	1765.94				
45.00	10.00	20.00	9.00	10.00	177.76	19.75	1784.18				
45.00	10.00	20.00	10.00	1.00	162.37	22.80	2507.23				
45.00	10.00	20.00	16.00	4.00	167.50	24.17	2563.81				
45.00	10.00	20.00	16.00	7.00	172.63	25.46	2601.36				
45.00	10.00	20.00	16.00	10.00	177.76	26.75	2619.60				
45.00	10.00	20.00	22.00	1.00	162.37	28.88	3223.31				
45.00	10.00	20.00	22.00	4.00	167.50	30.17	3279.88				
45.00	10.00	20.00	22.00	7.00	172.63	31.46	3317.43				
45.00	10.00	20.00	22.00	10.00	177.76	32.75	3335.67				
45.00	10.00	10.00	2.50	1.00	153.78	12.24	1251.47				
45.00	10.00	10.00	2.50	4.00	157.30	14.07	1379.12				
45.00	10.00	10.00	2.50	7.00	160.82	15.89	1469.30				
45.00	10.00	10.00	2.50	10.00	164.34	17.72	1581.59				
45.00	10.00	10.00	9.00	1.00	153.78	18.74	2027.22				
45.00	10.00	10.00	9.00	4.00	157.30	20.57	2154.87				
45.00	10.00	10.00	9.00	7.00	160.82	22.39	2265.05				
45.00	10.00	10.00	9.00	10.00	164.34	24.22	2357.34				
45.00	10.00	10.00	10.00	1.00	153.78	25.74	2862.64				
45.00	10.00	10.00	10.00	4.00	157.30	27.57	2990.29				
45.00	10.00	10.00	16.00	7.00	160.82	29.39	3100.47				
45.00	10.00	10.00	16.00	10.00	164.34	31.22	3192.76				
45.00	10.00	10.00	22.00	1.00	153.78	31.74	3578.72				
45.00	10.00	10.00	22.00	4.00	157.30	33.57	3706.36				
45.00	10.00	10.00	22.00	7.00	160.82	35.39	3816.54				
45.00	10.00	10.00	22.00	10.00	164.34	37.22	3908.63				

***** BLUNDER ANALYSIS - DUAL AIRCRAFT MANEUVER ***** PAGE = 55

BLUNDERED DEPARTURE ANGLE (DEG.)	BLUNDERED VELOCITY (KNOTS)	BLUNDERED BANK ANGLE (DEG.)	BLUNDERED SUMMED DELAYS (SEC.)	ADJACENT SUMMED DELAYS (SEC.)	CORRECTED PARALLEL HEADINGS (DEG.)	BLUNDER CORRECTION TIME (SEC.)	BLUNDER RECOVERY AIRSPACE (FT.)
45.00	120.00	40.00	2.50	1.00	169.47	7.01	777.15
45.00	120.00	40.00	2.50	4.00	175.93	7.86	798.90
45.00	120.00	40.00	2.50	7.00	180.00	8.39	802.72
45.00	120.00	40.00	2.50	10.00	180.00	8.39	802.72
45.00	120.00	40.00	9.00	1.00	169.47	13.51	1708.05
45.00	120.00	40.00	9.00	4.00	175.93	14.36	1729.79
45.00	120.00	40.00	9.00	7.00	180.00	14.89	1733.62
45.00	120.00	40.00	9.00	10.00	180.00	14.89	1733.62
45.00	120.00	40.00	16.00	1.00	169.47	20.51	2710.55
45.00	120.00	40.00	16.00	4.00	175.93	21.36	2732.30
45.00	120.00	40.00	16.00	7.00	180.00	21.89	2736.12
45.00	120.00	40.00	16.00	10.00	180.00	21.89	2736.12
45.00	120.00	40.00	22.00	1.00	169.47	26.51	3569.94
45.00	120.00	40.00	22.00	4.00	175.93	27.36	3591.59
45.00	120.00	40.00	22.00	7.00	180.00	27.89	3595.41
45.00	120.00	40.00	22.00	10.00	180.00	27.89	3595.41
45.00	120.00	30.00	2.50	1.00	165.56	8.31	934.66
45.00	120.00	30.00	2.50	4.00	171.30	9.40	978.91
45.00	120.00	30.00	2.50	7.00	177.03	10.49	1001.35
45.00	120.00	30.00	2.50	10.00	180.00	11.06	1004.32
45.00	120.00	30.00	9.00	1.00	165.56	14.81	1865.56
45.00	120.00	30.00	9.00	4.00	171.30	15.90	1909.80
45.00	120.00	30.00	9.00	7.00	177.03	16.99	1932.25
45.00	120.00	30.00	9.00	10.00	180.00	17.56	1935.22
45.00	120.00	30.00	16.00	1.00	165.56	21.81	2868.06
45.00	120.00	30.00	16.00	4.00	171.30	22.90	2912.31
45.00	120.00	30.00	16.00	7.00	177.03	23.99	2934.75
45.00	120.00	30.00	16.00	10.00	180.00	24.56	2937.72
45.00	120.00	30.00	22.00	1.00	165.56	27.81	3727.35
45.00	120.00	30.00	22.00	4.00	171.30	28.90	3771.60
45.00	120.00	30.00	22.00	7.00	177.03	29.99	3794.04
45.00	120.00	30.00	22.00	10.00	180.00	30.56	3797.01

***** HLUNDER ANALYSIS - DUAL AIRCRAFT MANEUVER ***** PAGE = 56

BLUNDERED DEPARTURE ANGLE (DEG.)	BLUNDERED VELOCITY (KNOTS)	BLUNDERED BANK ANGLE (DEG.)	BLUNDERED SUMMED DELAYS (SEC.)	ADJACENT SUMMED DELAYS (SEC.)	CORRECTED PARALLEL HEADINGS (DEG.)	BLUNDER CORRECTION TIME (SEC.)	BLUNDER RECOVERY AIRSPACE (FT.)
45.00	120.00	20.00	2.50	1.00	160.20	10.10	1176.25
45.00	120.00	20.00	2.50	4.00	164.92	11.53	1262.73
45.00	120.00	20.00	2.50	7.00	169.65	12.95	1326.24
45.00	120.00	20.00	2.50	10.00	174.37	14.38	1366.34
45.00	120.00	20.00	9.00	1.00	160.20	16.60	2107.15
45.00	120.00	20.00	9.00	4.00	164.92	18.03	2193.63
45.00	120.00	20.00	9.00	7.00	169.65	19.45	2257.13
45.00	120.00	20.00	9.00	10.00	174.37	20.88	2297.24
45.00	120.00	20.00	16.00	1.00	160.20	23.60	3109.66
45.00	120.00	20.00	16.00	4.00	164.92	25.03	3196.13
45.00	120.00	20.00	16.00	7.00	169.65	26.45	3259.64
45.00	120.00	20.00	16.00	10.00	174.37	27.88	3299.74
45.00	120.00	20.00	22.00	1.00	160.20	29.60	3968.95
45.00	120.00	20.00	22.00	4.00	164.92	31.03	4055.42
45.00	120.00	20.00	22.00	7.00	169.65	32.45	4118.93
45.00	120.00	20.00	22.00	10.00	174.37	33.88	4159.03
45.00	120.00	10.00	2.50	1.00	151.74	12.92	1612.87
45.00	120.00	10.00	2.50	4.00	154.88	14.87	1790.62
45.00	120.00	10.00	2.50	7.00	158.01	16.83	1948.75
45.00	120.00	10.00	2.50	10.00	161.15	18.78	2086.78
45.00	120.00	10.00	9.00	1.00	151.74	19.42	2543.77
45.00	120.00	10.00	9.00	4.00	154.88	21.37	2721.52
45.00	120.00	10.00	9.00	7.00	158.01	23.33	2879.65
45.00	120.00	10.00	9.00	10.00	161.15	25.28	3017.68
45.00	120.00	10.00	16.00	1.00	151.74	26.42	3546.28
45.00	120.00	10.00	16.00	4.00	154.88	28.37	3724.02
45.00	120.00	10.00	16.00	7.00	158.01	30.33	3882.15
45.00	120.00	10.00	16.00	10.00	161.15	32.28	4026.18
45.00	120.00	10.00	22.00	1.00	151.74	32.42	4405.57
45.00	120.00	10.00	22.00	4.00	154.88	34.37	4583.31
45.00	120.00	10.00	22.00	7.00	158.01	36.33	4741.44
45.00	120.00	10.00	22.00	10.00	161.15	38.28	4879.47

***** BLUNDER ANALYSIS - DUAL AIRCRAFT ***** PAGE = 57

BLUNDERED DEPARTURE ANGLE (DEG.)	BLUNDERED VELOCITY (KNOTS)	BLUNDERED BANK ANGLE (DEG.)	BLUNDERED SUMMED DELAYS (SEC.)	ADJACENT SUMMED DELAYS (SEC.)	CORRECTED PARALLEL HEADINGS (DEG.)	BLUNDER CORRECTION TIME (SEC.)	BLUNDER RECOVERY AIRSPACE (FT.)
45.00	140.00	40.00	2.50	1.00	167.92	7.53	977.24
45.00	140.00	40.00	2.50	4.00	174.10	8.47	1012.01
45.00	140.00	40.00	2.50	7.00	180.00	9.37	1022.97
45.00	140.00	40.00	2.50	10.00	180.00	9.37	1022.97
45.00	140.00	40.00	9.00	1.00	167.92	14.03	2063.29
45.00	140.00	40.00	9.00	4.00	174.10	14.97	2098.06
45.00	140.00	40.00	9.00	7.00	180.00	15.87	2109.02
45.00	140.00	40.00	9.00	10.00	180.00	15.87	2109.02
45.00	140.00	40.00	16.00	1.00	167.92	21.03	3232.88
45.00	140.00	40.00	16.00	4.00	174.10	21.97	3267.65
45.00	140.00	40.00	16.00	7.00	180.00	22.87	3278.61
45.00	140.00	40.00	16.00	10.00	180.00	22.87	3278.61
45.00	140.00	40.00	22.00	1.00	167.92	27.03	4235.38
45.00	140.00	40.00	22.00	4.00	174.10	27.97	4270.15
45.00	140.00	40.00	22.00	7.00	180.00	28.87	4281.11
45.00	140.00	40.00	22.00	10.00	180.00	28.87	4281.11
45.00	140.00	30.00	2.50	1.00	163.82	8.89	1178.41
45.00	140.00	30.00	2.50	4.00	169.22	10.09	1244.41
45.00	140.00	30.00	2.50	7.00	174.63	11.29	1284.18
45.00	140.00	30.00	2.50	10.00	180.00	12.48	1297.37
45.00	140.00	30.00	9.00	1.00	163.82	15.39	2264.46
45.00	140.00	30.00	9.00	4.00	169.22	16.59	2330.45
45.00	140.00	30.00	9.00	7.00	174.63	17.79	2370.23
45.00	140.00	30.00	9.00	10.00	180.00	18.98	2383.42
45.00	140.00	30.00	16.00	1.00	163.82	22.39	3434.05
45.00	140.00	30.00	16.00	4.00	169.22	23.59	3500.04
45.00	140.00	30.00	16.00	7.00	174.63	24.79	3539.81
45.00	140.00	30.00	16.00	10.00	180.00	25.98	3553.01
45.00	140.00	30.00	22.00	1.00	163.82	28.39	4436.55
45.00	140.00	30.00	22.00	4.00	169.22	29.59	4502.55
45.00	140.00	30.00	22.00	7.00	174.63	30.79	4542.32
45.00	140.00	30.00	22.00	10.00	180.00	31.98	4555.51

***** BLUNDER ANALYSIS - DUAL AIRCRAFT MANEUVER ***** PAGE = 58

BLUNDERED DEPARTURE ANGLE (DEG.)	BLUNDERED VELOCITY (KNOTS)	BLUNDERED BANK ANGLE (DEG.)	BLUNDERED SUMMED DELAYS (SEC.)	ADJACENT SUMMED DELAYS (SEC.)	CORRECTED PARALLEL HEADINGS (DEG.)	BLUNDER CORRECTION TIME (SEC.)	BLUNDER RECOVERY AIRSPACE (FT.)
45.00	140.00	20.00	2.50	1.00	153.35	10.72	1477.00
45.00	140.00	20.00	2.50	4.00	162.73	12.26	1598.25
45.00	140.00	20.00	2.50	7.00	167.11	13.80	1692.26
45.00	140.00	20.00	2.50	10.00	171.48	15.34	1760.56
45.00	140.00	20.00	9.00	1.00	158.35	17.22	2563.04
45.00	140.00	20.00	9.00	4.00	162.73	18.76	2684.30
45.00	140.00	20.00	9.00	7.00	167.11	20.30	2779.00
45.00	140.00	20.00	9.00	10.00	171.48	21.84	2846.61
45.00	140.00	20.00	16.00	1.00	158.35	24.22	3732.63
45.00	140.00	20.00	16.00	4.00	162.73	25.76	3853.89
45.00	140.00	20.00	16.00	7.00	167.11	27.30	3948.59
45.00	140.00	20.00	16.00	10.00	171.48	28.84	4016.19
45.00	140.00	20.00	22.00	1.00	158.35	30.22	4735.14
45.00	140.00	20.00	22.00	4.00	162.73	31.76	4356.39
45.00	140.00	20.00	22.00	7.00	167.11	33.30	4951.10
45.00	140.00	20.00	22.00	10.00	171.48	34.84	5018.70
45.00	140.00	10.00	2.50	1.00	150.10	13.47	1988.96
45.00	140.00	10.00	2.50	4.00	152.93	15.52	2220.68
45.00	140.00	10.00	2.50	7.00	155.76	17.58	2431.03
45.00	140.00	10.00	2.50	10.00	158.59	19.64	2619.49
45.00	140.00	10.00	9.00	1.00	150.10	19.97	3075.00
45.00	140.00	10.00	9.00	4.00	152.93	22.02	3306.73
45.00	140.00	10.00	9.00	7.00	155.76	24.08	3517.07
45.00	140.00	10.00	9.00	10.00	158.59	26.14	3705.53
45.00	140.00	10.00	16.00	1.00	150.10	26.97	4244.59
45.00	140.00	10.00	16.00	4.00	152.93	29.02	4476.31
45.00	140.00	10.00	16.00	7.00	155.76	31.08	4686.66
45.00	140.00	10.00	16.00	10.00	158.59	33.14	4875.12
45.00	140.00	10.00	22.00	1.00	150.10	32.97	5247.10
45.00	140.00	10.00	22.00	4.00	152.93	35.02	5478.82
45.00	140.00	10.00	22.00	7.00	155.76	37.08	5689.17
45.00	140.00	10.00	22.00	10.00	158.59	39.14	5877.63

***** BLUNDER ANALYSIS - DUAL AIRCRAFT ***** PAGE = 59

BLUNDERED DEPARTURE ANGLE (DEG.)	BLUNDERED VELOCITY (KNOTS)	BLUNDERED BANK ANGLE (DEG.)	BLUNDERED SUMMED DELAYS (SEC.)	ADJACENT SUMMED DELAYS (SEC.)	CORRECTED PARALLEL HEADINGS (DEG.)	BLUNDER CORRECTION TIME (SEC.)	BLUNDER RECOVERY AIRSPACE (FT.)
45.00	160.00	40.00	2.50	1.00	166.51	8.00	1193.46
45.00	160.00	40.00	2.50	4.00	172.42	9.03	1244.33
45.00	160.00	40.00	2.50	7.00	178.33	10.06	1266.78
45.00	160.00	40.00	2.50	10.00	180.00	10.35	1267.93
45.00	160.00	40.00	9.00	1.00	166.51	14.50	2434.66
45.00	160.00	40.00	9.00	4.00	172.42	15.53	2485.53
45.00	160.00	40.00	9.00	7.00	178.33	16.56	2507.97
45.00	160.00	40.00	9.00	10.00	180.00	16.85	2599.12
45.00	160.00	40.00	16.00	1.00	166.51	21.50	3771.33
45.00	160.00	40.00	16.00	4.00	172.42	22.53	3822.20
45.00	160.00	40.00	16.00	7.00	178.33	23.56	3844.65
45.00	160.00	40.00	16.00	10.00	180.00	23.85	3845.80
45.00	160.00	40.00	22.00	1.00	166.51	27.50	4917.05
45.00	160.00	40.00	22.00	4.00	172.42	28.53	4967.92
45.00	160.00	40.00	22.00	7.00	178.33	29.56	4990.36
45.00	160.00	40.00	22.00	10.00	180.00	29.85	4991.52
45.00	160.00	30.00	2.50	1.00	162.26	9.41	1439.88
45.00	160.00	30.00	2.50	4.00	167.38	10.71	1531.49
45.00	160.00	30.00	2.50	7.00	172.49	90	1592.66
45.00	160.00	30.00	2.50	10.00	177.60	30	1622.89
45.00	160.00	30.00	9.00	1.00	162.26	15.91	2681.07
45.00	160.00	30.00	9.00	4.00	167.38	17.21	2772.69
45.00	160.00	30.00	9.00	7.00	172.49	18.50	2833.86
45.00	160.00	30.00	9.00	10.00	177.60	19.80	2864.08
45.00	160.00	30.00	16.00	1.00	162.26	22.91	4017.75
45.00	160.00	30.00	16.00	4.00	167.38	24.21	4109.36
45.00	160.00	30.00	16.00	7.00	172.49	25.50	4170.53
45.00	160.00	30.00	16.00	10.00	177.60	26.80	4290.76
45.00	160.00	30.00	22.00	1.00	162.26	28.91	5163.47
45.00	160.00	30.00	22.00	4.00	167.38	30.21	5255.08
45.00	160.00	30.00	22.00	7.00	172.49	31.50	5316.25
45.00	160.00	30.00	22.00	10.00	177.60	32.80	5346.48

***** BLUNDER ANALYSIS - DUAL AIRCRAFT MANEUVER *****

BLUNDERED DEPARTURE ANGLE (DEG.)	BLUNDERED VELOCITY (KNOTS)	BLUNDERED BANK ANGLE (DEG.)	BLUNDERED SUMMED DELAYS (SEC.)	ADJACENT SUMMED DELAYS (SEC.)	CORRECTED PARALLEL HEADINGS (DEG.)	BLUNDER CORRECTION TIME (SEC.)	BLUNDER RECOVERY AIRSPACE (FT.)
45.00	160.00	20.00	2.50	1.00	156.75	11.25	1794.76
45.00	160.00	20.00	2.50	4.00	160.83	12.89	1954.97
45.00	160.00	20.00	2.50	7.00	164.91	14.33	2085.40
45.00	160.00	20.00	2.50	10.00	168.99	16.17	2185.39
45.00	160.00	20.00	9.00	1.00	156.75	17.75	3035.96
45.00	160.00	20.00	9.00	4.00	160.83	19.39	3196.16
45.00	160.00	20.00	9.00	7.00	164.91	21.03	3326.59
45.00	160.00	20.00	9.00	10.00	168.99	22.67	3426.59
45.00	160.00	20.00	16.00	1.00	156.75	24.75	4372.63
45.00	160.00	20.00	16.00	4.00	160.83	26.39	4532.84
45.00	160.00	20.00	16.00	7.00	164.91	28.03	4663.27
45.00	160.00	20.00	16.00	10.00	168.99	29.67	4763.26
45.00	160.00	20.00	22.00	1.00	156.75	30.75	5518.35
45.00	160.00	20.00	22.00	4.00	160.83	32.39	5678.56
45.00	160.00	20.00	22.00	7.00	164.91	34.03	5808.99
45.00	160.00	20.00	22.00	10.00	168.99	35.67	5908.98
45.00	160.00	10.00	2.50	1.00	148.75	13.92	2376.08
45.00	160.00	10.00	2.50	4.00	151.33	16.06	2664.71
45.00	160.00	10.00	2.50	7.00	153.91	18.20	2930.52
45.00	160.00	10.00	2.50	10.00	156.49	20.34	3172.98
45.00	160.00	10.00	9.00	1.00	148.75	20.42	3617.27
45.00	160.00	10.00	9.00	4.00	151.33	22.56	3905.91
45.00	160.00	10.00	9.00	7.00	153.91	24.70	4171.72
45.00	160.00	10.00	9.00	10.00	156.49	26.84	4414.17
45.00	160.00	10.00	16.00	1.00	148.75	27.42	4953.95
45.00	160.00	10.00	16.00	4.00	151.33	29.56	5242.50
45.00	160.00	10.00	16.00	7.00	153.91	31.70	5508.39
45.00	160.00	10.00	16.00	10.00	156.49	33.84	5750.85
45.00	160.00	10.00	22.00	1.00	148.75	33.42	6099.66
45.00	160.00	10.00	22.00	4.00	151.33	35.56	6388.30
45.00	160.00	10.00	22.00	7.00	153.91	37.70	6654.11
45.00	160.00	10.00	22.00	10.00	156.49	39.64	6896.57

APPENDIX L

BIBLIOGRAPHY

-, Airlines Electronic Engineering Committee, "Supplement No. 1 to ARINC Characteristic No. 547 Airborne VHF Navigation Receiver", Aeronautical Radio, Inc., April 20, 1966.

-, Airman's Information Manual, Part 1, DOT/FAA, November 1970.

-, ARINC Characteristic No. 547, Airborne VHF Navigation Receiver (Rev. 1), Aeronautical Radio, Inc., October 1, 1961.

Barucha-Reid, A. T., Elements of the Theory of Markov Processes and Their Applications, McGraw-Hill, New York, 1960.

Bekey, G. A., H. F. Meissinger and R. E. Rose, "Mathematical Models of Human Operators in Simple Two-Axis Manual Control Systems", IEEE Transactions on Human Factors in Electronics, September 1965, pp. 42-52.

Blakelock, John H., Automatic Control of Aircraft and Missiles, John Wiley and Sons, Inc., New York, 1965.

Blumstein, Alfred, "A Monte Carlo Analysis of the Ground Controlled Approach System", Operations Research, Vol. 5, No. 3, June 1967, pp. 397-408.

Callaway, E. E., "ILS Back Course and VOR Approach Data", DOT-FAA, FS-640, 5 August 1971.

Carnahan, B., H. A. Luther, and J. O. Wilkes, Applied Numerical Methods, John Wiley & Sons, Inc., New York, 1969.

Carter, Hobert L., "Revalidation of the Data Base Used in Establishing the Criteria for Simultaneous ILS Approaches to Parallel Runways", DOT-FAA-SRDS-ATC Development Division, No. 150-502, May 1970.

Clement, W. F., J. J. Best and R. L. Stapleford, "Analysis of Display-Pilot-Vehicle Dynamics for ILS Approach of a Large Jet Aircraft", Technical Memorandum 163-C, May 1967.

Clement, W. F., H. R. Jex, and D. Graham, "Application of a Systems Analysis Theory for Manual Control Displays to Aircraft Instrument Landing", Fourth Annual NASA-University Conference on Manual Control, NASA SP-192, March 21-23, 1968,

pp. 69-94.

-, Collins Maintenance Manual, Collins Radio Company, 34-35-0, 1969, pp. 6 - 8-B.

-, Collins Overhaul Manual, Collins Radio Company, 34-35-03, 1969, pp. 3-8.

-, Collins 51R-7A, -8A VHF NAV/COMM Receivers, Collins Radio Company, 5M-WP-1-68, 1968.

-, Collins 51R-7/8 VOR/LOC Receivers, Collins Radio Company, 1968, pp. 1-3 - 1-8.

-, Collins 51RV-1 Navigation Receiver, Collins Radio Company, 2.5-LP-3-67, 1967.

-, Collins 51RV-2B Navigation Receiver, Collins Radio Company, 5M-JPC-5-69, 1969.

-, Computer-Aided Metering and Spacing with ARTS III, Phase I Design Study, FAA-RC-70-82, December 1970.

Davison, E. J., "A Method for Simplifying Linear Dynamic Systems", IEEE Transactions on Automatic Control, Vol. AC-11, No. 1, January 1966.

Doanmasch, D. O., et al, Airplane Aerodynamics, Third Edition, Pitman Publishing Corporation, New York, 1961.

Dorf, Richard C., Modern Control Systems, Addison-Wesley Publishing Company, Reading, Massachusetts, 1967, p91.

Erwin, Ralph L., Jr., "Time-Synchronized Approach Control", Proceedings of the Institute of Navigation, April 1970, pp. 163-173.

Etkin, Bernard, Dynamics of Flight, John Wiley and Sons, Inc., 1959.

-, "Evaluation of Parallel Runway Spacing", FAA-ARDS, Task No. 412-3-2T, July 1961.

Eveleigh, V. W., Adaptive Control and Optimization Techniques, McGraw-Hill Book Company, New York, 1967.

-, FAA Air Traffic Activity, Fiscal Year 1970, DCT-FAA, Information and Statistics Division, Office of Management Systems, August 1970.

Faison, W., "Analysis of a Procedure for Conducting Instrument Approaches to Parallel Runways Spaced Less than 5000 Feet Apart", RD 66-35, 1966.

Feller, William, An Introduction to Probability Theory, Volumes I and II.

Filkins, Lyle D. and Joseph W. Little, "Study of Aircraft Separation Criteria", Report No. RD-64-113, AD 700-304, November 1964.

Gartner, Walter B., "A Simulator Study of Flight Management Task Performance During Low Visibility Approach and Landing Using Baseline Category II Flight Instrumentation", Contract NAS2-4406, N70-42037, December 1969.

Goldman, A. J., "Analysis of a Capacity Concept for Runway and Final-Approach Path Airspace", Proceedings of the Institute of Navigation, April 1970, pp. 119-131.

Grafton, Sue B., Lysle P. Parlett, and C. C. Smith, Jr., "Dynamic Stability Derivatives of a Jet Transport Configuration with High Thrust-Weight Ratio and an Externally Blown Jet Flap", NASA TN D-6440, September 1971.

-, "Ground Noise Measurements During Landing and Take-off Operations of the McDonnell-Douglas 188 (Breguet 941) STOL Airplane", Langley Working Paper, LWP-741, April 18, 1969.

Hall, G. Warren and Edward M. Booth, "An In-Flight Investigation of Lateral-Directional Dynamics for the Landing Approach", Technical Report AFFDL-TR-70-145, AD 715-317, October 1970.

Hanke, C. R., "The Simulation of a Large Jet Transport Aircraft, Volume I: Mathematical Model", NASA CR-1756, N11-19239, March 1971.

Helstrom, C. W., "Markov Processes and Applications", Communication Theory, Chapter 2.

Hershkowitz, Ronald, "Collision Risk Model for NAT Region", Report No. DOT-TSC-FAA-71-6, AD 733-754, May 1971.

Higgins, L. O. and P. Mpontsikaris, "Evaluation of Air Traffic Control Models and Simulations", Report No. DOT-TSC-FAA-71-7, AD 733-755, June 1971.

Hockaday, S. L. M., A Model to Investigate the Separation of Landing Aircraft, With Special Reference to Collision Risk, Ph.D. Dissertation in Engineering, Graduate Division of the University of California, Berkeley.

Holland, Frederick C., "Analysis Tools for Airport Capacity", Proceedings of the Institute of Navigation, April 1970, pp. 133-162.

Holt, John M., "Application of CAS Theory to Parallel Runway Separation", Proceedings of the Institute of Navigation, April 1970, pp. 215-222.

Irby, F. S., Milestone Report for the System Modeling Task, Contract No. DOT-FA-71WA-2609, Resalab, Inc., September 1971.

Jackson, A. S., Analog Computation, McGraw-Hill Book Company, Inc., 1960.

Johnson, E. W., D. L. Carmack and L. H. Hadley, "Psychological and Procedural Aspects Related to ILS Approaches and Landings in Visibilities Less Than 1200 Feet", AGARD Conference Proceedings No. 59 on Aircraft Landing Systems, AGARD-CP-59-70, AD 714-925, May 1969, pp. 3-1 to 3-8.

Kaplan, Wilfred, Advanced Calculus, Addison-Wesley Publishing Company, Reading, Massachusetts, 1959.

Karlin, J. E. and S. N. Alexander, "Communication Between Man and Machine", Proceedings of the IRE, May 1962, pp. 1124-1128.

Klesken, D. L., "PLACE-An Engineering Experiment for Air Traffic Control", EA-CON '69 Record, 1969, pp. 166-173.

Kozoil, Joseph S., Jr., Simulation Model for the Piper PA-30 Light Maneuverable Aircraft in the Final Approach, Memorandum Report, DOT-FAA, SRDS, Report No. DOT-TSC-FAA-71-11, AD 733-757, July 1971.

Kuethe, A. M. and J. D. Schetzer, Foundations of Aerodynamics, John Wiley & Sons, Inc., 1959.

Kuo, B. C., Automatic Control Systems, Second Edition, Prentice-Hall, Inc., Englewood Cliffs, N. J., 1967.

Levison, W. H., S. Baron and D. L. Kleinman, "A Model for Human Controller Remnant", IEEE Transactions on Man Machine Systems, December 1969, pp. 101-108.

Marks, Marvin D. and John E. Hosford, "STOL Terminal Area Operations", Proceedings of the Institute of Navigation, April 1970, pp. 175-181.

McDonald, R. A., Mel Garelick, and J. O'Grady, "Linearized Mathematical Models for DeHavilland Canada "Buffalo and Twin Otter" STOL Transports", Report No. DOT-TSC-FAA-71-8, AD 733-756, June 1971.

McFarland, R. H. and F. J. Kiko, "Results of VOR Path Stability Investigations", Eascon '68 Record, pp. 531-536.

McLeod, E. F., "An International Airline Views Automatic Landing Systems", AGARD Conference Proceedings No. 59 on Aircraft Landing Systems, AGARD-CP-59-70, AD 714-925, May 1969, pp. 2-1 to 2-4.

McRuer, D. T. and H. R. Jex, "A Review of Quasi-Linear Pilot Models", IEEE Transactions on Human Factors in Electronics, Vol. HFE-8, No. 3, September 1967, pp. 231-249.

McRuer, D. T. and H. R. Jex, "A Systems Analysis Theory of Manual Control Displays", Conference on Manual Control, 1967, pp. 9-28.

McRuer, D. T. and E. S. Krendel, "The Man-Machine System Concept", Proceedings of the IRE, May 1962, pp. 1117-1123.

-, Minimum Performance Standards, Airborne ILS Localizer Receiving Equipment, Radio Technical Commission for Aeronautics,

Paper 89-54/DO-59, July 15, 1954.

-, Navigation Equipment Capability Analysis Program, FAA, Standards Development Division FS-920, August 1964.

Papoulis, Athamassois, Probability, Random Variables, and Stochastic Processes, McGraw-Hill Book Co., New York, 1965.

Paskin, H. M., "A Discrete Stochastic Optimal Control Model of the Human Operator", 1970 Proceedings, National Aerospace Electronics Conference, May 18-20, 1970 (NAECON '70), pp. 270-276.

Pawula, R. F., Generalizations and Extensions of the Fokker-Planck-Kolmogorov Equations, Ph.D. dissertation from California Institute of Technology, 1965.

Pearson, E. S., and H. O. Hartley, Biometrika, Volume I, Cambridge University Press, Cambridge, England, 1954.

Perkins, C. D. and Hage, R. E., Airplane Performance Stability and Control, John Wiley & Sons, Inc., New York, 1965.

Pierce, J. R., Symbols, Signals and Noise, Harper and Row Publishers, New York, 1961.

Pitham, Leonard and Frank Parr, "Navigation Equipment Capability Program, NECAP II", DOT-FAA, Flight Standards Service, FS 66-250-57, SRDS 330-001-01N, December 1968.

Prabhu, N. U., Stochastic Processes, MacMillan Company, New York, 1965.

-, Report of Department of Transportation Air Traffic Control Advisory Committee, Volumes I and II, U. S. Government Printing Office, Washington, D. C., December 1969.

Rich, Paul H., et al, "Reactions of Pilots to Warning Systems for Visual Collision Avoidance", DOT-FAA, SRDS, Report No. FAA-RD-71-61, AD 735-141, December 1971.

Sage, A. P. and J. L. Melsa, Estimation Theory with Applications to Communications and Control, McGraw-Hill, New York, 1971.

Schwartz, Mischa, Information Transmission Modulation and Noise, McGraw-Hill Book Co., New York, 1959.

Seckel, E. and J. J. Morris, "The Stability Derivatives of the NAVION Aircraft Estimated by Various Methods and Derived from Flight Test Data", DOT-FAA, Report No. FAA-RD-71-6, AD 723-779, January 1971.

Senders, J. W., "A Re-Analysis of the Pilot Eye-Movement Data", IEEE Transactions on Human Factors in Electronics, Vol. HFE-7, No. 2, June 1966, pp. 103-106.

Skinner, R. W. and F. Parr, "Evaluation of Lower ILS Minimums for Light Aircraft", DOT-FAA, Flight Standards Service, Project No. FS-460-5, AD 708-294, June 1970.

St. John, O. B., "All Weather Landing", AGARD Conference Proceedings No. 59 on Aircraft Landing Systems, AGARD-CP-59-70, AD 714-925, May 1969, pp. 1-1 to 1-5.

Steinberg, Herbert A., "Collision and Missed Approach Risks in High-Capacity Airports Operations", Proceedings of the IEEE, March 1970, pp. 314-321.

Stevenson, Lloyd E., Preliminary Survey of Potential STOL Terminal Area Operational Requirements, DOT-FAA Technical Memorandum, Report No. DOT-TSC-FAA-71-9, June 1971.

-, "STOL Evaluation DeHavilland Buffalo DHC-5", FAA-SRDS, May 1970.

-, "STOL Operational Evaluation MDC-188 (Breguet 941S)", FAA-ADS, December 1969.

-, "STOL Steep Approaches in the Breguet 941", DOT-FAA, FS-640, November 1969.

-, "STOL Steep Approaches in the DeHavilland DHC-5 Buffalo", DOT-FAA, Memorandum Report FS-640, April 1970.

Stratonovich, R. L., Topics in the Theory of Random Noise, Volumes I and II, Gordon and Breach, New York, 1967.

Sveshnikov, A. A., Problems in Probability Theory, Math Statistics and Theory of Random Functions, W. B. Sanders Company, Philadelphia, 1968.

Takacs, Lojos, Stochastic Processes, Methuen and Company Ltd., London, 1960.

-, "Technical Facilities at NAFEC", FAA-DOT, National Aviation Facilities Experimental Center, June 1969.

Teper, G. L. and R. L. Stapleford, "An Assessment of the Lateral-Directional Handling Qualities of a Large Aircraft in the Landing Approach", J. Aircraft, Vol. 3, No. 3, May-June 1966, pp. 201-207.

-, Terminal Air Traffic Control, DOT-FAA, Air Traffic Service 7110.8A (Rev. 5), January 1, 1970.

Thelander, J. A., "Aircraft Motion Analysis", Douglas Aircraft Company, FDL-TDR-64-70, March 1965.

-, V/STOL Handling, Criteria and Discussion, AGARD-R-577-70, AD 715-553, December 1970.

Vinje, E. W. and D. P. Miller, "An Analysis of Pilot Adaptation in a Simulated Multiloop VTOL Hovering Task", Fourth Annual NASA-University Conference on Manual Control, (NASA SP-192), March 21-23, 1968, pp. 95-117.

Watkins, Jimmy, "Analysis of the Minimum Required Lateral Spacing Between Parallel Runways Used for Simultaneous IFR Approaches", DOT-FAA, SRDS, ATC Development Division, Subprogram No. 150-502, November 1970.

Weir, David H., "Compilation and Analysis of Flight Control System Command Inputs", AFFDL-TR-65-119, AD 483-621, January 1966.

Winick, A. B. and D. M. Brandewie, "VOR/DME System Improvements", Proceedings of the IEEE, Volume 58, No. 3, March 1970, pp. 430-437.

Winick, A. B. and D. M. Brandewie, "VORTAC System Improvements", FAA, Department of Transportation, Eascon '69 Record, pp. 153-160.